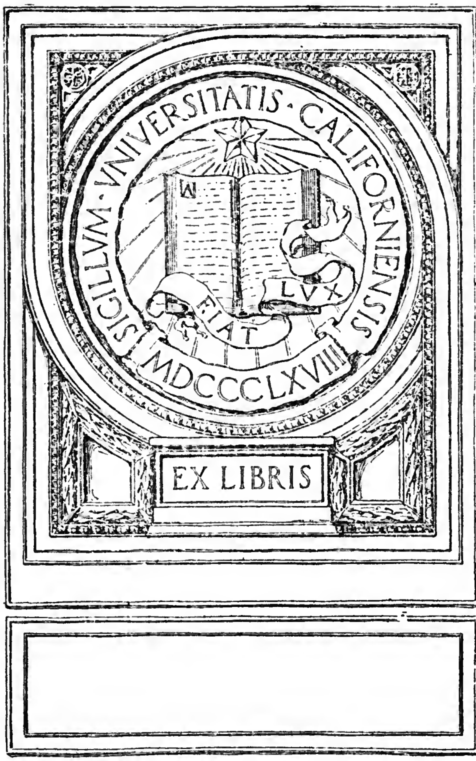
SIGILLVM · VNIVERSITATIS · CALIFORNIENSIS
FIAT LVX
MDCCCLXVIII
EX LIBRIS

Reproduced by courtesy of Messrs. Vickers, Ltd.

A Historic Machine.

The Vickers 'Vimy-Rolls' which crossed the Atlantic June 14th–15th, 1919.

Time: 15 hrs. 57 mins. Distance: 1890 miles.

Frontispiece

The Directly-Useful D.U. Technical Series

Founded by the late Wilfrid J. Lineham, B.Sc., M.Inst.C.E.

THE THEORY & PRACTICE

OF

AEROPLANE DESIGN

By

S. T. G. ANDREWS, B.Sc. (Engineering), London

Member of the Institute of Aeronautical Engineers,
Consulting Engineer;

AND

S. F. BENSON, B.Sc. (Engineering), London

Whitworth Exhibitioner,
Member of the Royal Aeronautical Society,
Consulting Engineer.

NEW YORK

E. P. DUTTON & COMPANY

681 FIFTH AVENUE

1920

PRINTED BY STRANGEWAYS AND SONS, TOWER STREET,
CAMBRIDGE CIRCUS, LONDON, ENGLAND.

EDITORIAL NOTE

The Directly-Useful Technical Series requires a few words by way of introduction. Technical books of the past have arranged themselves largely under two sections: the Theoretical and the Practical. Theoretical books have been written more for the training of college students than for the supply of information to men in practice, and have been greatly filled with problems of an academic character. Practical books have often sought the other extreme, omitting the scientific basis upon which all good practice is built, whether discernible or not. The present series is intended to occupy a midway position. The information, the problems and the exercises are to be of a directly-useful character, but must at the same time be wedded to that proper amount of scientific explanation which alone will satisfy the inquiring mind. We shall thus appeal to all technical people throughout the land, either students or those in actual practice.

AUTHORS' PREFACE

THE need of a reliable text-book in the theory and practice of aeroplane design has long been recognised by all those connected with aeronautical affairs. The present volume aims at supplying this want and will be found useful by designers, aeronautical draughtsmen, and students, besides containing much of interest to the general reader.

The study of Aeronautics can only be successfully attempted by those possessing a good knowledge of Mathematics and Physics. Aeroplanes are machines containing many differing elements. These elements demand a great or less knowledge of scientific matters according to their nature. In order to become an aeronautical engineer and designer it is necessary to have a thorough knowledge of—

(A) The Graphic Representation of Laws. From the practical point of view graphs are essential to the designer and engineer. Visualisation of the relationships existing between certain quantities, as for example Lift (Drag, or Lift/Drag), with change in the Angle of Incidence, is of the utmost importance. Graphs exhibit the variation of one quantity with another far more powerfully than any other method known. Again, the reverse process, namely, the establishing of an algebraical equation to satisfy the relationship existing between quantities whose graph has been drawn, is of considerable use in original work.

(B) The fundamental Theorems in Theoretical Mechanics such as those dealing with velocity, acceleration, gravity, moments of inertia, centrifugal force, fluid motion, work, energy, and power.

(C) Various Theorems in Applied Mechanics. The more important of these are considered in their bearing upon aeronautical problems in Chapters II. and IV., and at other places as occasion demands.

As will be seen from even a casual glance through this book, more than usual care has been devoted throughout to the preparation and production of the diagrams and tables, and it is confidently anticipated that they will prove of direct utility to those actively engaged in aeroplane design. A special feature has also been made of illustrative examples, and a large number of these will be found scattered throughout the text. It is hoped that their insertion will clear up all doubtful points. Furthermore, the whole subject has been presented in a complete and logical manner, and the principles enunciated have been applied in Chapter XIII. to the lay-out of a complete machine.

The authors desire to thank the following: Messrs. Vickers, who have spared no pains in supplying information and photographs relating to their machines; *Flight*, for their unfailing courtesy at all times, and permission to use the several blocks indicated in the text; Messrs. Handley Page, Ltd.; Boulton & Paul; Edgar Allen & Co., and Brunton's, for photographs and information where indicated; Messrs. Barling & Webb, for permission to use the tapered strut formula; and to the Advisory Committee for Aeronautics for permission to make extracts from their reports. In this connection we might add that we are still awaiting the photographs which the Secretary of the National Physical Laboratory promised in August, 1919.

We should also like to express our thanks to Miss G. E. Powers, Cambridge Mathematical Tripos; Mr. Lewis Curtis, M.A.; and Mr. H. J. Cardnell-Harper, A.M.I.C.E., for reading through the proofs; and to Mr. A. B. Tomkins, for assistance in preparing some of the illustrations.

In conclusion, while every precaution has been taken to guard against errors, the authors would be glad of notification of any which may be observed, or suggestions for improvements in future editions.

S. T. G. ANDREWS,
S. F. BENSON.

80 Shakespeare Crescent,
Manor Park, London, E. 12.
January, 1920.

CONTENTS

CHAPTER I

PAGE

THE PRINCIPLES OF DESIGN 1

The characteristics of an aeroplane — Weight — Aerofoil characteristics—The resistance of the machine — Horse-power available at the airscrew—Controllability and stability—General consideration of design.

CHAPTER II

THE MATERIALS OF DESIGN 13

Timber – Light alloys —Steel—Aeroplane fabric—Stress, strain, elasticity—Tests — Factor of safety — Wind pressure — Stress diagrams — Method of sections.

CHAPTER III

THE PROPERTIES OF AEROFOILS 38

Wind tunnel investigation—The N.P.L. four-foot tunnel—The balance—The Eiffel laboratory—The flat plate—The inclined flat plate—Flat plate moving edgewise —The aerofoil—Pressure distribution over an aerofoil—Aerofoil efficiency — Pressure distribution over the entire surface of an aerofoil — Full-scale pressure distribution experiments — Aspect ratio — The relative importance of the upper and lower surfaces of an aerofoil—Determination of the lift and drag of a series of aerofoils with plain lower surface and variable camber of upper surface—Determination of the lift and drag of a series of aerofoils with the same upper surface and variable camber of lower surface—Determination of the lift and drag of a series of aerofoils, the position of the maximum ordinate being varied — Effect of thickening the leading edge of an aerofoil — Effect of thickening the trailing edge of an aerofoil — Centre of pressure — Reflexed curvature towards the trailing edge—Interference of aerofoils—Gap—Decalage—Stagger—The choice of an aerofoil—Units—The law of similitude—Standard wing sections.

CHAPTER IV

PAGE

Stresses and Strains in Aeroplane Components . . 101

Moments of inertia—Shear force and bending moment—Stresses in beams—Relation between load, shear, bending moment, slope, and deflection—Struts—Eccentric loading—Streamlined struts—Tapered streamline struts.

CHAPTER V

Design of the Wings 130

Wing structures—Monoplane trusses—Biplane trusses—Wireless biplane trusses — Strutless biplane truss — Triplane trusses — Wireless triplane trusses—Quadruplane trusses—Drag and incidence bracing—Development of the single lift truss—Tractor and pusher machines—The factor of safety — Experimental investigation of the stresses upon a full-size machine during flight—Stresses — Stresses in the wing structure — Wing loading—Wing weights — Stresses due to downloading — Stressing of the wing structure — General procedure for design of the members of the wing structure — Change of direction of drag forces in the wing structure — Stagger—Detail design of the wing structure—The external bracing—The interplane struts—Tapered strut formula—The drag struts and bracing—Design of the spars—Practical example of wing structure design—Design of the wing ribs—Wing assembly.

CHAPTER VI

Resistance and Streamlining 208

Resistance—Variation from the (V^2) law—Streamlining—Inclination of struts—Resistance of the body or fuselage—Aeroplane bodies—Deperdussin monocoque fuselages—B.E. 2 and B.E. 3 fuselages—Resistance of wires—Resistance of flat plates—Resistance of landing gear—Effect of airscrew slip stream—Resistance of complete machine—Experimental Measurement of the resistance of full-size machines—Skin friction.

CHAPTER VII

Design of the Fuselage 238

Weights—The fuselage—Stressing the fuselage—Design of the engine mountings—Gyroscopic action of a rotary engine and the airscrew.

CHAPTER VIII

PAGE

DESIGN OF THE CHASSIS 260

Function of the chassis—Forces on chassis when landing—Method of locating fore and aft position of chassis—General principles of chassis design—Types of chassis—Stresses in chassis members—Shock absorbers—The tail skid—Streamlining the chassis.

CHAPTER IX

DESIGN OF THE AIRSCREW 280

Methods of design—Experimental method of design—Tractive power developed at the airscrew—Design of the airscrew by the blade element theory—Stresses in airscrew blades—Stresses due to bending—The construction of an airscrew.

CHAPTER X

STABILITY 303

Definition—Stability nomenclature—The equations of motion—The resistance and rotary derivatives—Longitudinal stability of the Bleriot machine—Lateral stability of the Bleriot model—Longitudinal stability of a biplane.

CHAPTER XI

DESIGN OF THE CONTROL SURFACES 346

Controllability and stability—The tail plane and elevator—Reduction of effectiveness of the tail plane due to wash from the main planes—The elevator—Tail plane design—Determination of dimensions of the tail plane and settings of the elevator—Fin and rudder lateral force due to the airscrew—Ailerons or wing flaps—Balance of the control surfaces—Construction of control surfaces.

CHAPTER XII

PERFORMANCE 381

Definition—The resistance of the machine—Horse-power required—Horse-power available—Rate of climb—Performance calculations—Measurement of performance—The airspeed indicator (anemometer)—Performance tests on full-scale machines—Rate of climb test—Theory of the aneroid barometer—Measurement of rate of climb.

CHAPTER XIII

PAGE

General Lay-out of Machines 403

The process of laying-out—General arrangement.

CHAPTER XIV

The General Trend of Aeroplane Design 424

The Bleriot machine—Avro machines—Airco machines—Armstrong-Whitworth machines—Bristol machines—Handley Page machines—Sopwith machines—Vickers machines—Boulton & Paul machines—Official machines—Wing design—Fuselages—Control surfaces—The airscrew—Performance.

THE THEORY & PRACTICE

OF

AEROPLANE DESIGN.

CHAPTER I.

THE PRINCIPLES OF DESIGN.

The Characteristics of an Aeroplane.—Practical flying is of very recent date, since it was only in 1903 that the Wright Brothers, in an aeroplane weighing 750 lbs. and mounting a 16 h.p. engine, succeeded in leaving the ground.

The work of the Wright Brothers is particularly interesting and instructive to the aeronautical student and engineer. They first of all learnt how to 'fly' a biplane glider—that is the wing structure only of an aeroplane—by launching themselves from the top of a slope (see Fig. 1, p. 8). In this way they discovered practically the elements of stability, and it is noteworthy that in their machines the controlling surface to give longitudinal stability was placed in front of the wing structure (see Figs. 1 and 2, p. 8), whereas modern practice places this member (the tail plane) at the rear. Another important detail in connection with the work of the Wright Brothers was the fact that they adopted the principle of warping the wings in order to maintain stability and do away with the necessity of moving their bodies on the glider, the method used by Lilienthal and Chanute. They also realised the fundamental basis of mechanical flight, namely, that the problem of the aeroplane is largely one of strength in relation to weight. There being no suitable power plant available combining the advantages of light weight with maximum power, they designed a special motor to fulfil these requirements, and this can justly be called the forerunner of modern aero engines.

The work of these pioneers, therefore, is an excellent example of the necessity for linking together into one homogeneous whole technical and scientific research.

To adjust the many details which enter into the design of a successful machine is a matter of compromise, and requires considerable care and judgment on the part of the designer. It is possible to-day to predict with considerable accuracy the performance of a machine before it leaves the ground; and in this connection Table I., dealing with a machine constructed in 1912, is instructive and worthy of notice.

TABLE I.—COMPARISON OF CALCULATED AND ACTUAL PERFORMANCE.

	Calculated.	Actual.	
Maximum speed ...	68 ...	69	miles per hour.
Minimum speed ...	39·5 ...	39·5	miles per hour.
Rate of climb	430 ...	400–450	feet per minute.
Minimum gliding angle	1 in 8·4 ...	1 in 7·4	

The problem before the manufacturer to-day is to supply, on a commercial basis, a machine which will carry a definite useful load over a given distance. The nature of this problem will be fully discussed in subsequent chapters. For a given type of machine the designer has to balance various conflicting factors so that the resulting machine may fulfil certain definite conditions with regard to efficiency, strength, stability, and convenience. For example, if a fast Scout is required, the reduction of resistance is a prime factor, and stream-lining must be carefully considered in all exposed parts. Again, if a cargo-carrying machine is wanted, great lifting capacity is necessary, and the choice of a suitable aerofoil is essential; for which purpose the designer must use the latest research work of the aeronautical laboratories.

There are, however, common to all types of machines certain basic considerations, namely:

Weight.
Aerofoil characteristics.
Resistance.
Horse-power available at the airscrew.
Controllability and stability.

Weight.—The question of weight is obviously an important one, and since a reduction in weight will always lead to improved performance, it will be useful to indicate in which directions a designer may hope to effect a saving. The necessity for obtaining maximum strength with a minimum of weight is one of the fundamental problems of aeroplane construction. In no branch of engineering is it more essential that weight should be economically distributed. The weight of an aeroplane can be considered under the following headings:

(*a*) Weight of the structural portion of the machine.
(*b*) Weight of the power plant, fuel, lubricant, etc.
(*c*) Weight of the useful load.

With present types of machines and constructional methods it is found that the weight of the structural portion amounts to about one-third of the total weight of the machine. The following figures, giving the weights of the principal elements of the aeroplane structure as a percentage of its total weight, are representative of modern practice.

TABLE II.—WEIGHTS OF STRUCTURAL COMPONENTS EXPRESSED AS PERCENTAGES OF THE TOTAL WEIGHT.

Wing structure complete	13 % of total weight.
Body complete	13 % " "
Tail unit complete	2 % " "
Landing gear	4 % " "

It is not likely that much improvement can be made on the above figures unless some other material, possessing greater strength per unit weight than wood, is made available.

The relative proportions of weight of power plant and useful load are necessarily dependent to a large extent upon the purpose for which the machine is to be used. The greater the flying range required the greater will be the quantity of fuel, lubricant, etc., required, and the smaller will be the useful load. Considering the power plant, it is useful to note the enormous advances which have been made in recent years in reducing the weight per horse-power of aero engines. Table III. illustrates this reduction.

TABLE III.—DIMINUTION IN WEIGHT PER H.P. OF AERO ENGINES.

Year ...	1901	1905	1908	1910	1912	1913
Wt/H.P. ...	12·7	9·5	5·2	5·7	5·3	4·7

Year ...	1914	1915	1916	1917	1918	1919
Wt/H.P. ...	3·9	3·85	3·1	2·8	1·9	1·5

Aerofoil Characteristics.—In Chapter III. we shall study the various characteristics of an aerofoil in detail, and show how to determine the aerofoil which is most suitable for a given set of conditions; and it is therefore sufficient for our present purpose to consider briefly the variation in section, form, number of surfaces used, and arrangement of those surfaces in relation to each other.

It is desirable to use a wing section with the maximum vertical reaction (or Lift) combined with a minimum horizontal reaction (or Drag); in other words, the Lift/Drag ratio must be high. The Wright Brothers, in their early machines, used a wing section with a Lift/Drag ratio of 12, and this figure represented a very great improvement on previous wing sections. To-day many aerofoils have a Lift/Drag ratio of 17, and in some cases this figure has been exceeded. But these results have been obtained partly at the expense of the maximum lift coefficient, and consequently for a given minimum speed we require a larger surface to support a given weight than with a section of lower maximum Lift/Drag ratio, but higher maximum lift coefficient. It will be instructive, and will serve to impress these facts more clearly on the mind if we study them with reference to the fundamental equation for the lifting capacity of a machine, namely—

$$W = K_y \frac{\rho}{g} A V^2 \quad \text{........ ... . Formula 1}$$

Where W = the total weight lifted.
K_y = the absolute lift coefficient.
ρ = the density of the air in lbs. per cubic foot.
A = the area of the supporting surface in square feet.
V = the velocity of the machine in feet per second.
g = the acceleration due to gravity.

A heavier-than-air machine will not leave the ground until the above relationship is satisfied. Hence for machines with equal supporting areas, the larger the maximum value of K_y for the wing section the smaller will be the value of V at which the machine leaves the ground, and the smaller will be the landing speed. Conversely, if the landing speed of two machines with aerofoils of different maximum lift coefficient be the same, then the machine with the wing section of lower maximum lift coefficient must have the larger area of supporting surface. A little time spent in examining this equation and its various factors will help to bring these points out, and will be time well spent.

It is desirable that a machine should have as large a speed range as possible, and be capable of landing at a comparatively low speed, so that the sacrifice of a high lift coefficient in order to obtain a better L/D ratio is not altogether an advantage. It is possible that some practical means of varying the camber of the wing section will be devised in the future, and this would furnish the best solution to the problem. Attempts have already been made in this direction, but the results have not justified the increased weight and complication of parts.

The planes are generally made rectangular in form, and this brings us to a consideration of aspect ratio, which is the ratio span : chord. The higher the aspect ratio, the better will be the L/D ratio of a plane. In Chapter III. it is shown that when the aspect ratio is diminished from 8 to 3, there is a diminution of 35% in the maximum value of the L/D ratio. This is due to the lateral escape of the air at the wing-tips, which causes a loss of lift, together with a large increase in the drag. This is an inherent defect of the modern wing section, and is very difficult to remedy. By suitably shaping the outer ends of the planes it is possible to reduce this loss considerably. It has been noted above that increase of aspect ratio means an improved L/D ratio over the wing. Unfortunately, however, increase of aspect ratio means increased mechanical difficulties in the construction of the wing structure, heavier wings and bracing, resulting in increased resistance. Moreover, the controllability of the machine and its ability to manœuvre rapidly will be diminished: hence it is necessary to compromise, and the aspect ratio of an aeroplane is therefore generally from 5 to 8. With increasing size of machine, the ratio appears to be advancing slightly, and in some cases approaches a value of 10; but this is quite unusual, and it is doubtful whether there is any advantage to be derived from it. This consideration of aspect ratio leads us on to another important consideration, namely, the arrangement of surfaces. Modern aeroplanes may be classified according to the number of the supporting surfaces: thus we have monoplanes, biplanes, triplanes, &c., but of these it may be said that the biplane group is by far the most important and numerous, and the tractor biplane is the form of aeroplane which at present approaches the nearest to a standardised type. It may be said generally that the most efficient plane from an aerodynamical point of view is the monoplane, for there is no possibility of interference of the planes as there is on the other types, and for small machines this is probably the best arrangement. With increasing size and weight, however, the large span required in this type to give the necessary supporting surface means a relatively heavy wing and increased complication of bracing, leading to a large increase in structural resistance; hence, for all but small machines, the multiplane arrangement is more efficient. Precisely the same argument holds with reference to the biplane and triplane. For the size and weight of the machines most generally used to-day the biplane arrangement is undoubtedly the most efficient one, but as the demand for larger and heavier machines increases, and particularly for the passenger and cargo-carrying machines, which will be increasingly developed in the near future, the triplane will become a serious competitor, and may prove to be a more efficient arrangement. Apart from this point of view, the difficulty of handling and housing a great structure of 100 feet span or more will become an important factor. In this connection, however, the practice of folding back the wings of a machine when not in use (as shown in Fig. 3, p. 8) will to some extent obviate this difficulty. It must also be remembered that it is relatively cheaper to increase the depth of a hangar than it is to increase its span.

The Resistance of the Machine.—This is usually regarded as made up of two parts—

1. The drift or drag of the wings.
2. The resistance of the remainder of the machine.

The first part will be very fully considered in Chapter III., and it therefore remains to say a few words with reference to the second part. The first designer to enclose the body from the wings to the tail plane was Nieuport, in 1909, and by this means he obtained a considerable improvement in speed without any corresponding increase in the horse-power used. All modern machines are stream-lined to the utmost possible extent, resulting in a great reduction in the total resistance of the exposed external parts. Table IV. gives the average resistances of the component parts of machines in general use to-day.

TABLE IV.—PERCENTAGE RESISTANCES OF AEROPLANE COMPONENTS.

	Percentage.
Body	60
Landing gear	17
Tail unit complete	8
Lift bracing and external fittings	15

As will be seen, the body accounts for the major portion of the total resistance of the machine, and it is impossible to avoid this with the usual arrangement of the radiator. Some German machines have had their radiators fixed in the surface of the top plane.

Horse-power available at the Airscrew.—The function of the airscrew is to transform the torque on the engine crankshaft into a propulsive thrust by discharging backwards the air through which it moves; and whose resultant reaction enables the necessary forward momentum to be secured. The horse-power available at the airscrew, therefore, depends upon the horse-power of the engine, the efficiency of the airscrew, and the efficiency of the transmission between the engine and the airscrew. The first two of these factors are largely influenced by the density of the air in which they are operating, and it is, therefore, desirable to say a few words concerning the effect of variation in altitude upon the performance of an aeroplane.

It is generally known that the density of the atmosphere diminishes with increase of altitude, the weight of a cubic foot of air at 15,000 feet being only ·59 of the weight of an equal volume at sea-level. What effect will this change of density have upon an aeroplane flying at this altitude? Considering, first, the power plant, it is found from the laws of thermodynamics that the power developed is directly proportional to the weight of the fuel burned per cycle, which weight in its turn depends upon the supply of oxygen available. Since the percentage of oxygen present in the atmosphere remains practically constant at all densities, it follows at once that the amount of oxygen available at 15,000 feet will only be ·59 of the quantity available at sea-level. Hence the combustion of fuel per cycle and the horse-power developed at this altitude will be in the same proportion. Therefore, increase in altitude will tend to a corresponding decrease in the horse-power developed, unless special devices have been incorporated in the engine.

The diminution in density also affects the resultant air pressure upon the wing surface and the body of the machine. Reference to the fundamental equation for lifting capacity shows that the Lift is directly proportional to the density of the air. It is, therefore, apparent that a diminution of the density (ρ) means a reduced lifting capacity of the wings. Similarly the horizontal component of the resultant air force, that is the Drag, will be reduced to ·59 of its value at ground-level; and at first sight it would therefore appear that the forward speed of the machine would be maintained. It is here, however, that the diminished lifting capacity of the planes steps in to modify the result. Since the horse-power has diminished in the same ratio as the drag, it will be impossible to obtain the increased lift necessary to support the weight of the machine by flying at a higher speed, and it is therefore necessary to alter the flight attitude of the machine. The increased lift obtained by flying at a larger angle of incidence will be accompanied by an increase in the drag of the wing surface, and hence the total drag of the machine will be greater than ·59 of its value at ground-level. As a result, the machine will fly at a somewhat slower speed at altitude than at ground-level. The reduction in speed will necessitate a further slight change in attitude of the machine until the reaction of the wings is just equal to the weight, and horizontal flight will then be possible.

Following this argument through, it will be seen that there will come a time when the machine is flying at the wing attitude which gives the maximum lift—corresponding to the critical angle of the aerofoil section—and therefore is unable to obtain an increase in reaction by alteration of attitude. Consequently at this stage it will be impossible to reach a higher altitude, and this height is known as the 'ceiling height' or 'ceiling' of the machine. This altitude varies considerably with different types of machines, the maximum height reached up to the moment being in the neighbourhood of 30,000 feet. For the majority of machines, however, 20,000 feet is a more usual 'ceiling.'

The efficiency of transmission depends upon the form which is employed. If a short shaft running in roller bearings is used, very little loss will occur between the engine and the airscrew, while a longer shaft will absorb somewhat greater power on account of the increase in the number of bearings. If the airscrew is geared down, as is frequently the case nowadays, there may be a considerable loss of power depending upon the efficiency of the gear employed.

From a consideration of the variation of the horse-power developed by the engine we turn to discuss the question of airscrew efficiency. The performance to be expected from an airscrew is dependent upon several factors, the chief being the engine and the machine to which the screw is fitted, and these factors should be considered when designing the airscrew. To illustrate these factors, consider an airscrew coupled to an engine of insufficient power to drive it. The resistance offered to rotation by the airscrew will be so great that the engine will be unable to develop its normal number of revolutions and consequently it will develop less power than it is capable of reaching under correct conditions. As will be seen in Chapter IX., the efficiency of an airscrew is proportional to its effective pitch, the latter quantity being directly proportional to the forward speed. An airscrew to exert its maximum

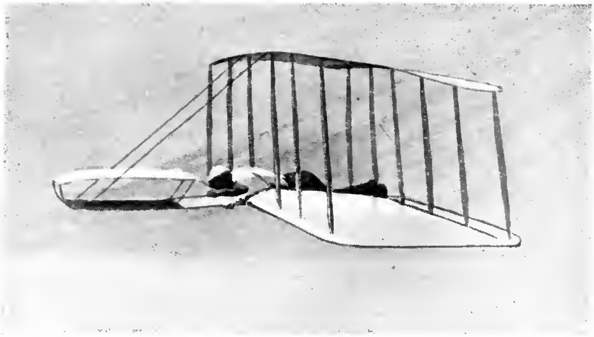

Fig. 1.—The Wright Glider.

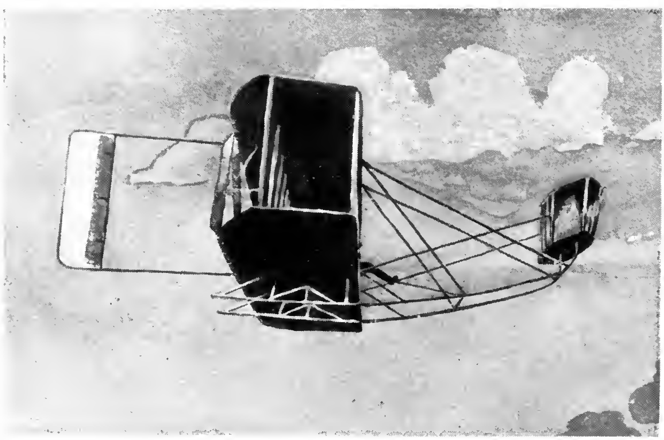

Fig. 2.—The Wright Biplane.

Reproduced by courtesy of Messrs. Handley Page, Ltd.

Fig. 3.—Method of folding Back Wings of a large Machine for Storage Purposes.

Facing page 8.

efficiency must be correctly designed in itself, and must also work under the conditions for which it is designed. A reduction in speed, such as occurs during climbing, will therefore lead to diminished efficiency. The angle of attack of the blade sections is fixed in accordance with the conditions for which it is desired to have maximum efficiency, and any departure from these conditions will alter the most efficient angle of the blade sections. Unfortunately the airscrew must operate under widely varying conditions during flight, and therefore cannot always be working at maximum efficiency. For instance, the variation in density with altitude has a similar effect upon the airscrew blade as it has upon the wing surfaces. Moreover, whereas in horizontal flight the whole of the lift is provided by the supporting surfaces, in climbing the airscrew thrust also contributes to the lift, that is, it takes part of the weight of the machine. An extreme case is shown in Fig. 4, p. 16. The thrust under these conditions will reach a maximum value, and the engine, being very heavily loaded, will tend to go slower, resulting in a further decrease in airscrew efficiency. The efficiency of an airscrew when working under the best conditions may reach as high a figure as 85%, but in climbing it is more frequently in the neighbourhood of 65%. If it were possible to adjust the angle of the sections in accordance with the speed of flight in a similar easy way to the manner in which the angle of incidence of the planes can be altered, the efficiency of the airscrew could be maintained at its maximum value under all conditions. Attempts have been made to realise this result by pivoting the blades so that they may be rotated about a radial axis, thereby permitting the angle of attack of the sections to be varied with relation to the axis of the screw itself. Up to the present time these efforts have achieved only moderate success, but there is little doubt that the problem will be satisfactorily solved in the future.

Controllability and Stability.—There are four forces acting on an aeroplane in flight:

1. Its weight acting downwards through the centre of gravity ... ... W
2. The lift of the supporting surfaces acting at the centre of pressure L
3. The resistance of the machine acting at the centre of resistance ... ... R
4. The thrust of the airscrew ... ... T

The distribution of these forces is shown diagrammatically in Fig. 5 below, and it is upon the way in which these varying quantities are disposed that the success or failure of the machine depends.

The weight of the machine does not remain constant throughout a flight because of the fuel consumption of the engine, and in the case of a bombing or a cargo-carrying machine the release of the bombs or discharge of the cargo produces a further variation. Wherever possible, the varying weights, such as the oil and petrol, etc., should be so arranged that the position of the C.G. of

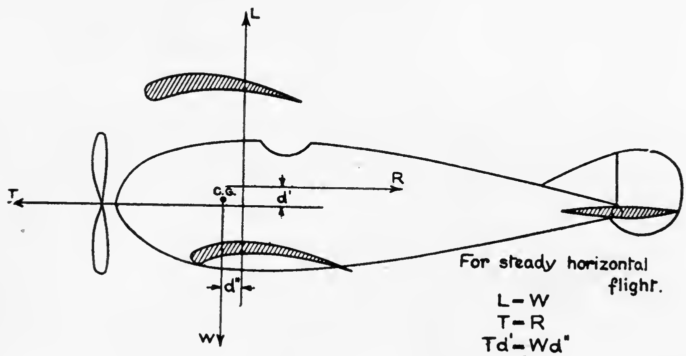

Fig. 5.—Equilibrium of an Aeroplane in Flight.

the machine remains unaltered. A further point to be noted is that the weights should be concentrated as much as possible, in order to reduce the moment of inertia of the machine, and thus allow of easy controllability. The lift of the supporting surfaces is equal to the weight of the machine in horizontal flight, but the position at which the resultant lift acts varies over a considerable range. The C.P. of a modern aerofoil travels, within the range of flying angles, from about ·3 to ·6 of the chord from the leading edge, and hence, while it is possible to obtain the C.P. of the wing and the C.G. of the weights in line with each other for one particular angle of incidence, yet for all the other angles there will be a weight/lift moment set up tending to produce a nose dive or a tail dive according as the C.P. is behind or in front of the C.G. In order to produce a restoring couple an auxiliary lift surface must be introduced, and this function is carried out by the tail unit. By raising or depressing the elevator a couple is produced tending to restore equilibrium. The tail plane fulfils a similar purpose in producing equilibrium when the line of thrust of the airscrew does not coincide with that of the total resistance of the machine. The position of the centre of resistance of the machine travels up and down in a vertical direction with variation of speed. This is due to the fact that at normal flying angles the drag of the wings remains almost constant over a considerable range of speed. The resistance of the remainder of the machine varies directly with the speed, and hence the resultant of the two will vary in its point of application.

The general question of controllability and stability has received much more attention in England during recent years than on the Continent or in America. The mathematical side of this problem has been developed by Bryan, and the practical application of Bryan's results has been demonstrated by Bairstow's work at the National Physical Laboratory. It is now possible, as a result of their work, to design a machine with any required degree of controllability or stability. Here, as in so many of the problems connected with Aeronautics, compromise is frequently necessary. If a machine is very responsive to the control lever it is not generally stable, while if a machine possesses a large amount of static stability it is heavy on the controls. The stability of an aeroplane is considered when the machine is in its normal flying attitude. It frequently happens, however, that when banking or performing some other evolution the wings assume a position approaching the vertical. When this is the case, the functions of the controlling surfaces are interchanged. There is need of extended investigation as to the effect of such reversion upon the behaviour of the machine.

Machines in the early days of aeronautics broke their backs under the strain of a sudden change in the direction of the flight path, and experiments have since been made to determine the increased loads likely to be encountered when doing sharply banked turns or loops. It has been found that the load is frequently increased to three or four times the normal, while even an ordinary banked turn will, under certain conditions, almost double the load. This brings us to a brief consideration of the factor of safety. Since fighting machines must be able to manœuvre rapidly, it is obvious that they must be strongly built, and they are not considered tolerably safe unless the wings can support at least six times the weight of the aeroplane. This question of the factor of safety makes large demands upon the resourcefulness of the designer, for he must obtain strength combined with minimum weight, and must therefore design his members as economically as possible, and yet retain sufficient material to carry the stresses. With large machines a lower factor of safety can be allowed, as there is not such a likelihood of sudden loads being thrown upon the members, and this will have an important bearing upon the possibilities of passenger and cargo-carrying machines. In fact, for commercial purposes generally a small machine will be of little use, and it is probable that the tendency of aeroplane design will be towards a machine considerably larger than those in most frequent use to-day, and hence the question of weight-saving will become increasingly important because of the inherent tendency of the weight to increase faster than the area of the supporting surfaces. This tendency may be simply explained as follows. For two aeroplane structures geometrically similar the stresses resulting from an equal rate of loading will be similar. The weight of such structures will increase as the cube of the similar dimensions, while the supporting area will increase only as the square of the similar dimension, so that the ratio of the weight to the supporting surface will increase as the linear dimension, and thus a definite limit would appear to be placed upon the size to which an aeroplane can be built.

General Consideration of Design.—The general method of procedure in designing an aeroplane can now be briefly outlined. A clear conception is necessary of the functions that the completed machine has to fulfil. An aerofoil must then be selected giving the necessary coefficients at the required speeds. A general arrangement of the machine should then be laid out and a preliminary balance effected. The total resistance of the machine can be estimated and an investigation made into the question of horse-power available at the airscrew. The amount of controllability and stability can next be decided and the areas of the controlling surfaces fixed. Details can be inserted in the design and the various performance curves drawn out for the machine. During construction the designer should check his estimated figures as opportunity offers, and revise his design accordingly. If this procedure be followed he will be able to predict the actual performance of his machine with reasonable certainty.

CHAPTER II.

THE MATERIALS OF DESIGN.

THE materials best suited for aeronautical purposes must combine strength with light weight. At the moment timber is the main material used, but research work has led to the rapid development of some very light alloys which are proving serious competitors to wood.

Timber.—Until the last few years little research work had been done upon this material of design, but much attention and scientific thought has been devoted to it recently, and more especially to the question of artificial seasoning. In former times natural seasoning was the chief method in vogue, but the speeding-up of production and the ever-increasing demand for all varieties of timber has led to great developments in artificial processes of seasoning. Green or unseasoned timber has only about 80% of the strength of dry or seasoned timber. There is great danger, however, that unless artificial seasoning is scientifically controlled, the process will be carried too far, with the result that certain varieties of timber—chiefly the coniferous varieties—will be rendered brittle. Age has a very similar effect upon mahogany and beech.

Wood varies in weight per cubic foot, that is in its density, according to its variety; the portion of the tree from which it is cut; the time of the year at which it is cut; and the amount of seasoning. Even after seasoning, which determines the amount of moisture present, variations occur according to the amount of protection upon the surface of the wood, which allows of or prevents the wood from absorbing moisture from the atmosphere or elsewhere.

As a general rule, the wood from the top portion of the bole is about 5% lighter than that from the bottom portion. In seasoning the wood shrinks considerably in width (some 4% to 8%), but very little in length. The percentage amount of moisture present in any given sample can be easily estimated by boring a hole with a twist bit through the sample. The borings should be weighed immediately, and then slowly heated in a crucible over a sand bath, great care being taken to see that they do not char. When thoroughly dry they should be weighed again without removal from the crucible, and the difference in the weighings enables the percentage amount of moisture present to be calculated.

Table V.—Strength and Weight of Timbers.

Kind.	Ultimate strength, lbs. per sq. in.			Specific gravity.	Weight, lbs. per cubic foot.	Modulus of elasticity. E.
	Tension.	Compression.				
		With grain.	Across grain.			
Ash	12,000	5,500	2,000	·7	44	1,400,000
Beech	12,000–20,000	8,000	—	·7	44	1,350,000
Birch	15,000	5,000	—	·72	44·5	1,600,000
Box	20,000	10,000	—	1·28	80	2,000,000
Elm—English ...	5,000–14,000	6,000–10,000	—	·55–·60	34–37	700,000–1,400,000
Fir—Baltic	4,000–10,000	3,000–5,500	—	·50–·70	30–44	1,000,000–2,000,000
Spruce—Grade A. ...	7,500	5,000	800	·5	31	1,400,000
„ Grade B. ...	6,000	4,000	700	·5	31	1,200,000
Kauri pine	10,000	6,000	—	·6	37·5	2,000,000
Larch	4,000–10,000	3,000–5,000	—	·54	33·5	1,000,000
Lignum vitae ...	11,000	10,000	—	1·33	83	2,000,000
Mahogany—						
Honduras	3,000–18,000	6,000–8,000	2,000	·55–·65	35–42	1,400,000–1,900,000
Spanish	3,000–16,000	7,000–8,000	—	·85	53	1,300,000–3,000,000
Oak—						
African	14,400	9,300	—	·99	62	2,000,000
American	10,000	6,500	—	·9	55	2,000,000
English	6,000–19,000	6,000–10,000	—	·8–·9	50–55	1,400,000–1,700,000
Pine—						
Yellow	2,000–10,000	4,000–8,000	—	·51	32	1,600,000
Baltic	3,000–10,000	6,000–8,000	—	·55–·65	34–42	1,600,000
Plywood	4,000–5,000	3,500	800	—	—	—
Teak	3,000–15,000	6,000–10,000	—	·65–·95	40–60	2,000,000
Walnut	18,000	6,000	1,300	·7	44	1,500,000

N.B.—Modulus of rigidity (G) for timber is 150,000 lbs. per sq. in. approx.

Table V. gives much useful and practical information concerning the most important timbers of commerce.

Light Alloys.—During recent years several light alloys have been placed on the market for which the makers have made various claims which have been more or less justified in use. The properties of the greatest importance in a light alloy are its strength, ductility, and permanence. It is frequently found that an alloy possessing great strength and a large degree of ductility lacks permanence. One of the most frequent erroneous claims made on behalf of the advertised light alloys is in connection with their relative density, it being often claimed that the density is less than that of pure aluminium. In order to obtain such a result, the aluminium—the basis of all these light alloys—must have been alloyed with some other metal of a less relative density than aluminium. Magnesium seems to be the only likely metal, and its addition to aluminium, unless in a very small percentage, renders the resulting alloy both weak and brittle.

Of the commercial alloys, Duralumin is the best known and has given very satisfactory service. Duralumin is composed of aluminium, copper manganese, and magnesium; variations in composition being made to meet particular requirements. The magnesium contributes to the hardness of the alloy, but increases the brittleness. Duralumin can be worked hot or cold, and its chief properties are given in Table VI.

Table VI.—Properties of Duralumin.

	Stress—Tons per square inch.		
	Rolled bar.	Tubes.	Wire.
Tensile ...	25	25	40
Compressive	32		
Elongation	20 %	$12\frac{1}{2}$ %	2 %
Specific gravity...	2·77 to 2·84		

This alloy has been very fully tested at the National Physical Laboratory by Dr. Rosenhain and Mr. S. L. Archbutt in connection with the Alloys Research Committee of the Institution of Mechanical Engineers. In their report they introduce the term Specific Tenacity, which is the constant obtained by dividing the tensile strength in tons per square inch by the weight of a cubic inch in pounds. As will be seen, this is quite an arbitrary conception, but it forms a very useful basis for comparison, and apart from questions of ductility, permanence, and cost, it is pointed out that the structural value of any alloy or other material is proportional to its specific tenacity. Using these units, the values shown in Table VII. have been obtained.

TABLE VII.—SPECIFIC TENACITY OF DIFFERENT MATERIALS.

Material.	Specific Tenacity.
Mild carbon steel	105
Special heat-treated steel	250
N.P.L. light alloys	up to 279
Duralumin	up to 290
Timber	up to 350

Another method of expressing the same property is obtained by using the length of the bar of the material, which, hanging vertically downwards, would just break under its own weight.

The use of these alloys for purposes connected with aircraft is a matter of great discrimination, as their properties are considerably affected by the way in which they are manipulated. Most of them machine easily, and are capable of taking quite a high polish. It may be noted in this connection that when highly polished they are more capable of resisting corrosion than when left rough. It should also be remembered that all the light alloys are injured by high temperatures, so that they should not, unless suitably protected, be used in places where they will be exposed to great heat, as near the engines, exhaust pipes, etc. According to the N.P.L. report, even a temperature of 200° C. reduces the strength materially.

In working aluminium the temperatures are important. If worked when too hot the aluminium becomes too soft, while if worked too cold brittleness results. Cast aluminium is popular, but not very satisfactory. Its strength is only about five tons per square inch, and there is very little elongation. It is much more useful as an alloy.

The brass or gun-metal alloys are formed by adding tin, zinc, and small quantities of other elements to copper.

Steel.—Steel is formed from iron by the addition of carbon and small quantities of other materials. Mild steel has a tenacity of under 26 tons per square inch, with an elongation of 30°/₀ on an 8″ gauge length. It is easy to get a strong steel, but increase of strength generally means increase of brittleness. Steel may be treated by heating to a high temperature and quenching it in oil. Its strength is increased to about 40 tons per square inch by the addition of nickel, with but little loss in elongation. With some sacrifice in ductility the strength may be further increased to between 50 and 60 tons per square inch. Chromium

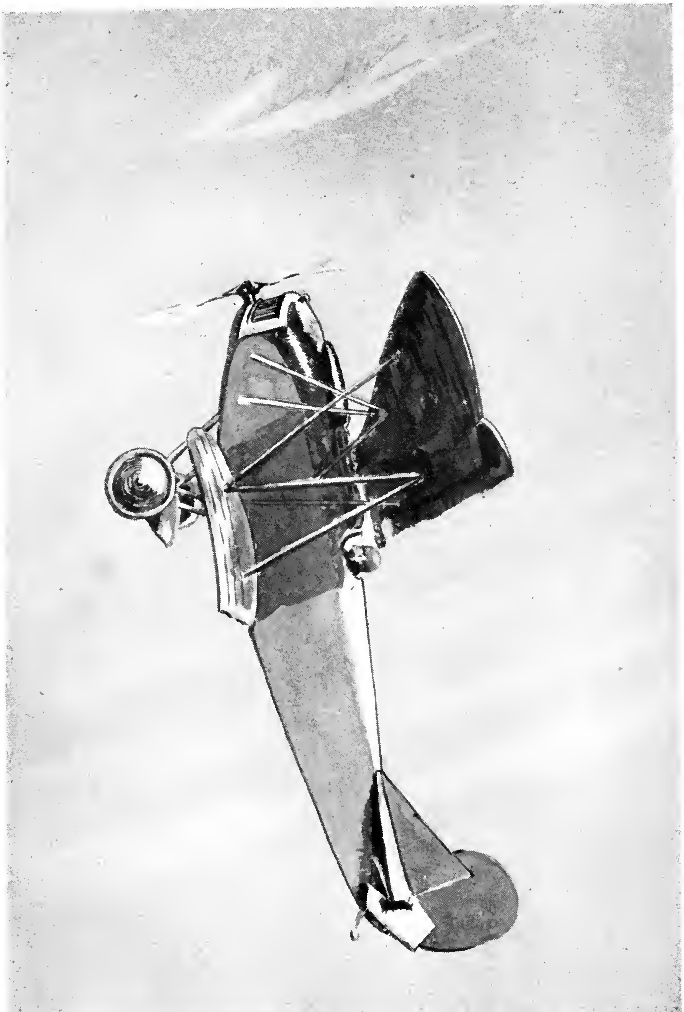

FIG. 4.—Fokker Biplane 'Hanging on the Prop.'

A stunt evolved by Fokker pilots during the War. To an observer in another machine the Fokker has the appearance of remaining stationary in the position indicated in the sketch. It is probable, however, that the aeroplane is losing height continuously, the airscrew thrust and air pressure being sufficient to reduce the fall to very small dimensions, as this position could be maintained for quite long periods. The Sopwith 'Camel' fitted with a Bentley engine can assume and retain a similar position.

Facing page 16.

and vanadium are also largely used for combining with steels to form high tensile strength alloys. When rolled into thin plates or drawn into wire the ultimate stress is still further increased, and it is possible to produce a wire $\frac{1}{16}''$ in diameter with a breaking stress of 150 tons per square inch. High tensile steels should not be subjected to punching for the purposes of lightening out, as the loss of strength may amount to 20 %. The metals most commonly used for additions in making steel alloys are aluminium, chromium, manganese, molybdenum, nickel, tungsten, vanadium, and combinations of these elements. The exact effect produced depends upon whether they are added singly or in combination. Their general effect is given below:

ALUMINIUM.—Usually added to increase the fluidity of cast steel, and by its great affinity for oxygen to reduce the formation of oxides. It also aids in the prevention of blow-holes.

CHROMIUM.—When added in small quantities it increases the tensile strength of the steel, but when added in large quantities it increases the brittleness. It is largely used for projectiles, railway tyres, and springs.

MANGANESE.—Added to make self-hardening steels. Increases the tensile strength and the elongation.

MOLYBDENUM.—Added for self-hardening purposes. Lowers the melting point somewhat.

NICKEL.—The commonest and best-known alloys are the nickel steels. An addition of 4 % nickel, 0·2 % carbon, results in an increase of tensile strength of about 10 % and an increase in the elastic limit of about 25 %. This increase continues with the addition of more nickel until the quantity of nickel present reaches 20 %, after which point a rapid decrease in strength takes place with the addition of more nickel. Nickel steels offer great resistance to corrosion, but when more than $1\frac{1}{2}$ % of nickel is present these steels are difficult to weld.

TUNGSTEN.—Another of the agents for obtaining self-hardening steels. It is also used for making magnets. Mushet steel—the forerunner of the modern high-speed steels—is a tungsten steel. Tungsten is a constituent of practically all the high-speed tool steels.

VANADIUM, generally speaking, increases the tensile strength and the elastic limit, but reduces the elongation slightly.

Table VIII. gives the chemical composition of various steels made to Air Ministry and Engineering Standards Committee specification, by Edgar Allen & Co., of Sheffield, and shows the results of tests upon bars $1\frac{1}{8}''$ in diameter turned down to the British Standard test-piece 'C.'

TABLE VIII.—STEELS TO STANDARD SPECIFICATIONS.

DESCRIPTION.	CHEMICAL COMPOSITION.						
	Carbon.	Silicon.	Manganese.	Sulphur.	Phos.	Nickel.	Chrome.
SELECTED AIR MINISTRY STEELS.							
S1. Part 2	·25–·40	·30	·40–·85	·06	·06	—	—
S2. H.T. Alloy bars	·28–·40	—	·50–·80	·04	·04	3·0–4·0	0·9–1·5
S8. 9 & 10.3% Nickel ...	—	—	—	·04	·04	2·5–3·5	—
S14. 15% Carbon Case-hardening	·12–·20	—	0·5–1·0	·04	·04	—	—
S17. 5% Nickel " "	·10–·20	—	·10–·40	·04	·04	4·50–6·0	—
S19. Chrome Valve	·2–·4	·50	·5	·06	·06	—	11·5–14·0
S24. Key Steel	·55–·80	—	·8	·04	·04	—	—
S26. 40-ton	·30–·45	·30	·50–·80	·06	·06	1·0	·5
S28. 100-ton Air-hardening ...	·35–	—	·50	·035	·035	3·75–4·75	1·0–1·8
ENGINEERING STANDARDS COMMITTEE'S STEELS.							
E.S.C. 10. Carbon Case-harden'g	·08–·14	·20	·60	·04	·04	—	—
E.S.C. 2% Nickel	·10–·15	·30	·25–·50	·05	·05	2·0–2·5	—
E.S.C. 5% "	·15	·20	·40	·05	·05	4·75–5·75	—
E.S.C. 20% Carbon	·15–·25	·25	·40–·85	·06	·06	—	—
E.S.C. 35% "	·30–·40	·30	·50–·85	·06	·06	—	—
E.S.C. 3% Nickel	·25–·35	·30	·35–·75	·04	·04	2·75–3·5	—
E.S.C. 1½% Nickel Chrome ...	·25–·35	·30	·35–·60	·04	·04	1·25–1·75	0·75–1·25
E.S.C. 3% " " ...	·20–·30	·30	·35–·60	·04	·04	2·75–3·50	0·45–0·75
E.S.C. Air hardening Nickel Chrome	·28–·36	·30	·35–·60	·04	·04	3·50–4·50	1·25–1·75

[EDGAR ALLEN & CO.

HEAT TREATMENT.		MECHANICAL TESTS.						
Normalising or hardening temperature.	Tempering or re-heating temperature.	Condition.	Max. stress tons per sq. in.	Yield point.	Elong. °/₀ on 2″	Reduc. of area °/₀	Izod impact ft. lbs.	BRINELL No.
Degrees Cent.	Degrees Cent.			Tons per sq. in.				
840–880	—	—	35	20	20	40	40	—
—	560–660	Treated.	55–65	45	18	55	40	402
840–880	—	Normalised.	45	32	24	50	—	—
—	—	Treated.	38	25	20	55	40	—
820–840	740–760	”	65	50	13	40	30	—
—	—	”	40	30	18	50	—	—
800–840	—	Normalised.	55	28	15	45	—	—
				Yield ratio.		Red. & elong.		
820–870	—	Treated.	40–50	60	22	70	30	—
790–830	—	”	90–110	—	13–6	40–16	418–269	—
				Yield ratio °/₀				
880–900	750–770	As rolled.	23–28	50	30	50	—	92–112
860–880	750–770	”	25–35	55	30	55	—	103–153
820–840	740–760	”	25–40	60	30	55	—	103–179
890–920	—	”	26–34	50	28	50	—	105–149
850–880	—	Treated.	30–40	50	25	45	—	121–179
840–880	—	”	35–45	55	24	45	—	140–202
850	600	”	45	70	15	50	—	179
820	600	”	45	75	15	50	—	175
820	—	”	100	75	5	13	—	418

Aeroplane Fabric.—This is cloth of a fairly closely woven texture, and is used for covering the wings, fuselage, and tail structure. The strength of this fabric is from 80 lbs. per square inch in the direction of the warp threads, to 120 lbs. per square inch in the direction of the weft threads. The warp threads are those running longitudinally, while the weft threads are the shorter ones crossing the warp threads at right angles. In order to make this fabric taut, air-tight, and unaffected by moisture, it is covered with 'dope.' Dope is a chemical preparation, the base of which is cellulose acetate, and from four to five coats are applied, the result being to increase the strength of the fabric by about 30 °/ₒ as well as rendering it weather-proof.

Stress, Strain, Elasticity.—When a bar of ductile material is tested in tension it stretches, and at first this stretching is proportional to the load applied, being practically uniform throughout the whole length of the bar. This proportionality of elongation to load is known as Hooke's Law, and continues

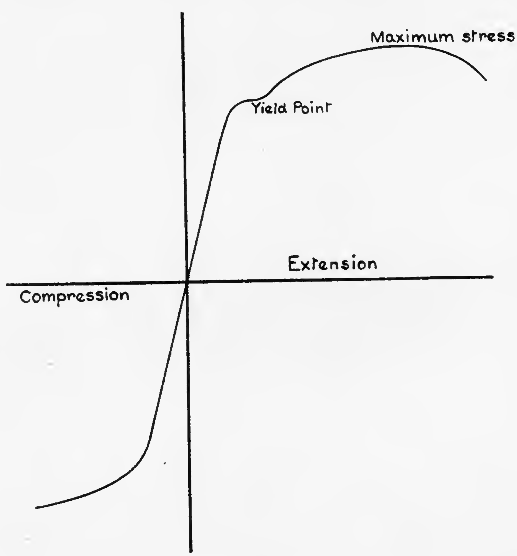

Fig. 6.—Stress Strain Diagram.

up to a point known as the elastic limit. At a load a little greater than the elastic limit the elongation increases more rapidly than the load, permanent deformation of the material occurs, this point being known as the yield point. Further increase of the load brings about a much greater increase in the elongation up to the maximum load, known as the breaking load. The bar, however, does not immediately break, but at one point a 'waist' is formed, and the load can now be reduced while the elongation continues, due to the reduction in the cross-sectional area of the bar. The bar finally breaks at the point where the waist formed.

Taking rectangular co-ordinates as in Fig. 6, the relation between stress and strain can be plotted as shown. It should be noted that this figure gives the nominal stress—that is, the stress upon the original cross-sectional area of the bar.

As a deduction from Hooke's Law we have the relationship

$$\text{Modulus of Elasticity} = \text{Stress/Strain} \quad \ldots\ldots\ldots\ldots \text{ Formula 2}$$

When a bar is subjected to a pull in one direction, there is, in addition to the longitudinal strain in the direction of the pull, a transverse strain set up in planes at right angles to the longitudinal strain, resisting the change in length. The ratio Transverse strain / Longitudinal strain is within the elastic limits a constant for any one material, and is known as Poisson's ratio, being frequently denoted by the Greek letter η. It has been suggested that Poisson's ratio is a constant for all materials, but recent researches have shown that this view is incorrect.

From Formula 2 the various Moduli of Elasticity are at once derived, namely:

Modulus of direct tension or compression, sometimes called

$$\text{Young's Modulus} = \frac{\text{Load/cross-sectional area}}{\text{extension or compression per unit length}},$$

$$\text{or} \qquad E = \frac{\frac{P}{A}}{\frac{X}{L}} \quad \ldots\ldots\ldots\ldots \text{ Formula 3}$$

Modulus of rigidity, or the shear modulus, or modulus of transverse elasticity

$$= G = \frac{\frac{P}{A}}{\text{Unital shear strain}} \quad \ldots\ldots\ldots\ldots \text{ Formula 4}$$

Modulus of volume or the bulk modulus

$$= K = \frac{\frac{P}{A}}{\text{Unital volume strain}} \quad \ldots\ldots\ldots\ldots \text{ Formula 5}$$

$$\text{Poisson's Ratio} = \eta = \frac{\text{Transverse strain}}{\text{Longitudinal strain}} \quad \text{........... Formula 6}$$

The relations between the elastic constants are best remembered in the following forms:—

$$\frac{9}{E} = \frac{3}{G} + \frac{1}{K} \quad \text{........... Formula 7}$$

$$\frac{E}{G} = 2\,(1 + \eta) \quad \text{........... Formula 8}$$

$$\frac{E}{K} = 3\,(1 - 2\eta) \quad \text{........... Formula 9}$$

Tests.—The general method employed for testing the mechanical properties of materials is to cut portions from selected pieces and to turn or shape them to standard forms. These pieces are then tested in special machines—the nature of the test depending upon the purpose for which the material is required. From the results, the elastic constants of the material under test can be evaluated by means of the formulæ given above.

An additional method of testing, which is being increasingly adopted in practice to-day, is known as the Brinell Hardness Test. In this method an indentation is produced in the flat surface of the material by applying a constant pressure upon it through a hardened steel ball. The diameter of the indentation is measured and the hardness is taken as being proportional to the area of the cavity made by a ball of definite size when subjected to a fixed load. The size of the ball is usually 10 millimetres in diameter, and the pressure 3000 kilograms.

The Brinell Hardness number is defined as the

$$\frac{\text{Total load}}{\text{Curved area of depression.}}$$

It is possible to form an approximate idea of the tensile strength of a material from a knowledge of its Brinell Hardness number, and as the test is so much simpler and quicker to perform than the ordinary tensile test, this method is frequently adopted in cases where it is not essential to have very accurate data.

Table IX. gives the Hardness number and corresponding approximate tensile strength of various qualities of steel.

TABLE IX.—BRINELL HARDNESS NUMBERS.

Diam. of impression. Mms.	Hardness number for the standard load of 3000 kilograms.	Approx. tensile strength. Tons.	Diam. of impression. Mms.	Hardness number for the standard load of 3000 kilograms.	Approx. tensile strength. Tons.
2·6	555	130	4·25	201	47·2
2·7	514	110	4·3	197	45·2
2·75	495	106	4·35	192	43·6
2·8	477	102	4·4	187	42·2
2·85	461	98	4·45	183	41.2
2·9	444	95	4·5	179	40·2
2·95	429	92	4·55	174	39·5
3·0	415	89	4·6	170	38·8
3·05	401	86	4·65	167	38·2
3·1	388	84	4·7	163	37·6
3·15	375	81·5	4·75	159	37
3·2	363	79	4·8	156	36·2
3·25	352	77	4·85	152	35·3
3·3	341	75	4·9	149	34·7
3·35	331	73·5	4·95	146	34·2
3·4	321	72	5·0	143	33·7
3·45	311	70	5·1	137	32·8
3·5	302	68	5·2	131	32
3·55	293	67	5·3	126	31·2
3·6	285	65·5	5·4	121	30·5
3·65	277	64	5·5	116	29·8
3·7	269	62·5	5·6	111	29·2
3·75	262	61·5	5·7	107	28·5
3·8	255	60	5·8	103	28·0
3·85	248	59	5·9	99·2	27·4
3·9	241	58	6·0	95·5	26·9
3·95	235	57	6·1	92	26·4
4·0	229	56	6·2	88·7	26·0
4·05	223	55	6·3	85·5	25·5
4·1	217	54	6·4	82·5	25
4·15	212	53	6·5	79·6	24·6
4·2	207	50			

N.B.—With the aid of the above table the Brinell Hardness number and approximate tensile strength can be obtained from a knowledge of the diameter of the impression formed in the material.

Factor of Safety.—The relationships between the elastic constants are obtained from the Theory of Elasticity. Theoretical considerations will generally produce a design, but whether such a design is practical or not depends upon a large number of varying factors, such as economy and facility in production, and economy in upkeep. In most cases some modification from the theoretical design will be necessary, and it is in this direction that experience and practice tell. In all design work using formulæ, and more especially in cases where a large number of empirical formulæ are used, it is exceedingly important, if these formulæ are to be used intelligently, to know and to understand the fundamental principles underlying the construction of such formulæ, and to realise and appreciate the various assumptions that have been made in arriving at any particular formula.

To allow for the effect of these assumptions and for accidental overloads that may occur in any portion of the structure, it is customary to design structures considerably stronger than an investigation shows to be necessary. This allowance is termed the Factor of Safety, and is of prime importance in aeronautical practice where weight-saving must be considered down to the last detail. Too high a factor of safety leads to a heavy structure, while too small a factor will probably result in an accident in mid-air. From theoretical considerations the ideal design would be that design in which such a factor of safety had been used in the various component parts that each of those component parts would be on the point of failure at the same moment. Table X. gives the Factors of Safety in general use to-day.

TABLE X.—FACTORS OF SAFETY.

Type of Machine.	Factor of safety C.P. forward.	Factor of Safety in terminal nose dive.
Fast Scout or Sporting Machine (that is, a machine liable to be stunted, etc.)—		
Up to 3,000 lbs.	8	1·5
3,000 to 10,000 lbs.	8 – 6*	
Over 10,000 lbs.	6	1·5
Commercial Machines (this type must not be stunted)—		
Up to 5,000 lbs.	6	1·5
5,000 to 10,000 lbs.	5	1·5
10,000 to 30,000 lbs.	5 – 4*	1·33
30,000 to 50,000 lbs.	4 – 3·5*	1·25
Over 50,000 lbs.	3·5	1·25

* Reduction in factor proportional to increase in weight.

Wind Pressure.—A large amount of research work has been carried out upon the subject of wind pressures during recent years. Anemometers, for example, are maintained upon the Tower Bridge, under the supervision of the National Physical

Laboratory, and the results and readings obtained are published from time to time. Generally speaking, the pressure varies approximately as the square of the velocity. Table XI. gives in a convenient form an idea of the velocities and pressures due to various types of winds.

TABLE XI.—WIND PRESSURES.

Velocity, m.p.h.	Pressure, lbs. per sq. ft.	Remarks.
4	·08	Light breeze.
10	·49	Fair breeze.
15	1·11	Strong breeze.
20	1·97	Very strong breeze.
30	4·43	Brisk gale.
40	7·87	High wind.
50	12·30	Very high wind.
60	16·70	Storm wind.
70	22·81	Great storm.
80	31·50	
90	39·4	
100	49·0	Hurricane.

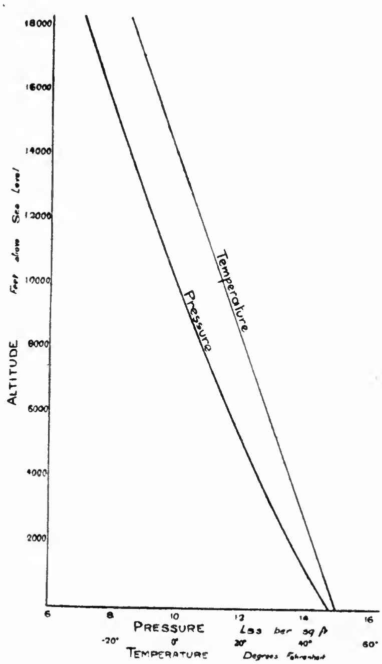

FIG. 7.—Variation of Pressure and Temperature with Change in Altitude.

The variation of pressure of the atmosphere at varying heights must also be borne in mind, not only in connection with its effect on the lifting capacity of the wings of a machine, but also in its effect upon the power developed by the engine.

Fig. 7 illustrates the change both of pressure and of temperature with varying altitude.

Stress Diagrams.—The preparation of stress diagrams for different components of an aeroplane constitutes a very large portion of the routine work of an aircraft designer, the draughtsman to whom this duty is delegated being frequently referred to in the drawing-office as a 'stress merchant.' The authors of this work have frequently found, in their experience, that the average draughtsman has but little conception of the fundamental principles underlying the construction of stress diagrams, so that he is quite unable to tackle a diagram for a case that is somewhat unusual. They therefore make no apology for dealing with this question fully, and hope that their explanations will lead to a clearer conception of the whole matter.

The fundamental theorem in connection with this subject is that known as the Triangle of Forces, which states: 'If three forces, acting at a point, be represented in magnitude and direction by the sides of a triangle taken in order, they will be in equilibrium.' It should be noted that the converse of this theorem is also true, namely, 'If three forces, acting at a point, be in equilibrium, they can be represented in magnitude and direction by the sides of any triangle drawn so that its sides are respectively parallel to the directions of the forces.' As an extension of this proposition we have the theorem known as the Polygon of Forces, which states: 'If any number of forces acting on a particle can be represented in magnitude and direction by the sides of a polygon taken in order, the forces are in equilibrium.' The construction of stress diagrams is based upon this theorem.

For equilibrium it will be noticed that the triangle or the polygon must be closed, hence the stress diagram must also close.

The formal treatment of statical problems by graphical methods is due to Clerk Maxwell, who published papers 'On Reciprocal Figures and Diagrams of Forces' in 1864, and subsequent years.

Two plane rectilinear figures are said to be reciprocal:

1. When they consist of an equal number of straight lines or edges, such that corresponding edges are parallel.

2. When the edges which meet in a point or corner of either figure correspond to lines which form a closed polygon or face in the other figure.

It will be observed that in order to obtain a reciprocal figure every corner must have at least three edges meeting at it, and since an edge can have only two ends, each of which represents a face in the other figure, two faces and two only intersect in each edge.

The best way of illustrating the fundamental principles enunciated above is by means of a concrete example. We will take as a first illustration the simple roof truss shown in Fig. 8.

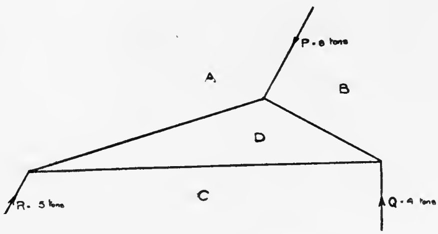

FIG. 8.—Frame Diagram.

It must be remembered in drawing stress diagrams that the following assumptions are made when the principle of reciprocal figures is applied to any framed structure:

1. That the members (or bars) of the structure are rigid.
2. That these members are connected together by means of frictionless pin-joints.
3. That the loads act at these pin-joints.

The first two assumptions are rarely justified in English engineering practice, and where the third assumption is not fulfilled it is customary, for the purpose of drawing the stress diagram, to divide up the load and place a portion at each joint.

In drawing a stress diagram there are two systems of forces to be considered, namely, the external forces and the internal forces. Thus in Fig. 8 the external forces are those shown by P = 8 tons, Q = 4 tons, R = 5 tons, and by drawing the stress diagram we determine the internal forces acting in the members of the frame. From the knowledge thus obtained we can proceed to the detail design of these members. The internal forces act along the neutral axes of the members.

The frame diagram (Fig. 8) is first lettered according to Bow's notation—that is, letters, figures, or other symbols are placed between the external forces acting and also between the members of the frame. The force P is now termed the force A B, the force Q is the force B C, and so on. The object of this notation will be apparent on the completion of the stress diagram. Commencing with the force A B, we set down the line *a b* parallel to the direction of the force A B and representing to some suitable scale its magnitude (8 tons). From *b* we draw *b c* parallel to the direction of the force B C to represent its magnitude (4 tons) to the same scale that *a b* represents the magnitude of A B. Joining *c a* gives the direction and magnitude of the force C A—namely, 5 tons. The triangle (polygon) of forces for the external loading of the frame under consideration has now been drawn. Through *a* we now draw a line parallel to the direction of the member A D, and through *c* a line parallel to the direction of the member C D. These lines intersect in *d*, and *a c d* is the polygon of forces for the corner where the

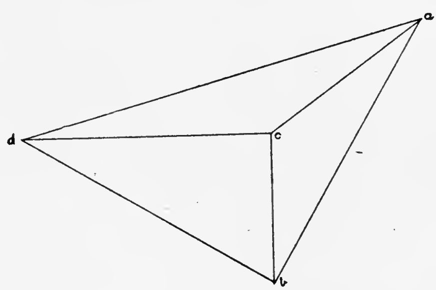

FIG. 9.—Stress Diagram.

force R acts. Through *b* we now draw a line (*b d*) parallel to the direction of the member B D. This should intersect the line *c d* in *d*, and its agreement or non-agreement provides a measure of the accuracy of the construction of the stress diagram. *b c d* is the polygon of forces for the corner where the force Q acts, and *a b d* is the polygon of forces for the corner where the force P acts.

The stress diagram can now be scaled for the forces acting in each member, and the advantage of Bow's notation is at once apparent, since the line *a d* (small letters) in the stress diagram gives the force acting in the member A D (large letters) ; the line *b d* in the stress diagram the force in the member B D ; and the line *c d* in the stress diagram the force in the member C D. It is next necessary to determine whether the members of the frame are in compression or in tension—that is, whether they are acting as struts or as ties ; because the manner of their subsequent design depends upon the way in which they are function-ing. The easiest way of determining this is to consider the polygon of forces for each corner of the frame separately, considering first the corner where the force P acts. The polygon of forces is given by the triangle *a b d*, and the direction of the force P is already known. Indicating this direction by an arrow-head as shown in Fig. 10 (*a*), we can insert arrows upon the remaining sides of the polygon, because we know from fundamental principles that these arrows must follow round the sides of the polygon in order, so that there may be equilibrium.

Fig 10

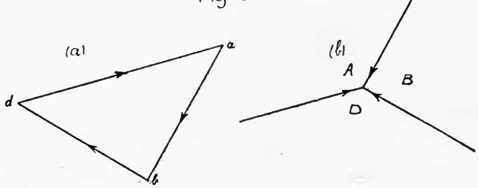

Fig. 11

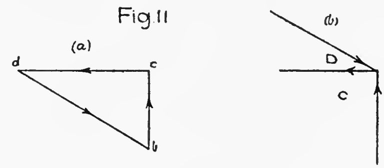

Fig. 12

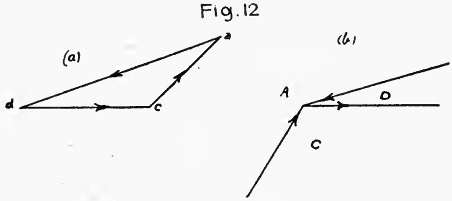

These directions can now be transferred to the frame diagram, as shown in Fig. 10 (*b*).

When an arrow so transferred points towards the corner, the member it belongs to is in compression; while if it points away from the corner, the member is in tension. We thus see that the members A D and B D are in compression—that is, that they must be designed as struts.

Dealing with the corner where the force Q acts, we proceed in exactly the same manner. *b c d*, Fig. 11 (*a*) is the polygon of forces, and the direction of the force B C is known, whence the remaining directions can be inserted. These directions can be transferred to the frame diagram, Fig. 11 (*b*), from which we see that the member B D is in compression, and the member C D is in tension. As will be observed, the result obtained for the member B D (compression) agrees with that obtained in Fig. 10.

We have now determined the nature of the stress in each of the members of the frame, but by way of a check we will deal with the remaining corner. The polygon of forces and the corner are shown in Fig. 12 (*a*) and (*b*), from which we see that the member A D is in compression, agreeing with the result obtained in Fig. 10; and the member C D is in tension, agreeing with the result obtained in Fig. 11.

Struts and ties are distinguished from each other on the

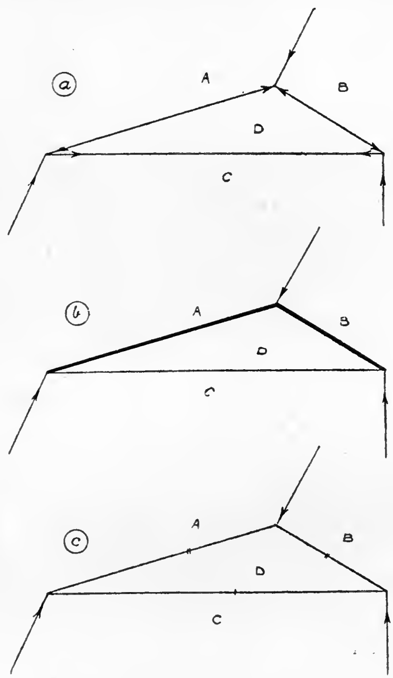

FIG. 13.—Methods of indicating Struts and Ties.

frame diagram in three different ways, as shown in Fig. 13 *a*, *b*, and *c*.

(*a*) By the use of arrows. Remember that, as pointed out above, an arrow pointing towards a joint indicates compression, while an arrow pointing away from the joint indicates tension.

(*b*) By thickening the compression members only.

(*c*) By two small cross lines upon the compression members, and one cross line upon the tension members, leaving those members in which there is no stress without any mark at all.

Having completed the stress diagram, the results obtained should be exhibited in a neat table upon the drawing. This table should also indicate those members which are in compression and those which are in tension. There are two methods of showing this, namely—

1. By underlining the compression members.
2. By placing a negative sign before the compression members, since compression tends to shorten a member; and by placing a positive sign before a tension member, since tension tends to lengthen a member.

The table for the frame under consideration will then appear in one of the two forms shown below.

TABLE XII.—MEMBER FORCE IN TONS.

AD	...	...	11·00
BD	...	...	7·75
CD	...	...	6·62

TABLE XIII.—MEMBER FORCE IN TONS.

AD	...	...	− 11·00
BD	...	...	− 7·75
CD	...	...	+ 6·62

We have taken a fairly general, though simple, example by way of illustration. Probably in an actual example the load P would act vertically, in which case the reactions Q and R would be vertical, and the triangle of external forces—*a b c*—would become a straight line.

As further exemplification of the fundamental principles, we will next consider the stress diagram for a framed structure such as is shown in Fig. 14, since the method of treatment—with variations, of course, to suit particular cases—is applicable to many forms of structures, including the wing-spars of aeroplanes, and the fuselages of aeroplanes. Such a structure as outlined is, strictly speaking, statically indeterminate, as it is a redundant frame, but for most practical purposes it can be treated by regarding it as made up of two perfect frames, the loads being equally divided between the two frames; and then finding the stress for each of these frames independently, and afterwards adding together algebraically the stresses obtained for the members common to both frames.

The division of this structure into two perfect frames is shown in Figs. 15 and 16. The stress diagram for the frame of Fig. 15

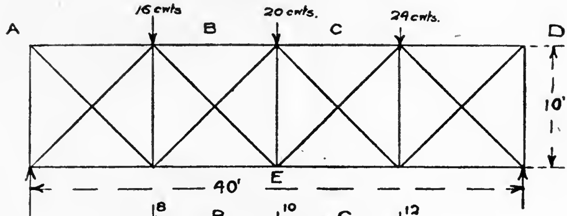

FIG. 14

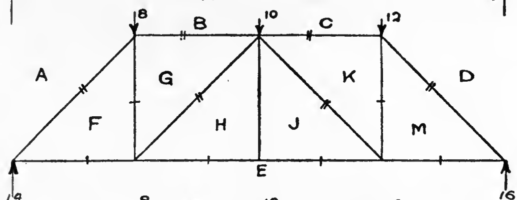

FIG. 15

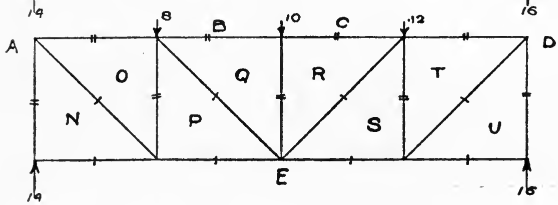

FIG 16

FIG. 17

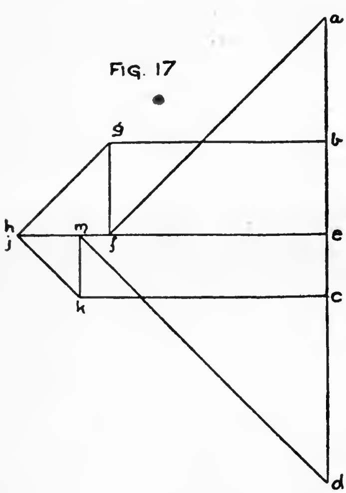

FIG. 18

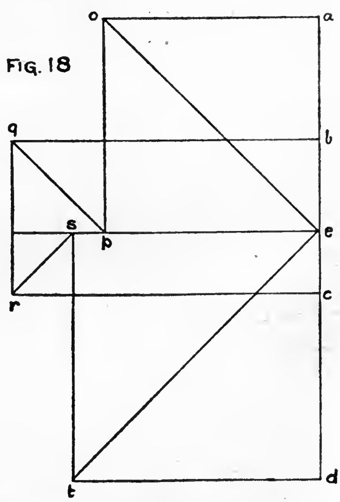

FIGS. 14 to 18.—Load, Frame, and Stress Diagrams.

is shown in Fig. 17; and that for Fig. 16 is shown in Fig. 18. In order to clear up any doubtful points, we will go through the construction briefly. The reactions in this case are found by taking moments about either support. For example, the reaction at the left-hand support is given by—

$$\text{Reaction left} = \frac{12 \times 10 + 10 \times 20 + 8 \times 30}{40}$$
$$= 14 \text{ cwt.}$$

The reaction for the right-hand support can be found in a similar manner, or, since the total load for Fig. 15 is 30 cwts., the reaction at the right-hand support can be found by subtraction, thus—

$$\text{Reaction right} = 30 - 14 = 16 \text{ cwt}$$

This practice is not to be recommended, however, as it does not afford any check upon the accuracy of the arithmetic of the first calculation, and such checks should always be introduced into practical calculations wherever possible. Thus, in the present case, the two reactions should be calculated separately, and then added together, to see that their sum is equal to 30 cwt.

Having calculated the reactions. the polygon of forces for the external forces—that, is the straight line *a b c d e a*—can be drawn to some suitable scale. *a f* is then drawn parallel to A F, and *e f* parallel to E F. The intersection of these two straight lines gives the point *f*. *b g* is next drawn parallel to B G, to meet *f g* drawn parallel to F G in *g*. *g h* is then drawn parallel to G H, to meet *e h* drawn parallel to E H in *h*, and thus half the diagram is completed. It is a good plan, in drawing complicated stress diagrams, to work from each end in turn, so that any drawing error is not continued through the whole of the stress diagram. It is therefore advisable to start now from the other end of the frame diagram, so that the amount of closing error—if any—may be kept as small as possible. Consequently, draw *d m* parallel to D M to meet *e m* drawn parallel to E M in *m*; and then *m k*, *c k*, parallel respectively to M K, C K, to obtain the point *k*. The line *k j* on the stress diagram tests the accuracy of your drawing, for a line through *k* parallel to K J on the frame diagram should pass through the point *h* already obtained on the stress diagram. If there is a big closing error, it is advisable to redraw the figure completely, and if the error is at all appreciable, it should be traced and corrected. The greatest trouble in drawing stress diagrams correctly in practice occurs where it is necessary to draw long lines on the stress diagram parallel to very short lines on the frame diagram. For important work it is desirable in such cases to calculate the inclination of such lines by trigonometrical methods, in which way a very fruitful source of error may be eliminated.

In an aeroplane the wings support the whole weight of the machine. They support both their own weight uniformly distributed over their length, and the weight of the other components

Fig. 19

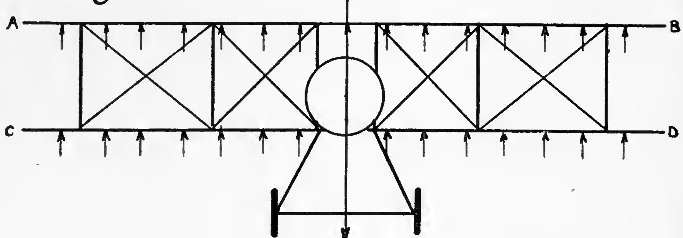

Fig. 20

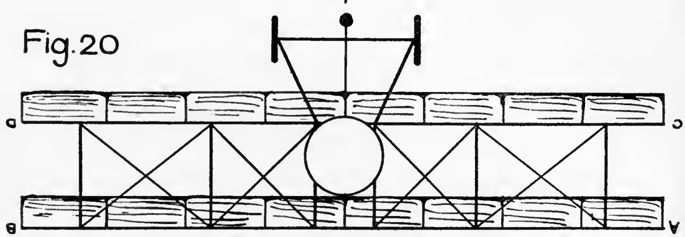

Fig. 21 Frame Diagram

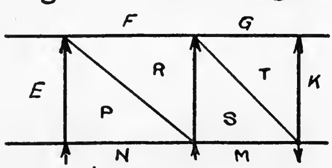

Fig. 22

Stress Diagram

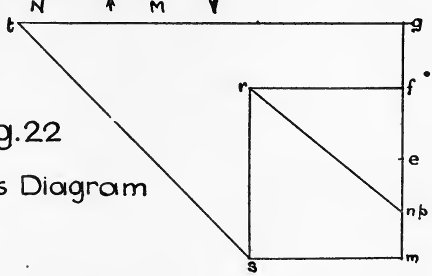

of the aeroplane concentrated at certain points. From a structural point of view they are therefore wide, flat beams stretching out on each side of the fuselage. To realise what the load on them really means, we can imagine the plane turned upside down.

Fig. 19 shows an aeroplane in its normal attitude, the wings A B, C D being loaded uniformly by upward wind forces, indicated by small arrows, the sum of these wind forces being equal to the total weight of the aeroplane acting downwards as shown. The strains and stresses in the wings of the machine would therefore be exactly the same if the machine were turned upside down as shown in Fig. 20, suspended from the centre of gravity, and weights placed uniformly along the wings as indicated, the sum total of these weights being equal to the total weight of the machine less the weight of the wing structure. In many circumstances the load on the wings will be many times the total weight of the machine, as for example when the aeroplane is being flattened out after a nose dive or in stunting. The biplane arrangement is essentially stronger than the monoplane, because it can be braced together until it forms a structure analogous to a bridge. The wings of a biplane can therefore be regarded exactly as a compound girder in bridge design. The panels are formed between the upper and lower spars, and as there are usually two sets of spars to each wing, there will be two sets of panels—a front and a rear set. Fig. 21 shows a front view of one half of the machine depicted in Figs. 19 and 20, one set of wires having been removed because it is assumed in aeroplane design that only one set of wires is acting at any given instant. This figure shows the simplest form of the frame of the machine illustrated, and in Fig. 22 the corresponding stress diagram is drawn. The method of drawing this diagram should be quite obvious from what has been said above with reference to such diagrams. The stress diagram for the other half of the machine will be exactly similar but reversed in direction. Further examples of the application of stress diagrams to the design of the wings will be given in Chapter V.

Method of Sections.—This method, which is also known as Ritter's method, or method of moments, generally entails much elaborate calculation, and in most cases the ordinary graphical method of obtaining the forces acting in the various members of a structure as outlined above is much to be preferred. In some few cases, however, the method of moments offers advantages, and the results obtained are of course more accurate than those obtained by reciprocal diagram work. On this account, in very important design work, it should be used as a check upon the accuracy of the graphical construction for the main members. By its aid, also, points of difficulty which sometimes arise in complicated frame structures can be overcome.

The method of moments will be illustrated by means of a worked example, as the writers are strongly of the opinion that 'Example is better than precept.'

We will take for our example the Warren frame of 30 feet span, shown in Fig. 23. It has five equal equilateral bays of 6 feet span, and is loaded at the lower flange with loads of 7, 5, and 2 cwt. at the first, second, and third nodes from the right-hand support as shown.

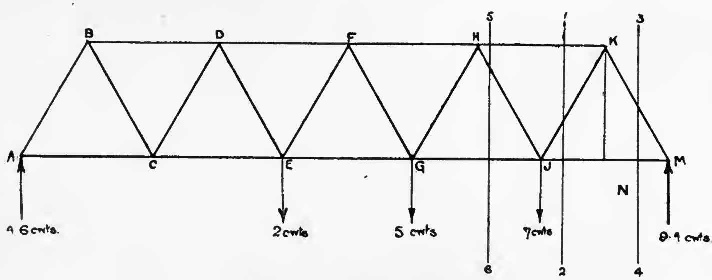

FIG. 23.—Method of Moments of Sections.

It may be noticed in passing that Bow's notation is not convenient for the method of moments.

We first find the reactions at A and M.

Taking moments about M, we have

$$R_A \times 30 = 2 \times 18 + 5 \times 12 + 7 \times 6$$

whence $R_A = 4{\cdot}6$ cwt.

and $R_M = 14 - 4{\cdot}6 = 9{\cdot}4$ cwt.

a value which should be checked by taking moments about A.

Consider the right-hand end bay J K M, and imagine that it is cut in two by some such line as 1–2, then the moment of the forces in the members J M, J K, H K about any point must be equal to the moment of the external forces acting either to the right or the left of the line 1–2 about the same point, for otherwise the structure would not be in equilibrium. Now, if we take moments about the point K, the moment of the forces in the members J K, H K about K is zero, and we are left with the moment of the force in J M about K, equal to the moment of the external forces to the right or left of 1–2 about K; that is, if we take the external forces to the right of the line 1–2, we have

Force in J M × K N $= 9{\cdot}4 \times 3$

or Force in J M $= 28{\cdot}2/5{\cdot}196 = 5{\cdot}43$ cwts. (Tension)

Again with the same cutting line, taking moments about J,

Force in H K × 5·196 = 9·4 × 6

or Force in H K = 10·85 cwt. (Compression)

Again with the same cutting line, taking moments about M,

Force in J K × 5·196 = Force in H K × 5·196

or Force in J K = Force in H K = 10·85 cwt. (Tension)

It will be noticed of course that for equilibrium here the force in J K must be of opposite sign to the force in H K, and since H K is in compression, J K must be in tension.

Next take a cutting line such as 3–4, and take moments about J, then

Force in K M × 5·196 = 9·4 × 6

or Force in K M = 10·85 cwt. and is in compression.

Again, with a cutting line such as 5–6, taking moments about G, we have

Force in H J × 5·196 = 9·4 × 12 − 7 × 6 − force in H K × 5·196

or Force in H J = 13·6 − 10·85
= 2·75 cwt.

With the same cutting line, taking moments about H,

Force in G J × 5·196 = 9·4 × 9 − 7 × 3

or Force in G J = 12·23 cwt.

In this manner, by taking fresh cutting lines along the girder and proceeding bay by bay, the whole of the forces in the various members can be evaluated. Of course it will be easier, when half-way along the girder, to commence from the left-hand end and work from that end towards the centre, just as in the case of stress diagrams it is best to work from each end.

CHAPTER III.

The Properties of Aerofoils.

Wind Tunnel Investigation.—In dealing with the subject of the aerofoil, it will be useful to commence by considering the method whereby most of our information concerning the characteristics of different aerofoils is obtained, namely, the wind tunnel method. By the use of the wind tunnel (or wind channel, as it is also called) it is possible to obtain both simply and accurately the particular qualities of various wing sections, and then by a comparison of their relative merits to deduce the one most likely to give the desired results upon a particular machine. Moreover, this method enables the effect upon aerodynamic characteristics of an alteration in the camber or shape of an aerofoil to be observed, and by its assistance the most efficient wing section for various specific duties can be evolved. To carry out such experiments upon a full-sized machine is practically impossible, besides being extremely dangerous and very expensive.

It will be appreciated that the application to a full-size wing section of the results obtained in a wind tunnel upon a small-scale model must necessarily be a problem of considerable difficulty, and this emphasises the importance of extreme accuracy in the measurement of the forces upon the model; for any slight error involved at this stage will naturally be greatly magnified when applied to full-scale machines. The question of scale effect has been the subject of close investigation, the results of which will be summarised at a later stage in this chapter.

The major portion of our knowledge of aerofoil characteristics is due to the splendid work of the National Physical Laboratory at Teddington, and to the work of Monsieur G. Eiffel in his laboratories at Auteuil, near Paris, so that a brief description of these two laboratories should suffice for a good understanding of the principles underlying the construction and use of wind tunnels. It may be remarked that there are also excellent aeronautical laboratories in the leading European countries and in the United States of America.

The N.P.L. Four-foot Tunnel.*—There are several wind tunnels at the N.P.L., including two of 7 feet diameter, but

* N.P.L. Report, 1912–1913.

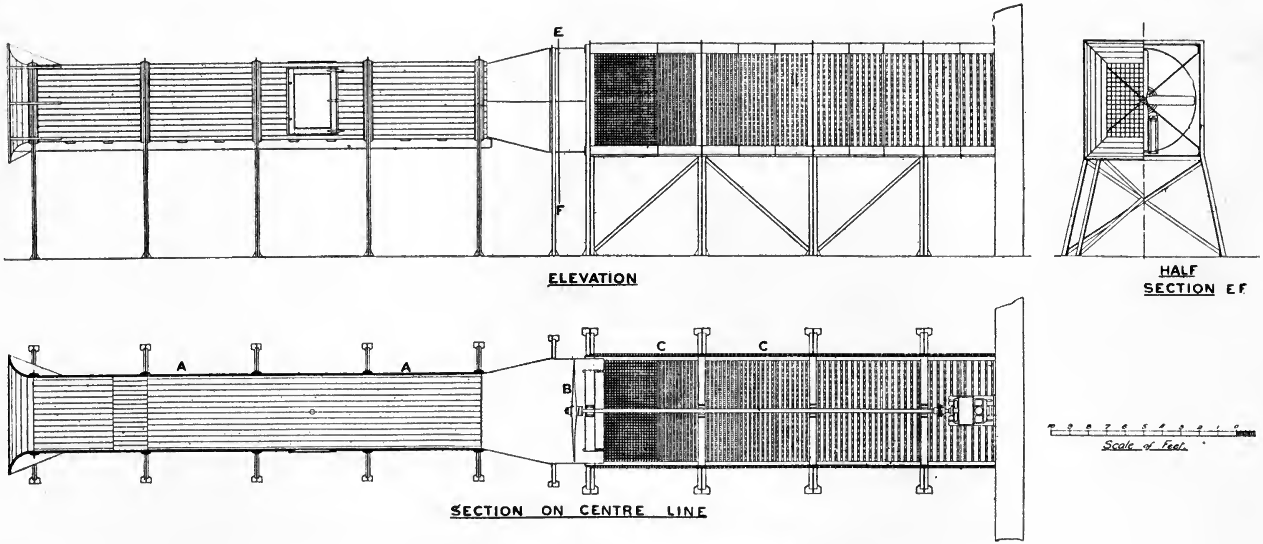

Fig. 24.—N.P.L. Four-foot Wind Tunnel.

from a room which is 60 feet long, 50 feet wide, and with an average height of 20 feet. The air, after entering the mouth of the tunnel, passes through a honeycomb, which can be seen in the half-section on EF, Fig. 24, and then along the main trunk portion, AA. This current of air is produced by the airscrew B (Fig. 24), this airscrew being driven by an electric motor through the line of shafting shown in the sectional plan (Fig. 24). Passing through the airscrew, the wind stream enters the specially perforated chamber, CC, and is squeezed through the walls of this chamber into the room again at a greatly reduced velocity. The airscrew has a pitch of 2 feet, and is made up of 4 blades of a constant width of 6 inches, the section being that of a previously tested aerofoil, and the pitch being calculated from the angle of no lift. It is possible to vary continuously the speed of the air stream through the working portion from 10 to 50 feet per second. At the highest speed the airscrew is making 1350 r.p.m., and absorbs about 8 h.p., 20% of this amount being lost in frictional resistance at the honeycomb. The wind velocity is measured by means of a Pitot tube, which is illustrated and fully described in Chapter XII. As a rough check upon this speed a recording speedometer is attached to the motor shafting.

It is very essential that the distribution of velocity over the central portion of the working part of the tunnel should be uniform. An investigation was made into this question by means of two anemometers, one of which was fixed and used as a standard of reference, while the other was moved from point to point in the cross-section. It was found that over a central square of 2·5 feet side, the velocity measurements did not differ more than 1% from the mean.

The Balance.—This balance has been designed for use under the most complex conditions, including investigations into the stability of a complete model. The arm of the balance which carries the model under test projects through the bottom of the channel. This arm is covered by a wind shield shaped like a low-resistance strut, and the hole where the arm passes through the floor of the tunnel is closed by means of an oil seal. Unless sealed, the gap between the balance and the arm and its shield would allow air at high velocity to enter the tunnel in the neighbourhood of the model, owing to the static pressure in the tunnel being less than the atmospheric pressure in the room outside. The use of a spindle to support the model introduces measurable disturbances in its own plane for some distance downwind, and corrections have to be applied. The balance is therefore arranged in such a way that any required measurement can be obtained without changing the spindle or its position relative to the model, so that any corrections which have to be made for the influence of the spindle on the air flow can be deduced from a second experiment on the same model, when held by the spindle in a different manner.

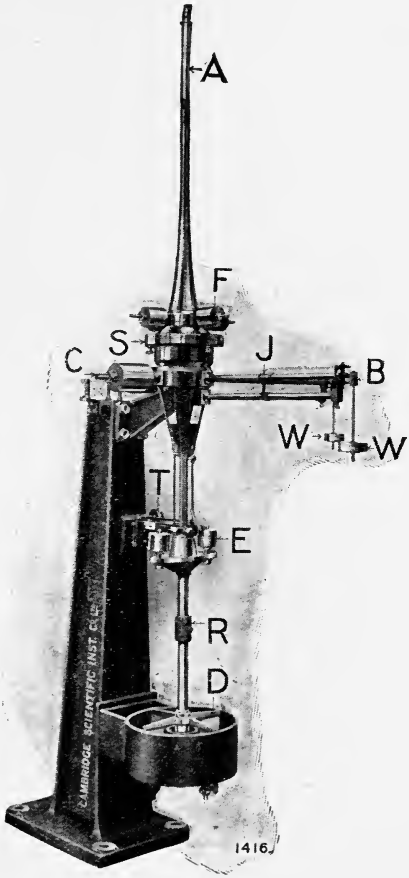

FIG. 27.

A photographic view of the balance is shown in Fig. 27, and an elevation of the balance is shown in Fig. 28. The arrangements of this balance allow for measurement of forces along, and moments about, three fixed rectangular axes. The main part of the balance consists of three arms mutually at right

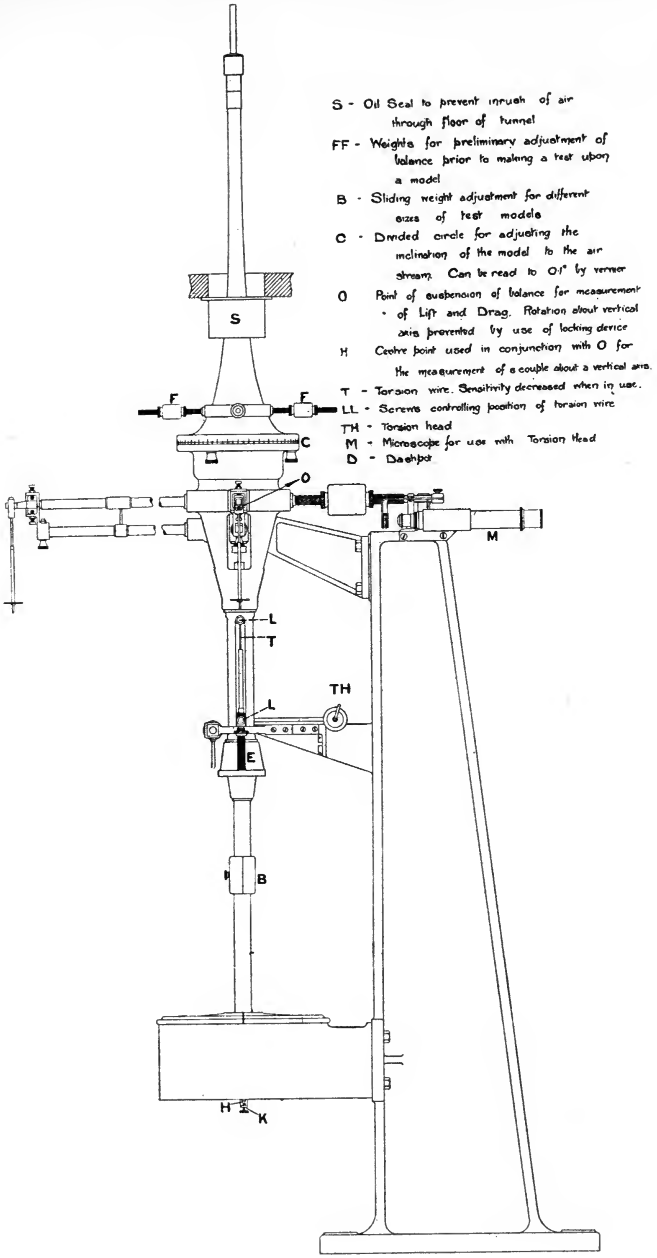

Fig. 28.—N.P.L. Aerodynamical Balance.

angles, each arm being counterbalanced. The centre lines of these arms meet in a point at which a steel centre is fixed. The weight of the balance is taken on this point, which rests in a hollow cone in a column fixed to the floor of the room. Three degrees of freedom are thus allowed, permitting measurements to be made of the moments about the centre lines of the three arms, which constitute a system of rectangular axes of reference. The vertical arm of the balance passes through the floor of the tunnel and supports the model under test. It can be rotated from the outside of the tunnel, and this rotation provides one of the two angle settings which have been shown to be necessary for general work. The two horizontal arms are set along and at right angles to the wind direction, and are used for determinations of lift and drag, or lateral force and drag, as may be required. The forces on the model are counterbalanced by dead weights hung from the ends of the horizontal arms, fine adjustment being provided by the movement of a jockey weight along the arm. The rotation of the balance about the vertical axis is prevented by a torsion wire, the twist in which is measured on a torsion head, and thus the moment about a vertical axis is determined.

The force along the vertical axis is measured on a horizontal weighing lever, the force on the model being transmitted to the lever through a vertical rod which slides freely inside the vertical arm of the balance. Two moments are also measured on this latter weighing lever. The model is held to the vertical balance arm by a special attachment, which allows rotation to occur about a horizontal axis in any desired direction, this axis being much nearer to the model than the axis of rotation of the main balance arms. The rotation of this special attachment is controlled by connecting it by a short arm to the top of the vertical sliding-rod. The immediate attachment to the model allows an alteration of angle to be made about a horizontal axis, which is fixed relative to the model. This adjustment can only be made from inside the tunnel.

Of the six force and couple measurements necessary for the examination of an unsymmetrically situated model, it is possible to make four simultaneously. Except in special circumstances, however, it is not desirable to make so many observations at the same time, and locking arrangements are therefore provided to reduce the number of degrees of freedom. A simple locking device also holds the balance from movement in any direction when not in use.

Rapid oscillations are damped out by means of dash-pots. On the lower part of the vertical arm, weights can be attached which allow changes to be made in the sensitivity of the balance, so that models of greatly varying size can be readily tested.

LIFT AND DRAG MEASUREMENTS.—For this purpose the balance is supported at the point O only, and a locking device prevents rotation about a vertical axis. The balance is then free to rotate about two horizontal axes only.

VERTICAL FORCE MEASUREMENT.—The vertical rod in the upper portion of the balance is guided by four rollers, so that it can slide in a vertical direction but not twist. The rod will move along its axis under a force of 0·0001 lb.

COUPLE ABOUT A VERTICAL AXIS.—For this purpose the centre H is held in a conical cup by the spring K, which is not sufficiently powerful to lift the upper centre O off its seating. The couples are therefore measured about an axis through O and H, and special precautions have been taken in the balance to ensure that the axis OH is in the vertical position. The rotation about this axis is controlled by the torsion wire T, the twist being measured on the torsion head TH by the amount of rotation necessary to bring a crosswire attached to the balance into alignment with a crosswire in the microscope M, which is fixed to the balance support.

MEASUREMENT OF DRAG ALONE.—For this purpose the support for the centre O is lowered until the balance rests on two points on either side, the centre point then being out of use. This measurement is used in those cases where there is no appreciable lift.

The Eiffel Laboratory.*—Eiffel's early wind-channel experiments were conducted in a laboratory erected in the Champ de Mars at Paris. These experiments were carried out to determine the force exerted upon a flat plate, and were made in conjunction with the method of dropping flat plates from the Eiffel Tower in Paris for a similar purpose. Much useful work was carried out in this early tunnel, but in order to be able to experiment at speeds more nearly approaching those of an aeroplane in flight there was built at Auteuil in 1912 a new laboratory and wind tunnel, of which illustrations are shown in Figs. 29–33.

The experimental chamber (see Figs. 30 and 32) is an air-tight room. Leading to this room are a pair of funnel-shaped collectors (see Fig. 31, p. 40) through which the air is drawn from the hangar outside (see Fig. 30, p. 46). In the new channel the

* From information communicated by Mons. G. Eiffel.

outer and inner diameters of the larger collector are 13 feet and $6\frac{1}{2}$ feet respectively, and it is 11 feet in length. The effect of so reducing the cross-sectional area is to raise the velocity of the

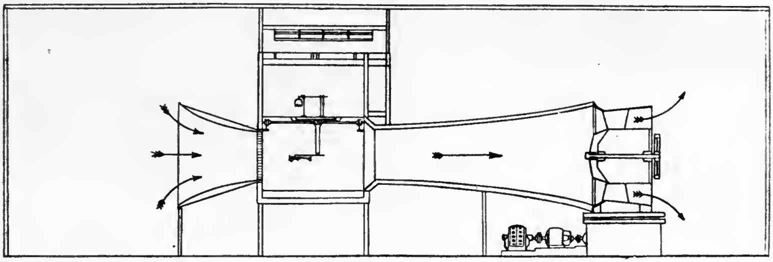

FIG. 29.—Sectional Elevation of Wind Tunnel in Eiffel Aerodynamical Laboratory.

air stream and diminish its pressure correspondingly. Consequently the model is under investigation in a region of high velocity and low pressure (see Fig. 33). By measuring the

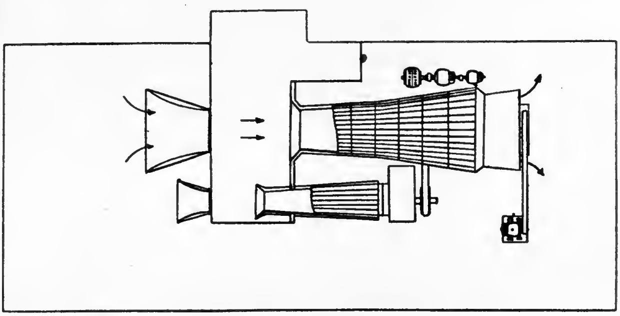

FIG. 30.—Sectional Plan of Wind Channel in Eiffel Aerodynamical Laboratory.

difference in pressure between the experimental chamber and the air in the hangar outside, the velocity of the air stream can be deduced from the formula

$$v^2 = 2gh \quad \text{............... Formula 10}$$

where h is the difference in pressure observed. Passing across the experimental chamber the air stream enters the discharger, which is an expanding chamber 30 feet long, leading to the airscrew. This airscrew is actuated by a 50 h.p. electric motor. This discharger serves to lower the velocity and raise the pressure of the air stream, thus reducing the power required to drive the airscrew and returning the air to the hangar without setting up pulsations. A maximum speed of 100 feet per second can be attained in the experimental chamber. The observers are situated on a platform above the air stream and model as shown in Fig. 32, a position which is very convenient for experimental purposes.

The investigations carried out by Eiffel include the determination of forces and moments upon flat plates and aerofoils, the resistances of wing structures, scale model tests, the application of results to full-sized machines, and the performance of model airscrews.

The Flat Plate.—The force exerted upon a flat plate suspended normally to a current of air is at the basis of experimental aeronautics. A very thorough investigation of this fundamental problem was carried out by Dr. Stanton at the N.P.L. As a result he found that the force (F) varied directly as the area of the plate (A), the square of the velocity of the plate relative to the wind (V), and that the relationship could be expressed by means of the formula

$$F = K \frac{\rho}{g} A V^2 \quad \text{........... Formula 11}$$

where K is a coefficient depending upon the units used and the size of the plate under investigation.

From Formula 11 we see that the pressure per unit area

$$= \frac{F}{A} = K \frac{\rho}{g} V^2 \quad \text{........... Formula 11 } (a)$$

These relationships are independent of the system of units used; if the units are the foot, pound, and second, the value of K increases from 0·52 for a plate 2 inches square to a value of 0·62 for plates between 5 and 10 feet square.

Eiffel obtained very similar results at his laboratory, and enlarged the scope of the investigation to include plates of varying aspect ratio, that is, ratio of span to chord. He found that the effect of increasing the span relative to the chord was to increase the normal pressure on the plate. His results are embodied in Table XIV.

TABLE XIV.—INFLUENCE OF ASPECT RATIO ON THE NORMAL PRESSURE OF A FLAT PLATE. (EIFFEL.)

Aspect ratio ...	1	1·5	3	6	10	14·6	20	30	41·5	50
Ratio of pressures $\frac{\text{Rectangle}}{\text{Square}}$	1·00	1·04	1·07	1·10	1·145	1·25	1·34	1·4	1·435	1·47

It will be seen from the above table that the normal pressure on a plate of aspect ratio 6 is 10%, and of aspect ratio 14·6 is 25% greater than that on a square plate of the same area at the same speed. This effect is due to the lateral escape of the air towards the ends of the plate, and will be more fully considered in relation to aerofoil sections.

The Inclined Flat Plate.—The next step was to investigate the effect of inclining the plate to the direction of the air stream, and this was undertaken both by the American experimenter,

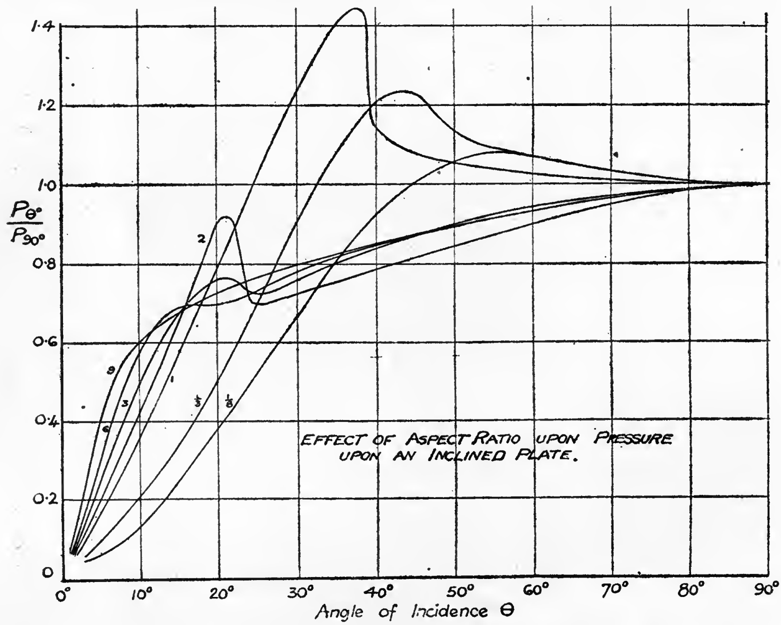

FIG. 34.—Effect of Aspect Ratio upon Pressure on Inclined Plane.

Langley, and Eiffel, from the latter of whom most of our information on this problem is derived. It was found that for small angles of incidence of the plate to the direction of the air stream the resultant force on the plate is given by the expression :

$$\text{Force} = F = C\frac{\rho}{g} A V^2 \theta \quad \text{.......... Formula 12}$$

and the pressure per unit area :

$$= \frac{F}{A} = C\frac{\rho}{g} V^2 \theta \quad \text{.......... Formula 12 } (a)$$

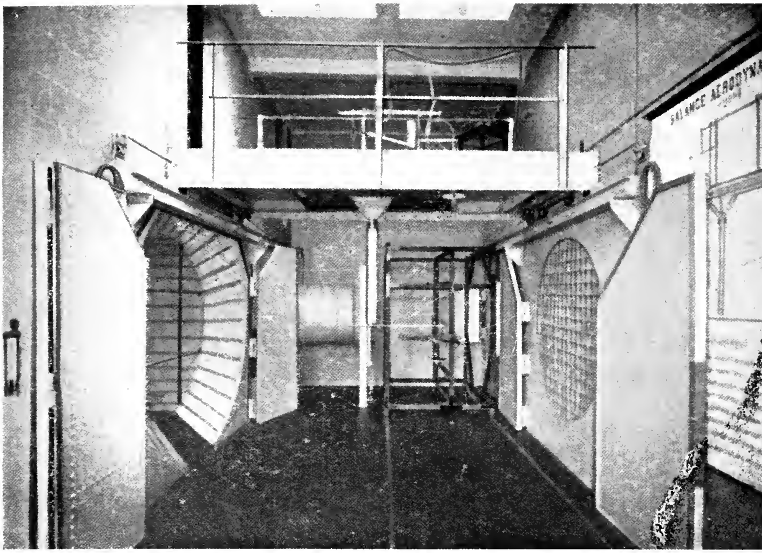

Reproduced by courtesy of M. Eiffel.

FIG. 32.—Experimental Chamber in Eiffel Laboratory.

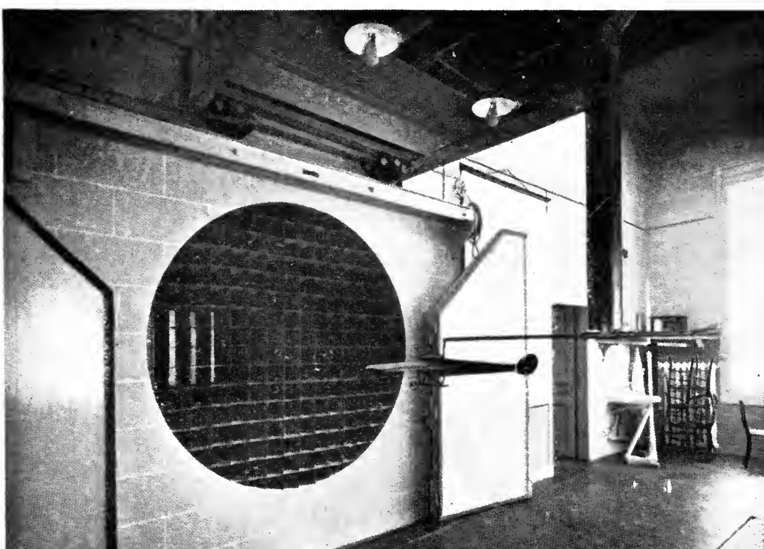

Reproduced by courtesy of M. Eiffel.

FIG. 33.—Model under Test in Eiffel Laboratory.

Facing page 48.

—that is, in this case the force is proportional to the angle of incidence θ of the plate.

As the angle of the plate relative to the air stream increases, Formula 12 ceases to hold good, and the force tends towards the value given by Formula 11. Fig. 34 shows that the pressure on a square plate between the angles of 25° and 90° is greater than that at 90°—that is, when the plate is normal to the wind direction. The effect of aspect ratio upon an inclined flat plate is very clearly exhibited by the graphs shown in Fig. 34. The series of curves there drawn are due to results obtained by Eiffel, and give the ratio between the pressure at any angle θ and the normal pressure, for all angles from 0° to 90°. It will be seen that increase of aspect ratio produces a smaller maximum normal pressure, but that for small angles of incidence the normal pressure is greatest for the largest aspect ratio.

The resultant force (F) on an inclined flat plate can be

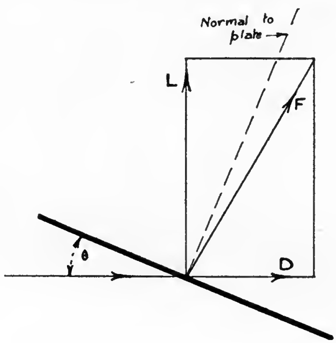

FIG. 35.

resolved into two particular components of great use in aeronautical problems. The first of these components is that perpendicular to the direction of the air stream, and is known as the Lift; while the second is the component in the direction of the air stream, and is known as the Drag. These components are illustrated in Fig. 35.

It is customary to express these components in the manner shown by the relationships in Formulæ 13 and 14.

$$\text{Lift} = K_y \frac{\rho}{g} A V^2 \quad \text{........... Formula 13}$$

$$\text{Drag} = K_x \frac{\rho}{g} A V^2 \quad \text{........... Formula 14}$$

where K_y and K_x, known as the Lift and Drag absolute coefficients respectively, are dependent upon the angle of incidence. Formulæ 13 and 14 may be regarded as the two fundamental equations of aerodynamics, and the ratio $\frac{\text{LIFT}}{\text{DRAG}}$ is a measure of the efficiency of the surface under test. The determination of the Lift and Drag coefficients for surfaces of various shapes is a function that has been admirably performed by the wind tunnel.

Flat Plate moving Edgewise.—The investigation of the forces in this case was carried out by Zahm, who expressed the results obtained in the relationship—

$$F = K\,A^{\cdot 93}\,V^{1 \cdot 86} \qquad \text{........... Formula 15}$$

We shall consider this question further when dealing with the subject of skin friction.

These fundamental data, while not directly applicable to practical aeronautical design work, provide an essential foundation for reference in the ever-growing field of aeronautical knowledge, and enable the true significance of the co-efficients for objects of special shapes, such as aerofoils and stream-line sections, to be more fully understood.

The Aerofoil.—Lilienthal was one of the first to investigate by means of scale models the properties of the cambered aerofoil, and to point out its much superior efficiency over that of the flat plate.

To-day, the analysis of a wing section enables the values of the lift and drag coefficients to be determined over a large range of angles and also provides information concerning the pressure distribution over the upper and lower surfaces.

These results are obtained from experiments carried out in wind tunnels upon carefully prepared scale models. The extreme accuracy with which the forces can be measured and the conditions of flight approximated, make wind-tunnel experiments of increasing importance and value. To-day, when a new type of machine is being designed, an accurate model is made and tested, and from the results information may be gathered leading to an increased efficiency in design.

From the point of view of aeroplane design, the determination of the lift and drag of an aerofoil for various angles of incidence is the most important measurement required, and it will therefore be useful to consider briefly the most general method of recording these characteristics of an aerofoil and their common features. Table XV. gives the results of tests in the wind tunnel made at the N.P.L. upon an aerofoil section known as the R.A.F. 6. It will be noted that the lift, drag, and Lift/Drag coefficients are given in absolute units. This is the method now adopted in England in giving the results of tests upon modern aerofoils, and expresses the values of K_y and K_x in Formulæ 13 and 14.

TABLE XV.—R.A.F. 6 COEFFICIENTS.

Angle of incidence.	Lift coefficient absolute.	Drag coefficient absolute.	Lift/Drag.
− 2	0·003	0·0201	...
0	0·074	0·0165	4·5
2	0·173	0·0159	10·9
4	0·275	0·0193	14·3
6	0·354	0·0252	14·1
8	0·423	0·0329	12·9
10	0·496	0·0433	11·4
12	0·564	0·0545	10·4
14	0·593	0·0640	9·3
16	0·605	0·0875	6·9
18	0·550	0·1336	4·1
20	0·500	0·1665	3·0
22	0·476	0·1845	2·6
24	0·456	0·2015	2·3

The curves obtained from the above results are shown plotted in Figs. 36, 37, and 38, and may be regarded as typical of the curves obtained from tests upon model aerofoils possessing no freak characteristics.

It will be observed that the point of no lift occurs at a small negative angle of incidence: that is, when the leading edge of the aerofoil is inclined downwards to the direction of the wind stream. The actual value of the point of no lift is of importance when considering questions of stability and control. The slope of the lift curve remains practically constant up to a point shown by C in Fig. 36, and is of importance in considering stability. The angle of incidence corresponding to this point is known as the critical angle. The value of the lift corresponding to the maximum Lift/Drag ratio is indicated by the point B (Figs. 38 and 36). The angle of incidence corresponding to this point will approximate very closely to that chosen for the most efficient flying position. Moreover, the value of the lift at this point should be high in order that the area of the planes may not be excessive. On the other hand, it should not approach the point of maximum lift C too closely, or there will be insufficient latitude for manœuvring. Upon the value of the critical angle depends the landing speed of the machine; and for

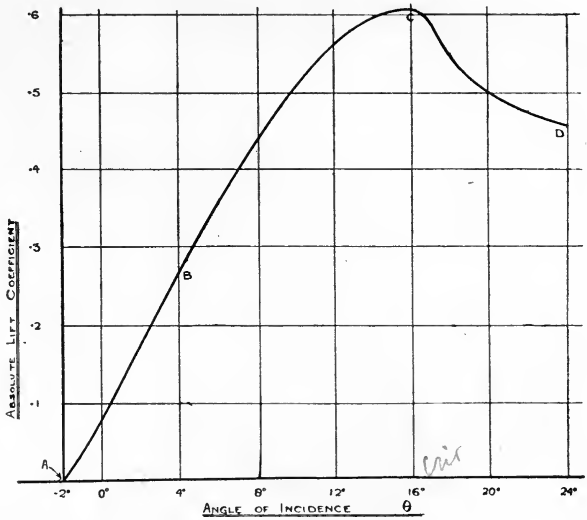

Fig. 36.—Lift Curve.

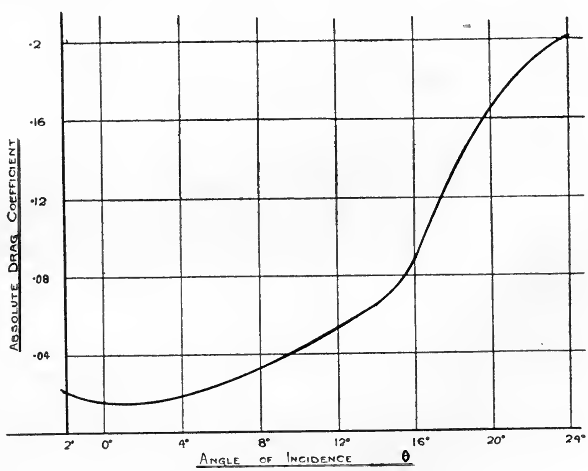

Fig. 37.—Drag Curve.

a given wing area the aerofoil having the maximum lift coefficient will give the slowest landing speed. The critical angle is influenced greatly by the shape of the aerofoil and slightly by the aspect ratio.

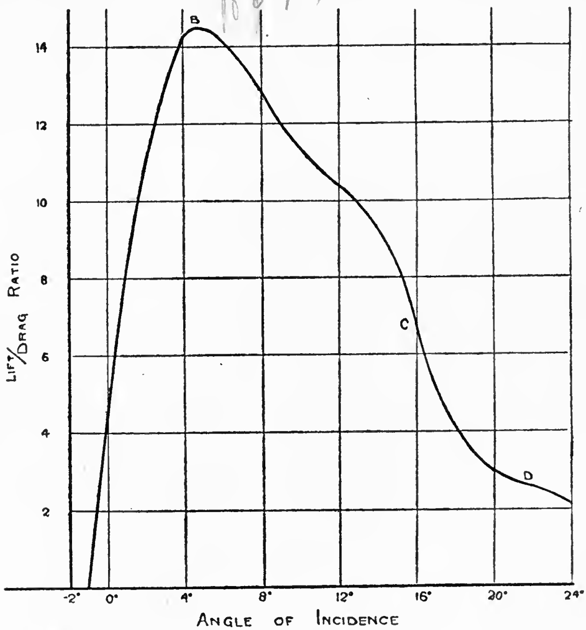

FIG. 38.—Typical Lift/Drag Curve for Aerofoil Section.

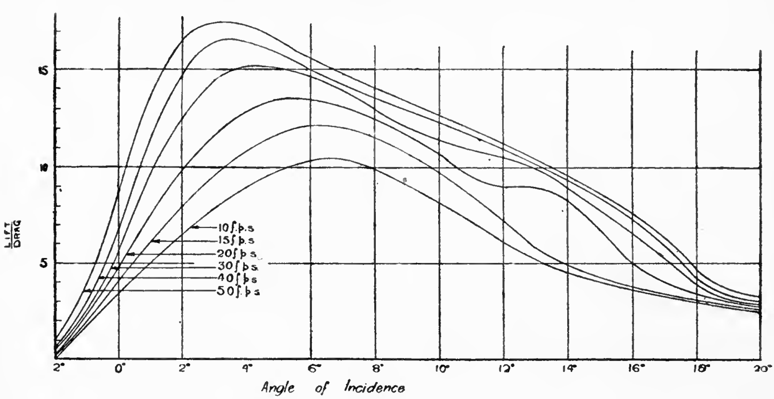

FIG. 39.—Variation of Lift/Drag Ratio with Increase of Speed.

After passing the critical angle, the lift diminishes sometimes slowly and sometimes rapidly, there being a corresponding increase in the drag. When testing model aerofoils at low speeds there is occasionally a rapid drop in the lift just after the critical angle, and then a second rise in the value of the lift

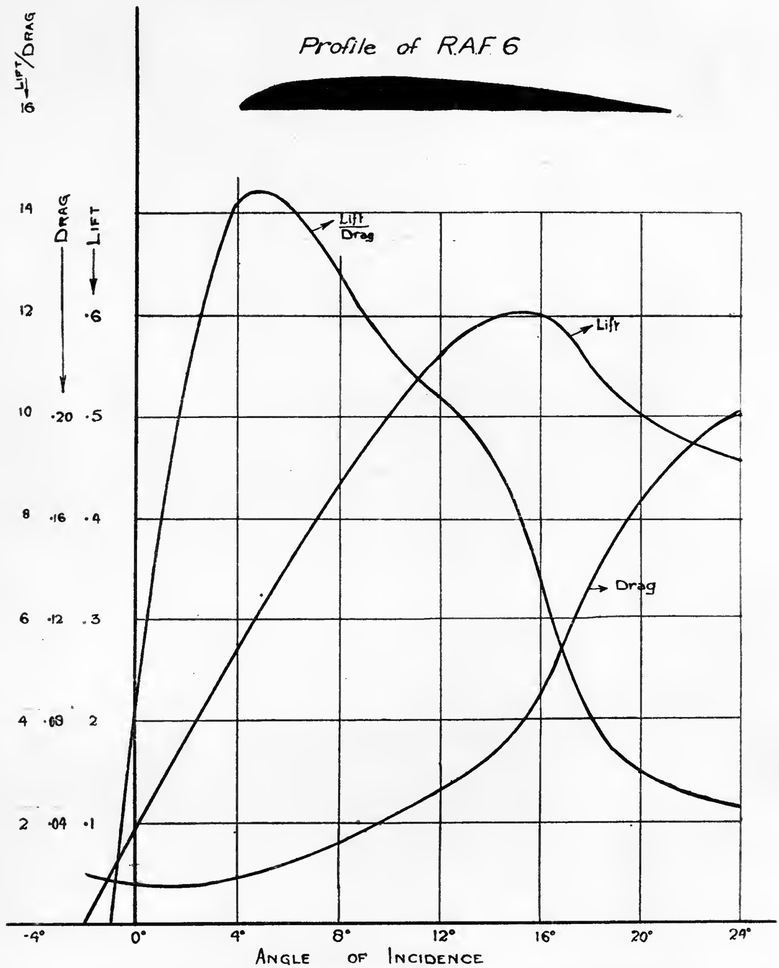

FIG. 40.—Typical Curves for an Aerofoil Section. Combination of Figs. 36, 37, 38.

coefficient to approximately the same value as that at first obtained. On increasing the speed of the air current, however, this temporary depression disappears.

Fig. 37 shows the drag curve, from which it will be seen that the drag diminishes to a minimum value between 0° and 2°, and that it remains fairly constant in this neighbourhood, and then follows approximately a parabolic law up to the critical angle, after passing which point there is a very rapid increase.

Fig. 38 shows the Lift/Drag curve for the aerofoil whose curves of lift and drag are given in Figs. 36 and 37, and is plotted from the calculated results shown in Table XV.

Fig. 39 shows the effect upon the Lift/Drag curve of increasing the speed of the air current in the wind tunnel for the same aerofoil.

For aerofoils in general use the critical angle is usually about 16°, the corresponding lift coefficient varying from ·45 to ·70. The maximum Lift/Drag ratio occurs at about 4° angle of incidence and varies in value between 15 and 18. The minimum drag so far obtained is about ·006. It is usual to incorporate all these three curves on one chart, as shown in Fig. 40.

Pressure Distribution over an Aerofoil.—Having considered the characteristic points of an aerofoil, it is desirable to investigate the nature of the airflow producing these characteristics, and to examine the effect upon this flow of changes in the shape of the aerofoil.

To establish the principles underlying the remarkable efficiency of a good aerofoil section as compared with an inclined flat plate, the N.P.L. investigated the distribution of pressure over the surface of an aerofoil. The following information is taken from the Reports for the years 1911–1912–1913.

In order to make a thorough analysis of the pressure distribution over a large range of angles of incidence, it was found advisable to limit the scope of the experiments to three different shapes, namely—

i. A flat plate.
ii. An aerofoil with both surfaces cambered.
iii. An aerofoil with the top surface only cambered.

The models used are illustrated in Fig. 41, the flat plate being made of thin steel ·02″ thick, 12″ long, and $2\frac{1}{2}$″ wide, while the other two models were moulded with wax upon thin brass sheet curved to the desired shape, 12″ long by $2\frac{1}{2}$″ wide, the upper surfaces of these two models being exactly similar. The pressure was observed at eight different points along the median section, the position of the holes being indicated in Fig. 41. These holes were 1/64″ in diameter and each communicated when under observation with a manometer by means of a length of tubing. All the holes except the one under test were plugged with plasticine, and the whole apparatus was designed to interfere as little as possible with the flow of the air around the aerofoil. The speed of the wind stream was measured in the usual way by observing the pressure difference shown by the Pitot tube, and was found to be about 17 feet per second.

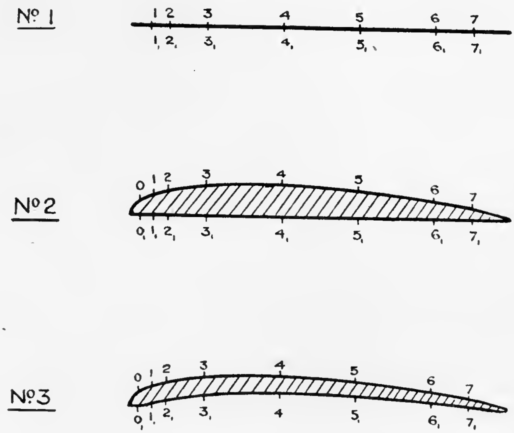

Fig. 41.—Aerofoil Sections.

The pressure diagrams obtained for these three model aerofoils are shown in Fig. 42. Ordinates below the datum line indicate negative pressure or suction, while those above indicate positive pressure. It will be seen that for ordinary flight angles both the negative pressure over the top surface and the positive pressure over the bottom surface reach a maximum very near to the leading edge and fall away almost to zero at the trailing edge, and for certain angles of incidence they even change sign. It is this phenomenon which accounts for the position of the centre of pressure—the point on the chord at which the resultant force acts—being much ahead of the centre of the chord for flight angles, and which points to the necessity for making the leading edge of an aerofoil very much stronger than the trailing edge. Applying these results to full-size wings, the force per square foot, at an angle of incidence of 10° and a speed of 60 miles per hour, is about 35 lbs. at the leading edge and only 2 lbs. at the trailing edge.

The observations show that for each aerofoil there is a critical angle above which the pressure over the upper surface, after passing through a period of extreme unsteadiness,

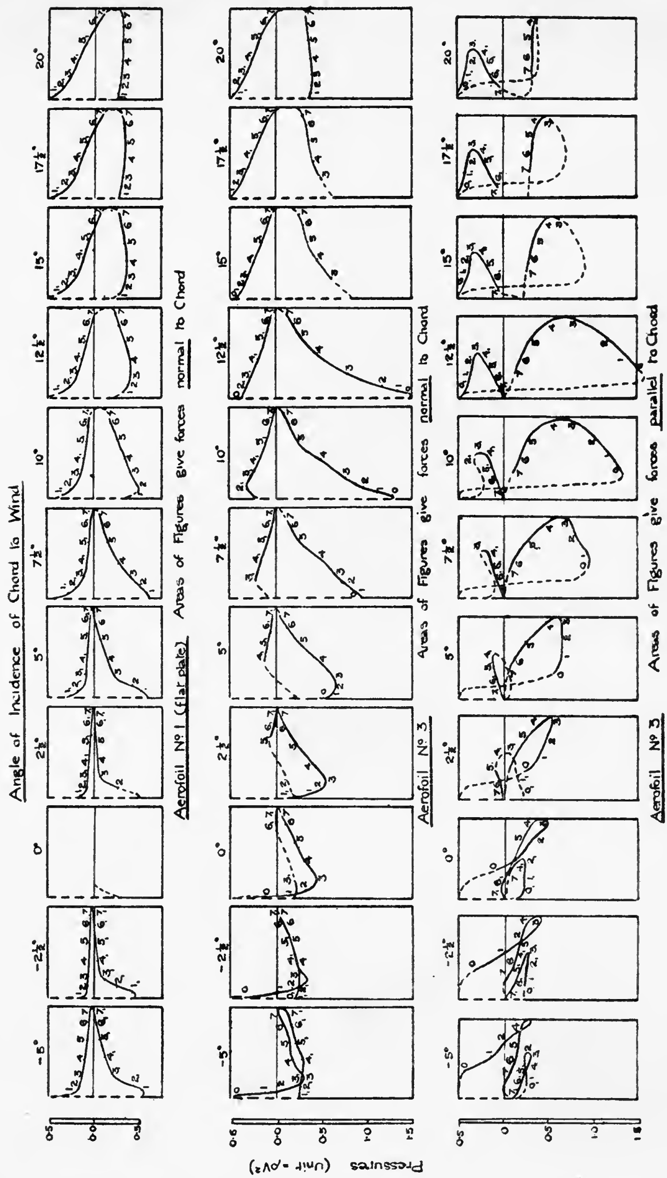

FIG. 42.—Distribution of Pressure on Median Section of Aerofoils Nos. 1 and 3.

becomes uniform. For angles below the critical angle the pressure over both surfaces varies with the angle of incidence according to definite laws, but after the unsteady region is passed the distribution over the upper surface becomes uniform, while pressure on the lower surface falls off to an extent sufficient to cause a change of sign near the trailing edge. A determination of the lift and drag on these aerofoils was also carried out, and the results are shown plotted in Fig. 43 (*a*) and (*b*). From these curves it appears that the critical angle, above which the pressure distribution becomes unsteady, corresponds to the critical angle of the lift curve at which there is a falling off in the lift and a large increase in the drag. This indicates that these phenomena are due to the sudden alteration in the

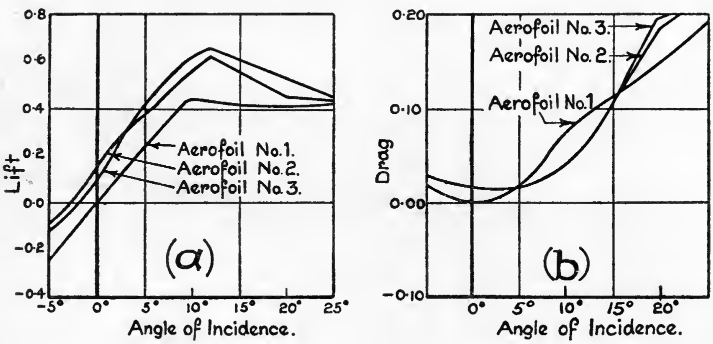

FIG. 43.—Lift and Drag Curves for three Aerofoils.

pressure distribution over the upper surface, owing to a breakdown in the character of the fluid flow in the neighbourhood of this angle. The value of the critical angle and the amount of change that occurs at this point is largely influenced by changing the position of the maximum ordinate of the aerofoil section, as will be seen shortly. A striking peculiarity illustrated by these pressure distribution curves is that it is possible to have a very high negative pressure or suction near the leading edge when the angle of incidence is such that a positive pressure would have been anticipated. The principle underlying this departure from expected conditions is known as the 'Phenomenon of the Dipping Front Edge,' the explanation being that the stream-lines approaching the leading edge are deflected upwards before reaching it, and consequently, although the local angle of incidence with the general wind direction may be positive, the actual angle made with the local wind is negative. This upward deflection of the stream-lines is accompanied by the formation of a general low-pressure region above

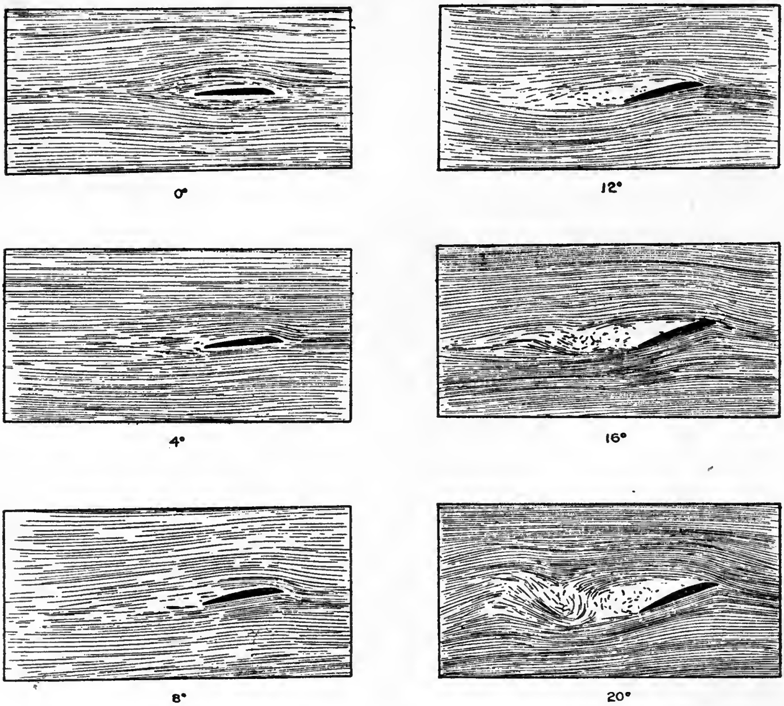

FIG. 44.—Flow past an Aerofoil Section, showing Development of Eddy Motion with Increase of Angle of Incidence.

and a high-pressure region below the aerofoil. The photographs reproduced in Fig. 44 show the effect of the disturbance for different angles of incidence.

Aerofoil Efficiency.—For an aerofoil to be of practical value it is essential that at some angle of incidence there should exist a high value of the ratio of L/D, accompanied by a high value of the lift coefficient. In the case of the flat plate, although the maximum ratio of L/D may be high at ordinary angles, the corresponding value of the lift, as shown by Fig. 43 (*a*), is much too low for practical purposes. The total lift on the aerofoil is seen from the same figure to be much greater than that for the flat plate, and there is also a much greater range between the angle of no lift and the critical angle, thus allowing much more latitude for adjustment during flight. The most important consideration leading to the greater efficiency of the aerofoil is as follows: Whereas the resultant force on a flat plate can never act forwards of a normal to itself, a good aerofoil section, on account of the upward deflection of the streamlines shown in Fig. 44, and the consequent pressure distribution over the front portion of the aerofoil, can and usually does have a resultant force upon it acting in a direction well forward of the normal to the chord. These cases are illustrated in Figs. 35 and 45. If the surface of the flat plate offered no resistance to

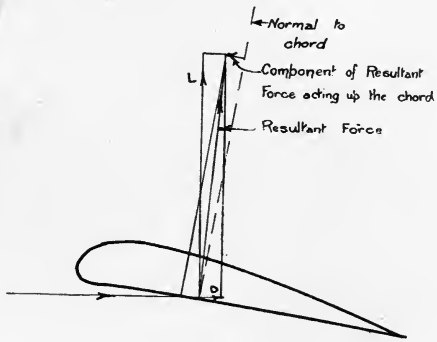

Fig. 45.

the airflow, which corresponds to a condition of maximum efficiency, the resultant would be exactly perpendicular to the plate. The effect of skin friction, however, is such that the resultant acts behind the normal to the chord. For the aerofoil the pressure distribution is such that the resultant acts forward of the normal to the chord. Resolving normally and along the chord, we therefore have a component acting along the chord practically in the opposite direction to the drag force, thus reducing the value of the total drag, and thereby increasing the value of the L/D ratio. The increased efficiency of an aerofoil is principally dependent upon the production of this component acting in opposition to the drag. Reference to the curves in Fig 42 shows that this is due to the uneven pressure distribution over the upper surface. If the pressure distribution were uniform, this opposing component would disappear entirely and the drag would be greatly increased, and this is actually what occurs after the critical angle is passed. The more pronounced this uneven pressure distribution effect can be made without causing a breakdown in the airflow, the more efficient the aerofoil becomes.

Pressure Distribution over the Entire Surface of an Aerofoil.—The experiments just described relating to the pressure distribution over the median section of a model aero-

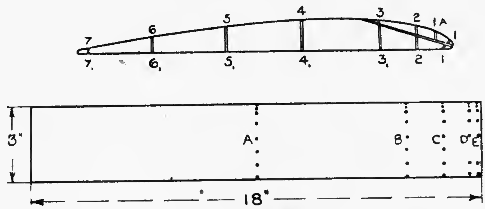

FIG. 46.—Plan and Section of Aerofoil, showing Observation Points.

foil were subsequently extended to cover the entire surface, the observations being made at four other sections, all comparatively near to the wing-tips, as well as at the median section.

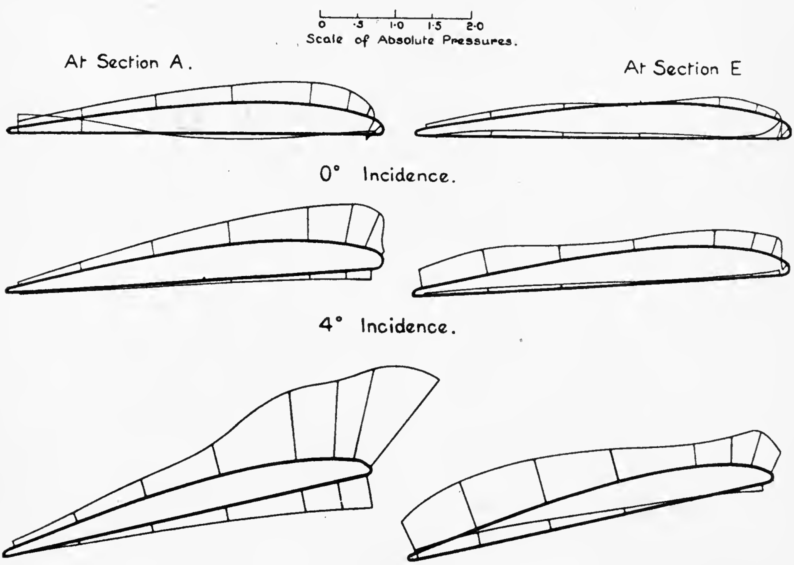

FIG. 47.—Curves showing Pressure Distribution over Aerofoil at Median and End Sections.

The positions of these observation points are indicated in Fig. 46, and the results obtained are shown in Fig. 47. Positive pressures are denoted by normals drawn downwards from the upper or lower surface, and negative pressures by normals drawn upwards. These pressures are given in absolute units. To convert to pounds per square foot at V miles per hour, multiply by $\cdot 00510\ V^2$.

The pressure distribution is shown for three angles of incidence, 0°, 4°, and 12°, for the median section and the extreme end section, side by side in order to give a clearer conception of the very different airflow existing at these two sections. It is found that the points of highest pressure on the aerofoil gradually recede from the leading edge, until in the neighbourhood of the wing-tip the maximum pressures occur close to the trailing edge and are due to suction entirely. As a result of this the direction of the resultant lift force instead of being inclined toward the direction of motion, is inclined in the opposite way, and hence its component in the direction of motion increases the drag force. The value of the drift is a minimum at the central section and increases gradually towards the wing-tips and then rises very rapidly at the extreme ends. The lift coefficient falls off considerably near the tips, its value only being about one-half that at the central section. This is due to the lateral escape of the air on the under side of the wing and the influx of air above the wing. The result of this variation in the characteristics of the aerofoil section at the wing-tips is a reduction in the L/D ratio of the wing as a whole; that is, the efficiency of the supporting surface is diminished owing to this effect, which is often called the 'End Effect.'

Full-scale Pressure Distribution Experiments.*—In a paper read before the Aeronautical Society, Captain Farren gave an account of the investigation of the distribution of pressure over the wings of a full size machine when in flight. The method adopted was very similar to that used for model aerofoils. A number of small tubes were run through the wings, with the outer ends open and fixed at the point in the surface of the wing at which it was desired to measure the pressure. The inner ends of the tubes were connected to manometer tubes so arranged that pressure differences could be recorded photographically. A diagrammatic sketch of the arrangement is shown in Fig. 48. As in the model experiments, all the holes except the one under observation at the moment were sealed up, and great difficulty was encountered in ensuring that there were no leaks in the tubes. Difficulty was experienced in comparing the results with those obtained in model aerofoil experiments, as it was not possible to determine the attitude

* *Aeronautical Journal*, February, 1919.

of the machine exactly, but by installing a yawmeter in a vertical plane, it may be possible to record the correct angle of incidence on the photographic record.

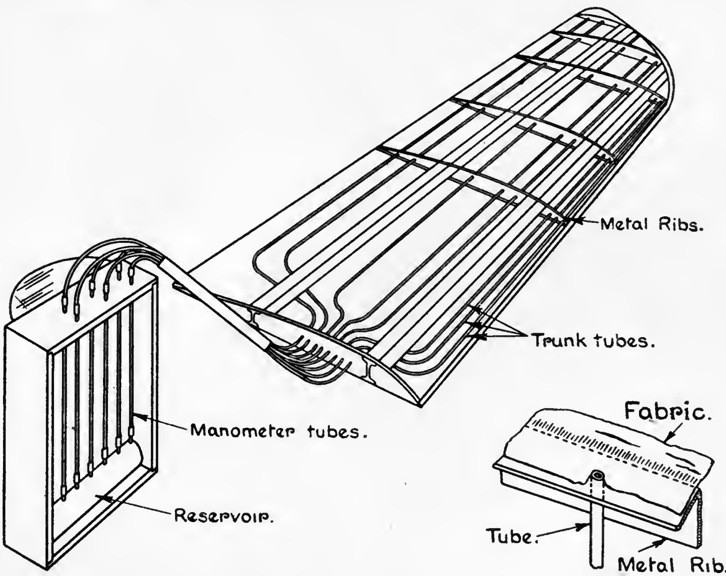

FIG. 48.—Arrangement of Manometer Tubes for Investigation of Pressure Distribution in Full-scale Machines.

Fig. 49 shows a comparison of the pressures obtained in a test upon a model biplane in the wind tunnel, and corresponding full-scale machine tested in the manner indicated above.

Aspect Ratio.—The pressure distribution diagrams given in Fig. 47 lead one to expect that the efficiency of a wing surface will be increased by an increase in aspect ratio. Table XVI. shows that this is precisely what occurs.

TABLE XVI.—INFLUENCE OF ASPECT RATIO.

Aspect ratio.	Angles of Incidence. 3° Lift	3° L/D	6° Lift	6° L/D	9° Lift	9° L/D
2	·60	·47	.62	·54	·60	·55
3	·70	·58	·73	·64	·78	·72
4	·84	·73	·85	·77	·90	·83
5	·94	·86	·95	·90	·96	·92
6	1·00	1·00	1·00	1·00	1·00	1·00
7	1·05	1·06	1·04	1·10	1·04	1·09
8	1·08	1·09	1·08	1·16	1·08	1·15

An aspect ratio of 6 has been taken as a standard of reference and the lift, and L/D of other aspect ratios expressed

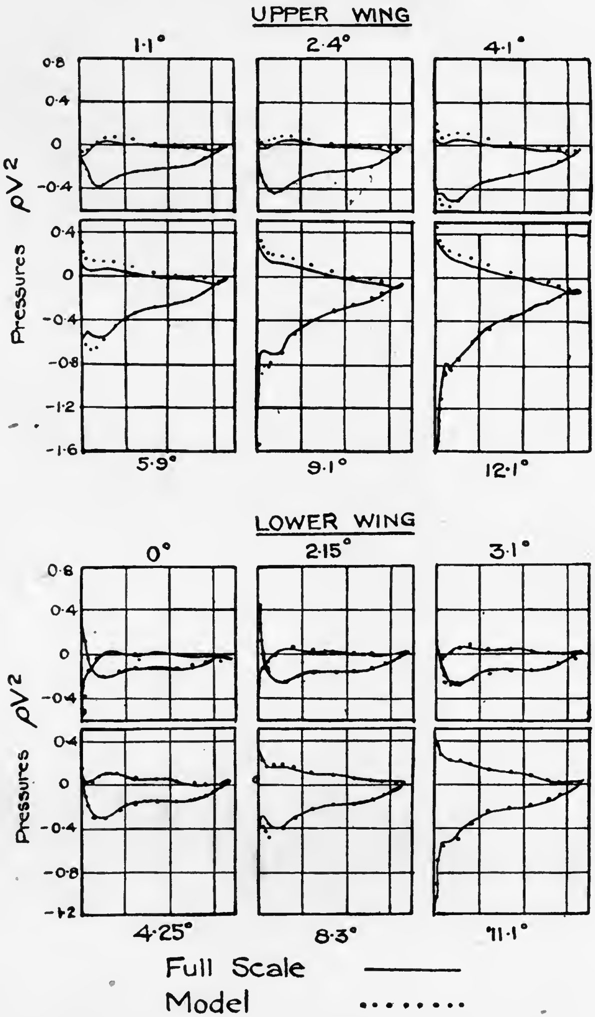

FIG. 49.—Comparison of Pressure Distribution on Model and Full-scale Biplane.

in terms of this unit. It will be seen that the L/D ratio increases continuously with aspect ratio. The actual figures are graphed in Fig. 50, from which it will be seen that the value is about 10 for an aspect ratio of 3, and increases to about 15·5 for an aspect ratio of 8. The maximum lift coefficient remains practically constant, the increased efficiency at high values of aspect ratio being due to reduced drag coefficients. It will also be seen from this figure that as the aspect ratio becomes less, the angle of no lift occurs earlier.

Since models of aerofoils and complete wing-spans are almost invariably tested with an aspect ratio of 6, it is only necessary to multiply the values given for the lift, and L/D

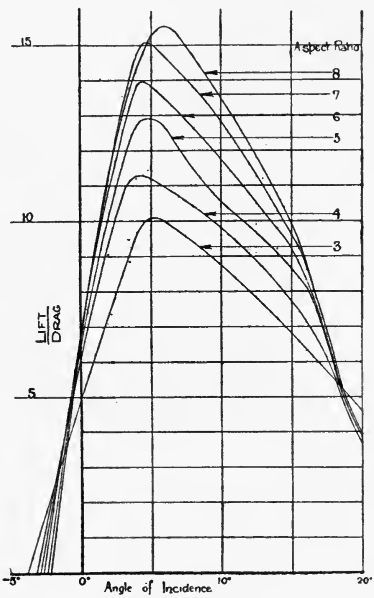

FIG. 50.—Effect of Aspect Ratio upon Lift/Drag Ratio.

coefficients by the appropriate factor in Table XVI., in order to obtain the correct value for any aspect ratio between 2 and 8.

The Relative Importance of the Upper and Lower Surfaces of an Aerofoil.—The pressure distribution curves given in Fig. 42 show that at ordinary angles of flight the negative pressure or suction over the upper surface is much greater numerically than the positive pressure on the lower surface. In the case of the flat plate, the upper surface contributes about 75% of the total force normal to the chord over the greater part of the range of angles under consideration, while for aerofoils the upper surface contributes practically all the normal force at from 0° to 4°, and quite 75% of this force at 12°. Since at these angles the force normal to the chord is scarcely distinguishable from the lift, it can be stated as a general rule that the lower surface of any aerofoil never provides more than 25% of the lift. This is an important consideration from the constructional point of view, in that it shows the necessity of securing the canvas forming the upper surface of the wing very firmly to the ribs in order to prevent it being torn away in an upward direction. There are no forces parallel to the chord in the case of the flat plate and in that of the aerofoil with flat undersurface excepting skin friction. For the cambered undersurface the lower surface contributes only 12½% of the total force at 12°, while for angles below 7° the force on it is in the direction of positive drag and is therefore disadvantageous.

An examination of the pressure distribution curves for the aerofoils and plate makes it possible to compare the variation of pressure distribution upon (*a*) a flat lower surface coupled both with a flat and a convex upper surface, and (*b*) a convex upper surface coupled both with a flat and a concave lower surface. As a result, it is found that the forces on the upper surfaces of aerofoils are only slightly affected by change of shape in the lower surface. For the lower surface, however, it is found that the percentage change due to variation of the form of the upper surface is considerable; but as these forces are small in magnitude, this change has very little influence upon the total forces. **These results demonstrate that the upper surface of an aerofoil contributes by far the greater part of the total force acting upon the aerofoil, and that the pressure distribution is practically independent of the shape of the lower surface, provided that it is not convex.**

As a corollary, the best form of upper surface can be determined in conjunction with some standard lower surface, say a flat one, and when this has been completed, the lower surface can be varied without appreciably upsetting the results obtained for the upper surface. A detailed investigation upon these lines was carried out by the N.P.L. in order to determine the best form of aerofoil.

The lift and drag of a series of aerofoils were measured, variations in the shape of these aerofoils being made according to the following plan:—

1. Aerofoils with a plane under surface, but with variable camber of upper surface.

2. Aerofoils possessing the same form of upper surface, but with variable camber of lower surface.
3. Aerofoils in which the position of the maximum ordinate was altered.

As the results of these experiments are of considerable practical value in the design of aerofoils for specific purposes, they will be given fully.

Determination of the Lift and Drag of a series of Aerofoils with plane lower surface and variable camber of upper surface.—The variation of camber of these aerofoils was obtained by varying the height of the maximum ordinate—

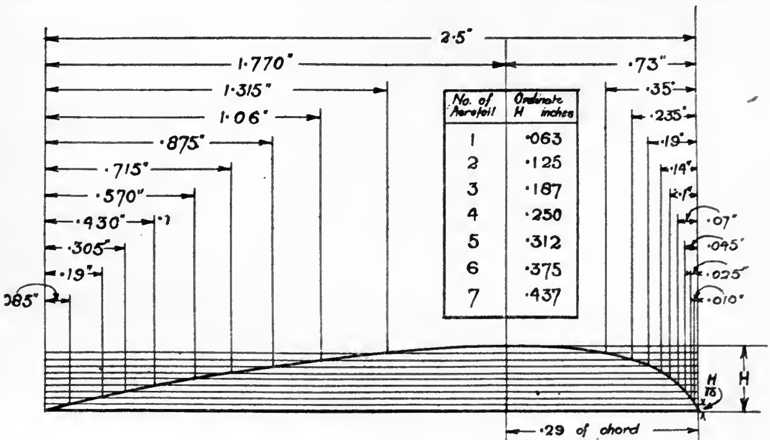

FIG. 51.—Dimensions of Aerofoils of Variable Camber.

kept in the same position at ·29 of the chord from the leading edge—from ·063″ to ·437″. This ordinate is then divided into ten equal parts and abscissæ drawn in the positive and negative direction from each point of division. The lengths of these abscissæ remained constant for the series of aerofoils. The scheme is shown in Fig. 51, and the resulting aerofoils are shown in Figs. 52 and 53. The numbers attached to the aerofoils are in order of the depth of the maximum ordinate. The length of each aerofoil was 15″ and the width was 2·5″. The velocity of the air stream in the wind tunnel during the tests was 20 miles per hour. The result of the observations is shown by Figs. 52 and 53. The aerofoil with the maximum ordinate begins to lift at an angle of $-7°$, the maximum lift being obtained at an angle of 6°. With diminishing camber the angles of no lift and of maximum lift become greater, and the decrease of the lift coefficient after passing the critical angle becomes much less marked. For all the aerofoils the L/D curves show maxima between 3° and 4°, but the actual values of these maxima vary greatly. As the camber changes, the L/D ratio approaches and passes a maximum in the neighbourhood of 15, the corresponding camber being about one in twenty.

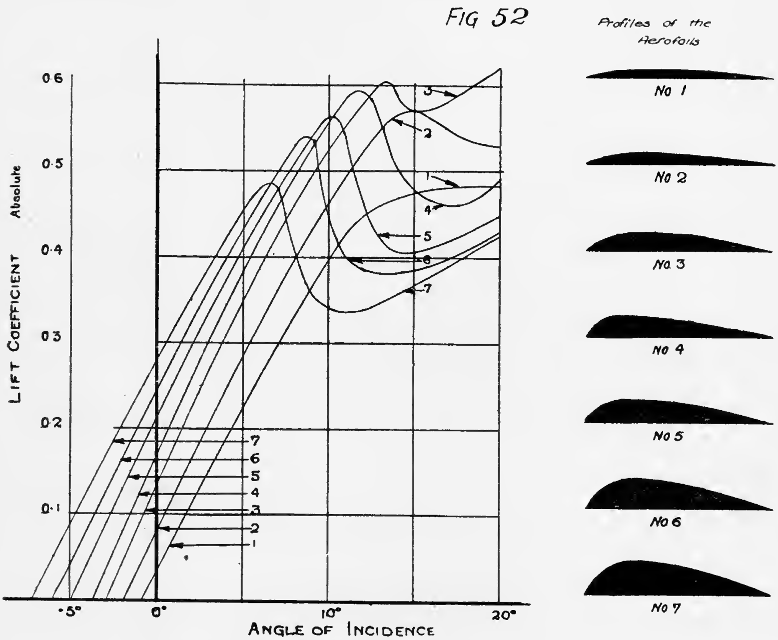

FIG. 52.—Aerofoils with Variable Camber of Upper Surface.

From an aerodynamical point of view, the most important characteristics of an aerofoil are:

(i) The maximum L/D ratio obtainable.

(ii) The value of the lift coefficient at the angle of maximum L/D.

(iii) The ratio of the value of the lift coefficient at the angle of maximum L/D to the value of the lift coefficient at the critical angle.

It will be seen from the curves that the aerofoils having a high maximum value for L/D ratio have a low value for the corresponding lift; but since the ratio of this lift value to the maximum lift coefficient is also low, such aerofoils are suitable for variable speed machines. Table XVII. was prepared to indicate the best camber. It was assumed that the aerofoils had been arranged at such angles of incidence as to give the same lift coefficient at the same speed. The lift coefficient corresponding to usual practice is about 0·25, and for this value the best L/D ratio is 15, and the camber required is ·055. If for constructional purposes it is desired to use a larger camber, column 5 shows the extent to which this may be done without decreasing the L/D ratio by more than 10%.

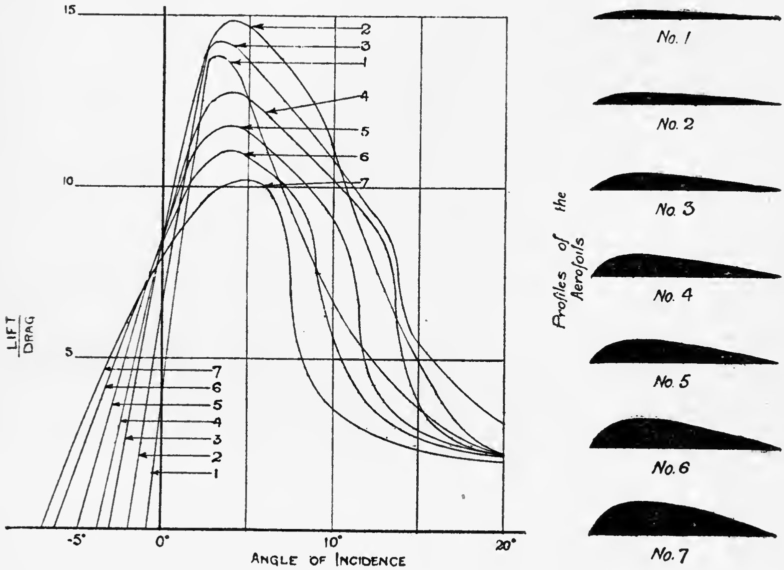

FIG. 53.—Aerofoils with Variable Camber of Upper Surface.

TABLE XVII.—CAMBER.

Lift coefficient absolute.	Camber for maximum L/D.	Corresponding maximum L/D.	Maximum lift.	Camber for L/D – 10% decrease.
·10	very small	—	—	—
·15	less than ·02	—	—	—
·20	·043	15·0	0·5	0·06
·25	·055	15·0	0·57	0·08
·30	·06	14·5	0·59	0·093
·35	·06	14·0	0·59	0·106
·40	·06	13·3	0·59	0·115
·45	·07	12·2	0·60	0·137
·50	·08	11·1	0·60	0·145

Determination of the Lift and Drag of a Series of Aerofoils with the same Upper Surface and Variable Camber of Lower Surface.—The scheme of these aerofoils is shown in Fig. 54, together with the resulting aerofoils. Aerofoil 4 of the previous series (see Figs. 52 and 53) was taken as the basis, and camber given to the lower surface by gradually increasing the height of the maximum ordinate from the chord line according to the dimensions attached to Fig. 54. It was

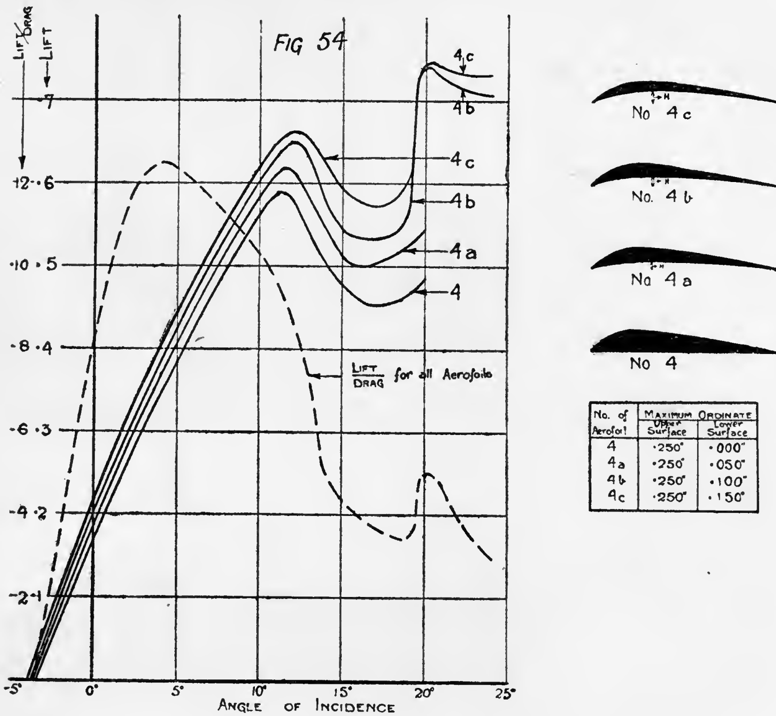

No. of Aerofoil	Maximum Ordinate Upper Surface	Maximum Ordinate Lower Surface
4	·250"	·000"
4a	·250"	·050"
4b	·250"	·100"
4c	·250"	·150"

FIG. 54.—Aerofoils with Variable Camber of Lower Surface.

found that the L/D ratios are practically unaltered by camber of the lower surface. The value of the lift coefficient, as will be seen from Fig. 54, increases steadily with increase of camber; but the variation is small, a maximum increase of 17% being obtained at the angle of maximum L/D. The critical angle is unaltered by increase of camber on the lower surface, and the fall in the lift coefficient after this angle is passed becomes less as the camber is increased.

Determination of the Lift and Drag of a Series of Aerofoils, the Position of the Maximum Ordinate being varied.—The sections were all developed from one chosen

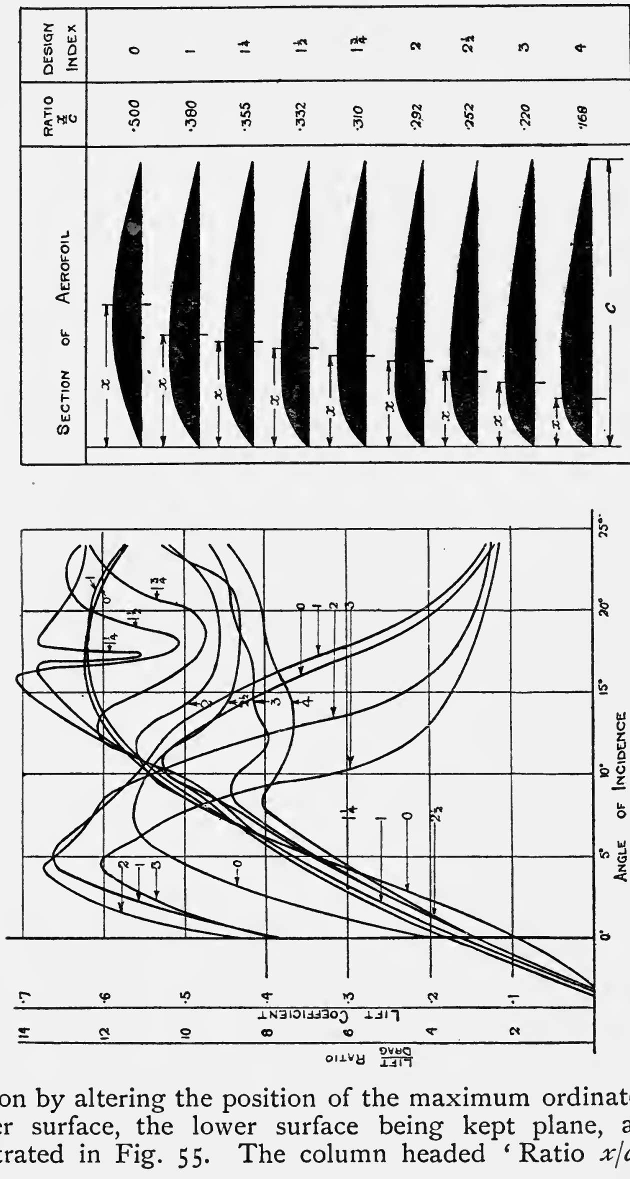

Fig. 55.—Aerofoils with Variable Position of Maximum Ordinate.

section by altering the position of the maximum ordinate of the upper surface, the lower surface being kept plane, and are illustrated in Fig. 55. The column headed 'Ratio x/c' gives the position of the maximum ordinate, and the column headed 'Design index' gives the value of the index 'a' in the expression $x = \frac{1}{2} c\,(0{\cdot}76)^a$. The original series contained only members whose design indices were 0, 1, 2, 3, 4, and the other members were introduced as occasion required in order to preserve continuity in the observations. The cuıves obtained from the observations on the nine aerofoils are also shown in Fig. 55. The most important deduction from the experiments is that for the particular camber adopted (0·100), the greatest maximum $\frac{K_y}{K_x}$ occurs when the position of the maximum ordinate is at about one-third of the chord from the leading edge. The main variations in the lift curves occur at angles above 10°. Below this angle the curves are of the same general character, although they differ widely at higher angles, and in certain cases are greatly changed by minute changes of the form of the section. It will be seen that for aerofoils 0 and 1 there is no defined critical angle, the lift following a continuous smooth curve having a flat maximum between 16° and 18°. In the next aerofoil, design index $1\frac{1}{4}$, a region corresponding probably to uncertain flow is observed between 17° and 18°, the lift coefficient oscillating between 0·67 and 0·54. The next aerofoil, design index $1\frac{1}{2}$, shows this effect more strongly marked; while succeeding aerofoils show this peculiar dip in the lift curves becoming steadily wider and shallower. The wind velocity for these experiments was 28 feet per second. With an increased velocity this dip was practically eliminated.

It is interesting to note that all the more complicated changes in the value of the lift coefficient occur with the aerofoils whose indices are between 1 and 2; that is, they correspond to a movement in the position of the maximum ordinate of ·012 of the chord, and that the form of the curve is very sensitive to minute changes of the section. The sudden change in the lift coefficient at the critical angle is always accompanied by a change in the drag, an increase in lift being associated with decrease of drag and *vice versâ*. This indicates that the change is due to a sudden alteration in the flow from an efficient to an inefficient type.

The ratio of $\frac{K_y}{K_x}$ increases as the maximum ordinate moves from the centre of the chord, until its position reaches a point about one-third of the chord from the leading edge. It would seem preferable, however, to avoid the uncertainty of flow above described and to use an aerofoil having its maximum ordinate at about ·375 of the chord from the leading edge. This results in a reduction of the maximum $\frac{K_y}{K_x}$, for this particular type of aerofoil, from 13·9 to 13·2.

Effect of thickening the Leading Edge of an Aerofoil.—These experiments were devised in order to show the way in which the behaviour of an ordinary aerofoil is influenced by substituting a thickened for a sharp leading edge. The sections

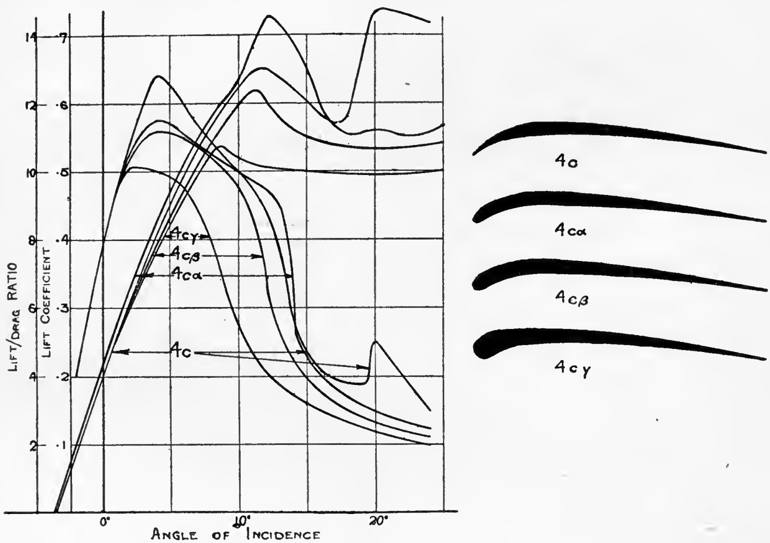

Fig. 56.—Aerofoils of Variable Thickness of Leading Edge.

of the aerofoils are shown in Fig. 56. All the aerofoils are identical behind the maximum ordinate, and the camber and chord remain unchanged throughout the series. The results of the observations are shown plotted in Fig. 56, from which it will be seen that the maximum L/D decreases steadily as the thickness of the nose increases, showing that the efficiency of an aerofoil section is impaired by thickening the leading edge. The lift is not greatly affected below angles of 8°, but above this angle the form of the curve is sensitive to the increasing thickness of the nose. The final effect on the lift is to cause the critical angle to occur much earlier and to flatten out the lift curve after this angle is reached.

Effect of thickening the Trailing Edge of an Aerofoil.—These experiments were undertaken in order to determine the extent to which an aerofoil can be thickened in the neighbourhood of the rear spar without materially affecting its aerodynamical properties, such extra thickness being very desirable in this region from a constructional point of view. The sections of the aerofoils used are shown in Fig. 57, No. 3 of the series being the same as the R.A.F. 6 aerofoil illustrated in Fig. 40. The observations are shown plotted in Fig. 57, from which it

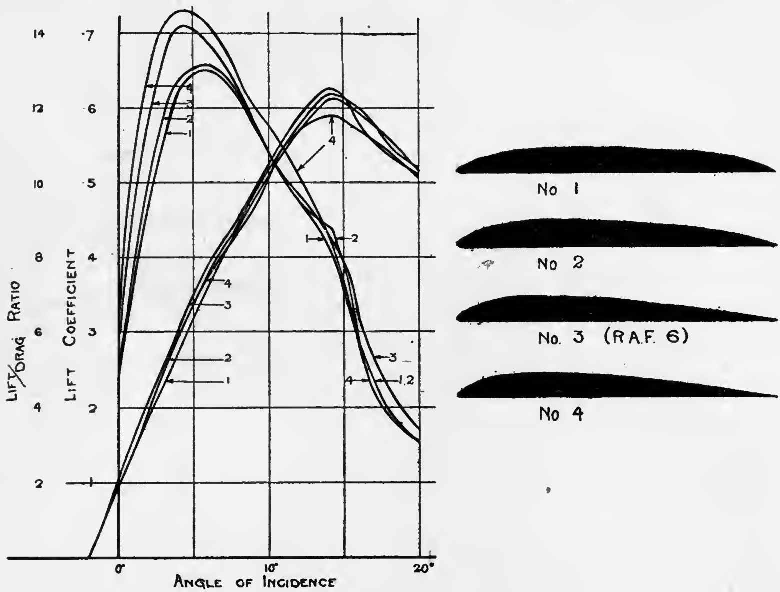

FIG. 57.—Aerofoils with Variable Thickness of Rear Portion.

appears that the lift coefficient is not much affected at angles greater than 7°, while the L/D curves show a steady improvement as the thickness diminishes.

Centre of Pressure.—The position of the centre of pressure (C.P.) of an aerofoil is defined as the point at which the line of resultant force over the aerofoil section cuts the chord. Since the pressure distribution, and hence the total force over the aerofoil, varies with the angle of incidence in the manner already described and illustrated in Fig. 47, it follows that the C.P. will also vary in its position along the chord-line. It has been seen that with increasing angle of incidence up to the critical angle, the pressure over the front portion of the aerofoil is greater than that over the rear portion, and as a result the C.P. moves forward. The importance of this fact from the practical point of view must be clearly realised, because the C.P. of a wing section may be regarded as the point at which the resultant lift of the supporting surfaces acts. The position of the centre of gravity (C.G.) of the machine, however, remains unaltered, hence, although for one particular angle of incidence the line of resultant lift can be arranged to pass through the C.G., for all

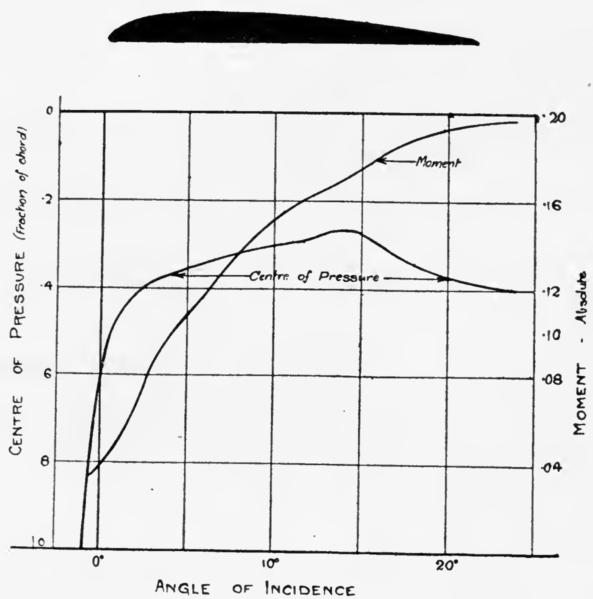

Fig. 58.—Travel of the Centre of Pressure.

other angles there will be a Lift/Weight couple introduced. Increasing divergence from the position of coincidence of the C.P. with the C.G. will tend to make this couple greater, and consequently the system will become unstable. The function of the tail plane is to provide the necessary righting moment, in order that the machine may be capable of steady flight over the required range of angle of incidence. A knowledge of the variation of the position of the C.P. is therefore essential for a correct setting of the tail in order to obtain stability. It is interesting to recall in this connection that Lilienthal, in his glider experiments, obtained stability by moving his body over the lower plane, thus countering the travel of the C.P. by a corresponding movement of the C.G. This travel of the C.P. has also an important bearing upon the design of the wing structure, for it gives rise to a variation in the stresses of the front and rear spar bracing systems as the angle of incidence increases. It is therefore necessary to stress the wing structure for the most extreme cases that occur over the range of flying angles, namely,

(*a*) The most forward position of the C.P.
(*b*) The most backward position of the C.P.

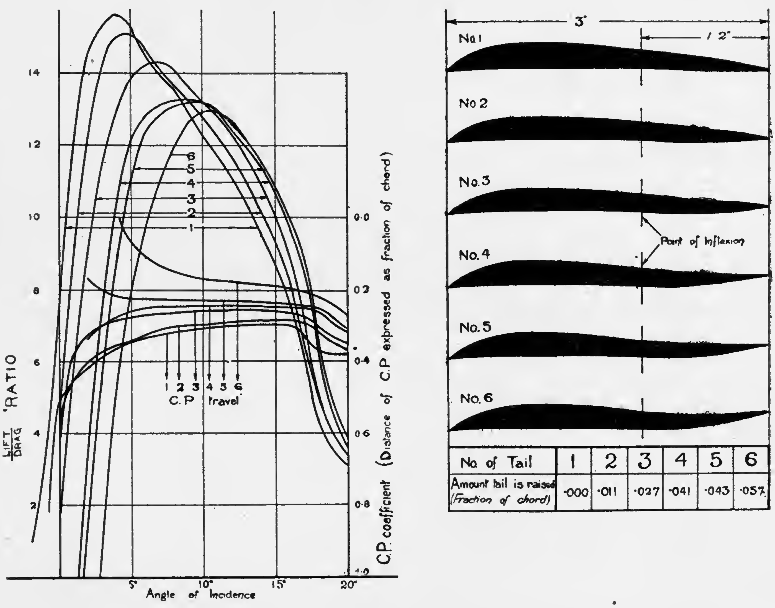

No. of Tail	1	2	3	4	5	6
Amount tail is raised (Fraction of chord)	·000	·011	·027	·041	·043	·057

FIG. 59.—Aerofoils with Variable Reflexure of Trailing Edge.

The position of the C.P. is determined experimentally by measuring the lift, drag, and the moment about the leading edge of the aerofoil under consideration for various angles of incidence. A knowledge of the magnitude of the lift and drag enables the direction of the resultant force to be obtained for each position, and the moment of this resultant force being known, it is a simple matter to calculate the leverage of the moment. This fixes the position of the line of resultant force, and consequently the position of the centre of pressure. The moment and C.P. curves for the R.A.F. 6 aerofoil are shown in

Fig. 58. The curves of lift and drag for this aerofoil were given in Fig. 40.

Reflexed Curvature towards the Trailing Edge.—This research was undertaken principally with a view to determining the extent to which a reflex curvature towards the trailing edge of an aerofoil would tend to neutralise the rapid movement of the C.P. due to the change of the angle of incidence. The sections of the aerofoils used are shown in Fig. 59, No. 1 of the series being in the form of the R.A.F. 6. The point in the sections at which reflexing was commenced was at 0·4 of the chord from the trailing edge. The same brass aerofoil was used for all the sections, the form being altered behind the point of reflexure by means of moulded wax. The curves for L/D and travel of the centre of pressure are shown in Fig. 59, from which it will be seen that a practically stationary C.P. can be obtained with an aerofoil of this type by elevating the trailing edge by about 0·042 of the chord, while the point of reflexure may be at any point between 0·2 and 0·4 of the chord from the trailing edge. This effect, however, is only obtained at the sacrifice of about 12% of the maximum L/D, and about 25% of the maximum lift. The elevation of the trailing edge, the rate of movement of the C.P., and the loss in the maximum value of the L/D ratio, are connected by approximate linear laws.

Interference of Aerofoils.—Mention has already been made of the superior efficiency of the monoplane from an aerodynamical standpoint, due to the absence of interference effects as compared with the multiplane. There are three variables to investigate when dealing with this question, namely, gap, decalage, stagger.

We have seen in Fig. 44 how the direction of flow of the air stream is affected when quite a considerable distance away from the leading edge of an aerofoil. It therefore follows that the placing of bodies or other aerofoils in close proximity to the first aerofoil will greatly affect the pressure distribution. When aerofoils are placed above one another, as in the biplane and triplane, interference and modification of the air forces at once results.

Gap.—The distance between the superimposed surfaces is known as the gap, and the ratio of gap/chord is used as a measure thereof. The negative pressure or suction upon the upper surface of an aerofoil has been found to be very much greater than the positive pressure upon the under surface (see Fig. 47), and consequently we should expect to find that the effect of placing one aerofoil over another is to reduce the lift and efficiency of the lower plane, and to leave the upper plane practically unaffected. This follows upon the consideration that the positive pressure on the under surface of the upper aerofoil, and the negative pressure on the top surface of the lower aerofoil, will tend to neutralise each other, whereas the negative pressure on the top surface of the upper aerofoil, and the positive pressure on the bottom surface of the lower aerofoil, will remain practically unaltered. The negative pressure or suction being so much more important, it follows that the upper aerofoil must be much less affected. This reasoning is borne out by the experimental investigations which have shown that practically the entire loss due to superposition is to be found in the reduction of the lift and L/D ratio of the lower plane. Further, it may be deduced from this that wing-flaps are very much more effective when placed on the upper plane than they would be if on the lower; also that in a combination of a high-camber upper plane, with a much flatter lower plane, the interference effects would be greatly reduced. Table XVIII. gives the biplane reduction factors for an average aerofoil, and is taken from an N.P.L. report.

TABLE XVIII.—REDUCTION COEFFICIENTS DUE TO BIPLANE EFFECT.

Gap/Chord.	Lift. 6°	Lift. 8°	Lift. 10°	L/D. 6°	L/D. 8°	L/D. 10°
0·4	0·61	0·63	0·62	0·75	0·81	0·84
0·8	0·76	0·77	0·78	0·79	0·82	0·86
1·0	0·81	0·82	0·82	0·81	0·84	0·87
1·2	0·86	0·86	0·87	0·85	0·85	0·88
1·6	0·89	0·89	0·90	0·88	0·89	0·91

To obtain values for a biplane, multiply values for a single aerofoil by the factors given. Note that there is quite a considerable effect when the Gap is equal to the Chord.

A more recent investigation carried out in the Massachusetts Institute of Technology* enables a comparison to be made between the lift and L/D coefficients and interference effects on the biplane and triplane. The biplane and triplane models had a constant gap between the planes equal to 1·2 times the chord length, and there was no stagger or overhang. A single aerofoil was first tested as a standard for reference, and then the additional surfaces were introduced. The lift, and drag, and L/D curves for each case are show in Fig. 60.

* Hunsaker and Huff. Reproduced by permission of Messrs. J. Selwyn & Co.

From comparison between the curves it will be seen that the triplane and biplane give nearly the same maximum lift at

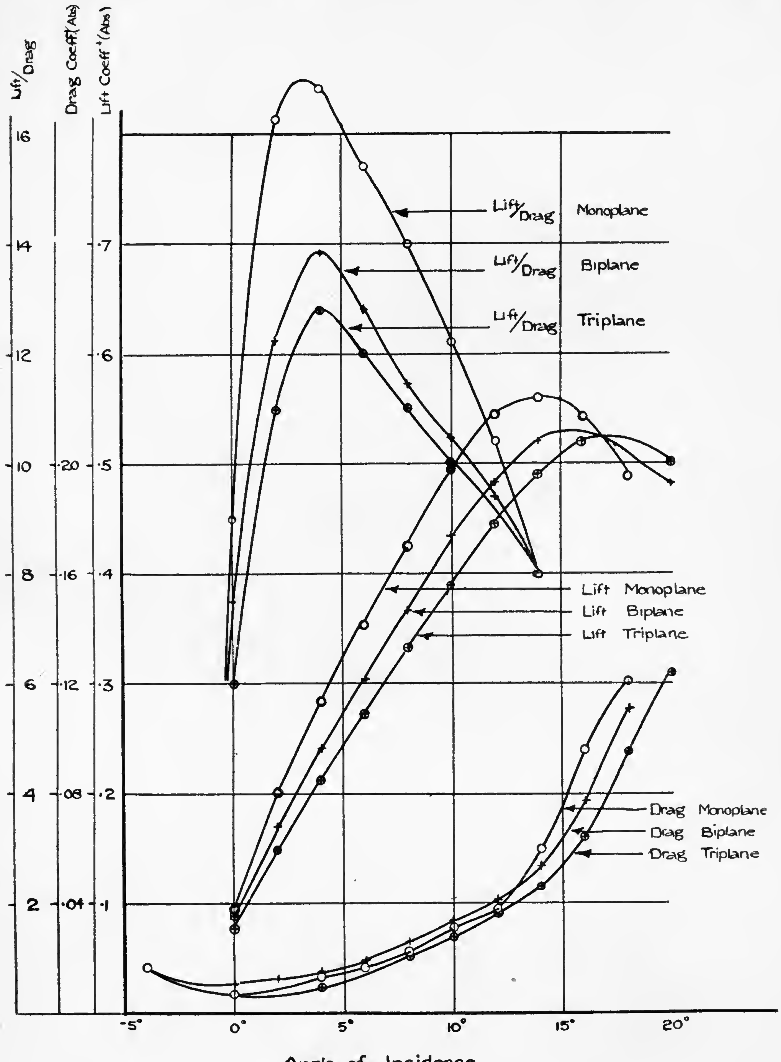

FIG. 60.—Aerodynamical Properties of Superimposed Aerofoils.

about 16°, but that for smaller angles of incidence the triplane lift is appreciably reduced. The lift coefficient for the monoplane is seen to be superior to the other cases at all angles above zero. The drag coefficient for angles below 12° is very similar in each case, but at large angles of incidence the triplane has a materially lower resistance. The curves of L/D show the relative effectiveness of the wings. Thus, the best ratio is 17 for the monoplane, 13·8 for the biplane, and 12·8 for the triplane. These values refer to small angles of attack, and therefore correspond to a high flight speed. Table XIX. illustrates these points clearly, the biplane and triplane lift coefficients being expressed as percentages of the monoplane coefficients.

TABLE XIX.—COMPARISON OF LIFT COEFFICIENTS.

Incidence.	Monoplane. Lift	Biplane. Lift %	Triplane. Lift %	Monoplane. L/D	Biplane. L/D %	Triplane. L/D %
0°	·096	88·8	83·0	8·6	73·2	70·8
2°	·202	83·8	75·4	16·8	74·7	69·8
4°	·284	85·4	75·7	16·8	82·0	76·1
8°	·427	85·2	77·4	13·8	81·9	80·4
12°	·545	87·6	81·2	10·0	95·0	89·0
16°	·543	98·5	96·4	4·5	124·0	145·0

Experiments were next undertaken to determine the distribution of load upon the three wings of the triplane made from aerofoils of R.A.F. 6 profile. The results are shown in Figs. 61 and 62. It appears that the upper wing is by far the most effective of the three, and that the middle wing is the least effective. This must be due to the interference with the free flow of air owing to the presence of the upper and lower wings. The results are conveniently tabulated as shown in Table XX. :—

TABLE XX.—COMPARISON OF THE WINGS OF A TRIPLANE.

Incidence.	Lift. Upper.	Lift. Middle.	Lift. Lower.	L/D. Upper.	L/D. Middle.	L/D. Lower.
0°	2·68	1·0	1·82	3·63	1·0	2·30
2°	2·14	1·0	1·75	3·18	1·0	2·13
4°	1·91	1·0	1·64	2·59	1·0	1·69
8°	1·56	1·0	1·36	1·49	1·0	1·37
12°	1·56	1·0	1·31	1·30	1·0	1·34
16°	1·49	1·0	1·20	1·22	1·0	1·17

It will be noticed that the middle wing has been taken as a standard of comparison, its lift and L/D being denoted by unity.

A further important instance of interference is to be found in the case of the tail plane. The air stream is deflected from the main wing planes of a machine and takes a downward

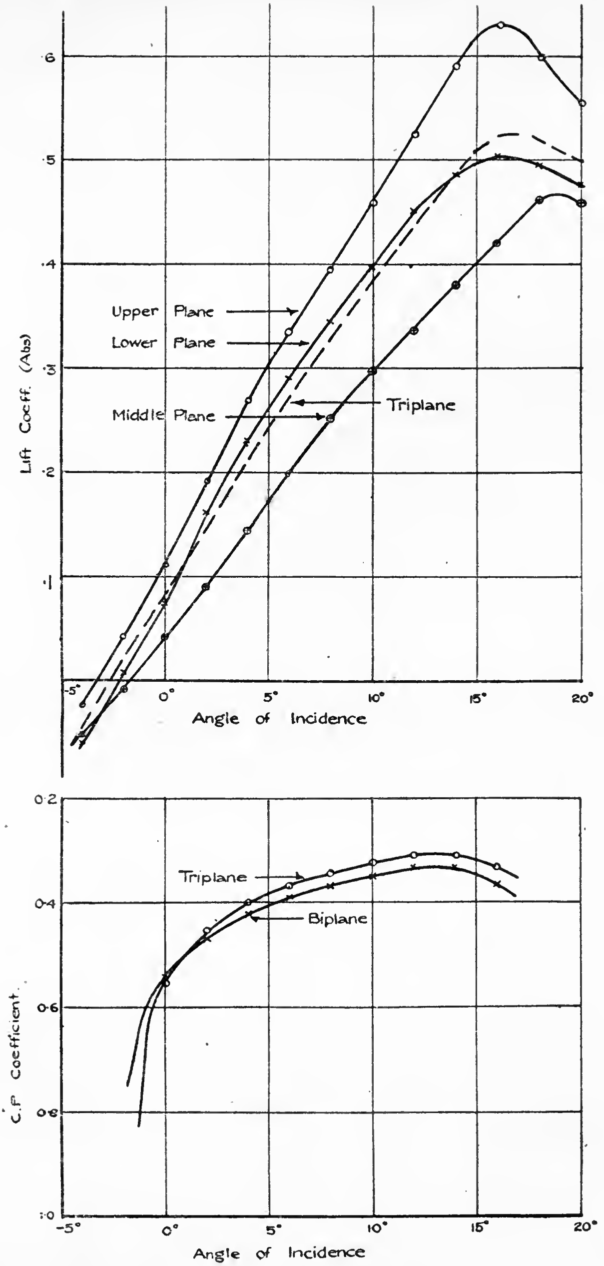

FIG. 61.—Lift and C.P. Coefficients for Superimposed Aerofoils.

course. Consequently the angle of attack of the surfaces behind the main planes must be reckoned with regard to the actual direction of this deflected air stream. The tail plane

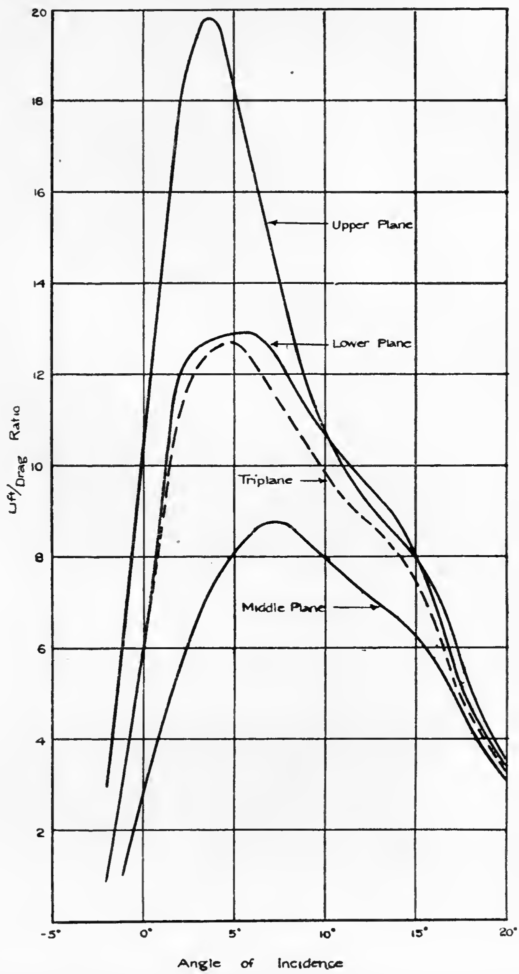

FIG. 62.—Lift/Drag Ratio for Superimposed Aerofoils.

operates directly in the downwash of the wings, and this effect must be carefully considered when the setting of the tail plane is being determined. Investigations made by Eiffel and the N.P.L. upon this problem show that the downward direction of the air stream persists for some distance behind the planes, and later experiments have shown that the angle of downwash is half the angle of incidence of the main planes measured from the angle of no lift.

Decalage.—The term decalage is used to define the difference in the angle of incidence between two aerofoils of the same machine. For example, the upper plane of a biplane may be set at a different angle to the lower plane; or the upper and lower planes of a triplane may be set at different angles to the middle plane; and, again, the setting of the tail plane may be different from the inclination of the main planes. Decalage is illustrated in Fig. 63.

It has been found experimentally that the effect of setting

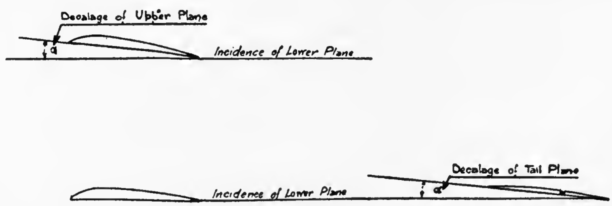

FIG. 63.—Decalage.

the upper surface of a staggered biplane at about 2° less incidence than the lower surface results in a pronounced increase in the lift, and a small increase in the L/D ratio over any other arrangement. Such a result, however, is modified when different wing sections are used; and there is room for considerable investigation into the problem of best wing combination, considering gap, stagger, decalage and interference effects. Decalage has the further advantage of reducing the instability of the C.P. curve, and even of stabilising the C.P. travel, if the angle between the surfaces is sufficiently great. Unfortunately this results in a loss in the aerodynamic efficiency of the system.

Stagger.—When the upper plane is set ahead of or behind the lower plane in the biplane or triplane arrangement the planes are said to be staggered, the amount of stagger being the horizontal distance between a vertical dropped from the leading edge of the upper plane and the leading edge of the lower plane or planes. Positive and negative stagger is illustrated in Fig. 64. In certain machines stagger has been adopted in order to give increased visibility, but the constructional difficulties are naturally greater than in the no-stagger arrangement. Positive stagger leads to a slightly increased efficiency over the no-stagger position, but this increase only becomes apparent when the stagger is about half the chord. Under these con-

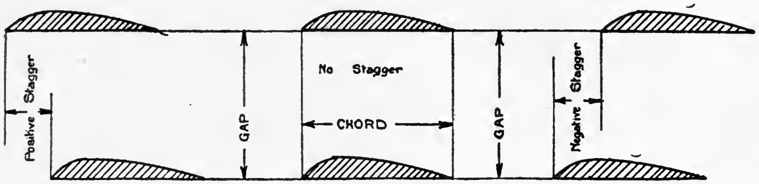

Fig. 64.—Stagger.

ditions there is a gain in the lift and the L/D of about 5%. Negative stagger, so far as present investigations go, would appear to be approximately of the same efficiency as the no-stagger arrangement.

From the designer's standpoint, the question of stagger must be treated in conjunction with the amount of gap desirable,

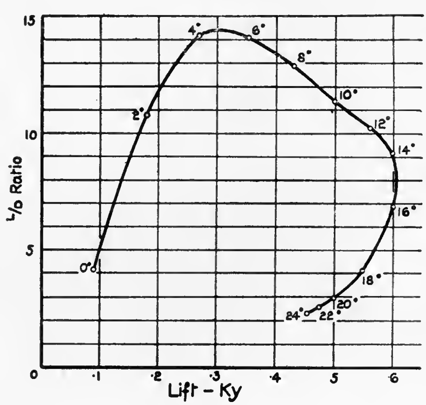

Fig. 65.

since stagger can be used to advantage when the gap is small in order to counteract the loss in aerodynamical efficiency due to interference.

The Choice of an Aerofoil.—Before concluding this chapter a short space can profitably be devoted to a brief outline of one or two simple methods of selecting an aerofoil which will be suitable for a wing section for various specific purposes. Curves of lift, drag, and L/D, and travel of the C.P., for some of the most successful aerofoils yet evolved, will be given at the end of this chapter; and a careful examination of these curves, together with the following matter, will enable the choice of the most suitable aerofoil for certain definite conditions to be made.

Having drawn the curves of lift and L/D ratio for an aerofoil as shown in Fig. 40, a further curve can be constructed by eliminating the angle of incidence. This is shown in Fig. 65. For the purposes of preliminary design work and for comparison this method of graphing wind-tunnel results is much more convenient than that shown in Fig. 40, as the angle of incidence is not of importance until the question of the actual position of the wing arises. The method of obtaining such curves is obvious from the figure, the corresponding value of the lift, and the L/D being taken at each angle of incidence.

A further method of plotting results useful for preliminary design work is obtained by remembering that the landing speed of a machine depends upon the maximum lift coefficient of the section used. Thus, if V be the landing speed and K the maximum lift coefficient,

$$W = K\rho A V^2/g$$

Also for any speed of horizontal flight V′

$$W = K'\rho A V'^2/g$$

where K′ is the lift coefficient at the corresponding angle of incidence. Hence, equating these two expressions we have

$$K V^2 = K' V'^2$$

$$\text{or} \quad V' = V\left(\frac{K}{K'}\right)^{\frac{1}{2}} \quad \ldots\ldots\ldots\ldots \text{ Formula 16}$$

By means of Formula 16 the speed at various angles of incidence can be determined if the corresponding values of the lift coefficients are known. For example, if we take the R.A.F. 6 aerofoil, we see from Fig. 65 that the maximum lift coefficient is ·6 approx., so that if a landing speed of 45 m.p.h. is desired, we have from Formula 16

$$V' = 45\left(\frac{\cdot 6}{K'}\right)^{\frac{1}{2}}$$

so that by substitution of K′ (the lift coefficient at any other angle of incidence), the speed at that angle can be obtained.

Formula 16 can also be put into the form

$$\frac{V}{V'} = \left(\frac{K'}{K}\right)^{\frac{1}{2}}$$

that is, the ratio of the landing speed to any other speed may be expressed in terms of the lift coefficients of the aerofoil section. Combining this ratio with the L/D ratio for the aerofoil, a further graph can be obtained as shown in Fig. 66, the calculations for which are arranged in tabular form below.

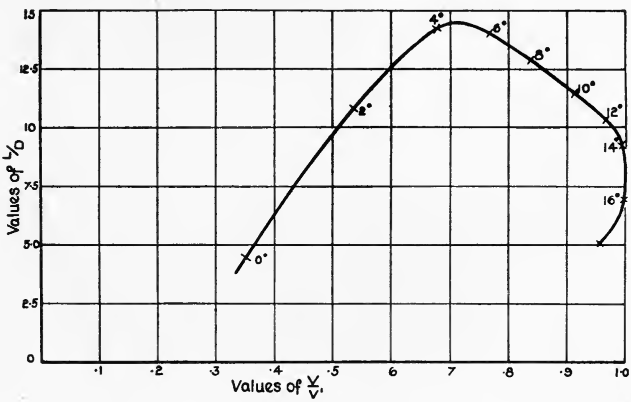

Fig. 66.

Table XXI.—Calculations of V/V′.

θ	0°	2°	4°	6°	8°	10°	12°	14°	16°	18°
K′	0·74	·173	·275	·354	·423	·496	·564	·593	·600	·55
$(V')^2$	16400	7030	4420	3440	2880	2450	2160	2050	2020	2210
V′	128	84	66·5	58·7	53·7	49·5	46·5	45·3	45	47
$\frac{V}{V'}$	·35	·535	·677	·767	·839	·91	·968	·994	1	·96
$\frac{L}{D}$	4·5	10·9	14·3	14·1	12·9	11·4	10·4	9·3	6·9	4·1

From this curve the most efficient speed and the value of the L/D ratio for the wings at the maximum flight speed required can at once be determined. For example, since the maximum L/D gives the value of V/V′ as ·72, the most efficient flying speed so far as the wings are concerned = 45/·72 = 62·5 m.p.h. Also if a maximum speed of 100 m.p.h. is required, the value of V/V′ is then = 45/100 = ·45, and for this value the curve shows that the L/D ratio is only just over 8, so that this section is not suitable for a high-speed machine.

The L/D ratio for the complete machine can only be determined when the drag of the body has been added to that of the wings, but the curve shown in Fig. 66 will indicate at a very early stage in the design whether the wing section chosen is suitable for the desired purpose. It is very convenient for design purposes to graph a large number of tests upon sections in this manner and to file them for future reference, indicating upon each graph the name of the section and the source from which the figures were obtained. All the curves should be drawn to the same scale upon good quality tracing linen, so that one curve can be readily compared with another for minute differences by superposition.

The curve in Fig. 66 also shows that a machine can only fly horizontally at a high speed if the angle of incidence of the wings is much smaller than that for which the L/D ratio is a maximum. From what has already been said, it follows that for a machine to have a large range of flying speeds the wings must possess the following characteristics :—

1. A large value for the maximum lift coefficient.
2. For small angles of incidence the value of the lift coefficient may be small, but the corresponding value of the L/D ratio must be large.
3. The section should have a large value of the maximum L/D, and the ratio of the maximum lift coefficient to the lift coefficient at the maximum L/D must be large.

Practical considerations necessitate that the movement of the centre of pressure over the range of flying angles should be small in order to obtain longitudinal stability, and from a constructional point of view the depth of the aerofoil section must be such that an economical spar section can be adopted.

Units.—The units which are used in the published results of aerodynamic research work in Great Britain are known as absolute units, or absolute coefficients. From Formulæ 13 and 14 we have

$$\text{Lift} = K_y \frac{\rho}{g} A V^2$$

whence K_y = Absolute lift coefficient

$$= \frac{\text{Lift}}{\frac{\rho}{g} A V^2} \quad \text{............ Formula 13 } (a)$$

and $\text{Drag} = K_x \frac{\rho}{g} A V^2$

whence $K_x = $ Absolute drag coefficient

$$= \frac{\text{Drag}}{\frac{\rho}{g} A V^2} \qquad \text{........... Formula 14 }(a)$$

Similarly the moment of an aerofoil

$$= M_c \frac{\rho}{g} A V^2 b \qquad \text{........... Formula 17}$$

where M_c represents the absolute moment coefficient and b represents the breadth of the wing chord.

It is desirable that all measurements should be made in terms of the same units, whether the C.G.S. or the F.P.S. system is employed. For example, in the C.G.S. system, metres, metres per second, kilograms, square metres, etc., should be used; and in the F.P.S. system, feet, feet per second, lbs., square feet, etc., should be used.

In order to obtain actual values from the absolute coefficients, the absolute values, which are of course independent of any system of units, must be multiplied by the remainder of the expression shown in Formulæ 13, 14, 17 expressed in appropriate units.

The value of $\frac{\rho}{g}$ in F.P.S. units for air at sea-level at a temperature of 15° C., and at normal pressure, is ·00237, while in the C.G.S. system under the same conditions it is ·125. Consequently in the F.P.S. system, if we wish to convert absolute values of the lift coefficient to actual values, we have

absolute value × ·00237 × area in sq. ft. × square of velocity in feet per second

while in the C.G.S. system we have

absolute value × ·125 × area in sq. ms. × square of velocity in ms. per second

The Law of Similitude.—Since the lift, drag, and L/D coefficients of an aerofoil vary with the speed, as shown by Fig. 39, it is not possible to pass directly from model tests to full-size machines. Lord Rayleigh called attention to this fact, and pointed out that the most general relationship between the quantities connected with aerodynamics could be expressed in the form

$$F = \frac{\rho}{g} V^2 L^2 \int \frac{V L}{\nu} \qquad \text{........... Formula 18}$$

where ν represents the kinematic viscosity of the air. For the condition of dynamic similarity to be satisfied $\frac{V\,L}{\nu}$ must be the same for the model test and the full-scale machine. With a four-foot wind tunnel the scale of the models tested is generally about one-twelfth. Consequently, since the kinematic viscosity may be regarded as constant for the two cases, it would be necessary, in order to preserve dynamic similarity, to test the models at a speed of 1000 m.p.h. This is obviously impossible, and it has therefore been suggested that a correction factor, known as the V L correction, should be applied to the results of model tests before they are applied to full-scale machines. The N.P.L. and others have investigated this question, but the results so far obtained are not conclusive. Although increase of L/D ratio was obtained with increase of speed, as shown in Fig. 39, this increase was not maintained, and a maximum value would appear to be reached with increase of speed. The latest work on the subject seems to suggest a motion in which the resistance decreases with an increase of viscosity, and Mr. Bairstow suggests that an increase of viscosity may render this possible by making a different type of motion stable, and so reducing the turbulence of flow.

Considering all the available data upon this point, it is apparent that it is at least on the safe side to test a model in the wind tunnel at a speed of from twenty to thirty miles per hour (30 to 44 feet per second), and then to apply the results so obtained without correction to full-scale design. This subject is essentially one upon which the designer must keep an open mind and modify his views as shown to be necessary by the results of the latest published researches into this subject, and by the results of his own applications of model figures to full-scale design. In this connection the findings of a special committee appointed to consider this matter are of interest. They are:

1. For the purpose of biplane design model aerofoils must be tested as biplanes, and for monoplane design as monoplanes. The more closely the model wing tested represents that used on the full-scale machine, the more reliable will the results be.
2. Due allowance must be made for scale effect on parts where it is known. In the case of struts, wires, etc., the scale effect is known to be large, but these parts can be tested under conditions corresponding with those which obtain on the full-scale machine.

3. The resistances of the various parts taken separately may be added together to give the resistance of the complete aeroplane with good accuracy, provided the parts which consist of a number of separate small pieces (*e.g.*, the under-carriage) are tested as a complete unit.
4. Model tests form an important and valuable guide in aeroplane design. When employed for the determination of absolute values of resistance, they must be used with discrimination and a full realisation of the modifications which may arise owing to interference and scale effect.

Wing Sections.—The dimensions and aerodynamic characteristics of some highly successful wing sections are shown in Figs. 67–76. All of these sections have been tested in actual aeroplanes and have proved themselves efficient in flight. They can therefore be confidently recommended for design purposes, the section for any particular machine being selected as explained in this chapter.

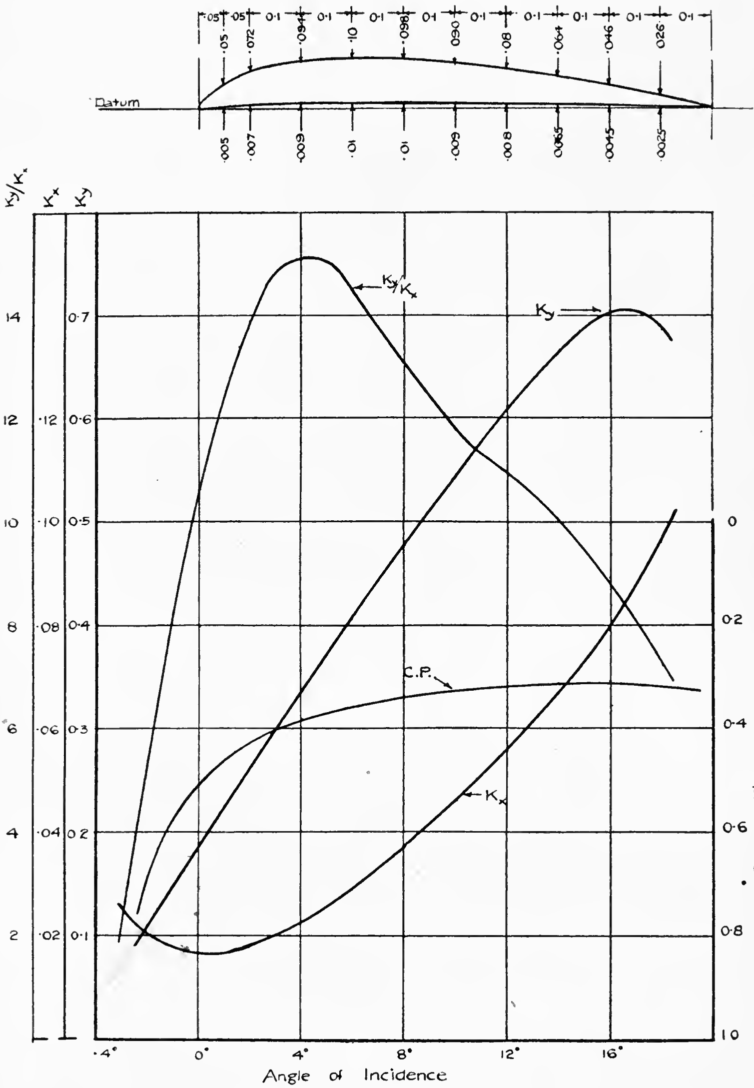

FIG. 67.—Wing Section No. 1.

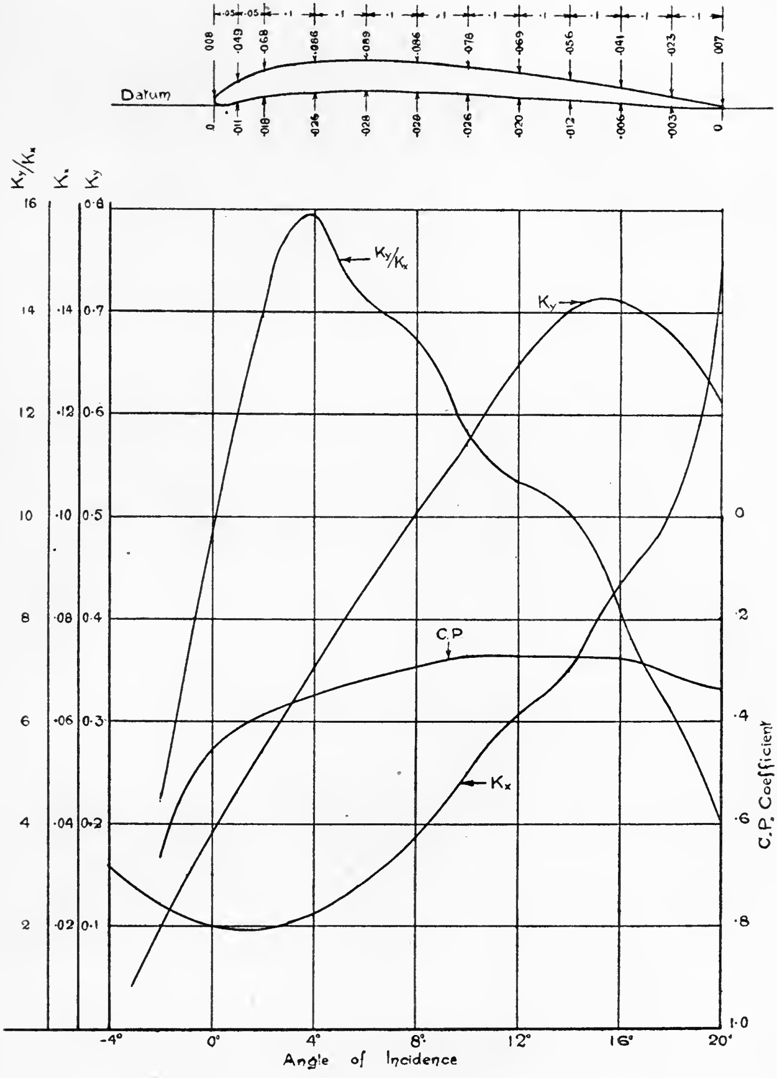

Fig. 68.—Wing Section No. 2.

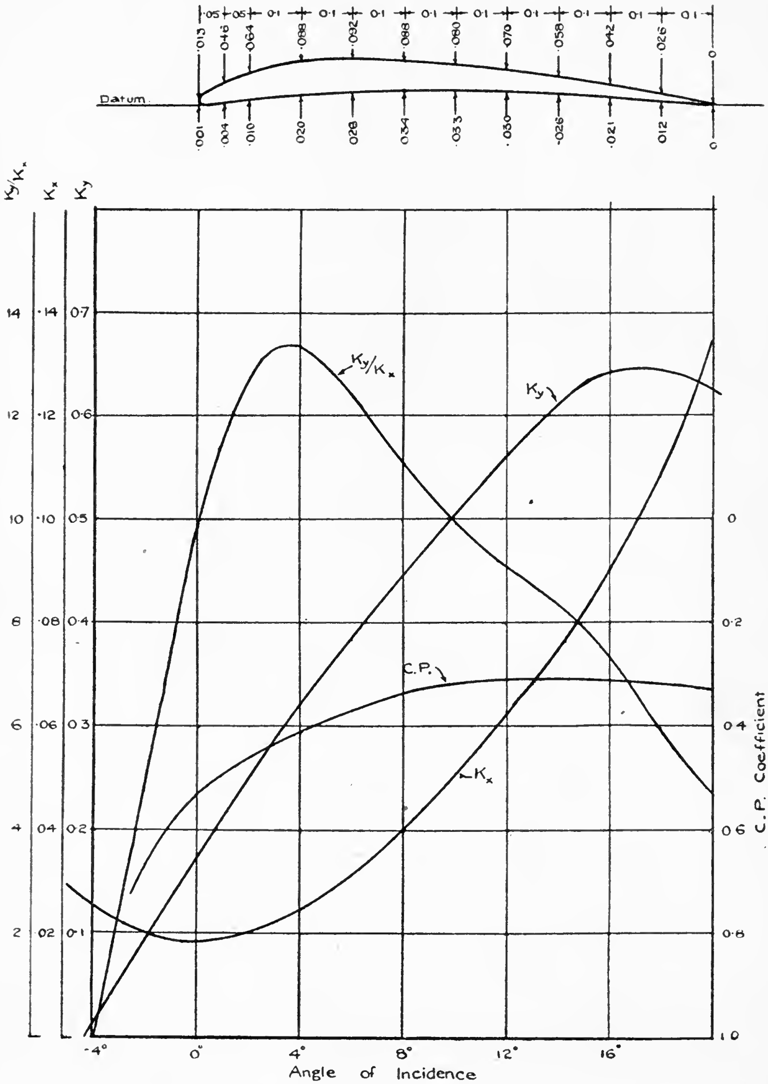

FIG. 69.—Wing Section No. 3.

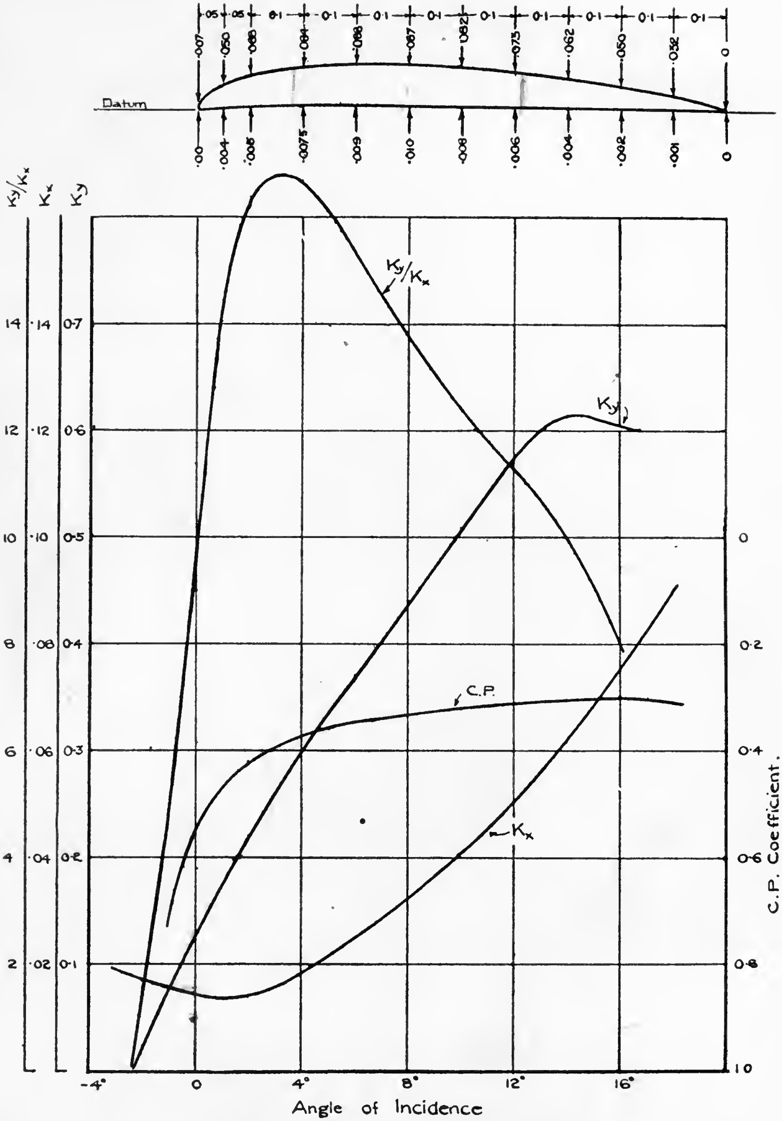

FIG. 70.—Wing Section No. 4.

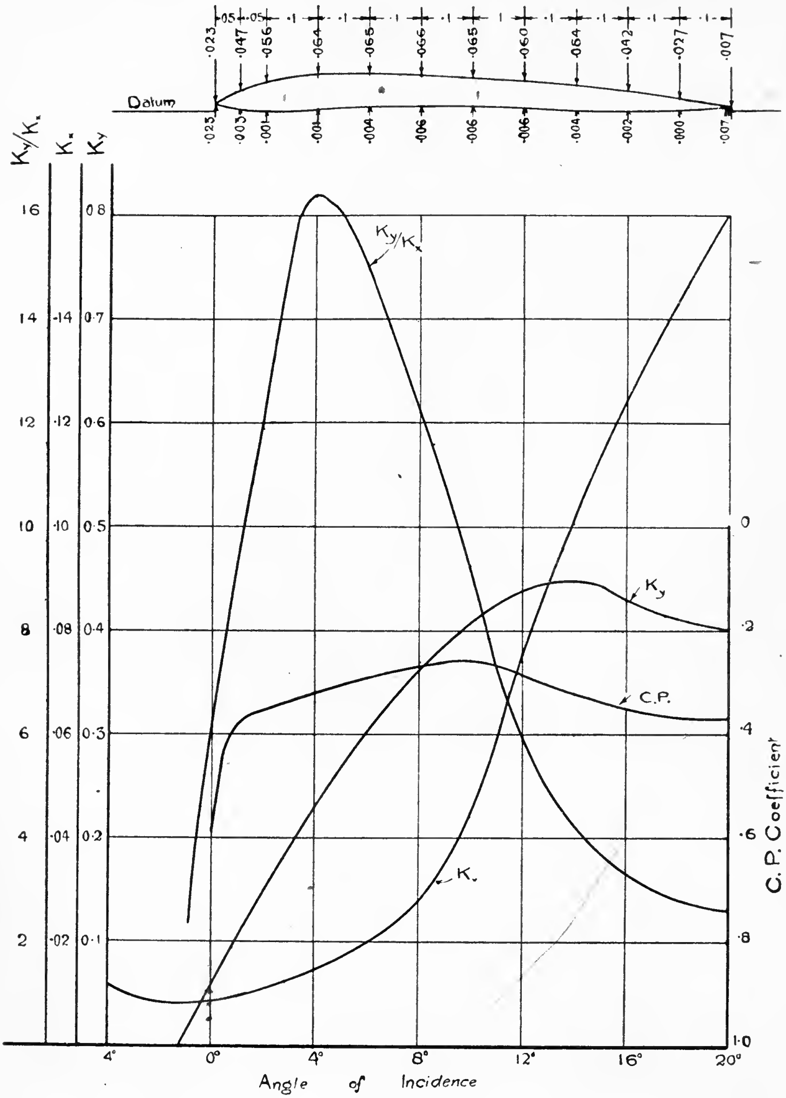

FIG. 71.—Wing Section No. 5.

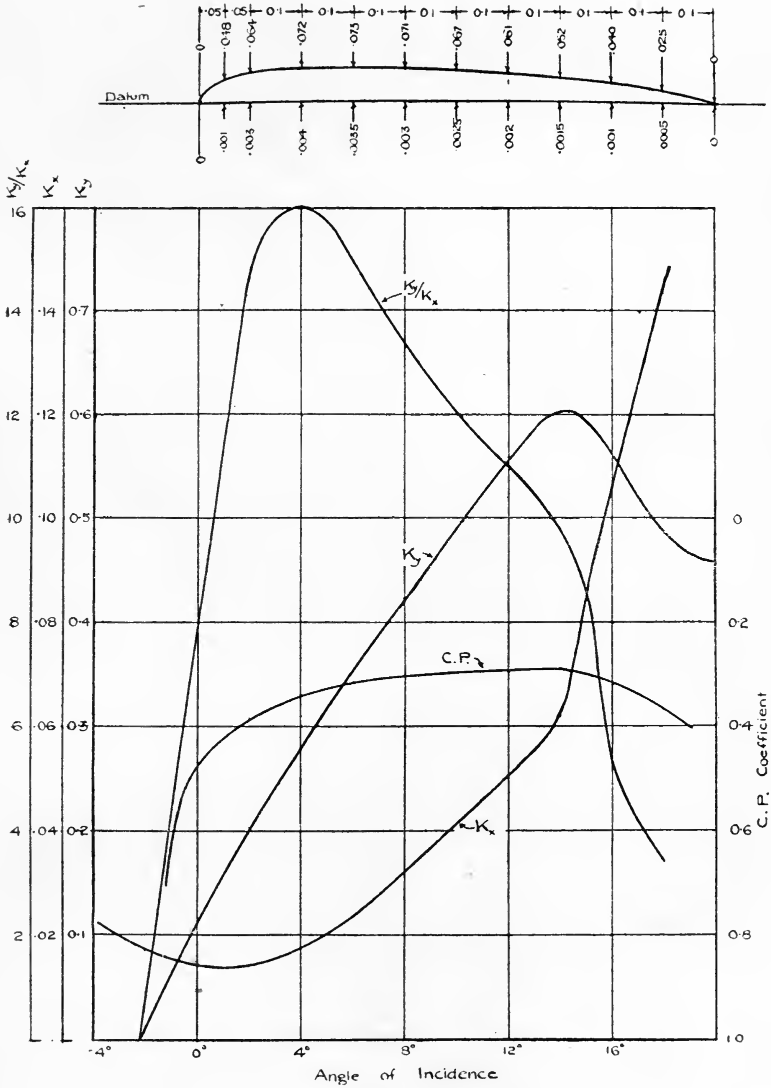

FIG. 72.—Wing Section No. 6.

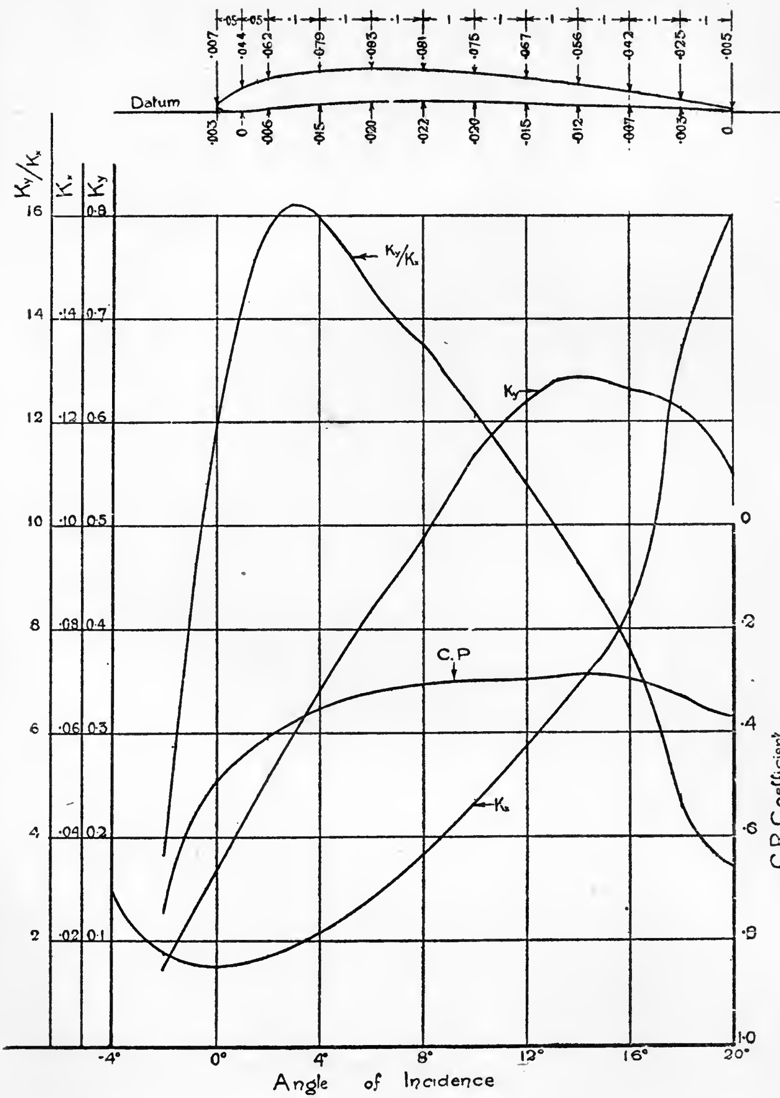

FIG. 73.—Wing Section No. 7.

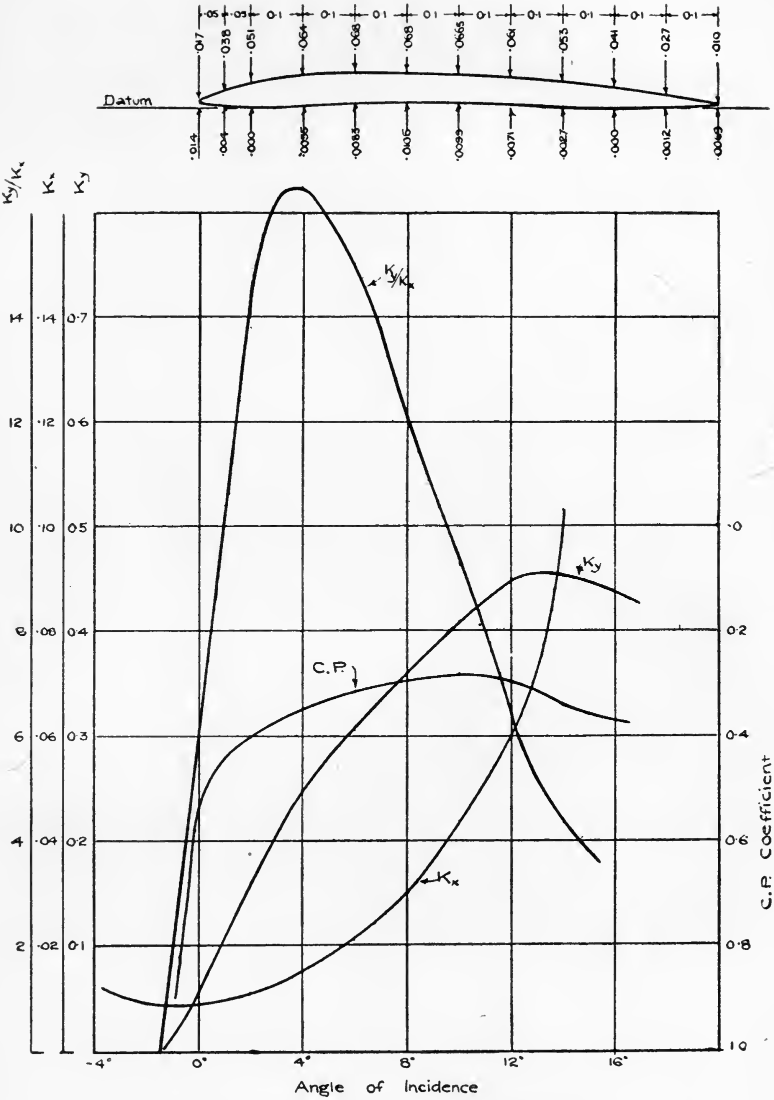

FIG. 74.—Wing Section No. 8.

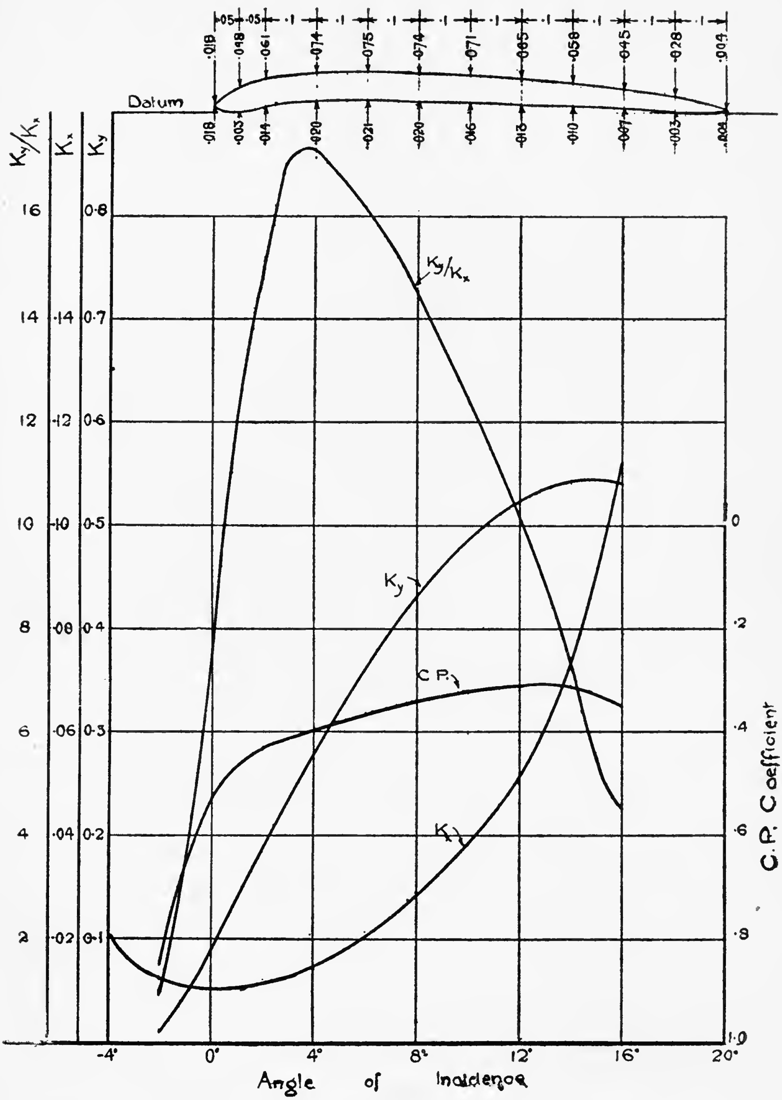

FIG. 75.—Wing Section No. 9.

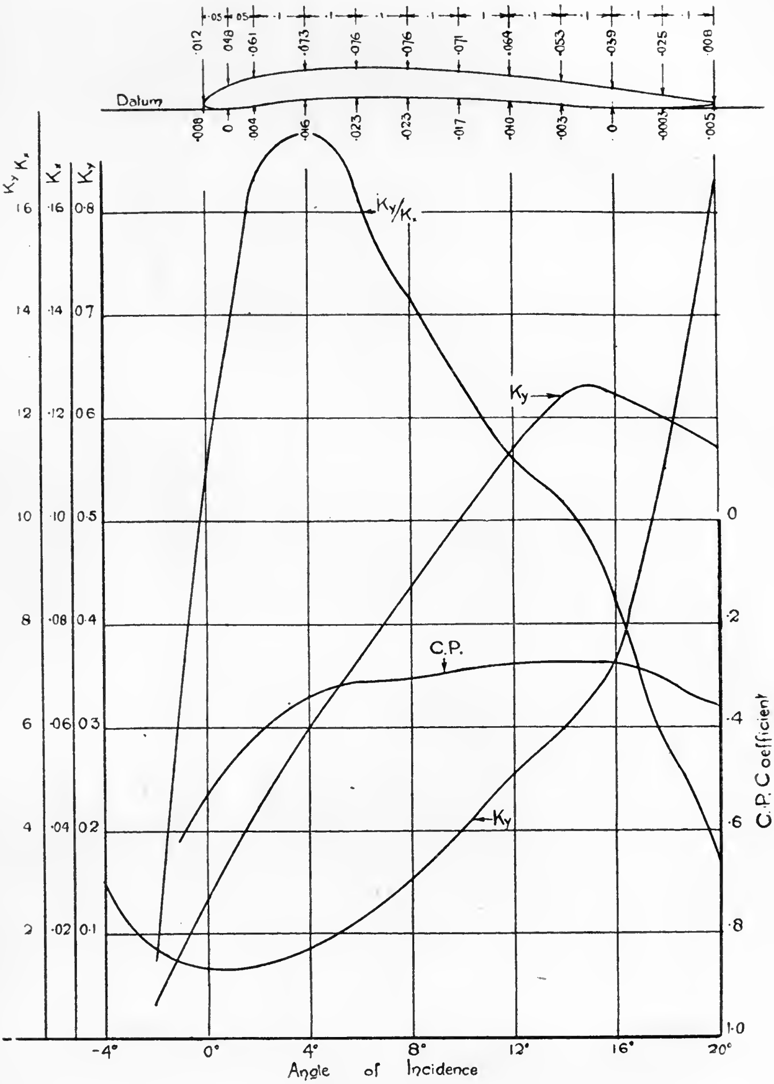

FIG. 76.—Wing Section No. 10.

CHAPTER IV.

STRESSES AND STRAINS IN AEROPLANE COMPONENTS.

Moments of Inertia.—The product of an area and its distance from a given axis is termed the moment of that area about the given axis. Thus in Fig. 77, if dA represent a small element of area of the surface S and y and x, the perpendicular distances of this area from the axes of x and y respectively, then

$dA . y$ = the moment of dA with reference to the axis of x
$dA . x$ = the moment of dA with reference to the axis of y

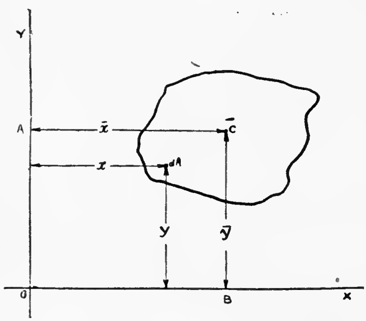

FIG. 77.—First Moment of Area.

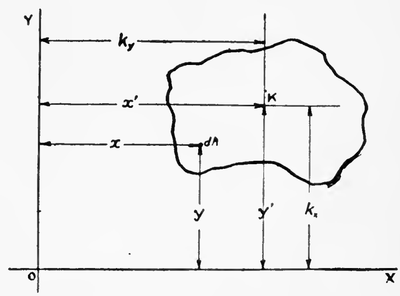

FIG. 78.—Second Moment of Area.

The total moment of the surface S about these axes is the sum of such elements as dA multiplied by the distance of each of these elements from the required axis, or

Moment of S about the axis OX = $\Sigma\, dA . y$ .... Formula 19
Moment of S about the axis OY = $\Sigma\, dA . x$ .... Formula 20

For many purposes the area of the surface S may be regarded as concentrated at a single point C, the position of the point C with reference to any axis being obtained from the relations

$$A \times \bar{y} = \Sigma\, dA . y$$

and $$A \times \bar{x} = \Sigma\, dA . x$$

or $$\bar{y} = \frac{\Sigma\, dA . y}{A}$$ .... Formula 21

$$\bar{x} = \frac{\Sigma\, dA . x}{A}$$ .... Formula 22

where A represents the total area of the surface S, that is the sum of such elements as dA, that is ΣdA.

The intersection of two such lines as AC and BC in Fig. 77, obtained by means of these two formulæ, gives the position of the centroid C, which for a homogeneous lamina corresponds to the centre of gravity.

The product of an area by the square of its distance from a given axis is termed the Moment of Inertia of the area about the given axis. Thus in Fig. 78, using the same notation as in Fig. 77, we have

$dA \,.\, y^2$ = moment of inertia of element dA about the axis of x
$dA \,.\, x^2$ = moment of inertia of element dA about the axis of y

and the total Moment of Inertia of the whole surface S is the sum of such elements multiplied by the squares of their respective distances from the given axis, whence

Moment of Inertia of S about OX $= \Sigma dA \,.\, y^2 = I_{XX}$ Formula 23
Moment of Inertia of S about OY $= \Sigma dA \,.\, x^2 = I_{YY}$ Formula 24

The term 'moment of inertia' is somewhat misleading, and, as will be apparent from Figs. 77 and 78, the term 'second moment' is much more applicable. The term moment of inertia is, however, in general use.

Now, in Fig. 78, if K be such a point that

$$A \times (y')^2 = \Sigma dA \,.\, y^2 = I_{XX}$$
$$A \times (x')^2 = \Sigma dA \,.\, x^2 = I_{YY}$$

then the point K in Fig. 78 is analogous to the point C in Fig. 77, and the distances y' and x' are known as the radii of gyration of the area A about XX and YY respectively. These radii of gyration are usually denoted by the symbols k_X and k_Y, so that

$$k_X = \sqrt{\frac{I_{XX}}{A}} \quad \text{.............. Formula 25}$$

$$\text{and} \quad k_Y = \sqrt{\frac{I_{YY}}{A}} \quad \text{.............. Formula 26}$$

Two very useful formulæ connecting moments of inertia about different axes are as follows:—

1. Principle of Parallel Axes.—If I_{CX} gives the moment of inertia through the centroid with reference to the axis of x, and I_{CY} the moment of inertia with reference to the axis of y, then

$$I_{CX} = I_{XX} - A\bar{y}^2 \quad \text{........... Formula 27}$$
$$\text{and} \quad I_{CY} = I_{YY} - A\bar{x}^2 \quad \text{........... Formula 28}$$

2. THE POLAR MOMENT OF INERTIA.—Knowing the moments of inertia about two axes at right angles to each other through the centroid as defined above, then the polar moment of inertia (I), that is, the moment of inertia about an axis perpendicular to each of the given axes, is given by the relationship

$$I = I_{CX} + I_{CY} \quad \text{.............. Formula 29}$$

TABLE XXII.—MOMENTS OF INERTIA—GEOMETRICAL SECTIONS.

Name	Form	Area A	Moment of Inertia I_{xx}	Radius of Gyration k^2	Modulus $Z = \frac{I}{y}$
Rectangle	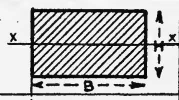	BH	$\frac{BH^3}{12}$	$\frac{H^2}{12}$	$\frac{BH^2}{6}$
Hollow Rectangle	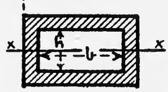	$BH-bh$	$\frac{BH^3-bh^3}{12}$	$\frac{BH^3-bh^3}{12(BH-bh)}$	$\frac{BH^3-bh^3}{6H}$
Pierced Rectangle	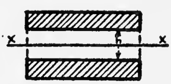	$B(H-h)$	$\frac{B(H^3-h^3)}{12}$	$\frac{H^2+hH+h^2}{12}$	$\frac{B(H^3-h^3)}{6H}$
Triangle	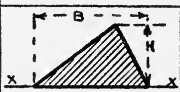	$\frac{BH}{2}$	$\frac{BH^3}{12}$	$\frac{H^2}{6}$	$\frac{BH^2}{4}$
Circle	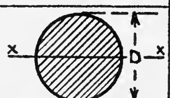	$\frac{\pi D^2}{4}$	$\frac{\pi D^4}{64}$	$\frac{D^2}{16}$	$\frac{\pi D^3}{32}$
Hollow Circle	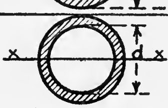	$\frac{\pi(D^2-d^2)}{4}$	$\frac{\pi(D^4-d^4)}{64}$	$\frac{D^2+d^2}{16}$	$\frac{\pi(D^4-d^4)}{32D}$
Ellipse		$\frac{\pi BH}{4}$	$\frac{\pi BH^3}{64}$	$\frac{H^2}{16}$	$\frac{\pi BH^2}{32}$
Hollow Ellipse	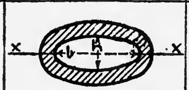	$\frac{\pi(BH-bh)}{4}$	$\frac{\pi(BH^3-bh^3)}{64}$	$\frac{BH^3-bh^3}{16(BH-bh)}$	$\frac{\pi(BH^3-bh^3)}{32B}$
Channel or I	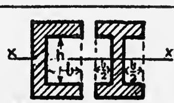	$BH-bh$	$\frac{BH^3-bh^3}{12}$	$\frac{BH^3-bh^3}{12(BH-bh)}$	$\frac{BH^3-bh^3}{6H}$

Table XXII. gives particulars with reference to the Moments of Inertia of some common geometrical sections. Of these, the solid rectangle, the box (or hollow rectangle), and the I are useful for the spars of wings and fuselage struts in aeronautical work. Unfortunately, however, in aeronautics many sections are employed to which the standard results cannot be directly applied with any degree of accuracy. In many such cases various empirical formulæ have been devised, but the graphical construction about to be described, and outlined in Fig. 79, gives results which are generally more accurate than those obtained by the use of these formulæ, while its use does not entail any advanced mathematical knowledge. Moreover, if the work is arranged in tabular form as shown, and if logarithms are employed for the multiplications, the labour involved is not so great as would appear at first sight. In using this method it is preferable to use decimal divisions of an inch, in order to reduce the calculations after summation of the columns. Fig. 79 shows the form of an interplane strut of a fineness ratio of 3·5 : 1, the Moment of Inertia of which is required about both axes.

Taking the line X′X′ as the axis of reference, the table shown in Fig. 79 is prepared. In this example a unit of ·05″ has been taken. The strut is next divided into any number of equal parts by lines drawn parallel to the axis of reference. In the example shown these lines were taken ·1″ apart. The mid-ordinate of each of these sections is then inserted as shown by the lines 1-1, 2-2, 3-3, 4-4, &c. The table shown to the right is next drawn up and the headings inserted. The first column, headed 'y,' represents the distance from the line of reference X′X′ of the mid-ordinate of each of the sections into which the strut has been divided. Since the strut is 7″ long, was divided by lines ·1″ apart, and since ·05″ has been adopted as the unit, the figures in the first column (y) will be the odd numbers commencing with 1 and running up to 139.

The second column, headed 'x,' shows the breadth of each of the mid-ordinates whose distance from the line of reference has been given in the first column. A diagonal scale can easily be constructed for reading off these lengths to any required degree of accuracy,

Column three, headed 'a,' represents the area of each of the sections, and is obtained from column two by multiplying each breadth by the depth of the section. Since, in the example, the depth of each section is constant, and equal to two units, column three is obtained from column two by multiplying by two. The total of column three gives $\sum a$, that is, the area of the section shown in terms of the unit employed. To obtain the area in square inches, we must therefore divide by the square of the unit, that is by 400, whence the area of the section is equal to 10·01 square inches, as shown. The empirical formula for finding the area of the section illustrated is

$$A = 2{\cdot}5\ t^4$$

whence $$A = 10 \text{ sq. ins.}$$

so that the agreement is very close.

The fourth column, headed 'ay,' gives the first moment of each section about the axis of reference X′X′. Its total therefore represents $\sum ay$, and by dividing this total by $\sum a$, we obtain the position of the centroid of the section with regard to the line X′X′. As shown, this distance is 3·87″.

Column five is obtained by multiplying column four by 'y,' and gives the second moment, or moment of inertia, of the sections with reference to the axis X′X′. Dividing the sum $\sum ay^2$ of this column by the fourth power of the unit used, gives the moment of inertia of the whole section about X′X′ in inch^4 units. The result, as shown in Fig. 79, is 178·18. Applying the principle of Parallel Axes to find the moment of inertia about the line through the centroid parallel to X′X′, the figure 29·26 is obtained, as shown.

The moment of inertia about an axis at right angles to X′X′ can be found in exactly the same manner. Since, however, the section is symmetrical about Y Y, it is only necessary to consider one-half of the section, and to multiply the results obtained by two, in order to obtain the correct results for the complete section. As will be seen from Fig. 80, the moment of inertia for the section about Y Y = 2·35 inch^4 units. The empirical formula for finding the moment of inertia of this section about Y Y is

$$\text{M.I.} = {\cdot}15\ t^4$$
$$= 2{\cdot}4 \text{ inch}^4 \text{ units.}$$

The accuracy obtained in Figs. 79 and 80 is far greater than is generally required in practical work, since a wooden strut cannot be made so accurately as these figures show, and even if made so accurately would not retain its accuracy unless fully protected from atmospheric effects. Consequently the labour involved in preparing a table such as is shown in Fig. 79 can be considerably reduced by taking the distance apart of the sections ·2″ instead of ·1″, since the form of the section with reference to the axis X′X′ does not change very rapidly. Since the form of the section changes fairly rapidly with reference to the axis Y Y, it is not advisable to increase the distances apart of the sections

FIG. 79.—Moment of Inertia of Streamline Section about Axis XX.

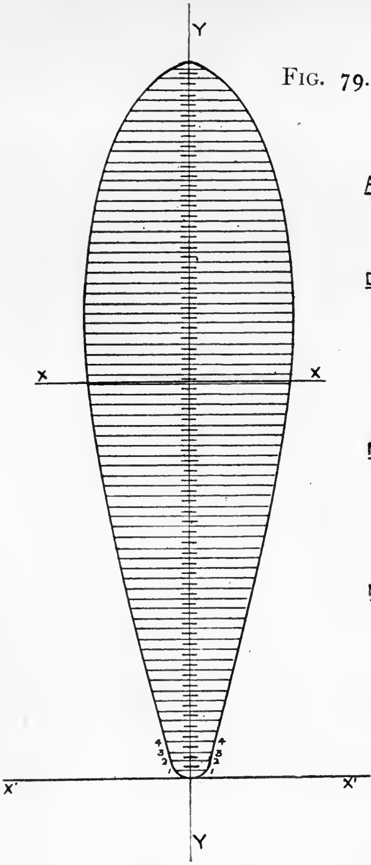

Area of Section

$= \frac{\Sigma a}{20^2} = \underline{10\cdot01 \text{ sq. ins}}$

Distance of Line through Centroid from X'X'

$= \bar{y} = \frac{\Sigma ay}{\Sigma a}$

$= \frac{309724\cdot8}{4005\cdot2 \times 20}$

$= \underline{3\cdot87 \text{ ins.}}$

Moment of Inertia about X'X'

$= \frac{\Sigma ay^2}{20^4} = \frac{28509652\cdot1}{20^4}$

$= \underline{178\cdot18 \text{ inch}^4 \text{ units}}$

Moment of Inertia about XX

$= I_{x'x'} - A\bar{y}^2$

$= 178\cdot18 - 149\cdot92$

$= \underline{29\cdot26 \text{ inch}^4 \text{ units}}$

y	x	a	ay	ay^2
1	5·8	11·6	11·6	11·6
3	7·6	15·2	45·6	136·8
5	8·4	16·8	84·0	420·0
7	9·4	18·8	131·6	921·2
9	10·8	21·6	194·4	1749·6
11	11·8	23·6	259·6	2855·6
13	12·8	25·6	332·8	4326·4
15	13·8	27·6	414·0	6210·0
17	15·0	30·0	510·0	8670·0
19	16·0	32·0	608·0	11552·0
21	17·2	34·0	722·4	15170·1
23	18·2	36·4	837·2	19255·6
25	19·4	38·8	970·0	24250·0
27	20·0	40·0	1080·0	29160·0
29	21·2	42·4	1229·6	35658·4
31	22·2	44·4	1376·4	42668·4
33	23·2	46·4	1531·2	50529·6
35	24·4	48·8	1708·0	59780·0
37	25·0	50·0	1850·0	68450·0
39	26·0	52·0	2028·0	79092·0

FIG. 79.—Moment of Inertia of Streamline Section (*continued*).

y	*x*	*a*	*a y*	*a y*²
41	27·0	54·0	2214·0	90774·0
43	28·0	56·0	2408·0	103644·0
45	29·0	58·0	2610·0	117450·0
47	29·4	58·8	2763·6	129889·2
49	30·4	60·8	2979·2	145980·8
51	31·2	62·4	3182·4	162302·4
53	32·0	64·0	3392·0	179776·0
55	32·6	65·2	3586·0	197230·0
57	33·6	67·2	3830·4	218332·8
59	34·4	68·8	4059·2	239492·8
61	35·0	70·0	4270·0	260470·0
63	35·6	71·2	4485·6	282592·8
65	36·2	72·4	4706·0	305890·0
67	36·8	73·6	4931·2	330390·4
69	37·4	74·8	5161·2	356122·8
71	38·0	76·0	5396·0	383116·0
73	38·4	76·8	5606·4	409267·2
75	38·8	77·6	5820·0	436500·0
77	39·2	78·4	6036·8	464833·6
79	39·4	78·8	6225·2	491790·8
81	39·5	79·0	6399·0	518319·0
83	39·6	79·2	6573·6	545608·8
85	39·7	79·4	6749·0	573665·0
87	39·8	79·6	6925·2	602492·4
89	40·0	80·0	7120·0	633680·0
91	40·0	80·0	7280·0	662480·0
93	40·0	80·0	7440·0	691920·0
95	40·0	80·0	7600·0	722000·0
97	40·0	80·0	7760·0	752720·0
99	39·8	79·6	7880·4	780159·6
101	39·6	79·2	7999·2	807919·2
103	39·0	78·0	8034·0	827502·0
105	38·4	76·8	8064·0	846720·0
107	38·0	76·0	8132·0	870124·0
109	37·6	75·2	8196·8	893451·2
111	37·0	74·0	8214·0	911754·0
113	36·6	72·2	8271·6	934690·8
115	35·4	70·8	8142·0	936330·0
117	34·6	69·2	8096·4	947278·8
119	33·4	66·8	7949·2	945954·8
121	32·6	65·2	7889·2	954593·2
123	31·0	62·0	7626·0	937998·0
125	29·6	59·2	7400·0	925000·0
127	27·6	55·2	7010·4	890320·8
129	25·6	51·2	6604·8	852019·2
131	23·2	46·4	6078·4	796270·4
133	20·4	40·8	5426·4	721711·2
135	17·2	34·4	4644·0	626940·0
137	12·2	24·4	3342·8	457963·6
139	4·6	9·2	1278·8	177753·2
		4005·2	309724·8	28509652·1

parallel to this axis, and as will be seen from Fig. 80, the labour involved in this case is not very considerable.

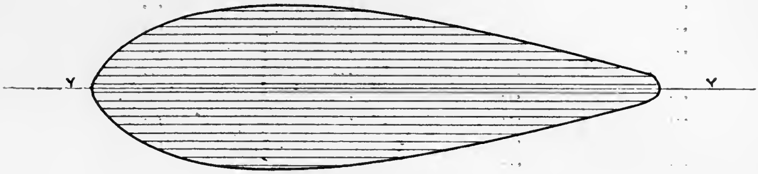

y	x	a	ay	ay^2
1	139·9	279·8	279·8	279·8
3	138·0	276·0	828·0	2484·0
5	129·9	259·8	1299·0	6495·0
7	120·8	241·6	1691·2	11838·4
9	110·8	221·6	1994·4	17949·6
11	103·7	207·4	2281·4	25095·4
13	87·4	174·8	2272·4	29541·2
15	76·0	152·0	2280·0	34200·0
17	58·2	116·4	1978·8	33779·6
19	36·0	72·0	1368·0	25992·0
		2001·4	16273·0	187655·0

Area of Section

$= \frac{2 \times 2001{\cdot}4}{20^2}$

$= 10{\cdot}007$ sq ins.

Moment of Inertia about YY

$= \frac{187655}{20^4}$

$= 2{\cdot}35$ inch^4 units

FIG 80.—Moment of Inertia of Streamline Section about Axis Y Y.

Nomograms, sometimes called alignment charts in England, can be prepared for some of the formulæ given in Table XXII. and many other formulæ in use in aeronautics, from which the value of the moment of inertia, or other quantity for which the nomogram has been constructed, can be read off immediately within the limits of the graduations.

Fig. 81 shows a nomogram constructed to give the moment of inertia of a rectangle, that is the quantity $\frac{b\,d^3}{12}$

To use nomograms it is very convenient to scribe a straight line on the under side of a large celluloid set square. Fig. 81 is then used in this manner. Suppose that it is required to find the moment of inertia of a rectangle whose breadth is ·6″ and whose depth is 2″. The line scribed on the set square is placed over the ·6 graduation on the breadth scale and swung round until it is over the 2″ mark on the depth scale. Where the line cuts the moment of inertia scale gives the answer, and as will be seen this gives the moment of inertia as ·4 inch^4 units. The same nomogram can also be used to find the moment of inertia of a square placed either with its axis parallel to or diagonal to the line of reference, remembering that the reading on the breadth scale must be the same as the reading on the depth scale. It can also be used to find the moment of inertia of a hollow rectangle, I beam, channel, or hollow square, by

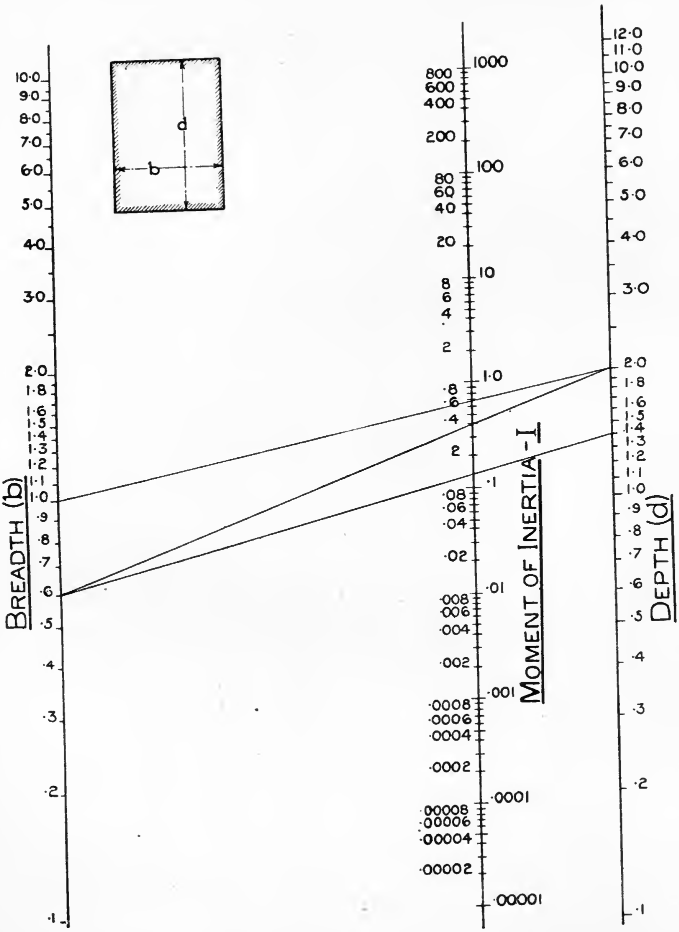

FIG. 81.—Nomogram for determining the Moment of Inertia of Rectangle, Square, Hollow Rectangle, Channel and 'I' Sections.

finding the difference between the moments for the whole and the missing portion. The following example will help to make this clear.

To find the M.I. of the box section illustrated in Fig. 82 :

M.I. of whole section = ·667 from nomogram.
M.I. of missing portion = ·137 " "

M.I. of the box section = ·53 inch^4 units.

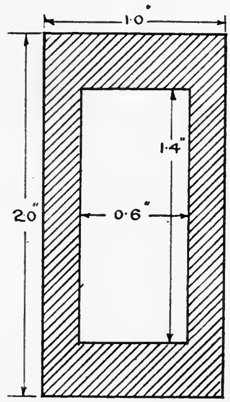

Fig. 82.

Shear Force and Bending Moment.—To obtain a clear idea of these quantities the following definitions must be carefully considered :—

The shearing force at any point along the span of a beam is the algebraic sum of all the perpendicular forces acting on the portion of the beam to the right OR to the left of that point.

The bending moment at any point along the span of a beam is the algebraic sum of the moments about that point of all the forces acting on the portion of the beam to the right OR to the left of that point.

Notice that since the beam is in equilibrium, the algebraic sum of the forces or the moments about any point considered on BOTH sides of the beam must be zero. Consequently the same value will be obtained for the shearing force or the bending moment, irrespective of whether we work from the right-hand end or the left-hand end.

The cases illustrated in Table XXIII., on pages 111–13, are of fundamental importance, and should be thoroughly well known before any attempt is made to apply the results to aeronautical design work.

TABLE XXIII.

LOAD, SHEAR FORCE, BENDING MOMENT, AND DEFLECTION.

A. CANTILEVERS.

	Type of Load	Load Diagram	Shear	Shear Force Diagram	Bending Moment	Bending Moment Diagram	Formula Number	Deflection	Formula Number	Remarks
1	Isolated Load at Free End	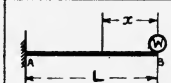	W Constant over whole span		Wx Increases as distance from load increases		30	$\frac{WL^3}{3EI}$ at free end B	31	
2	Isolated Load at any Point	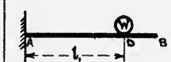	W from load to support D to A		Straight line increase from load to support		32	$\frac{Wl_1^3}{3EI}+(L-l_1)\frac{Wl_1^2}{2EI}$ at free end B	33	Deflection at B $=\frac{Wl_1^2}{2EI}\left(L-\frac{l_1}{3}\right)$
3	Uniform Load over whole span	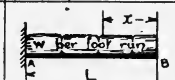	wx (st. line) increasing uniformly		$\frac{wx^2}{2}$ (parabola) Vertex at B		34	$\frac{wL^4}{8EI}=\frac{WL^3}{8EI}$ at free end B	35	wL = W = total load
4	Uniform Load over whole span plus an isolated load anywhere.	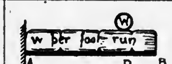	wx + W; wx only as far as D	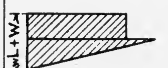	$Wx+\frac{wx^2}{2}$ from D to point of support A	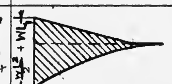	36	$\frac{Wl_1^2}{2EI}\left(L-\frac{l_1}{3}\right)+\frac{wL^4}{8EI}$ at free end B	37	Diagrams can be drawn on a horizontal base by using vertical ordinates
5	Gradually increasing Load from zero		$\frac{wx^2}{2}$ Parabola Vertex at B		$\frac{wx^3}{6}$ Cubic Parabola Vertex at B		38	$\frac{WL^3}{15EI}$ at free end B	39	Total load $=wL\times\frac{L}{2}=\frac{wL^2}{2}=W$

TABLE XXIII. (*continued*).

B. BEAMS . SIMPLY SUPPORTED.

	Type of Load	Load Diagram	Shear	Shear Force Diagram	Bending Moment	Bending Moment Diagram	Formula Number	Deflection	Formula Number	Remarks
6	Isolated Load at centre of span	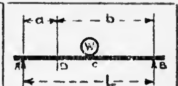	$\pm \frac{1}{2} W$ Sudden change of sign at centre	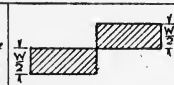	For load W at any point D B.M. $= \frac{Wab}{L}$	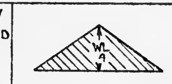	40	$\frac{WL^3}{48 EI}$ at centre C	41	For Load W at D Maximum Deflection $= \frac{Wb}{3EIL}\left[\frac{a(L+b)}{3}\right]^{\frac{3}{2}}$
7	Two isolated Loads at any points	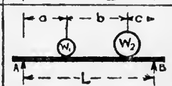	At A $= \frac{W_1(b+c)+W_2c}{L}$ At B $= \frac{W_1a+W_2(a+b)}{L}$		Obtained by adding together B.M. diagrams for W_1 and W_2	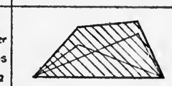	42			B.M. under W_2 $= \frac{W_2(a+b)c}{L} + \frac{W_1ac}{L}$
8	Uniform Load over whole span	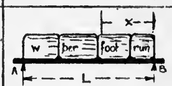	Straight line decrease to zero at centre from $\pm\frac{W}{2}$ at ends		$\frac{w}{2}[Lx - x^2]$ Parabola	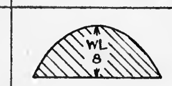	43	$\frac{5}{384}\frac{WL^3}{EI}$	44	Total load = wL = W
9	Uniform Load plus isolated load anywhere	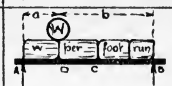	At A $= \frac{Wb}{L} + \frac{wL}{2}$ At B $= \frac{Wa}{L} + \frac{wL}{2}$		Maximum BM between C and D	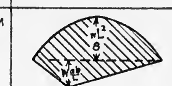				Bending Moment diagram can be redrawn on a straight line base by using vertical ordinates
10	Gradually increasing load from zero		Zero shear at $\frac{\sqrt{3}L}{3}$ from B	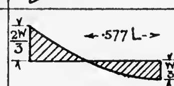	Maximum BM at point of zero shear Cubic parabola	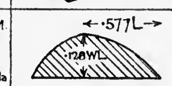				
11	Beam with overhanging ends loaded uniformly	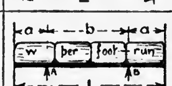	Treat overhanging ends as cantilevers	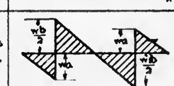	Support Moment $= \frac{wa^2}{2}$ Central B.M. $= \frac{wb^2}{8} - \frac{wa^2}{2}$	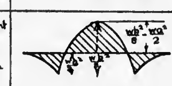				For maximum strength $\frac{wa^2}{2} = \frac{wb^2}{8} - \frac{wa^2}{2}$ whence $a = \frac{b}{2\sqrt{2}}$ and $\frac{b}{L} = 2 - \sqrt{2}$

TABLE XXIII. (*continued*).

	Type of Load	Load Diagram	Shear	Shear Force Diagram	Bending Moment	Bending Moment Diagram	Formula Number	Deflection	Formula Number	Remarks
C. FIXED BEAMS.										
12	Isolated Load at centre	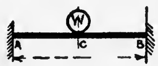	Same as for simply supported beam	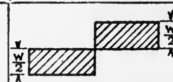		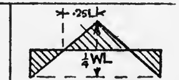		$\frac{WL^3}{192\,EI}$ at centre C	45	B.M. diagram obtained by considering beam as simply supported known as FREE B M DIAGRAM
13	Uniform Load over whole span		Same as for simply supported beam			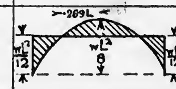		$\frac{WL^3}{384\,EI}$ at centre C	46	Difference between Free B.M. diagram and Support B.M. diagram gives the net B.M. at any point along span.
D. CONTINUOUS BEAMS										
14	Uniform Load over two equal spans	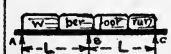	Zero Shear at ·375L from A and C	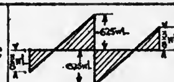	Maxm. B.M. at point of zero shear $= \frac{9}{128}wL^2$	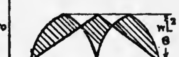		Remarks Clapeyron's 'Theorem of Three Moments' is $6\frac{A_2\bar{x}_2}{L_2} + 6\frac{A_3\bar{x}_3}{L_3} + M_B L_2 + 2M_C(L_2+L_3) + M_D L_3 + 6EI\left(\frac{\delta_2}{L_2} + \frac{\delta_3}{L_3}\right) = 0$ where A_1, A_2, A_3, etc. = Area of Free Bending Moment diagrams $\bar{x}_2, \bar{x}_3$ = distances of centroid of A_2, A_3, from left and right hand supports respectively M_A, M_B, M_C, etc. = Moments at supports A, B, C, etc δ_2 = distance support C falls below B δ_3 = distance support C falls below D		
15	General Case	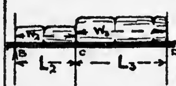	$F_B = \frac{M_A - M_B}{L_1} + \frac{w_1L_1}{2}$ $F'_B = \frac{M_C - M_B}{L_2} + \frac{w_2L_2}{2}$ $F_C = \frac{M_B - M_C}{L_2} + \frac{w_2L_2}{2}$ $F'_C = \frac{M_D - M_C}{L_3} + \frac{w_3L_3}{2}$ $F_D = \frac{M_C - M_D}{L_3} + \frac{w_3L_3}{2}$ $F'_D = \frac{M_E - M_D}{L_4} + \frac{w_4L_4}{2}$	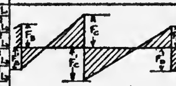	For a beam with n supports the general equation provides n-2 equations and the end supports supply 2 more equations	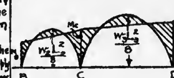	47			

Stresses in Beams.—The assumptions made in the Theory of Bending should always be remembered, because any formula derived from the Theory of Bending rests upon these assumptions. Consequently, when these assumptions do not hold good, the resulting formula cannot be applied with safety. Neglect of this almost obvious precaution is the root of practically all cases of discrepancy between theory and practice. In order to obtain a theory at all, certain assumptions have had to be made. Persons quite ignorant of theory find a formula in a pocket-book, apply it to a case (or cases) where the assumptions made in deriving the formula do not hold good, and when as a result failure occurs, the blame is laid at the door of theory.

The chief assumption made in the Theory of Bending is what is known as Bernouilli's Assumption, namely :

1. Transverse plane sections of a beam which are plane before bending remain plane after bending.

The other assumptions made are—

2. That Hooke's Law holds good.

3. That the modulus of Elasticity (E) is the same in tension as in compression.

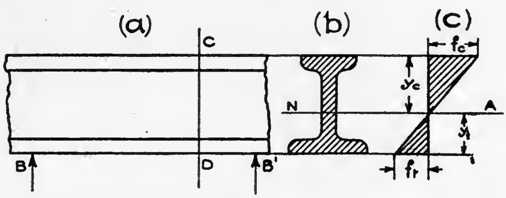

FIG. 83.—Distribution of Longitudinal Stress for **I** Section.

4. That the original radius of curvature of the beam is great compared with the cross-sectional dimension of the beam.

In simple bending, the external forces producing bending form a couple which is balanced by the internal forces in the fibres of the beam. These internal forces form another couple, and are the resultants of the tensile and compressive stresses in the beam.

Let Fig. 83 (*a*) represent a beam subjected to bending, whose cross-section is shown in Fig. 83 (*b*). Then, owing to the bending moment M at a cross-section such as C D, the distribution of longitudinal stress will be as shown in Fig. 83 (*c*). The line N A, which passes through the point of no stress, is known as the neutral axis of the beam. Since

$$\frac{f_t}{f_c} = \frac{y_t}{y_c}$$

the neutral axis (N A) must pass through the C.G. of the section.

Considering two transverse sections of a beam which are very close together, it will be seen from Fig. 86 that, in order to fulfil Bernouilli's assumption, after bending, the bounding lines are no longer parallel, but that a layer such as A D has been stretched, while a layer such as B C has been compressed. It is obvious that there must be an intermediate layer, such as M N, which is neither stretched nor compressed. This layer is known as the neutral axis (N.A.).

Produce A B, C D, Fig. 86 (*b*) to meet each other in O, and let the angle contained by these two lines contain α radians. Let the radius of curvature of the neutral surface M N = R, and let the height of any layer such as P Q from the neutral axis $= y$.

Then, from Fig. 86 (*b*)

$$\frac{\mathrm{PQ}}{\mathrm{MN}} = \frac{(R + y)\alpha}{R\alpha} = \frac{R + y}{R}$$

and the strain at a layer such as P Q, is equal to

$$\frac{\text{Extended length} - \text{Original length}}{\text{Original length}} = \frac{(R + y)\alpha - R\alpha}{R\alpha} = \frac{y}{R}$$

and the longitudinal tensile stress intensity at a distance y from the N.A. within the limits of elasticity

$$= f' = E \times \text{strain}$$

$$= E\frac{y}{R}$$

These longitudinal internal forces form a couple which is equal to the bending moment at every cross section, and is known as the Moment of Resistance. Expressing this couple in terms of the dimensions of the cross section and equating to the bending moment, we have

$$M = \frac{E}{R}I$$

Combining these several results in one expression, we have

$$\frac{E}{R} = \frac{M}{I} = \frac{f}{y} \quad \text{........... Formula 48}$$

From this equation we see that

$$M = f\frac{I}{y} = \frac{EI}{R}$$

The ratio I/y is known as the modulus of the section. This modulus is generally denoted by the letter Z, the suffix '*t*' or '*c*' being added according as the beam is in tension or compression.

SHEAR STRESS.—The complementary maximum horizontal shear stress generally occurs at the neutral axis, the distribution for any cross-section being given by the expression

$$q = \frac{F}{I b} \int_{y}^{Y} y \, . \, b \, . \, dy \quad \text{.......... Formula 49}$$

where

q = mean intensity of shear stress at a distance y from the N. A.
F = shearing force on the cross section of the beam.
I = moment of inertia of the cross section.
b = breadth of the cross section, having a particular value outside the integral, but varying with the distance y inside the integral.

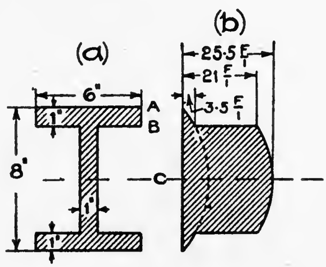

FIG. 84.—Distribution of Shear Stress for **I** Section.

A numerical example will make the use of Formula 49 clear. Consider the I section shown in Fig. 84 (a):

At A, $q = 0$

At B, $q = \frac{6 F}{I b} \int_{8}^{4} y \, . \, dy$

∴ for the inner edge of the flange

$$q = \frac{6 F}{6 I} \left[\tfrac{1}{2} (16 - 9) \right] \qquad = 3·5 \frac{F}{I}$$

and for the outer edge of web

$$q = \frac{6 F}{1 I} \tfrac{1}{2} (16 - 9) \qquad = 21·0 \frac{F}{I}$$

At C, on the neutral axis,

$$q = \frac{F}{1 I} \left[6 \int_{8}^{4} y \, . \, dy + 1 \int_{0}^{8} y \, . \, dy \right]$$

$$= \frac{F}{I} (21 + 4·5) \qquad = 25·5 \frac{F}{I}$$

and since the evaluation of the integral gives rise in each case to y^2, the curve of shear stress is a parabola, whence the distribution of shear stress can be drawn from these figures as shown

Fig. 85

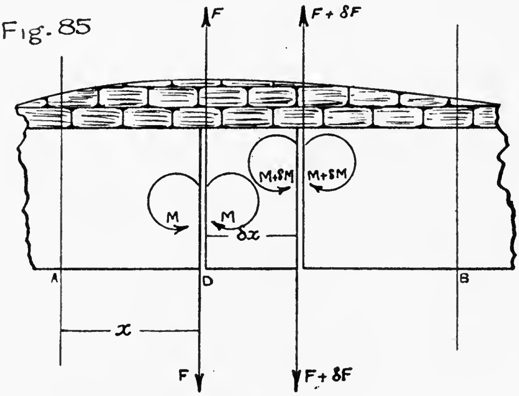

Fig 86

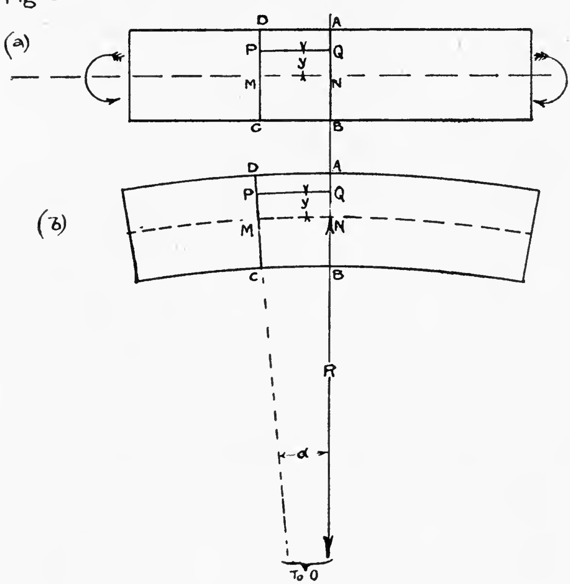

in Fig. 84 (*b*). From this figure it is clear that the web carries most of the shear, and it is usual on this account to design the web on the assumption that it carries all the shear, which gives a result on the safe side.

Relation between Load, Shear, Bending Moment, Slope, and Deflection.—Let A B, Fig. 85, represent a beam carrying a continuous load w per unit of length, and δx a length of this beam so small that whether w is constant or variable, for the distance δx it can be regarded as constant.

Then the forces acting upon this beam for the section considered are as shown in Fig. 85.

Equating upward and downward vertical forces, we have

$$F + \delta F = F + w \, . \, \delta x$$

whence $$\delta F = w \, . \, \delta x$$

or $$\frac{\delta F}{\delta x} = w \qquad \text{........... Formula 50}$$

that is, in words, the rate of change of the shearing force is numerically equal to the loading; and alternatively, the integration or summation of the loading diagram between the correct limits gives the shear force curve.

Again, equating moments about D for the external forces acting upon the section of length δx, we have

$$M + (F + \delta F)\,\delta x + w \, . \, \delta x \, . \, \tfrac{1}{2}\,\delta x = M + \delta M$$

and since δx represents a quantity of the first order of smallness, products containing two of these small quantities can be neglected.

Hence $$M + F \, . \, \delta x = M + \delta M$$

or $$\frac{\delta M}{\delta x} = F \qquad \text{........... Formula 51}$$

or in words, the rate of change of the bending moment is equal to the shearing force ; and alternatively, integration of the shear force curve gives the bending moment curve.

The curvature of a beam in accordance with the Theory of Bending is given by the relation

$$\frac{1}{R} = - \frac{\dfrac{d^2 y}{d x^2}}{\left[1 + \left(\dfrac{d y}{d x}\right)^2\right]^{\frac{3}{2}}} \qquad \text{........... Formula 52}$$

Neglecting second orders of smallness this expression reduces to

$$\frac{1}{R} = - \frac{d^2 y}{d x^2} \qquad \text{........... Formula 53}$$

and for the section δx shown in Fig. 85 we have by the combination of Formulæ 51 and 53

$$\frac{1}{R} = -\frac{d^2 y}{d x^2} = \frac{M}{E I} \qquad \text{......... Formula 54}$$

the negative sign being inserted to make the radius of curvature positive.

By adopting a suitable convention with regard to the sign of the bending moment, the last part of Formula 54 may be written

$$\frac{d^2 y}{d x^2} = \frac{M}{E I} \qquad \text{........... Formula 54 } (a)$$

Integrating Formula 54 (a) we have

$$\text{Slope} = \frac{d y}{d x} = \int \frac{M}{E I} d x \qquad \text{........... Formula 55}$$

Integrating Formula 55 we have

$$\text{Deflection} = y = \int\int \frac{M}{E I} d x . d x \text{........... Formula 56}$$

Combining Formulæ 50 and 51 we have

$$\frac{d^2 M}{d x^2} = w$$

which, combined with Formula 54 (a), gives

$$w = E I \frac{d^4 y}{d x^4} \qquad \text{........... Formula 57}$$

an expression which enables the shear, bending moment, slope, and deflection of a beam to be determined when the loading is constant or an integrable function of x.

For example, to take Case 8 of Table XXIII. shown on p. 112

$$\text{Load} = E I \frac{d^4 y}{d x^4} = w$$

$$\text{Shear} = E I \frac{d^3 y}{d x^3} = w x + A$$

$$\text{Bending Moment} = E I \frac{d^2 y}{d x^2} = \tfrac{1}{2} w x^2 + A x + B$$

But when $x = 0$, $M = 0$, $\therefore B = 0$

and when $x = L$, $M = 0$

$\therefore A L = -\frac{1}{2} w L^2$

or $A = -\frac{1}{2} w L$

Substituting

$$\text{Bending Moment} = \mathrm{E\,I}\frac{d^2 y}{d\,x^2} = \tfrac{1}{2}\,w\,x^2 - \tfrac{1}{2}\,w\,\mathrm{L}\,x$$

whence the bending moment at the centre

$$= \mathrm{M} = \tfrac{1}{2}\,w\,(\tfrac{1}{2}\,\mathrm{L})^2 - \tfrac{1}{2}\,w\,\mathrm{L}\,(\tfrac{1}{2}\,\mathrm{L})$$
$$= -\tfrac{1}{8}\,w\,\mathrm{L}^2$$

Integrating the bending moment expression

$$\text{Slope} = \mathrm{E\,I}\frac{d\,y}{d\,x} = \frac{w\,x^3}{6} - \frac{w\,\mathrm{L}\,x^2}{4} + \mathrm{C}$$

$$\text{Deflection} = \mathrm{E\,I}\,.\,y = \frac{w\,x^4}{24} - \frac{w\,\mathrm{L}\,x^3}{12} + \mathrm{C}\,x + \mathrm{D}$$

But when $x = 0$, $y = 0$, $\therefore\ \mathrm{D} = 0$
and when $x = \mathrm{L}$, $y = 0$,

$$\therefore\ \mathrm{C\,L} = \frac{w\,\mathrm{L}^4}{12} - \frac{w\,\mathrm{L}^4}{24}$$

$$\text{or}\quad \mathrm{C} = \frac{w\,\mathrm{L}^3}{24}$$

Substituting

$$\text{Deflection} = \mathrm{E\,I.}\,y = \frac{w\,x^4}{24} - \frac{w\,\mathrm{L}x^3}{12} + \frac{w\,\mathrm{L}^3\,x}{24}$$

whence the deflection at the centre

$$= y = \frac{w\,(\tfrac{1}{2}\,\mathrm{L})^4}{24} - \frac{w\,\mathrm{L}\,(\tfrac{1}{2}\,\mathrm{L})^3}{24} - \frac{w\,\mathrm{L}^3\,(\tfrac{1}{2}\,\mathrm{L})}{24}$$
$$= \frac{5\,w\,\mathrm{L}^4}{384\,\mathrm{E\,I}}$$

It will thus be seen that by successive integration and elimination of the constants of integration the shear, bending moment, slope, and deflection of a beam can be fully investigated from a knowledge of the loading, that is from Formula 57.

In addition, from a knowledge of these expressions different graphical methods can be devised to suit particular cases. It should also be noted that the bending moment curve bears the same relation to the slope and deflection curves, as the load diagram bears to the shear and bending moment curves.

A very easy method of summation which is frequently useful in practice for determining these quantities is the method of tabular integration. The advantage of this method is that the actual arithmetic of a table such as is shown below is very simple, and in addition the table can be dispensed with altogether by the use of squared paper diagrams. Particular attention must be paid to scales if the squared paper method of application is adopted. This graphical adaptation has been used in summing up (or integrating) the curves shown in the practical application of the theory of the tapered strut in Chapter V., and also in dealing with the airscrew in Chapter IX.

The tabular method of procedure will be illustrated by the following practical example :—

> Consider the spar of a wing, 8 feet long, loaded uniformly with 20 lbs. per foot run, and with the equivalent of a concentrated load of 20 lbs. at a distance of 5 feet from A, the fixed end.

The diagram of loading is shown in Fig. 87.

TABLE XXIV.—SHEAR, BENDING MOMENT, SLOPE, AND DEFLECTION BY TABULAR INTEGRATION.

Distance.	Load.	Shear.	B.M.	Slope.		Deflection.	
		$\int w\,dx$	$\int F\,dx$	$\int M\,dx$		$\int i\,dx$	
x	w	= F + A (A = O) = F	= M + B (B = O) = M	= $(i \times EI)$ + C	= $i \times EI$ (C = 1970)	= $(y \times EI)$ + D	$y \times EI$ (D = − 11815)
0		0	0	0	− 1970	0	− 11815·0
	20						
1		20	10	5	− 1965	1967·5	− 9847·5
	20						
2		40	40	30	− 1940	3920·0	− 7895·0
	20	60					
3	20	80	90	95	− 1875	5827·5	− 5997·5
	20						
4		100	180	230	− 1740	7635·0	− 4180·0
	20						
5		120	290	465	− 1505	9257·5	− 2557·5
	20						
6		140	420	820	− 1150	10585·0	− 1230·0
	20						
7		160	570	1315	− 655	11487·5	− 327·5
	20						
8		180	740	1970	− 0	11815·0	− 0

The first column in Table XXIV. contains the distances from the origin, which in this case has been selected at the free end B. The second column contains the load distribution. Since there is 20 lbs. per foot run, 20 lbs. is placed between each pair of figures in column 1; and as, in addition, there is a concentrated load of 20 lbs. at a distance of 3 feet from B, 20 is placed opposite the figure 3 in the first column. Formula 49 shows us that to obtain the shear we integrate (that is, sum up) the load. Column 3 contains this summation. At a distance of 0 feet it is obvious that there is no load, but from 0 feet to 1 feet it is seen that there is 20 lbs., hence opposite figure 1 in the first column we place 20 in the third column. From the first to the second foot there is another 20 lbs., which, added to the 20 already obtained, gives 40 as the figure to be placed opposite the second foot in the third column. Now at the third foot there is a concentrated load of 20, which means that there

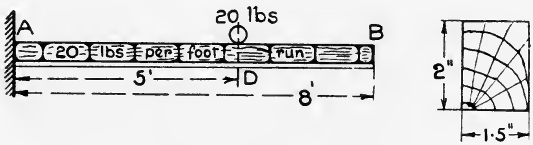

Fig. 87.—Load Diagram.

will be discontinuity in the shear force curve at that point. Consequently, in the third column, we require two figures: the first figure showing the shear an infinitesimal distance before reaching the concentrated load, and the second figure showing the shear just as the load is reached. Of course, in practice, the mathematical conception of a load acting at a point is impossible of realisation; and actually there is a rounding off of the corners of the shear force diagram where a load is applied, the rounding off being more or less gradual according as the load acts over a longer or shorter distance. The remainder of column 3 consists of adding on 20 for each foot length of the span, and is perfectly simple. As previously pointed out, when an expression is integrated an arbitrary constant appears, and this constant should be determined before proceeding further, if possible. On reference to Table XXIII., we see that the shear for a cantilever beam loaded as in this example is zero at the free end. This agrees with the value shown in Table XXIV., so that the constant of integration is zero, and the values shown in Table XXIV. represent the values of the shear in lbs. at each point along the span.

Integration of column 3 gives the bending moment. The process consists of finding the area of the shear force curve above each foot length of the span, and adding this area to the result already obtained. The area for the first foot $= \frac{1}{2}(0 + 20) \times 1 = 10$, for the second foot $= \frac{1}{2}(20 + 40) \times 1 = 30$. Adding to the bending moment already obtained for the first foot the bending moment at the second foot = 40.

For the third foot we have area ... ... $= \frac{1}{2}(40 + 60) \times 1 = 50$
whence bending moment at the third foot $= 40 + 50 = 90$.
Area for the fourth foot ... ... $= \frac{1}{2}(80 + 100) \times 1 = 90$
whence bending moment at the fourth foot $= 90 + 90 = 180$.
Area for the fifth foot ... ... $= \frac{1}{2}(100 + 120) \times 1 = 110$
whence bending moment at the fifth foot $= 180 + 110 = 290$.
Area for the sixth foot ... ... $= \frac{1}{2}(120 + 140) \times 1 = 130$
whence bending moment at the sixth foot $= 290 + 130 = 420$.
Area for the seventh foot ... ... $= \frac{1}{2}(140 + 160) \times 1 = 150$
whence bending moment at the seventh foot $= 420 + 150 = 570$.
Area for the eighth foot ... ... $= \frac{1}{2}(160 + 180) \times 1 = 170$
whence bending moment at the eighth foot $= 570 + 170 = 740$.

It now remains to eliminate the constant of integration. At the free end B the bending moment must be zero, therefore the constant of integration is zero, since the bending moment at that point is already zero.

Integration of the bending moment curve gives the slope, so column 5 is obtained from column 4 in exactly the same way that column 4 was obtained from column 3. To eliminate the constant of integration we notice that the slope must be zero at the fixed end A. Hence the constant of integration is − 1970 and column 6, which gives the slope multiplied by EI, is obtained by subtracting 1970 from column 5.

Integration of the slope gives the deflection, so column 6 is summed in exactly the same way as the previous columns. To eliminate the constant of integration we notice that the deflection is zero at the fixed end A. Consequently the constant of integration must be − 11815, and column 8, which gives the deflection multiplied by EI, is obtained from column 7 by subtraction of this constant.

Struts.—The use of struts enters very largely into aeroplane construction, hence it is important that the theory underlying the formulæ employed in their design should be clearly understood and appreciated. The classical theory is due to Euler, whose theory depends upon Formula 53. This formula, as we have just seen, rests upon the assumptions made in the theory of bending, and is further obtained by neglecting the denominator of Formula 52.

Considering a long rod A B, Fig. 88, Case I., pin-jointed at each end, but guided at A so that A remains vertically over B,

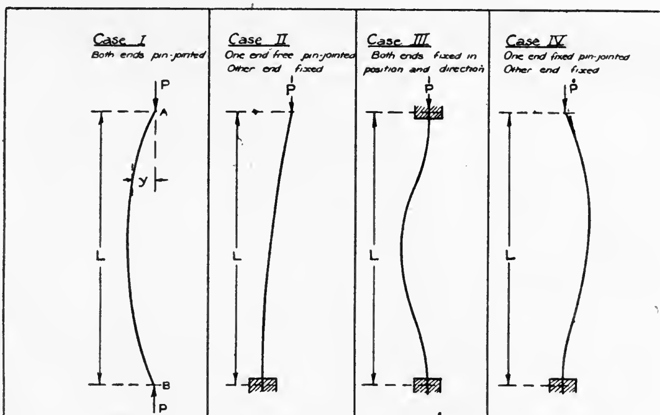

Maximum Load	$P = \frac{\pi^2 EI}{L^2}$	$P = \frac{\pi^2 EI}{4L^2}$	$P = \frac{4\pi^2 EI}{L^2}$	$P = \frac{9\pi^2 EI}{4L^2}$
Equivalent pin-jointed length	L	2 L	$\frac{L}{2}$	$\frac{2L}{3}$

FIG. 88.—Variation of Strut Formula, with Method of Fixing Ends.

with a force P applied at each end of the rod, then if the deflection at a distance 'x' from A is 'y,'

$$Py = M = \frac{-EI.d^2y}{dx^2}$$

or $$y = -\frac{EI.d^2y}{P.dx^2}$$

Let $$\frac{P}{EI} = p^2$$

then on substitution we have

$$\frac{d^2y}{dx^2} = -p^2y \quad \text{............} \quad 1$$

This is a differential equation satisfying the given conditions, and therefore a solution of this equation will also be a solution of the problem. Looking at this differential equation, we note that 'y' is a function such that its second derivative must be proportional to itself. This condition is satisfied by a sine or cosine function of the form

$$y = a \sin (b x + c) \qquad \ldots\ldots\ldots\ldots \qquad 2$$

where a, b, and c are constants to be determined by the conditions of the case. Since this is a function of the sine, we see that the shape into which the column will be bent must be sinusoidal.

Differentiating equation 2, we have

$$dy/dx = a\,b \cos (b x + c) \qquad \ldots\ldots\ldots\ldots \qquad 3$$

Differentiating equation 3, we have

$$d^2y/dx^2 = -\,a\,b^2 \sin (b x + c) \qquad \ldots\ldots\ldots\ldots \qquad 4$$

Substituting in equation 1 above the values obtained in equations 2 and 4, we have

$$-\,a\,b^2 \sin (b x + c) = -\,p^2 a \sin (b x + c)$$

Cancelling out common factors and taking the square root we obtain

$$b = p$$
$$= \sqrt{\frac{P}{EI}} \qquad \ldots\ldots\ldots\ldots \qquad 5$$

In order to eliminate the constant c, we must consider the end conditions.

When $x = 0$, we have $y = 0$, and on substitution in equation 3 we obtain

$$a \sin c = 0$$

whence $\qquad c = 0$

Again, when $x = L$, then $y = O$, which gives $b\,L = \pi \quad \ldots\ldots \quad 6$

Substituting the value thus obtained for b in equation 5, we have

$$\frac{\pi}{L} = \sqrt{\frac{P}{EI}}$$

$$\text{or} \quad P = \frac{\pi^2 EI}{L^2} \qquad \ldots\ldots\ldots\ldots \text{ Formula 58}$$

It should be noted that the value of the constant 'a' has not been determined. 'a' represents the amplitude of the sine curve, and since the fundamental equation is satisfied by any amplitude whatever, we have no restrictions upon the value of 'a,' which is therefore indeterminate.

If Formula 52 is used instead of Formula 53 for the derivation of this theory, the solution gives rise to an elliptic integral.

The theory that we have just outlined for long columns is known as Euler's Theory, and there are four standard cases to be considered.

CASE I.—The case we have just considered, namely both ends pin-jointed. This is the commonest case in practice.

CASE II.—One end fixed, the other end free to take up any angular position or to move laterally. In this case we have

$$P = \frac{\pi^2 E I}{4 L^2} \qquad \text{........... Formula 59}$$

The equivalent pin-jointed length of the strut is $= 2 L$

CASE III.—Both ends fixed in position and direction. In this case we have

$$P = \frac{4 \pi^2 E I}{L^2} \qquad \text{........... Formula 60}$$

The equivalent pin-jointed length of the strut is $= \frac{1}{2} L$

CASE IV.—One end fixed, the other end pin-jointed, but restrained from lateral movement.

$$P = \frac{9 \pi^2 E I}{4 L^2} \qquad \text{........... Formula 61}$$

The equivalent pin-jointed length of the strut is $= \frac{2 L}{3}$

In using Euler's formula the greatest working load is found by dividing by a factor of safety, and the load so obtained must not exceed the safe crushing load for the given material. Further, the given load must be applied axially, as Euler's formula does not apply if there is any eccentricity. Moreover the formula does not apply to struts which are not long in comparison with their cross-sectional dimensions. For aeronautical work the ratio

$$\frac{\text{length of the strut}}{\text{least radius of gyration}}$$

should be greater than 90 if Euler's formula is to be used.

For struts which are not long compared with their cross-sectional dimensions various empirical formulæ have been devised, the best known and most widely used of which is the Rankine-Gordon formula. This is of the form

$$p = \frac{P}{A} = \frac{f}{1 + a\left[\frac{L}{k}\right]^2} \qquad \text{........... Formula 62}$$

where

p is the crushing or crippling load on strut in tons (or lbs.) per square inch of cross-section.

P is the crushing or crippling load in tons (or lbs.).
A is the cross-sectional area in square inches.
f is the direct crushing strength of the material of the strut in tons (or lbs.) per square inch.
a is a constant.
L is the length of the strut—pin-jointed—in inches.
k is the least radius of gyration of the strut in inches.

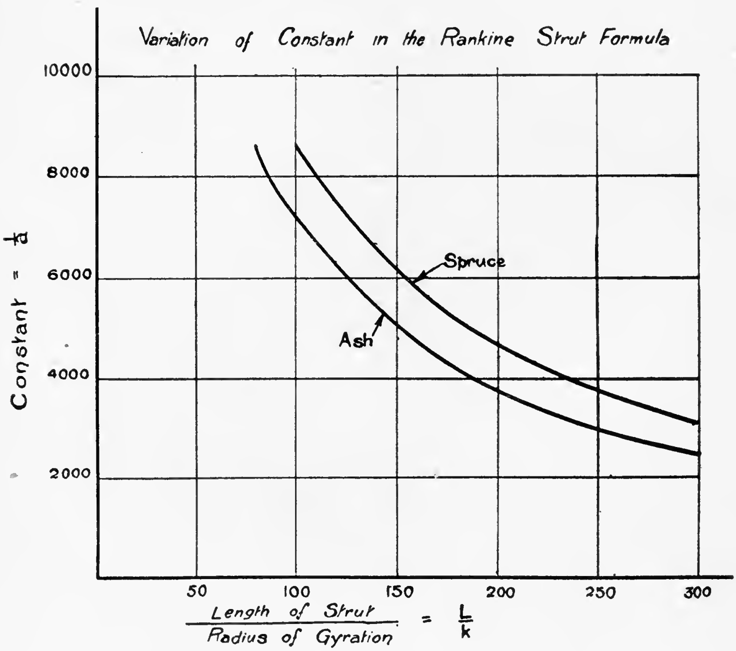

FIG. 89.

By experiment, the values of f and a have been determined. For aeronautical work Euler's formula is generally used for the Interplane Struts and the Spars, and for spruce the value of E is taken as

$$1{\cdot}6 \times 10^6$$

For the fuselage and similar short struts Rankine's formula is used, and for spruce f is taken as 5000 lbs. per square inch, and the value of the constant 'a' as 1/5200, when Rankine's formula becomes for spruce

$$P = \frac{5000 \times A}{1 + \frac{1}{5200}\left[\frac{L}{k}\right]^2} \qquad \text{............ Formula 62 } (a)$$

Strictly speaking, the value of the constant $1/a$ should vary with the value of L/k, and Fig. 89 gives the variation of this constant for value of L/k up to 300, according to data published by the R.A.F.

For ash, f is taken as 6200 lbs. per square inch.

Eccentric Loading.—We get an illustration of a combined direct and bending stress when a strut or column is loaded eccentrically. Let Fig. 90 represent such a case, where a load F is applied at a distance x from the centroid line of the column. Consider any section such as X Y. Without in any way affecting the stress at the cross-section X Y, we could insert equal and opposite forces F' F'', each equal to F, at points along

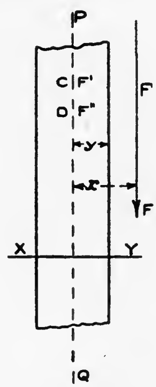

Fig. 90.—Strut loaded eccentrically.

P Q, such as C and D. Due to F' there will be a compressive stress on the cross-section X Y $= F'/A = F/A$, while due to the couple formed by F and F'', there will be a bending moment on the cross-section X Y $= Fx$. This bending moment will give rise to a compressive stress,

$$\frac{Fx}{Z_c} = \frac{F \times y}{Z_c y} = \frac{F \times y}{Ak^2}.$$

where k is the radius of gyration of the section in the plane of bending. Hence the total compressive stress at X Y

$$= f_c = \frac{F}{A} + \frac{F \times y}{Ak^2} = \frac{F}{A}\left[1 + \frac{xy}{k^2}\right]$$

$$\therefore \frac{F}{A} = \frac{f_c}{1 + \dfrac{xy}{k^2}} \qquad \text{........... Formula 63}$$

In aeronautical work the following formula, due to Professor Perry, is frequently used for struts with eccentric loading:

$$f = \frac{M}{Z}\left(\frac{Q}{Q + P}\right) + \frac{P}{A} \quad \text{........ Formula 63 } (a)$$

Where $Q = \frac{\pi^2 E I}{L^2}$

P = end load
M = maximum bending moment
f = maximum stress
A = cross sectional area
Z = modulus of section

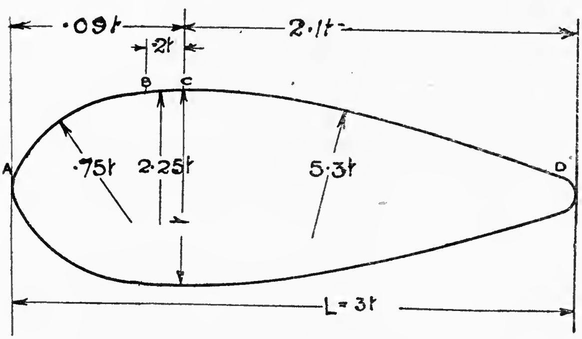

FIG. 91.—Dimensions of Stream-lined Strut, Fineness Ratio 3 : 1.

Streamlined Struts.—Fig. 91 gives the form and dimensions of a standard stream-lined strut.

The radius at A is ·08 t, from A to B is ·75 t, from B to C it is 2·25 t, from C to D it is 5·3 t, and at D it is ·1 t. The total length of the strut is 3 t.

The cross-sectional area	= 2·19 t^2
The Moment of Inertia	= 0·132 t^4
Ditto (transverse)	= 1·17 t^4
Distance of C.G. behind leading edge	= 1·34 t

Tapered Streamline Struts.—The development of large machines has led to the need for still greater economy in material and weight. In such machines considerable weight can be saved by the use of tapered interplane struts. The theory of the correct taper for such struts, and its application to actual design, will be fully treated in Chapter V.

CHAPTER V.

DESIGN OF THE WINGS.

Wing Structures.—The first man to develop a form of wing construction which contained all the essential elements of a modern aeroplane wing was Henson, who as early as 1842 adopted the Fink Truss for his wing construction. It is somewhat surprising, therefore, that the earlier experimenters did not adopt Henson's construction, which enabled a large reduction to be made in the number of exposed wires as compared with the umbrella type of wing which was used by Lilienthal and other pioneers. The first comparatively modern machine to be fitted with this type of wing structure was the Antoinette in 1909. This was somewhat similar in form to the type shown in Fig. 93A.

Monoplane Trusses.—Fig. 92A shows the most generally adopted form of monoplane bracing. The great objections to this type are—

(*a*) The large total resistance of the wires.
(*b*) The heavy compression set up in the spars.

The stress diagram of such a structure illustrates the latter objection very clearly, as shown by Fig. 92B. It will be noticed that the compression in the spars due to the angularity of the lift wires becomes very marked towards the centre of the span. Moreover, it is often difficult to place a direct strut across the fuselage, where the wing abuts. The advantages of this type are simplicity of construction and ease of adjustment.

The king-post method, shown in Fig. 93A, has the advantage of reducing the compression in the spars very considerably. The two cabane wires can be arranged at a good angle, and similarly the king-post wires can be at a greater angle than a wire from the cabane to the outer point. The compressions in the spars between the king-post bracing wires are self-contained, that is, they are not transmitted to the portion *b c*, which suffers so severely by the accumulation of compression in the most general arrangement shown in Fig. 92A. The maximum compression occurs in the portion *a b*. This arrangement is particularly useful when it is difficult to get in a sufficiently strong cross-fuselage strut such as would be required in the method of Fig. 92A.

In 1910 Bleriot adopted the Pratt Truss, already popular in biplane construction, for his monoplane, which was of considerable span and of the type shown in Fig. 94. A slightly different construction has survived until the present time in the German Taube. In the early days of aeroplane construction the monoplane achieved prominence in comparison with the biplane.

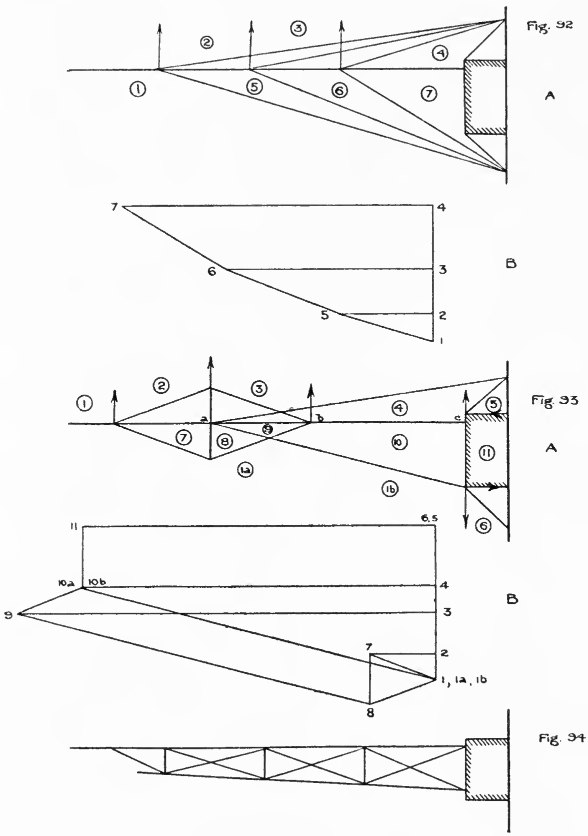

Monoplane Trusses.

The interference factor was absent, and the conception of the fuselage brought about a considerable decrease in the amount of head resistance. A greater margin of power became available, and the resulting increase of velocity enabled a reduction of area to be made; and to still further enhance the effect better wing sections were introduced. The popularity of the monoplane was short-lived, however, first on account of its inherent inferiority as a structure, and secondly owing to the disappearance of the aerodynamical disabilities of the biplane as finer flying angles were attained.

Biplane Trusses.—The first man to produce a simple and statically clear structure for the Biplane Truss was a bridge-builder, Chanute, one of the early pioneers in aeronautics. He applied the Pratt Truss to the biplane, and the idea was immediately adopted as the standard method of construction. Figs. 95–99 show the general form of biplane trusses, the number of panels varying from two to four in various constructions. By varying the width of the panels as shown, the structure can be made of lighter weight, or much stronger for the same weight. The forces acting in the spars increase from the wing tips towards the body, and it is advisable therefore to reduce the length of the spans towards the centre of the machine. This arrangement leads to a greater uniformity of forces in the members, since the outer struts and wires will be more heavily loaded and the inner members less heavily loaded than in the equally divided spans.

The next advance was the introduction of the overhung type of biplane truss by Henry Farman. This type is shown in Fig. 97. The overhang is treated either with lift wire bracing or with a landing strut. The latter arrangement is preferable, for it offers less resistance to motion. This is an important consideration, particularly for high-speed machines. Attention has already been drawn to the fact that aerodynamically the multiplane is less efficient than the monoplane, owing to the interference between superimposed planes, the lower planes being most affected. From this it follows that the greater the percentage of the total area formed by the upper plane, the greater will be the efficiency of the combination, other things being equal. Various other considerations, however, place a limit upon the reduction of the lower wing. For example, if the top wing be retained in its usual biplane position above the fuselage, while the area of the lower wing is reduced to zero, a monoplane of what has come to be known as the 'parasol' type results. In such a machine the C.G. is very much below the centre of lift, and the centre of thrust will probably be some distance below the centre of resistance. This is undesirable for several reasons, and hence, despite the unrestricted view downwards which such a type gives, the 'parasol' type has never developed. This case illustrates how practical requirements tend to lessen the aerodynamical efficiency of the monoplane. In order to overcome these disadvantages the French firm of Nieuport compromised between the theoretical efficiency of the monoplane and the practical advantages of the biplane. They effected this by making the area of the upper planes about

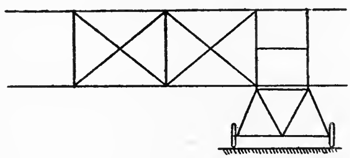

Fig. 95

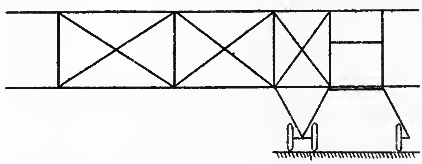

Fig. 96

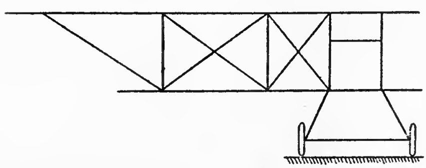

Fig. 97

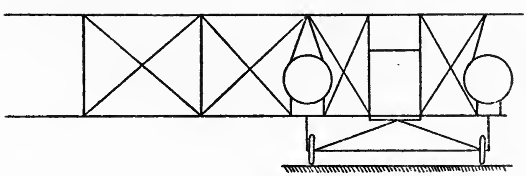

Fig. 98

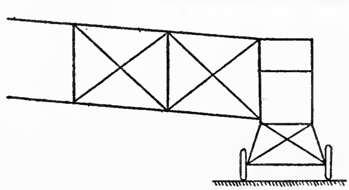

Fig. 99

Biplane Trusses.

twice that of the lower, thus closely approximating to the monoplane aerofoil efficiency while still retaining the biplane construction. The resulting machine has proved very successful. A side view of the wing structure is shown in Fig. 114.

At this point it will be instructive to examine the stress diagram for a general type of biplane of about the same size as the monoplane shown in Fig. 92A. The stress diagrams for the two cases are shown in Fig. 100, the monoplane at A and the biplane at B. The biplane has been arranged so that the aspect ratio of the wings is the same, but the combined area of the two wings is about 20% greater than that of the monoplane in order

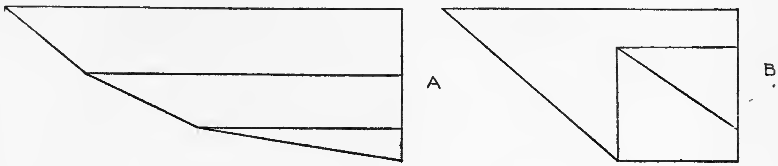

FIG. 100.—Comparison of Stress Diagrams for Monoplane (A) and Biplane (B).

to allow for the same landing speed, the maximum lift coefficient for the biplane being reduced by interference at large angles. The gap is equal to 1·2 × chord. A comparison of the two stress diagrams shows a considerably reduced compression in the lower spars of nearly 70%, so that these latter could be made very lightly. The biplane thus scores rather curiously perhaps

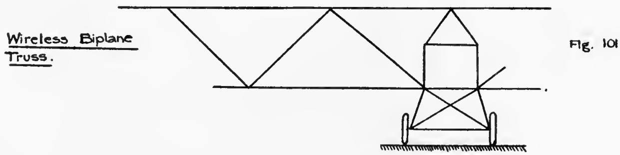

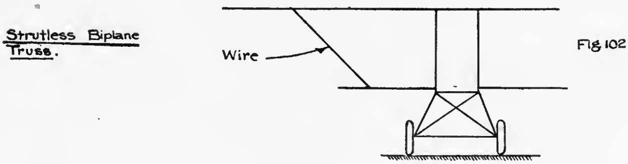

for high-speed work where the wings are necessarily thin and the maximum thickness of the spar must be small. Notice that as the compression due to angularity of the lift wires of a monoplane becomes pronounced as the span is increased, so also the compressions in the spars, even of a biplane, mount up if the span is unduly increased.

Wireless Biplane Trusses.—In 1913 the Albatross Company of Germany introduced what have come to be known as wireless trusses. An example is shown in Fig. 101. The advantage resulting from this construction is due to the reduction in resistance obtained by eliminating both lifting and landing wires and substituting members which will transmit both compression and tension. It is found that the total length of all the web members of a wireless truss can easily be made much less than one-half the total length of all the wires and

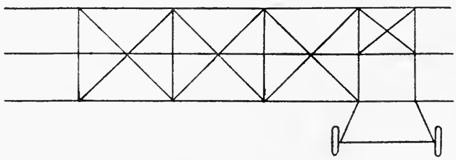

Fig. 103

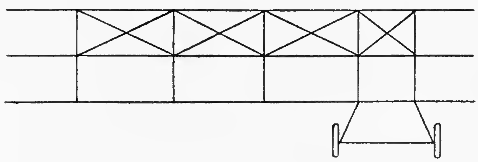

Fig. 104

Fig. 105

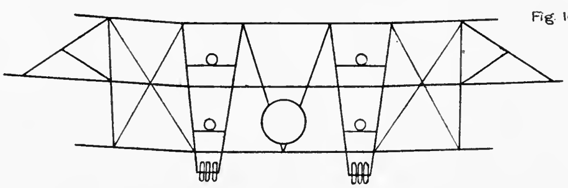

Triplane Trusses.

struts of the usual form of truss, so that the resistance of the web members can be reduced almost one-half with a very small increase of weight.

Strutless Biplane Truss.—The truss shown in Fig. 102 illustrates a very unusual departure from orthodox practice in biplane construction. This type of truss was designed by Dr. Christmas in order to imitate as far as possible the flexibility of the wings of a bird, the wing tips of this biplane having a range of movement of eighteen inches from a mean horizontal position in either direction. Thus the wings can assume a negative, neutral, or positive dihedral according to circumstances.

Triplane Trusses.—These may be treated in exactly the same manner as those of the biplane. Figs. 103–105 show various forms of bracing a triplane. It should be noted, however, that in the method of Fig. 103 the full height of the truss is not utilised, and as a result the strength of this construction is only about a quarter of that shown in Fig. 104. The triplane has the advantage of diminishing the length of the struts by half, which makes them relatively much stronger.

WIRELESS TRIPLANE TRUSS.

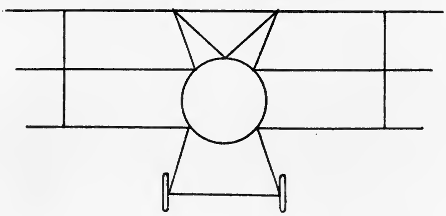

Fig. 106

QUADRUPLANE TRUSS.

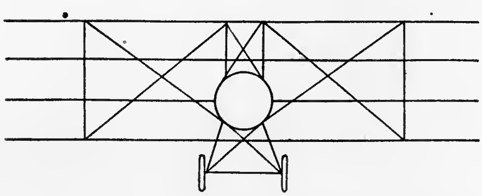

Fig. 107

Wireless Triplane Trusses.—Fig. 106 shows the latest Fokker triplane, which is of this type. As will be seen, all lift and landing wires are abolished, and the only wires used are the diagonal cross bracing wires between the centre struts sloping outwards and upwards from the body to the top wing. The designer of the Fokker seems to have sacrificed structural strength in order to cut down head resistance and interference to an absolute minimum. Such a wing structure as illustrated demands a very deep spar, in order to obtain a large moment of inertia coupled with a small area of section. In the spar construction adopted by the Fokker we find the two spars of an ordinary wing structure are placed rather closer together than usual. These spars are approximately of the ordinary box shape, and are made into one compound section by means of three-ply, and internal wing bracing is omitted. (See Fig. 141.)

Quadruplane Trusses.—The quadruplane truss shown in Fig. 107 illustrates an attempt made by Messrs. Armstrong, Whitworth, & Co. to supply a machine possessing good visibility in all directions, and therefore of great service as a fighting scout. The performance, however, is not so good as a comparatively small biplane, and pilots report that the machine is not an easy one to fly.

Drag and Incidence Bracing.—So far we have considered only the lift truss of an aeroplane. In order to stiffen the wings in the horizontal plane drag bracing is used. This in general takes the form shown in Fig. 108 for all types. The spars are braced together by means of the tie rods 'R' and compression members 'C.' For small machines specially constructed ribs, termed compression ribs, are sufficient to withstand the compressive forces between the two spars; but for large machines, and also in cases where the lift bracing is duplicated through the incidence wires, steel tubes or wooden-box struts are necessary to take the compression. The spars themselves transmit the components of the stress in the wires in the direction shown by the arrow, and these stresses must be added to those in the spars due to the lift forces. The lift and drag trusses are combined to form a rigid three-dimension structure by means of bracing in planes passing through the struts and parallel to the plane of symmetry of the whole machine. This side bracing is usually termed INCIDENCE BRACING. In the case of the monoplane, the most usual form is shown in Fig. 109. Each wing has two parallel or slightly converging spars—front and rear. The front pair of spars, together with some central pylon or the landing chassis taken as a kingpost, forms the front lift truss, the rear lift truss being formed in a similar manner.

For the biplane the most common types of incidence bracing are shown in Figs. 110 and 111, adapted to straight and staggered biplanes respectively. The incidence bracing may also be used to transmit the shear due to the lift or down forces from one frame to the other, if either of the bracing wires of the lift truss are broken. For example, suppose one of the front lift wires of a machine were shot away, the force which was originally transmitted to the body by this wire can be transferred by the incidence bracing to the rear frame and carried along to the body through this system. By this method it is possible to avoid the direct duplication of the main bracing wires, thereby considerably reducing the head resistance of the machine. It should, however, be observed that the stress in the incidence

Fig 108 DRAG BRACING

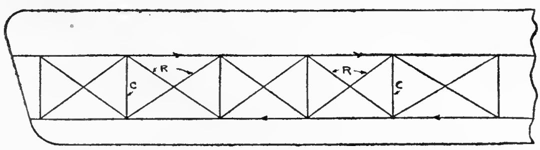

INCIDENCE BRACING

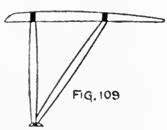

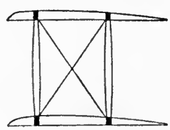

FIG. 110

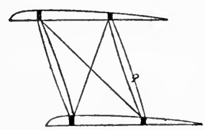

FIG. 111

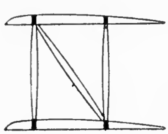

FIG. 112

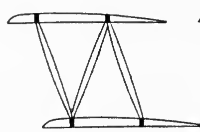

FIG. 113

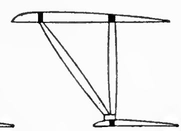

FIG. 114

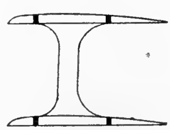

FIG. 115

Types of Drag and Incidence Bracing.

bracing will give rise to an increased force in the drag bracing, which must be made correspondingly stronger if this method is adopted. Figs. 112 and 113 show the 'N' type side bracing, with which again the resistance of the ordinary bracing can be decreased by half. This bracing, especially when combined with the wireless lift truss (Fig. 101), offers considerable possibilities for heavy large-span aeroplanes. Fig. 114 shows the 'v' type side bracing used in the Nieuport scouts. The two converging struts are fixed in a special socket fitted upon the spar of the lower plane. This construction is adaptable to both straight and staggered biplanes, but in both cases is especially good for an unequal chord biplane.

Development of the Single Lift Truss.—In 1909 Breguet produced a single lift truss biplane, and in 1914 the R.A.F. adopted this construction for a fast scouting machine. A side view of such a machine would be somewhat as shown in Fig. 115. The struts were fixed in sockets having long bases that reached from the front spar to the rear spar, and were fixed to the latter. The front and rear parts of the socket base may then be considered as a cantilever, subject to bending as the centre of pressure of the aerofoil moves in front of or passes behind the centre of the strut. The struts are thus subject not only to compression, but also to bending. The bending moments, however, are comparatively small for the ordinary size of machine, and can easily be accounted for.

The advantages of the single lift truss are :—

1. A reduction in weight and resistance of the struts.
2. A reduction in resistance of the bracing wires.
3. The forces acting are practically independent of the position of the C.P., whereas in the double lift truss in the extreme attitudes of flight one of the trusses is partly idle, and consequently contains excess strength and weight.

Generally the forces acting on a single lift truss will be about 30% less than the maximum load, thus leading to a further reduction of weight and air resistance.

Tractor and Pusher Machines.—All aeroplanes at present constructed may be classified under one of the above types, or as a combination of both types. As a generalisation it may be said that the fundamental difference between the two types is that in the tractor machine the airscrew is placed in front of the wing structure, whereas in the pusher machine it is placed behind. Side views of the two types are shown in Figs. 116 and 117 (page 144), from which it will be seen that the change in the position of the engine and airscrew considerably modifies the form of the body. In the case of the tractor, the body (or fuselage) extends from the airscrew at the extreme front right down to the control surfaces at the extreme rear of the machine. Such a body can with care be made of excellent streamline form, and if totally enclosed—which is likely to become standard practice in the near future—a comparatively low resistance can be obtained. In the case of the pusher, the presence of the airscrew at the rear of the wing structure necessitates a different form of construction in order to connect the control surfaces to the wing structure. This takes the form of what is known as an 'outrigger,' consisting usually of four longitudinal booms stretching from the wings at points where they are of sufficient distance apart to allow the airscrew to rotate between them, out to the tail unit. The body of a machine of this type is termed a nacelle, and is situated, as shown in Fig. 116, in front of the wings, thereby enabling an excellent range of vision and of gunfire to be obtained. It is comparatively short, however, and the position of the engine prevents a good streamline shape from being obtained.

In making a comparison of the aerodynamical efficiency of the two types, it must be noted that the fuselage of the tractor machine is operating in the slip stream of the airscrew, which leads to an increase in its resistance. In practice it is found that the presence of the fuselage in the wake of an airscrew increases the efficiency of the airscrew, and these two factors must therefore be considered in conjunction with one another. In the pusher type of machine, the less efficient type of the nacelle is coupled with a loss in efficiency of the airscrew due to the obstructed flow of the airstream in front of its path. It is therefore apparent that the tractor type is much more efficient aerodynamically. It is due to this fact, together with the more rigid structure that can be obtained by using a fuselage, that the pusher type of machine is rapidly disappearing.

The Factor of Safety.—The question of the factor of safety is of vital importance in aeroplane design. Contrary to general engineering practice, the structural parts of an aeroplane are designed to have a certain 'factor of safety' with reference to the normal flying load determined by the weight of the machine. Any excess stress due to manœuvring is taken account of in the factor of safety itself, so that in the engineering sense it is not a factor of safety at all, but merely an allowance for additional stresses set up under conditions other than ordinary horizontal flight. It is possible to determine approximately what the maximum stresses are likely to be, and from these determinations the aeroplane is designed so that its strength at all points is sufficient to withstand a reasonable value of this maximum stress, the actual 'factor of safety' being generally below 2. See Table X., page 24.

In no other branch of engineering is it so essential on the score of weight to use so small a margin of excess material, nor is there such a likelihood of greatly increased loads being placed suddenly upon the structure; while, generally speaking, failure in even apparently insignificant details leads to disastrous results. The requisite factor to adopt in any particular case follows more or less upon the selection of type; it is obvious, for instance, that a fairly heavy biplane will not be 'stunted' in the air to the same extent that a scout would be, while a heavy commercial or passenger-carrying machine will be most carefully handled in the air. Bearing these facts in mind we may examine the more important conditions common to all types in flight which tend to increase the normal load.

The load supported by the wings equals the weight of the complete machine only when the vertical component of flight is without vertical acceleration and the direction of the wind is steady. This second condition is necessary because a sudden change of the vertical component by the action of the wind might produce an overload by its impulsive action without causing any appreciable difference in the motion of the aeroplane. The maximum loading which can occur in this and similar cases is assessed by imagining the aeroplane to be flying at its fastest horizontal speed and to be suddenly pitched from the angle of incidence corresponding to that speed, to the angle of maximum lift. The loading would then be momentarily increased in the ratio approximately of the lift coefficients. As the maximum lift coefficient for any normal wing does not vary greatly from 0·6, the factor of safety necessary here will depend practically on the fastest flying speed. This is one reason why the fast machine should have a higher factor of safety than the slow machine. It is evident that such change of motion may take place from accidental causes and may be in the negative as well as in the positive direction, thus throwing a load on the 'down' bracing of a biplane, or on the upper wires of a monoplane.

Vertical motion due to the air may be classed under two heads:—

1. Alteration of wind velocity. In this case the effect is similar to pitching if the vertical component only of the wind velocity changes, but is more serious if combined with a change due to gusts.

2. The action of air pockets. Air pockets, which are really currents of air of different velocities from that of the main airstream, often occur over rivers, etc. The effect so far as concerns us here is that of dropping the aeroplane a certain

distance, and then dealing with the resistance of the wings as at 90° incidence, and having the velocity acquired by the fall. The distance fallen will not be large and as the aeroplane is continuously air-borne to some extent, this effect should not result in any considerable overloading

An illustrative example will make this clear.

A biplane of 300 sq. ft. wing area enters an air pocket and falls through a height of 25 ft. Find the increase of force on the wings when the machine emerges into air of normal density. Take the resistance of the wings as equal to ·003 A V^2

The vertical velocity downwards is given by the relationship

$$V^2 = 2gh$$
$$= 2 \times 32{\cdot}2 \times 25$$
$$\therefore V = 40 \text{ f.p.s.}$$
$$R = {\cdot}003\, A\, V^2$$
$$= {\cdot}003 \times 300 \times 40 \times 40$$
$$= 1440 \text{ lbs.}$$
$$= \text{increase of force on wings.}$$

Another condition in which loading may be augmented is in turning. During this manœuvre the machine is banked to prevent side-slipping outwards, hence the overloading depends entirely upon the sharpness of the turn, that is, upon its radius ; and the amount of banking.

Let W = the weight of the machine.
V = the velocity of the machine.
R = the radius of the turn.
β = the angle of banking proper to the turn. (See Fig. 118.)

Then, if circular turning is assumed, the force acting inwards towards the centre of turning = $W V^2 / g R$.

This force must be applied as a lift practically normal to the plane of the wings, and hence the force on the wings due to banking = $(W V^2 / g R) \sin \beta$.

When the wings are banked, however, the weight of the machine is taken by only a component of the forces on the wings. The load due to the weight = $W / \cos \beta$, so that the loading is increased from two causes. In a very sharp turn the the bank may be very steep and the machine may be allowed to fall during the very short time necessary for the turn.

The minimum possible radius of turning occurs when the centrifugal force exerted towards the centre of turning is the maximum aerodynamically possible. This obtains when the wing is banked approximately vertically and is inclined to the flight path at the angle of maximum lift. The question of overloading which occurs at about the commencement of the turn is then similar to the case of pitching already considered.

An illustrative example will help to make this condition clear.

A machine weighing 1800 lbs. is travelling at 100 m.p.h. and is suddenly banked to an angle of 60°. To find the approximate radius of turn required if the loading on the wings during the turn is not to exceed three times the weight of the machine.

$$V = 146 \cdot 7 \text{ f.p.s.}$$

Force acting inwards

$$= \frac{W V^2}{g R} \sin \beta$$

$$= \frac{W \times 146 \cdot 7 \times 146 \cdot 7 \times \sin 60°}{32 \cdot 2 \times R}$$

$$= 3 \times W \quad \text{from the stated conditions}$$

whence $R = 193$ feet.

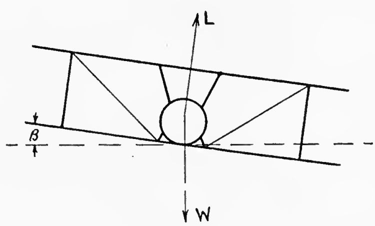

FIG. 118.

From what has been said it will be clear that the speed of a machine is an essential factor in the consideration of the overloading of wings, and hence it is natural to expect the overloading to be a maximum when the speed is greatest. This maximum speed will probably occur in a long nose dive. The following example is instructive. Suppose a machine weighing 1200 lbs. and fitted with a 100 h.p. motor is capable of attaining 100 m.p.h. in horizontal flight. Take the ratio of L/D of the wings at this speed as 10 and the airscrew efficiency as 80%. To find the terminal velocity at the end of a long nose dive. The lift of the wings must equal the weight of the machine, hence since the L/D ratio is 10, the resistance of the wings at this angle will be = 1200/10 = 120 lbs. The thrust of the airscrew equals

$$\frac{100 \times \cdot 8 \times 550 \times 3600}{100 \times 5280} = 300 \text{ lbs.}$$

Hence the resistance of the machine less the wings = 300 − 120 = 180 lbs.

The drift coefficient at the angle of no lift will be slightly greater than at fastest flying angle. A reasonable figure would be 15% greater, so that the drift of the wings at the angle of no lift = 120 × 1·15 = 138 lbs.

The machine will have acquired its maximum possible velocity downwards when the weight of the machine is equal to the resistance of the air; so that if V be this maximum velocity, we have 1200 = [(138 + 180) V × V] / 100 × 100, whence V = 194 m.p.h., say 200 m.p.h.

Since the speed of the machine is thus practically doubled, the drift of the wings will be increased four times during the last portion of the dive, thus causing considerable overload of the drift wires.

A more serious overloading will occur when the machine is flattened out at the conclusion of the nose dive. If we imagine it to have been flying with a lift coefficient of 0·15 and to have a maximum lift coefficient of 0·6; then the wings will be overloaded sixteen times for a sudden impulsive flattening out. The radius of the flattening-out curve will be

$$R = \frac{W V^2}{g \times 16 W} = \frac{294 \times 294}{32 \cdot 2 \times 16} = 170 \text{ feet.}$$

In actual flight a machine does not answer to its controls instantaneously, so that the impulsive overloading will not reach so high a figure as that indicated; nevertheless it may reach an overload as great as twelve times the weight of the machine.

In order that the overloading should not exceed four times the weight of the machine, the radius of the curve must therefore be 4 × 170 = 680 feet, which is quite a large radius; while the angle of the wings to the flight path must not exceed the fastest flying angle, the maximum lift coefficient being 0·15.

It is evident from this example that it is practically impossible to design an aeroplane which shall be sufficiently strong to be aerodynamically 'fool proof' in the hands of the pilot if ample control is provided. It is necessary therefore to compromise on the matter and to design a machine with a factor of safety sufficient to meet emergencies but with certain very definite limitations with which the pilot should be acquainted. This is particularly the case with machines having low head resistance and which as a consequence may develop an alarmingly high speed in a straight nose dive. The factor of safety hitherto dealt with is essentially an aerodynamic one. A further margin of strength is required to deal with—

Reproduced by courtesy of Messrs. Vickers, Ltd.

FIG. 116.—'Vickers Vampire': Armoured Trench Fighter, fitted with 200 h.p. B.R.2 Engine.

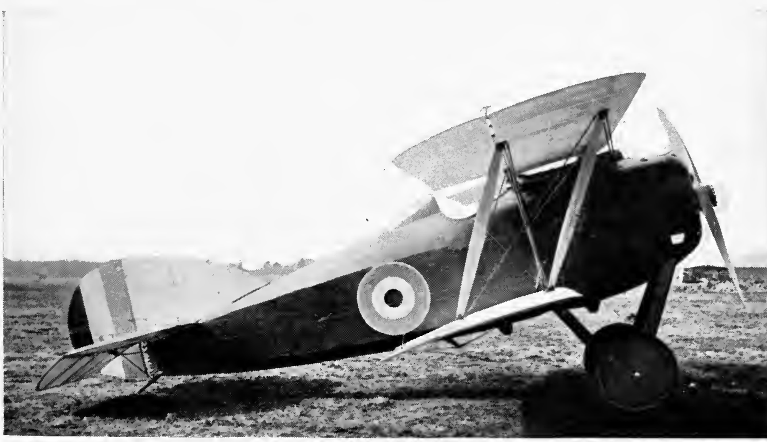

Reproduced by courtesy of Messrs. Vickers, Ltd.

FIG. 117.—'Vickers 16 D' Scout, fitted with 200 h.p. Hispano Engine.

1. The extra stresses produced by the failure of one of the members;

2. The extra stresses produced in the building of the machine.

The first requirement is of great importance in the case of military machines where an exposed part is liable to be shot away or seriously weakened by a bullet. The second is liable to occur owing to the uneven or excessive tightening up of the bracing system.

The general overloading produced in what may be termed abnormal flight is to be allowed for in the design of the wings and attachments by assuming the load to be several times the flying weight of the machine, the multiplying factor varying for different aeroplanes according to the purpose for which they are designed. Attention must be given to the stresses induced by the breaking of a part, and a good design will provide against this wherever possible. Stresses due to counterbracing must be allowed for, but in building the machine it is essential to take the utmost care that these stresses are not unduly increased, and that in 'tuning up' (a phrase sometimes used to describe the forcible straining of bad work into its correct shape), the mechanics are not given too free a hand.

Experimental Investigation of the Stresses upon a Full-size Machine during Flight.—One of the fundamental formulæ of applied mathematics, which follows directly as a deduction from Newton's Second Law of Motion, states that

$$\text{Force} = \text{Mass} \times \text{Acceleration}.$$

For an aeroplane in flight, the mass is practically constant, hence a determination of the forces set up in the wing structure will follow from a knowledge of the acceleration of the machine under various conditions. This principle has been adopted in the full-scale experiments carried out at the Royal Aircraft Establishment. An instrument called an Accelerometer is used to indicate photographically the acceleration of the machine in terms of the earth's attraction—that is, in terms of the force of gravity. In addition to giving a measure of the resultant air force on the machine, the instrument also measures the time of rapid manœuvres.

Figs. 119 and 120 show records obtained from this instrument in actual use. Fig. 119 indicates the accelerations set up on an S. E. 5 Scout machine and a Bristol Fighter during a mock fight, while Fig. 120 indicates the accelerations and speeds of flight of a Bristol Fighter during various manœuvres. It will be observed that in the case of the S. E. 5 the maximum stresses nowhere exceed three times the weight of the machine. In the case of the Bristol Fighter when manœuvring, the maximum

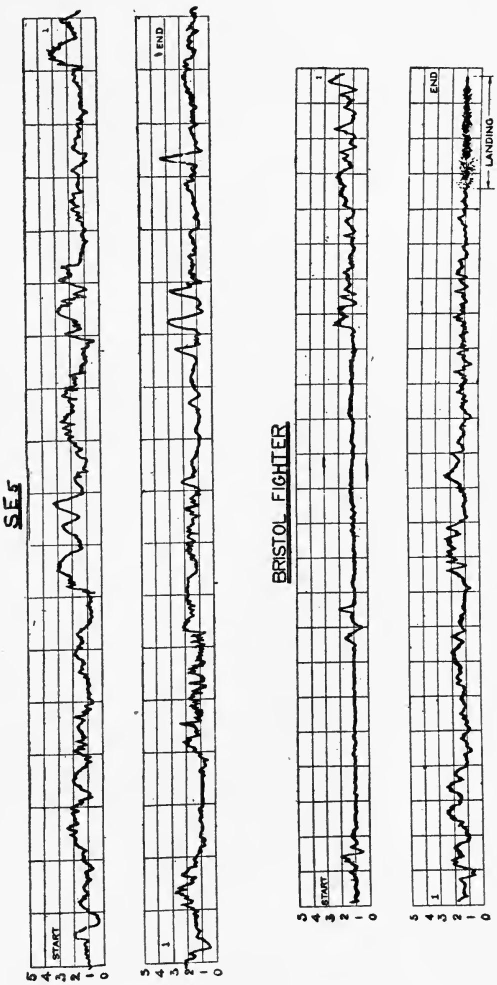

FIG. 119.—Accelerations on S. E. 5 and Bristol Fighter during a Mock Fight.

Accelerations in terms of *g*.

Vertical lines are drawn at intervals of approximately 15 seconds.

stress occurs during a loop, and is less than four times the weight of the machine. The diagrams indicate that the stresses in the machines keep remarkably steady during flight.

FIG. 120.—Accelerations and Air Speeds during Various Manœuvres on a Bristol Fighter.

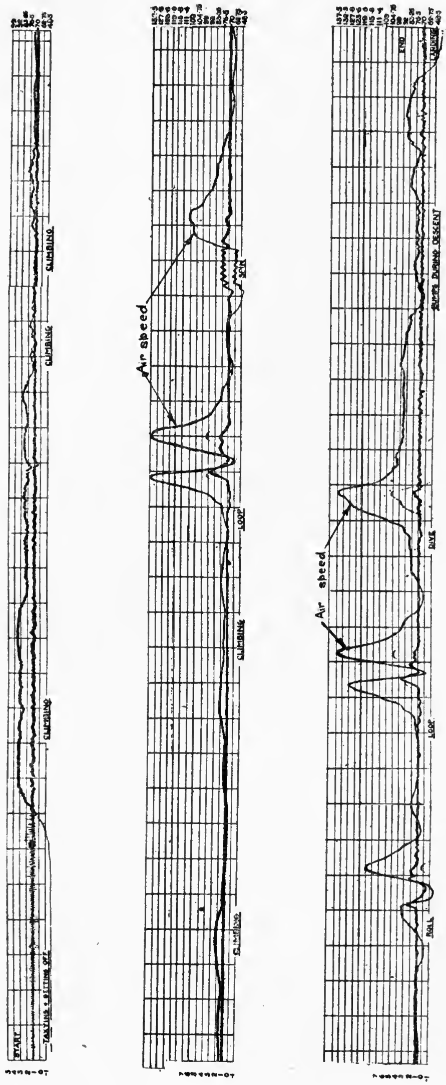

Air Speeds in M.P.H.

Accelerations in terms of *g*.

Vertical lines are drawn at intervals of approximately 15 seconds.

Accelerations in terms of *g*.

✓ **Stresses.**—The stresses to which the members of an aeroplane are subjected, and which it is necessary to consider in design, are as follows :—

1. Stresses set up in the wing structure during flight. These may be sub-divided into two classes :

(*a*) Those due to Lift and Down forces. These forces are principally transmitted by the external bracing of the machine.

(*b*) Those due to the Drag forces. These forces are transmitted by the internal (or the drag) bracing.

2. Stresses set up in the wing structure and under-carriage during landing. The resultant landing shock may be resolved into a vertical component known as 'down shock,' and a horizontal component known as 'end shock.' The extent of these forces is dependent upon the slope at which the machine descends, and the nature of the landing-ground.

3. Stresses set up in the fuselage due to the operation of the control surfaces, and to the thrust of the airscrew. When rotary engines are fitted, there are also gyroscopic effects developed.

The consideration of these stresses will be dealt with as follows : The stresses resulting from the various conditions arising in flight will be treated in this chapter ; those due to landing conditions will be considered in the chapter on the landing chassis ; while the fuselage stresses will be investigated in Chapter VII.

Stresses in the Wing Structure.—The process of determining the stresses in a wing structure consists of—

1. Finding what proportion of the load is carried by the various parts of the structure.

2. Determining what stresses these loads induce in the members of the structure.

In dealing with the first part of the problem it is necessary to know (*a*) the distribution of loading along the span of the wing ; (*b*) the distribution of the load over a section of the aerofoil.

The first of these two considerations is largely dependent upon what is termed 'end effect.' Unless specially determined data for the wing section to be used is known, it is customary to assume the load grading near the wing tips as being parabolic, the variation extending for a distance equal to the chord from the wing tips. We shall return to this point again later. The second consideration, the distribution of pressure over the wing section, has been fully considered in Chapter III. There remains to be determined what proportion of the load is carried by the spars at the minimum and maximum flying angles. This clearly depends upon the position of the centre of pressure of the section at these angles. The actual travel of the C.P. for the wing section adopted must be found by reference to its aerodynamical characteristics. In general, it is found that at large angles of incidence, corresponding to slow speeds, the C.P. is at about 0·3 × chord from leading edge, while at small angles and high speed it is at about 0·5 × chord. As an example, consider the wing section shown in Figure 121.

For a travel of the C.P. from 0·3 to 0·45 of the chord, we have—Maximum proportion of total load on front spar = (44 − 12·8)/44 = ·71; maximum proportion of total load on rear spar = (44 − 12)/44 = ·73.

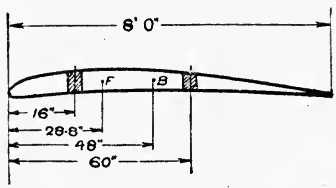

FIG. 121.

Care must of course be taken when determining these stresses that the most unfavourable condition is considered. Thus, in the above example, the front spars are stressed for the most forward position of the C.P.; while the rear spars are stressed for the most backward position of the C.P. In this manner the maximum possible stresses in either frame are determined.

Wing Loading.—Wing loading may be defined as the ratio weight of machine : area of supporting surface. Hence from the fundamental equation (Formula 1) we have

$$\frac{W}{A} = \text{loading} = \frac{\rho}{g} K_y V^2$$

The value of wing loading depends upon the maximum speed of the machine. For very fast machines the wing loading is high, while for a slow machine it is generally low. The advantage of a low value of wing loading is that it gives a large margin of safety against excessive loads. Such a machine will require more engine-power to fly at a given speed than will a machine with high wing loading. The general tendency to-day is to adopt a higher wing loading than was formerly used, and the majority of machines in present use have a wing loading factor of from 7 to 10 lbs. per square foot.

Table XXV., giving particulars of some of the leading machines of the day, is very instructive in this respect.

TABLE XXV.—WING LOADING OF MODERN MACHINES.

Machine.	Wing Area. Sq. feet.	Weight. Lbs.	Loading. Lbs. / sq. feet.
Airco 4	434	3340	7·4
Airco 9	438	3351	7·6
Airco 10	840	8500	10·12
A. R. (French)	484	2750	5·72
Avro	346	2680	8·23
A. W. Quadruplane	400	1800	4·5
Blackburn Kangaroo	868	8017	9·2
Breguet	528	3380	6·38
Bristol Fighter	405	2630	6·5
Bristol Monoplane	145	1300	8·97
Bristol Triplane	1905	16200	8·50
Bristol All Metal	458	2810	6·13
Caproni	990	8730	8·84
Caproni Triplane	2690	14630	5·45
Caudron	427	3170	7·42
Fokker Triplane	215	1260	5·9
F. F. Bomber (German)	750	6950	9·3
Handley Page O–400	1645	14000	8·5
Handley Page V–1500	2950	28000	9·5
Morane Parasol	145	1440	9·92
Nieuport	160	1200	7·47
S. E. 5	249	1980	8·0
Sopwith	344	2040	5·93
Sopwith Camel	231	1440	6·2
Sopwith Dolphin	258	1910	7·4
Sopwith Snipe	274	1950	7·1
Sopwith Triplane	251	1500	6·0
Spad	195	1550	8·08
Vickers' Commercial	1330	11120	8·4

Wing Weights.—The wing weight varies as the wing loading per square foot of surface, and ranges from 0·5 lbs. per square foot on small machines up to 1·4 lbs. per square foot on very large machines. The following formulæ for the weight of aeroplane wings are taken from the 1911–1912 N.P.L. Report:

1. Weight of Monoplane wing $= 0\cdot017\, W (A)^{\frac{1}{2}} + 0\cdot16\, A$
2. Weight of Biplane wing $= 0\cdot012\, W (A)^{\frac{1}{2}} + 0\cdot16\, A$

where W = weight of machine less the weight of the wings.
A = area of the wings in square feet.

The second term represents the weight of fabric in above formulæ. In Chapter I. we saw that the weight of the wing structure of modern machines is about 13 per cent. of their total weight. This figure represents the best that has been attained in practice so far, and is the result of much careful attention to detail, so that any improvement upon it will not be easy, but it should form a standard of reference to which to work.

Stresses due to Downloading.—In normal flight the resultant air force on the wings acts in an upward direction, thereby supporting the machine, in opposition to the force of gravity. Under certain circumstances, however, the pressure on the wings may be reversed in direction, as for instance when the elevator is depressed and the machine commences to dive. The force necessary to change the line of flight of the machine depends upon the radius of the turn with which the machine commences to dive. The centrifugal force upon the machine

$$= \frac{W V^2}{g R}$$

The reaction to this force must be provided by a down pressure on the wings. For example, let

P = force on wings.
W = weight of machine.
V = its velocity.
R = radius of flight path.

$$\text{Then} \quad P = W - \frac{W V^2}{g R} = W\left(1 - \frac{V^2}{g R}\right)$$

For the machine referred to in the consideration of factors of safety (p. 143), if flying at 100 m.p.h. and then suddenly directed downwards on a path of radius 170 feet, the downloading will be

$$= 1200\left(1 - \frac{147^2}{32\cdot2 \times 170}\right)$$

$$= 1200\,(1 - 3\cdot94) = -\,2\cdot94 \times 1200$$

or the downloading—indicated by the negative sign—is about three times the weight of the machine.

The effect of such downloading is to throw the downbracing wires, which are shown dotted in Fig. 122, into operation. A further instance of the occurrence of downloading stresses is during the time that the machine is resting on the ground, the downbracing wires then being loaded by the weight of the wing structure itself.

It is customary to design the wing structure for downloading on the assumption that the down forces are one-half as great as the maximum lift forces. This is conveniently accounted for by adopting a factor of safety equal to one-half that used for the lift forces.

Investigation of the stresses set up in the drag bracing of the wing structure will be dealt with later in this chapter, after the questions of duplication and stagger have been considered.

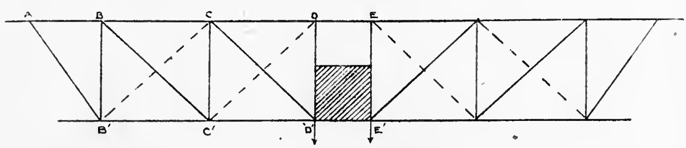

FIG. 122.

Stressing of the Wing Structure.—The method of drawing the stress diagrams for the external bracing system of an aeroplane is as follows.

The method adopted is similar for all types of machines, but as the biplane is the type in most general use, our attention will be confined to this type of structure for the present. The general procedure to be adopted will first be outlined, and then an example of its application to practice will be given.

(i.) NORMAL FLIGHT.—Let the total weight of the machine whose wing structure is to be designed be W, and let w be the weight of the wing structure alone. Then the load actually carried by the structure is $W - w$, since the wings themselves are directly supported by the air pressure, and thus relieve the struts and wires of having to transmit any stresses due to their weight. The air pressure is transmitted by the wing fabric to the ribs, which in turn transmit the load to the spars which are braced to the body.

An aeroplane being symmetrical about its longitudinal axis, it is only necessary to determine the stresses due to half the weight on one side of the machine. Consider a biplane as shown in Fig. 122. Let T be the area of top plane and B the area of lower plane.

We must first determine the proportion of the load carried by each plane. Owing to its greater area and also to biplane effect, the top plane will carry most of the load. Let e be the biplane coefficient, taken from the table given on page 78, for the particular ratio of gap/chord used.

$$\text{Then mean pressure over top plane} = P' = \frac{(W - w)}{(T + e\,B)}$$

$$\text{and mean pressure over lower plane} = P'' = e\,P'$$

$$\text{Therefore load on top plane} = W' = T\,P'$$

$$\text{load on lower plane} = W'' = B\,P''$$

The variation in load grading at the wing tips known as 'end effect' must now be taken into account. We shall assume the load grading over the outer section of the wing to be parabolic. The general result of this is to reduce the effective area of the planes. For this reason various shapes have been given to the wing tips in the endeavour to minimise this loss as much as possible; but it is very doubtful if these special shapes are worth the extra trouble and labour involved from the practical point of view. Let T′ and B′ be the effective areas of the top and bottom planes respectively, obtained from T and B by subtracting the area lost through end effect. Then we have

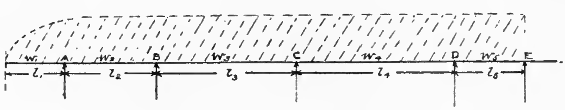

FIG. 123.

$$\text{Maximum pressure on top plane} = \frac{W'}{T'}$$

$$\text{Maximum pressure on bottom plane} = \frac{W''}{B'}$$

The curve of loading along the span can now be set out, since it is the product of the pressure per square foot and the chord length at that point. Curves for both the top and bottom planes must of course be drawn. They will be similar in nature to Fig. 123.

The next step is to determine the reactions at the supports. The spars approximate very closely to a continuous beam, and consequently the determination of the reactions involves the use of the Theorem of Three Moments as shown at D, Table XXII.

Graphical methods have been developed for determining these reactions, but for the simple loadings usually met with in aeronautical practice the Theorem of Three Moments is much quicker and simpler, and gives results which are quite satisfactory.

Let w_1, w_2, w_3, etc., be the loading per foot run over each bay, determined from the load curve previously drawn.

Considering first the top plane, let M_A, M_B, M_C, &c., be the bending moments at A, B, C, etc. See Fig. 123.

The bending moment at A is due to a varying upward load over a cantilever of length L_1, and must be determined by means of graphic integration if very accurate results are required. If the loading diagram be assumed parabolic over the outer section, the bending moment may be easily calculated. With this assumption, $M = W_1 L_1 \times 0.4 L_1$ where W_1 is the average loading over this span. Then bending moments at B, C, D, etc., are determined by applying the theorem of three moments.

For the spans A B, B C, we have, referring to Fig. 41,

$$M_A L_2 + 2 M_B (L_2 + L_3) + M_C L_3 - \tfrac{1}{4}(w_2 L_2^3 + w_3 L_3^3) = 0$$

For the spans B C, C D, we have, by a further application of the theorem,

$$M_B L_3 + 2 M_C (L_3 + L_4) + M_D L_4 - \tfrac{1}{4}(w_3 L_3^3 + w_4 L_4^3) = 0$$

For the spans C D, D E, by a further application,

$$M_C L_4 + 2 M_D (L_4 + L_5) + M_E L_5 - \tfrac{1}{4}(w_4 L_4^3 + w_5 L_5^3) = 0$$

Since the wing span is symmetrical, the support moment at D equals the support moment at E, and the support moment at A has previously been determined. Hence we have three equations to determine the three unknown moments at B, C, D. These can be easily obtained by successive substitution in the above equations.

Knowing the bending moments at the supports, it is now easy to determine the various reactions by taking moments.

Let R_A, R_B, R_C, &c., be the reactions. Then taking moments about B for the reaction at A, we have

$$w_1 L_1^1 (0.4 L_1 + L_2) + \frac{W_2 L_2^2}{2} - R_A L_2 = M_B$$

$$\text{or} \quad R_A = \frac{w_1 L_1 (0.4 L_1 + L_2) + \frac{W_2 L_2^2}{2} - M_B}{L_2}$$

Again taking moments about C for R_B, we have

$$w'_1 L_1 (0 . 4 L_1 + L_2 + L_3) + w'_2 L_2 \left(\frac{L_2}{2} + L_3\right) + \frac{W_3 L_3^2}{2}$$
$$- R_A (L_2 + L_3) - R_3 L_3 = M_C$$

Proceeding in this manner the reaction at each support can be obtained.

The formulæ look somewhat formidable, but their application is quite simple, and, with practice, both bending moments and reactions can be determined very quickly. The application of the theorem of three moments as used above assumes that the points of support are in the same straight line. In practice this is frequently not the case, the most notable difference being obtained after the process of tuning-up. Considerable errors are likely to be introduced in this manner, and if it is impossible to avoid this occurring a fresh set of bending moments must be obtained, assuming each point of support to be out of the straight line by say $\frac{1}{2}''$—this will produce large differences. In this case the more general form of the theorem of three moments must be used, namely:—

$$\frac{6 A_2 \bar{x}_2}{L_2} + \frac{6 A_3 \bar{x}_3}{L_3} + M_A L_2 + 2 M_B (L_2 + L_3) + M_C L_3$$
$$+ 6 E I \left(\frac{\delta_2}{L_2} + \frac{\delta_3}{L_3}\right) = 0 \quad \text{............ Formula 47}$$

where A_2, A_3 denote areas of free bending moment diagrams over second and third spans

$\bar{x}_2$ denotes the position of the C.G. of A_2 from the support A

$\bar{x}_3$ denotes the position of the C.G. of A_3 from the support C

δ_2 denotes the distance of B below A

δ_3 denotes the distance of B below C

A further proviso in the application of this theorem is that the bracing wires are attached in such a manner that the reactions pass through the neutral axis of the spar. In practice this is not always easy to obtain, and in such cases the Bending Moment diagrams will be somewhat modified.

Having determined the reactions at each support, the stress diagrams for the structure considered as a single vertical frame with pin joints can now be drawn as shown in Chapter II. An example of such a diagram is shown in Figs. 22 and 125.

(ii.) Downloading.—The procedure adopted in determining the stresses due to downloading is exactly similar to that outlined above for normal flight. In this case the reactions at the points of support will be downward.

Reference has already been made to the fact that it is customary to design the wing structure for downloading forces of one-half those obtained in normal flight. As the application of the centre of pressure and factor of safety is being left over until the question of detail design of the members is being considered, the reactions due to downloading may with advantage be set out equal in magnitude but opposite in direction to the lift reactions. The stress diagrams for downloading can now be drawn. It must be remembered in this case that it is the downbracing wires which are in operation. Fig. 126 illustrates a downloading stress diagram.

Illustrative Example.—Before proceeding to show how to determine the detailed stresses in each member of the wing structure, we will illustrate the methods just described by means of a practical example, and draw the stress diagrams for the external bracing of the biplane shown in Fig. 124 (*a*) and (*b*). The weight of the machine is 2000 lbs. and the weight of the wing structure is 300 lbs., the chord of the wings is 6 ft., span of top plane 40 ft., span of lower plane 31 ft.

Area of Top Plane.			Area of Bottom Plane.	
Overhang	$= 2\frac{1}{4} \times 6$	$= 13{\cdot}5$	Overhang 2×6	$= 12$
AB	$= 4 \times 6$	$= 24$	B′C′	$= 39$
BC	$= 6{\cdot}5 \times 6$	$= 39$	C′D′	$= 36$
CD	$= 6 \times 6$	$= 36$		
$\frac{1}{2}$ DE	$= \frac{1}{2}(2{\cdot}5 \times 6)$	$= 7{\cdot}5$		
		120		87

Distribution of load over upper and lower planes: Upward force to be distributed $= 2000 - 300 = 1700$ lbs.

$= 850$ lbs. per side.

Biplane effect: The ratio of gap/chord is unity, hence from Table on p. 78 the factor is $0{\cdot}82$

$$\therefore \text{ Average pressure top plane } = \frac{850}{120 + {\cdot}82 \times 87} = 4{\cdot}44 \text{ lbs./sq. ft.}$$

and average pressure on bottom plane $= 0{\cdot}82 \times 4{\cdot}5 = 3{\cdot}67$ lbs./sq. ft

and load on top plane $= 4{\cdot}44 \times 120 = 532$ lbs.

load on bottom plane $= 3{\cdot}67 \times 87 = 318$ lbs.

Total $= 850$ lbs.

FIG. 124

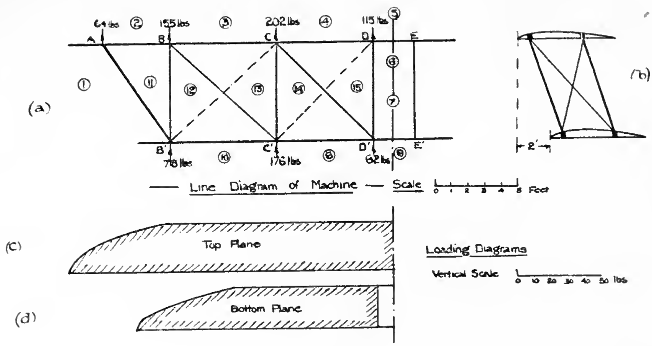

Fig. 125

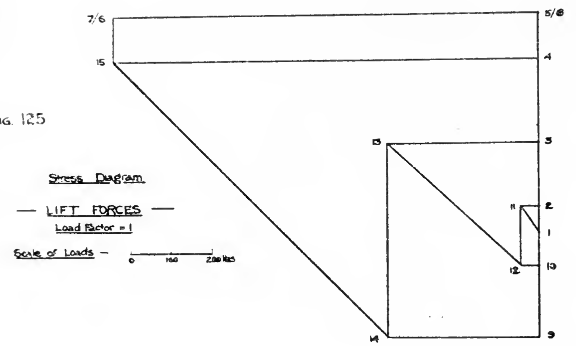

Member		Load
1 11	Strut	+ 80
11.12	"	− 142
13.14	"	− 472
15 6	"	+ 115
12 13	Lift Wire	+ 440
14 15	"	+ 950
2.11	Spar	− 45
3.13	"	− 370
4.15	"	− 1040
12 10	"	+ 45
14.9	"	+ 370
5 6	"	− 1040
7.8	"	− 1040

NB + Indicates Tension
− " Compn.

Fig. 126

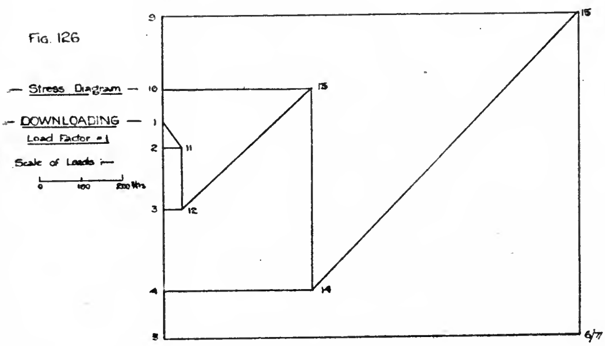

Member		Load
1 11	Strut	+ 80
11 12	"	− 155
13 14	"	− 490
15. 6	"	+ 790
12. 13	Down Wire	+ 456
14.15	"	+ 940
2. 11	Spar	+ 45
3 12	"	+ 45
4. 14	"	+ 360
5. 6	"	+ 1020
13. 10	"	− 360
15.9	"	+ 1020
7.8	"	+ 1020

FIGS. 124 to 126.—Method of setting-out Stress Diagrams.

Reduction of effective area due to end effect. Assuming parabolic loading over the outer 6 ft. (= chord) of each plane,

The equivalent loss in area $= 6 \times 6 \times \cdot 33 = 12$ sq. ft , and
hence the effective area of the top plane $= 120 - 12 = 108$ sq. ft.
and of lower plane $= 87 - 12 = 75$ sq. ft.

$\therefore$ Maximum pressure on top plane $= \frac{532}{108} = 4\cdot 94$, say 5 lbs./sq. ft.

Maximum pressure on bottom plane $= \frac{318}{75} = 4\cdot 25$ lbs./sq. ft.

The loading diagram for the planes can now be drawn as in Fig. 124 (*c*) (*d*), since load per foot run equals pressure at that point multiplied by the width of the chord, which in this example is constant and equal to 6 feet.

Having determined the load distribution, we can proceed to find the Fixing or Support Moments.

From Fig. 124 (*c*) the load on the overhang $= \frac{2}{3}(2\cdot 25 \times 30 \times \cdot 6) = 27\cdot 0$ lbs.

Bending Moment at A due to this load $= 27\cdot 0 \times \frac{2}{5} \times 2\cdot 25$
$= 24\cdot 3$ ft. lbs.
$= M_A$

Applying Theorem of Three Moments to the spans A B, B C, we have

$$4\,M_A + 2\,M_B\,(4 + 6\cdot 5) + M_C\,(6\cdot 5) - \tfrac{1}{4}\,(24\cdot 4 \times 4^3 + 30 \times 6\cdot 5^3) = 0$$

or $21\,M_B + 6\cdot 5\,M_C = 2350$ .... (1)

For the spans B C, C D, we have

$$6\cdot 5\,M_B + 2\,M_C\,(6\cdot 5 + 6) + 6\,M_D - \tfrac{1}{4}\,[30\,(6\cdot 5^3 + 6^3)] = 0$$

or $6\cdot 5\,M_B + 25\,M_C + 6\,M_D = 3675$ .... (2)

For the spans C D, D E, we have

$$6\,M_C + 2\,M_D\,(6 + 2\cdot 5) + 2\cdot 5\,M_E - \tfrac{1}{4}\,[30\,(6^3 + 2\cdot 5^3)] = 0$$

or $6\,M_C + 17\,M_D + 2\cdot 5\,M_E = 1730$ .... (3)

From symmetry $M_D = M_E$

$\therefore M_D = \dfrac{1730 - 6\,M_C}{19\cdot 5}$ .... (4)

Substituting for M_D in (2) we have

$$6\cdot 5\,M_B + 25\,M_C + 532 - 1\cdot 85\,M_C = 3675$$

$\therefore M_C = \dfrac{3143 - 6\cdot 5\,M_B}{23\cdot 15}$ .... (5)

Substituting for M_C in (1) we have

$$21\ M_B + 884 - 1{\cdot}83\ M_B = 2350$$

or $$19{\cdot}17\ M_B = 1466 \qquad \therefore\ M_B = 77 \text{ ft. lbs.}$$

Substituting this value in (5)

$$M_C = \frac{3143 - 500}{23{\cdot}15} = 114 \text{ ft. lbs.}$$

Substituting this value in (4)

$$M_D = \frac{1730 - 685{\cdot}}{19{\cdot}5} = 54 \text{ ft. lbs.}$$
$$= M_E$$

We can now determine the Reactions.

Taking moments about B for R_A

$$27\ \{4 + \tfrac{2}{3}\ (2{\cdot}25)\} + 100 \times 2 - 4\ R_A = M_B$$

or $$132 + 200 - 4\ R_A = 77$$

whence $R_A = 64$ lbs.

Taking moments about C for R_B

$$27\ \{4{\cdot}9 + 6{\cdot}5\} + 100 \times 8{\cdot}5 + \frac{30 \times (6{\cdot}5)^2}{2} - 10{\cdot}5\ R_A - 6{\cdot}5\ R_B = M_C$$

or $$308 + 850 + 634 - 672 - 6{\cdot}5\ R_B = 114$$

whence $R_B = 155$ lbs.

Taking moments about D for R_C

$$27\ (11{\cdot}4 + 6) + 100 \times 14{\cdot}5 + 30 \times 6{\cdot}5 \times 9{\cdot}25 + \frac{30 \times 6^2}{2}$$
$$- 16{\cdot}5\ R_A - 12{\cdot}5\ R_B - 6\ R_C = M_D$$

or $$470 + 1450 + 1800 + 540 - 1050 - 1940 - 6\ R_C = 54$$

whence $R_C = 202$ lbs.

Taking moments about E for R_D

$$27\ (17{\cdot}4 + 2{\cdot}5) + 100 \times 17 + 30 \times 6{\cdot}5 \times 11{\cdot}75 + 180 \times 5{\cdot}5$$
$$+ \frac{30 \times (2{\cdot}5)^2}{2} - 19\ R_A - 15\ R_B - 8{\cdot}5\ R_C - 2{\cdot}5\ R_D = M_E$$

or $$538 + 1700 + 2290 + 990 + 94 - 1215 - 2330$$
$$- 1720 - 2{\cdot}5\ R_D = 54$$

whence $R_D = 115$ lbs.

Sum total of Reactions = 64 + 155 + 202 + 115 = 536 lbs.

The load on the top plane was found to be 532 lbs. The slight difference is due to the fact that the loading was taken at 5 lbs. per square foot instead of the more accurate figure of

4·94 lbs. per square foot. The total sum of the reactions should always be checked in this manner.

In a similar manner the fixing moments and reactions at the lower plane supports can be determined. It should be noted that there are no lift forces over the portion D′E′, which represents the base of the fuselage. The reactions are:

$$R_{B'} = 78 \text{ lbs.}; \ R_{C'} = 176 \text{ lbs.}; \ R_{D'} = 62 \text{ lbs.}$$

The vertical reactions due to the lift forces being known, the next step is to draw the stress diagrams on the assumption that the frame is pin-jointed. The front elevation of the machine is set out to scale, and the stress diagram for the lift forces drawn in the usual manner, as shown in Fig. 125. In some cases it may be found more convenient to draw a diagram for both front and rear frames separately, by applying the requisite C.P. factor to give the maximum loading on each; but in this example a single diagram will suffice, and the stresses in each frame can be determined by applying the correct coefficients afterwards. Having completed the diagram, the stresses in each member due to the lift forces in horizontal flight should be tabulated.

The stress diagram for the downloading forces is shown in Fig. 126.

General Procedure for Design of the Members of the Wing Structure.—From the stress diagrams of the machine, considered as a single vertical frame and with a loading on the wings equal to its weight, the actual loads in the various members—upon which their design is, of course, based—are determined by applying the necessary centre of pressure coefficients and the requisite factor of safety. For all front-frame members of the wing structure the maximum stresses will be incurred with the most forward position of the centre of pressure during flight, and the maximum stresses in the members of the rear frame of the wing structure will be incurred with the most backward position of the centre of pressure during flight. As will be seen later, however, this condition of affairs may be modified by the method of duplication which is employed. By reference to the characteristics of the aerofoil which has been selected the travel of the C.P. is known, and hence the maximum proportion of the load which can fall on either front or rear frame can at once be determined in the manner shown on page 149.

As the factor of safety to be adopted is complicated by the method of duplication employed, this question will now be considered.

DUPLICATION OF THE EXTERNAL WING BRACING.—The possibility of having one or other of the wing-bracing members shot away, or otherwise rendered inoperative in flight, makes it necessary to consider this eventuality when designing a machine. In certain cases it is desirable to provide an alternative path whereby the lift reactions on the wing may be transferred to the body. Such duplication provides an additional safeguard against the failure of a bracing wire or fitting due to faulty material or bad workmanship. Two methods of duplication are in general use:—

1. *Direct duplication, in which method two wires are inserted one behind the other, and each one capable of taking two-thirds of the maximum load likely to fall on this member.* In the event of one wire failing, the other wire will transmit the load; but the system would now have a factor of safety of only two-thirds that

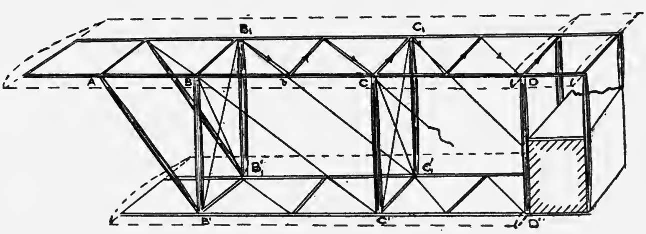

FIG. 127.—Transmission of Forces in Biplane Truss with Broken Wire.

of its previous value. In large machines these two wires should be faired off to an approximate streamline shape, in order to keep down the resistance, which would otherwise be considerably increased.

2. *Duplication through the Incidence Bracing.*—In this method the load originally carried by the broken wire is transmitted through the incidence wire to the corresponding unbroken frame, and from thence to the body. Reference to Fig. 127 will make this method clear. Suppose, for example, that the lift wire C D′ is broken. Originally this wire was transmitting the lift reactions at A, B, B′, C, C′, down to the body at D′. After it is broken these reactions are carried by the incidence wire C C′ down to the point C_1', whence they are transmitted up the rear strut $C_1 C_1'$, and thence by way of the rear lift wire $C_1 D_1'$ down to the body. In a similar manner if the rear wire $C_1 D_1'$ be broken, then the load previously carried by this wire is transmitted by the incidence wire $C_1 C'$ to the point C′, and thence by

way of the front strut and lift wire down to the body at the point D′. Since it is possible for any one of the external bracing wires, either 'lift' or 'down,' to be put out of action, it is necessary to consider the case of each wire separately and to examine what effect will be produced upon the remaining members of the structure in each contingency. The factor of safety with one wire broken is generally taken as two-thirds that when all the wires are intact. From the diagram it is clear that the main bracing, incidence bracing, and drag bracing are all affected, so each will be considered in turn.

(a) *Effect on the Main Bracing.*—It has already been shown that in the event of the lift wire C D′ being broken the lift reactions in the previous bays of the front frame will be transmitted to the rear frame by the incidence wire. This will result in a much greater load on the rear strut $C_1 C_1'$ the increased load being the sum of these reactions. The value of these reactions, however, depends upon the position of the centre of pressure of the air forces, and thus there are three cases to be considered in the design of wing structures when this method of duplication is adopted. For the biplane truss illustrated in Fig. 127 these cases are:—

i. With the C.P. forward and reduced factor of safety.

ii. With the C.P. rearward and reduced factor of safety.

iii. With the C.P. rearward, the structure intact, and the maximum factor of safety.

In case (ii.) the load transferred from the front frame will be less than in case (i.), but the loads due to the outer lift reactions on the back frame will be greater than in case (i.). Moreover, the reduced factor of safety used in the first two cases may lead to the conditions of case (iii.) being the criteria to adopt for design, and only a numerical determination will establish which condition produces the maximum stress in the strut and wire. The problem is not a difficult one, though somewhat more involved than that obtained when direct duplication is employed. The example given later in this chapter will help to clear up any difficulties.

(b) *Effect on the Incidence Bracing.*—When the wing structure is intact there are no stresses in the incidence bracing due to air forces. Their function under such conditions is principally to make the structure rigid. With one of the main bracing wires broken, however, the corresponding incidence wire is called upon to carry its load and it must therefore be designed for this purpose. The load in the incidence wire will be the sum of the reactions in the frame to the left of the broken wire resolved in its direction. For example, if *a b* (Fig. 128) represent the sum of such reactions, then *b c* will represent the corresponding stress in the incidence wire. The horizontal component *a c* of tension in the incidence wire is taken by the drag bracing which must now be considered.

(c) *Drag Bracing.*—The general form of the wing-drag bracing is shown in Figs. 108, 139.

It is general practice to assume the maximum drag force to be uniformly distributed on the wings of a machine, and to be equal to one-seventh of its total weight, and to design on this basis. Here again the method of duplicating the lift and down bracing wires will largely influence the design. With the incidence wires in operation, there will be a component of their tension acting in the plane of the drag bracing, and hence this must be sufficiently strong to transmit the resulting shear along to the centre section. The simplest method of determining the stresses in the drag bracing will be to draw the stress diagram,

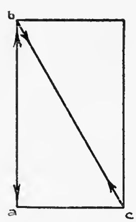

FIG. 128.

applying the forces due to the incidence bracing at the correct points of application. Referring to Fig. 127, if we suppose the front lift wire B C′ to be broken, and the incidence wire $B B_1'$ to be transmitting the lift forces from the front to the rear frame: the resulting tension in $B B_1'$ will cause an unbalanced force in the direction of the arrow, and the frame would therefore become distorted unless some means were provided to counteract this force. The drag bracing wire $B_1 b$ offers the best means of providing the necessary reaction and the shear will be transmitted along the path indicated by the arrows. The stresses set up in the drag bracing in this manner will be very much greater than those due to the drag forces alone, and the drag bracing will therefore need to be made correspondingly stronger.

Change of Direction of Drag Forces in the Wing Structure.—At first sight it would appear that the component of the drag forces in a wing structure always acted from the front to the rear of the wing. This, however, is not the case, as was pointed out on p. 60. The following example further illustrates this effect as influenced by the resistance of the bracing wires.

From the R.A.F. 6 aerofoil characteristics we find that the ratio L/D at 12° angle of incidence is 11. Making an allowance for the resistance of the bracing wires, this ratio will be taken as 10. Next set out the values of the lift and drag perpendicular and parallel to the air stream respectively. From Fig. 45 it will be seen that the resultant force on the section is forward of the normal to the chord line. For such an attitude of the wings, therefore, the component of the drag forces is acting in a forward direction. For the purposes of design work it is best to assume that the drag forces act in such a direction that they cause the greatest stress in the spars.

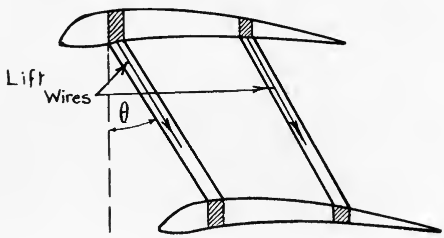

FIG. 129.

A moment's consideration will show that for the back spar design the drag forces should be acting in the direction shown in Fig. 127, and that for the front spar they should act in the opposite direction. This is because the spars are almost invariably designed to resist compression, and consequently the drag forces should act in such a manner as to increase this compression.

Stagger.—The effect of stagger upon the stresses set up in a wing structure is to introduce another factor to be applied to the loads obtained from the stress diagram of the vertical frame already discussed. Reference to Fig. 129 will make this clear. It will be seen from this figure that the vertical reaction of the lift forces is resisted by the lift bracing, which is inclined at an angle θ to the vertical. As a result of this the stresses obtained from the diagram for the vertical frame bracing must be multiplied by the factor $1/\cos\theta$ for the case of the staggered machine.

Moreover, it will be apparent that, on account of the line of pull of the lift wires not being in the same plane as that of the lift forces, there will result a horizontal component of the lift in the direction of the drag bracing $= L \tan \theta$, where L is the lift reaction at the joint considered; and the drag bracing must therefore be sufficiently strong to transmit the shear resulting from these horizontal components in addition to that due to the ordinary drag forces. This is illustrated in Fig. 129 (*a*).

Similarly at the lower plane joints the lift reaction is transmitted by means of the inclined strut to the top joint where the lift wire is attached. Hence the stress in the struts obtained from the vertical frame diagram must also be multiplied by the factor $1/\cos \theta$. Also there will be a backward component $= L' \tan \theta$ to be taken by the lower plane drag bracing where

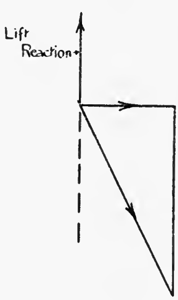

FIG. 129 (*a*).

FIG. 129 (*b*).

L′ is the lift reaction at any lower plane point of support. (See Fig. 129 (*b*).)

The method of determining the stresses in the wing structure of a staggered machine may therefore be summarised as follows :—

(i) *Lift Bracing and Interplane Struts.*—Multiply the loads obtained from the vertical stress diagram by the factor $\frac{1}{\cos \theta}$ where θ is given by the relationship $\tan \theta = \frac{\text{stagger}}{\text{gap}}$

(ii) *Drag Bracing.*—To the ordinary drag loads due to resultant air forces add a component equal to $L \tan \theta$ at each point of attachment of wing bracing, where L is the reaction at the joint considered, and draw stress diagrams for combined reactions. An example of this is shown in Fig. 146.

It should be noted that in the case of the downloading forces on a staggered machine the downbracing loads must be multiplied by the factor $1/\cos\theta$, while the horizontal component in the direction of the drag bracing will act in the opposite direction to that when the lift wires are in operation. A separate stress diagram for drag bracing of a staggered machine must therefore be drawn for downloading conditions.

Detail Design of the Wing Structure.—The various cases likely to be met with in stressing a wing structure having been considered, the detail design of the various members can be investigated. From the previous paragraph we see that the actual maximum loads for which it is necessary to design each member can be obtained by applying:

(*a*) The requisite C.P. coefficient;
(*b*) The necessary factor of safety; and
(*c*) Stagger coefficient in the case of a staggered machine, to the load obtained from the stress diagram drawn for unit load.

These detail members comprise:

1. The lift and down bracing.
2. The incidence bracing.

} These can be grouped together under the general heading of External Bracing.

3. The interplane struts.
4. The drag struts and drag bracing.
5. The spars.

The External Bracing.—The most common method of bracing the wing structure is by means of high tensile streamline wires or rafwires, of which particulars are given in Table XXVI.

These wires are rolled out of circular section, down to the shape shown in Fig. 130 (*a*) and (*b*), by means of specially shaped rollers, the process being termed 'swaging.' This process has the effect of making the steel very brittle, and also sets up initial strains in the material. It is therefore necessary to subject the wires to heat treatment, which consists of placing them in a bath of molten lead or in boiling salt solution, where they are allowed to remain until they have acquired the uniform temperature of the bath, after which they are removed and allowed to cool slowly. Previous to this heat treatment the yield point and the ultimate stress point are practically coincident, and there is no appreciable extension before fracture. The breaking stress of the wire in this condition is very often in the neighbourhood of 100 tons per square inch. After heat treatment the yield and ultimate stress points are much reduced, the latter being about 70 tons per square inch; but there is now an extension of from 15% to 20% on a gauge length of 8″.

TABLE XXVI.

SIZE		RAFWIRES		TIE RODS	TENSILE STRENGTH
Dia of Thread L.H. or R.H.	Length of Thread	Section of Streamline: Major Axis	Section of Streamline: Minor Axis	Dia of Rod (circular)	lbs
4 B.A	1·0″	0·17″	0·06″	0·10″	1050
2 B.A	1·1″	0·18″	0·07″	0·135″	1900
1/4″ B.S.F	1·3″	0·4″	0·09″	0·182″	3450
9/32″ "	1·4″	0·47″	0·10″	0·211″	4650
5/16″ "	1·5″	0·50″	0·11″	0·234″	5700
11/32″ "	1·6″	0·57″	0·13″	0·262″	7150
3/8″ "	1·7″	0·60″	0·14″	0·285″	8500
13/32″ "	1·8″	0·73″	0·15″	0·310″	10250
7/16″ "	1·9″	0·75″	0·16″	0·340″	11800
15/32″ "	2·0″	0·78″	0·17″	0·360″	13800
1/2″ "	2·0″	0·80″	0·18″	0·380″	15500

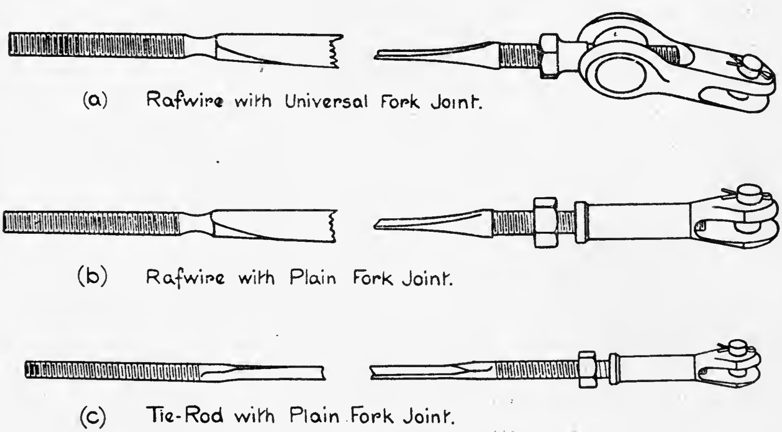

FIG. 130.—Bracing Wires and Tie-rods.

The ends of the wires are left circular, and are finally screwed with right- and left-hand threads respectively, which screw into plain or universal fork joints as shown in Fig. 130 (*a*) and (*b*). These fork joints are in turn pin-jointed to the wiring plates at the points of attachment to the wing structure.

Another method of external bracing is by means of stranded wires. The strands manufactured by Messrs. Bruntons, of Musselburgh, are illustrated in Fig. 131 : *a* is a section which should be used only in those places where little wear takes place. These strands combine strength and flexibility, and can be obtained in any required size. They do not deteriorate so rapidly as a rafwire, because in the latter type of bracing there is a certain amount of crystallisation due to the vibration. Further, if a single tie-rod has a slight nick upon its surface

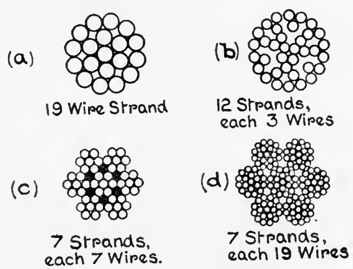

FIG. 131.—Bracing Cables (Brunton's).

it is liable to snap under a sudden accidental, but not necessarily severe, strain. In the case of a strand such a nick would mean the severance of one or two wires only, and would not greatly impair the strength of the complete strand.

Table XXVII. gives some details relating to the sizes, weights, and strength of the strands illustrated in Fig. 131.

TABLE XXVII.—PARTICULARS OF STRANDS FOR AIRCRAFT PURPOSES.

Size. Circumference in inches.	Weight per 100 feet. lbs.	Breaking strength. lbs.
$\frac{1}{4}$	1	784
$\frac{3}{8}$	2	1332
$\frac{1}{2}$	3·33	1904
$\frac{5}{8}$	5·5	2576
$\frac{3}{4}$	8·0	5152
$\frac{7}{8}$	12·5	7056
1·0	16·66	10080

These strands are tightened by the insertion of strainers or turnbuckles, a standard type of which is shown in Fig. 132. Details of these turnbuckles are incorporated in Table XXVIII.

An illustration of their use is given in Fig. 138 at *q*, *r*, *s*. In general the barrel portion is made of gun-metal, and the eye and fork portions of steel.

TABLE XXVIII.—STRAINERS.

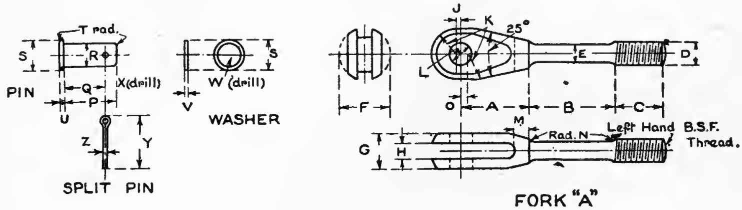

FORK A.

Diam. of Thread.	Dimensions.	A.	B.	C.	D.	E.	F.	G.	H.	J.	K	L.	M.
	Tolerances.	+ ·015 − 0.	+ ·04 − 0.	+ ·04 − 0.		+ ·002 − ·002.	+ ·015 − 0.	+ ·015 − 0.	+ ·015 − 0.			+ ·001 − 0.	+ ·015 − 0.
	Min. Strength.	Ins.	Ins.	Ins.	B.S.F. Ins.	Ins.	Ins.	Ins.	Ins.	Ins.	Ins.	Ins.	Ins.
$\frac{1}{2}$	95 cwt.	1·5	1·6	1·0	$\frac{1}{2}$	·418	1·08	·7	·3	·07	·54	·5	·2
$\frac{7}{16}$	72 ,,	1 4	1·5	·875	$\frac{7}{16}$	·365	·95	·65	·25	·06	·475	·438	·2
$\frac{3}{8}$	52 ,,	1·2	1·3	·75	$\frac{3}{8}$	·309	·8	·55	·2	·06	·4	·375	·2
$\frac{5}{16}$	34 ,,	1·0	1·2	·65	$\frac{5}{16}$	·252	·7	·475	·2	·05	·35	·312	·2
$\frac{9}{32}$	29 ,,	·9	1·1	·60	$\frac{9}{32}$	·23	·65	·45	·2	·04	·325	·281	·2
$\frac{1}{4}$	21·5 ,,	·8	1·1	·5	$\frac{1}{4}$	·20	·56	·42	·2	·04	·28	·250	·2
2 BA	11·5 ,,	·7	1·1	·4	2 BA	·147	·43	·31	·15	·04	·215	·187	·2
4 BA	6·7 ,,	·6	1.0	·35	4 BA	·11	·38	·26	·12	·04	·19	·156	·2

Diam. of Thread.	Dimensions.	N.	O.	P.	Q.	R.	S.	T.	U.	V.	W.	X.	Y.	Z.
	Tolerances.			+ ·01 − 0.	+ ·01 − 0.	+ 0 − ·001.	+ ·015 − 0.		+ ·01 − 0.	+ ·01 − 0.				
	Min. Strength.	Ins.	Ins.	Ins.	Ins.	Ins.	Ins.	Ins.	Ins.	Ins.	Ins.	Ins.	Ins.	Ins.
$\frac{1}{2}$	95 cwt.	·25	·17	·96	·86	·498	·64	·05	·1	·08	$\frac{1}{2}$	$\frac{3}{32}$	1	$\frac{3}{32}$
$\frac{7}{16}$	72 ,,	·2	·16	·91	·8	·436	·56	·05	·1	·07	$\frac{7}{16}$	$\frac{3}{32}$	$\frac{15}{16}$	$\frac{3}{32}$
$\frac{3}{8}$	52 ,,	·2	·16	·9	·7	·373	·52	·025	·1	·07	$\frac{3}{8}$	$\frac{3}{32}$	$\frac{7}{8}$	$\frac{3}{32}$
$\frac{5}{16}$	34 ,,	·15	·15	·71	·59	·310	·41	·025	·07	·05	$\frac{5}{16}$	$\frac{1}{16}$	$\frac{3}{4}$	$\frac{1}{16}$
$\frac{9}{32}$	29 ,,	·1	·14	·68	·56	·279	·38	·025	·07	·05	$\frac{9}{32}$	$\frac{1}{16}$	$\frac{5}{8}$	$\frac{1}{16}$
$\frac{1}{4}$	21·5 ,,	·075	·14	·65	·53	·248	·35	·025	·07	·05	$\frac{1}{4}$	$\frac{1}{16}$	$\frac{5}{8}$	$\frac{1}{16}$
2 BA	11·5 ,,	·075	.14	·53	·42	·185	·3	·025	·07	·05	$\frac{3}{16}$	$\frac{1}{16}$	$\frac{1}{2}$	$\frac{1}{16}$
3 BA	6· ,,	·07	·14	·48	·37	·154	·245	·025	·07	·05	$\frac{5}{32}$	$\frac{1}{16}$	$\frac{1}{2}$	$\frac{1}{16}$

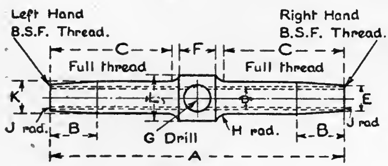

BARREL "B".

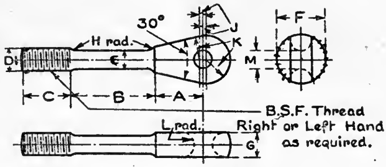

All holes must not be more than ·01" off ℄ of turnbuckle.

EYE "C".

Barrel B.

Dimensions.	A.	B.	C.	D.	E.	F.	G.	H.	J.	K.	L.
Tolerances.	+ ·08 − 0.	+ 0 − ·04.	+ ·04 − 0.		+ ·015 − 0.					+ ·015 − 0.	+ ·015 − 0.
Diam. of thread.	Ins.	Ins.	Ins.	B.S.F. Ins.	Ins.	Ins.	Ins.	Ins.	Ins.	Ins.	Ins.
$\frac{1}{2}$	5·75	1·0	2·35	$\frac{1}{2}$	·61	·75	$\frac{17}{32}$	·25	·07	·73	1·0
$\frac{7}{16}$	5·25	·875	2·1	$\frac{7}{16}$	·54	·6	$\frac{15}{32}$	·2	·06	·64	·86
$\frac{3}{8}$	4·5	·75	1·8	$\frac{3}{8}$	·45	·55	$\frac{13}{32}$	·2	·05	·55	·78
$\frac{5}{16}$	4·1	·65	1·6	$\frac{5}{16}$	·37	·5	$\frac{11}{32}$	·15	·05	·45	·64
$\frac{9}{32}$	3·7	·6	1·45	$\frac{9}{32}$	·35	·45	$\frac{5}{16}$	·1	·05	·42	·60
$\frac{1}{4}$	3·5	·5	1·4	$\frac{1}{4}$	·3	·4	$\frac{9}{32}$	·075	·05	·36	·52
2 BA	3·3	·4	1·4	2 BA	·23	·3	$\frac{7}{32}$	·075	·05	·28	·45
4 BA	3·0	·35	1·28	4 BA	·2	·24	$\frac{5}{32}$	·075	·05	·25	·37

Eye C.

Dimensions.	A.	B.	C.	D.	E.	F.	G.	H.	J.	K.	L.	M.
Tolerances.	+ ·015 − 0.	+ ·04 − 0.	+ ·04 − 0.		+ 002 − 002.	+ ·015 − 0.	+ ·015 − 0.			+ ·015 − 0.		+ ·015 − 0.
Diam. of thread.	Ins.	Ins.	Ins.	B.S.F. Ins.	Ins.	Ins.	Ins.	Ins.	Ins.	Ins.	Ins.	Ins.
$\frac{1}{2}$	1·0	1·6	1·0	$\frac{1}{2}$	·418	1·1	·55	·25	·07	·55	·275	·40
$\frac{7}{16}$	·9	1·5	·875	$\frac{7}{16}$	·365	·96	·48	·2	·06	·48	·24	·35
$\frac{3}{8}$	·8	1·3	·75	$\frac{3}{8}$	·309	·82	·41	·2	·06	·41	·205	·30
$\frac{5}{16}$	·65	1·2	·65	$\frac{5}{16}$	·252	·68	·34	·15	·05	·37	·17	·25
$\frac{9}{32}$	·55	1·1	·6	$\frac{9}{32}$	·23	·58	·29	·1	·04	·29	·145	·225
$\frac{1}{4}$	·5	1·1	·5	$\frac{1}{4}$	·20	·50	·23	·075	·04	·25	·115	·20
2 BA	·45	1·1	·4	2 BA	·147	·40	·19	·075	·04	·2	·095	·15
4 BA	·45	1·0	·35	4 BA	·11	·40	·19	·07	·04	·2	·095	·15

Fig. 132.—Complete Strainers.

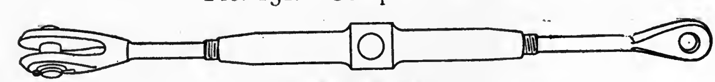

Forked one end.

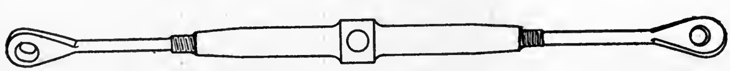

Double eye.

The Interplane Struts.—Investigations have been carried out in order to determine the best shape of strut for aeronautical work, and an account of some of these experiments will be given in Chapter VI. The essential features of such a strut are low resistance and small variation of resistance with change of angle of yaw of the machine. The researches have shown that the nose of the strut should not be too blunt, while the rear portion may be given an almost straight taper from the point of maximum thickness at about one-third the length of the strut from the leading edge, right down to the rear or trailing edge.

The type of strut most frequently met with in practice at the present time is the solid streamline spruce strut tapering from a maximum section at the centre of its length down to both of its ends. With large machines considerations of weight make it necessary that these struts should be made hollow, or that

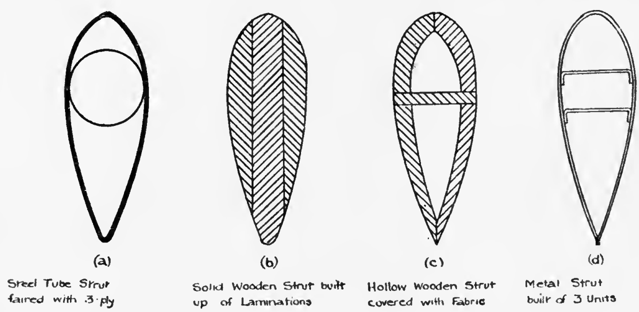

Fig. 133.—Types of Strut Sections.

an alternative form of construction should be adopted. This alternative form may consist of a steel circular tube faired to a streamline shape by means of three-ply wood—see Fig. 133 (*a*)—or a built-up section secured by glue and fabric—see Fig. 133 (*c*). Steel struts have also been designed, and Fig. 133 (*d*) shows such a strut. It is composed of three units, produced entirely by mechanical processes, the second diaphragm being added to give greater rigidity and strength. The units are blanked out and formed in presses, and then united by spot welding. The total weight is 3·15 lbs., against 3·25 lbs. for a wooden strut; while the failing load is ·77 tons, against ·475 tons for a wooden strut.

The design of a tapered strut is a matter requiring considerable care, for unless the correct taper is used throughout, the strength of the strut may be considerably reduced, so that the final result would be much worse than using a parallel strut.

With the correct taper, it is possible to obtain a reduction in weight of 13 %, and a reduction in resistance of 8 % over the parallel strut of the same strength. A theory for the design of

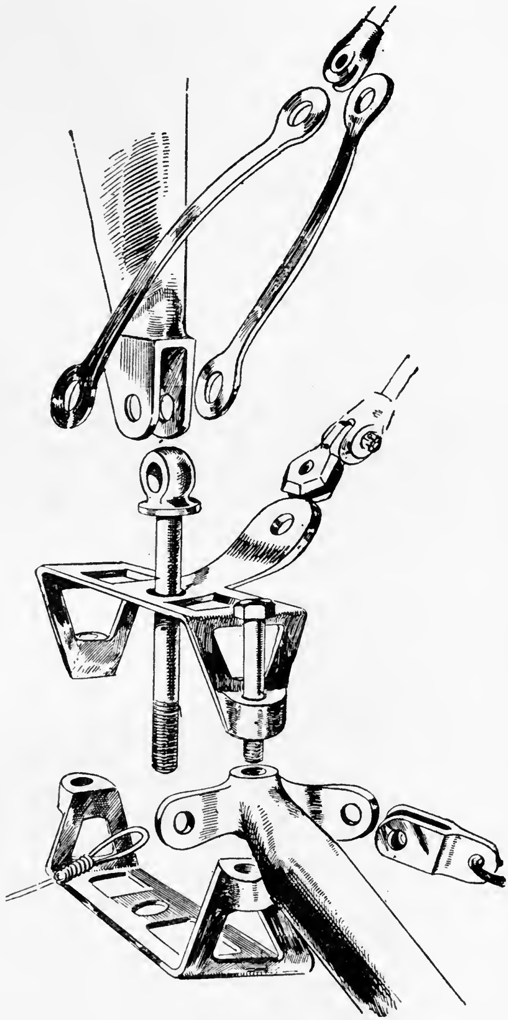

Reproduced by courtesy of 'Flight.'

FIG. 134 (*a*).—Analytical Sketch of Interplane Strut Attachment, Lift Wire Attachment, Internal Drag Bracing, and Drag Strut.

such struts which has been found to give good results in practice has been developed by Messrs. Barling and Webb, and an account is given in the *Aeronautical Journal* for October, 1918. As it

TYPES OF STRUT FITTINGS.

(*Reproduced by courtesy of 'Flight.'*)

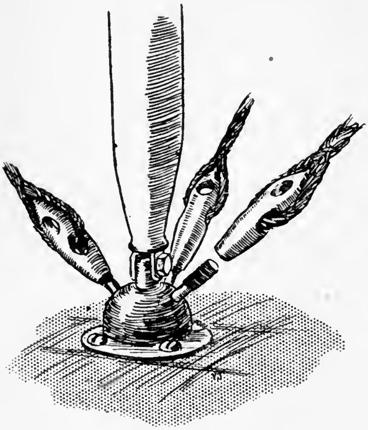

FIG. 134 (*b*).

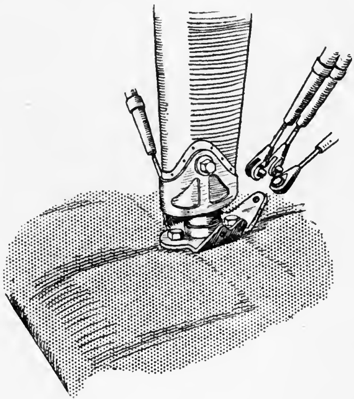

FIG. 134 (*c*).

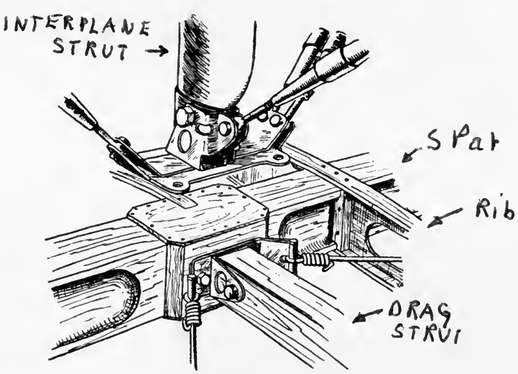

FIG. 134 (*d*).—Sketch showing Attachment of Interplane Strut and Drag Strut to Main Spar.

seems probable that this theory will be considerably used in the future design of tapered struts, the main outlines of this theory are included here, and later on in this chapter an example is given showing how to manipulate the complicated-looking equation in actual practice. It should be noted that the theory holds for struts of any regular cross section in which a curve can be drawn connecting the Moment of Inertia with thickness.

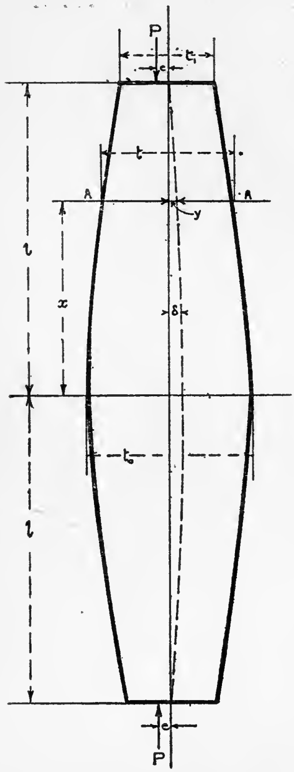

FIG. 135.—Tapered Strut.

Tapered Strut Formula.—*Derivation of Expression for the Meridian Curve.*—The strut is assumed to have frictionless pin-joints. It deflects under an end load of P lbs., the eccentricity of the load being e inches.

For a given cross section of the strut at a distance of x inches from the centre, the following notation is used. (See Fig. 135.)

Total length of strut ...	=	$2\,l$ ins.
Maximum thickness perpendicular to Neutral Axis	=	t ,,
Moment of Inertia of cross section about N.A.	=	I in.^{4} units
Area of cross section...	=	A sq. ins.
Deflection under the load P	=	y ins.

For any particular case, A and I will be functions of t.

The lateral load on strut = w lbs. per inch length of strut

$$\therefore \text{Total lateral load on strut} = \int_{x=-l}^{x=l} w\,t\,d\,x \text{ lbs.}$$

For the purposes of this investigation, w is supposed to be a function of x; if all the sections of the strut are similar, and the lateral load is due to wind pressure, then w is constant.

The *Meridian Curve* of the strut is defined as the curve whose ordinates are $t/2$, and whose abscissæ are x.

It is now required to find the shape of this curve, so that under the influence of the end load P, the maximum compressive stress at every cross section of the strut

$$= f \text{ lbs. per square inch}$$

The bending moment at a cross section such as A A

$$= \left\{ P(y + e - \int_0^x \int_0^x w\,t\,dx\,.\,dx \right\}$$

Maximum compressive stress at this cross section

$$= \frac{P(y+e) - \int_0^x \int_0^x w\,t\,dx\,.\,dx\}\,t}{2\,I} + \frac{P}{A}$$

$$= f \qquad \ldots\ldots\ldots\ldots \quad (1)$$

Omitting expression for lateral load, this becomes

$$= \frac{P(y+e)\,t}{2\,I} + \frac{P}{A} = f \qquad \ldots\ldots\ldots\ldots \quad (2)$$

That is $\quad yt + et = \frac{2\,I}{P}\left(f - \frac{P}{A}\right)$

or $\quad y = \frac{1}{t}\left\{\frac{2\,I}{P}\left(f - \frac{P}{A}\right) - et\right\}$

$$= \mathrm{f}(t) - e$$

whence $\quad \frac{d^2 y}{dx^2} = \frac{d^2}{dx^2}\left[\mathrm{f}(t)\right]$

The bending moment equation now becomes

$$= -\,E\,I\frac{d^2}{dx^2}\mathrm{f}(t) = P(y+e) = \frac{2\,I}{t}\left(f - \frac{P}{A}\right)$$

that is $\quad \frac{d^2}{dx^2}\mathrm{f}(t) = -\frac{1}{E}\cdot\frac{2}{t}\left(f - \frac{P}{A}\right) \qquad \ldots\ldots\ldots\ldots \quad (3)$

Let $\quad \mathrm{f}(t) = z$ and substitute,

then $\quad \frac{d^2 z}{dx^2} = -\frac{1}{E}\phi(z)$

To solve this differential equation,

let $\quad \frac{dz}{dx} = p$

then $\quad \frac{d^2 z}{dx^2} = \frac{dp}{dx} = \frac{dp}{dz}\cdot\frac{dz}{dx} = p\frac{dp}{dz}$

$\therefore \quad p\frac{dp}{dz} = -\frac{1}{E}\phi(z)$

or $\quad p\,.\,dp = -\frac{1}{E}\phi(z)\,dz$

integrating $\quad \frac{1}{2}p^2 = -\frac{1}{E}\int_0^t \phi(z)\,dz + C_1$

To determine C_1 we have from Fig. 135:

when $x = 0; \ \dfrac{dt}{dx} = 0$

and $t = t_0; \ p = \dfrac{dz}{dx} = \dfrac{dz}{dt} \cdot \dfrac{dt}{dx} = 0$

$\therefore$ $C_1 = \dfrac{1}{E}\displaystyle\int_0^{t_0} \phi(z)\,dz$

and $p = \sqrt{\dfrac{2}{E}\displaystyle\int_t^{t_0} \phi(z)\,dz}$

whence $x = \displaystyle\int \frac{dz}{\sqrt{\frac{2}{E}\int_t^{t_0} \phi(z)\,dz}} + C_2$

Also when $t_0 = t; \ x = 0$

$\therefore$ $C_2 = \displaystyle\int_t^{t_0} \frac{dz}{\sqrt{\frac{2}{E}\int_t^{t_0} \phi(z)\,dz}}$

Inserting value of z from (3), we get

$$x = \sqrt{\frac{E}{P}} \int_t^{t_0} \frac{\frac{d}{dt}\left\{\frac{1}{t}\left(1 - \frac{P}{fA}\right)\right\} dt}{\sqrt{\int_t^{t_0} \frac{1}{I} \cdot \frac{d}{dt}\left\{\frac{1}{t}\left(1 - \frac{P}{fA}\right)\right\}^2 dt}} \qquad (4)$$

.... Formula 64

Equation (4) will determine the cross section t at any distance x from centre. If the effect of the lateral load be included, this equation becomes

$$x\sqrt{\frac{P}{E}} =$$

$$\int_t^{t_0} \frac{\left[\frac{d}{dt}\left\{\frac{1}{t}\left(1 - \frac{P}{fA}\right)\right\}\right] dt}{\sqrt{\int_t^{t_0} \frac{1}{I}\frac{d}{dt}\left\{\frac{1}{t}\left(1 - \frac{P}{fA}\right)\right\}^2 dt + \int_0^{t_0} \frac{E\ wt}{Pf} \cdot \frac{d}{dt}\left\{\frac{1}{t}\left(1 - \frac{P}{fA}\right)\right\} dt}}$$

Formula 65 .... (5)

Since at the end of the strut $x = l$, and $y = 0$ we have from (1)

$$\frac{I_1}{t_1}\left\{1 - \frac{P}{fA}\right\} = \frac{Pe}{2f} \qquad \ldots\ldots\ldots\ldots (6)$$

an equation which gives t_1.

Substituting $x = l$ and $t = t_1$ in either (4) or (5), we have an equation which theoretically determines t_0

The percentage reduction of the crippling load of a tapered strut due to the lateral wind load w is given approximately by the expression

$$\frac{3}{4} \cdot \frac{fA_0}{P} \text{ if } \frac{P}{fA_0} > 0{\cdot}05 \qquad \ldots\ldots\ldots\ldots (7)$$

A_0 representing the area of the section where the thickness is t_0.

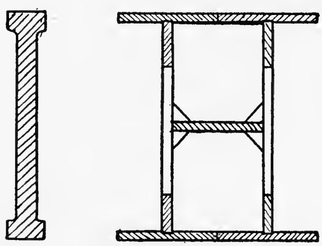

FIG. 136. FIG. 137.

Compression Rib Sections.

Investigations upon a number of struts have shown that this correction is practically negligible except for the wing struts of high-speed machines. For this reason the term containing w has been neglected in the illustrative example showing the practical application of the above theory to an actual strut, which is set out in full later in this chapter.

The Drag Struts and Bracing.—For small machines the general method of taking the shear due to the drag loads and components of the lift reactions is by means of compression ribs. These ribs have the correct contour of the wing section, and their web is made solid in order to resist the compression. The section of such a rib is as shown in Fig. 136.

A stronger and better method than this is illustrated in Fig. 137, in which two ordinary ribs with lattice webs are placed adjoining one another. Such an arrangement is considerably lighter than that shown in Fig. 136.

For larger machines it becomes necessary to build hollow wooden struts of circular or box section, or tubular steel struts may be used. It will generally be found that the wooden construction will prove the lightest for a given strength. Particulars of steel tubes which may be used for such purposes are given in Appendix.

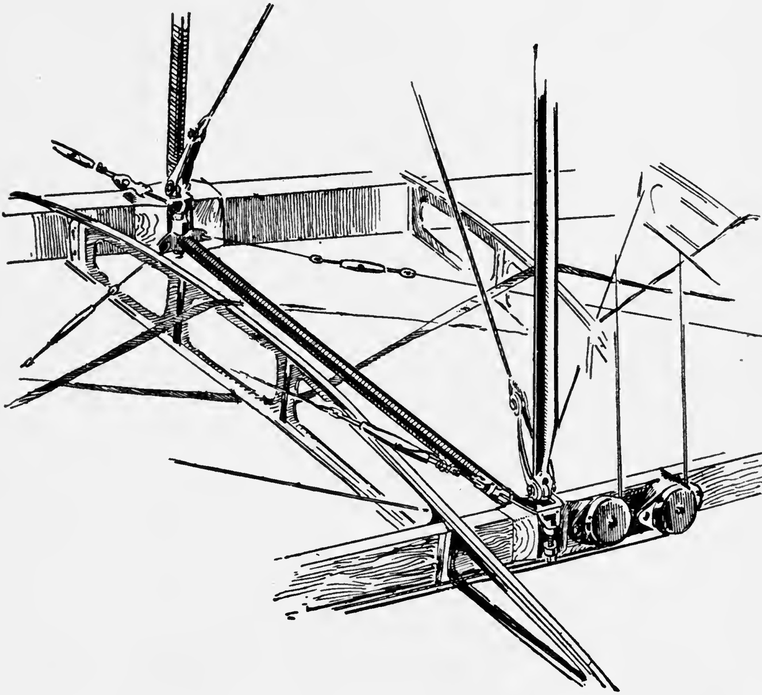

Reproduced by courtesy of 'Flight.'

FIG. 138.—General Sketch of Internal Bracing and of Interplane Strut Attachment.

Their use and mode of attachment is shown in Fig. 138.

The Drag Bracing wires usually take the form of small circular tie-rods screwed at each end, as shown in Fig. 130 (*c*), particulars of which are given in Table XXVI.

The general arrangement of a drag strut and fitting is shown in Figs. 138 and 139.

Design of the Spars.—The spars are the most important members of the wing structure, and much care must therefore be exercised in their design in order that the necessary strength may be obtained for the minimum possible weight. The larger the machine and the deeper the wing section employed the more economically can the spars be designed, but even in this case it is not easy to reduce the weight of the spars alone to less than one-third of the total weight of the wing structure. In

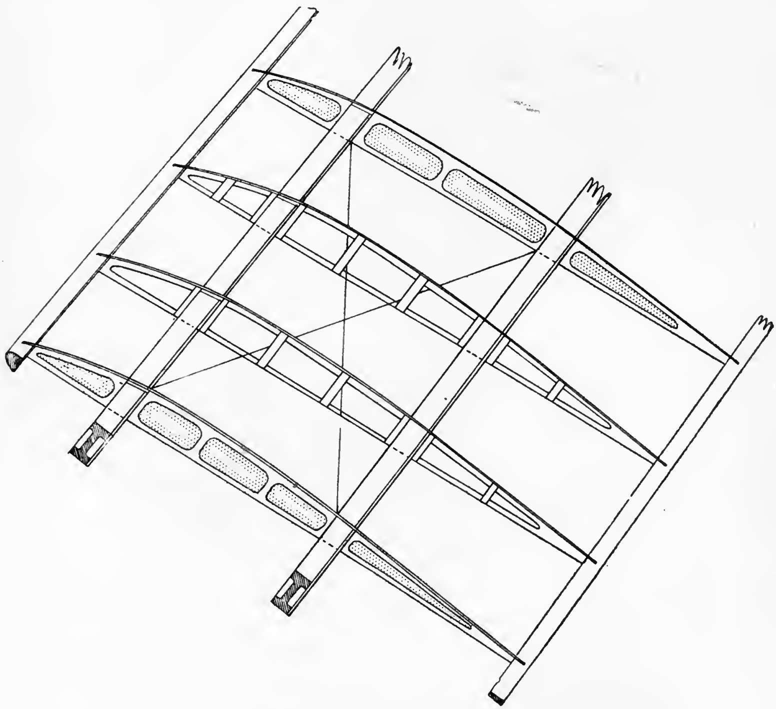

FIG. 139.—Internal Wing Structure.

small machines the weight of the spars may amount to as much as one-half of the total weight of the wing structure. A small percentage of saving in the weight of the spars will therefore be relatively of much more importance than a similar percentage saving in any other members of the wing structure.

Spars are subject to (*a*) Bending stresses, (*b*) Direct end loads.

The bending stresses result from the uniform distribution of the air forces along the wing section, and the spars therefore correspond, as shown in Chapter IV., to a continuous beam uniformly loaded and supported at various points by means of the wing bracing, and the complete bending moment diagrams are drawn upon this assumption by the methods outlined in that chapter. From the diagram so obtained the bending moment is shown at all points along the span, and the bending stresses can therefore be calculated from Formula 51.

Complete bending moment diagrams for the top and bottom plane spars of a small machine are shown in Fig. 147.

Bending stresses are set up by the lift forces, down forces, and drag forces. The drag forces are in the plane perpendicular to the other two forces, but they are usually so small that they can be neglected in ordinary practice.

Direct end loads are the horizontal components of the tension in the wing bracing both external and internal. A reference to the stress diagrams for vertical frames shows that in normal flight the top plane spars are in direct compression owing to these end loads while the lower plane spars are in tension. In cases of downloading these end loads are reversed in direction. For the end loads due to drag bracing it will be seen that with drag forces acting from front to rear, the rear spars are in compression and the front spars are in tension; and that these directions are reversed when the drag loads act from back to front. The actual loads are obtained from the stress diagrams for the respective cases from which the resultant stress at any section of the spar is obtained by dividing the load by the cross-sectional area at that point.

The total stress in the spar at the point considered is therefore

$$= f = \frac{My}{I} + \frac{F}{A} \qquad \text{............ Formula 66}$$

If the spars are made of silver spruce, the total stress obtained from Formula 66 must not exceed 4500 lbs. per square inch for compression, or 11,000 lbs. per square inch for tension.

Correction Factor to be applied to the Bending Moment at the Centre of Spans.—The effect of the distributed load along the spans will be to produce a deflection at the centre of each bay relative to the points of support where the external bracing is attached. As a result the bending moment at the centre of the span will be increased if the end load is compressive, and diminished if the load is tensile, by an amount which is equal to the end load multiplied by the deflection.

In order to allow for this a correction factor is applied to the bending moments at the centre of the spans, namely:

$$\frac{P_E}{P_E - P} \qquad \text{............ Formula 67}$$

where $P_E = \frac{2\pi^2 E I}{L^2} =$ crippling load of spars considered as a strut, using Euler's formula

and P = end load.

This factor will be greater than unity with compressive end loads and less than unity with tensile end loads.

Some typical wooden spar sections are shown in Fig. 140 ***a***, *b*, *c*. From the equation for bending stress (Formula 66) it is obvious that in order to keep the stress low the moment of inertia must be large, therefore the material must be concen-

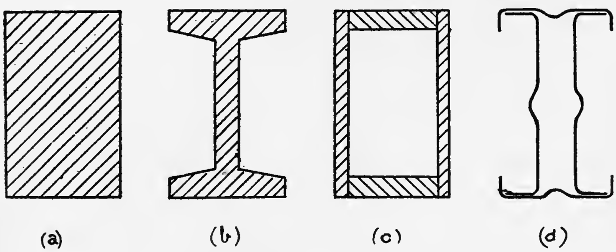

FIG. 140.—Typical Spar Sections.

trated as far as possible from the neutral axis. This is why an 'I' (see '*b*' in Fig. 140), or a 'box' (see '*c*' in Fig. 140) section is preferable to the rectangular section shown at '*a*' in Fig. 140. It is on this account that the thin wing possesses unduly heavy spans, and of course where the depth is small the rear span is very difficult to design. The spar shown at '*d*' in Fig. 140 is made of No. 22 S.W.G. sheet steel, being built up of two corrugated channel sections to form the web, and riveted to two corrugated flange plates at either end. Such a spar can be made very light, is easy to manufacture, and it is very probable that the near future will see a large development of steel spars built up in this manner.

A very interesting type of spar section and internal wing arrangement is that adopted on the Fokker wireless triplane, which is illustrated in Fig. 141. As will be seen from this figure, the two spars (each of the box type) are placed very close together, and then the two box sections are united by a sheet of three-ply covering. As a result of this uncommon arrangement all internal wing bracing has been avoided.

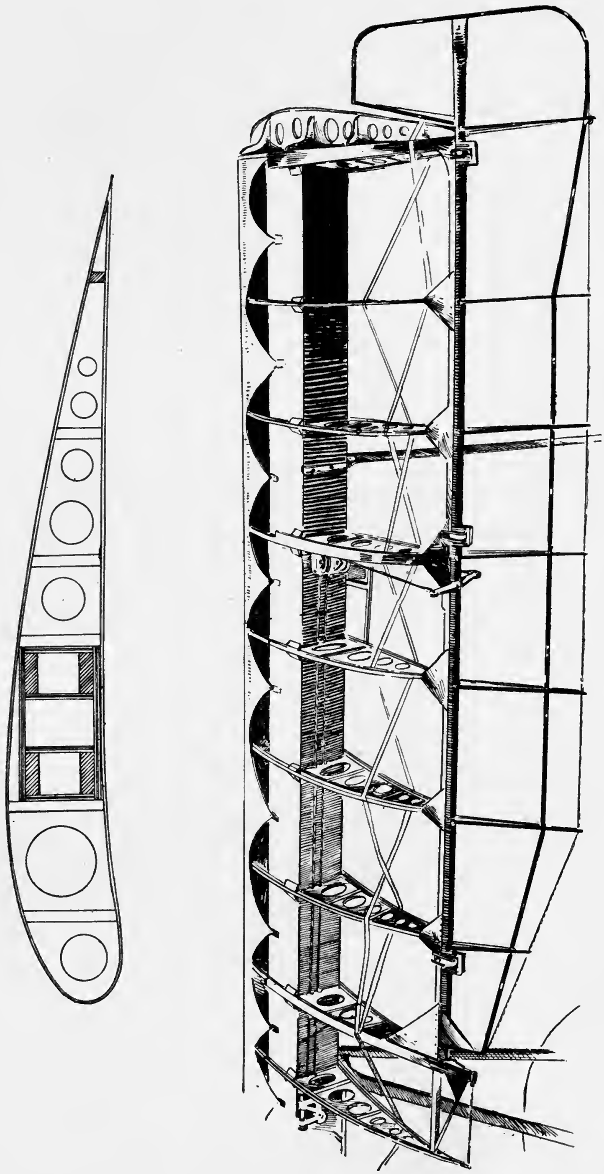

FIG. 141.—Wing and Rib of Fokker Machine.

Practical Example of Wing Structure Design.—The preceding work upon the detailed design of the wing structure members will now be applied to the machine for which the preliminary stress diagrams have already been drawn and shown in Figs. 125 and 126.

The wing section chosen for this machine is the R.A.F. 6, shown in Fig. 40.

NORMAL FLIGHT.—The travel of the C.P. is from ·3 to ·55 of the chord—that is, for a six-foot chord from 21·6″ to 39·6″ from the leading edge.

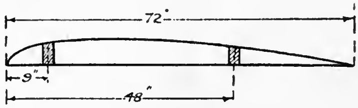

FIG. 142.

Spacing the spars as shown in Fig. 142,

The maximum proportion of the load on front spar

$$= \frac{39\cdot 0 - 12\cdot 6}{39} = 68\%$$

and the maximum proportion of load on rear spar

$$= \frac{39\cdot 0 - 8\cdot 4}{39} = 79\%$$

A factor of safety of 7 will be used throughout, and the method of duplication employed will be direct.

The factor due to stagger $= \frac{1}{\cos \theta} = \frac{1}{0\cdot 95} = 1\cdot 053$

Hence the maximum load in the front frame members

$=$ load in vertical frame from stress diagram $\times 7 \times \cdot 68 \times 1\cdot 053$

$= 5 \times$ stress diagram load

and the maximum load in the rear frame members

$=$ stress diagram load $\times 7 \times \cdot 79 \times 1\cdot 053$

$= 5\cdot 82 \times$ stress diagram load.

DOWNLOADING.—The position of the centre of pressure for downloading may be taken at ·25 chord, or at 18″ from the leading edge.

The maximum proportion of downloading on front frame

$$= \frac{39 - 9}{39} = 77\%$$

whence proportion for the rear frame $= 23\%$

The maximum load on the front frame downbracing

$$= \text{downloading stress diagram load} \times \frac{7}{2} \times \cdot 77 \times 1 \cdot 053$$

$$= 2 \cdot 84 \times \text{downloading stress diagram load}$$

and maximum load on rear frame downbracing

$$= \text{downloading stress diagram load} \times 3 \cdot 5 \times \cdot 23 \times 1 \cdot 053$$

$$= 0 \cdot 85 \times \text{downloading stress diagram load.}$$

Proceeding to detail design and inserting two wires each capable of taking two-thirds of the maximum load, we have

External Bracing.

Member.	Stress Diagram Load.	Front Frame.		Rear Frame.	
		Maximum Load.	Size of Wire.	Maximum Load.	Size of Wire.
		Factor 5·0		Factor 5·82	
Lift wire B C[1]	440	2200	2 – 2 B.A.	2560	2 – 2 B.A.
Lift wire C D[1]	950	4750	2 – ¼″ B.S.F.	5520	2 – 9/32″ B.S.F.
		Factor 2·84		Factor ·85	
Down wire C B[1]	435	1235	2 – 4 B.A.	370	2 – 4 B.A.
Down wire D C[1]	940	2670	2 – 2 B.A.	800	2 – 4 B.A.

Design of the Interplane Struts.—The load on the interplane struts for various flight conditions follows directly from the stress diagrams.

Interplane Struts.

Strut.	Load from Stress Diagram.		Maximum Loads.	
			Front Frame.	Rear Frame.
A B[1]	Lift forces	+ 80 lbs.	+ 400 lbs.	+ 465 lbs.
	Down forces	– 80 „	– 227 „	– 68 „
B B[1]	Lift forces	– 142 „	– 710 „	– 827 „
	Down forces	– 155 „	– 440 „	– 132 „
C C[1]	Lift forces	– 472 „	– 2360 „	– 2750 „
	Down forces	– 490 „	– 1390 „	– 417 „
D D[1]	Lift forces	+ 115 „	+ 575 „	670 „
	Down forces	– 790 „	– 2240 „	– 670 „

The loads for which it is necessary to design each strut are underlined. With regard to the strut A B[1], it is necessary to design this for the downloading forces because this strut is certain to fail under compression and not under tension.

In order that the theory of the tapered strut already outlined in this chapter may be fully appreciated, and the complicated results obtained made available for general design of struts, its use will be illustrated in the design of the strut C C[1].

Design of the Interplane Strut C C[1], according to the tapered strut formulæ given on pages 174–176 :—

Length of strut	...	...	6 ft. 4 ins.
Maximum compression		...	2800 lbs
Fineness ratio ...	...	...	3·5 : 1
Form of cross section as shown in Fig. 91.			
Area of cross section ...		...	$2{\cdot}5\,t^2$
Least moment of inertia		...	$= 0{\cdot}15\,t^4$

Taper to be from a maximum at the centre cross section down to the points of support.

In order to find t_0 and the correct taper of the strut, it is necessary to apply the theory shown on pages 174–176. At first sight this would appear to be a difficult process, but by taking each equation separately, and dealing with these portions in the manner indicated, the solution of the whole equation can be obtained without any knowledge of advanced mathematics, although, as will be seen, the process is somewhat lengthy.

Consider first the expression

$$\frac{d}{dt}\left\{\frac{I}{t}\left(1 - \frac{P}{fA}\right)\right\}$$

This expression represents the rate of change of the slope of the function

$$\frac{I}{t}\left(1 - \frac{P}{fA}\right)$$

with respect to t. In order to obtain this rate of change it is therefore necessary to draw the curve of this function, and measure its slope at various values of t. Alternatively, but by taking much smaller intervals, the value of this slope could be obtained by tabular integration in the manner shown for bending moments and deflections in Chapter IV. The work preparatory to graphing the function should be set out in the following manner:

t ...	1	1·25	1·5	1·75	2·0
t^2 ...	1	1·56	2·25	3·06	4·0
t^4 ...	1	2·44	5·06	9·40	16·0
$A = 2·5\,t^2$	2·5	3·92	5·63	7·65	10·0
$I = 0·15\,t^4$	0·15	0·366	0·76	1·41	2·4
$\frac{I}{t}$	0·15	0·293	0·506	0·805	1·2
$\frac{P}{fA} = \frac{2800}{5500\,A}$	0·204	0·13	0·0905	0·0665	0·051
$1 - \frac{P}{fA}$	0·796	0·87	0·9095	0·9335	0·949
$\frac{I}{t}\left(1 - \frac{P}{fA}\right)$	0·1193	0·255	0·46	0·751	1·14

The curve for this function can now be plotted from these figures. The next step is to draw the tangents to the curve for the values of t taken. These tangents give the slope of the curve at these points, that is, they give the value of the expression

$$\frac{d}{dt}\left\{\frac{I}{t}\left(1 - \frac{P}{fA}\right)\right\}$$

as below:

t ...	1	1·25	1·5	1·75	2·0
$\frac{d}{dt}\left\{\frac{I}{t}\left(1 - \frac{P}{fA}\right)\right\}$	0·44	0·72	0·94	1·35	1·82

and from these values the graph of the expression can be drawn. (See Fig. 143.)

The denominator of the equation

$$\sqrt{\int_t^{t_0} \frac{1}{I}\left[\frac{d}{dt}\left\{\frac{I}{t}\left(1 - \frac{P}{fA}\right)\right\}\right]^2 dt}$$

must next be considered, and examination of this expression shows that it is required to find the square root of the area of the curve represented by the expression

$$\frac{1}{I}\cdot\frac{d}{dt}\left\{\frac{I}{t}\left(1 - \frac{P}{fA}\right)\right\}^2$$

between the values of t and t_0. The value of t_0 is being sought, so that two or three other values of t must now be chosen and used to arrive at the value t_0 required. The method of procedure will be clear as the example progresses. Referring to the above expression it is seen that it represents the rate of change of slope of the square of the expression whose value has just been found multiplied by $1/I$.

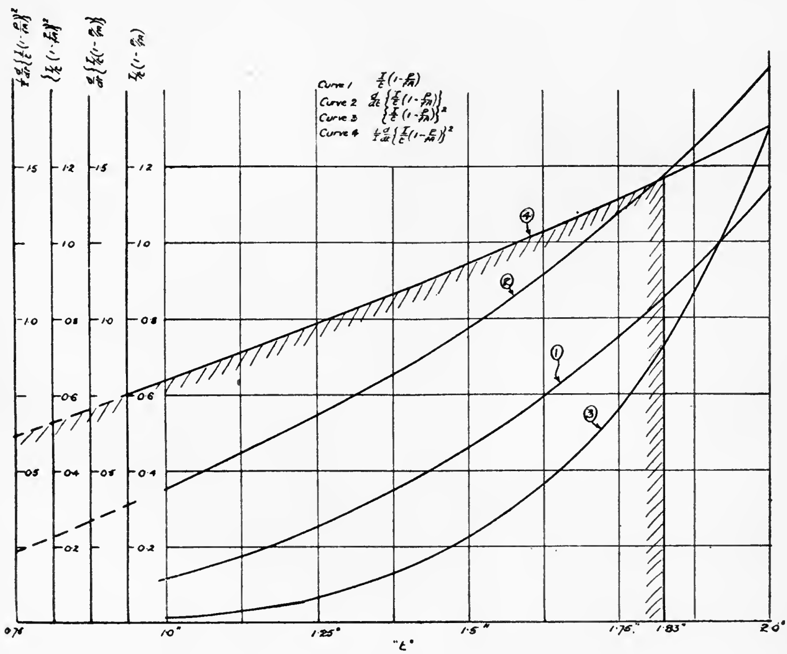

FIG. 143.

It is therefore necessary to square the various values obtained for

$$\frac{I}{t}\left(1 - \frac{P}{fA}\right)$$

and then to draw the curve for the results obtained, draw the tangents for the values of t under consideration, and then to measure the slopes of the tangents obtained as in the work dealing with the numerator. The values so obtained are then multiplied by $1/I$, and from the results the graph of the complete expression can be drawn. The tabular arrangement of the work is shown below, and the various curves are shown in Fig. 143.

t	...	1	1·25	1·5	1·75	2·0
$\left\{\frac{1}{t}\left(1-\frac{P}{fA}\right)\right\}^2$		0·1425	0·65	0·212	0·564	1·3
$\frac{d}{dt}\left\{\frac{1}{t}\left(1-\frac{P}{fA}\right)\right\}^2$		0·12	0·36	0·92	1·96	3·92
$\frac{1}{I}\cdot\frac{d}{dt}\left\{\frac{1}{t}\left(1-\frac{P}{fA}\right)\right\}^2$		0·8	1·00	1·21	1·39	1·63

For the remainder of this chapter we shall replace these complicated expressions by the following symbols:—

Expression.	Symbol.
$1-\frac{P}{fA}$	K
$\frac{1}{t}\left(1-\frac{P}{fA}\right)$	L
$\frac{d}{dt}\left\{\frac{1}{t}\left(1-\frac{P}{fA}\right)\right\}$	M
$\left\{\frac{1}{t}\left(1-\frac{P}{fA}\right)\right\}^2 = L^2 =$	N
$\frac{d}{dt}\left\{\frac{1}{t}\left(1-\frac{P}{fA}\right)\right\}^2 = \frac{dN}{dt} =$	P
$\frac{1}{I}\cdot\frac{d}{dt}\left\{\frac{1}{t}\left(1-\frac{P}{fA}\right)\right\}^2$	Q
$\int_t^{t_0}\frac{1}{I}\cdot\frac{d}{dt}\left\{\frac{1}{t}\left(1-\frac{P}{fA}\right)\right\}^2 dt$	R
$\sqrt{\int_t^{t_0}\frac{1}{I}\cdot\frac{d}{dt}\left\{\frac{1}{t}\left(1-\frac{P}{fA}\right)\right\}^2 dt}$	S

The values of Q are plotted against t as shown in Fig. 143. The area of this curve between t_0 and various values of t will give the value R. Selecting three values of t_0 and measuring the areas under the curve between the ordinates t_0 and each value of t considered, taking the square root of each of these areas, and then dividing each value so obtained into the corresponding value of M already determined, we arrive at the ordinates of the final curves. For this investigation the values 2·0″, 1·75″, and 1·5″ for t_0 have been selected. The tabular arrangement of the work is shown below, and it must be borne in mind in calculating these areas that the scales to which the graphs have been drawn are of prime importance.

$t_0 = 2·0''$

t	1·0	1·25	1·5	1·75	1·95	1·975	1·975
R	1·194	0·971	0·70	0·378	0·08	0·0405	0·0203
S	1·092	0·985	0·836	0·614	0·283	0·0201	0·0142
M	0·44	0·69	0·970	1·34	1·71	1·77	1·795
$\frac{M}{S}$	0·403	0·70	1·16	2·18	6·05	8·8	12·6

$t_0 = 1·75''$

t	1·0	1·25	1·5	1·70	1·725	1·7375
R	0·818	0·595	0·322	0·0685	0·0345	0·0173
S	0·904	0·771	0·568	0·262	0·186	0·1315
M	0·44	0·69	0·97	1·255	1·30	1·32
$\frac{M}{S}$	0·49	0·895	1·71	4·80	7·00	10·00

$t_0 = 1·5''$

t	1·0	1·25	1·45	1·475	1·4875
R	0·495	0·272	0·058	0·0294	0·0147
S	0·701	0·522	0·242	0·1715	0·121
M	0·44	0·69	0·91	0·94	0·95
$\frac{M}{S}$	0·625	1·32	3·76	5·49	7·85

The areas of the curves obtained by plotting these values against t_0 enable a value of t_0 satisfying the equation to be determined. The integral or area curves are shown in full lines, and those representing the complete function in chain lines. (See Fig. 144.) The maximum ordinates of the integral curves will be found to lie on a straight line, hence by joining up these points a straight line is obtained which represents the value of the integral

$$\int \frac{M \,.\, dt}{S}$$

for all values of t_0

The particular value of the integral required is determined by putting $x = l = \frac{1}{2}$ total length in the left-hand side of the equation 5.

Then area required $= \frac{76}{2}\sqrt{\frac{2800}{1{\cdot}6 \times 10^6}}$

$= 1{\cdot}59$ square inches.

From the curve the value of t_0 which gives this area is $1{\cdot}83''$, therefore the maximum thickness of the strut is $1{\cdot}83''$ and its length $= 1{\cdot}83 \times 3{\cdot}5 = 6{\cdot}4''$

SHAPE OF THE STRUT.—The value of t_0 thus found is now substituted in the general expression, and curve 4 integrated back from this point. The value of

$$\int_t^{1{\cdot}83} Q\,.\,dt$$

is determined for various values of t and the corresponding values of x obtained.

Arranged tabularly we have:

t	1·8125	1·80	1·75	1·625	1·5	1·25	1·0
$\int_t^{1{\cdot}83} Q\,.\,dt$	0·0182	0·0363	0·107	0·274	0·428	0·700	0·922
$\sqrt{\int_t^{1{\cdot}83} Q\,.\,dt}$	0·135	0·191	0·327	0·524	0·654	0·837	0·960
M	1·45	1·425	1·34	1·14	0·97	0·685	0·45
$\frac{M}{S}$	10·75	7·45	4·1	2·20	1·48	0·82	0·469
t	1·80	1·75	1·70	1·60	1·5	1·25	1·0
$\int_t^{1{\cdot}2} \frac{M\,.\,dt}{S}$	0·26	0·54	0·71	0·96	1·14	1·42	1·58
x	6·23″	12·9″	17″	23″	27·3″	34″	37·8″
$l = 3{\cdot}5\,t$	6·3″	6·125″	5·95″	5·6″	5·25″	4·375″	3·5″

$$\text{N.B.}\quad x = \frac{\displaystyle\int_t^{1{\cdot}2} \frac{\left[\frac{d}{dt}\left\{\frac{I}{t}\left(1 - \frac{P}{fA}\right)\right\}\right]dt}{\sqrt{\displaystyle\int_t^{1{\cdot}2}\frac{1}{I}\left[\frac{d}{dt}\left\{\frac{I}{t}\left(1 - \frac{P}{fA}\right)\right\}^2\right]dt}}}{\sqrt{\frac{P}{E}}}$$

The shape of the strut can then be drawn out from the values obtained above for x and l, as illustrated in Fig. 145.

DESIGN OF THE DRAG BRACING.—In accordance with standard general practice the total drag force to be distributed

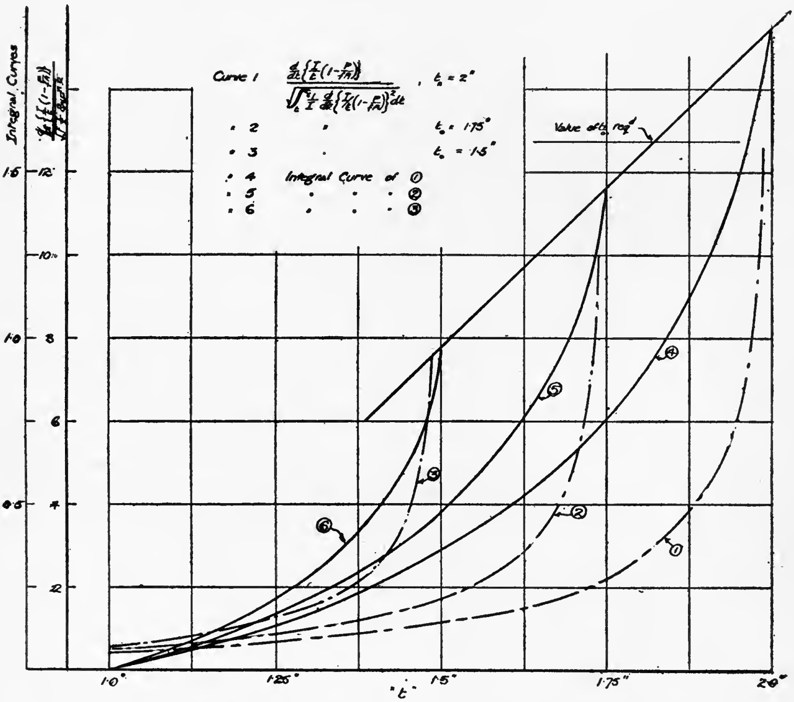

FIG. 144.—Graphical Evaluation of Tapered Strut Formula.

over the planes will be taken as one-seventh of the weight of the machine. Hence drag force

$$= \frac{2000}{7} = 286 \text{ lbs.}$$

$$= 0{\cdot}72 \text{ lbs. per square foot.}$$

This load is assumed equally carried by the front and rear spar. The plan of the wings must next be drawn out and the spacing of the drag struts decided upon. A suitable arrangement is shown in Fig. 146. The forces at the joints due to the drag forces is then determined in the following manner:—

Area of outer section of top plane from joint A to tip

$$= 14 \text{ sq. feet approx.}$$

Drag load on this area

$$= 14 \times 0{\cdot}72 = 10 \text{ lbs.}$$

This is equally distributed between the front and rear joints of A and A^1

Area of wing between A and B

$$= 4 \times 6 = 24 \text{ sq. feet.}$$

Drag load over this area

$$= 24 \times 0{\cdot}72 = 17 \text{ lbs. approx.}$$

Half of this acts at A and A^1, and the other half at B and B^1. Proceeding along the span in this manner the drag forces at each of the joints are obtained, and the results should be tabulated as under:—

TOP PLANE.

		a		*b*		*c*		*d*		*e*		*f*		*g*
Area of drag bay ...		14		24		21		18		18		18		15
Drag load—lbs. ...		10		17		15		13		13		13		11
Reactions ...	Front		9·0		8·0		7·0		6·5		6·5		6·0	
	Rear		9·0		8·0		7·0		6·5		6·5		6·0	

BOTTOM PLANE.

		j		*k*		*l*		*m*		*n*	
Area of drag bay ...		14		20		18		18		18	
Drag load—lbs. ...		10		15		13		13		13	
Reactions ...	Front		8·5		7·0		6·5		6·5		3·0
	Rear		8·5		7·0		6·5		6·5		3·0

In addition to these loads there will be horizontal components due to the inclination of the lift bracing owing to the stagger arrangement. These are obtained by multiplying the lift reactions at each point of support by the factor

$$\tan\theta = \frac{\text{gap}}{\text{stagger}} = \frac{2}{6} = \frac{1}{3}$$

The components thus obtained are added to the reactions due to the drag forces and the drag bracing stressed in the usual manner. In adding the lift components it is first necessary to apply both the C. P. and safety factors to

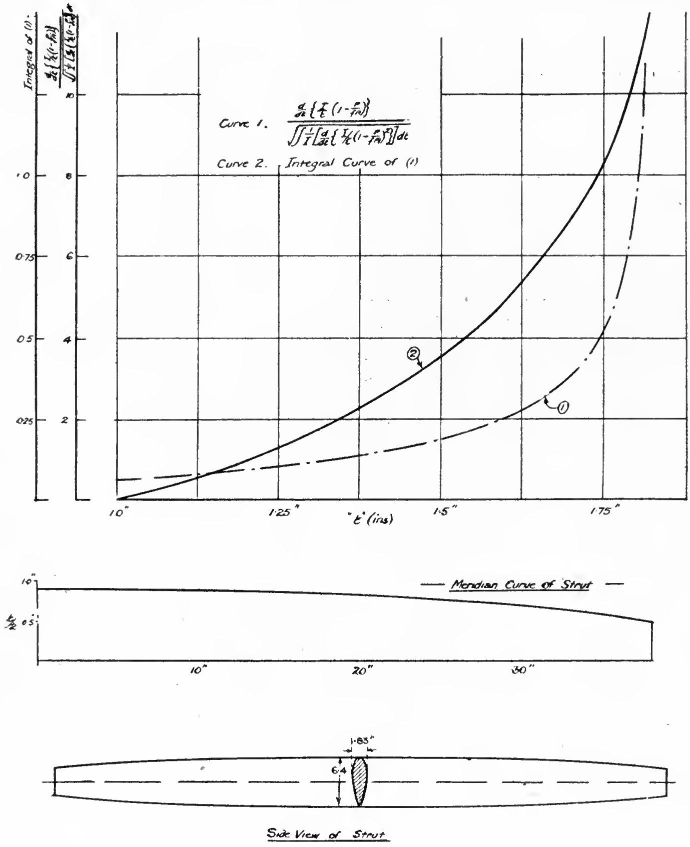

FIG. 145.

the original reactions. The coefficients to be applied are as follows:—

(*a*) Centre of pressure forward:

Front frame = 7 × ·68 × ·33 = 1·59
Rear frame = 7 × ·32 × ·33 = 0·75

(*b*) Centre of pressure backward:

Front frame = 7 × ·21 × ·33 = 0·49
Rear frame = 7 × ·79 × ·33 = 1·84

These coefficients applied to the lift reactions give the following horizontal loads which must be taken by the drag bracing :—

TOP PLANE.

Joint ...		A	B	C	D
Lift reaction on vertical frame		64	155	202	115
(*a*) C.P. forward, horizontal components	Front	102	246	321	183
	Rear	48	116	151	86
(*b*) C.P. back, horizontal components	Front	31	76	99	56
	Rear	118	286	372	212

BOTTOM PLANE.

Joint ...		B′	C′	D′
Lift reactions on vertical frame		78	176	62
(*a*) C.P. forward, horizontal components	Front	124	280	98
	Rear	58	132	46
(*b*) C.P. back, horizontal components	Front	38	86	30
	Rear	144	324	114

STRESS DIAGRAMS FOR DRAG BRACING.—The reactions thus obtained are added to the local drag reactions, and the stress diagrams for the drag bracing can then be drawn as shown in Fig. 146. It will be observed that in the case of normal flight the drag bracing wires shown in full lines will alone be in operation, whereas in the case of downloading the dotted bracing will be in action. It is customary to make the two bracing wires in each bay similar, so that it is not necessary to make a stress diagram for the drag bracing under downloading forces.

Further examination shows that it is only necessary to stress the drag bracing for the lift conditions with the centre of pressure forward. The stress diagrams therefore reduce to one for each plane. The factor having been applied to the reactions before drawing the diagrams, the individual stresses in the members can be read directly from the diagram and tabulated for reference as shown.

DESIGN OF THE DRAG BRACING.—Circular tie-rods, of which particulars have already been given in Table XXVI. and illustrations in Fig. 130 (*c*), may be used. From the table the sizes necessary are :

TOP PLANE.

Bracing wire ...	14–15	16–17	18–19	20–21	22–23
Load—lbs. ...	+ 280	+ 800	+ 770	+ 1450	+ 1470
Tie-rod size ...	4 B.A.	4 B.A.	4 B.A.	2 B.A.	2 B.A.

LOWER PLANE.

No. 4 B.A. tie-rods throughout.

DESIGN OF THE DRAG STRUTS.—For such a small machine as that under consideration it would be preferable in practice to insert compression ribs, but for purposes of further illustration we will assume that steel tubes of thin gauge are to be used as compression members. The size of tubes necessary will therefore be determined by use of Formula 62 (Rankine's Formula), where the constants have the following values:—

f_c = 21 tons per square inch.
a = 1/7500
L = length = 39″

TOP PLANE STRUTS.

Drag Strut ...	1–14	15–16	17–18	19–20	21–22	23–24
Load—lbs. ...	−110	−430	−560	−890	−1050	−1250
Diameter of tube, 22 S.W.G. ...	$\frac{1}{2}''$	$\frac{5}{8}''$	$\frac{3}{4}''$	$\frac{7}{8}''$	$\frac{7}{8}''$	1″

BOTTOM PLANE STRUTS.

Drag Strut ...	6–11	12–13	14–15	16–17
Load—lbs. ...	−130	−220	−490	−660
Diameter of tube, 22 S.W.G. ...	$\frac{1}{2}''$	$\frac{1}{2}''$	$\frac{3}{4}''$	$\frac{3}{4}''$

DESIGN OF THE SPARS.—The stresses in the spars are due to bending and direct end loads. In order to determine the bending stresses it is necessary to draw the complete bending moment diagrams for the top and bottom planes. The fixing moments at the supports have already been obtained. In order to complete the diagrams, the free bending moment diagrams are drawn upon each span for uniform loading. As shown in Chapter IV., these free B.M. diagrams will be parabolas with their maximum ordinates equal to $w\,l^2/8$

Hence in the case under consideration the maximum B.M. ordinates are:—

TOP PLANE.

Span	*a b*	*b c*	*c d*	*d e*
Maximum B.M.—lbs. ft ...	50	158	135	23·4

LOWER PLANE.

Span	*b′ c′*	*c′ d′*
Maximum B.M.—lbs. ft. ...	135	115

The parabolas and the fixing moments are set out to the same scale, and the net bending moment diagrams are shown shaded in Fig. 147, from which figures the value of the bending moment at any point along the span can be read off directly.

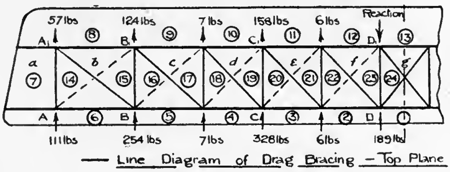

Reactions due to Stagger

Joint	A	B	C	D
Front Frame	102	246	321	183
Rear "	48	116	151	86

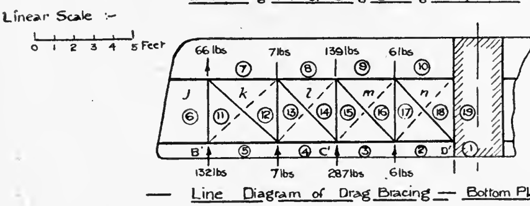

Reactions due to Stagger

Joint	B′	C′	D′
Front Frame	124	280	98
Rear "	58	132	46

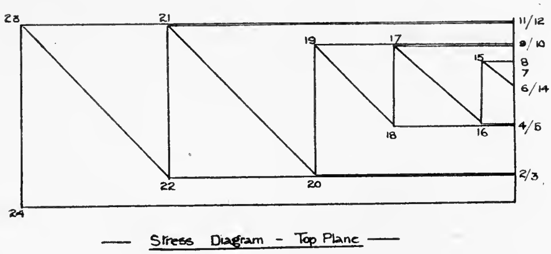

Member		Load
14.15	Bracing Wire	+ 280 lbs
16.17	"	+ 600 "
18.19	"	+ 770 "
20 21	"	+1450 "
22 23	"	+ 1470 "
7. 14	Drag Strut	− 110 "
15. 16	"	− 430 "
17.18	"	− 560 "
19.20	"	− 890 "
21.22	"	− 1050 "
23.24	"	− 1250 "

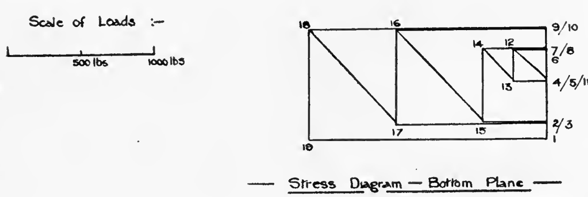

Member		Load
11. 12	Bracing Wire	+ 315 lbs
13. 14	"	+ 320 "
15 16	"	+ 870 "
17. 18	"	+ 880 "
6. 11	Drag Strut	− 130 "
12.13	"	− 220 "
14 15	"	− 490 "
16.17	"	− 660 "

FIG. 146.—Stress Diagrams for Drag Bracing.

To the values thus obtained the requisite factor of safety and the centre of pressure coefficients for the front and rear spars must be applied.

LIFT FORCE FACTORS.

Factor for front spar $= 7 \times \cdot 68 = 4 \cdot 76$
Factor for rear spar $= 7 \times \cdot 79 = 5 \cdot 53$

Tabulating the bending moments for various positions along the spans, we have the following tables :

TOP PLANE.

Position.	B.M. on diagram. lbs. ft.	Maximum B.M. Front spar. lbs. ft.	Maximum B.M. Rear spar. lbs. ft.
Joint A	25	119	138
Middle of span A B	negligible	—	—
Joint B	77	366	426
Middle of span B C	65	310	359
Joint C	114	543	630
Middle of span C D	50	238	276
Joint D	54	257	298
Middle of span D E	30	143	166

LOWER PLANE.

Position.	B.M. on diagram. lbs. ft.	Maximum B.M. Front spar. lbs. ft.	Maximum B.M. Rear spar. lbs. ft.
Joint B′	16	76	88
Middle of span B′ C′	75	357	415
Joint C′	105	500	580
Middle of span C′ D′	45	214	249
Joint D′	38	181	210
Middle of span D′ E′	38	181	210

DOWNLOADING.—The bending moments on the spars due to downloading forces follow in the same manner by applying the correct factors for the centre of pressure and safety. In general it is necessary to consider the lower spars only for downloading forces, as they will then be in compression, whereas in normal flight they are in tension. The much greater strength of spruce in tension as compared with compression, may result in the necessity of designing the lower spars for downloading forces in spite of the reduced factor of safety employed.

DOWNLOADING FORCE FACTORS.—LOWER PLANE SPARS.

Factor for front spar $= 3{\cdot}5 \times {\cdot}77 = 2{\cdot}69$
Factor for rear spar $= 3{\cdot}5 \times {\cdot}23 = {\cdot}805$

Position.	B.M. on diagram. lbs. ft.	Maximum B.M. Front spar. lbs. ft.	Maximum B.M. Rear spar. lbs. ft.
Joint B′	16	43	13
Middle of span B′ C′	75	202	60
Joint C′	105	283	85
Middle of span C′ D′	45	121	36
Joint D′	38	102	31
Middle of span D′ E′	38	102	31

The correction factor for end loads

$$\frac{P_E}{P_E - P} \qquad \text{............ Formula 67.}$$

has not been applied to the bending moments at the centre of the spans in this example. This correction should not be omitted in actual practice.

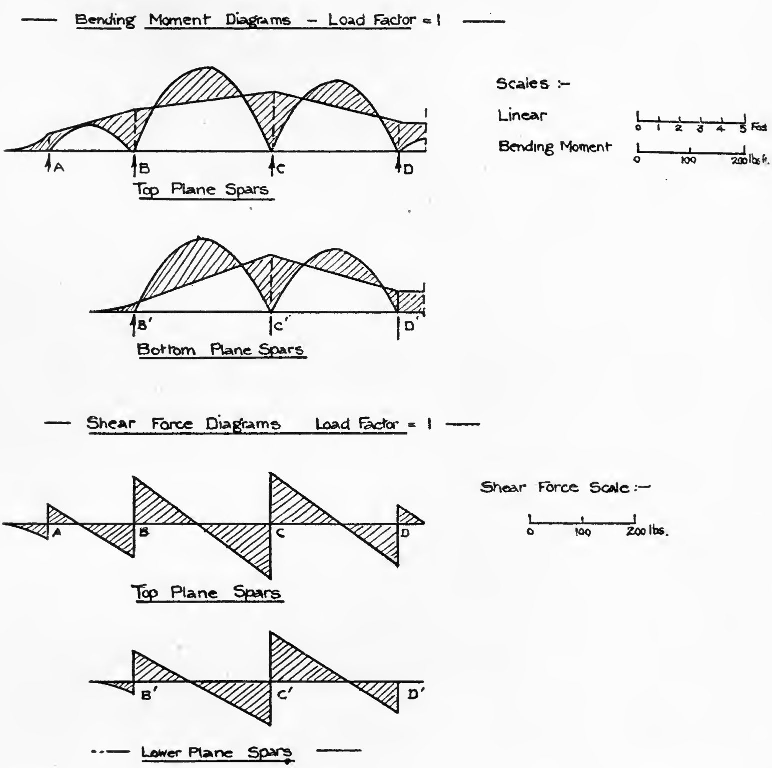

FIG. 147.—Design of the Wing Spars B.M. and S.F. Diagrams.

The bending moments along the spars having been determined, the next step is to deduce the direct end loads upon the spars resulting from the tension in the lift and drag bracing. These are read off from the stress diagrams. In the case of the loads obtained from the lift and downloading stress diagrams, factors must be applied as in the preceding work. The loads due to drag forces are read off directly. It will be observed that from the drag bracing stress diagram for the top plane, shown in Fig. 146, the front spar is in tension and the rear spar in compression. The result of this is that the drag forces on the front spar tend to reduce the direct load in the front spar, since the top plane spars are in compression due to the lift bracing, while they increase the direct load on the rear spar.

Direct End Loads on the Spars.

(Top Plane—Compression due to lift bracing.)

Span	AB	BC	CD	DE
Front spar	214	1760	4950	4950 lbs.
Rear spar	249	2040	5750	5750 lbs.

Loads due to Drag Bracing.

Span... ...	*b*	*c*	*d*	*e*	*f*	*g*
Front spar	0	+220	+820	+1360	+2360	+3360 lbs.
Rear spar...	−220	−820	−1360	−2360	−3360	−3360 lbs.

Resultant End Loads on Top Plane Spars.

Front spar—						
Lift ...	−214	−1760	−1760	−4950	−4950	−4950 lbs.
Drag ...	+ 0	+ 220	+ 820	+1360	+2360	+3360 lbs.
Total ...	−214	−1540	− 940	−3590	−2590	−1590 lbs.
Rear spar—						
Lift ...	−249	−2040	−2040	−5750	−5750	−5750 lbs.
Drag ...	−220	− 820	−1360	−2360	−3360	−3360 lbs.
Total ...	−469	−2860	−3400	−8110	−9110	−9110 lbs.

In a similar manner the direct loads upon the lower plane spars under normal flight conditions can be calculated. With downloading forces the same procedure is adopted, the end loads being read off the respective stress diagrams for the external and drag bracing under these conditions. The work should be set out in exactly the same manner as shown above for the top plane spars.

Design of the Spars.—The tables of direct loads in the spars indicate that the top rear spar will be the most heavily loaded, and therefore it is selected in order to illustrate the method to be adopted in the general design of a spar. The following figures relating to this spar have been obtained :—

Span	*b*	*c*	*d*	*e*	*f*	*g*
Maximum B.M.	426	426	630	630	298	298 lbs. ft.
Direct end load	−469	−2860	−3400	−8110	−9110	−9110 lbs.

It is necessary to select spar sections capable of carrying these loads safely. The depth of the spar is already fixed by the aerofoil section chosen. This in the present case is the R.A.F. 6 with a 6 ft. chord, and with the spars in the position shown in Fig. 142 the depth for the front and rear spars is limited to about 3·5″. This depth will therefore be taken, the spars will be made of I section, and will be lightened out towards the wing tips by diminishing the depth of the flange. The dimensions of the spar at various points along the span can now be determined, and a suitable series of sections are indicated in Fig. 148.

Considering the section for bay *e*,

$$\text{M.I.} = \frac{1}{12}(2 \times 3{\cdot}5^3 - 1{\cdot}5 \times 2^3)$$

$$= 6{\cdot}14 \text{ inch}^4 \text{ units}$$

$$\text{A.} = 7 - 3$$

$$= 4 \text{ inch}^2 \text{ units}$$

$$\text{Bending stress} = \frac{630 \times 12 \times 1{\cdot}75}{6{\cdot}14}$$

$$= 2155 \text{ lbs. per square inch.}$$

$$\text{Direct stress} = \frac{8110}{4}$$

$$= 2027 \text{ lbs. per square inch.}$$

$$\text{Total stress} = 4182 \text{ lbs. per square inch.}$$

The maximum compressive stress being 4500 lbs. per square inch for a spruce spar, this section is evidently satisfactory.

Considering the section for bays *f*, *g*, *d*,

M.I. = 5·2 inch^4 units
A. = 3·25 inch^2 units
Maximum bending stress in bays *f* and *g* = 1205 lbs. per sq. in.
Maximum = direct stress in bays *f* and *g* = 2805 lbs. per sq. in.
Total stress = 4010 lbs. per sq. in.

Maximum bending stress in bay *d* = 2540 lbs. per sq. in.
Maximum direct stress in bay *d* = 1045 lbs. per sq. in.
Total stress = 3585 lbs. per sq. in.

This section is therefore suitable for these bays.

Considering the section for bays *a*, *b*, *c*,

M.I. = 4·55 $inch^4$ units
A. = 2·87 $inch^2$ units
Maximum bending stress = 1965 lbs. per sq. in.
Maximum direct stress = 997 lbs. per sq. in.
Total stress = 2962 lbs. per sq. in.

As will be seen, this section is very much stronger than required; but as it is not practicable to make the thickness of the flanges less than that indicated in the figure, this section should be used over the outer portion of the wing. Finally, the strength

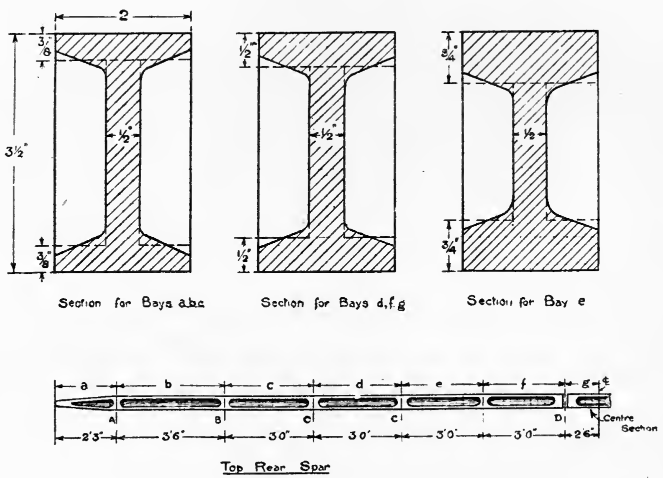

FIG. 148.—Design of Wing Spar.

of the spar in shear should be investigated. On referring to the shear force diagram shown in Fig. 147 it will be seen that the maximum shear occurs at the joint C, at which point the shear is equal to

$$202 \times \cdot 79 \times 7 = 1120 \text{ lbs.}$$

whence the shear stress approximately

$$= \frac{1120}{3\cdot 5 \times 2} = 160 \text{ lbs. per sq. inch}$$

since the section is rectangular at the joint in order to accommodate the fitting. A shear stress of 800 lbs. per square inch is permissible across the grain of spruce, so that the sections are quite safe as regards shear.

This completes the design of this spar, and by following a similar procedure in the case of the remaining spars the requisite sections can be determined and the spar detail drawings prepared.

Having settled the spar sizes, the design of the members of the wing structure is finished and a close estimate of the total probable weight when manufactured can be obtained. This should be compared with the weight assumed for the initial stressing of the wings, with which it should agree fairly closely.

Before leaving the question of wing-stressing, an example will be given of the alteration in the stresses when the method of duplication through the incidence bracing is adopted. It is supposed that the front lift wire C D′ (Fig. 127) is broken, and that the load originally carried by this wire is now transmitted by the incidence wire C C′ to the rear frame. What will be the effect of this upon the stresses in the members of the bay C D? There are three cases to consider :—

1. All wires intact, the C.P. back, and a factor of safety of 7.
2. Front wire C D′ broken, C.P. back, a factor of safety of ·66 × 7
3. Front wire C D′ broken, C.P. forward, factor of safety ·66 × 7

To determine the size of the incidence wire to transmit the load: the maximum load to be transmitted occurs with the C.P. forward and has a value

= sum of the front reactions as far as the bay C D
$= (64 + 155 + 78 + 202 + 176) \times \cdot 68 \times \cdot 66 \times 7$
$= 675 \times \cdot 68 \times \cdot 66 \times 7$
$= 2140$

Resolving this load in the direction of the incidence wire we have

$$\text{Maximum load} = \frac{2140}{\cos \theta} = 2250 \text{ lbs.}$$

and the size of the incidence wire must be sufficient to carry this load.

Maximum load in the rear lift wire $C_1 D_1'$. Considering the cases enumerated above separately we have

1. Vertical load to be taken by wire

$$= 675 \times \cdot 79 \times 7 = 3740 \text{ lbs.}$$

2. (i.) Load on the rear frame

$$= 3740 \times \cdot 66 = 2490 \text{ lbs.}$$

(ii.) Load transmitted from front frame by incidence wire

$$= 675 \times \cdot 21 \times \cdot 66 \times 7 = 661 \text{ lbs.}$$

$$\therefore \quad \text{Total load} = 2490 + 661 \doteq 3151 \text{ lbs.}$$

3. Load on rear frame

$$= 675 \times \cdot 32 \times \cdot 66 \times 7 = 1010 \text{ lbs.}$$

Load transmitted from front frame

$$= 675 \times \cdot 68 \times \cdot 66 \times 7 = 2140 \text{ lbs.}$$

$$\therefore \quad \text{Total load} \qquad = 3150 \text{ lbs.}$$

which is nearly the same as in the second case.

The maximum vertical load is therefore seen to be 3740 lbs., occurring when the C.P. is back and all the wires are in. This is consequently the condition for which the design must be carried through, and thus the design which has just been shown for direct duplication holds good because the broken wire does not alter the maximum load. There will also be an additional load to be carried by the drag bracing due to the horizontal component of the tension in the incidence wire. To determine which condition will produce the maximum load in the drag bracing the horizontal reactions for each of the three cases must be calculated as was done for the lift bracing, and separate stress diagrams must be drawn from which the maximum load occurring in the drag bracing members is determined. The direct end load in the spars will also be affected by the altered stresses in the drag bracing; and these must likewise be determined from the stress diagrams and the maximum load thus obtained combined with the correct bending moment in the manner previously described.

Design of the Wing Ribs.—In communicating the air forces from the wing surface to the spars, the ribs act as small girders, and it is necessary for design purposes to examine the loads acting upon them in flight. The load on each rib is obtained by determining the maximum load over the wing surface and dividing by the number of ribs (n). This load will be the sum of the reactions previously obtained multiplied by the factor of safety adopted. The distribution of the load over the wing section will be similar to that obtained upon an aerofoil tested in a wind tunnel, and the design of a rib is based upon the results of pressure distribution experiments such as have been described in Chapter III.

When applying these results to a wing rib the load curves must be drawn for the most unfavourable conditions of incidence which are likely to occur. For example, the maximum load on the leading edge of a wing will occur at large angles of incidence, whereas the maximum load on the rear portion of the wing will occur when the angle of incidence is small. In Fig. 149, obtained from pressure distribution experiments, the load curves over a wing section for angles of incidence of $2\frac{1}{2}°$ and $12\frac{1}{2}°$ are shown. During flight the wing loading W/n will be the same in each case. It is therefore necessary that the mean height of both diagrams should be the same, hence the pressure ordinates have to be altered in a constant ratio until this result is obtained.

The primary shear diagrams are next obtained by tabular-graphic integration from the load curves, commencing at the front of the section for the $12\frac{1}{2}°$ curve and at the rear of the section for the $2\frac{1}{2}°$ curve (Fig. 149 *b*). By further integration of the shear diagram the first bending moment curves are obtained as shown in Fig. 149 (*c*). The position of the spars having been decided upon, the final bending moment and shear force diagrams are obtained in the following manner :—

$12\frac{1}{2}°$ incidence.—The centre of pressure corresponding to this loading is at about ·28 chord.

Taking moments about B, see figure 149 (*c*),

$$R_1 (x + y) = P y$$

where P is the total load on the rib

$$\therefore \quad R_1 = \frac{P y}{x + y}$$

$$\text{and} \quad R = \frac{P x}{x + y}$$

The bending moment at the rear spar due to $R_1 = R_1 (x + y)$
$= P y$

From B set off a distance B C to represent $P y$ on the same scale as the bending moment diagram ordinates. Join A C. The bending moments on the rib between the spars are given by the difference in ordinates of the straight line A C and the bending moment curve. These have been drawn to an enlarged scale in Fig. 149 (*d*). Similarly the final shear force curve can be drawn now that the spar reactions are known. This is shown beneath the bending moment curve.

The same procedure must be carried through for the load distribution at $2\frac{1}{2}°$ incidence, and the final bending moment and shear force curves drawn preferably on the same base as those for the $12\frac{1}{2}$ incidence, as shown in Figs. 149 (*d* and *e*). The curve which indicates the maximum bending moment or shear

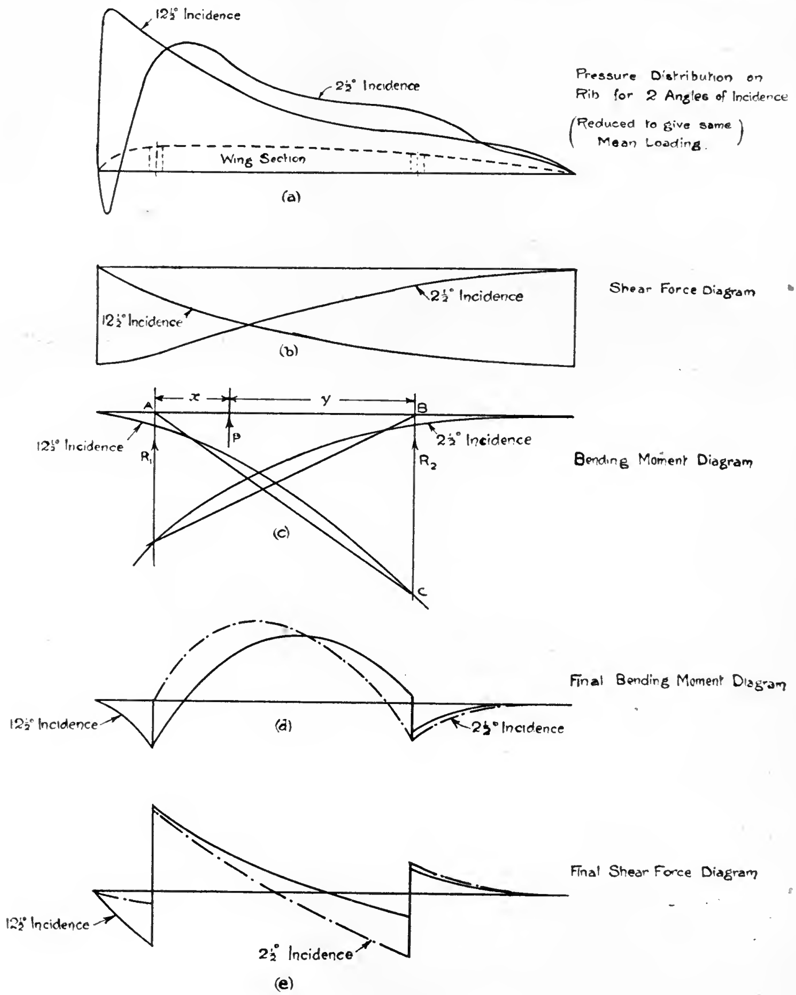

FIG. 149.—Determination of B.M. and S.F. Diagrams for Wing Ribs.

force at a particular section must be used when designing the rib at that section. In developing the bending moment and shear force diagrams along these lines, care is necessary with the various scales employed at each stage in order that the final diagrams may be correctly graduated.

Having determined the bending moment and shear force over the rib, the detail design follows in the usual way. If M be the bending moment at the section considered, f the maximum allowable stress in the material, y the distance of the outer fibre of the rib from the neutral axis, and I the required moment of inertia, then

$$\frac{My}{f} = I$$

A suitable section with this moment of inertia is then set out. It is customary to assume that the rib flanges alone take all the bending moment, while the web takes all the shear, as explained in Chapter IV., when dealing with the stresses in beams.

The web may be designed as follows :—

Let d be the depth of the web
t be the width or thickness
f_s the safe shear stress

Then the shear load that the web will carry

$$= d \times t \times f_s$$

whence

$$t = \frac{\text{Shear force at the section}}{d \times f_s}$$

This relation fixes the thickness of the web, while the wing section itself fixes d. Generally it will be found that in all machines, except very large ones, other practical considerations will fix the sizes of the rib, which, if then tested for shear strength, will be found to be amply strong.

Wing Assembly.—Several illustrations of typical aeroplane wings and their fittings have been shown in the illustrations given in this chapter, in order to show the various details and the method of assembly. The principles of construction are similar in every case. The wing is built up on the main spars. These main spars are fixed at the correct distance apart, and then the ribs, which have been constructed on special formers in order to give them the correct profile of the aerofoil selected, are slid along the spars until they reach their allotted place. A distance of from 15″ to 20″ is generally allowed between each main rib, but between the leading edge and the front spar a number of small intermediate ribs are fixed alternately with the main ribs in order to withstand the more intense pressure which occurs over this portion of the wing. Each rib is then glued and screwed to the spars. If compression ribs are used to take the drag loads, they must be strung on in their correct order with the other ribs; while if tubular or box struts are used, these are now inserted. A number of small stringers are threaded through the ribs, and serve to make them more rigid laterally. The drag bracing wires can next be attached to their respective fittings, and the skeleton wing is then complete and ready, as shown in Fig. 141, for its covering of fabric. This is bound round the wing and sewn to the ribs, and then covered with three or four coats of dope, in order to render the wing taut and weather-proof.

CHAPTER VI.

Resistance and Streamlining.

Resistance.—The total resistance of an aeroplane—that is the force which is balanced by the airscrew thrust at the flying speed of the machine—is made up of two parts:

1. The drag of the wings.
2. The resistance of the remaining parts of the machine.

Under the second heading is included the effect of the interplane struts, the external wires, the body, the chassis, the tail, and all other fitments exposed to the wind.

In a normal machine flying at the most efficient speed, these component resistances are approximately equal, so that in designing an aeroplane it is as important to assess the resistance of the exposed parts correctly as it is to know the drag of the wings. From one point of view it is more important, because, with increase of speed, the wings adjust their angle of incidence so as to keep $K_y \frac{\rho}{g} A V^2$ constant, and if the normal flying angle is not far from that giving maximum L/D, then the increase of wing drag may be small; but since the resistance of the exposed parts, other than the wings, varies approximately as the square of the velocity, a relatively small increase of speed produces a considerable increase in the magnitude of the resistance.

Unfortunately, it is much more difficult to estimate the second component than it is to calculate the first component, as very little is known of the manner in which the various parts of an aeroplane interfere with one another. For example, one part may effectually screen another from wind pressure, or the relative velocity with which one part engages the air may be more or less than the velocity of the machine. Also the slipstream from the airscrew increases the resistance of those parts of the machine placed in its stream. Further, it is necessary to correct an estimate of the value of the resistance of the remaining parts of a machine in the light of the actual performance of the machine in flight.

Of course, if the complete aeroplane were reproduced as a scale model, it would be possible to predict this body resistance accurately from wind tunnel tests, but the construction of the model is obviously a difficult and at the same time an expen-

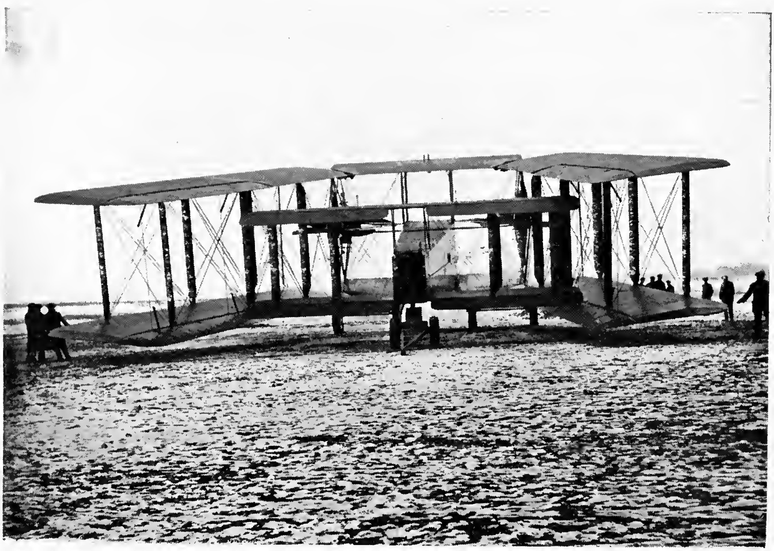

Reproduced by courtesy of Messrs. Handley Page, Ltd.

FIG. 151.—Front and Rear Views of V–1500 with Wings folded back.

Facing page 208.

sive matter. The designer should, therefore, try to arrange for the reduction of the second component to an absolute minimum. In so doing he will be guided by knowledge of the resistance of bodies of various shapes placed in the air-stream of the wind tunnel under more simple conditions.

A brief consideration of the following example will emphasise the importance of concentrating on minimising the second component, and will also show that if considerable weight has to be added in order to reduce the resistance of a given part, it may frequently be an advantage to tolerate this additional weight. Say a complete machine has a gliding angle of one in eight. This means that the *overall* efficiency or lift/drag ratio of the machine is 8. Now, if the second component can be reduced by 1 lb. by some means, then the machine will lift another 8 lbs. for the same speed. The overall efficiency of a

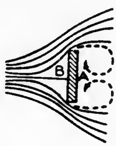

FIG. 152.—Flow past a Flat Plate.

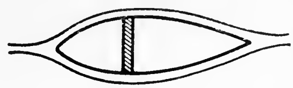

FIG 153.—Flow past a Streamline Shape.

machine must be borne in mind, therefore, when comparing struts, bodies, etc., of different resistances and different weights. It follows from this that the more efficient an aeroplane, the more it pays to improve its efficiency.

The resistance of any body placed in a current of air (this is, of course, equivalent to its resistance to motion through still air) is composed of two parts, namely:

1. The excess of air pressure in front of the body over that behind it, and
2. The skin friction.

It is shown subsequently that the amount of skin friction is small where the surface is small, and the considerable resistance therefore of some small bodies is almost wholly due to the first part. This excess of pressure is caused by a discontinuity of flow due to the abruptness of the body giving rise to a 'dead-air' region of diminished pressure in the rear of the body, and to increased pressure on the face of the body owing to the forward velocity of the air being reduced. This point will be made clear by reference to Fig. 152, which shows the flow of air past a normal flat plate. At B one streamline is evidently brought to rest, its velocity head being entirely converted into pressure, but the pressure thus set up will evidently diminish towards the edges of the plate as the stream divides to flow round the plate. A is the dead-air region of diminished pressure.

In seeking to diminish resistance, the principle is to eliminate as far as possible this region of 'dead air,' and to make the air flow round the body, thus preventing any discontinuity in the flow. The body is then said to be 'streamlined,' that is, it possesses a contour that the streamlines of flow can easily follow. Its limiting resistance is then the frictional resistance of the air flowing over the surface; and as this is a small quantity, the saving of resistance which can be obtained by efficient streamlining is large. Taking again the example of the normal flat plate of circular section, it is found necessary, in order to streamline it, to fit on both a nose and a tail, so that we arrive at a form somewhat similar to that of a fish or a bird. The more or less pointed nose eases the streamlines away from the disc without materially checking the flow, and a longer more or less pointed tail eases them back again after passing the plate or disc.

Fig. 153 depicts the flow past the plate streamlined by the addition of a nose and a tail. As will be seen, the region B has been eliminated, and the region A considerably reduced.

Variation from the (V^2) Law.—The resistance due to excess of air pressure varies with the square of the wind velocity (V), while that due to skin friction varies as $V^{1 \cdot 85}$. So long as the skin friction is small in amount in comparison with the resistance due to disturbance of the streamline flow, then the total resistance varies very approximately as the square of the velocity (V). In the case of a good streamline form, however, where the skin friction is comparable with the resistance due to the excess of air pressure, it may confidently be anticipated that the total resistance will vary according to an index of V much less than 2. Hence if it is assumed that the resistance of a streamline section is given by the general formula $R = K\,A\,V^2$, then the coefficient K will diminish as the velocity is increased. Experiments carried out on strut sections by Eiffel and the National Physical Laboratory have shown that this is actually the case.

Fig. 154 gives the results of tests carried out by Eiffel on the three strut sections shown. As will be seen, the drag coefficient diminishes in each case with increase of speed, but with the more perfect streamline shapes the diminution is very much greater than with those of a more imperfect form. This reduction of resistance at high velocities should be taken account of when estimating the resistance of good streamline shapes. Also in making a comparison between the efficiency of such shapes tested at different speeds, an allowance should be made for this effect.

The advantage to be derived in making a strut section of good streamline shape is well illustrated in Fig. 154, for it will be seen that the resistance of strut No. 3 is four or five times greater than that of struts Nos. 1 and 2 at the speeds of flight corresponding to those used in normal flying conditions.

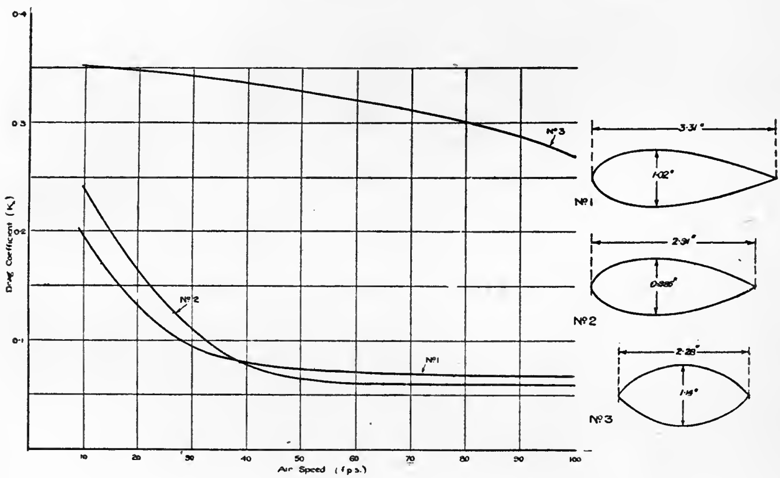

FIG. 154.—Variation of Drag with Change of Velocity.

Streamlining.—The designing of a good streamline form is an exceedingly delicate matter. The greatest scope is offered with airship bodies. The fuselage of a tractor aeroplane and the floats of a seaplane would offer an equally good field, but unfortunately the former has to accommodate an engine, and the latter have to be capable of easily leaving the water, both of which considerations result in a modified form. A fair field is, however, offered by the various struts of an aeroplane, and it is convenient to examine the matter from this point of view, although, of course, most of the following remarks apply almost equally well to any other solid body. Increase of resistance for small increases in size varies approximately as the increase of projected area upon a plane normal to the wind. It must be borne in mind that a very large change in size may involve a scale effect only to be investigated by experiment.

The strength of a strut depends on the moment of inertia of its section. The form of section giving a maximum value of this with minimum weight is the circular section of hollow form. The circle is a partly streamlined form of section, the resistance being, according to Eiffel, some 60% of the resistance of a flat rectangular plate of the same dimensions, for sizes usually obtaining with aeroplane struts. A further large reduction in resistance may be obtained by simply elongating the circle in the direction of motion into an ellipse, that is, by giving the section a 'fineness ratio.' Fineness ratio is defined as the ratio

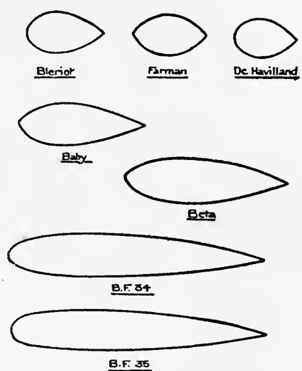

FIG. 155.—Strut Section.

of the length of the section to its maximum breadth. The saving to be effected in this way is about 50% of the resistance of the cylinder when the fineness ratio is 2, and a further 15% can be obtained by increasing the fineness ratio to 5. For a really good shape it is best to use a fineness ratio of about 3, or just a little over, and to keep the maximum thickness well towards the nose, say one-third of the length of the section back, and to keep the run of the 'contour' fairly flat at about this point. It is easy to produce a strut on these lines having a resistance of only 15% of the equivalent cylinder, or only 9% of the equivalent rectangular plane. It is of practically no importance whether the ends of the section are pointed or not, and it is usually most convenient to have well-rounded ends.

An instructive series of tests was carried out upon a number of struts by the N.P.L. in order to determine the best form of strut when taking into consideration both weight and strength as well as resistance. Some of the sections are shown in Fig. 155, and of these the Bleriot, Farman, and De Havilland were taken from struts in use on machines. The results are set out in Table XXIX.

It will be noted that there is a considerable range of shape of section for which the equivalent weights vary but little, while some of those sections which have been used on actual machines have an equivalent weight of from 150 to 180 lbs. The substitution of struts of 'Beta' section for those on the Farman biplane would have enabled it to carry 79 lbs. more useful load, without any addition to the horse power required.

TABLE XXIX.—RESISTANCES OF STRUTS.

Type of strut.	Resistance of 100 ft. of strut @ 60 ft /sec. Lbs.	Weight of 100 ft. of strut, maximum thickness 1″.	Maximum thickness for equal strength. Inches.	Equivalent weight of struts of equal strength. Lbs.
Circular, 1″ diam.	43	23·4	1·005	295
De Havilland	25·5	29·2	0·99	180
Farman	22·9	36·0	0·905	154
Bleriot	23·7	37·2	0·92	162
Baby	7·9	59·4	0·822	79
Beta	6·9	88·1	0·718	75
B.F. 34	7·2	133·0	0·65	84
B.F. 35	6·3	128·0	0·677	84

The effect of yawing is to increase the resistance of a strut considerably on account of the additional side force exerted by the air.

Inclination of Struts.—An investigation into the effect of inclining struts to the air stream, such as will occur for example in the struts of staggered machines, has also been made. It was found that for streamline shapes there is very little alteration in the resistance, but that for blunt-nosed sections the resistance was greatly reduced owing to the increased length of section in the air stream.

Resistance of the Body or Fuselage.—Since this forms the largest item in the consideration of resistance it will be considered at some length, so that when a fuselage of a new design has been drawn out, an estimate can be made of its probable resistance. The resistance of the body will vary approximately as the square of the velocity, and as has already been observed since the drag of the wings remains practically constant for various flight speeds, the question of the resistance of the body relative to that of the wings becomes of increasing importance as the speed of flight is increased.

This item must of course be reduced as much as possible, and more especially is this necessary in the case of very high-speed machines. The necessity for adopting good streamline shapes is at once evident, and it is to the realisation of this fact in practice that the modern development of high-speed machines

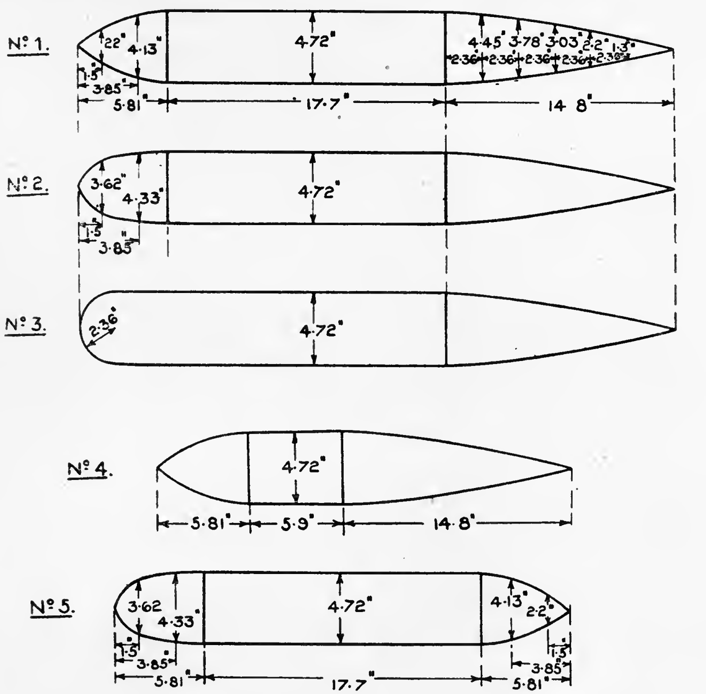

FIG. 156.—Shapes used by Eiffel in determining best form of fuselage.

is to a large extent due. A convenient method of comparing the resistance of various types of fuselages is to express these resistances in terms of a flat plane normal to the wind. For an efficient type of body the equivalent normal plane should be of a very much smaller cross section than the maximum cross section of the body. In many cases in practice, however, the resistance of the body is more than half the resistance of the equivalent flat plane, but with efficient design the maximum resistance should not be more than one quarter (25 per cent.). In order to obtain such a desirable result it is necessary to avoid, as far as is practically possible, all projections and corners likely to cause disturbances in the air flow. All members exposed to the air stream must be 'faired' to a streamline shape, a process which calls for the exercise of a considerable amount of care and patience, but which is amply repaid in the reduced resistance obtained.

In the absence of definite figures relating to the particular machine under design, the calculation of body resistance requires the computation of the resistance of each element, for which purpose it is convenient to have the tabulated results of the resistance of different kinds of fuselages, wires, chassis, wheels, and other components. Most of the data available for this purpose is the outcome of experiments carried out by M. Eiffel and by the National Physical Laboratory. Some experiments carried out by Eiffel upon the shapes shown in Fig. 156 will form a very useful introduction to this subject. These shapes consist of a nose, a cylindrical centre portion, and a conical tail. The results of the tests may be summarised—

(i) The blunter the nose the greater is the resistance. N.B.—Nose of section 1 is of streamline form.

(ii) For the same nose and tail the resistance diminishes as the length of the central portion is reduced.

(iii) Diminution in the length of the tail leads to a slightly increased resistance.

(iv) With streamline shapes the resistance varies with the velocity according to an index less than 2, the skin friction forming a considerable portion of the total resistance.

TABLE XXX.—RESISTANCE COEFFICIENTS FOR FUSELAGE SHAPES.

Body.	Equivalent normal plane coefficients. 32·8 f.p.s.	65·6 f.p.s.	98·4 f.p.s.	131·2 f.p.s.
I.	0·015	0·0139	0·013	0·012
II.	0·0147	0·0141	0·0133	0·0121
III.	0·170	0·0161	0·015	0·0135
IV.	0·0132	0·0123	0·0115	0·0103
V. Round end foremost...	0·0152	0·0143	0·0137	0·0103
V. Round end behind ...	0·0182	0·0167	0·0164	0·0103

N.B.—Observe that the resistance coefficient diminishes considerably as the air speed increases.

Turning from the general question of the resistance of bodies made up of geometrical solids, the question of the resistance of

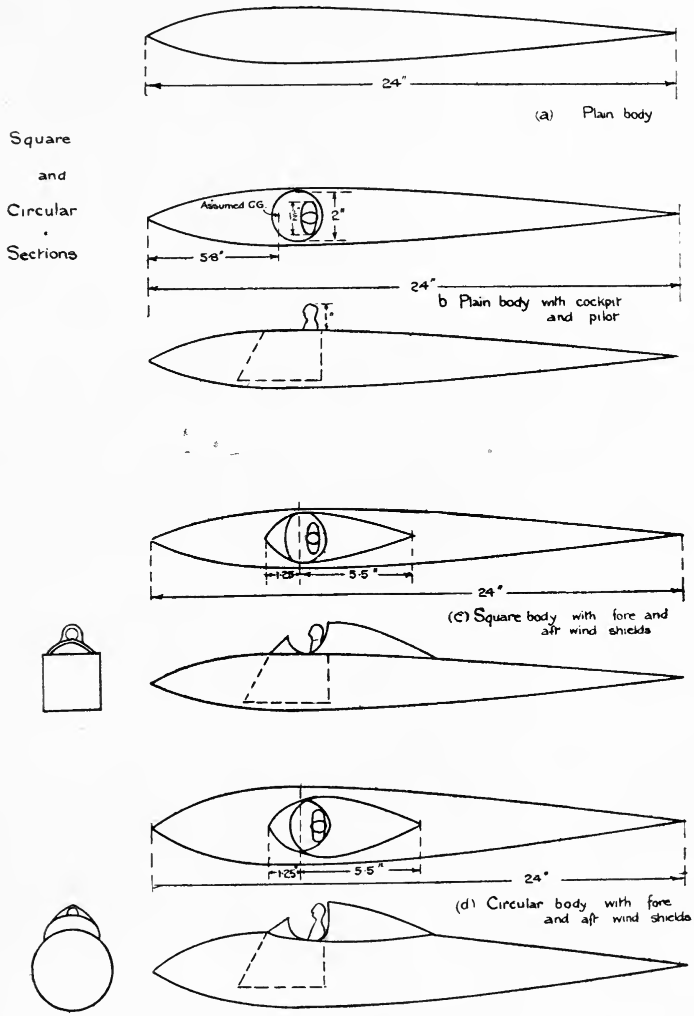

Fig. 157.—Aeroplane Bodies.

various types of fuselages met with in aeronautical practice will next be considered.

Aeroplane Bodies.—An investigation was made by the N.P.L. into the effect of various modifications of the form of aeroplane bodies upon the resulting forces and moments.

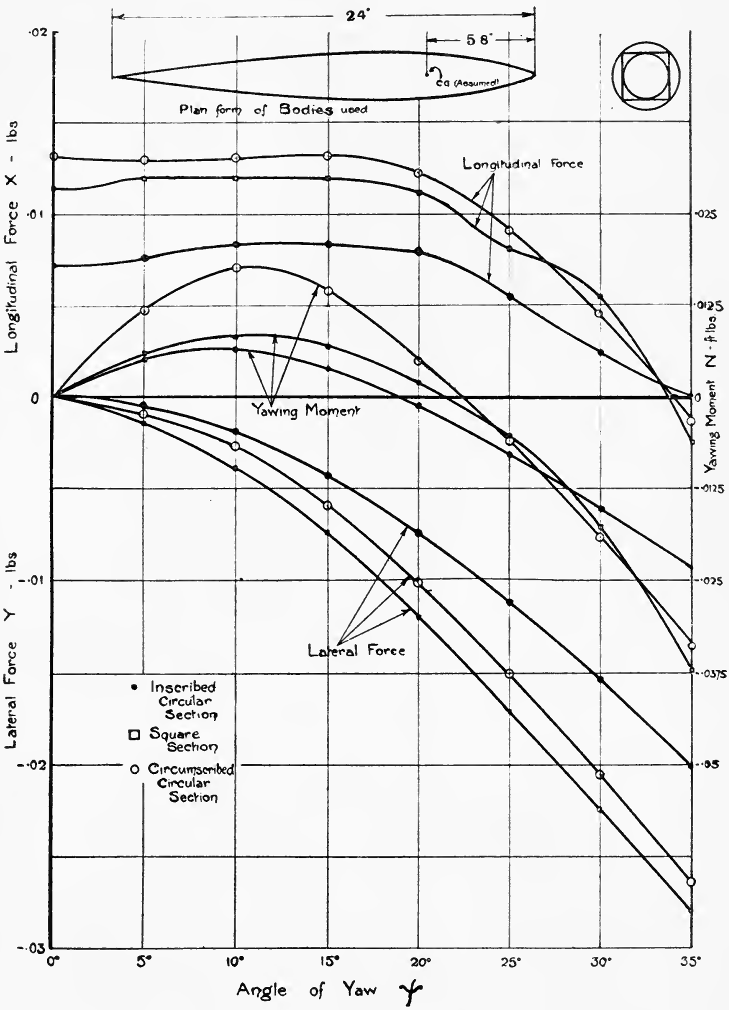

FIG. 158.—Comparison of Bodies of related Cross Section.

A comparison was first made of bodies of square and circular cross section, after which these bodies were modified by the addition of wind shields of various types. For the first comparison the square section body was taken as the basis. Then the relation between the three bodies was such that the circular sections at all points along bodies were respectively the inscribed and circumscribed circles of the square section. The

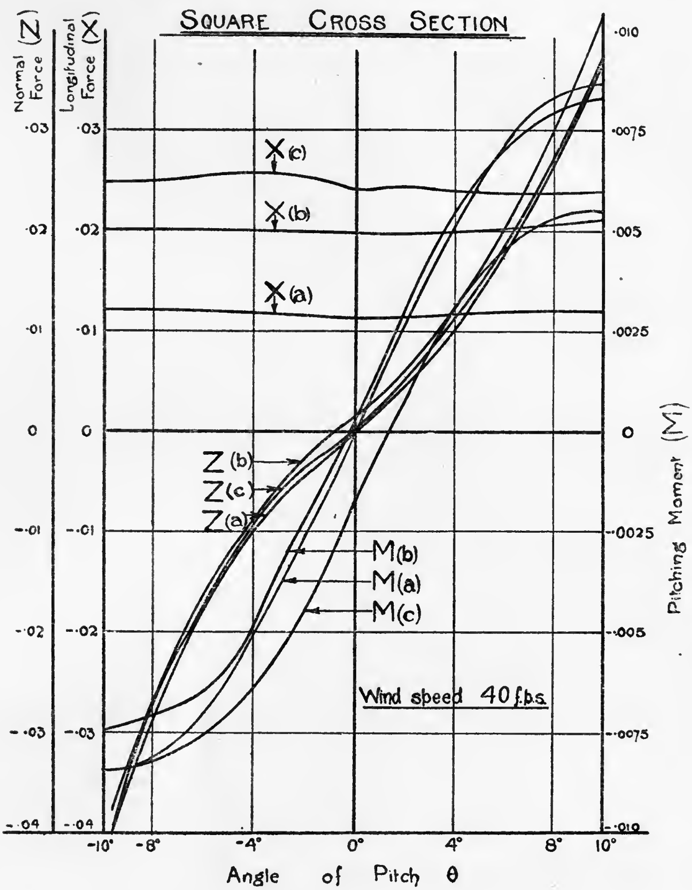

FIG. 159.

scheme is shown at the top of Fig. 158. Throughout this investigation it was assumed that the position of the centre of gravity was 5·8 inches behind the nose of the body, this figure being taken as a fair mean position after a consideration of a large number of types of existing machines.

The experimental results are shown plotted in Fig. 158, and it is somewhat surprising, taking into consideration the available amount of stowage space for engines, etc., the greater con-

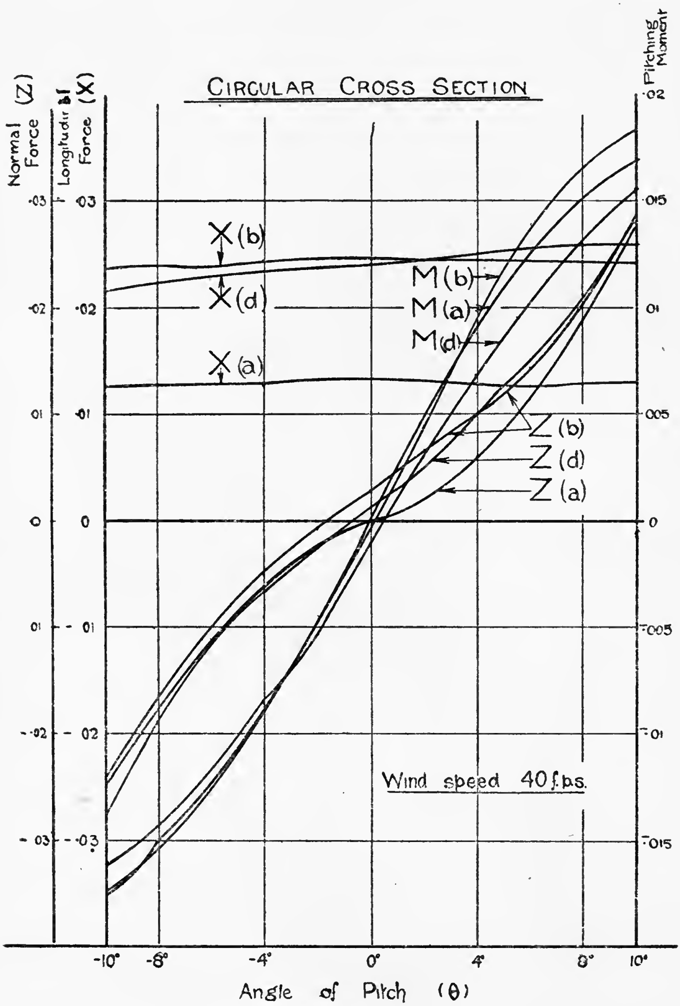

Fig. 160.

venience of attachment of such details as the wings and chassis, and the much greater ease with which it can be constructed, that the square section should prove to be the best type of body for general use. In order to obtain the same amount of stowage space it would be necessary to go to the size of the circum-

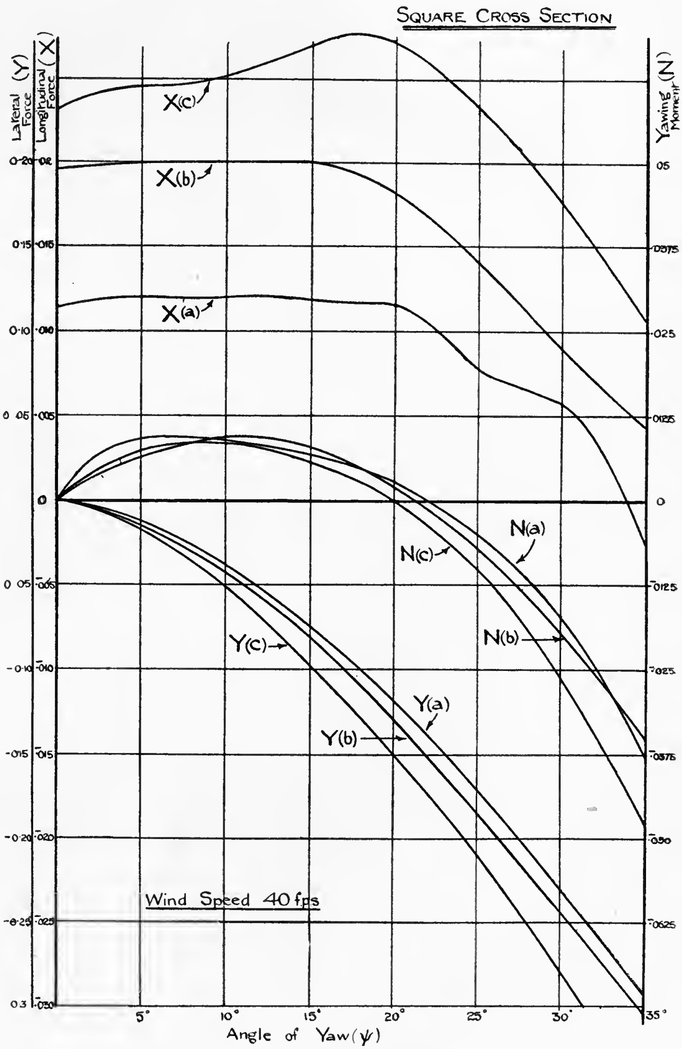

Fig. 161.

scribing circular section, and, as will be seen from Fig. 158, while this body is nearly as good as the square section generally, in the case of the Yawing Moment curve near the origin there is a much greater slope for the circular section, so that a much larger rudder would be necessary in order to counteract the negative righting moment due to the body. Moreover, the

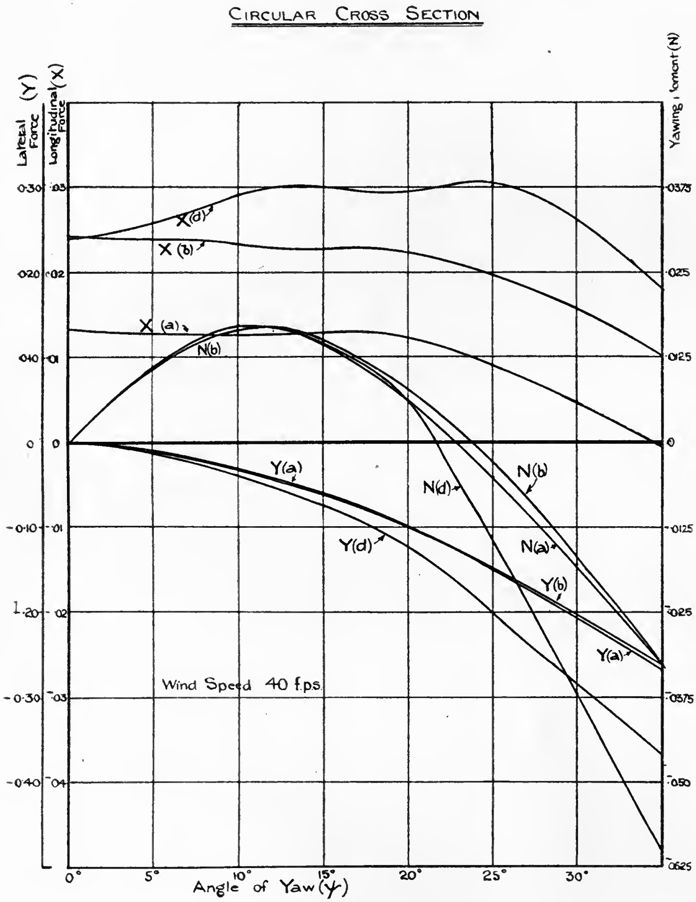

FIG. 162.

square section body possesses a much greater value for the lateral force than the circumscribing circular section, which in practice is equivalent to an addition to the area of the fin, and acts as a corrective to sideslip.

The models for the general series of tests are shown in Fig. 157, namely,

(*a*) Perfectly plain body—square and circular sections;
(*b*) Cockpit and pilot added—square and circular sections;
(*c*) Cockpit, pilot, fore and aft wind shields added—square section;
(*d*) Cockpit, pilot, fore and aft wind shields added—circular section.

Tests were also carried out upon models possessing a rear wind shield only, but, as was to be expected, the results showed that wind shields, both fore and aft, are preferable in all respects.

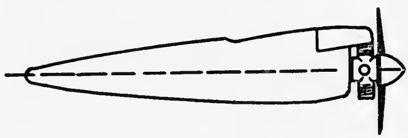

Fig. 163

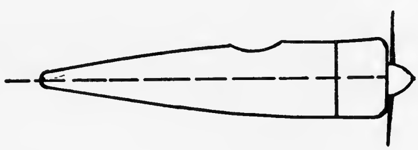

Fig. 164

Fig. 165

The curves plotted in Figs. 159–162 show that small modifications in the shape of the bodies do not affect either the forces or moments to any great extent, with the one exception of the longitudinal force. As will be seen from these figures, this force is particularly sensitive to small changes of shape, more especially so at large angles of yaw. The designer should therefore aim at keeping this longitudinal force as low as possible, while giving the pilot as much protection as possible from the wind, consistent with a good forward view. The development of a satisfactory transparent screen totally enclosing the pilot would be of considerable utility in ensuring his comfort upon long-distance journeys, and of distinct advantage from an aerodynamical standpoint, but mechanical or other means would have to be devised to keep it clear in all weathers.

Deperdussin Monocoque Fuselages.—Eiffel has tested two types of fuselage similar to those shown in Figs. 163 and 164. It will be seen that the bodies differ in the arrangement of the nose portion, the one being fitted with a rotary engine and top cowl only; while in the other the engine was totally enclosed save for a small aperture between the propeller boss and cowl to admit the cooling air. The models were to one-fifth scale and of the following dimensions:—Length, 2·94 ft.; diameter of No. 1 (Fig. 163), 0·525 ft.; diameter of No. 2 (Fig. 164), 0·588 ft. The tests were made at speeds varying from 80 to 90 f.p.s. In the first series of tests no airscrews were fitted to the models, and the results were as follows:—

TABLE XXXI.—MONOCOQUE FUSELAGES WITHOUT AIRSCREWS.

Fuselage.	Resistance at 60 m.p.h.
No. 1	22·6 lbs.
No. 2	19·0 lbs.

In the second series of experiments made upon these models, airscrews were fitted and allowed to rotate with the engine under the influence of the moving air, the conditions thus approximating to those occurring during a glide with the engine switched off but rotating. The results were as follows:—

TABLE XXXII.—MONOCOQUE FUSELAGES WITH AIRSCREWS.

Type of fuselage.	Resistance at 60 m.p.h.
No. 1	65 lbs.
No. 2	43·8 lbs.

It will be seen that the introduction of the airscrew increases the resistance very considerably. This is due to the increased pressure on the fuselage resulting from the airscrew wake and to the disturbance in the air flow over the entire surface.

Fig. 165 represents another type of body in which the model was fitted both with a tail plane and an under-carriage, and was to one-twelfth scale. The resistance of the model was found to be 0·1365 lbs. at 30 m.p.h. The corresponding resistance of the full-size body—24·5 ft. long—complete is 218 lbs. at 100 m.p.h.

B.E. 2 and B.E. 3 Fuselages.—A very complete investigation was made by the National Physical Laboratory into the forces and moments acting upon the models shown in Figs. 166 and 167. Since the results are also of great utility in considering questions of stability in addition to their value in estimating body resistance, they will be given in entirety.

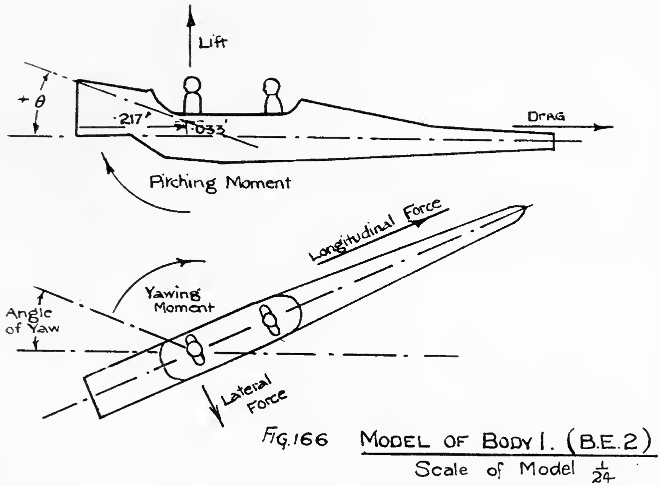

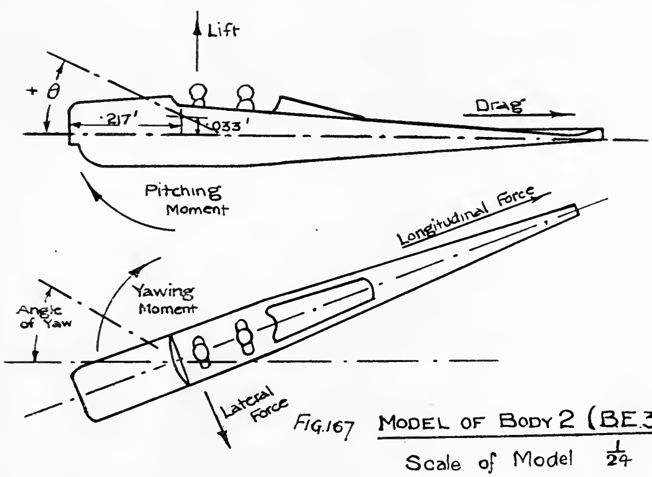

Figs. 166 and 167.—Forces and Moments on Model Fuselages.

Measurements were made of—

(i.) Lift and drag for various pitching angles with zero angle of yaw;

(ii.) Pitching moment about a horizontal axis perpendicular to the wind, with zero angle of yaw;

(iii.) Drag, lateral force, and yawing moment, about a vertical axis for different angles of yaw with the pitching angle zero.

The results are exhibited graphically in Fig. 168. It will be noted, in the case of the longitudinal force curves, how the longitudinal force rises rapidly with increase of angle of yaw in the case of the B.E. 2 body. This is probably due to the projecting head and shoulders of the aviators when there is a small angle of yaw. In the B.E. 3 there is no such effect, and the longitudinal force varies very little for small angles of yaw. The curves show that the B.E. 3 body is of a much better form than the B.E. 2, its drag at zero angle being only half that of the

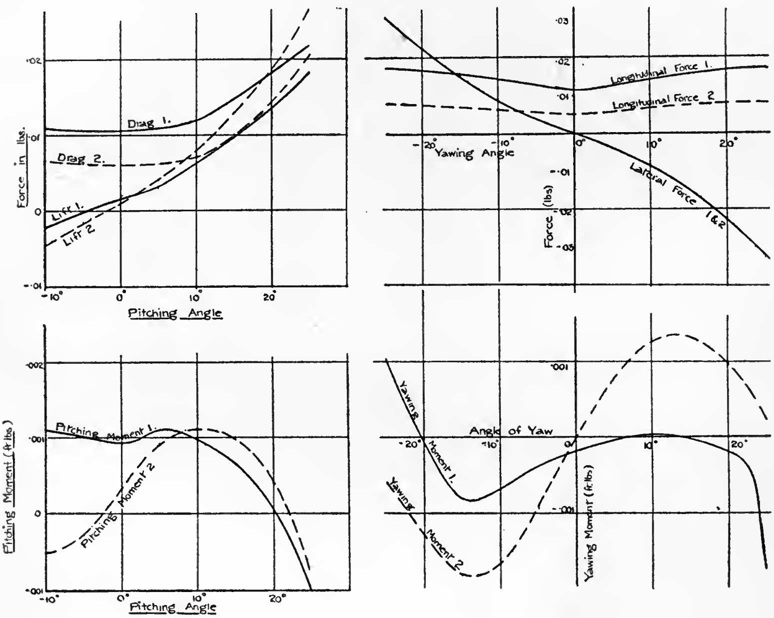

Fig. 168.—Forces and Moments on B.E. Fuselages.

latter in the same position. The moment curves show that in all cases the bodies are unstable in their symmetrical position if supported at the C.G., that is, for small angular displacements there is a moment tending to increase the angle of displacement. The wind speed throughout all these tests was 30 f.p.s.

A further series of experiments was carried out on the two models shown in Figs. 169 and 170. Both these models were tested with and without the rudder, and readings were taken of the lateral force, drag, and yawing moment for various angles of yaw. After these tests had been completed on the model shown in Fig. 169, the recesses round the crank case were faired with plasticine and the drag at zero yawing angle determined. The drag was found to be reduced from 0·016 lb. to 0·0148 lb., a reduction of 7·5%.

The general results indicate that model, Fig. 169, is slightly better than the B.E. 2, but not so good as the B.E. 3 body. The curves of model, Fig. 170, are similar to the others in general form, the chief difference being in the curve of yawing moment without rudder. For this body a restoring moment is obtained

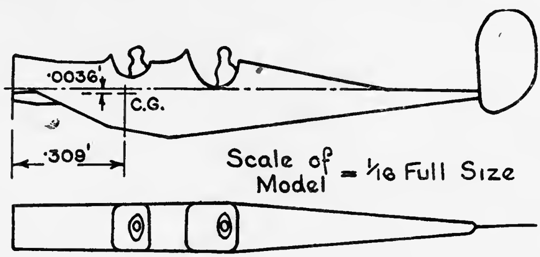

Fig. 169

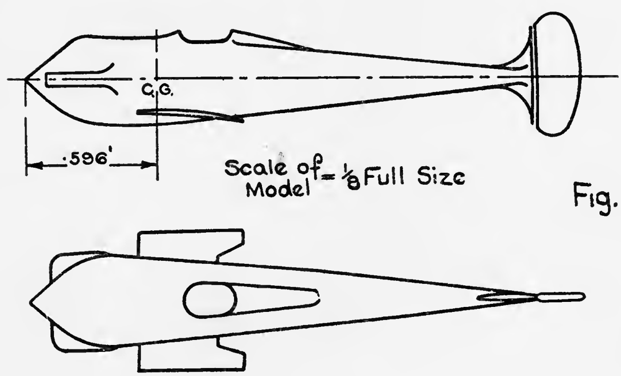

Fig. 170

for displacements from the symmetrical position as regards yawing motion about the C.G. This is probably due to the two small fins just in front of the rudder itself, which were not removed in the test without the rudder.

In Table XXXIII. the resistance in pounds of the four full-sized bodies at 60 m.p.h. without rudder or elevator planes is given. The four bodies are not very different in over-all length, but in order to allow for this difference the value of the resistance, divided by the square of the over-all length, has been given. The figure so obtained is a fair criterion of the relative

FIG. 171.

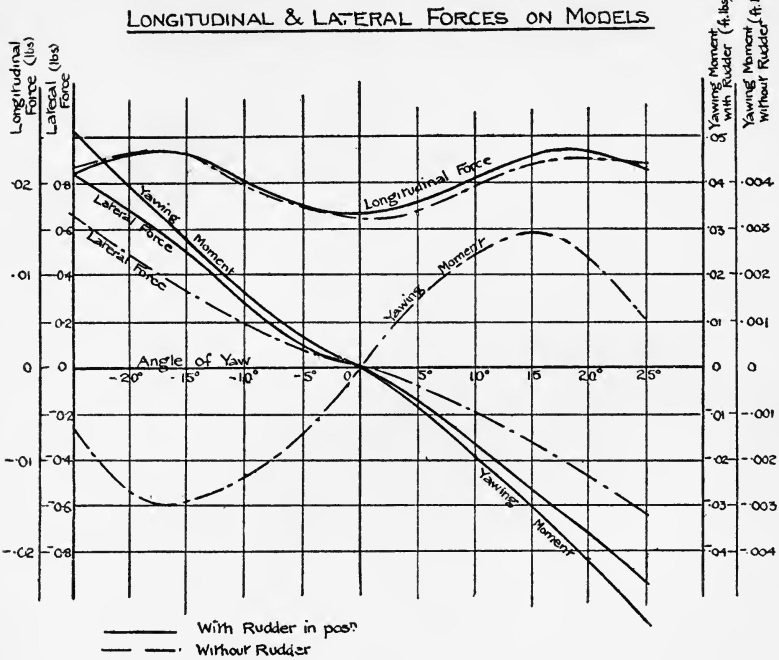
LONGITUDINAL & LATERAL FORCES ON MODELS
Longitudinal Force (lbs)
Lateral Force (lbs)
Yawing Moment with Rudder (ft.lbs)
Yawing Moment without Rudder (ft.lbs)
Longitudinal Force
Yawing Moment
Lateral Force
Lateral Force
Yawing Moment
Angle of Yaw
Yawing Moment
With Rudder in posn
Without Rudder

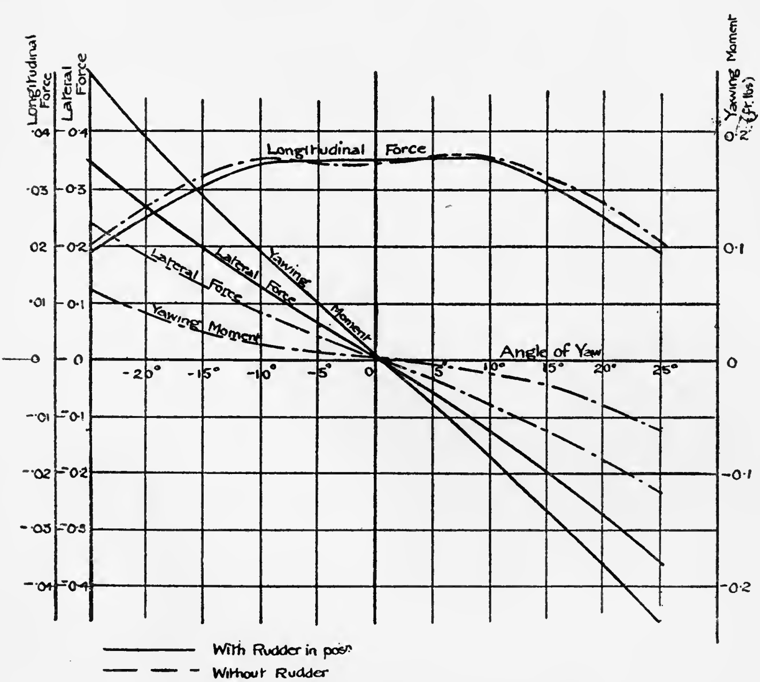
Longitudinal Force
Lateral Force
Yawing Moment N. (ft.lbs)
Longitudinal Force
Yawing
Moment
Lateral Force
Lateral Force
Yawing Moment
Angle of Yaw
With Rudder in posn
Without Rudder

efficiency of the bodies as regards resistance in the normal flight position. The actual resistances were calculated by assuming the drag to vary as the square of the velocity and as the square of the linear dimensions.

TABLE XXXIII.—COMPARISON OF FOUR FUSELAGE BODIES.

Body.	Drag at 60 m.p.h.	Drag/Length^2.
B.E. 2	54·0 lbs.	0·102
B.E. 3	25·8 ,,	0·041
Model 4	35·3 ,,	0·080
Model 5	18·4 ,,	0·054

Resistance of Wires.—The results of a large number of tests show that the resistance of a wire may be expressed in the form,

$$R = K d V^2 \qquad \text{............... Formula 68}$$

where d = the diameter of the wire,
V = the velocity of the air relative to the wire in feet per second,
R = the resistance per foot run,
K = a multiplying constant, which depends upon the product dV, in accordance with the principle of dynamic similarity.

For values of dV less than 0·15, K decreases with increase of dV, and for values of dV greater than 0·15, K increases with dV. It is with the latter portion that we are chiefly concerned in aeronautics. Table XXXIV. gives the values of K for increasing values of dV, and is taken from results of tests at the N.P.L.

TABLE XXXIV.—VALUES OF K WITH INCREASE OF dV.

dV	0·5	1·0	1·5	2·0	2·5	3·0
K	·0012	·0013	·00137	·00141	·00144	·00145

These experiments covered a range of speed of from 9 to 25 feet per second, and the diameters of the wire varied from ·04″ to 0·25″.

More recent experiments at the N.P.L. have been made at speeds up to 50 feet per second and upon wires up to $\frac{3}{4}''$ in diameter. The results are shown graphically in Fig. 172, where the value of the constant K is plotted against the product dV in F.P.S. units.

For example, to find the resistance of a $\frac{1}{4}''$ wire at 100 m.p.h.,

$$d = \cdot 25'' = \cdot 02083'$$
$$V = 100 \text{ m.p.h.} = 146 \cdot 7 \text{ f.p.s.}$$
$$dV = 146 \cdot 7 \times \cdot 02083 = 3 \cdot 06$$

From Fig. 172, the value of K corresponding to 3·06 = ·00145.

$$\therefore \text{ Resistance of } \tfrac{1}{4}'' \text{ wire}$$
$$= \cdot 00145 \times \cdot 02083 \times 146 \cdot 7 \times 146 \cdot 7$$
$$= 0 \cdot 65 \text{ lb. per foot run}$$

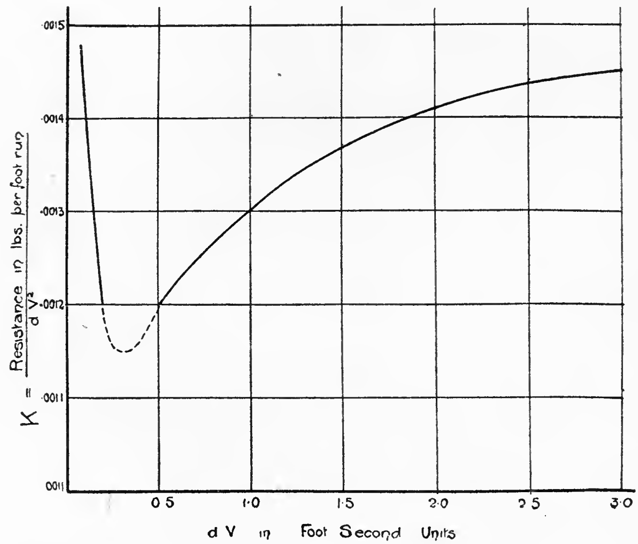

FIG. 172.—Values of k with increase of dV

The values given in Table XXXIV. are for smooth wires. For stranded cables or ropes these values must be increased 20%.

If the struts or wires are inclined to the direction of motion of the air, the resistance may be very much diminished owing to the change in shape of section, as the following table shows.

TABLE XXXV.—RESISTANCE OF INCLINED STRUTS AND WIRES.

Inclination of strut to wind ...	90°	80°	70°	60°	50°	40°	30°	20°
Percentage of Normal Resistance for Constant Projected Length.								
Circular section ...	100	96	88	76	61	45	31	21
Streamline section	100	97·5	91	83	70·5	55·5	45·5	44

The percentage resistance for the struts at all angles is given in terms of their resistance when normal. The last line shows, as was to be expected, that for a streamline strut or wire there is not such a large gain due to inclination as for a strut or wire of circular section.

Resistance of Flat Plates.—The resistance of a flat plate normal to the wind, apart from scale effect, depends upon the compactness of its outline. For example, the best form of

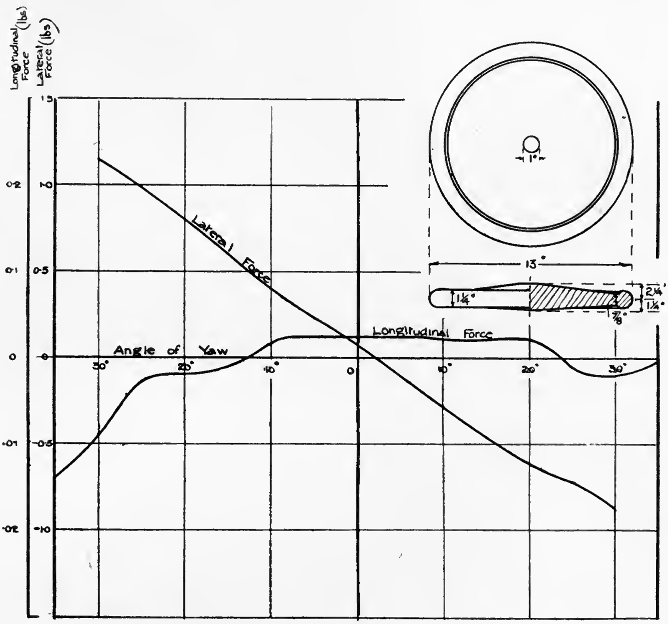

FIG. 173.—Wind Forces on Wheel of Landing Chassis.

outline is a circle, while the worst form is one having many re-entrant angles. The following formula by the N.P.L. gives the resistance of square plates for values of V L between 1 and 350, where V is the velocity in feet per second, and L is the length of the side in feet.

$$R = \cdot 00126\,(V\,L)^2 + \cdot 0000007\,(V\,L)^3 \quad \ldots\ldots\ldots \text{ Formula 69}$$

For rectangular plates the results obtained by this formula must be corrected by the use of the factors in Table XIV.

Resistance of Landing Gear.—When designing a landing gear, care should be taken that all struts and tubes are enclosed in a streamline fairing in order to cut down the resistance as far as possible.

M. Eiffel has measured the resistance of several full-sized landing chassis wheels, the results of which are embodied in Table XXXVI. below.

TABLE XXXVI.—RESISTANCES OF LANDING WHEELS.

Type of wheel.	Dimensions of tyre (mms.)	Resistance at 82 f.p.s.	Equivalent normal plane constant.
Deperdussin	725 × 65	3·88	0·92
Farman (uncovered)	610 × 77	4·19	1·00
Farman (covered)	610 × 77	2·07	0·49
Dorand	530 × 80	2·57	0·68
Astra Wright	450 × 53	1·27	0·80

It will be observed from this table that the effect of covering the Farman wheel is to reduce its resistance by 50%. Tests at the National Physical Laboratory to find the resistance and the lateral force upon the wheel shown in Fig. 173 gave the results shown in that figure.

Effect of Airscrew Slip Stream.—The effect of the airscrew slip stream upon those members situated within it is to increase the velocity of the air impinging upon them. This means a corresponding increase in their resistance, which must be allowed for when making an estimate of their resistance and the total resistance of the machine. The slip stream effect is not easy to estimate, the relative increase in resistance being much greater at low speeds than at high. The slip stream is regarded by some designers as a tubular body of air of external diameter of approximately 0·95 times the airscrew diameter, and internal diameter of 0·2 times the airscrew diameter. All members included within this annular cylinder are exposed to the increased velocity. In the absence of more definite results bearing upon any particular design under consideration, the curve shown in Fig. 174 can be used to give a rough estimate of the increase in resistance. The value of the Tractive power of an airscrew at a given speed is obtained from the equation,

$$\text{Tractive power} = k\left[1 - \left(\frac{V}{Np}\right)^2\right] N^3 D^5 \quad \ldots\ldots \text{Formula 70}$$

where N = number of revolutions per second,
D = diameter of the airscrew,
V = forward speed of the machine,
p = experimental mean pitch of the airscrew,
k = constant whose value can be determined experimentally.

If D be the diameter of the airscrew used, then the value of the fraction $\frac{\text{Tractive power}}{(\text{Diameter})^2}$ can be calculated for the speed under consideration. The value of the corresponding slip stream coefficient is at once obtained from the curve in Fig. 174, and the resistance of each component falling within the slip stream must be multiplied by this coefficient.

Resistance of Complete Machine.—The following table shows the estimation of the resistance of the various parts of an aeroplane. The machine under consideration is the B.E. 2, total weight 1650 lbs., with a speed range of 40–73 m.p.h.

TABLE XXXVII.—ESTIMATE OF BODY RESISTANCE OF B.E. 2 AT 60 M.P.H.

STRUTS.—8—6′ 0″ × 1¼″ @ ·85 lbs./sq. ft. ...	4·2 lbs.	
4—4′ 0″ × 1¼″ @ ,, ,, ...	1·4	
6—3′ 0″ × 1¼″ @ ,, ,, ...	1·6	
		7·2
WIRING.—220 feet cable @ 10 lbs./sq. ft. ...	29·5	
70 feet 12 G.H.T. wire @ 10 lbs./sq. ft.	5·6	
52 strainers, estimated	3·0	
		38·1
Rudder and elevators	2·0	
Body with passenger and pilot	40·0	
Axle @ ·85 lbs./sq. ft.	2·0	
Main skids and axle mounting, estimated ...	1·0	
Rear skid, estimated	·5	
Wheels ,, ...	3·5	
Wing skids, etc. ,, ...	10·0	
		59·0
		104·3

Exposed to a slip stream of 25 feet per second.

Body	40 lbs.	
4—4′ 0″ struts	1·4	
⅔ of 3′ 0″ ,, ...	·8	
50′ 0″ cable	6·7	
30′ 0″ H.T. wire	2·4	
Rudder and elevator	2·0	
Rear skid	0·5	
Fittings	2·0	
	55·8	
Increase in resistance due to slip stream	= 35·7	35·7

Whence total resistance of machine = 140·0 lbs.

The following data will be found useful in estimating the resistance of the different members of a machine.

TABLE XXXVIII.—RESISTANCE OF AEROPLANE COMPONENTS.

Component.	Resistance at 100 f.p.s. Normal area.
Streamline struts ...	1·3 lbs. per sq. ft.
Streamline axle ..	1·5 ,,
Round smooth cable	10 ,,
Stranded cable ...	12 ,,
Landing wheels ...	4·0 ,,
Fuselage ...	3·4 ,,
Tail skid ...	5·9 ,,
Tail plane and rudder	1·0 ,,
R.A.F. wires	3·25 ,,
Wing skids	5·0 ,,
Tail plane and aileron levers	2·5 ,,

Experimental Measurement of the Resistance of Full-size Machines.—Two methods have been adopted for the measurement of the resistance of actual machines—

(i) By measuring the gliding angle of the machine with the engine switched off and the propeller stopped.

Let θ = the gliding angle

then we have $\tan\theta = \dfrac{\text{Lift}}{\text{Drag}}$ .... Formula 71

In gliding flight the lift is given by the relationship

$\text{Lift} = W\cos\theta$ .... Formula 72

so that the drag is very easily calculated.

The value of the drag thus obtained represents the total resistance of the machine, that is the wings and the body, at the speed of flight considered. The resistance of the wings can be calculated directly from the area of the supporting surface and the characteristics of the aerofoil used by applying Formula 14.

Corrections must be applied for speed and scale effect and also for interference effects. By subtracting the resulting resistance of the wings from the total resistance obtained previously, the body resistance is determined, and may be compared with that used in the original estimate for the purposes of preliminary design. The principal difficulty encountered in this method results from the very rapid change which occurs in the density of the atmosphere as the machine descends, and which will give rise to serious errors unless its effect is eliminated.

(ii) By determining the thrust of the airscrew during a series of climbs.

The direct measurement of this thrust by means of a thrust meter offers the most convenient and accurate method of determining the resistance of a machine, but the difficulty of obtaining a reliable instrument has so far prevented the results secured from being of an entirely satisfactory nature. It has therefore been necessary to deduce the thrust from particulars of the horse-power and the airscrew efficiency of the power unit employed, under conditions similar to those encountered during the test.

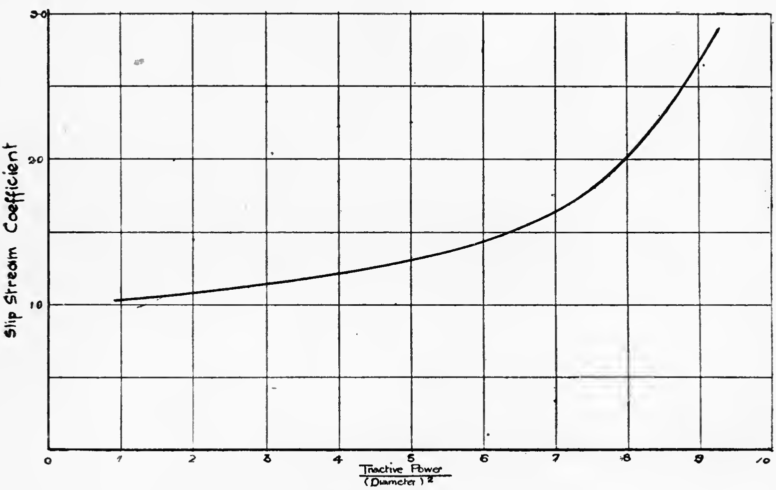

FIG. 174.—Slip Stream Coefficient.

Having obtained this information and carried out the climbing tests, the thrust necessary to overcome the drag of the machine can be determined and the body resistance deduced, as in case (i).

Skin Friction.—When a fluid flows smoothly over a stream-line body such as an efficient airship envelope, or a thin flat plate placed edgewise and assumed to have no head resistance, a certain resistance is still felt against the relative motion of the body and the fluid, which is termed the skin or surface friction. A thin film of air covers the actual surface of the body, being entangled in the 'roughness' of its outer layers, and imprisoned there by the outer pressure of the air. The frictional force felt is partly due to the continuous shearing which takes place between this film and the stratum of fluid adjacent to it. It is therefore a function of the viscosity of the fluid. The coefficient of viscosity is defined as the force required to maintain a plate of unit area at unit velocity when it is separated from another plate by a layer of fluid of unit depth.

Stokes showed that so long as the motion was sufficiently slow to avoid eddies the frictional resistance varied as the first power of the velocity. Allen showed that this stage was followed by one in which the index of the velocity was 1·5. In the range of velocity common in aeronautical practice the index appears to lie between 1·5 and 2. Lanchester and Zahm further developed the fundamental equation, and from the experiments carried out by the latter, in which the skin friction of a large number of smooth surfaces in a current of air was measured, it was found that the resistance increased according to the power 1·85 of the velocity. Zahm therefore developed the following equation, connecting skin friction with the length of the plane and the velocity.

$$p \propto L^{-.07} V^{1.85} \quad \text{........... Formula 73.}$$

V = the velocity in feet per second.
L = the length of the planes in feet.
p = the tangential force per square foot.

Lanchester has shown that to express the resistance of a plane in terms of the linear size and kinematic viscosity, the relation

$$R \propto \nu^q L^r V^r \quad \text{........... Formula 74}$$

Where R = resistance per unit density

ν = kinematic viscosity $= \dfrac{\mu}{\rho} = \dfrac{\text{coefficient of viscosity}}{\text{density}}$

L = linear size

V = velocity

holds for an incompressible fluid when $q + r = 2$.

Expressing Zahm's equation (Formula 73) in terms of R, it becomes

$$R \propto L^{1.93} V^{1.85} \quad \text{........... Formula 73 } (a)$$

whereas, in order to satisfy Lanchester's equation (Formula 74), the indices of L and V should be equal.

Lanchester has therefore adopted the following expression for a smooth surface :—

$$R \propto \nu^{.1} L^{1.9} V^{1.9} \quad \text{........ Formula 74 } (a)$$

Assuming that the exponent varies with the nature of the surface, as has been found to be the case by actual experiment, Formula 74 (*a*) may be written in the form

$$R \propto \nu^{2-n} L^n V^n$$

Whence $$F = R\rho = K\rho\nu^{2-n} L^n V^n \quad \text{...... Formula 75}$$

For any one surface it is convenient to neglect the length and embody its value and the value of ρ and v in one constant, when the equation becomes

$$F = K \,.\, V^n \quad \text{............ Formula 75 }(a)$$

The value of K depends, of course, on the units employed, and both n and K may vary with the surface for even so-called 'smooth' surfaces.

An exhaustive series of experiments have been carried out at Washington to determine the values of F, n, K in the simplified Formula 75(*a*) above. Plate glass was used as a standard surface, since it is very smooth, and can be readily duplicated. The various fabrics were attached to this surface by a special varnish, to obtain as smooth a surface as possible; and experiments were made at velocities of 30 to 70 m.p.h., and the forces measured with great accuracy. The results obtained are shown in Table XXXIX., where F is in lbs. per sq. ft., and the resistance factor (R.F.) is the ratio Observed resistance : Resistance of Glass Plate.

TABLE XXXIX.—SKIN FRICTIONAL RESISTANCES.

Nature of surface exposed.	PLATE GLASS.	FINE LINEN, uncoated.	One coat of aero varnish.	Three coats of aero varnish.	Three coats of aero varnish one coat of spar varnish.	AEROPLANE FABRIC, rubber surface.
n	1·81	1·94	1·84	1·89	1·84	1·83
$K \times 10^7$ ...	166	128	163	129	153	165
m.p.h.						
30 F ...	·0079	·0095	·0085	·0082	·0081	·0084
R.F. ...	1·0	1·205	1·081	1·042	1·031	1·070
40 F ...	·0133	·0161	·0141	·0138	·0135	·0142
R.F. ...	1·0	1·234	1·080	1·060	1·034	1·082
50 F ...	·0199	·0249	·0218	·0208	·0204	·0215
R.F. ...	1·0	1·254	1·098	1·048	1·028	1·083
60 F ...	·0276	·0361	·0309	·0295	·0287	·0299
R.F. ...	1·0	1·305	1·118	1·067	1·038	1·081
70 F ..	·0364	·0496	·0424	·0403	·0387	·0393
R.F. ...	1·0	1·362	1·162	1·108	1·061	1·079

With the aid of this table the actual skin friction of an aeroplane wing surface can be easily calculated. It will be found that it is a very small quantity. It is only in the case of airships where relatively low head resistance is combined with a large surface area that the effects of skin friction are found to be considerable.

Zahm's experiments upon a series of surfaces of width w resulted in the following equation :—

$$F = \cdot 00000778\, w\, L^{0 \cdot 93}\, V^{1 \cdot 85} \quad \ldots\ldots \text{ Formula 76}$$

where F is the friction in pounds at a speed of V feet per second. For double-sided planes this value must be doubled, but when estimating the surface friction of streamline shapes the single value alone may be employed.

Zahm's formula for the skin friction of a fuselage is

$$F = \cdot 00000825\, A^{0 \cdot 925}\, V^{1 \cdot 85} \quad \ldots\ldots \text{ Formula 77}$$

where A is the superficial area in square feet, and V the velocity in feet per second.

CHAPTER VII.

DESIGN OF THE FUSELAGE.

Weights.—Before proceeding to consider the general and detail design of the fuselage, it is necessary to examine more closely the question of the weights of the various components of an aeroplane.

With this object in view Table XL. has been prepared from an analysis of a large number of machines of various types, and gives the percentage weights of the different portions of the machine arranged in groups. The weights of the individual members of a group will, of course, vary considerably in different designs.

TABLE XL.—PERCENTAGE WEIGHTS OF AEROPLANE COMPONENTS.

1. *The Power Plant.*		
(*a*) Engine	20·0	
(*b*) Radiator	2·5	
(*c*) Cooling water	2·0	
(*d*) Tanks and pipes	3·0	
(*e*) Airscrew	2·5	
	——	30·0
2. *The Glider Portion.*		
(*a*) Wings	13·0	
(*b*) Wing bracing	3·0	
(*c*) Tail unit	2·0	
(*d*) Body	13·0	
(*e*) Chassis or undercarriage	4·0	
	——	35·0
3. *Useful Load.*		
(*a*) Fuel	20·0	
(*b*) Passengers and cargo	14·0	
	——	34·0
4. *Instruments, etc.*		1·0

Table XLI. gives particulars concerning the chief Modern Aero Engines of various types.

TABLE XLI.—WEIGHTS AND PARTICULARS OF LEADING AERO ENGINES.

NAME OF ENGINE.	At ground level.		Method of cooling.	Type of engine.	No. of cylinders.	Fuel consumption. lbs. per B.H.P. hr.		Weight of engine dry.		Weight of engine with fuel and tanks for 6 hours running.		Overall dimensions of engine. Length.	Width.	Height.
	Normal B.H.P.	R.P.M.				Petrol.	Oil.	Lbs.	Lbs./B.H.P.	Lbs.	Lbs./B.H.P.	Inches.	Inches.	Inches.
A B.C. Wasp	170	1750	Air	Radial	7	·495	·019	260	1·53	820	4·82	35·7	42·2	42·2
„ Dragon Fly ...	320	1650	„	„	9	·560	·020	600	1·88	1801	5·64	42·1	48·5	47·5
B.R. 1	154	1250	„	Rotary	9	·59	·10	405	2·6	1130	7·8	43·5	47·5	41·6
B.R. 2	238	1300	„	„	9	·63	·074	475	2·0	1544	6·5	—	—	—
Clerget	127	1250	„	„	9	·60	·123	400	3·15	1009	8·0	36·2	40·15	40·15
Cosmos Jupiter	450	1800	„	Radial	9	—	—	662	1·47	—	—	—	—	—
Gnome	103	1200	„	Rotary	9	·72	·18	270	2·7	848	8·25	19·6	38·5	38·5
Hispano Suiza	150	1450	Water	V. 90°	8	·52	·05	440	2·93	1018	6·8	51·5	33·6	32·8
„ „	208	2000	„	„	8	·52	·056	510	2·32	1492	6·7	51·5	33·6	32·8
„ „	300	1600	„	„	8	·52	·056	596	1·98	—	—	—	—	—
Liberty 8 A	270	1700	„	V. 45°	8	·547	·050	575	2·12	1637	6·06	—	—	40·2
„ 12 A	400	1700	„	V. 50°	12	·509	·037	845	2·11	2276	5·68	69·0	27·8	40·2
Mercedes	150	1250	„	Vertical	6	·60	·028	618	3·86	1270	8·5	—	—	—
„	252	1400	„	„	6	·605	·032	935	3·75	2040	8·06	—	—	—
Napier Lion	450	2000	„	V. 60°	12	·48	·020	850	1·89	2670	5·95	—	—	—
Rolls Royce, Falcon 3 ...	270	2200	„	„	12	·53	·026	723	2·68	1880	6·9	72·0	37·24	42
„ „ Eagle 8 ...	350	1800	„	„	12	·50	·028	933	2·66	2406	6·9	76·0	42·5	48·03
Siddeley	240	1400	„	Vertical	6	·50	·062	625	2·6	1678	7·0	69·9	24·1	43·6
Sunbeam...	350	2000	„	V. 60°	12	·50	·038	1118	3·2	2598	7·1	61·8	37·8	38·9
B.H.P.	240	1400	„	Vertical	6	·52	·035	605	2·52	1650	6·9	66·7	19·0	43·8

When considering the question of design it will be found very convenient in the preliminary stages to remember the approximate weights in groups of items which are associated together in an aeroplane. One method is to divide up the total weight into the three main divisions or groups shown in Table XL., namely:

1. The weight of the power plant.
2. The weight of the glider portion.
3. The weight of the useful load carried.

The proportion of these components to the total weight of the machine is set out in this table, and the figures given there will serve as a useful basis from which to start.

Another method is to group together the power plant, fuel, and accessories, and consider them concentrated at the engine bearers. A second group is made up of the pilot, instrument board, control levers, and other fittings of the cockpit. A third group is formed by the tail unit, and comprises the tail plane, elevators, rudder, fin, and tail skid. This is a light group, but as it acts at a long leverage from the C.G. it is of importance for balancing purposes. In this method, the chassis and wings being close to the C.G., may sometimes be neglected in obtaining a preliminary balance, but the effect of these weights must not be overlooked when the design is finally considered.

In disposing of the weights it is a good rule to concentrate them as much as possible in order to reduce the moment of inertia of the machine. Some latitude also must be allowed so that after the complete design of the wings, chassis, tail unit, etc., has been got out, a heavy weight such as the engine or pilot may be moved a short distance so as to compensate for any initial errors of estimation in weight or leverage. All fluctuating loads such as fuel, bombs, cargo, should be concentrated as near the C.G. as possible, so that balance may be preserved after unloading.

The Fuselage.—The fuselage has to be strong enough to stand up to difficult conditions in its function as a structural member. Its duties are—

1. To act as a double cantilever in flight, supporting the weights of the engine and pilot through the agency of the wings.
2. To support the same two weights when the chassis strikes the ground in a fairly bad landing.
3. To withstand the compression in the spars of the wings.
4. To act as a vertically loaded beam when it transmits the pitching moment due to moving the elevators, or that due to the tail plane in a longitudinal oscillation.

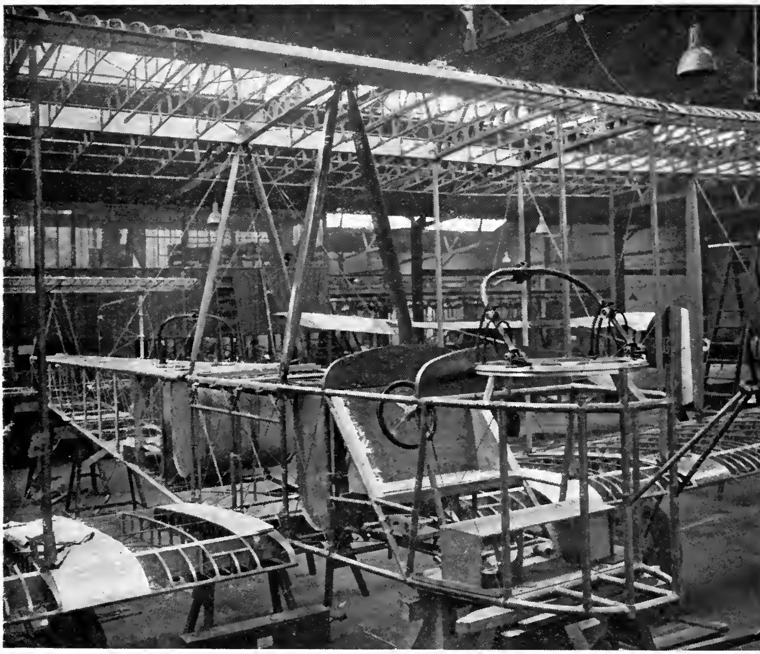

Reproduced by courtesy of Messrs. Vickers, Ltd.

FIG. 178.—Fuselage of the 'Vimy' Bomber.

Facing page 240.

5. To act as a horizontally loaded beam when directional moments are applied by the rudder or the vertical fin.

6. To resist any torsion due to the warping arrangements or the power plant.

Such a complexity of systems of loading leads to a symmetrical method of construction.

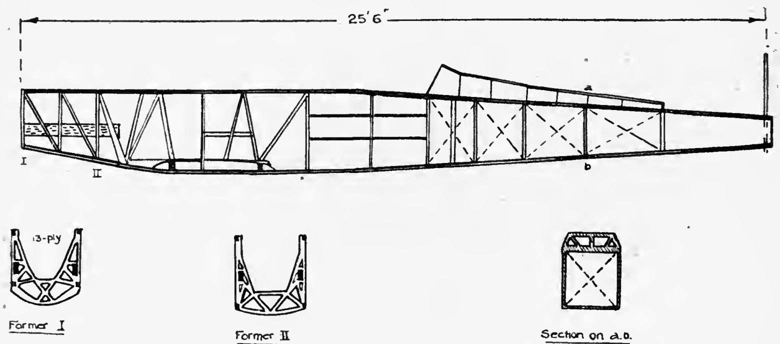

FIG. 175.—Example of Wooden Fuselage.

In general four main longerons run from end to end of the fuselage. Transverse, horizontal, and vertical struts divide the main structure up into a series of panels, each of which is cross-braced by means of small tie-rods (see Fig. 176). For machines fitted with stationary engines the vertical struts at the forward end are frequently replaced by plywood formers cut to the

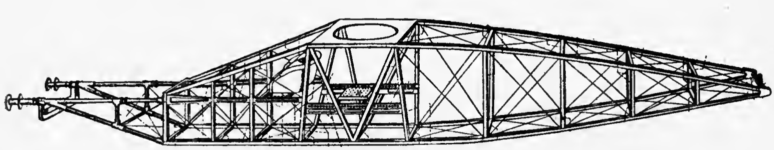

FIG. 176.—Wooden Fuselage with tubular Engine Bearers.

cross-sectional shape of the body, and lightened out wherever possible (see Fig. 175). These formers transmit the direct weight of the power plant to the fuselage. In this manner a very strong structure is obtained without the addition of a large amount of weight. The longerons may be of ash, spruce, or steel tubes. The section adopted depends upon the material used, and also upon the need for achieving minimum weight.

The finished longeron represents a number of small struts, joined together at the ends, and bent to obtain a streamline form. If lightened out the longeron must be bent very carefully in order to prevent the introduction of initial strains. For machines of about a ton in weight the longerons may be made of wood of $1\frac{1}{4}''$ square section in the important part, tapering away at both ends. If a single length of good quality is not obtainable, two pieces may be spliced together or connected by a clip. Wherever exposed to wearing conditions such as foot-rubbing, engine heat, etc., they should be sheathed or otherwise protected. As far as possible, holes in the longerons should be avoided, in fact it is good practice not to pierce them at all. If pierced to carry any strain-bearing bolt, the bolt should be supported externally by means of flitch plates. A form of clip can be easily devised which satisfies the requisite conditions to take the wires which radiate from the junction of the longeron with strut, and further keeps the strut in position. From the general arrangement made in the drawing office the fuselage will usually be set out full size on a large board in the shops. The longerons may be bent and the size of the struts cut off to the very accurate shapes and dimensions given by the latter drawing, which also supplies the local angles of the longeron and struts.

The longerons are bound in pairs at their rear ends to the sternpost, which provides a strong fixing for the rudder and the hinge spar for the elevators (the rear spar of the tail plane). The sternpost may be either of wood or a steel tube, and may also conveniently serve for the fixing of the tail skid and of the vertical fin. At their forward end the longerons are bound to the corners of a square or rectangular plate, which, if the engine is overhung, serves as an engine bearer plate (see Fig. 183), or provides a fixing for the extension shaft for the airscrew.

The square section given to the fuselage by the longerons and struts is far from ideal from the standpoint of streamlining, especially on the top. The flat top may be rounded off by means of fabric stretched over formers. These formers may be built up very lightly out of reinforced plywood, lightened out until there is very little material left. They may be mounted over the top struts, and connected together by means of a few longitudinal strips. Fabric should be used wherever possible as a fuselage covering, and three-ply should be avoided owing to its much greater relative weight.

In this connection it is important to remember the results of the experimental investigation into the relative merits of the square and circular cross-section aeroplane bodies given in the preceding chapter. As will be seen from Fig. 184, it is possible to build up a fuselage of streamline shape without using a square section as the basis.

Two or three of the top bracing-panels will require to be omitted on account of:

1. The pilot.
2. The passenger, if any.
3. The fuel tanks.
4. Perhaps the engine.

This means collectively a serious weakening, and the panels thus mutilated should be strengthened by all convenient means.

Points of attachment of heavy weights, such as pilot, passenger, tanks, etc., should be made to the longerons at the cross panels. This principle must be the chief guide in setting out the fuselage, and it should be remembered that bending moments are to be avoided as far as possible in any member of the body. Further, where a compressive force, as from the wings, comes on the fuselage a specially strong strut should be arranged to take the strain directly, and, where a tension may be applied, a special tension member should be introduced. The sizes of these members are calculated in the usual manner.

The general arrangement of the fuselage may be conveniently set out by drawing a section longitudinally, and then making drawings of each cross panel. The formers, wherever used, should be included in the transverse sections.

It is useful to have cardboard models of a pilot to the scales most generally used in the office, as there is frequently a question as to clearance between some portion of the pilot's body and the various fittings in the cockpit.

The engine is the limiting factor in considering the design of the fuselage aerodynamically. If a radial engine is used it may be hung on the nose of the fuselage and partially protected by a cowl, or it may be totally enclosed some way back. The second method gives much greater scope with regard to the streamlining of the fuselage, although it is impossible—owing to considerations of balance—to get the engine back far enough. It has the great drawback, however, that it greatly increases the weight owing to the extension of the airscrew shafting, bearings for same, and extra engine-bearing plates of large size. It is further liable to accidental fires. In the case of the heavier type of the fixed cylinder engine its greater weight will necessitate a less forward position, leading to greater ease in aerodynamic design. On account, however, of the shaft, and consequently the airscrew, being at the bottom of the engine instead of in the middle, it will be difficult to totally enclose the engine without unduly increasing the height of the chassis, still keeping to the minimum section of body. The cylinder heads are often left exposed in this type of engine and may spoil an otherwise good design, more especially if the heads happen to be placed in the airscrew slip-stream. In important cases, and in fact whenever possible, different designs should be tested in the wind tunnel and compared from the point of view of weight and cheapness to manufacture. As we have previously seen, a small saving in head resistance is likely to be of great importance in high-class work. When considering the question of skin friction of a fuselage, Zahm's formula may be used, namely:

$$\text{Skin-friction} = \cdot 00000825\ A^{0 \cdot 925}\ V^{1 \cdot 85}$$

where A is the superficial area in square feet
V is the velocity in feet per second.

Assuming ordinary dimensions, it will be seen on applying this formula that air friction accounts for about half of the total resistance of a good fuselage shape. The total head resistance of the fuselage will then vary as a power of the velocity between 1·85 and 2. Wind-tunnel tests would be useful to a designer in assessing the true value of this index for a particular case.

The importance of keeping the maximum cross-sectional area low should not be lost sight of. It is frequently argued, and it is often true, that it is better to waste space by increasing the maximum cross dimensions of the fuselage, if by so doing the 'lines' of the fuselage may be improved. The principle is a sound one within certain prescribed limits, but it is easy for an enthusiast in streamlining to increase the maximum section of the fuselage by 2″ to 3″ all round, thus increasing the maximum cross-sectional area by some 30%. This means that the coefficient of head resistance of the thicker shape would have to be improved by the same amount (30%) in order that the enlarged body should have as small a resistance as the original body, and more than this amount if improvement is to be attained. The size, therefore, should be kept as small as possible consistent with housing the engine and pilot and without unduly exposing parts of either to the wind. This last consideration will limit the size of the cockpit opening and lead to a small shield, a few inches only in height, being placed on the forward half of the cockpit opening in order to spill the air over the opening.

It is interesting to note in this connection that totally enclosing the fuselage cockpits results in a greatly reduced resistance. For example, the Vickers' Commercial machine, the fuselage of which will be shown later in this chapter, is 10% faster than its prototype, the Vickers' Vimy Bomber. This and other types of fuselage used in modern practice are shown in Figs. 175-184.

In the fuselage shown in Fig. 175 it will be observed that the longerons are supported in their correct position by means of three-ply formers in the front portion and by means of struts and wires in the rear portion.

An excellent type of fuselage is that of the Bristol Fighter, which is shown in Fig. 176. The front portion, comprising the engine-bearers, is composed of tubular steel, while the remaining portion of the structure is built up of wood braced together with small tie-rods. The depth of the beam increases towards the centre of the machine and thereby helps to keep the bending stresses low throughout.

In order to afford a comparison between the fuselages of two

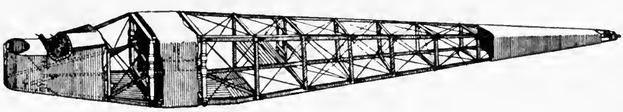

FIG. 177.—Fuselage of Handley-Page (0–400) Machine.

machines which are being largely adopted for commercial work, and to illustrate the different methods employed in practice in building large fuselages, the fuselages of the Handley-Page and the Vickers' machine are shown in Figs. 177 and 178.

As will be seen, the Handley-Page follows the construction of the types already illustrated, while the Vickers' machine exhibits a totally different type of construction. As adapted to commercial uses the passenger cabin of the latter machine is of considerable interest. It may be mentioned in passing that the sole modification of the well-known war machine of the Vickers Company, the Vimy Bomber, for commercial purposes, lies in the use of a different fuselage. As will be seen from Fig. 179, the shell of the cabin is built up of oval wooden rings of three-ply box section, the formers being shown in the background of Fig. 179. The cover of the cabin is made according to the 'Consuta' patent of Saunders, of Cowes, and is constructed of thin layers of selected wood, the grain being placed diagonally, and then glued and sewn together, the rows of stitching running in parallel lines about $1\frac{1}{2}''$ apart. The strength of this material is very great, giving a high factor of safety to the cabin, and enabling all cross-bracing wires to be dispensed with in the interior of the cabin, as shown in Fig. 180. An exterior view of the completed cabin is shown in Fig. 181.

Fig. 182 illustrates the fuselage of the Fokker Biplane. It will be seen that it is built up of thin steel tubes which are welded together. The longerons are fixed relatively to one another by means of cross struts butt-welded to the longerons and by means of bracing wires. This method of construction has not proved very successful up to the present, mainly on account of the difficulties of welding and brazing, and it is found

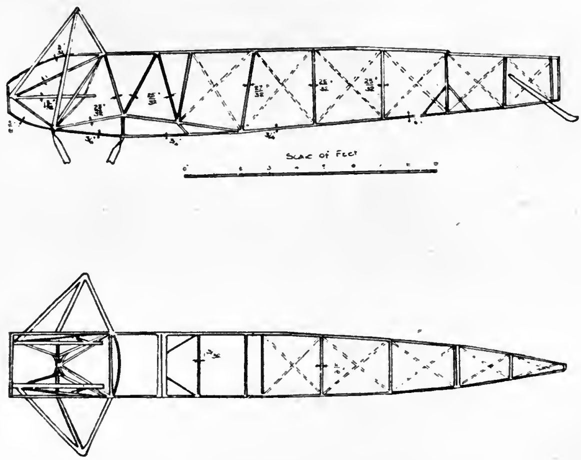

FIG. 182.—Example of Steel Fuselage.

that for a given weight a wooden fuselage is stronger. It is more probable that the steel fuselage of the future will be constructed by the methods usually adopted in other engineering structures, namely, by means of steel channels and angle irons. By this means the expensive steel sockets and fittings necessary at the joints of a wooden structure can be avoided, while the work involved in pressing out a steel channel or angle iron to the desired shape is very much less than the process of producing such a member in wood. Moreover, it can readily be lightened when necessary and desirable by punching holes in it. The Sturtevant Company of America have already produced fuselages upon these lines, and apparently with some success. One type of their large battle-planes is fitted with a steel fuselage which, complete with steel engine-bearers and bracing, weighs only 165 lbs. It is estimated that a wooden structure of equal strength would weigh over 200 lbs. The Sturtevant fuselage has been found quite satisfactory in a series of prolonged tests, and there is little doubt that in process of time the use of steel or light alloys in this direction will be very greatly extended.

Fig. 183 illustrates the fuselage of a small scout machine, namely, the Sopwith Camel. It follows the usual girder type of construction. The longerons at the forward end fit into a pressed steel engine bearer which carries the rotating engine with which this machine is fitted. The engine cowl is attached to the circular tube seen at the fore end.

Fig. 184 illustrates the fuselage of the German Pfalz, and gives an excellent idea of the body formers and the position of the longerons for obtaining a good streamline shape.

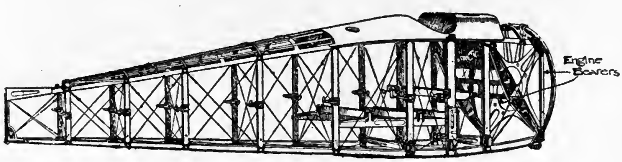

FIG. 183.

Stressing the Fuselage.—The method of stressing the fuselage will now be briefly considered. For the general type of fuselage structure such as is shown in Figs. 176, 177, 178, 182, 183, the determination of the stresses in the various members is not a difficult matter once the external loads upon the structure have been estimated. It is customary to stress the rear portion of the fuselage for the tail load alone, this being considered as an isolated load acting at the point of attachment of the tail plane to the fuselage. The tail plane may be subject either to lift or to down load, thus causing the fuselage members to be subject to reversed stresses. The usual method of designing the tail plane is to assume it to be subject to a uniform load per square foot of area. This having been decided upon, the total load applied by the wind forces through the tail plane upon the fuselage is easily determined. It is common practice to assume a loading of from 15 to 25 lbs. per square foot of tail surface, either up or down forces, the larger figure being adopted where a high factor of safety is desired. The principal load upon the front portion of the

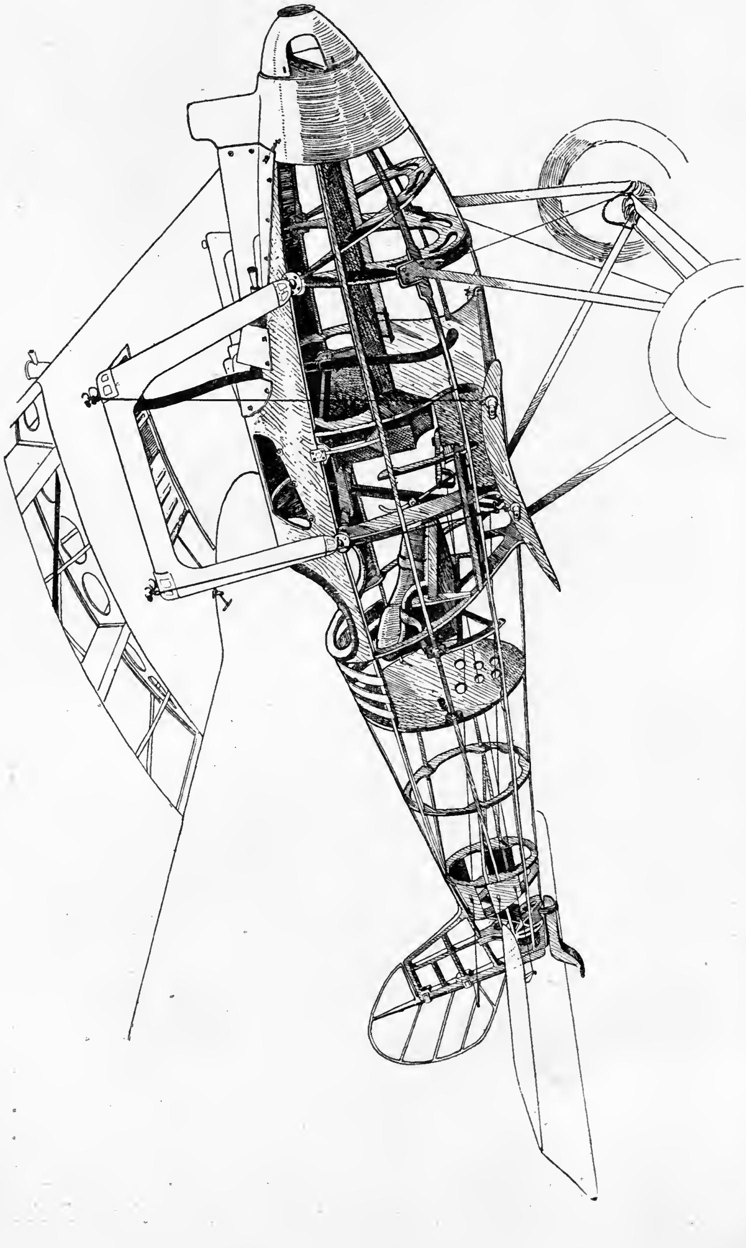

FIG. 184.—Fuselage of the Pfalz Machine.

Reproduced by courtesy of 'Flight.'

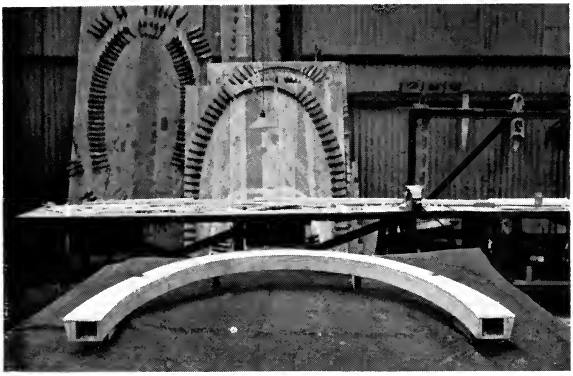

FIG. 179.

FIG. 180.

FIG. 181.

Reproduced by courtesy of Messrs. Vickers, Ltd.

Construction of Passenger Cabin for Vickers' Commercial Machine.

Facing page 248.

fuselage is that of the power plant, which includes engine, radiator, fuel, tanks, etc. Having decided upon the position in which these items are to be fixed, the structure can be stressed in the usual manner. An example of stressing the fuselage is shown in Fig. 185. It has been assumed that the machine is fitted with a tail plane of 35 square feet in area, and of weight 40 lbs. The maximum down load on the tail plane is to be 25 lbs. per square foot. The total load acting at the rear end of the fuselage is therefore $35 \times 25 + 40 = 915$ lbs. This is distributed equally on each side of the structure, making 458 lbs. to be applied on each girder. A side elevation of the fuselage

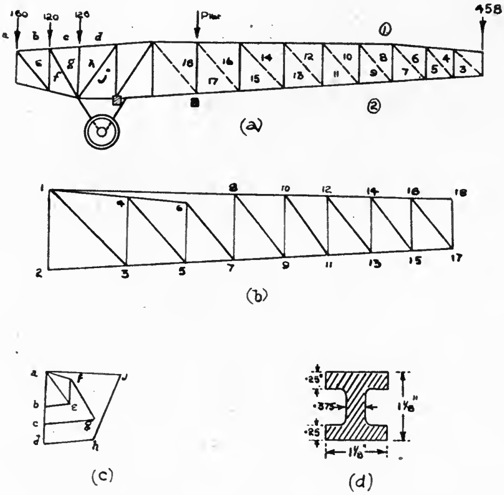

FIG. 185.—Stress Diagram for Fuselage.

is next drawn out as in Fig. 185 (*a*), and the stress diagram for the rear section then follows, as shown in Fig. 185 (*b*).

From the table of stresses prepared from this diagram the necessary sizes of the members in the rear portion of the fuselage can be determined. Referring first to the longitudinal members, it will be found that they must be designed for compressive loads. For this purpose the Rankine Strut formula may be used, the constants being taken from Fig. 89.

In using Rankine's formula, it generally happens that the area chosen gives a crippling load much above or much below the value required. To obtain a close approximation, several values have to be tried, though other considerations frequently intervene to fix the sizes.

The vertical struts are generally of the same thickness as the longerons at their junction to the latter, but may with advantage be spindled out intermediately. A section such as that shown in Fig. 185 (*d*) will be suitable. The sizes should be checked by means of Rankine's formula modified as in the case of the longerons; in fact, it is a good plan if one is engaged on much strut work to graph this formula for various standard sections, so that much tedious computation is avoided.

The front portion of the fuselage may next be considered. The principal load occurring on it is the engine and radiator. For this design the weight is about 800 lbs. Half of this load is carried by each side and in turn distributed over the struts which carry the engine bearers. The stress diagram can then be drawn as in Fig. 185 (*c*). It will be seen that the loads are so light that the longerons will take them comfortably, and in practice the nose portion is very rarely stressed. It must be remembered, however, that they have also to take the vibration due to the engine, so that it is inadvisable to reduce them in size, as the structure might shake to pieces.

The fuselage shown has three-ply wood $\frac{1}{8}''$ thick over the entire front of the structure.

There remains to be considered the stresses in the centre portion of the body when the machine lands. Half the maximum landing shock will be taken by each landing wheel. This force may be resolved into two components along the under-carriage struts, and these components will set up a direct compression in the vertical struts of the fuselage, and place the portion of the longeron between them in tension. When designing this portion of the fuselage, the effect of this tension must be considered, and care taken to see that the longeron is sufficiently strong for this purpose. Where possible it should always be arranged that the principal loads act upon the vertical struts so that the longerons are not called upon to act as beams, but are only subject to direct tensile or compressive stresses.

Design of the Engine Mountings.—Before commencing to examine the various types of engine mountings, a few notes as to the problems involved will be useful. We shall first consider the stationary vertical type of engine, this being perhaps in most general use. The engine itself consists of 4, 6, or sometimes 8 cylinders placed one behind the other in a straight line on top of a common crankcase. This arrangement of cylinders makes for a somewhat long engine bed, which must be very rigid if misalignment is to be avoided. Some types of engine have been supported by transverse members running through the crankcase from side to side, but in the majority of cases the two sides of the crankcase are provided with horizontal flanges running the whole length of the engine, or else with brackets projecting out from the sides at intervals, designed to be bolted on to longitudinal engine bearers resting on the body structure of the aeroplane.

The problem confronting the designer is to provide a structure which, while rigid enough to ensure that the engine itself is not subjected to any bending stresses, is yet sufficiently flexible to transmit the vibration of the engine to the mounting, and yet damp out these vibrations before they reach the structure of the aeroplane 'fuselage' proper.

In this connection it should be remembered that apart from such minor considerations as vibration, which should be reduced to a minimum in a modern engine, there are two main loads to be considered. One is the weight of the engine, which is always acting, while the other is the thrust or pull of the airscrew acting only when the engine is running, and varying from a maximum when the engine is going 'all-out' to a minimum when it is throttled right down. There is also the reverse thrust when the machine is diving and the air pressure on the back of the screw is driving the engine.

It will thus be seen that these two main loads give one vertical component and one horizontal component. Neither is constant, for during a vertical nose-dive with engine running, the weight of the engine is acting along the same line as the thrust, both tending to pull the engine out of the fuselage in a forward direction. Moreover, as we have already seen, the horizontal component varies both in magnitude and direction. In general, however, we may consider the two components as being vertical and horizontal respectively.

In normal flight the resultant of these two components will have a forward inclination of approximately 45°. This may be illustrated as follows :—Consider an engine of the average vertical type weighing, say, 5 lbs. per h.p.—this is somewhat high, but will illustrate the point—and the thrust obtained with an airscrew of average efficiency as 5 lbs. per h.p., it will be seen that the vertical and horizontal components are approximately equal in magnitude, and their resultant will therefore have an inclination of approximately 45°.

For a 100 h.p. engine weighing 5 lbs. per h.p. and giving a thrust of 5 lbs. per h.p., the resultant will therefore be about 700 lbs. acting at an angle of 45°. During a vertical dive the weight component will be parallel to the thrust component, and hence for the same engine the pull tending to tear it out of the fuselage will be about 1000 lbs., that is, twice the weight of the engine. When diving with engine off, the thrust will operate against the weight and thus reduce the forward pull on the engine bearers.

There are several different ways in use for transmitting the load from the longitudinal bearers to the body structure proper. In some machines the engine is supported at each end only, while others have three or four points of support. The question

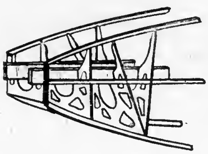

Reproduced by courtesy of 'Flight.'

FIG. 186.

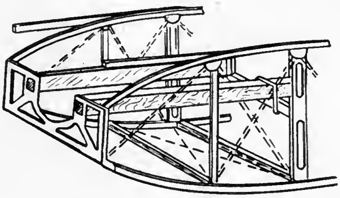

FIG. 187.

of the number of supports to employ depends largely upon the size of the engine.

Wood is the most common material used for the direct support of the engine, this being largely on account of its greater resiliency, which acts to a certain extent as a 'shock absorber,' and thereby lessens the vibration.

We shall now consider several practical examples of engine

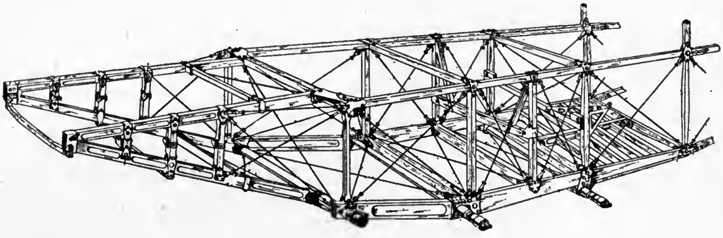

FIG. 188.

mountings. The arrangement of engine bearers on an Albatross biplane is shown in Fig. 186. The two longitudinal members are of ash, and are supported by transverse members connecting them to the upper and lower longitudinals of the fuselage. The front transverse member takes the form of a pressed steel frame lightened in places and joining a capping plate over the ends of the four longitudinals which converge somewhat at this point. The next support is joined by a ply-wood member 20 mms. thick, cut out in places for lightening purposes. From the point on the lower longitudinals where the front landing chassis struts are attached, two supporting transverse members radiate. One of these, which is of the same thickness and general construction as the preceding one, slopes forward, while the other, supporting the rear end of the engine, has a backward slope. The thickness of the latter member is 25 mms.

In the Curtiss biplane the engine is supported by two transverse members only, and for the comparatively light engine employed this is quite adequate (see Fig. 187). The front support takes the form of a steel plate lightened out, and with the edges turned in to stiffen the plate against buckling. At the rear the engine bearers rest on a transverse member, which is in turn secured to the upright body struts. Each bearer is clamped to the transverse beam by two bolts as shown in sketch.

As the engine overhangs the front chassis struts, the bracing

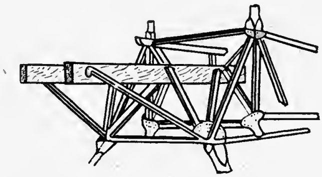

Reproduced by courtesy of 'Flight.'

FIG. 189.

of the sides of the fuselage has to be sufficiently strong to withstand landing shocks, and for this reason the wiring of the front bays is in duplicate.

An excellent type of engine bearer for either vertical or V-type stationary engines is shown in Fig. 188.

Another interesting type of mounting is that fitted to the all-steel Sturtevant biplane (Fig. 189). Here it will be observed that the engine bearers are of ash, supported by members of channel steel. Four supports carry each bearer, three running to the point where the under-carriage struts are attached to the fuselage longerons. In addition to their forward slope the channel steel supports are inclined inwards, thus effecting a very rigid bracing of the engine in every direction.

An additional consideration in the mounting of air-cooled stationary engines is that of providing the necessary cooling effect. It seems probable that ultimately the air-cooled engine will, on account of the large reduction in weight resulting from the absence of radiators and water tanks, supersede the water-cooled type, so that, although the water-cooled engine is now used almost universally, it is well to keep in sight the advantages to be derived from an efficient air-cooled engine. It will be realised that since the cylinders are usually placed in two rows of 4, 6, or 8 each, according to size of engine, the front cylinders will have a shielding effect upon the rear ones, which, as a consequence, will be insufficiently cooled, and this will lead to trouble. The method usually adopted in the tractor type of machine is to direct the air by means of deflector plates so that it enters the space between the two rows of cylinders from the front, is prevented by a vertical partition from escaping at the rear, and is thus forced by the pressure of the incoming air out through the spaces between the adjacent cylinders.

In the pusher type of machine the difficulty was overcome by mounting a large enclosed centrifugal fan on the front end of the crankshaft. The space between the cylinders was covered by an arched roof of aluminium running from the tops of the cylinders on one side to the tops of the cylinders on the other. The Vee between the last two cylinders was covered by a vertical aluminium plate. When the fan sucked the air into the space between the rows of cylinders the only escape for the air was the small spaces between adjoining cylinders, which were thus cooled on three sides—the inner side, the front, and the back—while the outer sides of the cylinders were cooled by the air current due to the forward speed of the machine. This method proved very satisfactory for the 'pusher' machine.

Considerable diversity of practice occurs with the mounting of rotary engines, but the different methods may be divided into two categories: (1), those in which the motor is supported between two plates; (2), those in which the motor itself is overhung. This latter method allows of ready accessibility of the engine when repairs are necessary, but is probably slightly heavier than the double bearer mounting, owing to the necessity of using a thicker gauge material.

Fig. 190 illustrates an example of the first method. The plates are pressed from sheet steel and all the edges are flanged in order to prevent buckling. The front plate takes the ball race through which the airscrew shaft runs, while to the rear bearer is bolted the back plate of the engine. Great care is necessary in cutting out the lightening holes, and these should be such as not to materially diminish the strength of the plates. The general arrangement of the front part of the fuselage will be clear from the drawing.

An example of the overhung method is shown in Fig. 191. In this case the back plate of the engine is attached to the front of the front engine bearer, while the rear bearer acts as a support to an extension shaft which passes through both bearers. The plates are pressed out of sheet steel either by machine or hand, and care is necessary to ensure that they are attached to the longerons in a suitable manner.

A problem of considerable importance in connection with the housing of rotary engines is that of obtaining sufficient cooling effect with a minimum of head resistance. The method generally adopted is to fit a cowl or sheet metal shield over the engine. In the majority of machines only the upper part of the engine is covered.

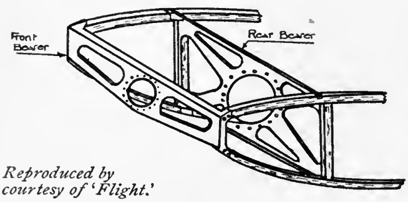

Reproduced by courtesy of 'Flight.'

FIG. 190.

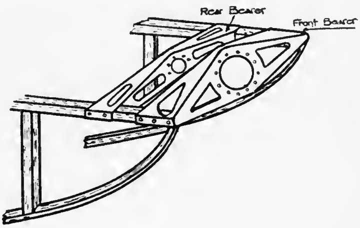

FIG. 191.

Radiators.—With the increasing demand for larger engine power and the difficulties encountered in air-cooling methods the question of water-cooling has become of great importance, and it will be useful to consider this subject briefly. The type of radiator in most general use for aero engines has developed principally from the motor-car radiator. According to the present practice there can be but little doubt that the honeycomb type of radiator holds the lead, whether it is mounted in the fuselage or elsewhere. In the absence of wind-tunnel tests it is difficult to say whether the square tube, round tube, or other formations are best as regards the ratio of cooling capacity to wind resistance.

COOLING AREA OF RADIATORS.—The following method was adopted by Lanchester in order to determine the area of cooling surface required. The heat units disposed of per square foot of single service may be expressed by the equation :

$$H = \frac{0{\cdot}24\ ECPVT}{2} \quad \text{.............. Formula 78}$$

where E = double surface coefficient of skin friction = ·008
C = normal plane resistance coefficient = ·6
V = velocity of air stream,
T = temperature difference, say 120° Fahr.
P = ·078

Taking velocity of the air stream equal to 50 ft./sec. then the heat units disposed of per sq. ft. of surface

$$= \frac{\cdot24 \times \cdot008 \times \cdot6 \times \cdot078 \times 50 \times 120}{2} \text{ Fahr. H.U. per sec.}$$

$$= \cdot27$$

and the horse-power equivalent $= \dfrac{\cdot27 \times 780}{550} = \cdot4$ nearly

(Note that 780 is the work equivalent of 1 Fahr. Heat Unit. Hence under the above conditions, and for a velocity of 50 ft. /sec., about $2\frac{1}{2}$ square feet of radiator surface are required per h.p.)

The above values for the coefficients were obtained from experiments carried out on a motor-car radiator, and the results were in good agreement with general practice.

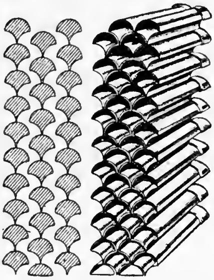

FIG. 192.

The increased speed with which the radiator on an aeroplane meets the air stream will bring down the cooling surface area inversely as the speed, and the above formula may be used to determine the necessary radiator surface required.

It is found practically that if the radiator is placed immediately behind the airscrews, about 1·6 to 1·8 square feet of area per 100 h.p. is required; whereas, if it is placed so that it gets the full effect of the slip stream, about 1 square foot of area per 100 h.p. is necessary. In the Airco 9, the radiator is arranged in the floor of the front portion of the fuselage, so that a greater or less portion can be exposed at will, according to the prevailing conditions.

A form of honeycomb radiator which is being largely used on modern aeroplanes is shown in Fig. 192. The water spaces consist of a series of semi-circles and quarter-circles. Each air channel is formed of a strip of brass, the ends of which are folded over and joined by a machine. The strips are then placed in a press and given their correct shape, after which the honeycomb is completed by soldering the ends of the adjoining strips together. A point in favour of this type of radiator is that it can be built up in units or sections of almost any size. Further, repairs can be quickly and cheaply effected, a damaged section being simply removed and a new one substituted.

The Denny Jointless Honeycomb Radiator is constructed by the electro-deposition of pure copper, so that the resultant radiator is all in one piece, thus eliminating soldered joints.

A useful system which has recently been taken up is one in which a radiator is built up of a number of standardised units in such a manner that for a given engine a certain number of units are employed. If the same engine is used on a faster machine fewer units are employed; if on a slower one, more units. The advantage of such a system is that instead of a different size and shape of radiator varying for each type of machine, and even in the same machine according to the engine fitted, the standard unit can be turned out in quantities irrespective of the machine to which it is to be fitted. This naturally leads to rapidity and economy of production.

Some German machines have been fitted with radiators in the top centre section of the main planes, but it is very doubtful whether the increased complications of such a system are worth while, either from a practical or an aerodynamical standpoint.

Gyroscopic Action of a Rotary Engine and the Airscrew.—Before concluding this chapter it is desirable to say a few words upon this subject, since the effect is to produce a sideways twist upon the engine-bearer end of the fuselage. From the practical point of view this twist can be easily provided for, and from the pilot's point of view it is found that the usual controls are ample so far as handling is concerned.

This gyroscopic action will arise in the case of an aeroplane when for example a tractor machine whose airscrew and engine, viewed from the C.G. of the machine is rotating in a clockwise direction, attempts a right-handed turn. An external couple about a vertical axis is set up owing to the applied air forces, and the axis of the engine and the airscrew tries to set itself in a line with this axis, so that there will be a tendency for the machine to dive.

The magnitude of this gyroscopic couple is given by the expression

$$\text{Couple} = \frac{I\,\Omega\,\omega}{g} \text{ ft. lbs.} \quad \ldots\ldots\ldots \quad \text{Formula 79}$$

where I is the moment of inertia of engine and airscrew about its axis of revolution in absolute units.

Ω is the angular velocity of the engine and airscrew about their axis of revolution in radians per second.

ω is the angular velocity of the machine in radians per second at which precession is forced.

Experiments were carried out at the Royal Aircraft Establishment in order to determine the magnitude of the gyroscopic couple upon an aeroplane fitted with a 100 h.p. Gnome Engine. The moment of inertia of the engine was found by weighing the parts and measuring their distance from the centre, the result being checked experimentally by measuring the period of oscillation of the engine when suspended by three wires. Similarly the moment of inertia of the airscrew was determined by suspending it bifilarly and measuring its period of oscillation. The results obtained for a 100 h.p. Gnome Engine were:—Weight, 270 lbs.; M.I., 114 lbs. feet^2; Speed, 1200 r.p.m. And for an airscrew: Weight, 30 lbs.; M.I., 150 lbs. feet^2; whence total moment of inertia for engine and airscrew is 264 lbs. feet^2.

The gyroscopic couples due to the precessional movements involved both in turning and pitching were determined as under.

(a) *Gyroscopic Moment due to Turning.*—In the first of these cases the aeroplane was turned completely round in 20 seconds, involving severe banking and a very sharp turn.

Angular velocity of machine

$$= \omega = \frac{2\pi}{20} = \cdot 314 \text{ radian per sec.}$$

Angular velocity of engine and airscrew

$$= \Omega = 2\pi \times \frac{1200}{60} = 125 \cdot 8 \text{ radians per sec.}$$

whence

Moment due to gyroscopic couple

$$= \frac{264 \times 125 \cdot 8 \times \cdot 314}{32 \cdot 2} = 324 \text{ ft. lbs.}$$

(b) *Gyroscopic Moment due to Pitching.*—The problem in this case necessitates the determination of the maximum angular velocity about the axis of pitch when the elevator is suddenly deflected to its full extent. The limit of this will be determined by that velocity at which the pilot is just about to be lifted from his seat.

Let M' be the mass of the pilot.
θ angle of the path.
V the velocity of the machine along the path.
r the radius of curvature of the path.

Then $$M' g \cos \theta = \frac{M' V^2}{r}$$

whence angular velocity

$$= \frac{V}{r} = \frac{g \cos \theta}{V}$$

This is a maximum when θ is zero.

For the machine considered in case (a) V is 100 f.p.s.

$$\therefore \quad \omega = 32{\cdot}2/100 = {\cdot}322 \text{ radian per sec.}$$

and the moment due to gyroscopic couple

$$= \frac{264 \times 125{\cdot}8 \times {\cdot}322}{32{\cdot}2}$$

$$= 330 \text{ foot lbs.}$$

which is of approximately the same magnitude as that due to turning.

These figures indicate that there is a twist set up in the engine structure which will be communicated to the wings and must be opposed by a movement of the control surfaces. As previously pointed out, this must be borne in mind when designing the fuselage.

CHAPTER VIII.

Design of the Chassis.

Function of the Chassis.—The most important duty of the chassis is to provide for the attainment along the ground of a sufficient speed to lift the aeroplane into the air. This is very easy to design for, but the other duties of a chassis are in some respects equally important, and must not be lost sight of. They are:

1. To make easy a good landing.
2. To protect the airscrew at all times from contact with the ground.
3. To provide and permit of easy 'taxying' along the ground.
4. To form a firm base upon which the machine may safely stand at rest in a wind.
5. To save the machine from damage, as far as possible, in the case of a bad landing.

Forces on Chassis when landing.—The design of the Chassis is one of the most difficult problems confronting the aeronautical designer, for, while it is desirable to obtain sufficient strength in the landing gear for the machine to be able to land itself when gliding down at its normal gliding angle, it must at the same time be comparatively light and must offer as little resistance to the air as possible.

It will be useful first to enumerate the forces acting upon a machine when landing. Referring to Fig. 193 (*a*) they are:

1. The weight of the machine—W—acting vertically downwards through the C.G.
2. The lift—w—remaining on the wings by virtue of the forward velocity.
3. The head resistance—R.
4. The resistance of the ground acting at the point of contact of the wheels and equal to μ P where μ is the coefficient of ground friction, and may be taken as 0·16, and P is the reaction at wheel.
5. The force due to the momentum—M—depending upon the velocity and the weight, and acting through the C.G. of the machine.

The fifth force causes a couple M . d (d being the perpendicular distance from the line of action of M to the point of contact with the ground), about the point of contact tending to overturn the machine. It is clear, therefore, that the position of the wheels is an important factor in this connection. The higher the C.G. of the machine, the farther forward must the wheels be placed.

Method of locating Fore and Aft Position of Chassis.—It will be sufficiently accurate for our present purpose to assume that both the lift of the wings and the resistance of the machine act through the C.G. Then with the notation shown in Fig. 193 (a), in order to prevent nose-diving of the machine on landing, it is necessary that the moment P x must be at least equal to the moment μ P y.

Consequently we have the condition

$$P . x > \mu . P y$$

that is $$\frac{x}{y} > \mu \quad \text{......... Formula 80}$$

or $$\tan \theta > \mu$$

Taking the value of μ given above and substituting

$$\tan \theta = 0{\cdot}16$$

whence $$\theta = 9^\circ$$

In order to allow for landing on soft ground or upon a slope this angle is generally made equal to about 14°, with the axis of the body in the horizontal position.

A second method of determining the fore and aft position of the wheels of the chassis is to utilise the gliding angle of the machine in the following manner:

Let C (Fig. 193 b) represent the position of the C.G. of the machine under consideration. From C drop a perpendicular C A upon the ground line X X. The distance of the ground from the horizontal line through the C.G. is governed by the amount of clearance given to the airscrew, twelve inches being a usual allowance for the purposes of preliminary design. Then set out the angle A C B equal to the gliding angle of the machine. As in the first method, an extra allowance must be made for unforeseen contingencies, 5° being a common figure in this respect. Therefore set out the angle B C D equal to 5°, the point of intersection D with the ground line X X giving the required position.

A third, but still more empirical method, is illustrated in Fig. 193 (*c*). In this method an angle of 75° is set off from the chord of the lower main plane in order to arrive at the required position.

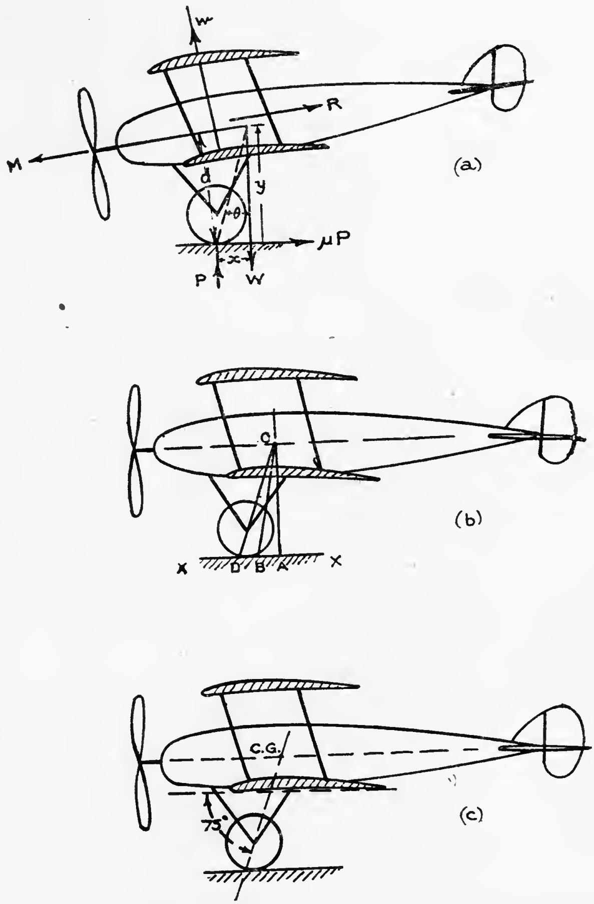

Fig. 193.—Methods of locating the Fore and Aft Position of the Chassis.

General Principles of Chassis Design.—The first point to decide is the necessary factor of safety. A chassis cannot be made strong enough—for aerodynamic reasons—to stand up to everything that may possibly occur. Provided that the pilot lands squarely on the two wheels, shock occurs in one of two ways :—

1. He does not flatten out quick enough ; or
2. He flattens out too early, and so 'pancakes' down from a height.

Considering the first case and assuming that the machine comes into contact with the ground as in a natural glide without having flattened out at all,

Let v be the vertical component of V, the forward velocity of the machine,
f be the vertical retardation on meeting the ground,
d be the give of the landing gear in feet,
a the angle of descent to the horizontal,
P be the mean reaction at the wheels during landing,
w be the lift remaining on the wings, equal say to two-thirds of W, the weight of the machine,

we have
$$P = W + \frac{Wf}{g} - \frac{2W}{3}$$
$$= W\left(\cdot 33 + \frac{f}{g}\right)$$

Now the vertical retardation is given by $v^2 = 2fd$

that is
$$f = \frac{v^2}{2d} = \frac{V^2 \sin^2 a}{2d}$$

whence
$$P = W\left(\cdot 33 + \frac{V^2 \sin^2 a}{2gd}\right) \quad \ldots\ldots\ldots \text{Formula 81}$$

By the use of this formula the reaction at the wheels during landing can be ascertained. Suppose a machine of weight W to be descending at a slope of 1 in 6 at a speed of 50 m.p.h. To find the reaction at the wheels for a give of 10″ in the landing gear :

Substituting in Formula 81 we have

$$P = W\left(0{\cdot}33 + \frac{73{\cdot}3^2 \times 0{\cdot}164^2}{64{\cdot}4 \times \cdot 834}\right)$$
$$= 3{\cdot}03\ W$$

Assuming the shock absorber to be of rubber and the force to decrease uniformly from a maximum to zero, the maximum force on landing will be twice the average force. Hence maximum force on landing

$$= 6{\cdot}06\ W$$

that is, the landing gear must be sufficiently strong to withstand a ground reaction of about six times the weight of the machine.

From Formula 81 it is obvious that the mean reaction will decrease according as the give of the landing gear increases, and hence it is necessary to provide a material capable of absorbing the maximum amount of energy. This may take the form of rubber cord, steel springs, or pneumatic cylinders. Rubber cord is to be preferred for small machines, because it is light, cheap, easily workable, and easily replaced; and it has the further great advantage of not causing an elastic rebound as in the case of steel springs, owing to the energy of the shock being sufficiently absorbed by the viscosity of the rubber.

Formula 81 also shows the advisability of adopting as low a value as possible for the landing speed of any machine under design.

It will also be observed from the above example that while it is a comparatively simple matter to design a chassis for a machine possessing a low landing speed, it becomes increasingly difficult to do so as the landing speed increases.

An efficient chassis becomes heavy as the loading of the wings is increased, ample wing area leading to a saving in weight and resistance. A compromise must evidently be made in most designs, and the latitude to be allowed the pilot must be assessed according to the particular experience and practice of the designer. An important consideration to bear in mind is the necessity to preserve the machine, even if the chassis is smashed. In this connection the skid type of chassis would be very advantageous were it not for its great resistance at high speed.

Types of Chassis.—The various designs may be roughly divided into two groups:

(*a*) Those with a longitudinal skid placed in front of, and forming part of, the chassis; and

(*b*) Those without such skids.

Of these two groups by far the greater number of modern machines belong to the second group, while most of the earlier types of machines possessed chassis belonging to the first group.

In the earlier types the skid stretched from behind the C.G. of the machine to either just behind of, and in some cases even in front of, the airscrew, thus forming a backbone to the chassis. This skid was fixed just a few inches above the ground, and provided a rigid stop to the elasticity of the chassis, thereby preventing the airscrew from touching the ground. This type is illustrated in Fig. 194.

The objection to its use is the heaviness and large air resistance of the type of chassis involved, and the danger, either in a bad landing due to the pilot not flattening out soon enough, or the presence of rather rough ground, of the nose of the skid striking the ground directly, or even impaling itself. In the event of this happening, it is easy for the aeroplane to turn completely over, owing to the high position of the C.G. above the ground. The best way of guarding against this contingency is to protect the forward part of the skid or skids with small extra wheels. These wheels may be very much smaller than the landing wheels proper, but a considerable addition to the weight, and, more important still, a great increase in the head

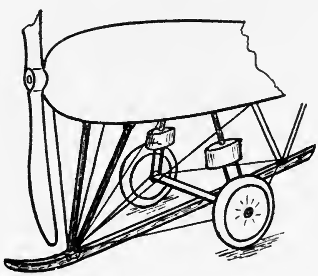

FIG. 194.—Central Skid Chassis.

resistance, cannot be avoided, and therefore these wheels are seldom used.

The longitudinal skid may be either a single central skid fixed between the two landing wheels, or may be made up of two lighter skids placed one in front of each wheel.

The single or central skid type of chassis has the long central skid fastened to the longerons of the fuselage by two pairs of struts which form a V, one just behind the airscrew, and the other just in front of the C.G. (See Fig. 194.) The forward struts should be given a rake, so that their lower ends are in front of their upper ends, and the panels formed by skid, fuselage, and struts should be cross-braced by cables. This will provide for the longitudinal backwards component of the force of a bad landing. The axle can also be made divided, each half being hinged at the skid, and having a cable or swivelling-rod connection from just inside the wheel to about half-way along the skid. With this arrangement, a telescopic shock absorber is needed from the axle to the longerons. The skid should be well curved up in front so as to minimise the chances of impaling.

This type of chassis is suitable for heavy work, and can be made strong enough to withstand rough handling and very bad landings. The V struts and shock absorbers at the axle together form a triple V or M shaped girder, which can be designed to withstand a large sideways force, such as occurs in a bad landing on one wheel. High resistance is unavoidable owing to the multiplicity of its parts, so that it is unsuitable for high-speed work unless great strength is required. If the skid is continued under the airscrew, protection is afforded to that member. There is one point of weakness which requires attention: that is, the inability of the forward chassis struts to withstand any considerable transverse force. As wide an angle

FIG. 195.—Double Skid Chassis.

V as possible should be sought for here, and consequently, if the longerons converge considerably towards the front of the fuselage, the forward struts may require to be attached to them some distance back from the engine plate or fuselage nose, at a position where the fuselage is still wide. Although the forward rake of these struts helps in this respect, their bottom ends may nevertheless be a long way behind the airscrew in the case of an overhung rotary-engined machine. Consequently it is not always possible to prolong the skid under the airscrew, owing to the large bending moment which may occur in the skid due to this leverage. Apart from this, it will be found advisable to use a strong skid in this central type.

The double skid type of chassis (Fig. 195) is comprised of two lighter longitudinal skids, connected to each other and the fuselage with struts, the whole structure being braced together in the usual manner.

Telescopic shock absorbers are out of place in this design, elasticity being provided by wrapping rubber cord round the outer ends of the axle, just inside the wheel and the fixed transverse strut. This type is lighter, and has less resistance than the central skid type, owing to the decreased number of parts, and to the abolition of the telescopic shock absorber; but it is not so flexible, and is weaker in many ways, and therefore not suitable for heavy rough work. On the other hand it is stronger than the central design as regards side force well forward, as its braced square panel forward is much superior to the simple V; but it may be argued on the contrary that it is more liable to such a force. It is not much use to prolong the double skids

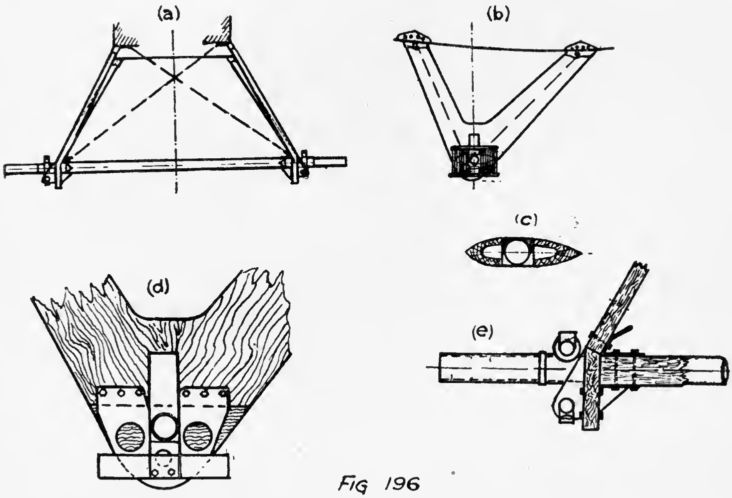

FIG 196

Landing Chassis Details.

forward past the airscrew. The prolonged central skid is a protection chiefly against a localised hillock on the ground; the double skids, if prolonged, would only be useful against a bank, as a small hillock might easily pass between them and cause an accident.

The chassis just considered is a half-way house between the heavy, single skid type, and the light, skidless design which constitutes the second group. (See Figs. 197 and 198.) In this group there is no limit stop or positive protection for the airscrew. The axle is connected to the lower longerons by a pair of struts on each side, forming two V's longitudinally placed. The two struts forming each V are united at their lower ends by a steel fitting, which also provides a vertical slot for up-and-down movement of the axle. See Fig. 196 (*d*). If this slot be made with a beaded edge, and the axle fitted with four collars, the axle can be arranged to act the part of a transverse strut. The resistance and weight are, in this case, reduced to a minimum for a fixed chassis; there are, indeed, only five members, and two of these are in protected positions. Skill, however, is required in manœuvring over the ground so as to keep the airscrew safe, and, with this end in view, the wheels may with advantage be set somewhat further forward than with the other types, in order to give a larger tail moment.

When landing on one wheel there is generally a resulting side blow on the chassis, and in order to resist this it is customary to introduce cross bracing between the axle and the fuselage.

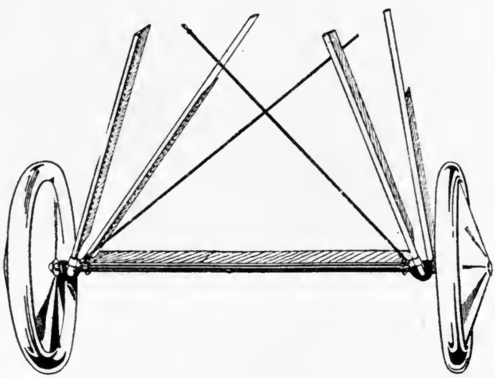

Fig. 197.—Landing Chassis of Bristol Fighter.

This type is eminently suitable for light, high-speed work, and owing to its great advantages as regards light weight and low resistance, its use should always be carefully considered before another type is adopted. Some excellent examples of this type of chassis are shown in Figs. 196, 197, 198.

Fig. 196 shows the details of the chassis of the Airco 4 machine. Each pair of side struts is made of solid wood, and at their lower ends vertical strut shoes, which carry the wheel, axle, and fittings for the rubber shock absorbers, are fixed. The axle itself—Fig. 196 (*c* and *e*)—rests between two cross struts of wood, which are shaped to a streamline form as shown. The total weight of this chassis is 119 lbs.

The landing chassis for the Bristol Fighter is shown in Fig. 197, and Fig. 198 shows this type as used in a standard American training machine. The method of construction is

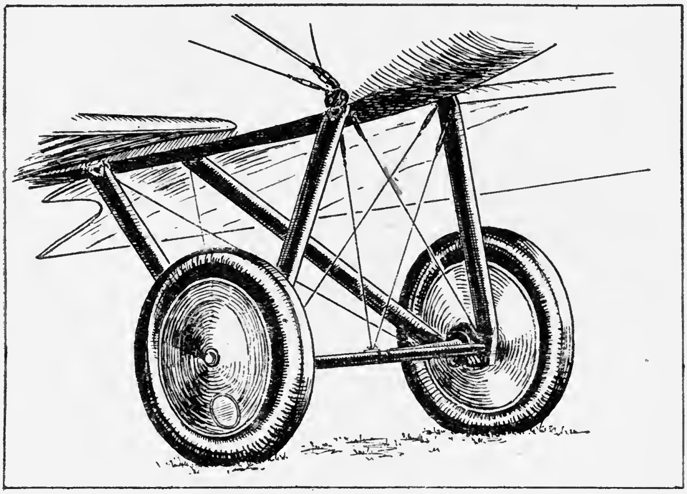

Reproduced by courtesy of 'Flight.'

FIG. 198.—Wright-Martin Landing Chassis.

clearly shown in these figures. An illustration of a chassis suitable for heavy machines is shown in Fig. 199, which depicts the complete chassis of the Handley-Page machine O-400.

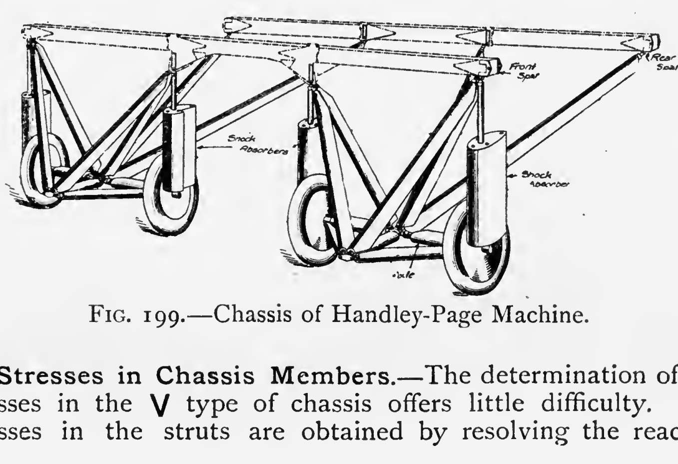

FIG. 199.—Chassis of Handley-Page Machine.

Stresses in Chassis Members.—The determination of the stresses in the V type of chassis offers little difficulty. The stresses in the struts are obtained by resolving the reaction

$\frac{1}{2}$ P at the wheel along the required direction, or by drawing a stress diagram as shown in Fig. 200, care being taken to use the component of the reaction in the plane of the struts, as determined by means of Formula 81.

The maximum side shock likely to occur on the machine may be taken as one-fifth of the maximum vertical reaction at each wheel. The cross bracing should be designed to withstand this load.

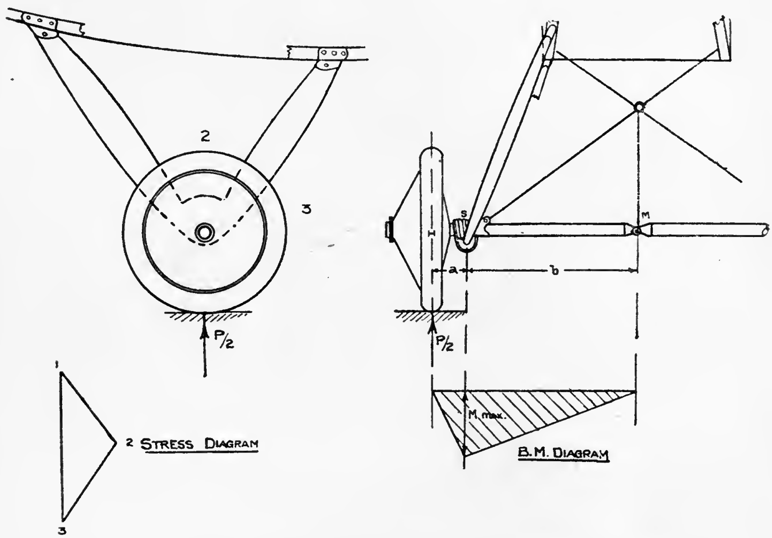

FIG. 200.—Stress Diagram and Bending Moment Diagram for Landing Chassis with Divided Axle.

The stress on the axle may be simply determined in the following manner :—

1. *Continuous Axle* (Fig. 201).—Let the distance between the centre H of the hub and the centre S of the shock absorber elastic be *a*, and that between the latter point and the central longitudinal plane of the machine be *b*. The bending moment on the axle is due to the couple $\frac{1}{2}$ P *a*, and increases from zero at the hub centre to $\frac{1}{2}$ P *a* at the point S. From S it is constant until the other shock absorber centre is reached, whence it decreases to zero at the centre of the other hub. The axle in this case may well be made of uniform strength, except for the portions H to S, which may be strengthened against shear. In

the event of landing on one wheel, if Q be the load on the wheel, the bending moment increases from zero at H to

$$\frac{Q \times a \times 2b}{2b + a}$$

at S, and from there decreases again to zero at the point of attachment of the other shock absorber. There is then a tension in the other shock absorber equal to $Q a / (2b + a)$, which must be provided for.

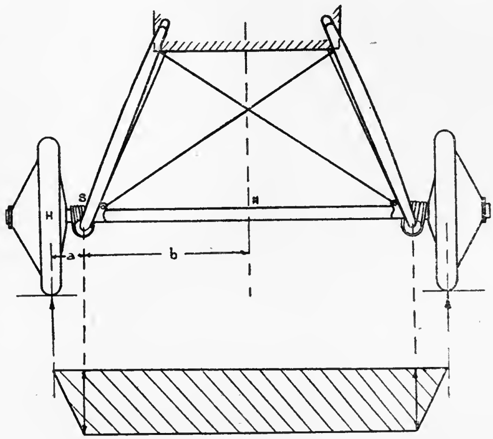

FIG. 201.—B.M. Diagram for Landing Chassis with Continuous Axle.

2. *Divided Axle* (Fig. 200).—In this case the bending moment gradually diminishes from $\frac{1}{2} P a$ at S to zero at M. The axle may therefore be made lighter towards the centre so long as it is able to take the constant shearing force between the central plane and S, equal in magnitude to $Q a / (a + b)$. Alternatively the portion on each side of S subjected to large bending moment may be reinforced. It is important to keep S as near to H as possible. With a divided axle it is necessary to have a wire leading from the junction of the cross bracing wires to the central hinge fittings, in order to counteract the downward force at the hinge due to the load on the wheels.

Shock Absorbers.—The two main types of shock-absorbing devices are—

(*a*) Rubber shock absorbers.
(*b*) Oleo shock absorbers.

The first type is used much more extensively than the second, principally on account of its lightness, ease of construction, and its cheapness. It has this disadvantage, however, that the mechanical properties of rubber vary very considerably, and are likely to deteriorate with time. Some interesting experiments upon a rubber shock-absorbing device were carried out by Hunsaker at the Massachusetts Institute of Technology.

A shock absorber of the type shown in Fig. 202 was fitted with twelve rubber rings 2″ × 2″ × 5/16″ each passing over a ¼″ steel pin. Table XLII. shows the elongation corresponding to a series of loads.

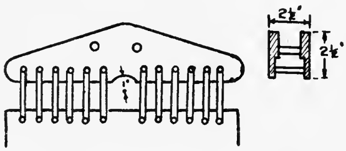

FIG. 202.

TABLE XLII.—ELONGATION OF SHOCK ABSORBER.

Load.	First loading.	Second loading.	Third loading.
1000 lbs.	·22″	·48″	·52″
2000 "	·78″	1·25″	1·37″
3000 "	1·40″	1·98″	2·12″
4000 "	2·08″	2·45″	2·60″
3000 "	1·98″	2·26″	2·45″
2000 "	1·57″	1·74″	1·91″
1000 "	·68″	·70″	·78″

Finally the absorber was tested to destruction and failed at 9750 lbs., with a corresponding extension of 5·06″. The pins failed by shearing with the rubber rings still unbroken. The effect of hysteresis is brought out clearly in the above figures, the rubber not contracting as rapidly as it extends. The area of the hysteresis loop represents the work done on the rubber which is not restored and is a measure of the shock-absorbing quality of the rubber. Moreover, it will be seen that the hysteresis loss diminished with each loading. The stress in the rubber rings when the bridge failed was 650 lbs. per square inch. In a subsequent test they failed at a stress of 900 lbs. per square inch.

Reference to Formula 81 shows that an increase of 'give' of the shock-absorbing device reduces the reaction at the wheels, hence greater elasticity of the rubber is needed to reduce landing shock on the chassis. Such increase of elasticity would have the further advantage of relieving the jolting of the machine when running along the ground.

DESIGN OF A RUBBER SHOCK ABSORBER.—In order to determine the number of rubber rings required to absorb the landing shock of a machine it is necessary to equate the work done in stretching the rubber to the energy of the machine at the instant of landing. For example, to take the case of the machine referred to on page 263.

Kinetic Energy of the machine on landing

$$= \frac{(W - w)(V \sin \alpha)^2}{2g} = \frac{\cdot 33\, W \times 12^2}{64}$$

$$= \cdot 74\, W$$

Potential Energy of the machine on landing

$$= (W - w) \times \text{'give' of gear} = \cdot 33\, W \times \cdot 834$$

$$= \cdot 275\, W$$

$$\text{whence Total Energy} = 1\cdot 015\, W$$

To determine the stretch of the shock-absorbing device we apply Formula 3, so that

$$\text{Extension} = \frac{PL}{AE}$$

and if n be the number of rings of rubber cord of $\frac{3}{4}''$ diameter, and the diameter of each ring assumed to be 6″, we have

$$x = \frac{P \pi 6}{\frac{\pi}{4}(\cdot 75)^2 n E}$$

$$= \cdot 142 \frac{P}{n}$$

For good quality shock absorber elastic E is taken as 300 lbs. per square inch.

In the above expression

$$P = \text{average load on the shock absorber}$$
$$= \text{half total reaction at wheels}$$
$$= \tfrac{1}{2}(3\cdot 03\, W)$$
$$= 1\cdot 51\, W$$

$$\text{whence} \quad x = \frac{\cdot 142 \times 1\cdot 51\, W}{n}$$

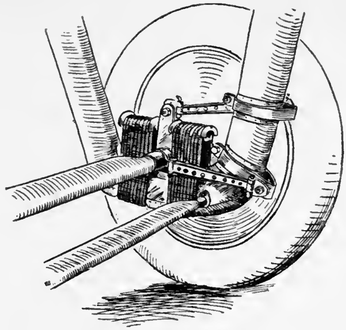

FIG. 203 (*a*)

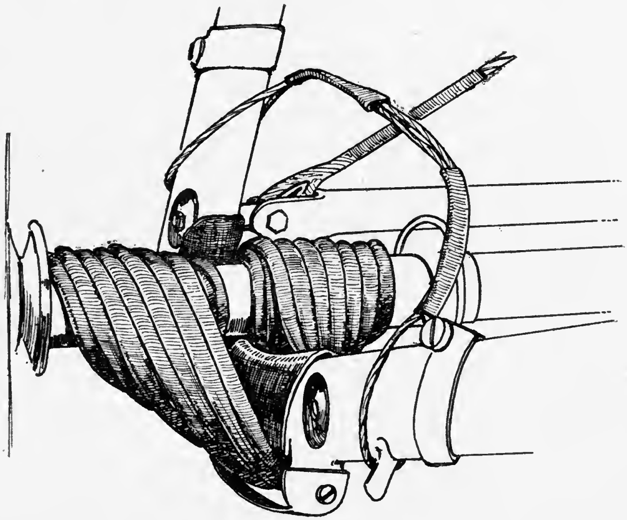

Reproduced by courtesy of 'Flight.'

FIG. 203 (*b*).

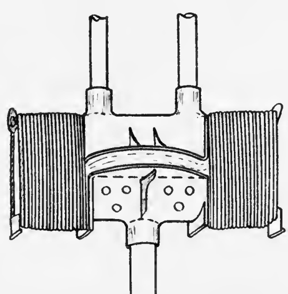

FIG. 203 (*c*)

Types of Shock Absorbers.

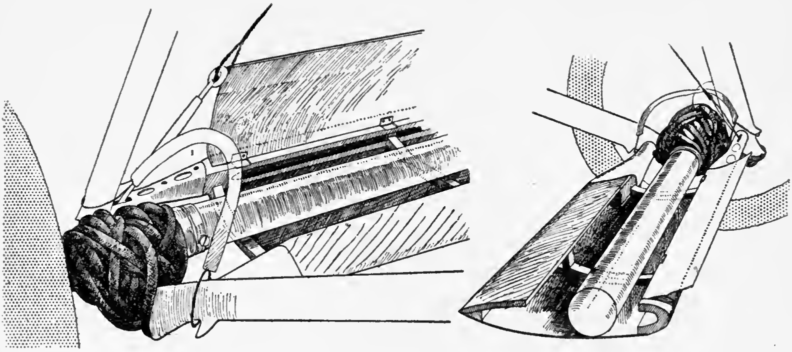

Fig. 203 (*d*).—Shock Absorber Device, and Streamlining of Axle of Landing Chassis.

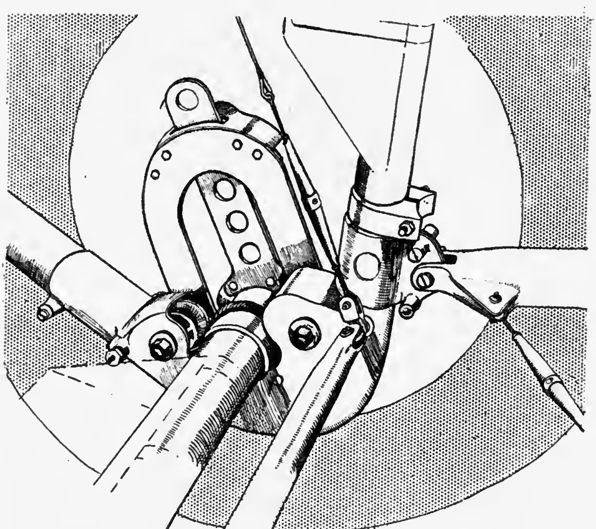

Reproduced by courtesy of 'Flight.'

Fig. 203 (*e*)

Further equating the total energy to the work done

$$1{\cdot}015\,W = P \cdot \frac{x}{12}$$

Substituting for x and P

$$1{\cdot}015\,W = \frac{1{\cdot}51\,W\,({\cdot}142 \times 1{\cdot}51\,W)}{12\,n}$$

whence $$n = {\cdot}0267\,W \quad \text{........... Formula 82}$$

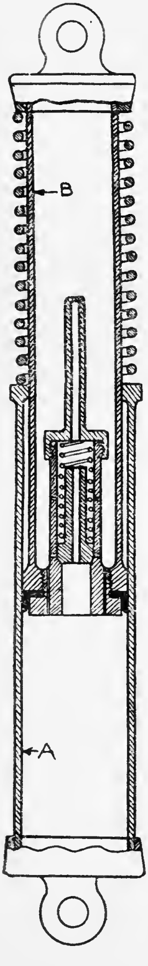

FIG. 204.

Therefore, for a machine weighing 2000 lbs., 54 rings of rubber of the size mentioned would be required. In this calculation no allowance has been made for the energy absorbed by the resilience of the pneumatic tyres.

In practice, the most general method of applying the rubber is to coil a long length around the axle and the main chassis struts respectively. The number of turns required will correspond to the number of rings as calculated from the above formula, plus any turns necessary for starting and ending.

Illustrations of rubber shock-absorber devices are shown in Fig. 203.

OLEO SHOCK ABSORBERS.—These in general consist of two telescopic steel tubes, the outer one serving as a cylinder in which oil is maintained at a fixed level, whilst the inner tube is attached to the body and acts as a piston. The inner tube or piston—see Fig. 204 (B)—carries a spring-loaded valve which covers ports round the lower part of the tube. The cylinder below the valve is filled with oil. When landing occurs and the tubes are compressed, the oil passes through a series of small holes into the upper cylinder. If the shock of landing exceeds a certain figure, the spring-loaded valve opens and provides an additional passage.

Particulars of an Oleo Leg, designed by the R.A.F., are given in the Report of the Advisory Committee for Aeronautics, 1912–13, as follows: During flight the lower tube or cylinder containing the oil drops through 11 inches. When the machine (a B.E. 2) strikes the ground the oil first passes into a small central air chamber and afterwards through three 4 millimetre exit holes. If the velocity of impact with the ground is sufficiently great so that the resistance of the oil passing through these holes is enough to raise the oil pressure to 640 lbs. per square inch, the spring-loaded valve opens and allows the oil an additional passage.

The arrangement was designed so that after the first two inches of travel the resistance remains constant, and equal to two and a half times the weight of the machine. The vertical travel, excluding the first 2″, was 13″, so that if the pressure remained constant the total energy absorbed was 4300 ft. lbs., and consequently the machine could land without damage with a vertical velocity of 13 feet per second. In addition to the oil and air gear, strong spiral springs carry the weight of the machine when running along the ground.

The Tail Skid.—The tail skid, which is situated at the rear end of the fuselage, provides the necessary point of support for the rear portion of an aeroplane when the machine is resting on

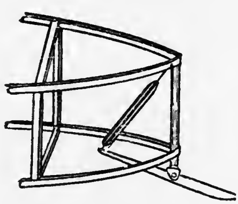

FIG. 205.

the ground. There are several different types of skids in actual use, examples of which are shown in Figs. 205–208.

The simplest form is that shown in Fig. 205. In this type the movement of the tail skid relative to the body of the machine is confined to the vertical plane. The skid itself is usually made of ash, and is provided with a steel shoe. The shock absorber device is composed of rubber cord. Another example of this type is shown in Fig. 206.

Another type of tail skid is that in which the tail skid is free to rotate about a vertical axis. The skid can then set itself at any angle laterally, and can therefore follow the curve traced out by the aeroplane in its motion over the ground. Such movement makes it much more convenient to manœuvre the machine when 'taxying' before flying or after alighting. Examples of this type of skid are shown in Figs. 207, 208.

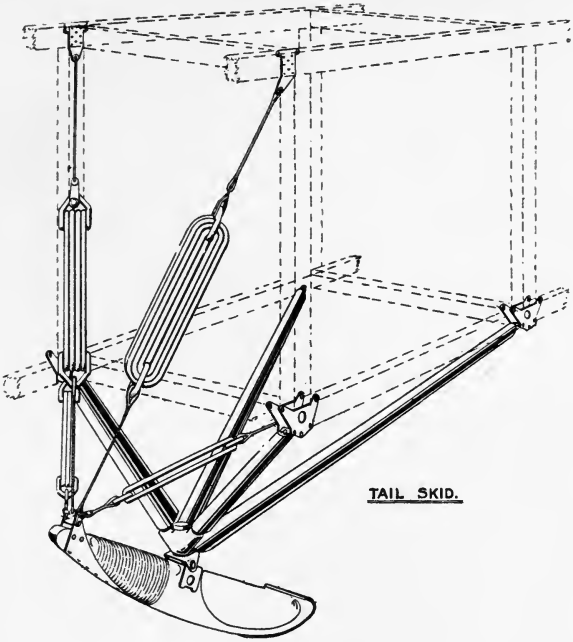

FIG. 206.—Example of Tail Skid for Large Machine.

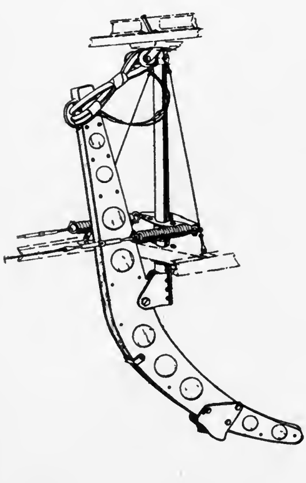

FIG. 207.

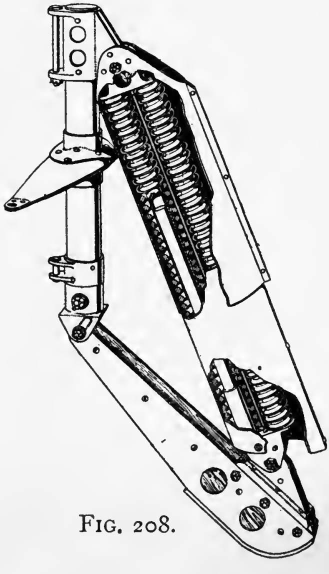

FIG. 208.

In Fig. 207 the shock absorber device is of rubber, which is placed in tension when the machine is upon the ground. A variation of this type is shown in Fig. 208. In this skid the shock-absorbing device is composed of steel springs which are subject to compression when in use. Such an arrangement is more efficient mechanically than the previous types shown, for it leads to a much smaller reaction at the fulcrum.

Streamlining the Chassis.—In general, the question of streamlining the chassis must be carefully considered, and all parts should be given a streamline form wherever possible. The resistance of the under-carriage is generally an important item, particularly in the case of high-speed scouts. Attempts have also been made to design a chassis which can be drawn within the fuselage during flight.

CHAPTER IX.

Design of the Airscrew.

Methods of Design.—The problem of airscrew design has been approached by analytical and by empirical methods The two principal methods of analytical attack are:

(i.) Examination of the air flow through the airscrew and the determination of expressions for its change in momentum and energy.

(ii.) Consideration of the actual forces set up upon the blades.

The first method may be called the classical method, and was the method developed by Rankine, Froude, and others for application in the first instance to the design of marine propellers.

The second method is known as the blade element method, and has been specially developed for application to airscrews, the pioneers in this case being Drzewiecki and Lanchester.

In both cases the premises are somewhat obscure, and the conclusions therefore correspondingly uncertain. It should be noted, however, that the second method is concentrated on the airscrew itself from first to last, and so leaves the designer with something definite to work upon, even if the data are not sufficiently accurate for his purpose. The design of airscrews, therefore, is best attempted along the more modern line of thought, which is generally known as the **Blade Element Theory.** This method is based upon laboratory experiments upon aerofoils, about which a vast amount of information is available from the force shape point of view; whereas very little definite information concerning the flow of air past an aerofoil is available in a quantitative form that can be applied to the design of an airscrew.

The first principles of the method are familiar to most engineers: an element of the blade is taken at any radius from the centre of rotation, say a section of width dr at a radius r, as shown in Fig. 209; and this section is then studied separately while still considered as joined to the whole. It is assumed that this element operates like a small aerofoil, the aerodynamic properties of which can be easily determined, as explained in

Chapter III. The whole airscrew is then treated as a summation of such elements, and the forces on the whole airscrew as a summation of the forces such as those upon the small element studied, applying to successive subdivisions of the blade such corrections for velocity, leverage, &c., as may be necessary.

It is first essential to realise the path of the blade. This, being a motion of uniform rotation and of uniform translation, is a helix, similar to a very deep-cut coarse pitch screw thread. Fig. 210 is a sketch of such a path. It should be noticed that as the radius is increased, so the resultant or helical velocity is increased. The forward velocity of the airscrew, however, is uniform for every point on it, and therefore the pitch is constant,

FIG 209

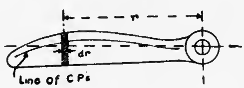

FIG 210

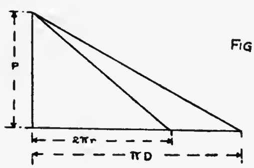

FIG 211

unless expressly made otherwise. The geometric pitch is the length along the axis which the airscrew would move for one revolution, if the fluid through which it moved suffered no translation, as for example if the screw worked in a fixed nut. If the fluid behaved in this manner we could represent the motion of our element as taking place along the hypotenuse of the triangle shown in Fig. 211; having for its sides the pitch (D), and the length of the particular circumference chosen ($2\pi r$). The motion of the wing tip would of course be given by substituting π D for the latter side, where D is the diameter of the airscrew. The above conditions of working are most nearly realised in practice when the airscrew is so working that there is no thrust on the shaft. The axial advance for one revolution under these circumstances is termed the experimental mean pitch (p). In practice, however, the airscrew is usually exerting a pull, and the axial advance per revolution is considerably less owing to the velocity impressed on the air. If V feet per second be the translational velocity of the airscrew, revolving at N revolutions per second, the actual effective pitch is V/N feet. The amount by which this quantity is less than P is termed the 'slip,' and averages between 20% and 30%. It is convenient to think of this in terms of the dimensions of the airscrew, and so the term 'slip ratio' is introduced, and we have

$$\text{Slip ratio} = \frac{P - \frac{V}{N}}{P}$$

The true path of the blade element is as represented in

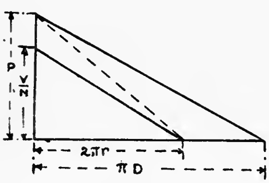

FIG. 212.

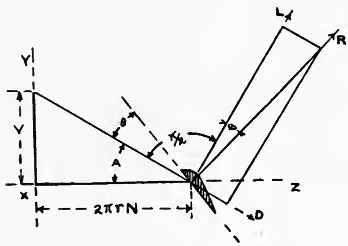

FIG. 213.

Fig. 212, where the dotted lines show the variation from Fig. 211.

Now the blade element theory is built upon aerofoil data, and remembering this, we may define the position of the element as shown in Fig. 213. A is the angle of the helix, and is equal to the angle whose tangent

$$= \frac{V}{2 \pi r N}$$

θ is the angle of incidence of the aerofoil element to its path, R is the resultant air force upon it, ϕ is its inclination to the perpendicular to its path, L is the aerofoil lift along this perpendicular to the path, D is the drag or component of R along the path. The thrust t is the component of R, along the direction of the translational velocity, that is, along X Y. Hence we have

$$t = R \cos (A + \phi)$$

The resistance to rotation, that is, the torque q on the shaft, is proportional to the component of R along the line XZ (the direction of rotative velocity), so that

$$q = R \sin (A + \phi) r$$

and the efficiency of the element

$$= \eta = \frac{R \cos (A + \phi) V}{R \sin (A + \phi) 2 \pi r N}$$

$$= \cot (A + \phi) \tan A \quad \text{.......... Formula 86 } (a)$$

Aerofoil data are given in the form of the absolute coefficients of the Lift and the Drag. From these we can obtain the values of the absolute coefficients of resultant force, K_r and of ϕ, by making use of the following relationships :—

$$K_r = \sqrt{K_x^2 + K_y^2}$$

$$\text{and} \qquad \phi = \tan^{-1} \frac{K_x}{K_y}$$

If b is the breadth of the blade where the element is chosen, the thrust on each element may be written

$$dT = K_r \cdot \frac{\rho}{g} \cdot b \cdot dr \cdot v^2 \cdot \cos (A + \phi)$$

where v = velocity along helical path

$$= \sqrt{V_1^2 + 2 \pi r N^2}$$

$$= \sqrt{V_1^2 + \frac{V_1^2}{\tan^2 A}} = \frac{V_1}{\sin A}$$

$$\text{whence } dT = K_r \frac{\rho}{g} b . dr \frac{V_1^2}{\sin^2 A} \cos (A + \phi)$$

$$= K_y \sqrt{1 + \left(\frac{K_x}{K_y}\right)^2} b \frac{\rho}{g} V_1^2 \frac{\cos (A + \phi)}{\sin^2 A} dr$$

and total thrust =

$$T = n \frac{\rho}{g} V_1^2 b_{max} \int_0^{\frac{D}{2}} K_y \sqrt{1 + \left(\frac{K_x}{K_y}\right)^2} \frac{b}{b_{max}} \cdot \frac{\cos (A + \phi)}{\sin^2 A} dr$$

Formula 83

where n = number of blades.

Similarly the torque q on any element is given by

$$q = \mathrm{K_r} \cdot \frac{\rho}{g} \cdot b \cdot dr \cdot v^2 \sin(\mathrm{A} + \phi) \cdot r$$

$$= \mathrm{K_y} \sqrt{1 + \left(\frac{\mathrm{K_x}}{\mathrm{K_y}}\right)^2} \cdot \frac{\rho}{g} \cdot b \cdot r \cdot \frac{\mathrm{V_1}^2}{\sin^2 \mathrm{A}} \cdot \sin(\mathrm{A} + \phi) \cdot dr$$

and total torque =

$$\mathrm{Q} = n \cdot \frac{\rho}{g} \cdot \mathrm{V_1}^2 \, b_{\max} \int_0^{\frac{\mathrm{D}}{2}} \mathrm{K_y} \sqrt{1 + \left(\frac{\mathrm{K_x}}{\mathrm{K_y}}\right)^2} \, \frac{b}{b_{\max}} \, r \, \frac{\sin(\mathrm{A} + \phi)}{\sin^2 \mathrm{A}} \, dr$$

Formula 84

An examination of these expressions for the total thrust and the total torque of an airscrew indicates that in order to evaluate

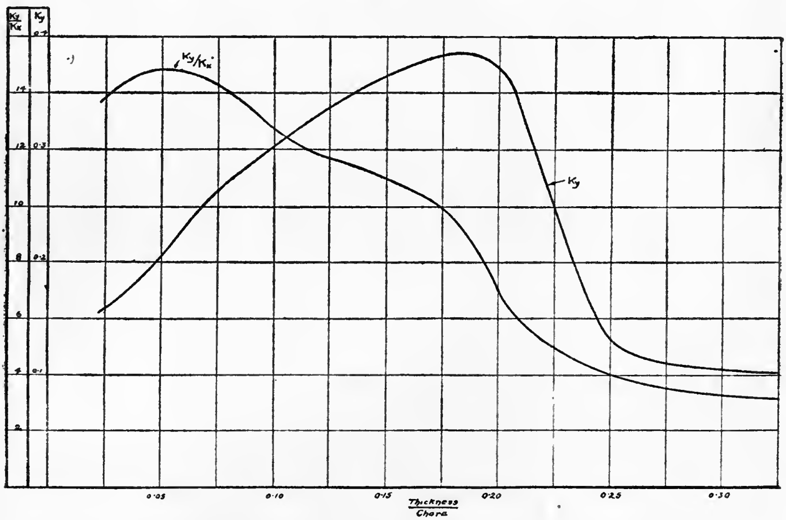

FIG. 214.—Aerodynamic Characteristics for Airscrew Sections.

the integrals, it is necessary to know the aerodynamic characteristics of a number of suitable aerofoil sections. The data given on pages 67 – 70 relating to the sections illustrated will be found very useful in this connection. From the data there given the curves shown in Fig. 214 have been drawn. It is seen from Fig. 53 that the most efficient angle of incidence, that is, the angle giving the maximum ratio $\mathrm{K_y}/\mathrm{K_x}$, for these sections, is in the neighbourhood of 3°. Consequently the angle of attack (θ) for the airscrew elements, if these sections be used, should be 3°. Using this angle of incidence, the curves shown in Fig. 214 have been drawn, giving the values of K_y and K_y/K_x plotted against the ratio Thickness/Chord. The value of this proceeding will be evident shortly. It should be observed here that on account of the loss in efficiency of an airscrew when climbing, it is sometimes advisable to adopt a smaller angle of attack than the angle of maximum efficiency, in order to minimise this loss when climbing. Such an arrangement leads to reduced efficiency at top speed, which is counterbalanced by an increased efficiency when climbing. The advisability of such procedure naturally depends upon the desired performance, and the designer must compromise in order to get the results desired

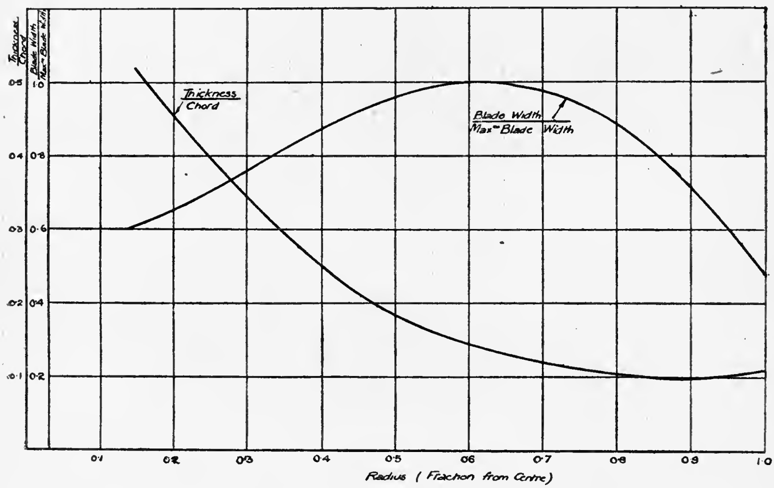

Fig. 215.—Design Data for 2-bladed Airscrews.

in any particular case. It is on this account that an airscrew in which the angles of the blade are adjustable in accordance with the conditions of flight prevailing would offer considerable advantages, and would lead to a much-increased all-round efficiency. This problem of the variable pitch airscrew is receiving much attention, and will undoubtedly be solved in the very near future.

A second factor involved in the evaluation of the integral is the ratio b/b_{max}. This ratio represents the width of the blade at any section in terms of the maximum width of the blade, and its value is dependent upon the plan form adopted.

Figs. 215 and 216 represent an analysis of several types of airscrews which have proved successful in practice, the curves showing—

(a) The ratio b/b_{max}

(b) The ratio maximum thickness/chord,

for all points along the blade. These curves, together with those shown in Fig. 214 give all the necessary data for the design of a successful airscrew, and their application to such design will be fully explained in this chapter.

Referring to the expression for total torque (Formula 84), it is seen that by inserting the values of K_y, K_x, b/b_{max} for a number of sections along the blade, the various values of the

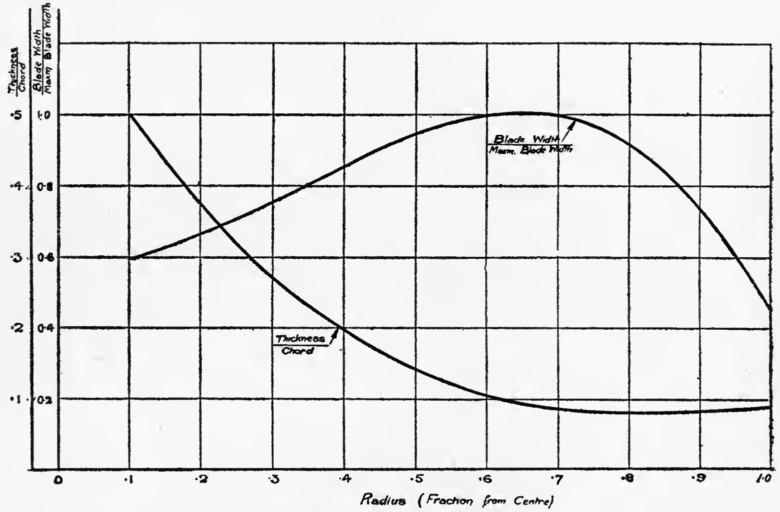

FIG. 216.—Design Data for 4-bladed Airscrews.

expression at these sections can be evaluated, and the torque curve for the airscrew can then be drawn. The torque available from the aero-engine at maximum efficiency is given by the relationship

$$\text{Torque} = \frac{\text{H.P.} \times 550}{2\pi N} \quad \text{............ Formula 85}$$

where N = number of revolutions per second

H.P. = horse-power of engine.

By equating this torque to that given by Formula for torque of the airscrew, the requisite value of b_{max}, the maximum blade width is determined. Having determined the maximum blade width, the width at all sections immediately follows from Figs. 215, 216.

Further, when the maximum blade width has been determined, the thrust can be calculated by the use of the expression for total thrust (Formula 83).

Finally, the overall efficiency of the airscrew will be given by the expression

$$\varepsilon = \frac{T\,V}{2\,\pi\,N\,Q} \qquad \text{........... Formula 86}$$

where V = translational velocity of the machine
T = thrust of the airscrew
Q = torque of the airscrew
N = revolutions of the airscrew.

Unfortunately the premises are not so adequate as a superficial glance at the above formulæ would seem to indicate. The chief causes of error may be summarised as under, and must be taken into account by the designer.

1. Air is set in motion by the airscrew before the disc of the airscrew is actually reached.
2. Aerofoil data may not be directly applicable in the case of the very high speeds obtaining with airscrews.
3. 'Wing tip losses' are very important, as the tip is the most effective part of the blade of the airscrew.
4. Allowances are necessary for the root of the blade, partly because it must be designed primarily for strength, and not for efficiency, and partly because of the boss and other obstructions.

It may be observed that research work is in progress upon all these doubtful points. To allow for the first it is necessary to measure the 'velocity of inflow' at various radii, and then modify the analysis to suit. Information was given on this point in a paper read before the Aeronautical Society by M. A. S. Riach in 1917. In this connection Formula 86 (*a*) should be plotted for various values of A, when it will become apparent that the efficiency of the element depends upon the radius.

The second point will become clearer the more model experiments are carried out upon airscrews having blades of known aerofoil sections.

The third point suggests a rounded tip in preference to a square end; and the fourth point indicates that it will in most cases be hardly worth while to trouble about obstructions to flow massed round the shaft.

When setting out the plan form of the blade, care should be taken to eliminate twisting as far as possible. This is effected by arranging the moments of the forces on the blade elements about a line drawn along the length of the blade, so that these moments balance one another. For this purpose the aerofoil data giving the C.P. position for each blade element used must be employed.

Experimental Method of Design. — When using this method of design, small model airscrews are constructed and tested experimentally, and from the results obtained the probable performance of a full-sized airscrew of similar design is deduced from the laws of geometrical similitude. The following formulæ are assumed to hold good for geometrically similar airscrews :—

$$\text{Thrust} = C\,N^2\,D^4$$
$$\text{Horse-power} = K\,N^3\,D^5$$

where N = airscrew revolutions per second
D = airscrew diameter in feet.

C and K are constants depending upon the ratio of the circumferential blade tip velocity to the translational velocity—that is, they are proportional ND/V.

Also since the efficiency of the airscrew

$$= \frac{\text{Thrust} \times \text{Forward Velocity}}{\text{Horse-power}}$$

$$\therefore \qquad \epsilon = M\,\frac{V}{N\,D}$$

where M is a constant.

It is thus seen that for any airscrew it is possible to draw curves in which thrust, torque, and efficiency are plotted against the ratio V/N D. These quantities may be determined experimentally for a number of similar types of airscrews in which the ratio pitch/diameter is different, and from the experimental results so obtained the required curves can be plotted. The efficiency curve for each airscrew is then plotted on the same sheet, and an envelope of all these curves is drawn. Each point on this envelope corresponds to a particular pitch ratio member of the series, and can therefore be applied to the design of an airscrew which is required to fulfil certain given conditions. For example, if an airscrew of this type is required of diameter D, with maximum efficiency at a certain definite forward velocity V, corresponding, say, to top speed or best climbing speed, and to have a rotational speed of N revolutions per second, the ratio V/N D is easily calculated, and from the point on the envelope of the efficiency curve corresponding to this value, the correct pitch ratio can at once be read off.

This principle can be extended further in order to find the best blade width ratio for the required conditions. A number of airscrews having the correct pitch ratio may be constructed with varying blade width ratios, and from the experimental results a further series of curves can be drawn, each corresponding to a particular blade width ratio. The envelope of these curves will enable the best value of the blade width ratio for the particular conditions under which the airscrew is to work to be read off.

In cases where it is possible to carry out tests upon model airscrews, this method leads to very good results, and is much more reliable than the method of calculation. It is probable, however, that a combination of the two methods will form the final basis for airscrew design, the experimental results being used to give the necessary correction factors which the purely theoretical method requires.

Tractive Power developed at the Airscrew.—The tractive power developed by an airscrew (P) was given in Formula 70, Chapter VI., namely

$$P = k\left[1 - \left(\frac{V}{Np}\right)^2\right]N^3 D^5$$

The expression $(V/Np)^2$ is the slip-stream factor, and it will be observed that when the product Np is equal to the forward speed of the aeroplane there will be no power developed by the engine save that required to overcome friction.

Again, when the velocity is zero—that is, when the machine is standing—the power developed reduces to the expression

$$P = k N^3 D^5$$

The constant k depends upon the construction of the airscrew, but it can be determined experimentally by flying the machine and noting the power P required at a certain definite speed. This for horizontal flight at speed V is given by the expression

$$\frac{\frac{\rho}{g} A V^3 K_x}{550}$$

where K_x is the drag of the machine, A the wing area, and ρ the density of air per cubic foot.

Naturally the efficiency of the airscrew varies considerably under different conditions, owing to the variation in its effective pitch. It has its maximum efficiency when its effective pitch is largest—that is, when the machine is travelling fast; and its minimum efficiency when the effective pitch is smallest—that is, when the machine is climbing.

Design of an Airscrew by the Blade Element Theory. —It is customary to commence from the following data, which have already been fixed by outside considerations, namely:

1. The horizontal velocity of the machine V.
2. The speed of the airscrew in revolutions per second N.
3. The diameter of the airscrew D, which is usually fixed by the question of ground clearance, and which should be as large as the machine under construction will permit, so that tip velocity does not exceed 1000 f.p.s.
4. The B.H.P. available from the engine.
5. The aerodynamical properties of the aerofoil sections it is proposed to employ.

It is intended to design a four-bladed airscrew of 10 feet diameter, with a speed of 1000 r.p.m. The aeroplane is fitted with a 375 h.p. engine, and is required to do 130 m.p.h. at an altitude of 10,000 feet. It will be assumed that the engine power diminishes with atmospheric pressure, the pressure at 10,000 feet being 70% of that at ground level, and the density at that altitude being 72% of that at ground level.

The aerofoil characteristics will be those taken from Fig. 214, and the blade proportions will be taken from Fig. 216. It is first necessary to determine the angle A for each section, from the relationship

$$\tan A = \frac{V}{2\pi N r} \quad \text{...... ... See Fig. 213}$$

$$V = 130 \text{ m.p.h.} = 190{\cdot}8 \text{ f.p.s.}$$

$$N = 1000/60 = 16{\cdot}67$$

$$\therefore \quad \tan A = \frac{190{\cdot}8}{33{\cdot}33\,\pi r}$$

from which expression the values of A can be tabulated as below:

Section ...	A	B	C	D
Radius r feet ...	1·25	1·75	2·25	2·75
Tan A ...	1·46	1·04	0·81	0·664
A ...	55° 36′	46° 87′	39°	33° 35′

Section ...	...	E		F		G		H
Radius r feet ...	3·25	...	3·75	...	4·25	...	4·75
Tan A ...	..	0·561	...	0·486	...	0·429	...	0·384
A ...	...	29°18′	...	25°55′	..	22°13′	...	21°

The blade width ratios b/b_{max} and the aerofoil characteristics are now taken from Figs. 216 and 214, remembering that the latter correspond to the angle of attack of 3°.

The evaluation of the torque and the thrust can now be proceeded with, using the relations already established in this chapter, namely, formulæ 83, 84.

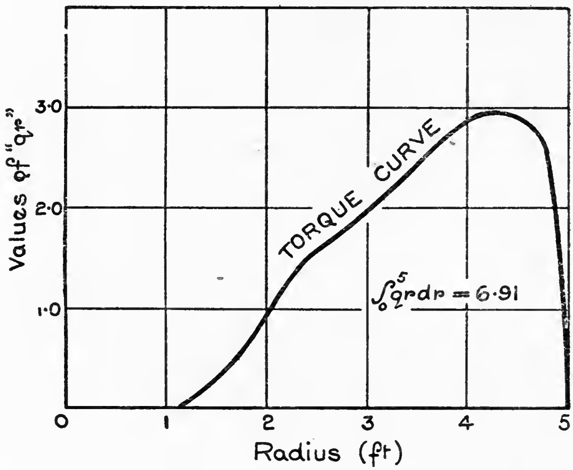

FIG. 217.—Torque Curve for Airscrew.

$$\text{Torque} = 4 \times ·00237 \times ·72 \times 190·8 \times 190·8$$

$$\times\, b_{max} \int_0^5 K_y \sqrt{1 + \left(\frac{K_x}{K_y}\right)^2}\, \frac{b}{b_{max}} \frac{\sin(A + \phi)}{\sin^2 A}\, r \,.\, dr$$

$$\text{Thrust} = 4 \times ·00237 \times ·72 \times 190·8 \times 190·8$$

$$\times\, b_{max} \int_0^5 K_y \sqrt{1 + \left(\frac{K_x}{K_y}\right)^2}\, \frac{b}{b_{max}} \frac{\cos(A + \phi)}{\sin^2 A}\, dr$$

The determination of these integrals is best effected in practice by adopting the tabular method of procedure as shown on next page.

Section	A	B	C	D	E	F	G	H
$\frac{r}{R}\left(\frac{\text{radius}}{\frac{1}{2}\text{ diameter}}\right)$	·25	·35	·45	·55	·65	·75	·85	·95
b/b^{max}	0·71	0·80	0·90	0·975	1·0	0·97	0·84	0·60
$\frac{\text{Thickness}}{\text{Chord}}$	0·32	0·23	0·165	0·12	0·092	0·082	0·08	0·085
K_y	0·10	0·22	0·375	0·33	0·29	0·28	0.275	0·282
K_x/K_y	0·28	0·208	0·096	0·084	0·076	0·072	0.0715	0·072
$\phi = \tan^{-1}\frac{K_x}{K_y}$	15°39′	11°45′	5°29′	4°48′	4°21′	4°7′	4°5′	4°7′
$(A + \phi)$	71°15′	57°52′	44°29′	38°23′	33°39′	30°2′	27°18′	25°7′
$\sin(A + \phi)$	·947	·847	·701	·621	·554	·500	·459	·424
$\cos(A + \phi)$	·321	·532	·713	·784	·832	·866	·888	·905
$\sin^2 A$	·681	·520	·395	·305	·239	·190	·154	·128
$\sqrt{1 + \left(\frac{K_x}{K_y}\right)^2}$	1.038	1·021	1·005	1·004	1·003	1.003	1·003	1·003
$K_y\sqrt{1 + \left(\frac{K_x}{K_y}\right)^2}\frac{b}{b_{max}}\frac{\sin(A + \phi)}{\sin^2 A}r$	0·128	0·512	1·355	1·810	2·195	2·70	2·94	2·68
$K_y\sqrt{1 + \left(\frac{K_x}{K_y}\right)^2}\frac{b}{b_{max}}\frac{\cos(A + \phi)}{\sin^2 A}$	0·0347	0·184	0·613	0·830	1·015	1·242	1·335	1·200
A+Θ	58°36′	49°7′	42°	36°35′	32°18′	28°25′	26°13′	24°

These values are next plotted against the radius r as shown in Figs. 217 and 218, and the areas enclosed by the curves very carefully measured. From these curves it was found that

$$\int_0^5 K_y \sqrt{1 + \left(\frac{K_x}{K_y}\right)^2} \frac{b}{b_{max}} \frac{\sin(A+\phi)}{\sin^2 A} r.dr = 6{\cdot}91$$

$$\int_0^5 K_y \sqrt{1 + \left(\frac{K_x}{K_y}\right)^2} \frac{b}{b_{max}} \frac{\cos(A+\phi)}{\sin^2 A} dr = 3{\cdot}17$$

hence the torque required to drive the airscrew

$$= 4 \times {\cdot}00237 \times {\cdot}72 \times 190{\cdot}8 \times 190{\cdot}8 \times 6{\cdot}91 \times b_{max}$$

but the torque available from the engine

$$= \frac{{\cdot}70 \times 375 \times 550}{2\pi \times \frac{1000}{60}}$$

$$= 1375 \text{ lbs. ft.}$$

Equating these values

$$b_{max} = 1375/1720$$
$$= 0{\cdot}8 \text{ feet} = 9{\cdot}6 \text{ inches}$$

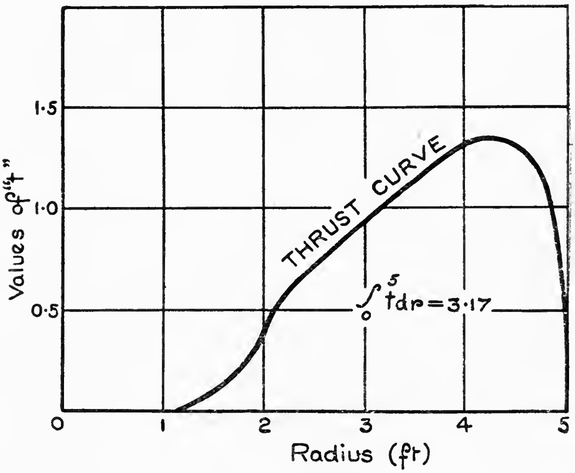

FIG. 218.—Thrust Curve for Airscrew.

The maximum blade width having thus been determined, the dimensions of each section follow at once from the third and fourth lines of table on page 292, namely :

Section	A	B	C	D	E	F	G	H
Blade width—ins.	6·81	7·69	8·64	9·36	9·6	9·31	8·06	5·76
Thickness—ins....	2·18	1·77	1·43	1·12	0·88	0·76	0·65	0·49

The thrust of the airscrew

$$= 4 \times \cdot 00237 \times \cdot 72 \times 190 \cdot 8 \times 190 \cdot 8 \times 0 \cdot 8 \times 3 \cdot 17$$
$$= 630 \text{ lbs.}$$

Therefore the efficiency

$$= \frac{630 \times 190 \cdot 8}{2\pi \cdot \frac{1000}{60} \cdot 1375}$$
$$= 83 \cdot 5\%$$

In practice it is found that the efficiency of an airscrew is generally slightly higher than its calculated value; hence it is probable that this figure would be more than realised if tested under the conditions assumed.

The general lay-out of the airscrew can now be developed as shown in Fig. 219. Each section must be drawn in its correct position along the blade and with the required angle, A + 3°, to the axis of the blade.

The following points should be observed when sketching the aerofoil sections :—

(*a*) The centre of area of the sections should lie on the blade axis.

(*b*) The respective positions of the centre of pressure of the sections should be arranged about the blade axis so as to eliminate as far as possible all twist upon the blade. For this reason a symmetrical blade is unsuitable, because the centres of pressure in this case would all lie on one side of the centre line of the blade. By adopting some such shape as that shown, this unbalanced effect is avoided.

(*c*) Sections near the boss of the airscrew are designed chiefly from considerations of strength, and the adoption of a convex instead of a flat face is a help in this direction, while the aerodynamical loss resulting from such alterations at these sections is practically negligible.

The contour lines of the blade can now be constructed. This is an operation which demands great skill, and depends for its success principally upon the experience of the designer. Indeed, it may be said that after the design of a few successful airscrews an airscrew designer will no longer need aerodynamical data to assist him, but will be able to produce an efficient airscrew merely by 'eye.'

In normal flight the 'slip' of the airscrew may be somewhat greater than that corresponding to maximum efficiency, in which case small variations in the rotational speed will be accompanied by appreciable variations in the value of the thrust. By adjusting the torque of the engine, allowance can be made for any small discrepancy between the calculated and the actual behaviour of the airscrew.

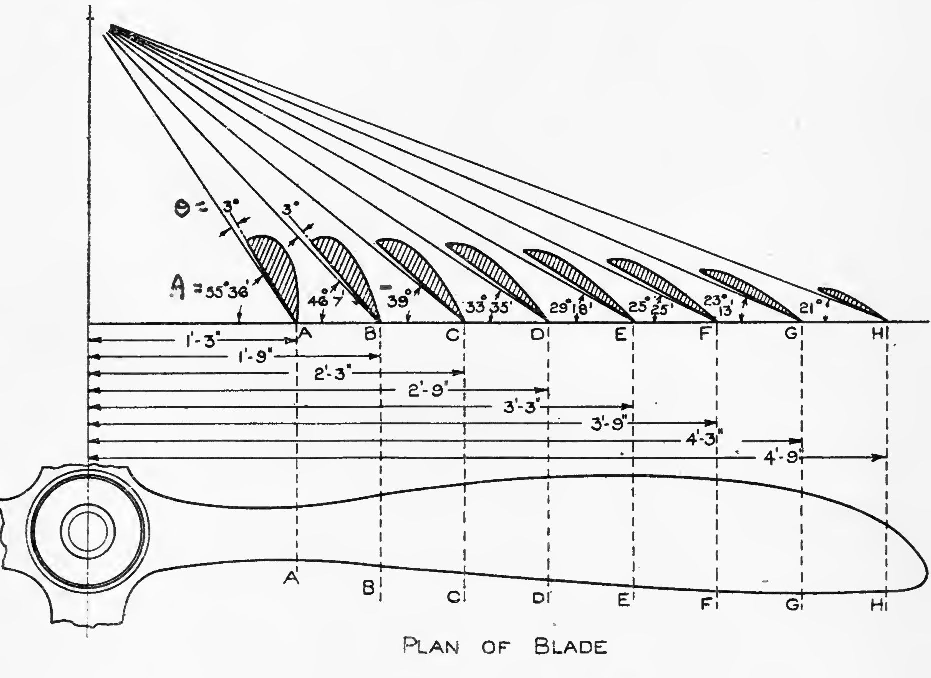

FIG. 219.—Lay-out of an Airscrew.

Stresses in Airscrew Blades. — An airscrew blade is generally subjected to the following forces :—

1. A tension due to centrifugal force.
2. A bending moment.
3. A twisting moment.

It is therefore obvious that an accurate calculation of the combined stresses at any point along the blade is a matter of considerable difficulty. We can, however, obtain satisfactory results by considering each stress separately. In a well-designed airscrew the stresses due to twist will be quite small, since particular care will have been taken in the design to eliminate all twist as explained previously. The stresses due to centrifugal force and bending moment may be determined as follows: Let Fig. 220 represent the airscrew blade, and let 'a' be the cross-sectional area of a section of the blade distant 'x' from

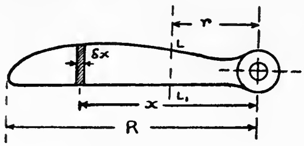

FIG. 220.

FIG. 221.

the centre. Then the centrifugal force set up by a small element of the blade at this distance

$$= \frac{\text{weight of element} \times (\text{velocity})^2}{g\,x}$$

Let w be weight in lbs. of a cubic foot of the material of which airscrew is made

Then volume of element $= a\,.\,d\,x$

weight of element $= w\,a\,.\,d\,x$ lbs.

velocity of element $= 2\,\pi\,n\,x$ feet per second,

hence centrifugal force due to element

$$= \frac{w\,a\,.\,d\,x \quad 4\,\pi^2\,n^2\,x^2}{g \qquad\qquad x}$$

The stress at any section L L[1] of cross-sectional 'a''

$$= f = \frac{4\,\pi^2\,n^2\,w}{g\,a'} \int_{x=r}^{x=R} a\,x\,.\,d\,x$$

The value of the integral can best be determined graphically by taking values of the product $a\,x$ along the blade and plotting them on an 'x' base. The area of the curve thus obtained will enable the stresses due to centrifugal force to be determined with considerable accuracy. A simpler but not so accurate a method is to assume the blade of constant section over a certain distance, and to treat each such length separately by determining its weight and mean distance from the centre of rotation.

Adopting this method, the stresses due to centrifugal force in the airscrew just designed are obtained by tabulation as shown

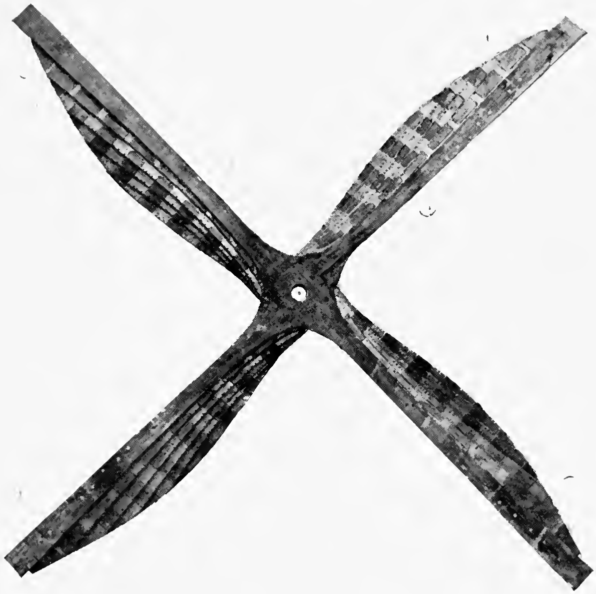

FIG. 225.—Appearance of Airscrew Laminations before shaping.

Reproduced by courtesy of Messrs. Oddy, Ltd.

FIG. 228.—Finished Airscrew.

Facing page 296.

below. The area of each section should be determined by graphical summation, Simpson's rule, or by the use of a planimeter. The weight of a cubic foot of mahogany is taken as 35 lbs.

TABLE XLIII.—STRESSES DUE TO CENTRIFUGAL FORCE.

Section	A	B	C	D	E	F	G	H
Area sq. ins. ...	9·94	9·05	8·24	6·98	5·64	4·72	3·49	1·88
Volume cu. ins.	59·6	54·3	49·4	41·9	33·8	28·35	20·95	11·28
Centrifugal force	514	655	767	794	758	732	613	369
Σ C	5202	4688	4033	3266	2472	1714	982	369
Stress $= \frac{\Sigma C}{A}$ ...	524	519	490	469	438	364	282	196

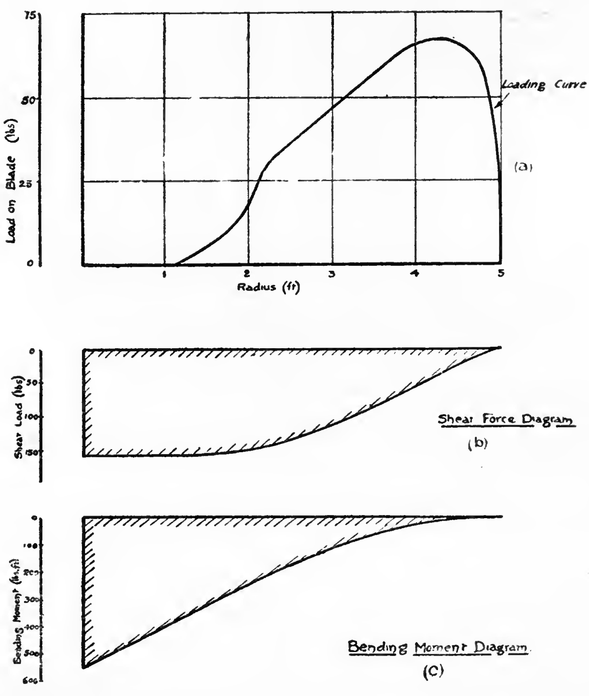

FIG. 222.—S. F. and B. M. Diagrams for Airscrew.

Stresses due to Bending.—The stresses in the blade due to bending are set up by the air pressure exerted upon each element of the blade. Consider a section of the blade such as is shown in Fig. 221. The maximum tensile and compressive stresses will occur in the outer layers of the material, and to find their values we require to know the bending moment at the section considered. The value of this bending moment is determined by drawing the load grading curve. The ordinates of this curve are obtained from the thrust grading curve by dividing the thrust at each section by cos $(A + \phi)$. Since this is a mere ratio the thrust grading curve can evidently be used with a different vertical scale. The curve of shear force over the blade follows directly from the load grading curve by graphic or tabular integration, whichever is preferred. Similarly integration of the shear force curve gives the bending moment curve. This work is quite straightforward, but if graphical integration is used care must be taken to see that the correct scales are obtained. Fig. 222 (*a b c*) shows these curves for the airscrew under consideration.

The bending moment at each section is then read off from the curve, and the stresses obtained from Formula 51.

The moment of inertia of the sections and their centre of gravity can be readily determined by the use of the graphical method outlined for a streamline strut in Chapter IV.

The stresses due to bending are tabulated in Table XLIV. below.

TABLE XLIV.—STRESSES DUE TO BENDING.

Section ...	A	B	C	D	E	F	G	H
I/y_c in.^{3} ...	2·46	1·83	1·34	0·89	0·565	0·41	0·26	0·105
I/y_t in.^{3} ...	3·70	2·75	2·02	1·34	0·85	0·614	0·39	0·16
B.M. lbs. ft....	365	286	214	146	87	40	15	4
B.M. lbs. in....	4390	3440	2570	1750	1040	480	180	48
Compressive Stress.								
My_c/I lbs. per sq. in.	1790	1880	1920	1970	1840	1170	690	460
Tensile Stress.								
My_t/I lbs. per sq. in.	1190	1250	1270	1310	1225	780	460	300

The maximum stresses at each section can now be obtained by adding together the centrifugal and the bending moment stresses of Tables XLIII. and XLIV.

It will be observed that the tension due to centrifugal force will diminish the compressive stress in the blade, but increase the tensile stress. For mahogany or walnut the maximum permissible working stress is 2000 lbs. per square inch. The stresses obtained are seen to be well within this figure.

TABLE XLV.—MAXIMUM STRESSES IN THE AIRSCREW BLADE.

Section	A	B	C	D	E	F	G	H
Compressive stress	1266	1361	1430	1501	1402	806	408	264
Tensile stress	1714	1769	1760	1779	1663	1144	742	496

The best materials at present available for the construction of airscrews are walnut (black) and mahogany. Walnut is heavier than mahogany, but is not so liable to warp; on the other hand, mahogany takes the glue better. The ultimate tensile strength of either material is about 4 tons per square inch, so that a working stress of 2000 lbs. per square inch may be considered as quite satisfactory.

The method of building up an airscrew will be apparent from a study of Fig. 223. The thickness of the laminæ varies from $\frac{3}{4}''$ to $1\frac{1}{4}''$.

Much controversy has raged round the question of the relative merits of the two- and the four-bladed airscrew. The four-bladed airscrew is probably better balanced and slightly more efficient than the two-bladed variety, but the latter type is easier to build, and can also be made stronger at the boss.

The Construction of an Airscrew.—As already stated, the timber most frequently used for the construction of an airscrew is either mahogany or walnut. The wood should be thoroughly seasoned, straight-grained, and quite free from knots. The use of curly-grained timber will cause the blades to cast, and should therefore be avoided. The planks from which the laminæ are to be cut should be stored for several weeks in a room where the temperature and atmospheric conditions are the same as those prevailing in the workshop. The first operation is the sawing out of the laminæ. The dimensions at the various sections are obtained from the drawing. A template giving the shape of each lamina should be prepared in either three-ply wood or in aluminium sheet. A margin of about $\frac{1}{2}''$ in the case of a four-bladed airscrew and of about $\frac{1}{4}''$ in the case of a two-bladed airscrew should be allowed all round to compensate for any errors in gluing in position or change of position due to warping. The planks should then be marked off from the templates, the grain running longitudinally and parallel to the flat surface. The laminæ are best cut out with a band saw and then planed to the correct thickness.

In the case of the four-bladed screw the laminæ are half lapped at the centre, as shown in the sketch, Fig. 224. The surfaces which receive the glue should be 'toothed' lengthwise along the blade. The laminæ are then supported at their centre on a balance and the heavier ends marked. The gluing together of the laminæ can now be commenced. The first two laminæ are thoroughly warmed by placing them in contact with a hot plate, and then their adjacent surfaces are quickly covered with best Scotch, French, or Lincoln glue, after which they are clamped together in their correct relative positions by means of a number of hand-screw clamps. Clamping should be commenced at the centre of the block, working outwards to the tip. In this manner a failure of the glued joints at the boss is avoided. It is also very essential that the temperature of the glue room should be maintained at a uniform temperature of about 70° F. throughout the entire process of gluing, otherwise an opening of the joints is

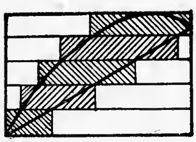

FIG. 223.

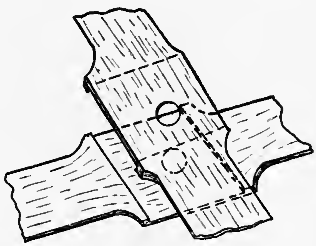

FIG. 224.

probable after the airscrew has been completed. The remaining laminæ are then glued in position one at a time, a period of at least eight hours being allowed between the addition of each lamina. The process of warming the lamina and clamping it down on to the block is exactly similar to that described above for the first two laminæ.

In order that the position of each lamina relatively to the block may be correct, it is customary to locate it by measurement from the preceding one, and then a small piece of wood is glued on the projecting portion of the lower lamina, and the side of the freshly added lamina is pressed up tight against this small block. Before the addition of each lamina the block is checked for balance and then the light end is balanced up by placing the heavier end of the next lamina upon it. In this manner the block is comparatively well balanced at the completion of the gluing-together stage. After gluing, a number of small pegs are driven into the blades at positions which have been indicated upon the drawings. They should be a moderate driving fit, and glued into position. The boring of the hole in the boss is the next operation. This is best performed upon a boring machine, the cutter being run at a high speed in order to obtain accuracy. The block is then set aside for several days in a room the temperature of which is exactly the same as that prevailing in the glue room. During this period the tendency of the blades to cast or warp will be taken up. Fig. 225 shows a 4-bladed airscrew at this stage of construction.

The 'roughing-out' stage is now commenced, and the blades are shaped down to within about $\frac{1}{4}''$ of their final dimensions. A further period of several days is then allowed for the timber to take up any change of state. In this manner a more accurate and more permanent contour is finally obtained. Lastly, the final shaping of the airscrew is proceeded with. The correct shape and angle of the blade sections are obtained by the use of

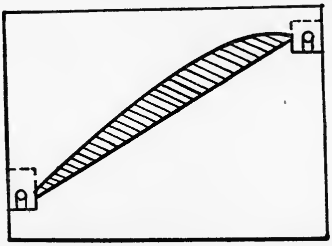

Fig. 226.—Template for checking Airscrew Section.

steel or aluminium templates such as are shown in Fig. 226. The balance of the airscrew should be frequently tested during this latter process and more material removed from the heavier blades. The blade surfaces are finally smoothed up by means of glass-paper and the airscrew should now be almost perfectly balanced. One type of balance for testing airscrews is shown in Fig. 227. A thin steel tube is passed through the airscrew hub, and the airscrew is then lifted on to the balance, the outer ends of the tube resting on two knife-edged plates. Another method is to support the tube inside roller bearings carried on a wall bracket. The remaining operations are

(*a*) The drilling of the bolt holes through which pass the bolts which attach the airscrew to the steel boss, which in turn is serrated and fits on to a correspondingly serrated shaft attached to the engine shaft.

(*b*) The final varnishing of the airscrew in order that it may withstand climatic conditions.

The first of these operations necessitates the use of a drilling jig for which a standard airscrew boss can be used ; while for the second, two or three coats of good boat varnish with an oil base should be used. The final balance of the airscrew is effected by adding extra varnish to the lighter blades. A completed airscrew is shown in Fig. 228.

The practice of adding brass tips to the airscrew blades was

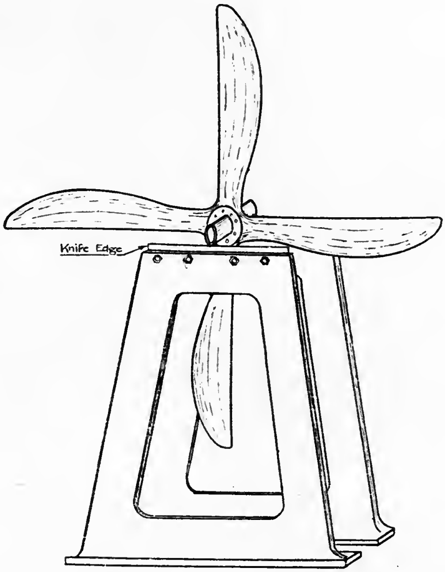

FIG. 227.—Testing the Balance of an Airscrew.

largely adopted during the war. These tips are bent to the correct shape on a former, and then riveted to the blades by means of copper rivets. They serve as a protection to the outer leading edges of the airscrew, but greatly increase the stresses at the roots of the blades due to centrifugal force. The sheathing of the blades with fabric has also been largely adopted.

CHAPTER X.

STABILITY.

Definition.—The stability of an aeroplane considered from the most general point of view would involve a discussion of all those qualities which enable a machine to be flown in safety under all the varying conditions likely to be met with in flight in all weathers.

The stability of an aeroplane as studied in this chapter will be considered from the more limited standpoint of the following definition: 'If a body be moving in a uniform manner relative to the surrounding medium, then the motion is said to be **stable,** if when any small disturbance takes place in the medium, the forces and reactions set up in the body tend to restore the body to its original state of motion; while if the forces due to a small initial disturbance tend to produce a further departure from the original state of motion, then the motion is said to be **unstable.**'

Applying this definition to an aeroplane, it is seen that a machine will be **inherently stable** if after a sudden disturbance in its flight path it is able to regain correct flying attitude without any assistance on the part of the pilot.

For an aeroplane to be completely stable it must possess both statical and dynamical stability. An aeroplane is statically stable if righting moments are called into play which tend to bring the machine back to its normal flying attitude if deviated therefrom temporarily. These righting moments will, however, set up oscillations, and the machine will be dynamically stable only if these oscillations diminish with time and ultimately die out, leaving the machine in its normal flight attitude. It is therefore essential to establish statical stability before making an investigation of dynamical stability.

The question of stability is closely inter-connected with the question of controllability. A machine possessing a large amount of inherent stability is sometimes difficult to control, or in the words of the pilot, is said to be 'heavy on the control.' It is generally necessary to make a compromise between the two factors. For fighting purposes manœuvrability is of the utmost importance, and it is essential that a war machine should answer very rapidly to its controls, and consequently the question of inherent stability is not of such vital importance as in the case of the commercial machine. Reference to the particulars given in Chapter XIV. with regard to the Bristol Fighter and the S.E. 5 illustrates that fighting machines have been designed possessing a large degree of both inherent stability and manœuvrability. It will be readily appreciated that in the case of long distance flights an aeroplane which continually tends to depart from the normal flight path, owing to minor disturbances, requires constant attention on the part of the pilot, and imposes upon him a very severe strain, which it is both possible and desirable to avoid.

The mathematical theory of stability, with respect to an aeroplane in the restricted sense of the above definition, has been developed principally by Lanchester* and Bryan.† The application of Bryan's theoretical results to a particular machine was very ably carried out by Bairstow,‡ and much of the subsequent matter is based upon his work.

The theory is very complex and those desiring a fuller treatment of the subject should consult the references given below. Our aim in this chapter is to outline the theory and to show its application to the results of tests upon models, and then to indicate the method whereby the stability of a completed machine may be predicted from these wind channel tests.

The investigation of stability can be summarised as under:—

Summary of Procedure:

A. Theoretical determination of the equations of motion by mathematical reasoning in terms—

(i.) Of the velocities of the C.G. of the machine along the axes of reference;

(ii.) Of the angular velocities of the machine about the same axes.

B. These expressions contain a number of constants termed Derivatives, which can be divided into two classes—

(i.) **Resistance Derivatives** which depend merely on the shape and size of the machine, and not on its motion;

(ii.) **Rotary Derivatives** which depend upon the motion of the machine.

Both classes of derivatives can be determined analytically, and also by means of model tests.

* *Aerodonetics* (Constable & Co.). † *Stability in Aviation* (Macmillan).
‡ *N.P.L. Report*, 1912–1913.

C. Substitution of the values obtained for the derivatives in the general equations of motion developed under A leads to a solution in many important cases, and consequently the nature of the motion can be investigated.

D. The investigation of the small oscillations occurring about the steady motion of an aeroplane leads to a classification into two groups, each determined by three equations of motion. These groups are:

(i.) The group representing motion in a vertical plane, and determining the nature of the longitudinal oscillations upon which the longitudinal stability of the machine depends.

(ii.) The group representing motion about the plane of symmetry, and determining the nature of the rolling and yawing oscillations upon which the lateral stability of the machine depends.

Stability Nomenclature.—The N.P.L. system is illustrated in Fig. 229 and tabulated in Table XLVI.

The axis O x corresponds to the axis of drag of the machine in normal flight.
The axis O z corresponds to the axis of lift.
The axis O y is perpendicular to the plane x o z.
O is the centre of gravity of the machine.

Rotation about the axis O x is termed ROLLING.
Rotation about the axis O y is termed PITCHING.
Rotation about the axis O z is termed YAWING.
The linear velocities in the directions of the axes are denoted by u, v, w respectively, and the angular velocities about these axes are denoted by p, q, r respectively.

TABLE XLVI.—STABILITY NOMENCLATURE.

Axis.	Name of axis.	Name of force.	Symbol for force.	Name of angle.	Symbol for angle.	Name of moment.	Symbol for moment.
O x	Longitudinal	Longitudinal	X	Roll	ϕ	Rolling	L
O y	Lateral	Lateral	Y	Pitch	θ	Pitching	M
O z	Normal	Normal	Z	Yaw	ψ	Yawing	N

The signs of the forces are positive when acting along the positive directions of the axes indicated by arrows in Fig. 229; the angles and moments are positive when turning occurs or tends to occur from Oy to Oz; Oz to Ox; Ox to Oy.

In order to define the angular position of an aeroplane, Euler's 'System of Moving Axes' is adopted, the motion of the machine being referred to a system of axes fixed in the machine itself. If the motion of these axes be known with reference to

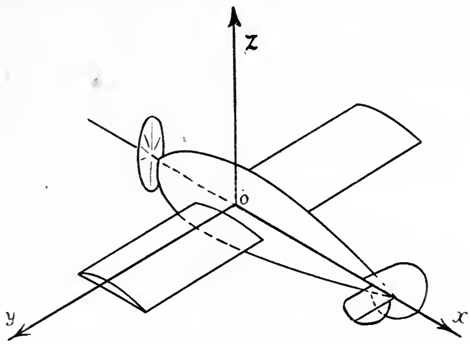

FIG. 229.—Axes of Reference.

any set of axes fixed in space, then the motion of the aeroplane is completely known. In Euler's method this fixed set of axes is chosen so as to coincide with the moving body axes at the

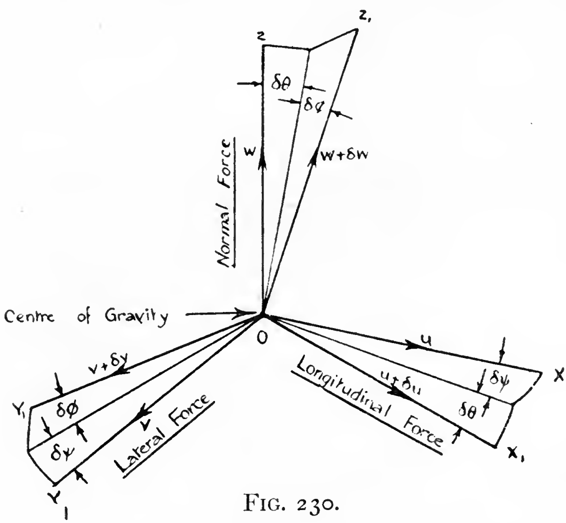

FIG. 230.

instant under consideration. Hence the fixed axes are continually being selected and discarded during motion. This method has the advantage of enabling the difficulties of referring the motion to a set of axes fixed in space to be avoided, but possesses the disadvantage that it cannot be used for allowing the flight path of the machine to be continuously traced out.

The Equations of Motion.—(*a*) LINEAR ACCELERATIONS.—Let O X, O Y, O Z be axes fixed in the machine occupying positions O X, O Y, O Z, and O X_1 O Y_1 O Z_1 at successive instants, as in Fig. 230.

Let u, v, w be the velocities of the machine along the axes O X, O Y, O Z; and $u + \delta u$, $v + \delta v$, $w + \delta w$ the velocities of the machine along the axes O X_1, O Y_1, O Z_1. The position of the axes relative to each other is obtained by first rotating the machine through an angle $\delta \psi$ about O Z, secondly rotating the machine through an angle $\delta \theta$ about the new axis of Y, and lastly by rotating the machine through an angle of $\delta \phi$ about the new axis of X.

Increment of velocity along fixed direction O X

$$= (u + \delta u) \cos \delta \theta \cos \delta \psi + (w + \delta w) \sin \delta \theta - (v + \delta v) \sin \delta \psi - u$$

$$= u + \delta u + w \, \delta \theta - v \, \delta \psi - u$$

whence neglecting second and higher orders of small quantities.

Acceleration in the direction O X

$$= \frac{\delta u + w \, \delta \theta - v \, \delta \psi}{\delta t}$$

$$= \frac{d u}{d t} + w \frac{d \theta}{d t} - v \frac{d \psi}{d t}$$

Similarly the increment of velocity along O Y

$$= (v + \delta v) \cos \delta \phi \cos \delta \psi + (u + \delta u) \sin \delta \psi - (w + \delta w) \sin \delta \phi - v$$

$$= v + \delta v + u . \delta \psi - w . \delta \phi - v$$

Acceleration in the direction O Y

$$= \frac{\delta v + u . \delta \psi - w . \delta \phi}{\delta t}$$

$$= \frac{d v}{d t} + u \frac{d \psi}{d t} - w \frac{d \phi}{d t}$$

And increment in velocity along O Z

$$= (w + \delta w) \cos \delta \theta \cos \delta \phi + (v + \delta v) \sin \delta \phi - (u + \delta u) \sin \delta \theta - w$$

$$= w + \delta w + v . \delta \phi - u . \delta \theta - w$$

Acceleration in the direction O Z

$$= \frac{\delta w + v . \delta \phi - u \, \delta \theta}{\delta t} = \frac{d w}{d t} + v \frac{d \phi}{d t} - u \frac{d \theta}{d t}$$

Now $\frac{d\phi}{dt}$ is the angular velocity of machine about axis $Ox = p$

$\frac{d\theta}{dt}$ " " " $Oy = q$

$\frac{d\psi}{dt}$ " " " $Oz = r$

Hence the acceleration of the machine along the three axes of reference may be written

$$\text{Acceleration along } Ox = \frac{du}{dt} + wq - vr = X$$

$$\text{,, \quad ,, \quad } Oy = \frac{dv}{dt} + ur - wp = Y$$

$$\text{,, \quad ,, \quad } Oz = \frac{dw}{dt} + vp - uq = Z$$

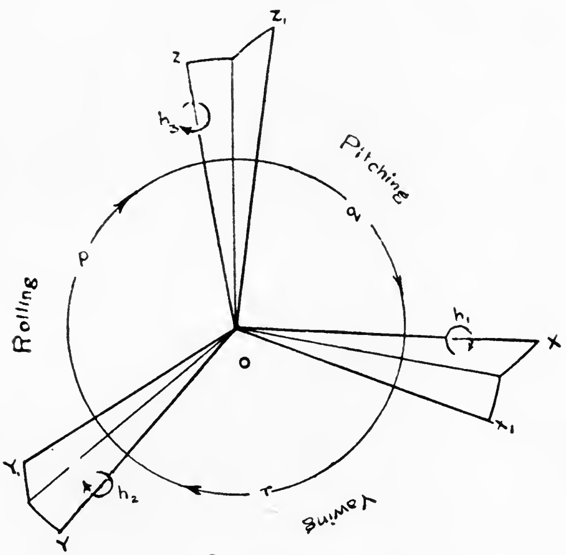

FIG. 231.—Angular Accelerations.

(*b*) ANGULAR ACCELERATIONS.—The angular velocities of the system of moving axes Ox, Oy, Oz, about any instantaneous position are represented by p, q, r respectively.

Let h_1, h_2, h_3 represent the angular velocities of the machine about these axes.

It is first necessary to find what angular acceleration, if any, is entailed in the superposing of the above angular velocities.

Consider a body moving in the plane Z O X (see Fig. 232) with an angular velocity q about the axis $o\,y$, and rotating with an angular velocity h_1 about the axis $o\,x_1$.

At a time 't' the axis $O\,x_1$ makes an angle $q\,t$ with $O\,x$. Mark off a distance $O\,f$ along axis $O\,x_1$ to represent the angular velocity h_1. Then component of angular velocity about axis $O\,x = o\,g = h_1 \cos q\,t$. Also component of angular velocity about axis $O\,z = o\,e = h_1 \sin q\,t$. Differentiating to determine the angular accelerations,

$$\text{Angular acceleration about } O\,x = -\,q\,h_1 \sin q\,t$$
$$\text{,,} \quad \text{,,} \quad \text{,,} \quad O\,z = q\,h_1 \cos q\,t$$

Compounding to determine the resultant angular acceleration,

$$\text{Resultant angular acceleration} = \sqrt{(q\,h_1)^2\,(\sin^2 q\,t + \cos^2 q\,t)}$$
$$= q\,h_1$$

This acceleration takes place about an axis $O\,a$, which rotates with angular velocity q about $O\,y$, the axis $O\,a$ always being at right angles to $O\,y$ and $O\,x_1$.

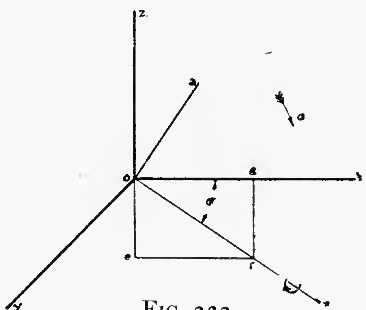

FIG. 232.

Applying this result to the general figure shown in Fig. 231, it is seen that the resultant angular acceleration about each axis contains three terms, two being due to the angular velocities about the other two axes, and the third being due to the rate of change of its own angular velocity. The angular accelerations about each of the axes can consequently be written down in the following manner :—

$$\text{Angular acceleration about } O\,x = \frac{d\,h_1}{d\,t} - r\,h_2 + q\,h_3$$
$$\text{,,} \quad \text{,,} \quad \text{,,} \quad O\,y = \frac{d\,h_2}{d\,t} - p\,h_3 + r\,h_1$$
$$\text{,,} \quad \text{,,} \quad \text{,,} \quad O\,z = \frac{d\,h_3}{d\,t} - q\,h_1 + p\,h_2$$

Considering the case of an aeroplane whose position in space at any moment is indicated by the axes O x, O y, O z, making angles of θ, ϕ, ψ, with the fixed axes O x_1, O y_1, O z, as shown in Fig. 233.

Let the velocity of the C.G. of the machine along the body

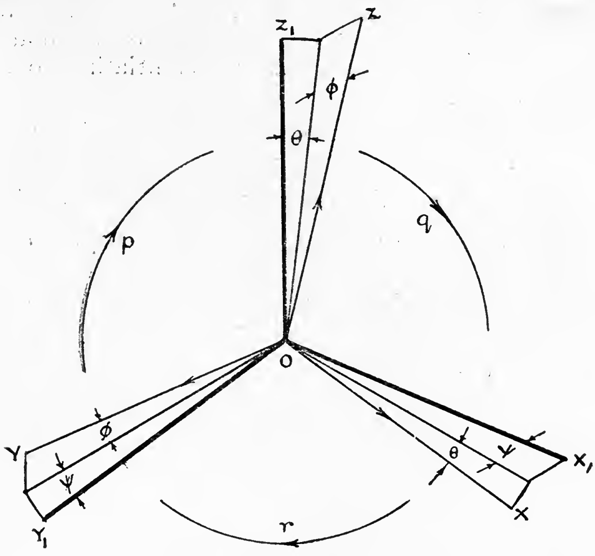

FIG. 233.

axes be u, v, and w respectively, and the angular velocity of the machine about these axes be p, q, r.

The general equations of motions will then be

$$\left.\begin{aligned} m\,(\dot{u} + w\,q - v\,r) &= m\,\mathrm{X} \\ m\,(\dot{v} + u\,r - w\,p) &= m\,\mathrm{Y} \\ m\,(\dot{w} + v\,p - u\,q) &= m\,\mathrm{Z} \\ \dot{h}_1 - r\,h_2 + q\,h_3 &= m\,\mathrm{L} \\ \dot{h}_2 - p\,h_3 + r\,h_1 &= m\,\mathrm{M} \\ \dot{h}_3 - q\,h_1 + p\,h_2 &= m\,\mathrm{N} \end{aligned}\right\} \quad \text{......... Formulæ 87}$$

where $\dot{u} = \dfrac{d\,u}{d\,t}$, and similarly for $\dot{v}$, etc.

m = mass of the aeroplane

$$h_1 = p\,\mathrm{A} - q\,\mathrm{F} - r\,\mathrm{E}$$
$$h_2 = q\,\mathrm{B} - r\,\mathrm{D} - p\,\mathrm{F}$$
$$h_3 = r\,\mathrm{C} - p\,\mathrm{E} - q\,\mathrm{D}$$

A B C D E F are the moments and products of inertia.

In the general problem the air forces X, Y, Z, and the air moments L, M, N, are functions of the velocity components, and of θ, ϕ, and ψ, and a disturbance from the normal flying speed and attitude causes a change in each of these quantities. If U be the normal flying speed and the disturbance be small, then $u, v, w, p, q, r, \theta, \phi, \psi$ are small compared with U, so that we can write

$$\mathrm{X} = f(\mathrm{U}, u, v, w, p, q, r, \theta, \phi, \psi),$$

which can be expanded into the approximate form

$$\mathrm{X} = u\,\mathrm{X_u} + v\,\mathrm{X_v} + w\,\mathrm{X_w} + p\,\mathrm{X_p} + q\,\mathrm{X_q} + r\,\mathrm{X_r} + \mathrm{X_o} + g\sin\theta$$

which is a linear function of the small quantities u, v, w, p, q, r, θ. The coefficients of these small quantities are the derivatives, which represent physically the slope of the curve of X upon a base of $u, v, w, p; q, r$ respectively. In a similar manner we have

$$\left.\begin{aligned}
\mathrm{Y} &= u\,\mathrm{Y_u} + v\,\mathrm{Y_v} + w\,\mathrm{Y_w} + p\,\mathrm{Y_p} + q\,\mathrm{V_q} + r\,\mathrm{Y_r} + \mathrm{Y_o} - g\cos\theta\sin\phi \\
\mathrm{Z} &= u\,\mathrm{Z_u} + v\,\mathrm{Z_v} + w\,\mathrm{Z_w} + p\,\mathrm{Z_p} + q\,\mathrm{Z_q} + r\,\mathrm{Z_r} + \mathrm{Z_o} - g\cos\theta\cos\phi \\
\mathrm{L} &= u\,\mathrm{L_u} + v\,\mathrm{L_v} + w\,\mathrm{L_w} + p\,\mathrm{L_p} + q\,\mathrm{L_q} + r\,\mathrm{L_r} + \mathrm{L_o} \\
\mathrm{M} &= u\,\mathrm{M_u} + v\,\mathrm{M_v} + w\,\mathrm{M_w} + p\,\mathrm{M_p} + q\,\mathrm{M_q} + r\,\mathrm{M_r} + \mathrm{M_o} \\
\mathrm{N} &= u\,\mathrm{N_u} + v\,\mathrm{N_v} + w\,\mathrm{N_w} + p\,\mathrm{N_p} + q\,\mathrm{N_q} + r\,\mathrm{N_r} + \mathrm{N_o}
\end{aligned}\right\}\ \text{Formulæ 88}$$

Before proceeding to form the equations for small oscillations, it should be observed that from considerations of the symmetry of the aeroplane, eighteen of the derivatives will be zero. For this reason the derivatives X, Z, M disappear when the suffix is v, p, or r, and the derivatives Y, L, N disappear when the suffix is u, w, or q.

Separating the equations of steady motion from those for small oscillations by writing $(\mathrm{U} + u)$ for u, $(\mathrm{V} + v)$ for v, $(\theta + \theta^1)$ for θ, etc., and omitting those derivatives whose value is zero, and combining formulæ 87 and 88, the equations become

$$\left.\begin{aligned}
&m\,[\dot{u} + (\mathrm{W} + w)(\mathrm{Q} + q) - (\mathrm{V} + v)(\mathrm{R} + r)] = m\,[u\mathrm{X_u} + w\mathrm{X_w} + q\,\mathrm{X_q} + \\
&\qquad\qquad \mathrm{X_o} + g\sin(\theta' + \theta)] \\
&m\,[\dot{v} + (\mathrm{U} + u)(\mathrm{R} + r) - (\mathrm{W} + w)(\mathrm{P} + p)] = m\,[v\,\mathrm{Y_v} + p\,\mathrm{Y_p} + r\,\mathrm{Y_r} + \\
&\qquad\qquad \mathrm{Y_o} - g\cos(\theta' + \theta)\sin(\phi' + \phi)] \\
&m\,[\dot{w} + (\mathrm{V} + v)(\mathrm{P} + p) - (\mathrm{U} + u)(\mathrm{Q} + q)] = m\,[u\,\mathrm{Z_u} + w\,\mathrm{Z_w} + q\,\mathrm{Z_q} + \\
&\qquad\qquad \mathrm{Z_o} - g\cos(\theta' + \theta)\cos(\phi' + \phi)] \\
&\dot{p}\,\mathrm{A} - \dot{q}\,\mathrm{F} - \dot{r}\,\mathrm{E} - r\,h_2 + q\,h_3 = m\,[v\,\mathrm{L_v} + p\,\mathrm{L_p} + r\,\mathrm{L_r} + \mathrm{L_o}] \\
&\dot{q}\,\mathrm{B} - \dot{r}\,\mathrm{D} - \dot{p}\,\mathrm{F} - p\,h_3 + r\,h_1 = m\,[u\,\mathrm{M_u} + w\,\mathrm{M_w} + q\,\mathrm{M_q} + \mathrm{M_o}] \\
&\dot{r}\,\mathrm{C} - \dot{p}\,\mathrm{E} - \dot{q}\,\mathrm{D} - q\,h_1 + p\,h_2 = m\,[v\,\mathrm{N_v} + p\,\mathrm{N_p} + r\,\mathrm{N_r} + \mathrm{N_o}]
\end{aligned}\right\}\ \text{Formulæ 89}$$

By limiting the conditions to those occurring in steady flight in a straight line in the plane of symmetry $x\,O\,z$, this plane being vertical, these equations can be still further simplified. For such conditions

$$V = 0;\ \phi' = 0;\ \psi' = 0;\ P = Q = R = 0;\ D = F = 0$$

the dash attached to an angle being used to denote the angles for flight under such conditions.

The terms such as X_0, Y_0, Z_0, &c., are included in the conditions of steady motion. For equilibrium in steady flight X_0 and Z_0 are balanced by the thrust of the airscrew and force of gravity respectively, and since there is no side force on the machine the various moments are zero. For steady motion, therefore, when axis of machine is at an angle θ' to the direction of flight,

$$X_0 + g \sin \theta' = 0;\quad Z_0 - g \cos \theta' = 0;\quad Y_0 = 0;$$
$$L_0 = M_0 = N_0 = 0;\quad \theta = \phi = 0$$

Hence, neglecting small quantities of the second order, the equations of small oscillations reduce to

$$\left.\begin{aligned}
\dot{u} + Wq &= uX_u + wX_w + qX_q + \theta g \cos \theta' \\
\dot{v} + Ur - Wp &= vY_v + pY_p + rY_r - \phi g \cos \theta' \\
\dot{w} - Uq &= Z_u + wZ_w + qZ_q + \theta g \sin \theta' \\
\dot{p}A - \dot{r}E &= m\,[vL_v + pL_p + rL_r] \\
\dot{q}B &= m\,[uM_u + wM_w + qM_q] \\
\dot{r}C - \dot{p}E &= m\,[vN_v + pN_p + rN_r]
\end{aligned}\right\} \ldots \text{Formulæ 90.}$$

The oscillations being small, it can be assumed that the displacements are proportional to $e^{\lambda t}$, so that the rate of change of each of the quantities u, v, w, p, q, r, is proportional to

$$\lambda, \text{ or } \frac{du}{dt} = \dot{u} = \lambda u \text{ and so on.}$$

Also by a suitable choice of axes W can always be made zero, and the generality of the equations is not affected thereby.

Further, by writing the moments and products of inertia, represented by A, B, etc., in the form $m k_A^2$, $m k_B^2$, etc., where k_A, k_B, etc., represent the radii of gyration about the respective axes, it is possible to eliminate the mass of the machine from the equations, Formulæ 89.

The resulting equations can be divided into two groups representing the Longitudinal and the Lateral Oscillations respectively, and are best expressed in the form of two determinants, namely—

1. Longitudinal Oscillations.

$$\begin{vmatrix} \lambda - X_u \ , & - X_w \ , & - \lambda X_q - g \cos \theta' \\ - Z_u \ , & \lambda - Z_w \ , & - \lambda (U + Z_q) - g \sin \theta \\ - M_u \ , & - M_w \ , & \lambda (- M_q + \lambda k_B^2) \end{vmatrix} = 0$$

Formula 91.

2. Lateral Oscillations.

$$\begin{vmatrix} \lambda - Y_v \ , & g \cos \theta - \lambda Y_p \ , & \lambda (U - Y_r) + g \sin \theta' \\ - L_v \ , & \lambda (- L_p + \lambda k_A^2) \ , & - \lambda (L_r + \lambda k_E^2) \\ - N_v \ , & \lambda (- N_p - \lambda k_E^2) \ , & - \lambda (N_r - \lambda k_C^2) \end{vmatrix} = 0$$

.... Formula 92.

Bryan has shown that the solution of these equations can be written in the form

$$A \lambda^4 + B \lambda^3 + C \lambda^2 + D \lambda + E = 0$$
$$A_1 \lambda^4 + B_1 \lambda^3 + C_1 \lambda^2 + D_1 \lambda + E_1 = 0 \quad \text{Formula 93.}$$

For stability the quantity λ must be negative if real, or have its real part negative if it is complex, in which cases the amplitude of the oscillations diminish with time. The condition that the real roots and the real parts of imaginary roots of Formula 93 may be negative, is that the coefficients A, B, C, D, E, shall each be positive, and also that the quantity $BCD - AD^2 - B^2E$—generally known as Routh's Discriminant—shall be positive. In this manner Bairstow has derived the following values for the coefficients from Formulæ 91, 92.

Longitudinal Oscillations.

$$A = K_B^2$$

$$B = - [M_q + X_u k_B^2 + Z_w K_B^2]$$

$$C = \begin{vmatrix} Z_w \ , & U + Z_q \\ M_w \ , & M_q \end{vmatrix} + \begin{vmatrix} X_u \ , & X_q \\ M_u \ , & M_q \end{vmatrix} + k_B^2 \begin{vmatrix} X_u \ , & X_w \\ Z_u \ , & Z_w \end{vmatrix}$$

$$D = - \begin{vmatrix} X_u \ , & X_w \ , & X_q \\ Z_u \ , & Z_w \ , & U + Z_q \\ M_u \ , & M_w \ , & M_q \end{vmatrix} - g \begin{vmatrix} M_u \ , & - \sin \theta' \\ M_w \ , & \cos \theta \end{vmatrix}$$

$$E = - g \begin{vmatrix} X_u \ , & X_w \ , & \cos \theta' \\ Z_u \ , & Z_w \ , & \sin \theta' \\ M_u \ , & M_w \ , & \theta \end{vmatrix}$$

.... Formulæ 94.

LATERAL OSCILLATIONS.

$$A_1 = \begin{vmatrix} k_A^2, & -k_E^2 \\ -k_E^2, & k_C^2 \end{vmatrix}$$

$$B_1 = \begin{vmatrix} Y_v, & o, & o \\ L_v, & -k_A^2, & -k_E^2 \\ N_v, & k_E^2, & k_C^2 \end{vmatrix} - \begin{vmatrix} k_A^2, & L \\ -k_E^2, & N \end{vmatrix} - \begin{vmatrix} L_p, & -k_E^2 \\ N_p, & k_C^2 \end{vmatrix}$$

$$C_1 = \begin{vmatrix} Y_v, & Y_p, & o \\ L_v, & L_p, & -k_E^2 \\ N_v, & N_p, & k_C^2 \end{vmatrix} - \begin{vmatrix} Y_v, & o, & Y_r - U \\ L_v, & -k_A^2, & L_r \\ N_v, & k_E^2, & N_r \end{vmatrix} + \begin{vmatrix} L_p, & L_r \\ N_p, & N_r \end{vmatrix}$$

$$D_1 = - \begin{vmatrix} Y_v, & Y_p, & Y_r - U \\ L_v, & L_p, & L_r \\ N_v, & N_p, & N_r \end{vmatrix} + g\cos\theta' \begin{vmatrix} L_v, & -K_E^2 \\ N_v, & -K_C^2 \end{vmatrix} + g\sin\theta' \begin{vmatrix} L_v, & -k_A^2 \\ N_v, & k_E^2 \end{vmatrix}$$

$$E_1 = -g\cos\theta \begin{vmatrix} L_v, & L_r \\ N_v, & N_r \end{vmatrix} + g\sin\theta \begin{vmatrix} L_v, & L_p \\ N_v, & N_p \end{vmatrix} \quad \text{......... Formulæ 95.}$$

The application of these formulæ to the investigation of the stability of an aeroplane appears a formidable task, but it will be shown subsequently that several of the derivatives included in the above expressions are of minor importance and may be neglected. This results in much simpler expressions.

The Resistance and Rotary Derivatives.—Before proceeding to the solution of the biquadratic equations it is necessary to consider the manner in which the resistance derivatives depend upon the dimensions of a machine. Simple mathematical expressions can be deduced for most of these derivatives, enabling a much clearer conception to be formed as to their dependence upon the form of the machine. The experimental value of the derivatives for the model of a Bleriot monoplane constructed to a scale of one-twentieth full size, its shape and leading dimensions being shown in Fig. 234, was carried out by the N.P.L. The model experiments were carried out at a speed of 30 feet per second, while the normal speed of the prototype was 65 m.p.h. (95·4 f.p.s.). The weight of the actual machine was 1800 lbs.

To convert the model results to the full-size machine the following conversion factors were therefore used :—

$$\text{Force on machine} = \text{force on model} \times \left(\frac{95{\cdot}4}{30}\right)^2 \times 20^2$$

$$= 4040 \times \text{force on model}$$

$$\text{Moment on aeroplane} = \text{moment on model} \times \left(\frac{95{\cdot}4}{30}\right)^2 \times 20^3$$

$$= 80800 \times \text{moment on model}$$

It should be noted that the methods to be adopted in the investigation of the stability of any machine will be upon similar lines to those outlined here for the Bleriot monoplane. The various derivatives will be considered in turn and the method of their determination fully explained.

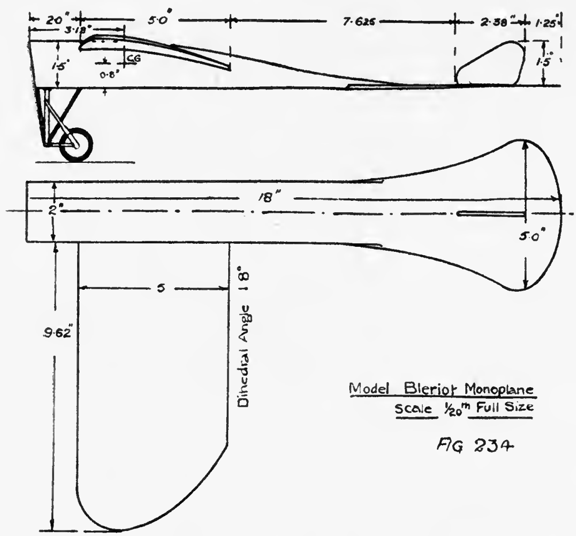

Model Bleriot Monoplane
Scale 1/20th Full Size

FIG 234

A. Derivatives affecting Longitudinal Stability.—X_u This is the rate of change of horizontal force with forward speed. Let the forward speed of the machine increase from 'U to U + u

It may here be pointed out that as the motion of the aeroplane is in the negative direction along the axis of X, the sign of U will always be negative in actual flight. It is also convenient to have an expression for wind velocity relative to the aeroplane, although it only varies from the velocity of the machine in its sign. For this purpose we shall use the symbol 'U, which, of course, is connected with U by the relation 'U = − U

The equilibrium forces other than those due to the airscrew vary as the square of the forward velocity, hence the horizontal force or drag $m\,X_o$ becomes

$$m\,X_o\left\{\frac{('U - u)^2}{'U^2}\right\} = m\,X_o\left(1 - \frac{2\,u}{'U}\right)$$

Differentiating this expression with respect to u, we get

$$\frac{d}{d\,u}\left(m\,X_o\left\{1 - \frac{2\,u}{'U}\right\}\right) = -\frac{2\,m\,X_o}{'U} = m\,X_u$$

whence $X_u = \dfrac{-2\,X_o}{'U}$ where X_o is the drag per unit mass.

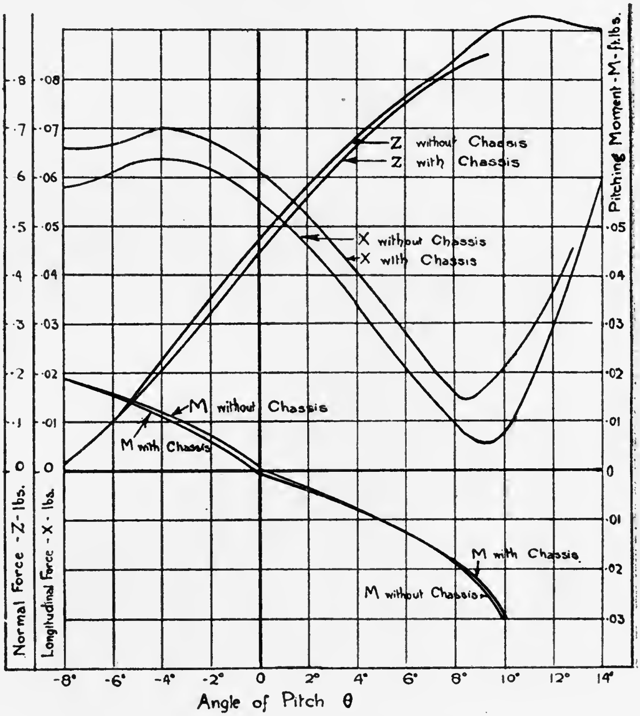

FIG. 235.—Forces and Moments on Model Bleriot-type Monoplane.

The experimental determination of X_o is carried out as follows: The model is supported in the wind channel, and measurements are made of the longitudinal force X—that is, the force along the airscrew axis—for varying angles of incidence.

The observations made upon the Bleriot model covered a range of pitch from -8° to $+14^\circ$, and are shown graphically in Fig. 235.

The value of X when the angle of pitch is zero is the required value of X_0 From Fig. 235 this is seen to be 0·062 lbs. for the Bleriot monoplane, and therefore it will be $4040 \times \cdot 062 = 250$ lbs. for the full-size machine. Consequently

$$X_u = \frac{2 \times 250}{-95 \cdot 4} \times \frac{32 \cdot 2}{1800}$$
$$= -0 \cdot 0935$$

Generally X_u may be expected to lie between $-0 \cdot 05$ and $-0 \cdot 25$.

X_w Variation of longitudinal force due to a normal velocity of the machine relative to the wind. The effect of a small upward velocity of the machine is to reduce the angle of incidence of the wings. If w be this small normal velocity, then the reduced angle of incidence

$$= \tan^{-1} \frac{w}{U}$$

This variation is equivalent to a small angle of pitch $d\theta$ away from the equilibrium position, and in the limit we may write

$$d\theta = \frac{w}{'U} \quad i.e., \; w = {'U}\, d\theta$$

whence since $\quad X_w = \dfrac{dX}{w}$ (from definition)

we have $\quad X_w = \dfrac{dX}{'U\, d\theta}$ where $d\theta$ is in radians

or $\quad = \dfrac{57 \cdot 3}{'U} \dfrac{dX}{d\theta}$ where $d\theta$ is in degrees

$dX/d\theta$ is the slope of a curve of X on a base of angles of pitch. and when this curve has been drawn its slope where θ is zero may be ascertained.

It is thus seen that X_w is proportional to the slope of the longitudinal force curve. Referring to the curves for the model given in Fig. 235, the value of the slope of the curve for X for zero angle of pitch is $-\cdot 0035$. For the full-size machine we therefore have

$$\frac{dX}{d\theta} = -4040 \times \cdot 0035 = -14 \cdot 12$$

$$X_w = \frac{57{\cdot}3}{-95{\cdot}4 \times 56} \times -14{\cdot}12 = 0{\cdot}152$$

Note $$56 = \frac{1800}{32{\cdot}2} = \text{mass of machine}$$

Generally X_w may be expected to lie between 0 and ·4.

Z_q The variation of longitudinal force due to pitching. This derivative cannot be traced to any definite part of the machine, but is apparently of small importance, and may be neglected in the stability equations.

Z_u The rate of change of normal force with forward velocity. In a similar manner to that adopted above for X_u, it can be shown that

$$Z_u = -\frac{2g\cos\theta'}{'U}$$

In horizontal flight Z_u may be expected to vary between $-1{\cdot}3$ and $-0{\cdot}4$, the higher value corresponding to a low speed.

Z_w The variation of the normal force due to a normal velocity of the machine relative to the wind. Exactly as in the case of X_w it can be shown that

$$Z_w = \frac{57{\cdot}3}{'U}\frac{dZ}{d\theta}$$

The value of $dZ/d\theta$ is obtained by measuring the air forces on the model normal to the airscrew for varying angles of pitch. Measurement of the slope of the curve of Z for zero pitch angle gives the required value. The normal force does not differ much from the lift of the machine for the usual range of flying angles.

For the Bleriot model the value of $dZ/d\theta$ for $\theta = 0$, as obtained from the curve shown in Fig. 235, is ·055. For the full-size machine

$$\frac{dZ}{d\theta} = 4040 \times {\cdot}055 = 222$$

whence $$Z_w = \frac{57{\cdot}3}{-95{\cdot}4 \times 56} \times 222 = -2{\cdot}43$$

Z_w is generally found to vary between $-1{\cdot}5$ and -4.5.

Z_q Variation of the normal force with pitching. The value of this derivative is not important, as the terms depending upon it in the stability equations are small. It can therefore be neglected.

M_u The rate of variation of pitching moment with variation of forward speed. Since there is no pitching moment upon the machine in steady flight the value of this derivative is zero.

M_w The variation of pitching moment with normal velocity. Similarly to X_w it can be shown that

$$M_w = \frac{57{\cdot}3}{U} \frac{dM}{d\theta}$$

$dM/d\theta$ being the slope of the pitching moment curve at zero angle of pitch. In order to determine this curve the model is suspended in the wind channel and the pitching moment observed for various angles of pitch. The curve of M for the model is shown in Fig. 235.

From this curve the value of the slope for zero pitch is found to be $-{\cdot}00255$, whence

$$M_w = \frac{57{\cdot}3 \times -{\cdot}00255 \times 80800}{-95{\cdot}4 \times 56}$$
$$= 2{\cdot}21$$

This moment is principally due to the action of the elevator and tail plane, modified by the couple due to movement of the centre of pressure of the main planes and by a couple due to the fin action of the body. Generally it is found to vary between 2 and 6 for horizontal flight.

M_q The variation of pitching moment with pitching. It is not possible to develop a simple expression for this derivative, and the method adopted for determining its value is to oscillate a model in the wind channel. The model is supported by a spindle passing through its centre of gravity and by means of a spring a slight angular displacement is communicated to the machine, which commences to oscillate about the position of equilibrium corresponding to the angle of attack. These oscillations are recorded photographically, and from a comparison of the damping with and without the wind the value of M_q can be evaluated. Its value is affected by the tail planes, body, and main planes, and for the average size of machines will vary from -100 to -300. For the Bleriot monoplane M_q was found to be -175.

B. Derivatives affecting Lateral Stability.—**Y_v The variation of lateral force with side slip.** This derivative is almost entirely due to the resistance of the side area of the body and fin, and may be expressed very simply in the form

$$Y_v = \frac{57 \cdot 3}{'U} \frac{dY}{d\psi}$$

where $dY/d\psi$ is the slope of the lateral force curve at zero angle of yaw. As the machine side-slips, the direction of the wind relative to it no longer acts along the axis of x, but has a small component along the axis of y. This component will set up a lateral force on the machine tending to make it yaw. The magnitude of this force must be determined by direct experiment, and then the value of Y_v can be calculated.

The experimental method is to support the model in the wind tunnel by means of a spindle attached to the balance arm and then to rotate the model through various angles of yaw from the symmetrical position, the angle of pitch being kept at zero. Proceeding in this manner the lateral force Y on the Bleriot model was determined, the results being shown in Fig. 236. It will be seen that Y is negative, thus indicating that its tendency is to oppose side-slipping. This naturally is the general case, but it should be noted that the lateral force due to certain parts, particularly the struts, increases the side-slipping. The lateral force becomes greater and greater as the side-slipping increases, an effect which makes for safety.

By measuring the slope of the curve of Y at the origin, the variation of lateral force per degree of yaw is determined. This is found to be $-\cdot 0025$ for the Bleriot model, whence

$$Y_v = -\frac{57 \cdot 3}{95 \cdot 4 \times 56} \times \cdot 0025 \times 4040$$
$$= -0 \cdot 108$$

Y_v may be expected to vary between $-0 \cdot 1$ to $-0 \cdot 4$

L_v Variation of rolling moment due to side slip. This can be expressed in the same manner as Y_v, namely,

$$L_v = \frac{57 \cdot 3}{'U} \frac{dL}{d\psi}$$

where $dL/d\psi$ is the slope of the curve of rolling moment at zero angle of yaw. The model is suspended in the wind channel and the rolling moment on the machine for various angles of yaw is observed. The results for the Bleriot model are shown in Fig. 236. The slope at the origin is seen to be $\cdot 0008$, whence

$$L_v = \frac{57 \cdot 3}{95 \cdot 4 \times 56} \times \cdot 0008 \times 80800$$
$$= 0 \cdot 70$$

The value of L_v varies from $0 \cdot 4$ to 5.

It is possible to develop a mathematical expression for the value of this derivative in a fairly simple manner, and as it is probable that mathematical expressions will be available for all

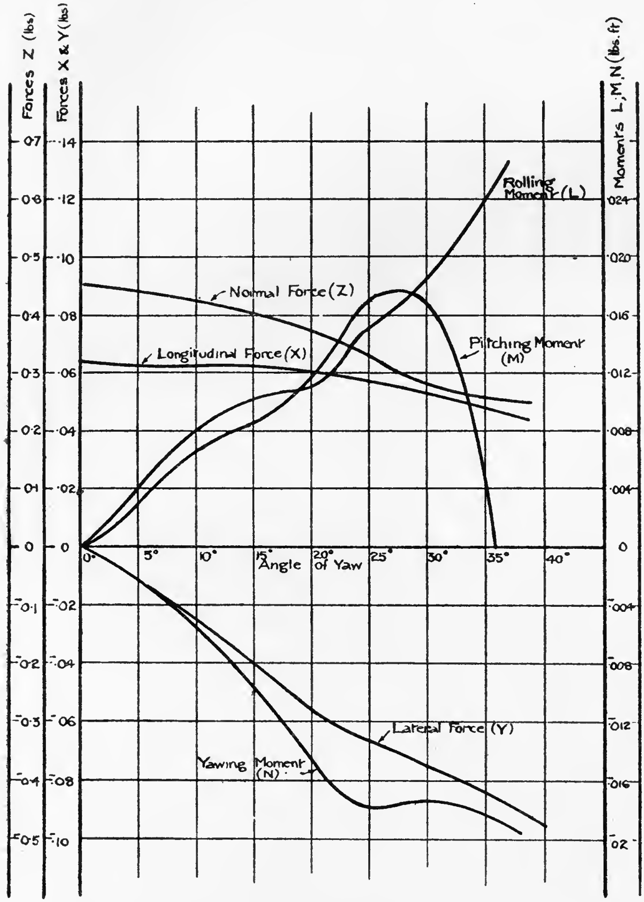

FIG. 236.—Forces and Moments on Model Bleriot-type Monoplane.

the derivatives in the near future, we outline below the necessary steps in developing such formulæ on a logical basis.

The damping of the rolling moment on a machine depends almost entirely upon the wings and tail plane. Let us consider the effect of each in turn.

Consider the wings of a machine as shown in Fig. 237. The dihedral angle is β as shown. Suppose that the machine is moving along the axis of x with a velocity U, and that a side gust strikes it with a velocity v. Then the direction of the relative wind will be along O P. The angle of incidence of the right-hand surface will be increased from i to $i + \delta i$; while that of the left-hand surface will be diminished by δi. From the geometry of the figure it will be seen that

$$\delta i = \pm \frac{v}{'U} \beta$$

This alteration in the angle of incidence of the wings will set up a moment on the machine tending to turn it about the axis of x.

Let $d K_y / d i$ be the slope of the Lift Incidence curve for the

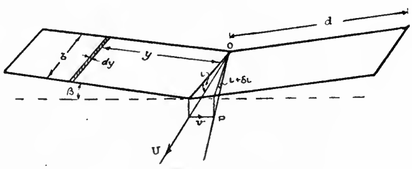

FIG. 237.

wing section used, then the increase of lift upon any element considered is

$$= \frac{\rho}{g} b \cdot dy \cdot \delta i \frac{d K_y}{d i} \cdot 'U^2$$

$$= \frac{\rho}{g} b \cdot dy \cdot v . 'U \cdot \beta \cdot \frac{d K_y}{d i}$$

and the moment of the element

$$= \frac{\rho}{g} b \cdot dy \cdot v \cdot 'U \cdot \beta \cdot \frac{d K_y}{d i} \cdot y$$

whence Total Moment

$$= \int_o^d \frac{\rho}{g} \cdot v \cdot \beta \cdot 'U \cdot \frac{d K_y}{d i} \cdot b \cdot y \, dy$$

$$= \tfrac{1}{2} m \cdot v \cdot L_v$$

whence, for wings of rectangular plan form

$$L_v = \frac{2 \rho}{g m} \beta \cdot 'U \cdot \frac{d K_y}{d i} \cdot \frac{b d^2}{2}$$

$$= \frac{\rho}{g m} \cdot 'U \cdot \beta \cdot \frac{d K_y}{d i} \cdot b d^2$$

In a similar manner L_v due to the tail

$$= \frac{\rho}{g\,m}\,'U\,\beta'\,\frac{d\,K_y'}{d\,i}\,b'\,d'^2$$

where β = dihedral of tail

$\frac{d\,K_y'}{d\,i}$ = slope of lift/incidence curve for tail

b' = chord of tail

d' = span of tail

The total value of the derivative L_v will be approximately the sum of these two expressions.

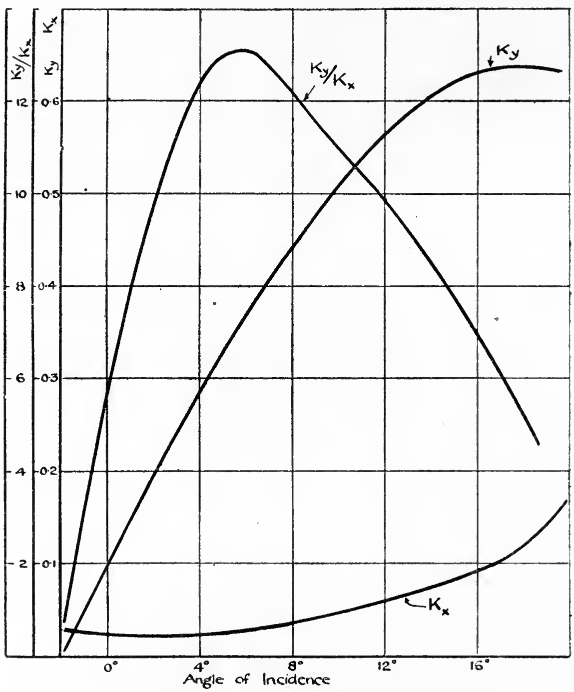

FIG. 238.—Characteristics of Bleriot Aerofoil.

It will be seen that the value is directly proportional to the dihedral angle of the planes, and since the 'end effect' causes a variation in $d\,K_y/d\,i$ at the wing tips, this effect must be taken into account if a strictly accurate result is to be obtained by the use of the above formulæ.

In applying these formulæ to the case of the Bleriot machine, it is necessary to know the characteristics of the wing section employed. These are shown in Fig. 238. The angle of incidence of the wings throughout the test was 6°, the dihedral angle is 1·8°

$$\text{whence} \quad L_v = \frac{\cdot 00237}{56} \times 95\cdot 4 \times 1\cdot 8 \times \cdot 045 \times \frac{5}{12} \times \left(\frac{9}{12}\right)^2 \times 20^3$$
$$= 0\cdot 62$$

The experimental value of L_v was 0·7

It will be observed that the span of the wings has been taken in the calculation as 9·0″ instead of the actual 9·7″ in order to allow for the variation in chord at the wing-tip; also that no term due to the tail plane has been added, owing to the fact that there is no dihedral angle on the tail. The body and the fin would have a slight effect upon the value of this derivative, and would account for the discrepancy shown.

N_v The variation of Yawing Moment due to Side-slip.—This derivative may be determined by suspending the model in the wind channel at zero angle of pitch and measuring the variation in yawing moment over a range of angles of yaw. From the resultant curve the value of N_v may be calculated from the relationship

$$N_v = \frac{57\cdot 3}{'U} \cdot \frac{dN}{d\psi}$$

The curve of yawing moment for the Bleriot model is shown in Fig. 236, from which curve the value of the slope for zero angle of yaw is found to be $-\cdot 0005$, whence

$$N_v = \frac{57\cdot 3}{95\cdot 4 \times 56} \times (-\cdot 0005 \times 80800) = -0\cdot 44$$

In general N_v varies from $-0\cdot 4$ to $-1\cdot 0$

A mathematical expression can also be deduced for N_v but whereas in the case of L_v the effect of the body and fins is very small in comparison with that of the wings, and can therefore be neglected for most cases, such is not the case with N_v, the fin surfaces having a very important effect upon the value of this derivative. The yawing moment due to side-slip depends primarily upon the body and fins, and its value is determined by the proportion of body and fin surface before and behind the C.G. The mathematical expression will therefore contain a term very similar to that due to the wing surfaces in L_v, together with terms in which the position of the fin surfaces relative to the C.G. is taken into account.

Y_p Variation of Lateral Force with Rolling.—The lateral force produced by rolling is principally due to the dihedral angle between the main planes, and is unimportant in the stability equations.

L_p The variation of Rolling Moment due to Rolling.—The value of this derivative depends almost entirely upon the wings, and can be calculated with sufficient accuracy from the results of the usual aerofoil tests in the manner shown below. This is the method most frequently adopted. A roll increases the angle of incidence of the falling wing and decreases that of the rising wing. Let p be the angular velocity of wings about the axis of x: then the increase in the angle of incidence due to this velocity (p)

$$= \delta i = \pm \frac{p\,y}{'U}$$

and increased lift on falling element

$$= \delta i \frac{d\,K_y}{d\,i} \cdot \frac{\rho}{g} b \,.\, d\,y \,.\, 'U^2$$

$$= p\,y \,.\, b \,.\, d\,y \,.\, \frac{\rho}{g} \,.\, 'U \,.\, \frac{d\,K_y}{d\,i}$$

Moment of element

$$= -\,p \,.\, y \,.\, b \,.\, dy \,.\, \frac{\rho}{g} \,.\, 'U \,.\, \frac{d\,K_y}{d\,i} \,.\, y$$

Total Moment $= \frac{1}{2}\, m \,.\, p \,.\, L_p$

$$= -\,p\frac{\rho}{g} \,.\, 'U \,.\, b \,.\, \frac{d\,K_y}{d\,i} \int_0^d y^2 \,.\, dy$$

That is, for wings of rectangular plan form

$$L_p = -\,\tfrac{2}{3}\,\frac{\rho}{g\,m} \,.\, 'U \,.\, \frac{d\,K_y}{d\,i} \,.\, b \,.\, d^3$$

The value of L_p will be considerably affected by 'End Effect,' and in order to obtain the most accurate results it is necessary to take this loss into account. The greater the aspect ratio of the wings the less important does this correction become.

For small machines L_p varies from -200 to -400, while for machines of 20,000 lbs. in weight its value approaches -2000.

An example of this is shown by applying formula to the case of the Bleriot machine. Then

$$L_p = -\,\frac{2}{3} \times \frac{\cdot 00237}{56} \times 95\cdot 4 \times \cdot 045 \times 57\cdot 3 \times \frac{5}{12} \times \left(\frac{9}{12}\right)^3 \times 20^4$$

$$= -\,195$$

The experimental value of the derivative was -167 and the discrepancy is largely due to the fact that no correction was made for 'end effect.' The aspect ratio of the Bleriot machine is low, and consequently there would be a considerable reduction in the average dK_y/di over the wing surface. Assuming the value of the lift coefficient to vary in accordance with a parabolic law over the outer section for a distance equal to the wing chord, the average value of K_y for the Bleriot wing surface will be approximately $0{\cdot}83 \times$ max. K_y. The value of the derivative L_p would now become $-195 \times 0{\cdot}83 = -162$, which is in very close agreement with the experimental value. A much more accurate method of taking into account 'end effect' is to solve the integral

$$\int \frac{dK_y}{di} by^2 \, dy$$

graphically, and to substitute the value thus obtained in the general formula. Such a method would of course necessitate an accurate knowledge of the variation of the lift coefficient over the whole span.

The experimental method of determining L_p is to mount the model of the machine upon the balance in such a manner that it is free to rotate about a horizontal axis. The model is oscillated by means of a spring against the damping present due to the wind forces and frictional losses in the apparatus for a period of from 20 to 40 seconds. The oscillations are photographically recorded for several wind speeds and provide a means of estimating the damping coefficient due to the relative wind, and this is the derivative required.

N_p The variation of Yawing Moment due to Rolling.—It has been seen that the value of L_p depends upon the slope of the lift curve for the wing section employed. It follows that the yawing moment due to rolling must depend chiefly upon the slope of the drag curve. The value of N_p may therefore be written

$$N_p = \frac{2}{3} \frac{\rho}{gm} \, 'U \frac{dK_x}{di} \cdot b d^3$$

The effect of the body and fins will be very small in most machines.

The ratio of the slopes of the Lift and Drag Curves at angles slightly greater than those giving maximum Lift/Drag is usually in the neighbourhood of 10, hence the value of N_p will be about one-tenth that of L_p at these angles. Also since the slope of the drag curve may become zero, the value of

N_p when the machine is flying at the angle of minimum drag of the wings must be zero. N_p is found to vary between 0 and 40 for small machines, and increases up to 300 in large machines.

The experimental determination of N_p is a somewhat difficult matter, the method adopted being similar to that used for the determination of L_r which will be described later. For the Bleriot machine the experimental value was 24.

Using the formula we have

$$\frac{dK_x}{di} = \cdot005 \times 57\cdot3$$

whence

$$N_p = \frac{2}{3} \times \frac{\cdot00237}{56} \times 95\cdot4 \times \cdot005 \times 57\cdot3 \times \frac{5}{12} \times \left(\frac{9}{12}\right)^3 \times 20^4$$
$$= 22$$

Y_r Variation of Lateral Force due to Yawing.—This derivative has practically no effect upon the stability of an aeroplane, and its value can therefore be neglected.

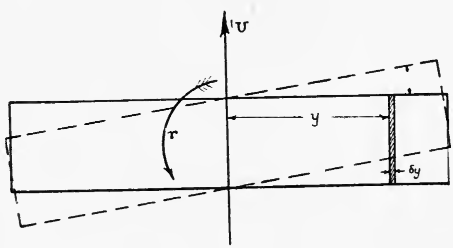

FIG. 239.

L_r Variation of Rolling Moment due to Yawing.—The value of this derivative is largely dependent upon the wing surfaces of a machine. Its experimental determination is not easy, as it is necessary to produce a forced oscillation of known magnitude about one axis of rotation, and to measure the corresponding oscillation about a second axis of rotation perpendicular to the first. The model is arranged to be free to rotate about the axes of roll and yaw, the rolling motion being controlled by a stiff spring so that the model can oscillate in sympathy with an impressed force of suitable period. An oscillation is then set up about the axis of yaw, and the period of oscillation about the axis of roll is adjusted until resonance is obtained; the required data can then be deduced from a knowledge of the amplitude of the oscillations. The experimental value for L_r for the Bleriot model is found to be 54.

MATHEMATICAL DERIVATION OF L_r—In yawing, the outer wing of the machine is moving faster than the normal speed of the machine, while the inner wing is moving slower. This will cause an increased lift on the outer wing and a diminished lift on the inner wing. If r be the angular velocity of yaw, then the increased speed of any element distant y from the axis of $z = d'U = ry$ (see Fig. 239), and the increased lift on this element

$$= K_y \frac{\rho}{g} \left\{ (U' + du)^2 - U^2 \right\} b \,.\, dy$$

$$= K_y \frac{\rho}{g} 2 \,.\, 'U\, ry\, b \,.\, dy$$

and Moment of Element

$$= K_y \frac{\rho}{g} 2 \,.\, 'U\, ry^2\, b \,.\, dy$$

whence $\frac{1}{2} m r L_r = K_y \frac{2\rho}{g} 'U\, r \int_0^d b \,.\, y^2 \,.\, dy$

That is, for wings of rectangular plan form

$$L_r = \frac{4}{3} \frac{\rho}{gm} K_y 'U\, b\, d^3$$

For the Bleriot machine the calculated value of L_r

$$= \frac{4}{3} \times \frac{\cdot 00237}{56} \times 0{\cdot}38 \times 95{\cdot}4 \times \frac{5}{12} \times \left(\frac{9}{12}\right)^3 \times 20^4$$

$= 58$ as compared with the experimental value 54.

L_r varies from 50 in small machines to 600 in large machines.

N_r Variation of Yawing Moment due to Yawing.—This derivative depends upon wings, body, and fins, and its value must therefore be determined experimentally. The method adopted is similar to that used in the determination of L_p. Its value may be expected to vary between -20 and -100. For the Bleriot machine its value was found to be -31.

Application of Derivatives to Stability Equations.—From this enumeration and consideration of the derivatives it is now necessary to turn to the question of the method of their application to the stability equations.

A. LONGITUDINAL STABILITY (Period of Oscillation).—Bairstow has shown, from an examination of the relative numerical values of the coefficients in the biquadratic equation, that it can be factorised to a first approximation and expressed in the form

$$\left[\lambda^2 + \frac{B}{A}\lambda + \frac{C}{A}\right]\left[\lambda^2 + \left(\frac{D}{C} - \frac{B\,E}{C^2}\right)\lambda + \frac{E}{C}\right] = 0 \quad \ldots\ldots \text{ Formula 96}$$

This approximation is sufficiently accurate if

$$\frac{B}{C} \text{ and } \frac{A\,E}{C^2} \text{ are less than } \frac{1}{20}$$

$$\text{and } A\,D \text{ is less than } \frac{B\,C}{20}$$

These conditions are generally satisfied by modern machines, but should be checked before proceeding further with an analysis of stability.

In Formula 96 the first factor represents a short oscillation which in most aeroplanes rapidly dies out and is not of much importance. The second factor represents a relatively long oscillation, involving an undulating path with changes in pitch, forward speed, and attitude. It is termed by Lanchester the "phugoid oscillation." These long oscillations should diminish in amplitude with time, in which case the motion is stable and the aeroplane will return to its original flight attitude if temporarily deviated therefrom by accidental causes. The motion is unstable if the amplitude increases with time.

Eliminating the various resistance derivatives of negligible value, the formula for the coefficients in longitudinal stability (Formula 94) can be written.

$$\begin{aligned}
A &= k_b^2 \\
B &= -\left(M_q + X_u k_b^2 + Z_w k_b^2\right) \\
C &= Z_w M_q - M_w U + X_u M_q + k_b^2\left(X_u Z_w - X_w Z_u\right) \\
D &= -X_u M_w U + Z_u M_q X_w - X_u Z_w M_q \\
E &= -g M_w Z_u \qquad \ldots\ldots\ldots\ldots \text{ Formula 94 } (a)
\end{aligned}$$

By substitution of the values of the various derivatives in the above formula, the periodic time of each oscillation is easily determined. A very short oscillation indicates great statical stability, and the machine will very rapidly resume its normal flying attitude. Such a machine would be very uncomfortable for flying purposes on account of the violent changes in motion. It is preferable that an aeroplane should have a heavily damped oscillation of long period, such that the resumption of the normal flying attitude takes place very gradually. The aim in design should therefore be to ensure that the righting moments on the machine are just sufficient to give static stability, and to depend upon large damping surfaces for dynamic stability. It is probable that longitudinal stability may be secured at all speeds by the use of a sufficiently large tail plane.

Longitudinal Stability of the Bleriot Machine.—Collecting together the various quantities and the values of the derivatives affecting the longitudinal motion of this machine, we have

$m = 56$	$X_w = 0{\cdot}152$
$k_b = 5$ feet	$Z_w = -2{\cdot}43$
$X_u = -0{\cdot}935$	$M_w = 2{\cdot}21$
$Z_u = -0{\cdot}672$	$M_q = -175$

The values of the coefficients are therefore

$$A = 5^2 = 25$$

$$B = -(-175 + -0{\cdot}0935 \times 25 + -2{\cdot}43 \times 25) = 236$$

$$C = (-2{\cdot}43 \times -175) - (2{\cdot}21 \times -95{\cdot}4) + (-0{\cdot}0935 \times -175) + 25(-0{\cdot}0935 \times -2{\cdot}43 - 0{\cdot}152 \times -{\cdot}672) = 636$$

$$D = (0{\cdot}0935 \times 2{\cdot}21 \times -95{\cdot}4) + (-0{\cdot}672 \times -175 \times 0{\cdot}152) - (-0{\cdot}0935 \times -2{\cdot}43 \times -175) = 77$$

$$E = -32{\cdot}2 \times 2{\cdot}21 \times -0{\cdot}672 = 48$$

Substituting these values in Routh's Discriminant

$$236 \times 636 \times 77 - 25 \times 77^2 - 236^2 \times 48 = 8{\cdot}7 \times 10^6$$

Since all the coefficients and Routh's Discriminant are positive, the aeroplane is longitudinally stable.

The periodic time of the short oscillation is determined from the first factor of Formula 96.

Substituting the values obtained above

$$\lambda^2 + \frac{236}{25}\lambda + \frac{636}{25} = 0$$

that is $\lambda^2 + 9{\cdot}44\lambda + 25{\cdot}4 = 0$

whence $\lambda = -4{\cdot}72 \pm 1{\cdot}76i$

The imaginary roots indicate an oscillation of periodic time

$$= \frac{2\pi}{1{\cdot}76} = 3{\cdot}6 \text{ seconds approximately}$$

and the time to damp 50%

$$= \frac{0{\cdot}69}{4{\cdot}72} \text{ seconds} = 0{\cdot}15 \text{ seconds.}$$

The periodic time of the long oscillation is determined from the second factor of Formula 96.

Substituting the values obtained above

$$\lambda^2 + \left(\frac{76}{636} - \frac{236 \times 48}{636^2}\right)\lambda + \frac{48}{636} = 0$$

or $$\lambda^2 + 0{\cdot}092\,\lambda + 0{\cdot}0754 = 0$$

whence $$\lambda = -\,0{\cdot}046 \pm 0{\cdot}271\,i$$

The period of the longitudinal oscillation is therefore

$$\frac{2\,\pi}{0{\cdot}271} = 23 \text{ seconds}$$

and the disturbance is reduced to half its value in

$$\frac{0{\cdot}69}{0{\cdot}046} \text{ seconds, that is in about 15 seconds.}$$

The mathematical treatment given in the foregoing paragraphs has been extended by the N.P.L. to show the motion of this aeroplane during recovery from gusts and movements of the controls. Fig. 240 shows the disturbed longitudinal motion due to a single horizontal gust. As a result, the velocity of the aeroplane relative to the air is increased by a small amount, u_0. This increase rapidly dies away, and after 5 seconds becomes zero; the velocity goes on decreasing for a further 5 seconds, reaching its minimum value at the end of 10 seconds. This velocity then increases again for a period of about 10 seconds before commencing to diminish again. The changes appear to follow a periodic curve of rapidly decreasing amplitude, such as would be obtained, for example, from the projection of a logarithmic spiral, and after about 50 seconds are completely damped out. The change of velocity of the machine normal to the air is w, and, as will be seen from Fig. 240, this commences from zero, reaches a maximum value of about $\cdot 2\,u$, and then dies away rapidly in the same manner as u. Curves for q the angular velocity of the machine (shown dotted), and for θ the angle of pitch, are also shown to a greatly enlarged scale. It will be seen that the pitch angle increases for about 5 seconds and then diminishes again, being finally brought to zero through a series of periodic changes of decreasing amplitude and of 22 seconds period.

The corresponding case in practice arises when the machine is struck by a horizontal gust. The lift on the wings will be momentarily increased and the machine will begin to climb; that is, there will be a component of velocity w normal to the direction of flight. The nose of the machine will be inclined upwards; that is, an angular velocity q is set up, and the angle of incidence of the wings is increased by an amount θ. The result of the gust, however, will be to reduce the velocity of the machine, and after it has passed the lift on the wings will be insufficient to support the machine. It therefore commences to

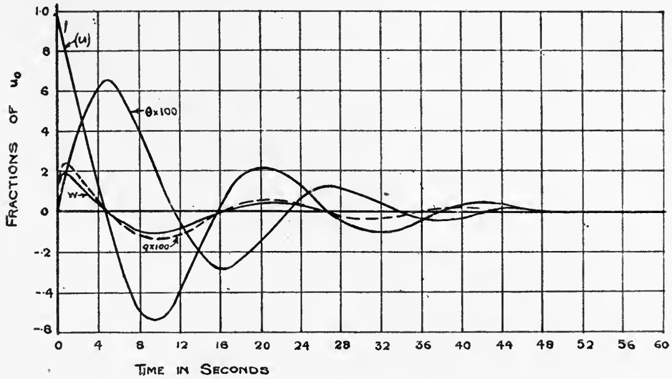

FIG. 240.—Disturbed Longitudinal Motion of an Aeroplane (Single horizontal gust).

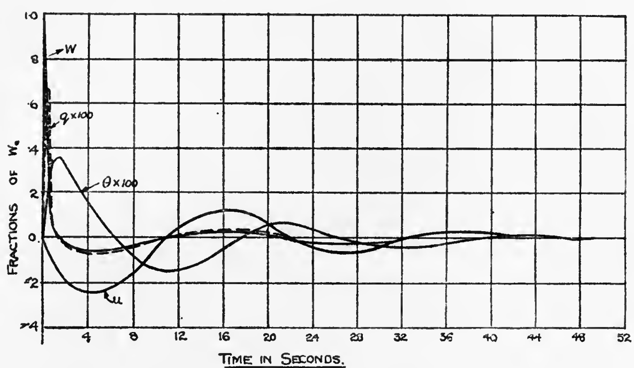

FIG. 241.—Disturbed Longitudinal Motion of an Aeroplane (Single downward gust).

fall, and in so doing picks up speed again. On account of its momentum, however, its velocity increases to a greater extent than is required for equilibrium, and the machine will then flatten out and commence to climb again, the cycle of operations being repeated until the oscillation dies away through the damping out, owing to the action of the control surfaces. The motion is therefore seen to be stable, and the machine settles down to its original speed relative to the wind in less than a minute.

A second curve, Fig. 241, was prepared to show the effect of a downward gust upon the machine. By combining the results of these two diagrams, it is possible to find the effect of a steady gust of wind striking the machine in any direction in the plane of symmetry.

Recent investigations upon the stability of full-size machines by the use of cinematography, show that the mathematical theory is borne out with considerable accuracy in practice.

B. Lateral Stability.—The factorisation of the biquadratic equation for lateral stability as deduced by Bairstow is

$$\left(\lambda + \frac{E'}{D'}\right)\left(\lambda + \frac{(B')^2 - A'C'}{A'B'}\right)\left[\lambda^2 + \left(\frac{C'}{B'} - \frac{E'}{D'}\right)\lambda + \frac{B'D'}{(B')^2 - A'C'}\right] = 0$$

Formula 97

which approximation is sufficiently accurate if

$$\frac{E'}{B'} \text{ and } \frac{E'}{D'} \text{ are less than } \frac{1}{20}$$

$$\text{and } B'D' - (C')^2 \text{ is less than } \frac{(C')^2}{20}$$

The value of the coefficients for lateral stability in horizontal flight given in Formulæ 95 be can reduced to the simpler expressions

$$\begin{aligned}
A' &= k_A^2 k_C^2 \\
B' &= -Y_v (L_p N_r - N_p L_r) + L_p k_C^2 + N_r k_A^2 \\
C' &= Y_v (L_p k_C^2 + N_r k_A^2) - U_0 N_v k_A^2 + L_p N_r - N_p L_r \\
D' &= U_0 (L_v N_p - L_p N_v) - Y_v (L_p N_r - N_p L_r) \\
&\quad + g (L_v k_C^2 - N_v k_A^2) \\
E' &= -g (L_v N_r - N_v L_r)
\end{aligned}$$

.... Formulæ 95 (*a*)

By far the most important item in the biquadratic (Formula 97) is the first factor, namely, $(\lambda + \frac{E'}{D'}) = 0$. If the machine be stable this factor represents a subsidence the amplitude of which will be reduced 50% in $\dfrac{0{\cdot}69}{\frac{E'}{D'}}$ seconds. If E′ and D′ be of opposite sign, instability will arise, and for present-day machines the criterion that E′ is positive is the most important consideration for lateral stability, and is also the most difficult condition to obtain. In order that E′ may be positive, it will be seen from the signs of the various derivatives that numerically L_v/N_v

should be greater than L_r/N_r. The physical explanation of this result is comparatively easy to understand. L_v and L_r are the rolling moments due to side-slip and yawing respectively, the former, as will be seen from the mathematical expression, being dependent on the dihedral angle, and the latter on the increased lift of the outer wing when turning. A side-slip inwards tends to reduce the banking whilst the turn tends to increase it, and instability occurs when the latter becomes the greater. L_v can be increased by making the dihedral angle greater, but L_r is difficult to control.

The derivatives N_v and N_r depend upon the relative rates of side-slipping and turning of the body surface and rudder area. N_v can be reduced by using a small rudder, but this has obviously the disadvantage of reducing the control, and would tend to produce a form of instability known as 'spin,' in which the machine will rotate about a vertical axis through its centre of gravity. Too large a fin area will produce instability of a different and more dangerous kind. This is shown mathematically by N_v assuming a large negative value, and this will make E' negative. The physical explanation is as follows.

Suppose the machine to be accidentally banked. It commences to move in a circular path, the axis of the body no longer lying along the direction of flight. This introduces a large lateral force if the rear fin surface is great, and the body will be swung round and tend to coincide with the direction of flight. This will involve a still greater velocity of the outer wing, and the increased lift obtained thereby will further increase the banking. The large fin area continuously operating therefore continually reduces the radius of the turn, and at the same time the lift on the wings will be constantly diminishing, so that the machine will be gradually falling. A continuation of these conditions leads directly into the dangerous motion known as the 'spiral nose dive,' and a machine liable to such motion is said to be spirally unstable.

In order to avoid spiral instability it is necessary that the arrangement of fin surfaces is such that when the machine side-slips to one side it will bank suitably to make a turn in the opposite direction. This will cause it to resume its normal attitude. [Such an effect may be produced by having the major portion of the fin surface, including the side area of the body, above the C.G. of the machine.]

From the preceding paragraph it will be seen that the fin surface of a machine must be within certain definite limits if instability is to be avoided, and it is in this connection that the mathematical analysis will be of increasing value.

The readiest means of producing stability occurs in the changes which can be made in the value of N_r and this can be increased without affecting N_v by putting equal areas before and behind the C.G., a part played to some extent by the fuselage of most machines.

The second factor $\lambda + \frac{(B')^2 - A'C'}{A'B'} = 0$ represents for stability a subsidence of which the amplitude is reduced 50% in $\frac{\cdot 69 \, A'B'}{(B')^2 - A'C'}$ seconds, and for instability to occur $\frac{(B')^2 - A'C'}{A'B'}$ must be negative. None of the quantities involved in A′, B′, C′ is liable to vary in such a way as to render this expression negative for ordinary conditions of flight, and the equation represents a rolling of the aeroplane, which is heavily damped by the wing surfaces. In the case of a stalled machine, however, this motion would lead to trouble, since the damping effect produced by the increased lift on the downward-moving wing will no longer operate. Under such circumstances a movement of the wing flaps will no longer produce any righting moment.

The third factor may be written approximately

$$\left[\lambda^2 + \frac{C'}{B'}\lambda + \left(\frac{C'}{B'}\right)^2\right] = 0$$

and the motion represents a damped oscillation of period

$$2\pi\sqrt{\frac{4\,B'}{3\,C'}}$$

and damping $\frac{C'}{2\,B'}$

The third oscillation consists of a combined yawing and rolling motion, and for stability the amount of fin surface above the C.G. should not be excessive, while there should be sufficient fin surface on the tail. It will be seen that these requirements clash with those for spiral stability, but it is possible by a careful adjustment of the surfaces to satisfy both conditions.

Lateral Stability of the Bleriot Model.—Applying the equations of motion to the case of the Bleriot Model, its lateral stability may be investigated. The derivatives concerned are—

$Y_v = -0{\cdot}108$	$N_p = -0{\cdot}44$
$L_v = 0{\cdot}7$	$L_p = 167$
$N_p = 24$	$L_r = 54$
$N_r = -31$	

The radii of gyration of a machine can be calculated from the scale drawings in the manner indicated for a streamline strut in Chapter IV., and in the case of the Bleriot were found to be

$$k_A \text{ (radius of gyration about axis of roll)} = 5'$$
$$k_C \text{ (radius of gyration about axis of yaw)} = 6'$$

Substituting these values in the stability equation, the values of the coefficients are found to be

A′ is 900; B′ is 6780; C′ is 5580; D′ is 6640; E′ is − 68

whence Routh's discriminant

$$= B'C'D' - A'D'^2 - B'^2 E'$$
$$= 21{\cdot}5 \times 10^{10}$$

The coefficient of E′ being negative, the machine is laterally unstable.

Considering the first factor of the equation, we have

$$p = -E'/D' = -(-68/6640) = {\cdot}0102$$

As p is positive, the motion is not oscillatory, and the amplitude will increase and double itself in time,

$$= 0{\cdot}69/{\cdot}0102 = 68 \text{ seconds.}$$

Considering the second factor, we have

$$p = -6{\cdot}71$$

This represents a steadily damped motion, which will be reduced to half its value in

$$0{\cdot}69/6{\cdot}71 = 0{\cdot}1 \text{ seconds.}$$

The third factor of the equation becomes

$$p^2 + 0{\cdot}833\,p + 1{\cdot}10 = 0$$

and the roots are

$$p = -0{\cdot}416 \pm 0{\cdot}963\,i$$

The period of oscillation will be

$$\frac{2\pi}{0{\cdot}963} = 6{\cdot}5 \text{ seconds}$$

and the amplitude will be reduced to one-half in

$$0{\cdot}69/0{\cdot}416 = 1{\cdot}65 \text{ seconds.}$$

We thus see that the machine under consideration is spirally unstable, which is shown by the fact that the coefficient E′ is negative, that is, L_v/N_v is less numerically than L_r/N_r Reference to the mathematical expressions for these derivatives will show that in order to eliminate the spiral instability it is necessary to have

L_v large, that is a good dihedral.
N_v small, that is a smaller rudder.

The other two derivatives are difficult to control, but N_r may be increased by adding equal fin areas in front of and behind the centre of gravity of the machine, and this will not affect the value of N_v

A graphical representation of this lateral or asymmetric motion, prepared upon the same lines as for the longitudinal motion, is shown in Figs. 242, 243. Since this lateral motion is unstable, they differ essentially from those shown for the longitu-

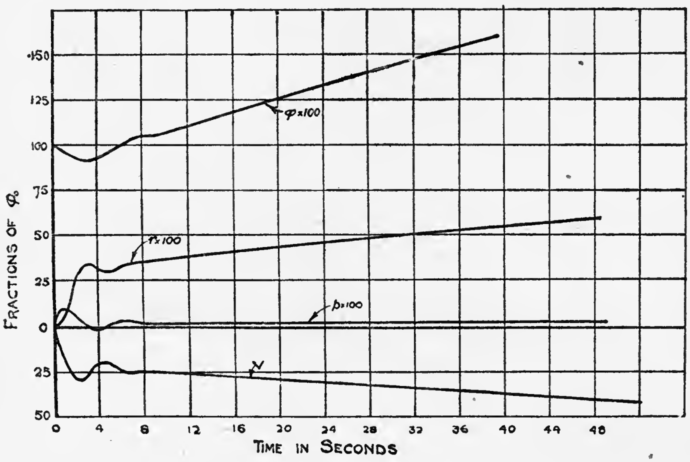

FIG. 242.—Disturbed Lateral Motion of an Aeroplane.

dinal motion. Fig. 242 shows the effect of suddenly banking the machine through an angle ϕ. It will be seen that after a slight subsidence the angle of bank increases continuously, and after 40 seconds exceeds its original value by more than 60 per cent. At the same time the velocity of side-slip (v) also increases rapidly in a negative direction. The machine therefore turns to the right, the angle of bank together with the velocity of side-slip increasing, and the machine falls with increasing speed.

Fig. 243 shows the effect of a side wind v'' striking the machine on the left-hand side. The sideways motion is very rapidly damped down, but after about seven seconds commences

TO INCREASE.

to increase again very gradually, and unless the controls are altered this velocity of side-slip will continue to increase. The velocity of roll (p) grows very rapidly at first, but after two or three oscillations is reduced almost to zero before commencing a gradual increase, which will necessitate an alteration of the controls if it is to be checked.

Longitudinal Stability of a Biplane.—A more recent investigation of the longitudinal stability of a machine was carried out at the Massachusetts Institute of Technology by Hunsaker, and is described in the U.S.A. Advisory Committee Report for 1914. The machine was a Curtiss Biplane, and the

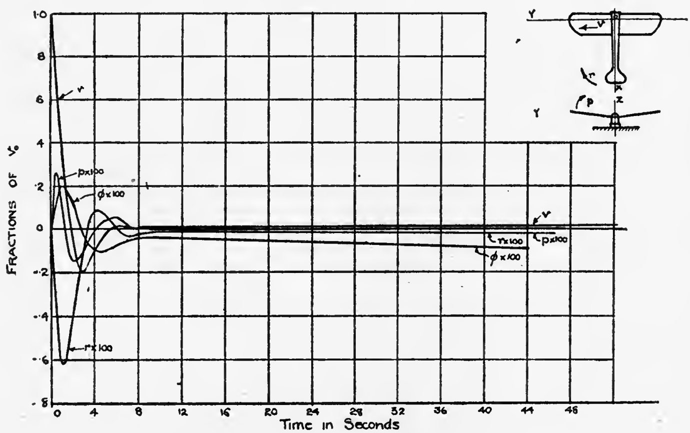

FIG. 243.—Disturbed Lateral Motion of an Aeroplane.

model which is shown in Fig. 244 (a b c) was made one-twenty-fourth full size, and geometrically similar to its prototype.

The leading dimensions of this machine are as follows :—

Weight, 1800 lbs.	Span, 36 ft.
Total wing area, 384 sq. ft.	Chord, 5 ft. 3 ins.
Area of tail, 23 sq ft.	Gap, 5 ft. 3 ins.
Area of elevator, 19 sq. ft.	Length of body, 26 ft.
Area of rudder, 7·8 sq. ft.	

The model was mounted on the balance, with its wings in the vertical plane, and the Lift, Drag, and Pitching Moment were measured for various angles of wing chord to the wind.

These results are exhibited graphically in Fig. 245, the forces being given direct in lbs., and the moments in lbs. inches. The wind velocity was 30 m.p.h.

The axes of reference are assumed fixed in the aeroplane

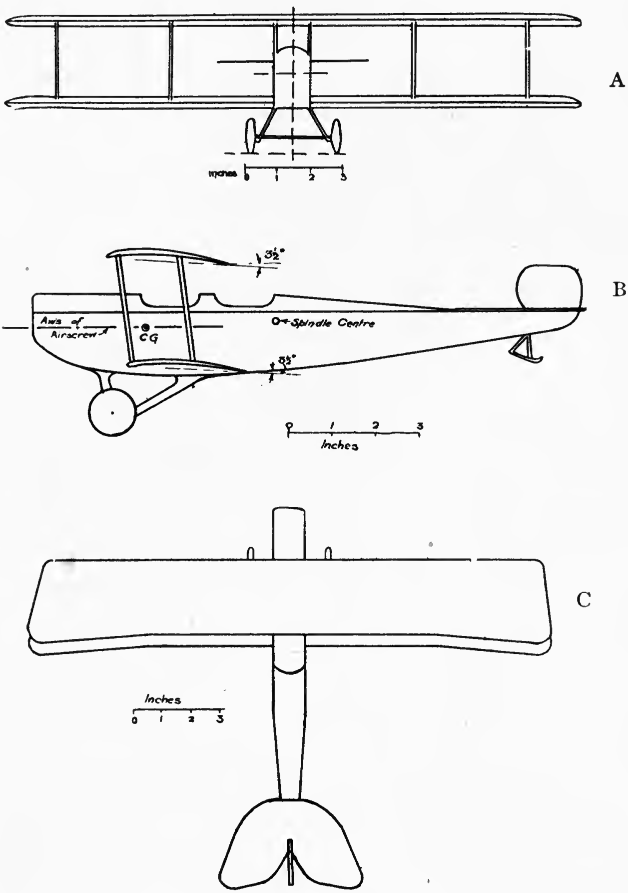

Fig. 244.—Model Curtis Biplane.

and moving with it in space, with the origin at the centre of gravity. For steady horizontal flight at a given attitude the axis of 'z' is vertical, and the axis of 'x' is horizontal. Angles of pitch departing from the normal flying attitude will be denoted according to the table by θ. For equilibrium θ is, of course, zero.

At high speed (79 m.p.h.) the axis of 'x' was horizontal,

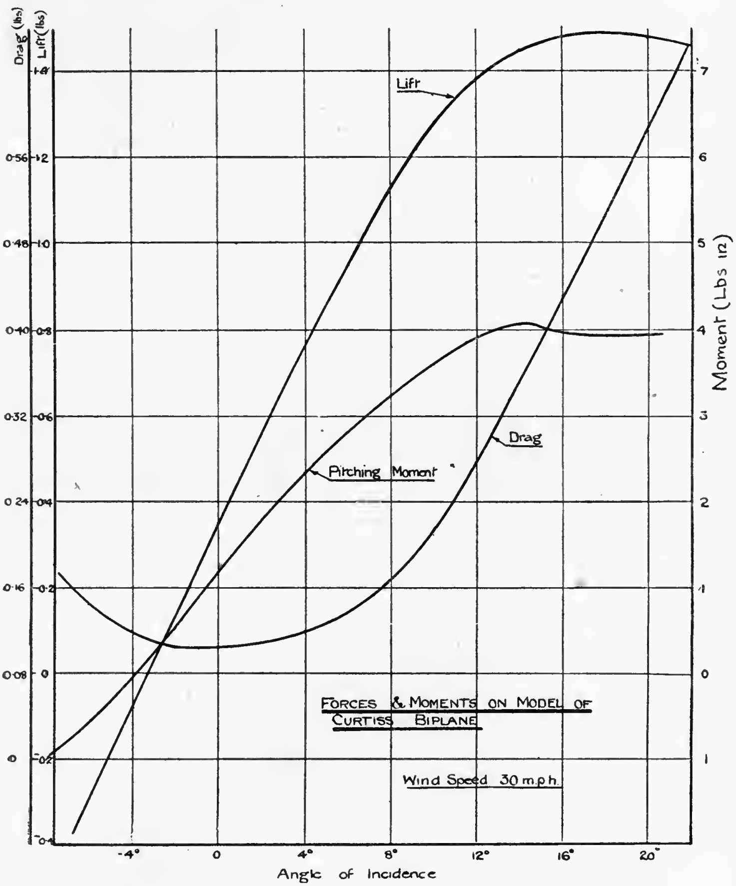

FIG. 245.—Forces and Moments on Model of Curtis Biplane.

and made an angle of 1° with the wing chord; while at low speed (45 m.p.h.), with the axis of 'x' still horizontal, this axis made an angle of 12° with the chord. The axes are fixed by the equilibrium conditions for flight, and differ for each normal flying attitude

It was found convenient for wind-tunnel purposes to measure the lift and drag about axes always vertical and horizontal in space. To transform these axes to those re-

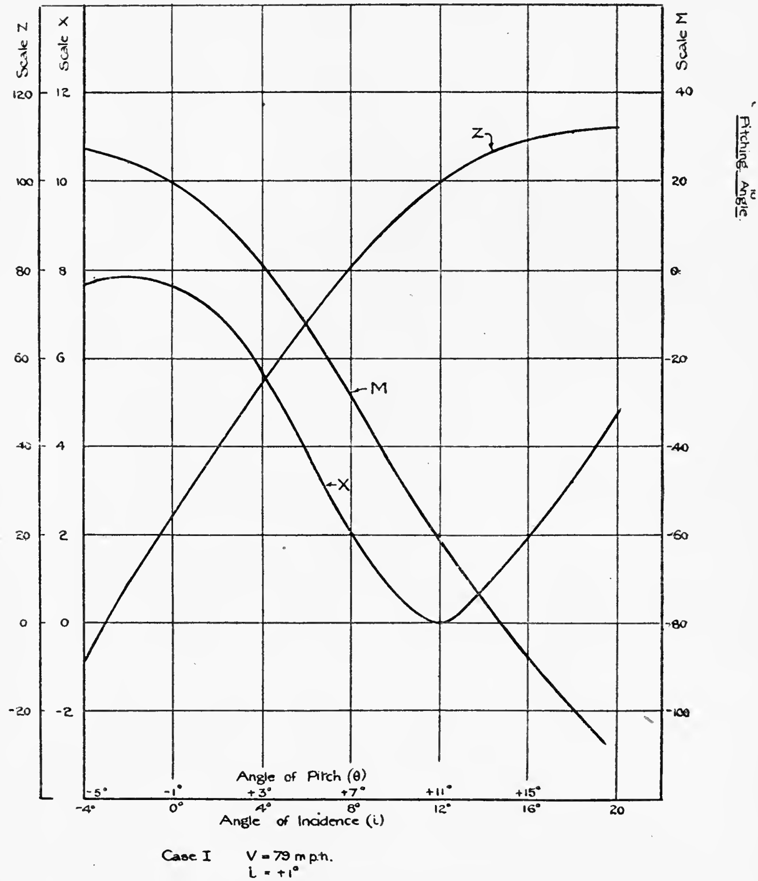

FIG. 246.—Forces and Moments on Model of Curtis Biplane.

quired for stability investigation the following relationships are used:

$$m\,Z = L \cos\theta + D \sin\theta$$
$$m\,X = D \cos\theta - L \sin\theta$$

By the use of these formulæ and reference to Fig. 245, Tables XLVII. and XLVIII. were calculated.

TABLE XLVII.—(CASE I.)

Speed, 79 m.p.h. Angle of attack (i) 1°.

i	θ	L	D	Z	X
− 4	− 5	− 0·08	·115	− 6·4	7·7
0	− 1	·35	·102	24·9	7·76
4	3	·765	·118	54·9	5·6
8	7	1·13	·165	81·0	1·9
12	11	1·39	·270	100·0	− ·7
16	15	1·48	·428	109·0	− 2·05

TABLE XLVIII.—(CASE II.)

Speed, 45 m.p.h. Angle of attack (i) 12°.

i	θ	L	D	Z	X
8	− 4	1·13	·165	26·1	5·68
10	− 2	1·28	·21	29·6	5·83
12	0	1·39	·27	32·4	6·29
14	2	1·45	·348	34·0	6·92
16	4	1·48	·428	35·2	7·56

These results are shown graphed in Figs. 246 and 247 From these curves the values of

$$\frac{dX}{d\theta} \quad \frac{dZ}{d\theta} \quad \frac{dM}{d\theta} \quad \text{where } \theta = 0$$

are read off, and the values are then inserted in the formulæ for derivatives X_w, Z_w and M_w

Case I.—

$$X_w = \frac{57 \cdot 3}{U} \frac{dX}{d\theta}$$
$$= \frac{57 \cdot 3 \times - \cdot 65}{- 115 \cdot 5 \times 2}$$
$$= \cdot 162$$

Note that U is negative, as explained previously.

$$Z_w = \frac{57 \cdot 3}{U} \frac{dZ}{d\theta}$$
$$= \frac{57 \cdot 3 \times 31}{- 115 \cdot 5 \times 4}$$
$$= - 3 \cdot 95$$

$$M_w = \frac{57{\cdot}3}{U}\frac{dM}{d\theta}$$
$$= \frac{57{\cdot}3 \times -14}{-115{\cdot}5 \times 4}$$
$$= 1{\cdot}74$$
$$X_u = \frac{2 \times \text{Drag}}{mU}$$
$$= \frac{2 \times {\cdot}104 \times 24^2 \times (V/30)^2}{32 \times -115{\cdot}5}$$
$$= {\cdot}128$$
$$Z_u = \frac{2 \times g}{U}$$
$$= \frac{2 \times 32{\cdot}2}{-115{\cdot}5}$$
$$= -{\cdot}557$$

By experiment the value of M_q was found to be -150.

The radius of gyration of the machine about the axis of pitch was experimentally found to be 5·8 feet, which gives us at once the value of k_b.

By substituting in the various values of the derivatives the values of the coefficients are found to be

$A = {\cdot}5{\cdot}8^2 = 34$

$B = -(-150 - {\cdot}128 \times 34 - 3{\cdot}95 \times 34)$
$= 289$

$C = 3{\cdot}95 \times 150 + 1{\cdot}74 \times 115{\cdot}5 + 34({\cdot}12 \times 3{\cdot}95 + {\cdot}162 \times {\cdot}557)$
$= 834$

$D = {\cdot}128 \times 1{\cdot}74 \times 113{\cdot}5 + {\cdot}557 \times 150 \times {\cdot}162 + {\cdot}128 \times 3{\cdot}95 \times 150$
$= 115$

$E = 32{\cdot}2 \times 1{\cdot}74 \times {\cdot}557$
31

Substituting these values in Routh's Discriminant we get that the discriminant

$$= 289 \times 834 \times 115 - 34 \times 115^2 - 289^2 \times 31$$
$$= 18 \times 10^6$$

Since Routh's Discriminant and all the coefficients are positive, the machine will be longitudinally stable at the speed considered, namely 79 m.p.h.

The short oscillation

$$= \lambda^2 + 8{\cdot}5\lambda + 24{\cdot}5 = 0$$

whence $\lambda = -4{\cdot}25 \pm 2{\cdot}54\,i$

The period = $P = 2\pi/2{\cdot}54 = 2{\cdot}5$ seconds

The time to damp out 50°/。

$$= 0{\cdot}69/4{\cdot}25 = {\cdot}16 \text{ seconds}$$

The long oscillation

$$= \lambda^2 + {\cdot}125\lambda + {\cdot}0374 = 0$$

whence $p = -{\cdot}063 \pm {\cdot}183\,i$

The period of this long oscillation

$$= P' = 34{\cdot}3 \text{ seconds}$$

and time to damp 50 °/。

$$= t = 10{\cdot}8 \text{ seconds}$$

The small oscillations are thus seen to be unimportant while the long oscillations are strongly damped. The aeroplane should therefore be very steady at this speed.

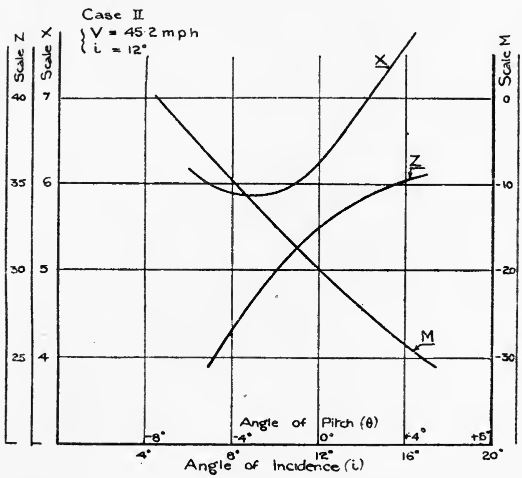

FIG. 247.—Forces and Moments on Model Curtis Biplane.

Case II.—Speed, 45 m.p.h (66 f.p.s.); incidence, 12°. Proceeding in a similar manner, the values of the derivatives at this speed are found to be

$$X_u = -{\cdot}189 \qquad Z_u = {\cdot}972 \qquad M_w = 2{\cdot}15$$

$$X_w = -{\cdot}236 \qquad Z_w = {\cdot}736 \qquad M_q = -106$$

and the values of the coefficients are

$$A = 34 \qquad C = 243 \qquad E = 67{\cdot}2$$
$$B = 137{\cdot}5 \qquad D = 17{\cdot}4$$

whence Routh's Discriminant

$$= 137{\cdot}5 \times 243 \times 17{\cdot}4 - 34 \times 17{\cdot}4^2 - 137{\cdot}5^2 \times 67{\cdot}2$$
$$= -7 \times 10^5$$

which being negative indicates that the machine will be unstable at this speed.

The short oscillation

$$= \lambda^2 + 4{\cdot}04\lambda + 7{\cdot}14 = 0$$

whence $\lambda = -2{\cdot}02 \pm 1{\cdot}75\,i$

and the period $= 3{\cdot}59$ seconds

and the time to damp out 50°/₀ = 0·342 seconds

The long oscillation

$$= \lambda^2 - 0{\cdot}085\lambda + {\cdot}276 = 0$$

whence $\lambda = 0{\cdot}043 \pm {\cdot}524\,i$

and the period $= 12{\cdot}0$ seconds

and the time to double amplitude = 16 seconds.

The machine is thus seen to be unstable at a speed of 45 m.p.h., and it is essential that the pilot should keep a firm hold on his elevator control.

CHAPTER XI.

Design of the Control Surfaces.

Controllability and Stability.—The question of the relation between the control and stabilising surfaces was briefly considered in the preceding chapter on stability, and it was stated that the degree of controllability of a machine was determined generally by the duties for which it was to be used. For fighting purposes it is necessary that the machine should answer very quickly to the controls, and hence its static stability must be small; whereas in the case of a large commercial machine with which long journeys must be undertaken, the static stability can with great advantage be considerably increased.

In general it is preferable to keep the static stability as low as possible, and to obtain dynamic stability by using large wings and stabilising surfaces. The problem of static stability can be considered as under. In nearly all the modern machines the stabilising surfaces are:

(*a*) The Tail Plane and Elevator.
(*b*) The Rudder and Fin.

Of these the elevator is also the control surface for longitudinal flight and the rudder for directional flight, while ailerons or wing-flaps control the rolling motion of a machine.

The Tail Plane and Elevator.—The tail plane and elevator in an aeroplane of normal design are essentially those members which are intended to give the machine that longitudinal stability which the wing surface alone lacks. It will be remembered from Chapter III. that over the range of normal flying angles the C.P. of an aerofoil moves forward as its angle to the wind direction is increased. The resulting effect upon the machine is illustrated by the diagrams in Fig. 248.

If it be assumed, as shown in case (*b*), that at that particular instant the line of lift passes through the C.G. of the machine, then there will be no moment upon the machine, and consequently no load upon the tail. If, however, a upward gust of wind strikes the machine, the angle of incidence of the wings to the resultant wind direction will for a very short time be reduced, the C.P. will move backward to the position shown in case (*a*), and a pitching moment will be set up upon the machine which must be counterbalanced by the tail plane surface if equilibrium is to be restored. Similarly in case (*c*), if the angle of incidence relative to the wind direction has been temporarily increased, then a stalling moment will be set up and the tail plane will be called upon to produce a righting moment.

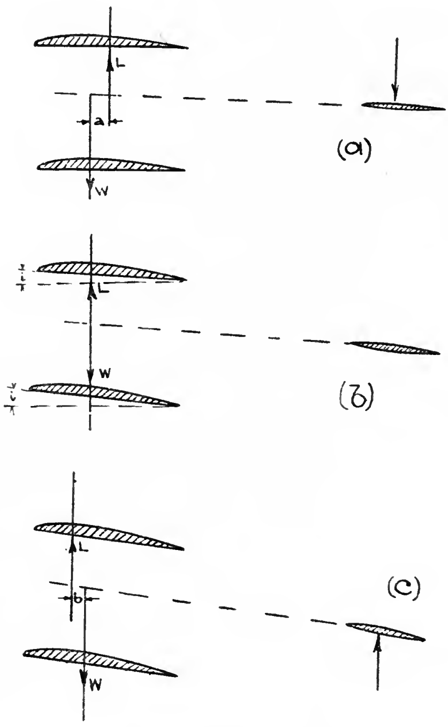

FIG. 248.—Direction of Load on the Tail Plane.

Moreover, by reference to the fundamental equation (Formula 1), it will be seen that

$$\text{Normal force} = K_y \frac{\rho}{g} A V^2$$

$$= W \cos i \qquad \text{...... ... for case } (b)$$

or

$$V = \sqrt{\frac{W \cos i}{K_y \frac{\rho}{g} A}}$$

from which it follows that the attitude of the machine for equilibrium varies with the speed. The righting moment to be exerted by the tail plane and elevator will therefore depend upon the speed at which the machine is flying. Conversely, an adjustment of the tail plane and elevator will alter the pitching moment upon the machine, and so lead to an alteration in its attitude and speed.

A further deduction from the preceding paragraph is that the successful design of a tail plane for a particular machine will depend largely upon its speed range; for it is easy to see that, in a fast machine with a wide speed range, if the tail plane is sufficiently large for the upper limits of speed, then it will be inadequate for slow flight unless more weight and head resistance are allotted to it than would in most cases be advisable. In the absence of an easy method of making a variable-area tail—the real solution to the above difficulty—some compromise must be made in practice.

In certain cases it is sometimes found necessary to displace the line of thrust of the airscrew so that it no longer passes through the C.G. of the machine. The unbalanced moment resulting will need to be corrected, and this duty also falls to the lot of the tail plane. It will thus be seen that a large number of factors enter into the design of the tail plane and elevator.

The duty of the tail plane does not require it to be cambered, a flat plane being all that is necessary, though some streamlining at the leading and trailing edges may help towards lessening resistance. A streamlined tail plane can generally be designed that will offer no extra head resistance, but will afford greater thickness and greater strength, combined with better accommodation for a strong hinge-spar for the elevator lift. The tail, moreover, need normally exert no lifting force; but this non-lifting or 'floating' tail will only be so at certain angles—that is, at certain speeds of the machine.

When the disposition of the tail plane is such that the tail exerts a downward force, it is found that the stability of a machine is increased, and this arrangement is frequently adopted in modern design. Should, however, the line of thrust of the airscrew fall below the horizontal line through the C.G. of the machine, an upward load on the tail is necessary. Either arrangement causes an increase of gliding angle, and may, if carried to excess, decrease the useful angular range of the machine, owing to the proximity in one direction of the critical angle. In considering the tail plane as a stabilising surface the area of the elevators should be added to the area of the fixed part. If the fixed part is symmetrical in section, the elevators, in the case of a floating tail, will exert zero lift when in the same straight line. A floating tail is not at 0° angle of incidence to the flight path, but positively inclined at some less angle than the wings owing to the downwash, the rate of change of momentum vertically of which is the lift for horizontal flight. Again, the drag of the whole machine is the rate of change of momentum horizontally of the disturbed air. Thus the tail operates in a region where the air is in a state of motion downwards and forwards relative to the surrounding

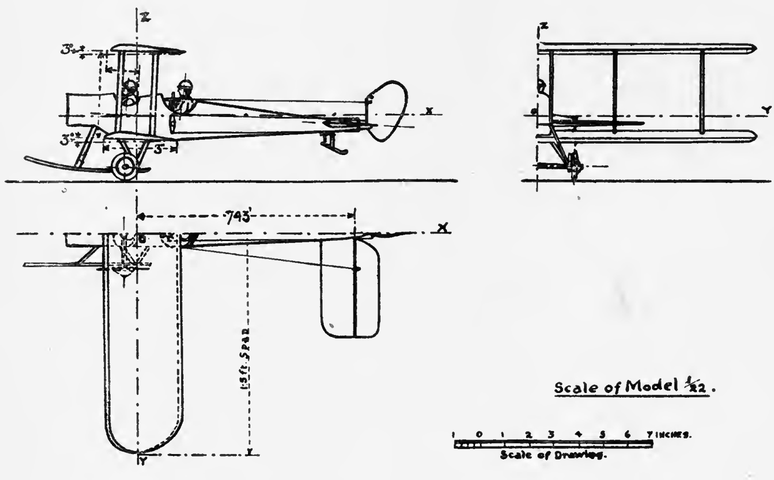

FIG. 249.—Model of B.E. 2 Biplane.

atmosphere in gliding flight. It has been found experimentally that the angle of downwash from the main planes is approximately one-half the angle of incidence of the main planes measured from the angle of no lift. This will give the position of the tail plane when 'floating.'

Reduction of Effectiveness of the Tail Plane due to Wash from the Main Planes.—A method of investigating the effect of the downwash of the main wing surface upon the moment exerted by the tail plane was to determine experimentally the pitching moment upon the model of a complete machine for a large number of angles of pitch. The tail plane was then removed from the model, and a similar series of experiments conducted in order to determine the pitching moment on the model without its tail plane. Measurements were then made of the longitudinal and normal forces upon the tail plane and elevator alone at various angles of incidence. A comparison between the results obtained in these three cases enables the effect of the downwash of the main planes to be determined. From an investigation of this nature the N.P.L. found that both the normal force and pitching moment for the tail plane in its normal position are reduced approximately to one-half the values they show when the tail plane is tested separately—that is, interference due to the downwash from the main planes reduces the slope of the pitching-moment curve in this ratio, and consequently the necessary area of the tail

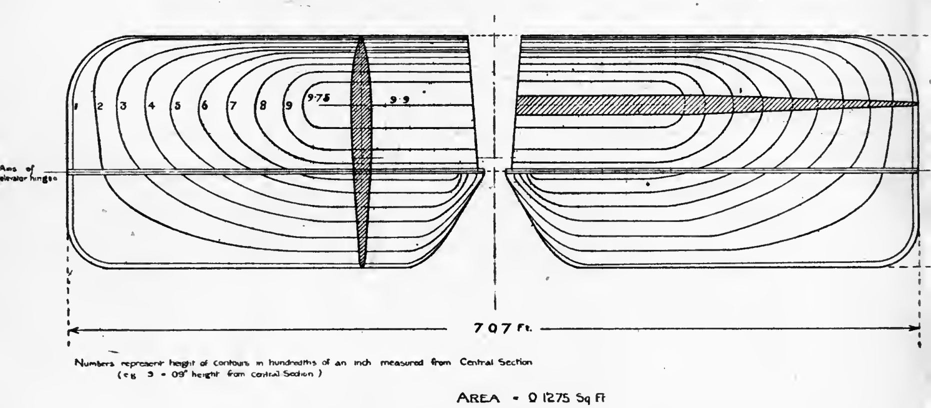

FIG. 250.—Contoured Plan and Sections for Tail Plane 3.

plane is double that to be otherwise expected. These results are of such practical importance that they are reproduced here for the purposes of reference. A scale drawing of the model is shown in Fig 249, from which it will be seen that it is of the B.E. type. Experiments were carried out with a series of different tail planes, the results obtained being of a very similar character, those given here referring to the tail-plane section designated T.P. 3, the contours of which are shown in Fig. 250. As will be seen, this section is very similar to that adopted in general practice upon modern machines.

The effect upon the value of the pitching moment on the model of a change in the position of its C.G. was also observed, and the indications showed that in order to obtain a machine of reasonable longitudinal stability without unduly increasing the length of the fuselage and the area of the tail plane it is necessary to have a down load on the tail. The position of the C.G. of the model relative to the chord in the experiments herewith recorded was at ·41 of the chord from the leading edge. In the first series of tests the longitudinal force, normal force, and pitching moment were measured for the complete machine for angles of pitch ranging from $-23°$ to $+17°$ at a wind speed of 40 feet per second. These tests were repeated with the elevator

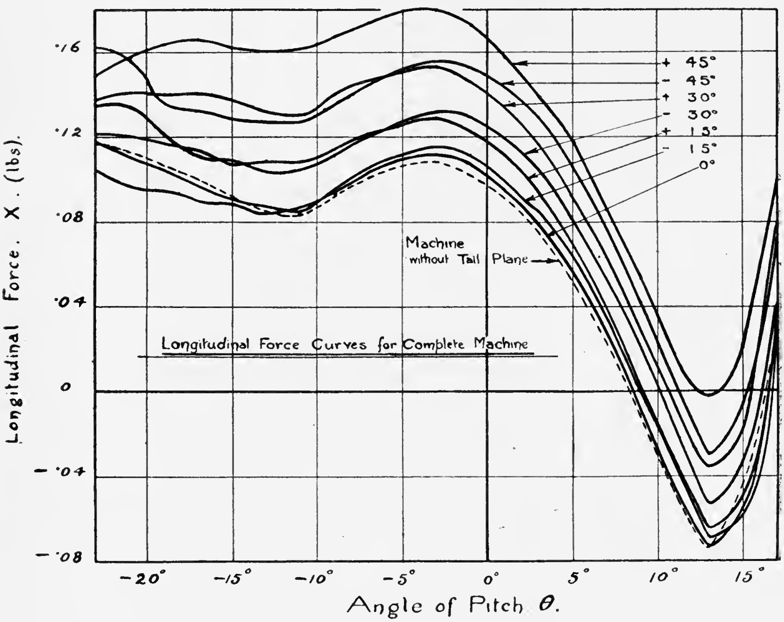

FIG. 251.—Longitudinal Force Curves for Complete Machine.

set at inclinations of $-45°$. $-30°$, $-15°$, $-10°$, $-5°$, $0°$, $+5°$, $+10°$, $+15°$, $+30°$, $+45°$, respectively. The curves corresponding to inclination $\pm 5°$, $\pm 10°$ follow the general lines of $0°$ and $\pm 15°$, and are omitted for the sake of clearness. The inclination of the elevator is taken to be positive when it is turned downwards. The tail plane and elevator were then removed from the model and tested separately over the same angular range at the same wind velocity. The results are shown graphically in Figs. 251–259.

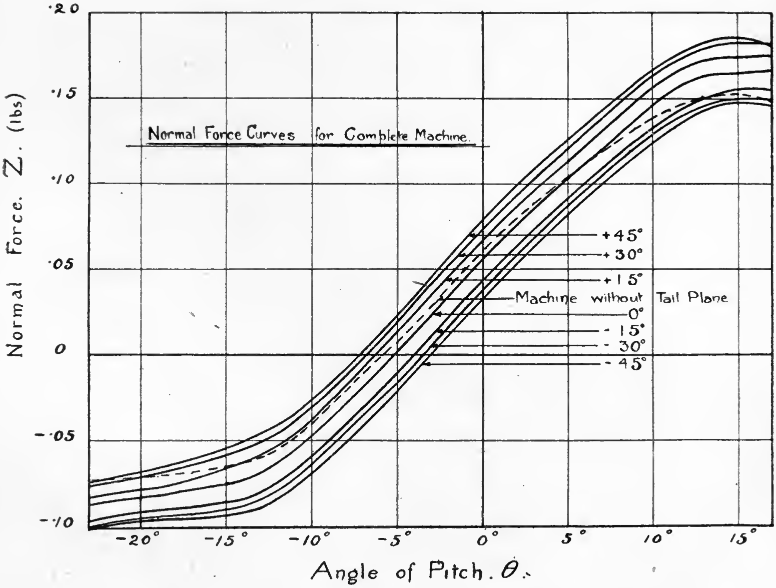

FIG. 252.—Normal Force Curves for Complete Machine.

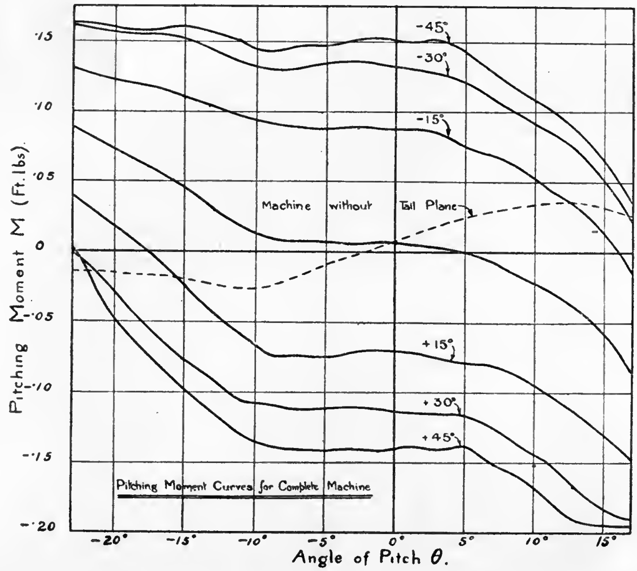

FIG. 253.—Pitching Moment Curves for Complete Machine.

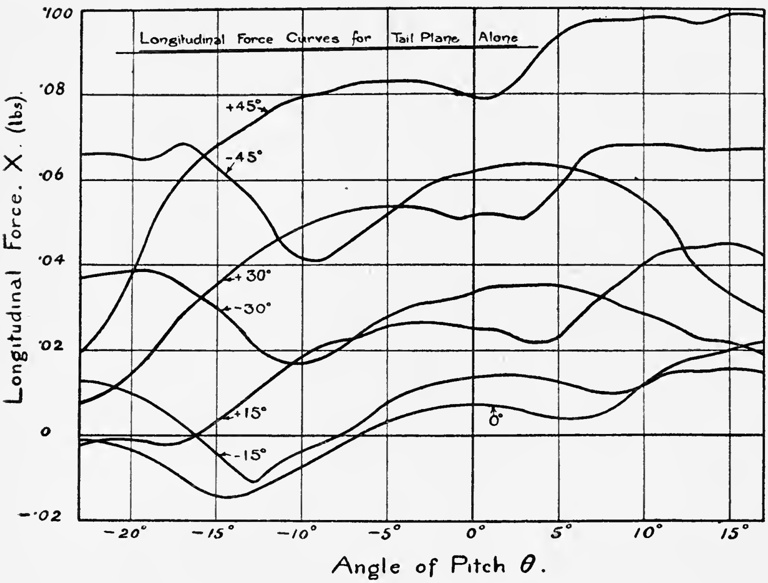

FIG. 254.—Longitudinal Force Curves for Tail Plane Alone.

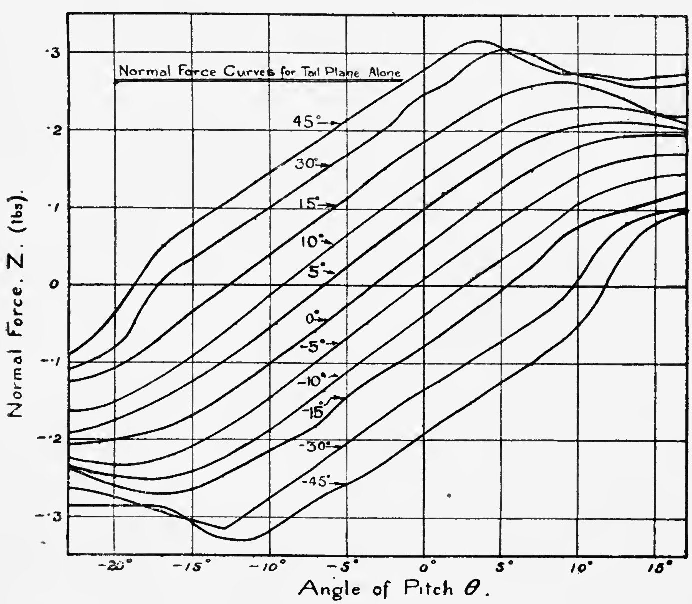

FIG. 255.—Normal Force Curves for Tail Plane Alone.

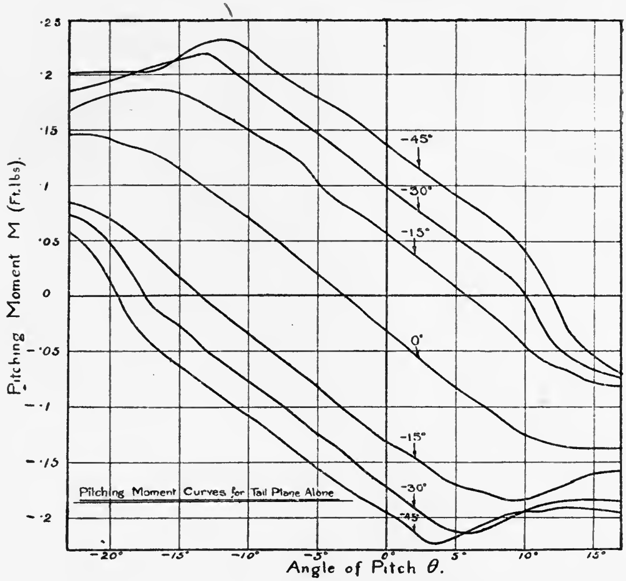

FIG. 256.—Pitching Moment Curves for Tail Plane Alone.

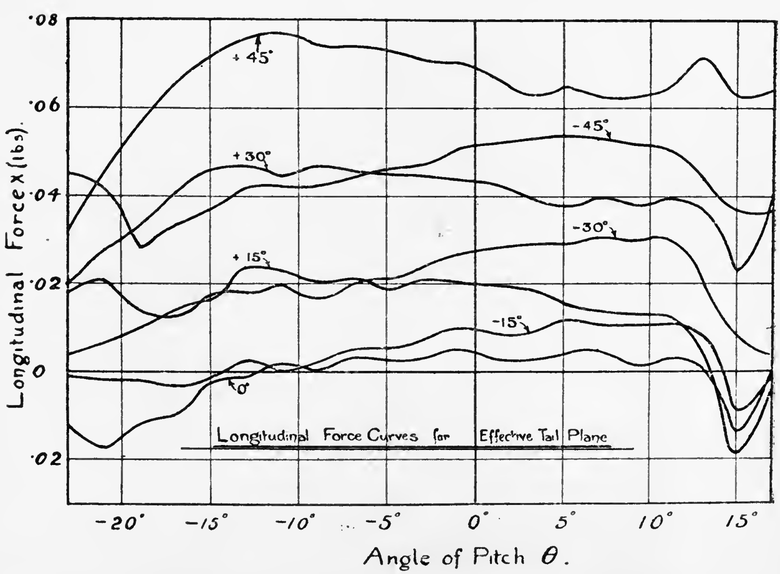

FIG. 257.—Longitudinal Force Curves for Effective Tail Plane.

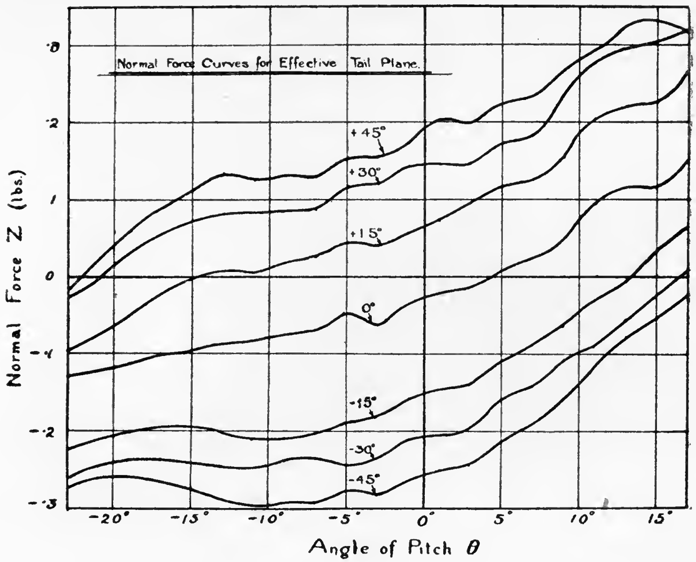

FIG. 258.—Normal Force Curves for Effective Tail Plane.

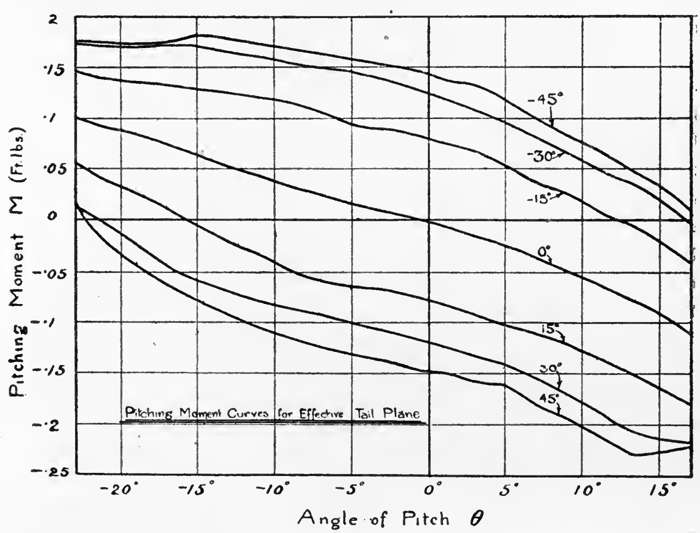

FIG. 259.—Pitching Moment Curves for Effective Tail Plane.

The Elevator.—From the preceding remarks it will have been observed that the function of the elevator is of a twofold nature:

(i.) To regulate the speed of flight;

(ii.) To correct any variation in the attitude of the machine which may arise from the action of gusts or other causes.

It will be apparent that the position of the elevator required to maintain equilibrium when the machine is flying at its top speed will generally be quite different from that required when stalling. In addition it is necessary to have a range of positions in order to correct for disturbances at these speeds, hence the maintenance of the elevator in such attitudes involves a considerable strain upon the pilot. Two methods have been adopted in practice to reduce this strain, namely:

(*a*) The elevator is balanced by means of an extension projecting in front of the hinge spar, or by placing the hinges close to the C.P. of the elevator load.

(*b*) The function of the elevator in regulating the speed of flight may be transferred to the tail unit as a whole by making the latter adjustable. This method is now common practice on most machines, and reference will be made to it subsequently.

The elevators are fitted to the rear of the tail plane, and elevate or depress the tail of the machine as actuated by the pilot. They do not provide the whole of the lifting force themselves by virtue of their inclination to the wind, but are very much more efficient because they induce a lift of like sign in the surface to which they are fixed, owing to the fact that when rotated from their mean position they form, with the fixed surface, a kind of rudimentary aerofoil. The centre of pressure of this lift which forms the controlling force is not, therefore, necessarily upon the elevators at all: it may be somewhat in front of the hinge spur. This does not mean that the force required to be exerted by the pilot for turning the elevators is in any way diminished; the distance between the C.P. of that part of the total force which is distributed over the elevator itself from the hinge spar must be considered separately in this connection. The form of elevator which will be easiest to turn will be that variety which is not hinged to a fixed surface; the total area being sufficient to provide for the stabilising moments required. In this case the pivot should be arranged at the mean position of C.P. travel during rotation.

Owing to the intervention of the critical angle, it is of no use to arrange for a greater angle of incidence being given to the elevators than 25°, and even this amount may well be reduced. The elevators are likely to be called upon most when the tail plane itself is already set, by reason of the general inclination of the machine, at a large angle in the direction in which rotation of the elevators is carried out by the pilot. A considerably smaller rotation than 25° will then bring about the critical angle. In some cases it may be necessary to guard against this, as a considerable fall in lift may occur from over-rotation, a calamity the cause of which the pilot in time of emergency cannot be called upon to appreciate. For this reason the rotation may well be limited to between 15 and 20 degrees. It is of course better to provide ample surface with small rotation than a meagre surface with a large rotation. There is one great danger which must be guarded against, namely, that the pilot should be able to exert too great a control longitudinally. This is of fundamental importance in the case of nose-diving; in which case, as we have already seen in Chapter V., the wings may be very greatly overstressed if the pilot should intentionally or accidentally flatten out the nose-dive too quickly.

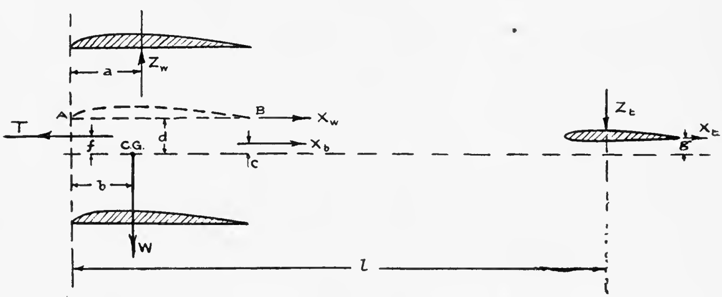

FIG. 260.—Equilibrium of a Machine in Flight.

Tail Plane Design.—From these experimental results we can with advantage consider their application to general design, and for this purpose it is necessary to draw a diagram of the various forces acting upon a machine in normal flight. (See Fig. 260.)

Let A B represent the mean chord of the wings;
X_w the resistance of the wings;
X_b the resistance of the body, chassis, &c.;
X_t the resistance of the tail;
Z_w the normal load on the main planes;
Z_t the normal load on the tail plane;
T the thrust of the airscrew.

Of these quantities the mean chord of a biplane is determined in the following manner. First find the length and position of the mean chord of the wing surfaces, taking into account the variation of chord over the surface and the amount of the dihedral angle. Let C D (Fig. 261) represent the mean chord of the top wing surface, and E F the mean chord of the bottom wing surface.

Join A E, D F. Then draw the line A B such that

$$CA : AE = DB : BF$$

$$= \frac{\text{effective area of bottom plane}}{\text{effective area of top plane}}$$

the effective areas of the top and bottom planes being determined as shown in Chapter III. This mean chord represents the chord of an imaginary monoplane surface equivalent aerodynamically to the several planes of a multiplane.

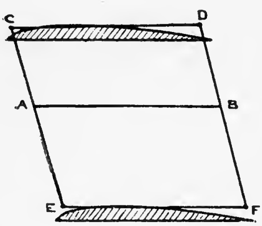

FIG. 261.—Equivalent Chord.

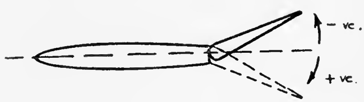

FIG. 262.

The values of the resistances of the wings and tail are easily determined from a knowledge of their aerodynamic characteristics. The resistance of the body and the point at which its resultant may be taken to act is determined by summing up the resistance of the various components included for a given speed, as shown in Chapter XIII. By taking moments of the various resistances about some fixed point, the position of the resultant is found. The airscrew thrust at any speed is determined from particulars of the airscrew which is to be used. The normal force on the wings can be calculated from the wing characteristics and the area.

Now taking moments about the C.G. of the machine (see Fig. 260)

$$Z_t (l - b) = Z_w (a + b) + Tf - (X_w d + X_b c + X_t g)$$

Formula 98

This formula gives the requisite moment to be exerted by the tail plane to secure equilibrium. By substituting the values of the quantities for the range of speeds over which the machine is required to operate, a series of tail moments are obtained, from which it is possible to choose the tail-plane area and setting which will best satisfy the given conditions.

The moments set up by the tail plane when the machine is disturbed from its position of equilibrium must be such that they always tend to restore the position of equilibrium, but for ease of control it is essential that the righting moments should be comparatively small with small displacements from the position of equilibrium, while they should increase with increase of displacement.

It is necessary in deciding on the size of tail plane required for a given machine to consider it in conjunction with the length of the fuselage. As will be seen subsequently in relation to the rudder, there is an advantage in a fairly long distance between the C.G. of the machine and the tail; but for stabilising quality of the tail plane, moment only is of importance. A curve may be drawn representing the moments of lift of wings at various angles of incidence — owing to the travel of the centre of pressure—about the C.G. of the machine, assuming the machine to swing while in a straight path under its inertia. A similar curve will show the correcting couples due to the change of angle of the tail. The first curve may be subtracted geometrically from the second, and thus may be obtained a righting couple curve which is an index to the statical stability of the machine.

Determination of Dimensions of the Tail Plane and Settings of the Elevator.—In the following paragraphs the design of a tail plane is fully carried out, since it is only by such a method that the nature of the problem involved can be fully understood and grasped. The machine for which this tail unit is designed will be the one for which the wing-bracing stresses were worked out in Chapter V., the weight being 2000 lbs., the effective area of the supporting surfaces 366 square feet, and the wing characteristics those given in Table XLIX. The C.G. of the machine is assumed to be at ·32 of the chord from the leading edge of the wing, the distance between the C.G. of the machine and the centre of pressure of the tail being 16 feet. The tail-plane section to be used will be the T.P. No. 3, for which the contours are given in Fig. 250. The chord of the wing is 6 feet, and the angle of incidence relative to the body axis is 4°.

TABLE XLIX.—WING CHARACTERISTICS.

Inclination of wing to wind ...	0°	2°	4°	6°
Absolute lift coefficient (K_y) ...	0·09	0·205	0·298	0·37
Pos^n of C.P. (fraction of chord)	0·575	0·425	0·358	0·329
Pos^n of C.P. relative to C.G. chord (− behind, + in front)	−0·255	−0·105	−0·038	−0·009
Ditto (feet)	−1·53	−0·63	−0·228	−0·054
Pitching moments (lbs. ft.) ...	−3060	−1260	−456	−108
Inclination of wing to wind ...	8°	10°	12°	14°
Absolute lift coefficient (K_y) ...	0·441	0·514	0·573	0·598
Pos^n of C.P. (fraction of chord)	0·312	0·302	0·292	0·28
Pos^n of C.P. relative to C.G. chord (− behind, + in front)	+0·008	+0·018	+0·028	+0·04
Ditto (feet)	+0·048	+0·108	+0·168	+0·24
Pitching moments (lbs. ft.) ...	+96	+216	+336	+480

The normal force on the wing may, with sufficient accuracy, be assumed to be equal to the weight of the machine. The small variation in the load due to the tail-plane pressure is also ignored. The pitching moments on the machine due to the travel of the C.P. are shown in Table XLIX.

The function of the tail plane is to introduce opposing moments to these, so that the total pitching moment upon the machine in normal flight is zero. Other forces besides the wings and the tail plane modify the pitching moment on a machine, as is seen by reference to Fig. 260; but, for the sake of simplicity and clearness, these will be neglected in the present case. In an actual design, however, they must not be ignored, and each of the forces shown must be considered.

It is therefore assumed that the C.G. of the machine lies along the mean chord of the wings, and that the line of thrust and body and wing resistance passes through the C.G. Hence c, d, f, g in Formula 98 are each equal to zero, so that the only forces producing a pitching moment upon the machine are the normal forces upon the wings and the tail plane respectively.

Moment due to the tail = Normal force on tail × distance of tail C.P. from C.G. of machine

$$= \theta' \frac{d\,K_y}{d\,\theta'} \frac{\rho}{g} A' V^2 l$$

Where θ' = angle of incidence of tail plane to relative wind

A' = area of tail plane

$\frac{d K_y}{d \theta'}$ = rate of change of normal force on tail plane with angle of incidence.

l = distance from C.P. of tail plane to C.G. of machine.

From the experiments on the tail plane No. 3 it was observed that the angle of downwash from the main planes is approximately one-half the angle of incidence of the main planes measured from the no lift position. This for the section employed is $-2°$, so that the following table can be prepared :—

TABLE L.

Inclination of wings to wind ...	0°	2°	4°	6°	8°	10°	12°	14°
Inclination of wings measured from angle of no lift ...	2°	4°	6°	8°	10°	12°	14°	16°
Angle of downwash	1°	2°	3°	4°	5°	6°	7°	8°

At this stage it is necessary to determine A' and θ' by trial. A value of A' must be assumed and the necessary tail setting θ' calculated as in the following manner. If the result obtained by this assumed value is unsatisfactory, a fresh value for A' must be taken, and the calculations repeated until a satisfactory setting results. In this connection it is very useful to refer to some such table as that given on page 439, in which the dimensions of the tail plane for several successful machines are shown. From this table an estimate can be formed in most cases of a probable suitable size. A tail plane of span 16 feet and a chord 4 feet will be assumed for the tail plane under consideration. Two cases will be considered :

(*a*) A tail plane of variable angle of incidence relative to the body axis.

(*b*) A tail plane of fixed angle of incidence relative to the body axis.

(*a*) In this method, by adjusting the angle of incidence of the complete unit, equilibrium at varying speeds of flight is obtained without the use of the elevator, the latter being used solely to perform corrective manœuvres about the position of equilibrium.

$$\text{Moment due to tail} = \theta' \frac{d K_y}{d \theta'} \times \cdot 00237 \times 64 V^2 \times 16$$

By reference to the curves shown in Fig. 255, it will be seen that the normal force on the tail plane increases with the angle of incidence according to a straight-line law and the value of the slope

$$\frac{dZ}{d\theta} = \cdot 0158$$

This refers to the model of area ·1275 square feet at a wind speed of 40 feet per second

$$\therefore \quad \cdot 0158 = \frac{dK_y}{d\theta} \times \cdot 00237 \times \cdot 1275 \times 40^2$$

whence $$\frac{dK_y}{d\theta'} = \cdot 033$$

that is, the rate of change of the absolute lift coefficient for the Tail Plane Section No 3 when interference effects are absent is ·033. Interference effects reduce this figure by approximately one-half. Hence we may write the moment due to the tail

$$= \theta' \times \frac{\cdot 033}{2} \times \cdot 00237 \times 64 \times 16\, V^2$$

$$= \cdot 04\, \theta'\, V^2 \qquad \ldots\ldots\ldots\ldots \quad A$$

Also $$V^2 = \frac{W}{K_y \frac{\rho}{g} A} = \frac{2000}{K_y \times \cdot 00237 \times 366}$$

$$= \frac{2300}{K_y} \qquad \ldots\ldots\ldots\ldots \quad B$$

From the values given by the relationships A and B a table of the following nature can be prepared :

Table LI.

Angle of incidence of wing.		V^2		Moment due to tail.		Moment required.		$\theta' = \frac{\text{Moment required}}{\text{Moment}}$
0°	...	25600	...	1024 θ'	...	− 3060	...	3
2°	...	11200	...	448 θ'	...	− 1260	...	− 2·82
4°	...	7740	...	310 θ'	...	− 456	...	− 1·47
6°	...	6220	...	249 θ'	...	− 108	...	− 0·43
8°	...	5200	...	208 θ'	...	+ 96	...	+ 0·46
10°	...	4480	...	179 θ'	...	+ 216	...	+ 1·2
12°	...	4020	...	161 θ'	...	+ 336	...	+ 2·08
14°	...	3850	...	156 θ'	...	+ 480	...	+ 3·08

The angle of the tail plane relative to the downwash of the machine must therefore vary between -3° and $+3^\circ$. The angle required for determining the travel of the variable gear is that relative to the body axis. The angle of the body axis is 4° less than that of the wings, whence Table LII. can be prepared from Tables L. and LI.

TABLE LII.

Angle of wing to wind	0°	2°	4°	6°
Angle of body axis	−4°	−2°	0°	2°
Angle of downwash relative to body axis	−5°	−4°	−3°	−2°
Angle of tail plane relative to body...	2·0°	1·18°	1·53°	1·57°
Angle of wing to wind	8°	10°	12°	14°
Angle of body axis	4°	6°	8°	10°
Angle of downwash relative to body axis	−1°	0°	1°	2°
Angle of tail plane relative to body...	1·46°	1·2°	1·08°	1·08°

It is thus seen that a variation in the angle of incidence of the tail plane and elevator relative to the body axis of from $+2^\circ$ to $+1^\circ$ is sufficient to ensure equilibrium at all angles of flight with no deflection of elevator relative to the tail plane. Examples of Tail Plane Incidence Gears are shown in Figs. 274 and 275.

(*b*) Tail-plane setting fixed relative to the body. With this method equilibrium at various speeds is obtained by the use of the elevator. It is therefore necessary to choose some intermediate position for the tail-plane setting in order that the requisite elevator deflection may be small, thereby ensuring that sufficient additional moment may be secured for manœuvring.

From an examination of the tail-plane settings in the case just considered it is probable that a fixed angle of incidence of $1\frac{1}{2}^\circ$ relative to the body will be suitable. Using this figure the angle of downwash relative to the tail plane is as shown in Table LIII.

TABLE LIII.

Angle of incidence of wings ...	0°	2°	4°	6°
Angle of downwash relative to tail plane θ'	$-3\frac{1}{2}^\circ$	$-2\frac{1}{2}^\circ$	$-1\frac{1}{2}^\circ$	$-\frac{1}{2}^\circ$
Moment due to tail plane ...	−3590	−1120	−464	−124
Moment required	−3060	−1260	−456	−108
Moment to be exerted by elevator	+ 530	− 140	+ 8	+ 16

Angle of incidence of wings ...	8°	10°	12°	14°
Angle of downwash relative to tail plane θ'	$\frac{1}{2}$°	$1\frac{1}{2}$°	$2\frac{1}{2}$°	$3\frac{1}{2}$°
Moment due to tail plane ...	+ 108	+ 358	+ 402	+ 540
Moment required	+ 96	+ 216	+ 336	+ 480
Moment to be exerted by elevator	− 12	− 142	− 66	− 60

Additional Moment due to Deflection of Elevator.—Referring to Fig. 255 it will be seen that the increase in normal force due to the deflection of the elevator at a fixed angle of pitch is approximately proportional to the angle of deflection over the range of angles of pitch from $-11°$ to $+5°$. On plotting this increase of normal force the variation of lift coefficient for the section per degree movement of elevator is found to be ·018. Allowing a decrease of 50% due to its operation in the downwash of the main planes, a value of

$$\frac{d\,K_y}{d\,\theta''} = \cdot 009$$

is deduced. Hence the increase of normal force on the tail due to the deflection θ'' of the elevator

$$= \theta'' \times \cdot 009 \times \cdot 00237 \times 64\,V^2$$

whence additional moment

$$= \cdot 0219\,V^2\,\theta''$$

and the required deflection of elevator at each speed in order to produce equilibrium

$$= \theta'' = \frac{\text{Moment to be exerted by elevator}}{\cdot 0219\,V^2}$$

$$\therefore \theta'' = +0\cdot 95° \quad -0\cdot 57° \quad +0° \quad +0\cdot 12° \quad -0\cdot 10 \quad -1\cdot 45° \quad -0\cdot 75 \quad -0\cdot 70°$$

It will be seen that the deflection of elevator required for equilibrium is almost negligible when a correct tail-plane setting has been secured. Consequently, in a case such as the present no advantage is to be derived by installing a tail-incidence gear, such a device being generally of more value in the case of large machines.

So far the method of design has been limited to the determination of the righting moments necessary to produce equilibrium at a particular angle of incidence. Before finally deciding upon the tail plane it is essential to examine whether equilibrium will be restored should the machine be temporarily deflected from its normal flight attitude by a gust or other cause. For stable equilibrium it is necessary that the moments set up by the tail plane in the event of such disturbance are sufficient to overcome the unbalanced moment set up by the wings and to restore the machine to its original flight attitude. For such to be the case, the moment due to the tail plane must increase at a faster rate than that due to the wings. Now, from Fig. 260

$$\text{Moment due to wings} = K_y \frac{\rho}{g} A V^2 (a-b)$$

and

$$\text{Moment due to tail} = K'_y \frac{\rho}{g} A' V^2 l$$

Since ρ/g (V^2) is common to both expressions, it follows that the moment due to the wings is proportional to $K_y A (a-b)$ and the moment due to the tail proportional to $K'_y A' l$. By plotting these expressions on a pitch-angle base, curves such as are shown in Figs. 263 and 264 result, and an examination of such curves enables conclusions to be drawn as to the probable dynamic stability of the machine.

For the machine previously considered, the values for $K_y A (a-b)$ for different wing angles are shown in Table LIV., and for the tail plane the values of $K'_y A' l$ are shown in the same table, where

$$K'_y = \theta' \frac{d K'_y}{d \theta'}$$

for fixed angles of $1\frac{1}{2}°$ to body.

TABLE LIV.

Incidence of wings	0°	2°	4°	6°
K_y	·09	·205	·298	·37
$(a-b)$ feet	−1·53	−·63	−·228	·054
$K_y A (a-b) \times 366$	−50·4	−47·4	−24·9	−7·3
Angle of tail plane relative to downwash θ'	$-3\frac{1}{2}°$	$-2\frac{1}{2}°$	$-1\frac{1}{2}°$	$-\frac{1}{2}°$
$K'_y = \theta' \times ·0165$	−·0578	−·0413	−·0248	−·0082
$K'_y \times 16 \times 64$	59·2	42·3	25·4	8·4
Incidence of wings	8°	10°	12°	14°
K_y	·442	·514	·573	·598
$(a-b)$ feet	·048	·108	·168	·24
$K_y A (a-b) \times 366$	7·76	20·3	35·2	52·5
Angle of tail plane relative to downwash θ'	$\frac{1}{2}°$	$1\frac{1}{2}°$	$2\frac{1}{2}°$	$3\frac{1}{2}°$
$K'_y = \theta' \times ·0165$	·0082	·0248	·0413	·0578
$K'_y \times 16 \times 64$	−8·4	−25·4	−42·3	−59·2

These values are shown plotted in Fig. 263. The moment due to the tail plane is a straight line, whose position may be shifted (corresponding to a movement of the elevator) such that equilibrium may be obtained at each angle of incidence of the wings. The slope of the resultant curve obtained by combining the two curves will indicate the nature of the equilibrium at the various attitudes of flight.

These curves are shown in Fig. 263, and it will be observed

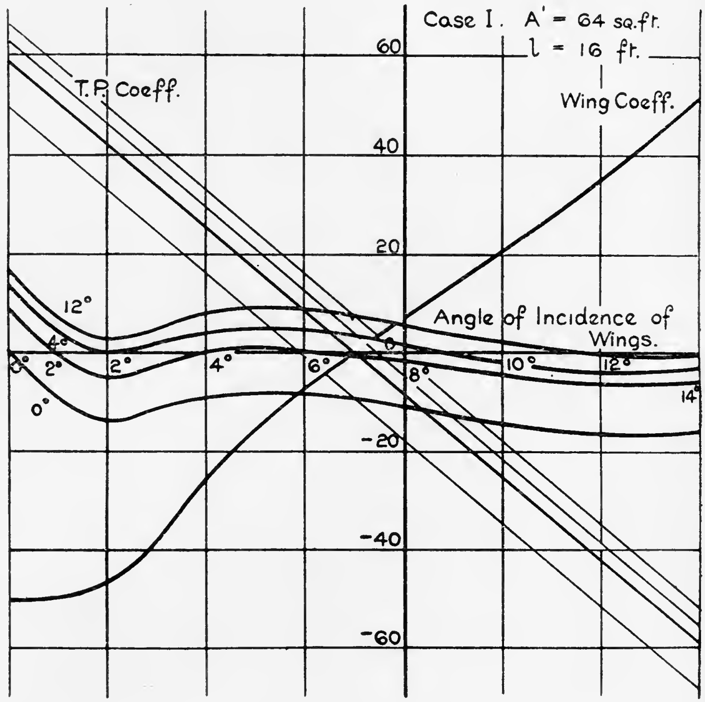

FIG. 263.—Case I.

that the slope of the resultant curve for which equilibrium is obtained at angles of from 5° to 12° is of opposite sign to that for angles 2° to 5°. Between angles of 5° to 12° the equilibrium is such that an alteration in the angle of incidence of the wings sets up a pitching moment which causes the machine to revert to its original position—that is, the equilibrium is stable. Between angles 2° to 5° an alteration in attitude of the machine sets up a pitching moment which tends to increase the deviation from the equilibrium position, hence the equilibrium is unstable, and unless a correcting moment is introduced by a movement of the elevator, the attitude, and consequently the speed, will be permanently altered. It is therefore apparent that, to secure stable equilibrium at all angles of incidence, the slope of the curve due to the tail plane must at all points be greater than that of the curve due to the wings. The slope of the tail-plane curve is directly proportional to the area of the tail A′, and the length

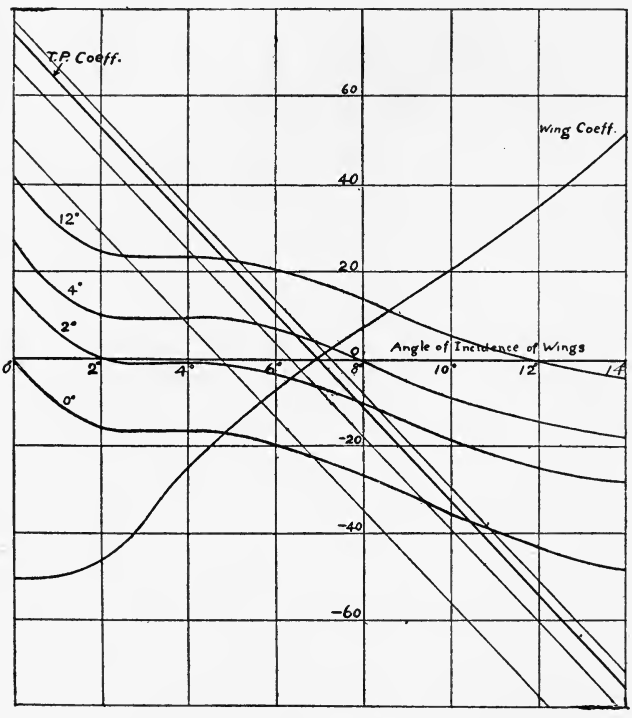

FIG. 264.—Case II.

from the C.G. at which it is acting (l); therefore by increasing either of these factors stable equilibrium can be secured in the above case. For the present purpose an increase in l from 16 to 20 feet will be adopted. The values of $K'_y A' l$ will then be as shown in Fig. 264. In this case the equilibrium is stable throughout the complete range of flying angles.

In actual design work this latter operation must be carried out before determining the tail settings, otherwise in the event of any alteration in the main dimensions being necessary, as was the case in this example, the whole of the preceding work would have to be repeated. The order in the present chapter is due to reasons of clarity, it being easier to understand the principles involved after the treatment of the tail settings.

Having thus secured a tail plane to give stable equilibrium at all speeds, an investigation into the longitudinal stability of the machine should be carried out according to the method shown in Chapter X. A satisfactory result will in all probability be secured, and the dimensions of the tail plane can then be embodied in the general design of the machine.

Fin and Rudder.—The fin and rudder form the stabilising and control surfaces for directional flight. In certain cases the

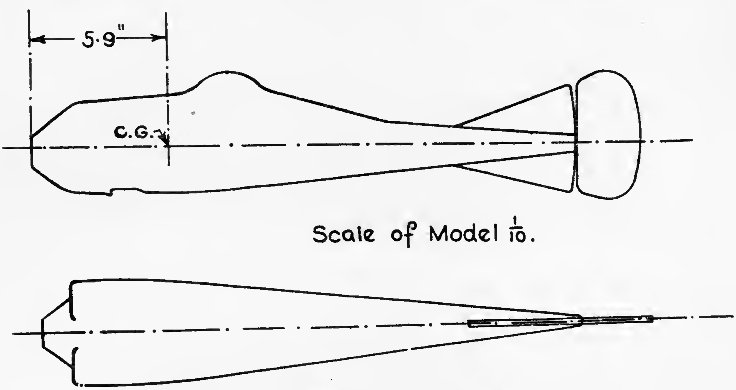

FIG. 265.—Model of S. E. 4 Body.

rudder may be used without a fin, and under these circumstances it performs the dual function of a stabilising and controlling surface. Such an arrangement, however, should be limited to small machines. On rotation of the machine about the axis of yaw, the rudder and fin, together with all members of the aeroplane which present a side area to the line of flight upon rotation, produce a horizontal force transverse to the line of flight which is known as the lateral force.

Just as curves can be drawn for longitudinal 'static' stability, so also can curves be drawn in the case of members contributing lateral force during or owing to directional change; the moments of lateral forces about the C.G. of the machine being plotted. The rudder, and fin if any, must then be sufficiently large to ensure that there is always a small positive residual moment—

that is, a moment which tends to restore the machine to its proper direction. The balance should be right in the case of a tractor machine when the engine is working, as then the propeller exercises more fin effect than in gliding flight. Lateral force is to be avoided as far as possible, owing to the fact that it produces side-slip. For this reason, therefore, a long fuselage carrying a small rudder is an advantage. The same remarks as were made in reference to the elevators are applicable, but to a less extent, owing to the smaller area, with regard to the interaction of the rudder and fin. The rudder may with advantage be given a moderate amount of aspect ratio, particularly in the case where there is no fin.

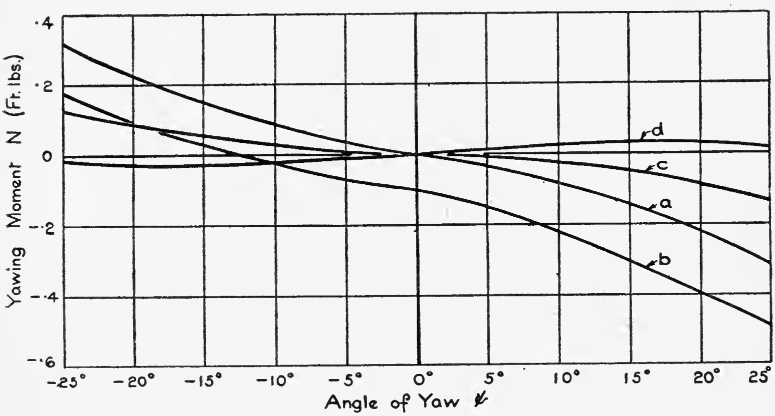

FIG. 266.—Yawing Moment on Model of S. E. 4 body.

Wherever possible, the lateral force on a machine should be deduced from experiments on a model of the machine being designed. An example of the experimental determination of the lateral force and yawing moment upon a model is shown in Figs. 266 and 267.

The model was of the S. E. 4 body, and was one-tenth full size, the overall length with rudder in position being 25″. This model is shown in Fig. 265. Measurements of the lateral force and yawing moment about the C.G. of the machine were made for four modifications of the model, namely:

(*a*) With fins and rudder straight.
(*b*) With rudder set over at 10°.
(*c*) With fins on and rudder off.
(*d*) Without fins and rudder.

The curves (*a*), (*b*), (*d*) in all figures show the progressive effect of the decrease of rudder and fin area. The lateral force is reduced to about 70% of its value by removing the rudder, and to about 40% of its value by removing fins as well The yawing moment is reduced to about 35% by removing the rudder, and changes sign when the fins are also taken off, showing that the body is unstable as regards yawing about the C.G. when there is no fin area at the after-end.

In the event of such experimental information being unob-

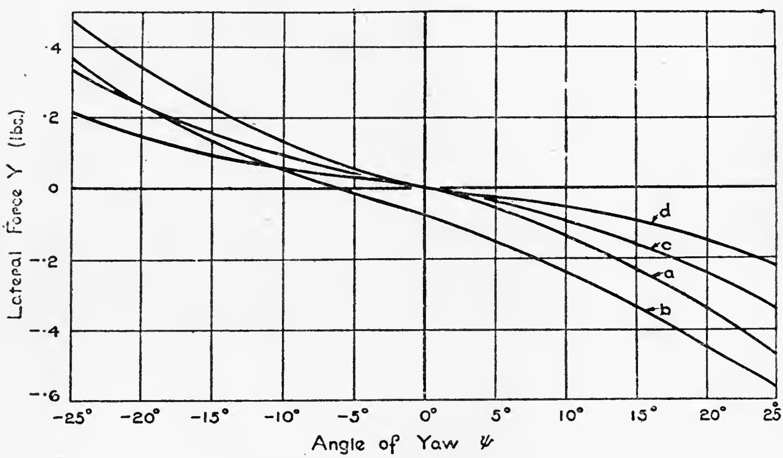

FIG. 267.—Lateral Force on Model of S. E. 4 body.

tainable for a machine under design, the following figures may be used :—

TABLE LV.

ITEM.	Lateral Force in lbs. per Degree Yaw at 100 f.p.s.
Streamline wires	0·8 lbs. per square foot side area.
Streamline struts	0·7 lbs. per square foot side area.
Fuselage	0·11 lbs. per square foot side area.
Rudder and fin	0·6 lbs. per square foot side area.
Landing chassis and wheels ...	0·8 lbs. per square foot side area.

From a side elevation of the machine the amount of side area presented by the various members may be assessed and the lateral force then calculated.

Lateral Force due to the Airscrew.—When investigating the lateral stability of the B.E. 2 machine it was found experimentally that the total side force upon the machine when the airscrew was rotating was considerably greater than a calculation of the known lateral forces had indicated. This led to an investigation of the possible action of the airscrew as a fin, and a mathematical theory was developed by Mr. T. W. K. Clarke, B.A., A.M.I.C.E., from the following considerations. Referring to Fig. 268, it will be seen that the effect of a side wind will be to cause a difference in the velocity of the airscrew blades relative to the air according as to whether they are moving in the direction of the side wind or moving towards it—that is, if u be the velocity of the side wind, and v the velocity of the blade, then the velocity of the blade relative to the wind will be $v - u$ and $v + u$ respectively. The result of this will be that the angle of

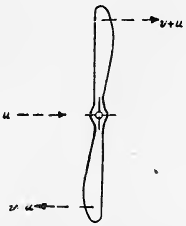

Fig. 268.—Lateral Force on Airscrew.

attack for the lower blade will be increased (see Chap. IX.), while that for the upper blade will be diminished. This increase in the angle of attack and the increased velocity of the lower blade relative to the air produce a greater pressure on the lower blade, while upon the upper blade there is a decrease in pressure: hence the side components of the forces on the blades no longer balance each other, and it is this unbalanced force which causes the variation of total side force according as the airscrew is rotating or motionless relative to the machine.

An experimental verification of the theory was carried out by the N.P.L., and it was found that the results were in good agreement with those calculated. For an airscrew of 9 feet diameter and speed of 900 r.p.m., such as was used on the B.E. 2, the lateral force was found to be 10·3 lbs., with an angle of yaw of 5° and a translational speed of 100 f.p.s. For angles up to 25° the force is approximately proportional to the angle of yaw.

After an estimate of the lateral force per degree of yaw upon the various members of a machine has been made, the yawing moment about the C.G. can be determined, it being the sum of the various lateral forces multiplied by their respective distances from the C.G. This calculation will enable the 'minimum' size of fin and rudder area required to give directional stability to be estimated. The maximum size of fin is fixed by considerations relating to spiral instability, as was indicated in Chapter X. The condition for spiral instability there stated was that the numerical value of the ratio of the derivatives L_v/N_v should be greater than the ratio of the derivatives L_r/N_r. The limiting condition for stability will therefore be reached when

$$\frac{L_v}{L_r} = \frac{N_v}{N_r}$$

and this will give a value for the maximum fin permissible. The value of L_v is dependent upon the dihedral angle of the machine, and hence this forms the readiest means of securing spiral stability, as in most cases it is simpler to assume a size of fin by reference to successful machines of a similar size. The dihedral angle can then be varied, if necessary, to give the required degree of stability. The determination of the above derivatives necessitates model experiments for the best results, though in the absence of such data they may be calculated to a fair degree of approximation in the manner shown in Chapter X.

Ailerons or Wing Flaps.—Control about the axis of roll is provided generally by means of hinged ailerons or flaps. In the early stages of aviation the method of warping the wings was adopted, but this practice has now been almost abandoned. When dealing with the elevator, it was stated that the effect of rotating the elevator with reference to the tail plane was to increase or decrease the lift of the combined surface. In the case of the aileron a continuous high lift/drag ratio is of prime importance. The angle of rotation must therefore be small and the flaps consequently large.

In actual practice we find a wide range of aileron areas according to the width and the amount of rotation employed. The moment required depends upon the span, the area of the wings, and the transverse moment of inertia of the whole machine. The area itself also depends upon the speed and the speed range. In designing the ailerons, attention must be paid to the yawing moments induced by using the flaps. We have previously seen that a reflexed trailing edge diminishes the resistance of a wing. If the flaps are interconnected, therefore the resistance of one wing will be diminished while that of the other is increased, thus necessitating simultaneous use of the rudder. When the rudder is used to produce a turning movement, banking is necessary to prevent side-slip. If the machine be banked by use of ailerons or warping of the wings, the upper wing-tip will have the flap pulled down and so will have an increased resistance ; while the reverse is the case for the lower wing-tip. But the upper wing-tip is required to travel faster

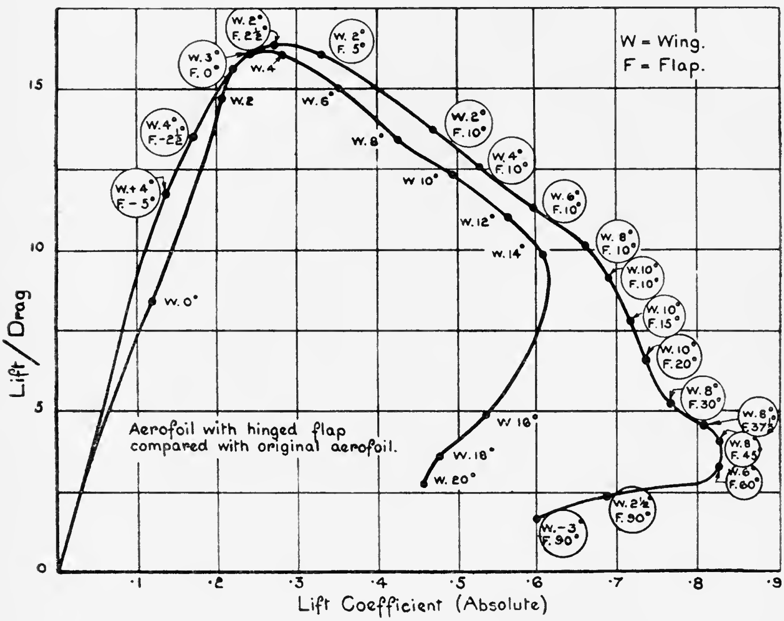

Fig. 269.—Comparison of Lift Drag Rated for Aerofoil with and without Flaps.

than the lower one, and thus the rolling control opposes the rudder action. In an extreme case the size of the rudder might have to be increased to take account of this.

Experiments relating to an aerofoil with a hinged flap are described in the 1913-1914 Report of the Advisory Committee for Aeronautics. Although these experiments were not made in connection with the question of aileron surface, they are of considerable interest in this respect, and therefore the most important results are here given. The section of the aerofoil used in these experiments was similar in form and aerodynamic characteristics to that shown in Wing Section No. 6. The dimensions were 18″ by 3″, and the flap extended over the whole length of the rear part of the section, being 1·155″ wide (·385 chord). The gap in the aerofoil due to the hinges was filled with plasticine, as it was found that the drag was greater if this was not done. Angles of pitch were in all cases measured from the chord of the original aerofoil, so that when the flap angle was zero the section corresponded exactly with that shown in Fig. 72.

Fig. 269 represents the value of the L/D ratio plotted against lift coefficient for the most efficient equivalent aerofoil—that is, the combination of angle of incidence of chord with

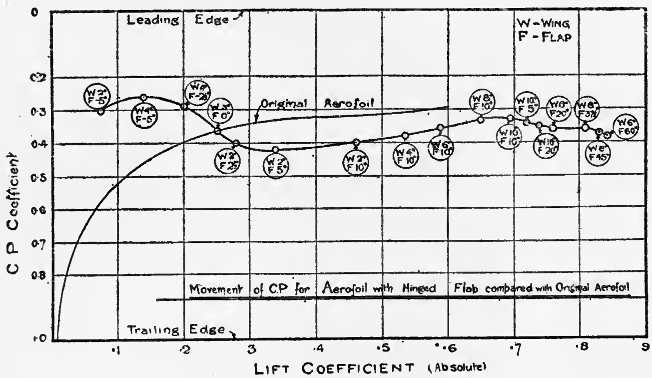

FIG. 270.—Movement of C.P. for Aerofoil with Hinged Flap compared with Original Aerofoil.

angle of flap to give maximum efficiency as compared with the original section. The angle of pitch of the wing and the relative pitch for the flap are marked on the figure, and the corresponding curve with zero angle of pitch of flap are shown on the same figure. In the neighbourhood of points of greatest efficiency it will be noticed that an alteration of flap angle gives a better lift without alteration of the pitch angle of the wing itself, while maximum lift is obtained with the flap at a large angle of pitch and the incidence of the wing itself smaller than at the corresponding point for the original section. The centres of pressure for these most efficient combinations are shown in Fig. 270. For values of lift coefficient between ·13 and ·3 the C.P. moves backward with increase of lift coefficient. The equivalent aerofoil is therefore stable over the most important portion of the range of lift coefficient used at ordinary flying speed.

From these experiments the following important conclusions as to the advantages of using a wing with a hinged rear portion can be deduced :

1. That the increased maximum lift coefficient obtained permits of a considerable reduction in the landing speed.
2. That by adjusting the flap to correspond with the minimum drag for the particular angle of incidence at which the machine travels over the ground, the distance necessary to take off may be reduced by 13%.
3. The distance required to pull up after having landed can be diminished by setting the flaps at a large angle of pitch.
4. The maximum flying speed can be increased by giving to the flaps a small negative angle at the corresponding angle of flight for maximum speed.
5. A slight gain in climbing speed can be obtained by the use of flaps.

The mechanical difficulties involved in securing a hinged wing section are considerable, but it is apparent from these experiments that a considerable gain would accrue in aerodynamical efficiency.

Balance of the Control Surfaces.—When referring to the elevator it was stated that, in order to reduce the strain upon the pilot when working the controls, the method of balancing the control surface was desirable. Similar considerations make it advisable to balance both the rudder and the ailerons upon large machines—*i.e.*, machines of greater weight than 5000 lbs. This may be effected in two ways (see Fig. 272) :

(i.) By adding an extension which projects in front of the main portion of the surface.

(ii.) By placing the hinge about which the control rotates some distance behind the leading edge.

In both these methods the air forces upon the surface in front of the hinge produce about the hinge a moment of opposite sign to that of the main control surface, and therefore reduce the effort required to move it by twice this amount. The first method has been most frequently employed in practice in this country, but the second method possesses many more advantages, and has been used on the latest Handley-Page machine (V-1500). In order to decide upon the area of the extension required, it is necessary to determine the moment of the main surface about the hinge for various angles of deflection and then to select an extension which will produce the necessary degree of balance over this range of angles. For most accurate results a model of the wing and flap with extension should be made and tested in the wind tunnel, the size of the extension being altered until satisfactory.

If such a procedure is not possible, the size of the extension must be deduced from whatever results are available. The

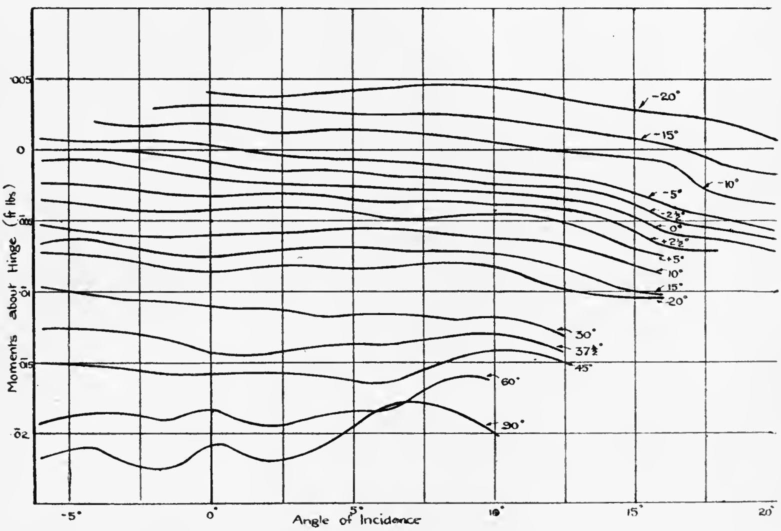

FIG. 271.—Moments about Hinge of Wing Flap.

following example indicates a rough method of arriving at the necessary dimensions of an extension to a wing flap for balancing purposes. Fig. 271 gives the moments about the hinge for the wing flap described on page 374. The increase of moment per degree of deflection of flap at 0° pitch of wing = ·0004 ft. lbs. The section of the extension used will be that of the Tail Plane No. 3, whose $d\,K_y/d\,\theta$ = ·033, and the average position of whose C.P. will be taken at 0·23 chord from the leading edge.

Then for balance the moment of the extension about the hinge must equal ·0004 ft. lbs. per degree—that is, the load on the extension × 2 × c = ·0004 ft. lbs.

The C.P. coefficient is ·23; therefore the distance from hinge at which the resultant force upon the extension may be assumed to act is

$$= (1 - \cdot 23)\, a - 1 \cdot 155''$$
$$= \cdot 77\, a - 0 \cdot 0963 \text{ feet}$$

whence $2 \times \cdot 033 \times \cdot 00237 \times 40^2 \times a \times b\,(\cdot 77\, a - 0 \cdot 0963) = \cdot 0004$

Taking an approximate value for b of 1·5, we have

$$0 \cdot 313\, a\,(\cdot 77\, a - 0 \cdot 0963) = \cdot 0004$$

or $$\cdot 77\, a^2 - 0 \cdot 0963\, a = 0 \cdot 00128$$

Solving this quadratic

$$a = \cdot 206 \text{ feet} = 2 \cdot 47''$$

so that the dimensions of extension necessary to balance the flap upon the assumptions made = 1.5″ × 2·47″. In practice

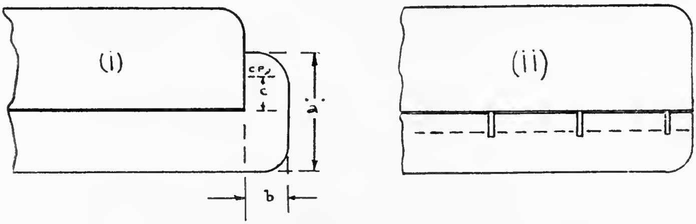

FIG. 272.—Balanced Ailerons.

the dimensions 1·5″ × 2·5″ would be adopted. Such an extension increased to the same scale as the wing and flap would give the required balance upon a full-size machine.

The above calculation is given to indicate the method to be used for calculating the size of a balancing extension.

It is obvious that the assumptions made cannot be strictly justified, since the position of the C.P. of the extension varies with the angle of incidence. Moreover, end-effect will be important at the wing-tips. Nevertheless, such a calculation is extremely useful in the initial stages of a new design as affording an indication of the probable size required. This can be altered subsequently, if experience shows it to be necessary after a trial flight has been made.

For securing balance by the second method, recourse must also be made to wind-channel experiments. An examination of the pressure-distribution diagrams over the rear portion of a wing section will be of much assistance in this direction. In general the shape is found to be approximately triangular, as will be seen by reference to Fig. 48. For a triangle the C.P. will be at one-third the altitude from the base line, hence it can be inferred that the position of the hinge for full balance in this method should be at one-third the chord of flap from its leading edge. In order to avoid the possibility of the flap being over-balanced, and hence tending to increase its deflection relative to the remainder of the section, it would be advisable to place the hinge at about 0·3 times the flap chord from the leading edge.

These methods of balancing are applicable to each of the control surfaces.

Construction of Control Surfaces.—The controlling surfaces are built up much as portions of wings. A strong leading edge serves to take the hinges, and forms as it were a 'back-

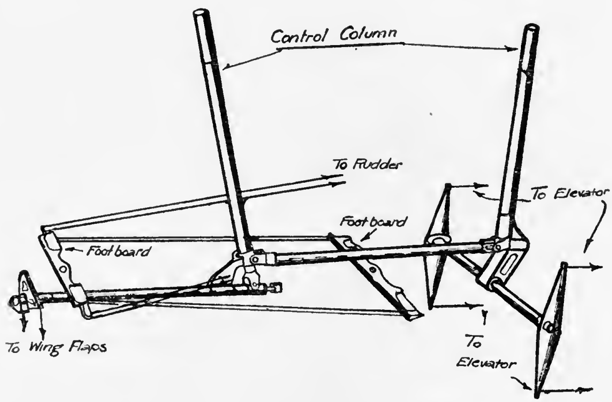

FIG. 273.—Dual Control System.

bone' from which may radiate ribs of light construction to the trailing edge. The trailing edge, in the case of the wing-flaps, will be similar to the rigid part of the wings. In the case of the elevators, and more especially in the case of the rudder, thin tubing of about 10 mm. diameter will be found useful. Short levers of streamlined section are fixed to the backbone or spars, and connected by wires to the control lever in the pilot's cockpit. The wires, or rather thin cables, may be guided round corners by pulleys or bent copper tubing. They should be covered as much as possible, so as to diminish head resistance, and should therefore be placed inside the wings, inspection doors being provided where necessary in the wings; and for the

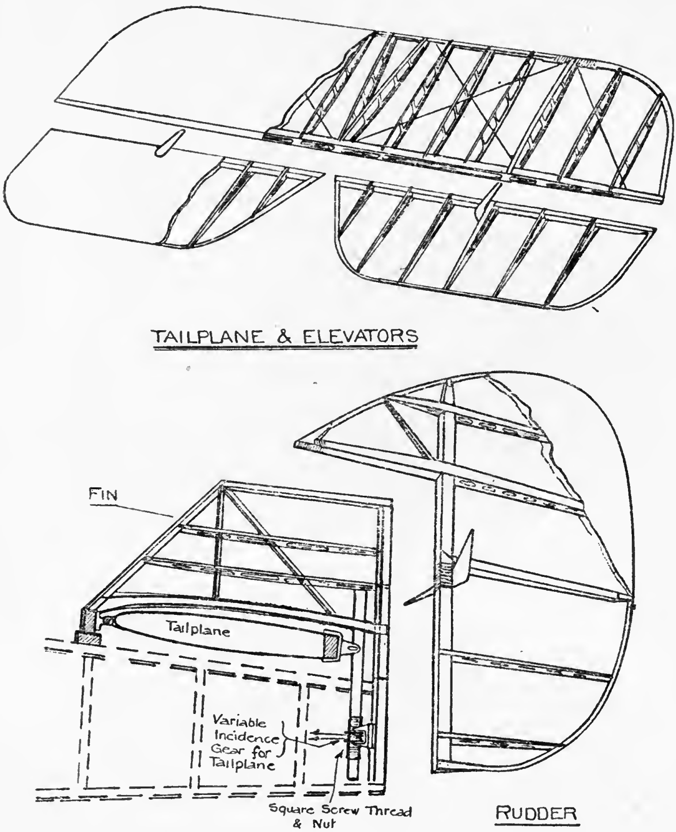

FIG. 274.—Tail Unit Components. (See also p. 412.)

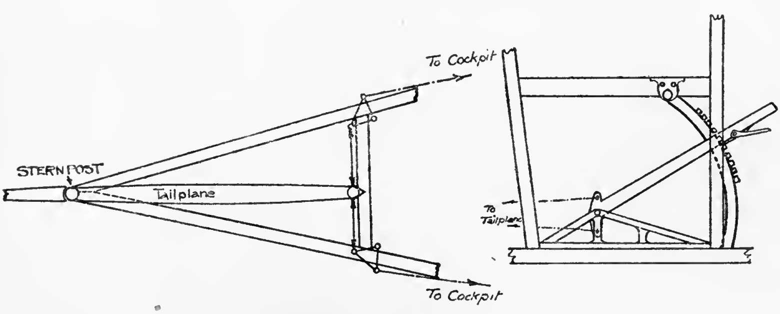

FIG. 275.—Variable Incidence Gear for Tail Plane.

tail unit should enter the fuselage as soon as convenient. The success with which the designer balances his controlling surfaces is shown by the consequent lightening of the control lever, and more especially is this the case with large machines.

The design of the control is a simple matter when the loads spread over the control surfaces have been assessed for the highest speeds and the greatest angles, and their moments about their hinges obtained by locating the c.p. The pulls in the connecting wires follow at once, and the problem of the

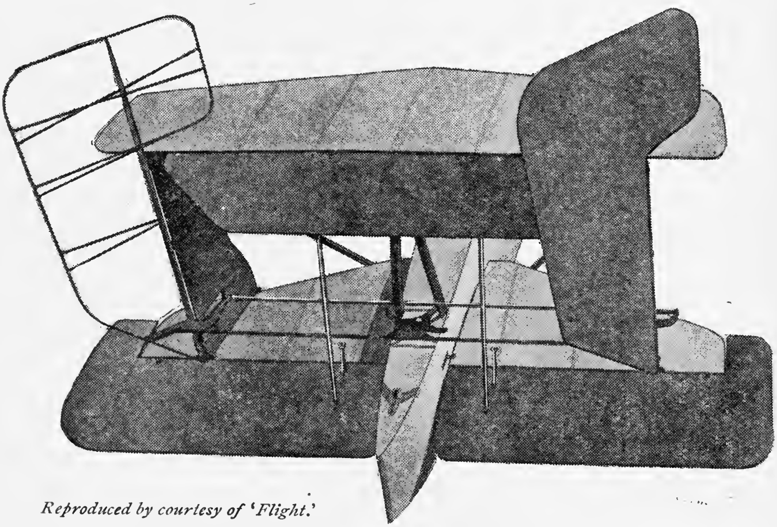

Reproduced by courtesy of 'Flight.'

FIG. 276.—Double Tail Unit for Large Machine.

control lever reduces to the question of a short cantilever projecting vertically from a horizontal pivot tube. If the elevators are attached to levers at the ends of this tube—that is, near the sides of the fuselage—the tube must be designed for combined torsion and bending.

The fuselage should be strengthened where it takes the strain of the control lever and rudder bar. The rudder bar, arranged for the feet, may be conveniently made of wood with metal fittings. The vertical pivot should be made adjustable along the fuselage, with lengthened strips for the rudder cables, so as to be available, without any inconvenience, for pilots of different sizes.

CHAPTER XII.

Performance.

Definition.—The factors upon which the performance of a machine depends—that is, the maximum speed which it is able to attain at varying altitudes and the time it takes to reach such altitudes—were considered at some length in Chapter I., and those pages should be again consulted at this stage. In this chapter the relation between these various factors will be investigated in their effect upon the increase or decrease of the efficiency of the aeroplane, and some practical methods of actually determining the performance of machines in flight will be given.

The primary object of the aeroplane is to transport a certain useful load from one point to another, using the air as a medium of travel. It must therefore be provided with a surface capable of developing the necessary reaction to overcome the force of gravity, while offering at the same time a minimum resistance to forward motion through the air. The development of the modern wing section, as outlined in Chapter III., had for its aim the accomplishment of this purpose. The area of the supporting surfaces—that is, the wings—must obviously be such that the reaction upon them is equal to the weight of the machine. This reaction, as we have already seen, is termed the lift of the wings. Such lift is always accompanied by a resistance or drag at right angles to it. The drag of the complete machine is made up of two parts—namely, the wing resistance and the body resistance. It is the aim of the designer to obtain a wing section in which the ratio of L/D is a maximum for the speed at which he proposes the machine under consideration should fly.

The efficiency of the wing surfaces is largely influenced by 'end effect,' and in order to obtain a highly efficient wing the aspect ratio must be high. Increase of aspect ratio leads to a corresponding increase in the weight and constructional difficulties, so that apparently a definite limit for greatest efficiency is soon reached. The maximum aspect ratio adopted to-day is in the neighbourhood of 10.

All resistances other than that of the wings are grouped together under the term 'body resistance.' This resistance varies approximately as the square of the speed, but a factor which leads to considerable uncertainty in this direction is the slip stream from the airscrew. In the case of the tractor machine the body moves directly in this slip stream, and its resistance is thereby increased relative to the remainder of the machine. Moreover, interference between the various components leads to a further modification, which it is very difficult to estimate. The body resistance becomes of increasing relative importance as the speed of flight becomes greater and greater. Examination of the resistance curves for the wings shown in Fig. 278 indicates that the wing resistance remains fairly constant over a considerable range of speeds, whereas the body resistance increases as the square of the speed. The minimum total resistance will occur when the wing and body resistance are approximately equal in amount, and the speed corresponding to this will be the most economical for flight.

Turning next to a consideration of the Engine power, the first point to be observed is that the thrust exerted by the engine must be sufficient to propel the wing surfaces through the air at such a speed that their reaction overcomes the weight of the machine. The forces tending to prevent the attainment of such speed are the wing and body resistances referred to above, hence for horizontal flight at a particular speed it is necessary that the engine thrust must be at least equal to the drag of the machine. An estimate of the horse-power required necessitates, therefore, a knowledge of the resistance to be overcome at the various speeds of flight. It is also essential that a reserve of power is available in order that the machine may climb. The excess of power supplied over that required for horizontal flight is the horse-power available for climbing, and this being known a simple calculation will enable the rate of climb to be determined. The maximum rate of climb will correspond with that speed at which the excess power is greatest.

The prediction of performance necessitates a knowledge of the resistance of the machine at various flight speeds, together with the excess horse-power available at that speed. The following paragraphs show one method of determining these quantities for a machine of new design.

The Resistance of the Machine.—(*a*) *Wing Resistance.*—The wing resistance is deduced directly from the aerodynamic characteristics of the section employed. It is first necessary to determine the lift coefficient corresponding to various speeds of flight. For this purpose the fundamental equation (Formula

13) is used. This gives K_y for varying values of V. From the wing-section characteristics the value of the drag coefficient corresponding to each K_y is obtained, which gives the corresponding flight speed. The drag coefficient and the speed of flight being known, the wing resistance follows from the fundamental equation (Formula 14). These values should be plotted on a speed base.

(*b*) *Body Resistance.*—The estimation of the body resistance is a matter of some difficulty, and recourse must be had to wind-tunnel data wherever available. It is advisable to make a point of collecting resistance data whenever an opportunity occurs, particularly the resistances of a complete machine, such as that, for example, given in Chapter VI. for the B.E. biplane. The figures given in Chapter I. will also be useful in this connection, and will serve as a base upon which to make comparisons. The accuracy of the entire performance calculation is directly dependent upon this estimate of body resistance, and hence it is essential that it should be carried out as carefully as possible, due allowance being made for those parts in the airscrew slip stream.

If the machine has already been built, it is possible to determine the body resistance by noting the gliding angle. If this be θ we then have the relationship $\tan \theta = D/L$ where D represents the total drag of the machine, and L the lift of the wings. From the total drag the resistance of the wings is subtracted, and the remainder will be the body resistance. This is in most cases the more accurate method, it being usually found that the estimated 'body resistance' is higher than the observed body resistance. The body resistance (R) being known for any speed v, then at any other speed (V) the resistance is obtained from the equation

$$\text{Resistance at speed V} = \frac{R \cdot V^3}{v^2}$$

Add the body resistance at any speed to that of the wings for the same speed, and the total resistance of the machine for that speed is obtained. A curve of total resistance against speed can then be drawn.

In determining the wing resistance of a machine, allowance must be made for the following factors:

1. Effect of slip stream of airscrew.
2. Interference effects.
3. The stagger and aspect ratio of the wings.

Horse-power required.—(*a*) To overcome wing resistance:

$$\text{H.P required} = \frac{\text{Resistance} \times \text{Velocity}}{550}$$

$$= K_x (\rho/g) A V^2 \times V/550$$

$$= \frac{(\rho/g) A V^3}{550} \times K_x$$

Knowing K_x corresponding to each flight speed V, the wing H.P. can be calculated.

(*b*) To overcome body resistance: similarly,

$$\text{H.P. required} = \frac{R V^2}{v^2} \cdot \frac{V}{550}$$

$$= \frac{R V^3}{550 v^2}$$

From this equation the 'body' H.P. can be determined for several values of V. It will be found most convenient in calculating the total horse-power required to use the tabular method of setting out the work.

Horse-power available.—As stated in Chapter I., this depends both upon the engine and the airscrew. The efficiency of each of these units depends largely upon the conditions under which it is working, and data respecting the variation of engine-power, with altitude and revolutions per minute, should be obtained from tests carried out independently or by the manufacturer. It is found that the brake horse-power of an engine varies almost directly as the density of the air, and is practically independent of its temperature.

The efficiency of the airscrew varies with its forward speed, and may be calculated with a considerable degree of accuracy in the manner set forth in Chapter IX. The horse-power required to drive the airscrew at various speeds can be determined from its torque curve. If Q be this torque, then the horse-power required to drive the airscrew at n revolutions per second

$$= \frac{2 \pi n Q}{550}$$

This horse-power should then be plotted on the base of 'n' and superposed on the B.H.P. curve of the engine similarly plotted on a base of 'n.' The intersection of these curves gives the maximum horse-power available at that translational speed of the airscrew. The efficiency of the airscrew being known, it is then an easy matter to determine the maximum available horse-power to drive the machine.

On plotting (1) total H.P. required to overcome resistance of machine at ground level; (2) power available at ground level, on a speed base, it can be seen from the curve what power is available for climbing, and also the fastest climbing speed.

Similarly, by calculating the above quantity for the density corresponding to the maximum height it is desired to fly at, it will be seen what is the highest speed attainable at this height.

Rate of Climb.—The difference between the ordinates of the H.P. required and the H.P. available curves shows the H.P. available for climbing at each speed. The maximum difference will give the maximum rate of climb to be expected, which can be calculated thus:—

Let P represent the horse-power available for climbing. Then rate of climb in feet per minute

$$= r = \text{P} \times 33000/\text{weight of machine}$$

The points at which the H.P. curves intersect determine the maximum and minimum flying speeds respectively, and thus a calculated estimate of the performance of the machine is obtained. The nearness with which these results approach those experimentally obtained will be a measure of the accuracy of the estimated resistances and other assumptions.

Performance Calculations.—An example of the method of predicting the performance of an aeroplane, such as should be carried out when designing a new type of machine, will now be given. For this purpose the particulars of the machine referred to in Chapter V. will be used. It is required to determine the maximum speed and rate of climb of this machine at ground level when fitted with a 150 H.P. engine and an airscrew possessing an efficiency of 80%. The estimated resistance of the machine less wings—that is, its body resistance—is equal to 150 lbs. at 100 feet per second. The characteristics of the wing section are as follows:—

CHARACTERISTICS OF THE WING SECTION.

θ	0°	2°	4°	6°	8°	10°	12°	14°
K_y ...	·097	·192	·273	·347	·421	·492	·555	·59
K_x ...	·0167	·0165	·0199	·0261	·0355	·0452	·0551	·0742

From these characteristics the wing resistance at varying speeds is calculated in the following manner. From formula

$$V^2 = \frac{W}{\frac{\rho}{g} A' K_y}$$

Substituting $= \dfrac{2000}{\cdot 00237 \times 366 \times K_y} = \dfrac{2300}{K_y}$

Notice that the effective supporting wing area—A′—is used in this formula. From this relationship the velocity of flight corresponding to varying values of K_y, and consequently of the angle of incidence, can be calculated, whence the determination of the wing resistance is obtained by using the formula

$$R_W = K_x \frac{\rho}{g} A V^2$$

where R_W represents the wing resistance and A the total area of the wing surface = 414 square feet. Tabulating the results we obtain

TABLE LVI.

θ	0°	1°	2°	4°	6°
V^2	23700	15800	11980	8430	6630
V (f.p.s.) ...	154	126	109·2	91·8	81·4
$\frac{\rho}{g} A V^2$	23250	15400	11750	8260	6500
R_W	388	253	194	164	170

θ	8°	10°	12°	14°
V^2	5460	4670	4150	3900
V (f.p.s.) ...	73·9	68·4	64·4	62·5
$\frac{\rho}{g} A V^2$	5350	4580	4070	3820
R_W	190	207	224	284

Body Resistance.—The resistance of the rest of the machine is proportional to the square of the speed of the machine, consequently the resistance can be obtained from the formula

$$R_B = \frac{150}{(100)^2} \times V^2 = 0{\cdot}015\, V^2$$

The figure used for the body resistance of the machine, which in this case has been assessed at 150 lbs. at 100 f.p.s., should be most carefully estimated from all available data, the resistance of each member and detail being checked wherever possible by reference to full-scale results. The accuracy of the predicted performance depends to a large extent upon this estimate. Tabulating the results for the body resistance we have

V^2 ...	23700	15800	11980	8430	6630	5460	4670	4150	3900
R_B ...	356	237	180	126	100	82	70	62	49

Adding together R_w and R_B the total resistance of the machine for varying flying speeds is obtained, namely,

$R_W + R_B$ ...	744	490	374	290	270	272	277	286	333

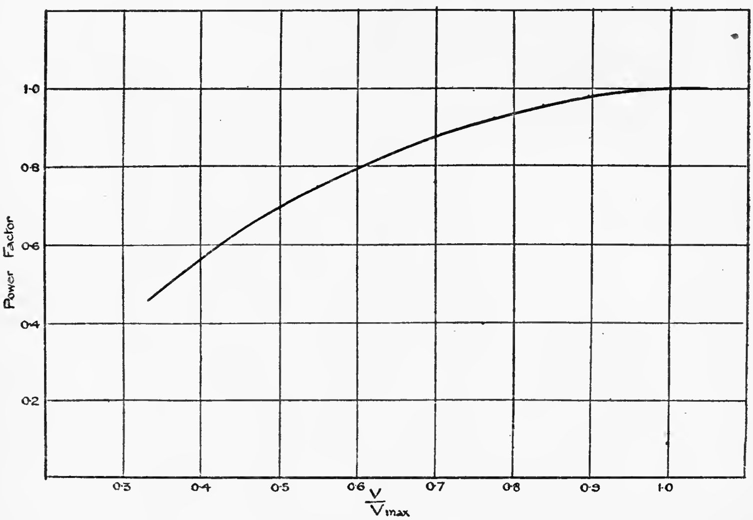

FIG. 277.—Power Factors from Typical Engine and Airscrew Curves.

Horse-power required.—Having obtained the total resistance, the horse-power required is obtained by multiplying by V/550. The results are tabulated below:—

V/550 ...	·288	·229	·199	·167	·148	·134	·124	·117	·114
H.P. ...	208	112	74·5	48·5	40	36·5	34·4	33·5	38

Horse-power available.—It will be assumed that the engine and airscrew are designed to give the maximum efficiency at a forward speed of 100 m.p.h., and that the variation in power at other speeds follows a curve similar to that shown in Fig. 277.

TABLE LVII.

V (m.p.h.) ...	100	90	80	70	60	50	40
V (f.p.s) ...	146·8	132	117·2	102·8	88	73·4	58·7
V/V_{max}	1·0	·9	·8	·7	·6	·5	·4
F_p from curve ...	1·0	·98	·94	·88	·80	·70	·56
H.P. available ...	120	118	115	106	96	84	67

In the above table the horse-power available is obtained by multiplying F_p by the horse-power of the engine (150) and by the maximum efficiency of the airscrew (0·8). The curves of

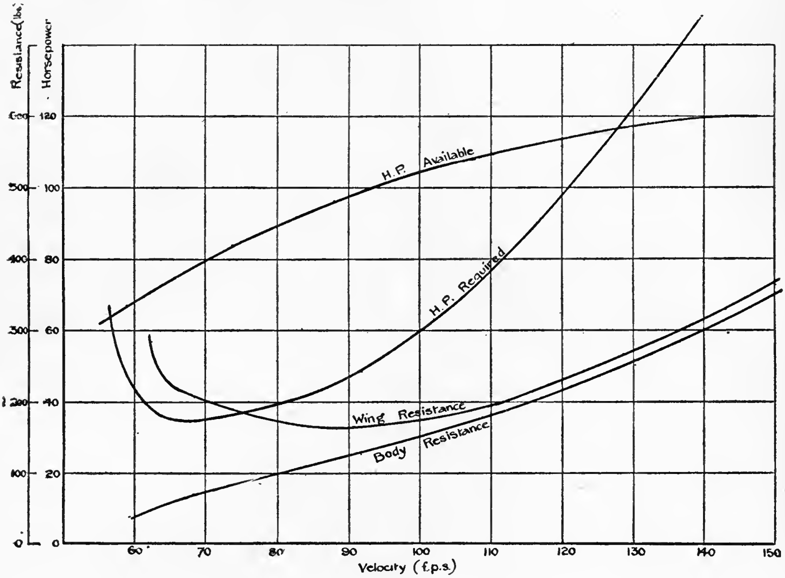

FIG. 278.—Performance Curves.

horse-power required and horse-power available must now be plotted on a speed base, as shown in Fig. 278. The intersection of the curves shows the maximum speed which the machine is capable of attaining—namely, 128 f.p.s. or 87 m.p.h. The maximum horse-power available for climb is 52 at a forward speed of 85 f.p.s., whence the maximum rate of climb

$$= \frac{52 \times 33000}{2000} = 860 \text{ feet per minute.}$$

A further practical example of the calculation of the performance of a machine is given in Chapter XIII.

Measurement of Performance.—Having dealt with the method of predicting performance for a machine of new design, it is desirable to consider various experimental methods whereby the actual performance of such a machine when built can be checked. The chief difficulty met with in making these measurements is due to variation in the medium in which flight occurs. As is generally known, the pressure, and consequently the density of the atmosphere, diminishes with increasing altitude. Further, as has already been shown in Fig. 7, there is also a fall in the temperature. The instruments for the measurement of performance are directly dependent upon the condition of the air, and it is this fact which renders the accurate measurement of the performance of a machine a difficult operation. In addition to the above variations, it must also be borne in mind that the temperature may vary very considerably at the same altitudes, owing to up and down air currents, to seasonal changes, and to change of latitude. Much of our knowledge of this subject is due to Mr. W. H. Dines, F.R.S., who has carried out and controlled observations for several years. Table LVIII. is a summarised result of his labours.

TABLE LVIII.—MEAN ATMOSPHERIC PRESSURE, TEMPERATURE, AND DENSITY AT VARIOUS HEIGHTS ABOVE SEA LEVEL.

Height in kilometres.	Feet.	Mean pressure millibars.	Mean temp. C° abs.	Mean density kgm/cu. metre.
0	0	1014	282	1·253
1	3280	900	278	1·128
2	6560	795	273	1·014
3	9840	699	268	0·909
4	13120	615	262	0·818
5	16400	568	255	0·735
6	19680	469	248	0·658
7	22960	407	241	0·589

It is convenient to choose some density as a standard and to call it unity, and then to refer all other densities to this standard by expressing them as percentages of this standard density. The standard taken by the R.A.E. is the density of dry air at a pressure of 760 mm. and at a temperature of 16° C., where the density is 1·221 kgm. per cubic m. In order therefore to obtain a strict basis of comparison, all observed aeroplane performances must be reduced to this standard.

TABLE LIX.—PERCENTAGE OF STANDARD DENSITY DUE TO CHANGE OF ALTITUDE.

Height.	Percentage of standard density.	Height.	Percentage of standard density.
0	102·6	11000	71·7
1000	99·4	12000	69·5
2000	96·3	13000	67·3
3000	93·2	14000	65·3
4000	90·3	15000	63·0
5000	87·4	16000	61·0
6000	84·6	17000	59·1
7000	81·9	18000	57·1
8000	79·2	19000	55·2
9000	76·5	20000	53·3
10000	74·0		

The Airspeed Indicator (Anemometer).—The measurement of the speed of a machine is the first essential of a performance test. This may be made either by direct measurement of the time taken to cover a measured distance or by using a speed indicator, which must, however, have been calibrated by the direct test. The method of carrying out the direct test will be considered subsequently.

Briefly summarised, the requirements and conditions of aeronautical airspeed indicators are as follows:

1. *Weight and Head Resistance.*—Must both be small.

2. *Mechanical Strength.*—The severe conditions of vibration preclude the possibility of using instruments which are not mechanically strong, or which cannot be made so without the addition of undue weight. Both the head proper, and the transmitting and indicating parts, must be simple, light, strong, and free from the need of delicate adjustment or frequent testing.

3. *Position.*—The head must, so far as practicable, be out of reach of irregular currents or eddies, and therefore at some distance from the indicator, which of course must be placed in the pilot's cockpit. The best position would appear to be towards the end of a wing-tip if the transmission gear can be made satisfactory.

4. *Influence of Gravity.*—On account of the very considerable angles of heeling and pitching which occur in flight, any instrument which depends for its action upon weights or a liquid manometer is useless. Any required forces must be applied by means of springs, or if pressures are to be registered it must be

by means of spring gauges. Further, all parts of the instrument must be so balanced that in any position the readings are independent of the effect of gravity.

The ordinary form of speed indicator is the Pitot Tube, which is an instrument measuring the pressure difference between a current of moving air and the corresponding stationary air. It consists essentially of two tubes, namely, the dynamic tube, the end of which is open to and faces the moving air stream; and the static tube, which carries a ring of concentric holes over which the air stream flows. The underlying theory of the Pitot tube is fairly simple.

Let V = velocity of the air stream
w = weight of 1 cubic foot of air
p = static or barometric pressure
h = potential pressure head

Then by Bernouilli's theorem:

$$h + \frac{p}{w} + \frac{(V)^2}{2g} = \text{constant}$$

Now for horizontal motion the potential pressure head h remains constant; hence we may write

$$\frac{p}{w} + \frac{(V)^2}{2g} = \text{constant}$$

Let P be the so-called dynamic pressure transmitted by the inner tube. At the mouth of this tube the velocity is reduced to zero, hence

$$\frac{P}{w} + 0 = \frac{p}{w} + \frac{(V)^2}{2g}$$

Or

$$\frac{P - p}{w} = \frac{(V)^2}{2g}$$

The quantity $(P - p)/w$ is the difference in pressure measured by the manometer. Denoting this by H, the above expression may be written

$$(V)^2 = 2gH$$

In order to allow for errors in construction, the law of the Pitot tube is generally written

$$(V)^2 = K \cdot 2gH \text{ .... Formula 99}$$

where K is a correction factor to be determined by calibration of the actual tube. It is generally equal to unity.

The advantages of the Pitot tube over other instruments are:

1. Absence of any kind of friction, as there is practically no displacement of air along the the tube.
2. Comparative ease of reproducing exactly similar tubes, thus obviating the necessity of individual calibration.
3. Very small wind resistance.

If the potential pressure head in Formula 99 is read on a gauge containing a liquid of density '*d*,' while the density of the air current is ρ, the above equation takes the form

$$V^2 = K \cdot 2gH\frac{d}{\rho}$$

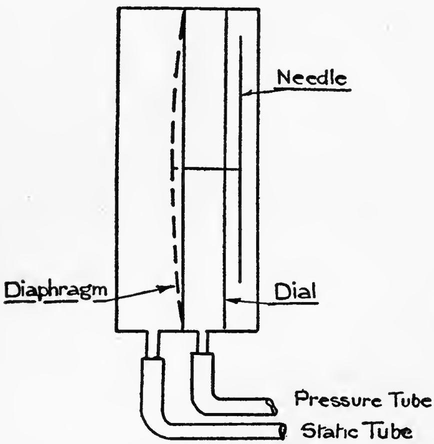

FIG. 279.—Airspeed Indicator.

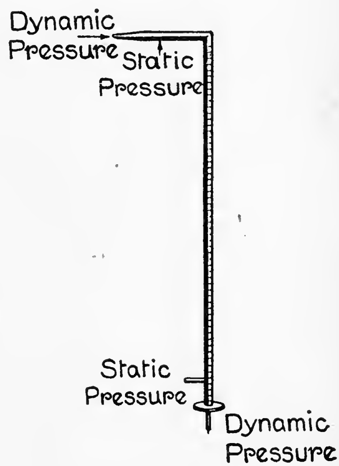

FIG. 280.—Pitot Tube.

Recent investigations have shown that almost any form of dynamic opening is satisfactory, but that the static opening must be specially designed in order that the coefficient K may be equal to unity.

When used on an aeroplane, the Pitot tube is generally fitted to the leading edge of the top wing and to one side of the centre line of the machine, so as to be out of the slip stream of the airscrew. The speed-indicator dial is fixed in the pilot's cockpit, the general arrangement being shown in Fig. 279. The dynamic pressure of the air is transmitted to a small airtight cylinder divided into two parts by a rubber diaphragm, the space on the opposite side of the diaphragm being connected to the static tube. The movement of this diaphragm under the action of the air forces is communicated to a needle which registers the air speed. These instruments are carefully calibrated by means of the ordinary type of Pitot tube, shown in Fig. 280.

Another form of airspeed indicator depends upon the principle of the Venturi meter, familiar to students of hydraulics. The Venturi tube consists of a short converging inlet followed

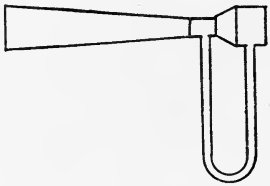

FIG. 281.—Venturi Airspeed Indicator.

by a long diverging cone, the entrance and exit diameters being usually made equal, so that the instrument may be inserted as part of a pipe line. (See Fig. 281.) As shown, there is generally a short cylindrical throat, and the converging part has somewhat the shape of a 'vena contracta,' but its exact form is not important. The exit cone has a total angle of about 5°, this angle having been found to give the minimum frictional loss for a given increase of diameter. When a current of fluid passes

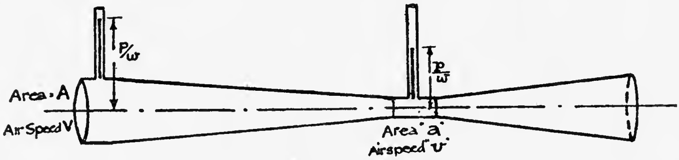

FIG. 282.—Venturi Tube.

through the tube the pressure in the throat is less than at the entrance to the converging inlet by an amount that depends upon the ratio between the entrance area and the throat area, the density of the fluid, and the speed of flow. If the tube is provided with side holes and connections to a differential gauge by which this pressure difference may be observed, it constitutes a Venturi meter. The ratio between the areas is a known constant for a given instrument, so that when the density of the fluid is known the observed pressure difference may be used as a measure of the speed of flow. Such an instrument may be used as an anemometer by pointing it so that the wind blows directly through it, and the observed 'head' may then serve as a measure of the wind speed. This method has recently been adopted in an aeroplane anemometer.

Theory of the Venturi Tube (see Fig. 282).

Applying the Bernouilli Theorem to a horizontal tube, we have

$$\frac{v^2}{2g} + \frac{p}{w} = \frac{V^2}{2g} + \frac{P}{w}$$

or $$\frac{v^2 - V^2}{2g} = \frac{P - p}{w} = H$$

whence $$v^2 - V^2 = 2gH$$

Further $$VA = va$$

therefore $$\left(\frac{VA}{a}\right)^2 - V^2 = 2gH$$

or $$V = \frac{a}{\sqrt{A^2 - a^2}}\sqrt{2gH} = B\sqrt{2gH}$$

.... Formula 100.

Now if $A = a\sqrt{2}$, B will be equal to unity, and the observed Venturi pressure difference will be the same as that shown by a Pitot tube.

It is obvious, however, that the Venturi pressure difference can be made very much larger than the Pitot pressure difference at the same entrance speed, and consequently the gauge reading with a Venturi tube anemometer can be made more sensitive.

At high speeds the compressibility of the air must be taken into account and allowed for in the development of the equation. Since the pressure difference may be made so much greater than with the Pitot tube, the problem of making a satisfactory spring gauge for indicating the pressure is much simpler, and this type will probably be considerably developed in the near future.

It will be observed that the measurement of velocity by the use of instruments such as have just been described introduces consideration of the density of the air. This we have already shown varies with the altitude, hence the indicator will only give correct readings at one particular altitude where the density is such as to agree with that for which the scale on the instrument was calibrated. It is therefore necessary to introduce a correction factor in order to make allowance for this. Reference to the formula for the pressure head on these instruments shows that this correction is proportional to the density, and the square of the velocity, that is to say,

$$H \propto \rho V^2$$

To correct the indicator reading for any altitude at which the density (ρ') differs from the standard it is necessary to divide the reading by the square root of the percentage density at the height in question, that is

$$\text{True speed} = \frac{\text{Indicated speed}}{\sqrt{(\text{Percentage density at altitude considered})}}$$

Performance Tests on full-scale Machines. — Having enumerated the various factors to be considered in making an observation of the velocity of a machine in flight, the manner in which the direct test method is carried out will now be indicated. The tests about to be described are those used at the Royal Aircraft Establishment, and are taken from lectures read before the Royal Aeronautical Society by Captains Tizard and Farren. The simplest test is that known as the ground speed course, in which the aeroplane is flown over a measured distance (of 1000 yards) at a height of a few feet from the ground. Observation stations are placed at each end of the course. At each station an observer is stationed, with a stop watch and an electric bell switch connected to a bell placed in the other station. Upon the leading edge of the aeroplane passing the sight of the first observer, he starts his stop watch and presses the bell switch simultaneously. When the observer at the other end hears his bell ring, he starts his watch. The reverse series of operations are carried out at the end of the course, the second observer stopping his watch and pressing the switch of the first observer's bell as the leading edge of the machine passes his sight. The actual time taken for the aeroplane to fly over the distance between the stations will be very accurately given by the mean of the times indicated by the two stop-watches. To take into account a light side wind, the machine is allowed to drift with the side wind away from the measured line, such variation from the exact distance making practically no difference to the accuracy of the result.

A second method is known as the altitude speed test. In this case the machine flies over a measured distance of about 4000 yards at an altitude of approximately 3000 feet. The flight path is observed by means of a reflecting prism and telescope, the combined instrument being capable of rotation about an axis such that the aeroplane can be kept in view throughout unless the deviation exceeds 800 feet. The observations are similar to those of the first method. As the aeroplane passes across the telescopic sight of the first instrument, the time is observed by the first observer, who proceeds to follow the flight of the machine by rotation of his instrument. When the machine passes over the second station, the observer there signals to the first station, and automatically fixes the position of the instrument of the first observer. The times in this case are all recorded automatically at one end of the course. The disadvantage of this method is the difficulty of accurately measuring the velocity and direction of the wind.

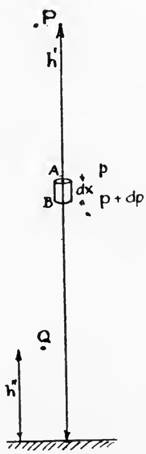

Fig. 283.

This is approximately achieved by firing a smoke puff from a Verey pistol, and tracing its subsequent path by means of a camera obscura, the velocity of the wind being assumed constant along the course. In order to increase the accuracy of this test, the machine flies up and down the course several times.

A third method is to apply the camera obscura observation of the smoke puff to the observation of the flight of the machine itself.

Rate of Climb Test.—The measurement of rate of climb is generally carried out by observing the time taken to climb a given distance, this distance being measured by means of an aneroid barometer. This instrument is really a pressure indicator, and measures the height in terms of the variation of pressure due to change of altitude, the scale of the instrument being graduated to read height instead of pressure.

Theory of the Aneroid Barometer.—Let P and Q be two points at altitudes h' and h'' respectively (see Fig. 283). It is required to find the vertical height between them in terms of the pressure of the atmosphere.

Take two points, A and B, situated very close to one another, and let the pressure per square inch at A be p and at B be $p + dp$, and the distance between A and B be dx. Then the increase in pressure at B is due to the weight of the small column of air, of height dx and one square inch in cross section, that is

$$(p + dp) - p + \rho g dx = 0$$

where ρ is the mean density of the air between A and B. If the air be at constant temperature, the density is proportional to the pressure, that is

$$\rho \propto p$$

Or $$\rho = kp$$

Substituting in equation above

$$dp + kpg dx = 0$$

Or $$\frac{dp}{p} + kg dx = 0$$

Integrating

$$\log_e p + kgx = \text{constant.}$$

If p' be the pressure at P, and p'' the pressure at Q, then

$$\log_e p' + kgh' = \log_e p'' + kgh''$$

Or $$h' - h'' = \frac{1}{kg} \log_e \frac{p''}{p'}$$ .... Formula 101.

That is, the difference in altitude is equal to difference between the Napierian logarithms of the pressures multiplied by a constant.

Formula 101 has been obtained on the assumption that the temperature of the atmosphere remains constant, but since this is not the case, it is necessary to introduce a temperature correction factor for the aneroid readings, unless a temperature correction device has been incorporated in the instrument.

The aneroid or altimeter (see Fig. 284) consists essentially of a shallow corrugated metal drum from which the air has been exhausted. A strong spring attached to the top of the drum enables it to withstand the atmospheric pressure tending to crush it. With increase of altitude the pressure on the exhausted chamber diminishes, thereby allowing the spring to distort it.

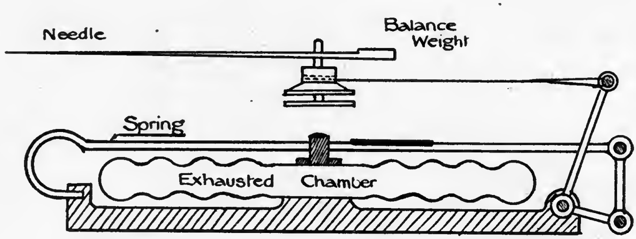

FIG. 284.—Aneroid Altimeter.

The ensuing movement of the drum is communicated to the indicator by means of a delicate mechanism of the nature shown in Fig. 284.

In order to provide for the variation of atmospheric pressure at ground level, a thumbscrew is provided whereby the needle can be adjusted to zero position on the scale. The variation in temperature is allowed for by means of a steel and brass

FIG. 285.

compensating device fixed to one of the levers. The unequal expansions of these two metals provides the necessary correction.

Measurement of Rate of Climb.—This measurement is made in several different ways. Either the time to climb a definite height, or the height attained in a definite time, may be measured. The horizontal speed is varied over definite steps ranging from the minimum to the maximum possible at the altitude in question, and the rate of climb measured in each case with the engine at full throttle. By plotting the results obtained it is easily seen at which speed the maximum climb is attained and the corresponding value. An instrument called a climb-meter has also been devised. It consists of a Dewar vacuum flask, which communicates with the outer air through a piece of glass tubing which is arranged with an air trap at

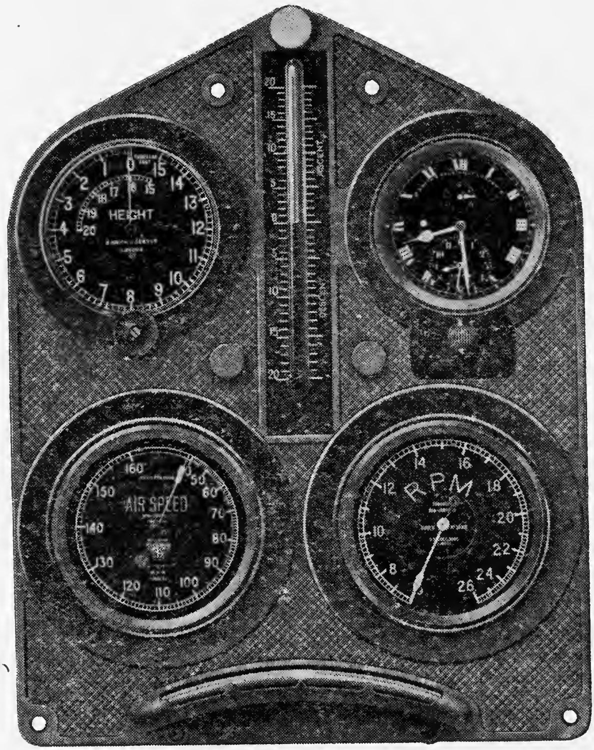

Fig. 286.—Aviation Instrument Board.

(By courtesy of Messrs. S. Smith & Sons, Ltd.)

each end. The trap serves to limit the path of a small drop of liquid, which acts as an air seal when the internal and external air pressures are equal. (See Fig. 285.) A manometer tube connected to the flask serves to indicate the difference between the internal pressure and that of the atmosphere. As soon as the machine commences to climb, the pressure of the atmosphere is diminished, and the greater pressure inside the flask forces the drop of liquid to the trap furthest away from it, thus allowing the air to escape. During climbing, therefore, the internal pressure always tends to be greater than the external, and the enclosed air escapes through the trap. When the machine is climbing at its maximum rate the difference of pressure between the inside and outside of the flask is greatest, and this will be indicated by the maximum difference in level of the manometer tube attached to the flask. The pilot therefore adjusts the attitude of his machine until this condition is attained. To indicate when the machine is flying horizontally a Statoscope is used. This instrument is similar in principle to the Climbmeter. In this case, however, the pilot will adjust the drop of liquid (Fig. 285) until it is in the central position.

From the foregoing remarks it will be seen that the number of instruments requiring attention on the part of the pilot for flying the machine are fairly numerous, in addition to which further instruments are required for controlling the engine. In order to arrange these instruments conveniently for use and observation, various types of instrument boards have been devised. Fig. 286 shows an instrument board designed by Messrs. S. Smith & Sons.

A summary of the various measurements to be made in the test of performance may now be given.

1. Flying speed.
   - (*a*) The engine revolutions and the airspeed are noted when flying level with full throttle.
   - (*b*) From the aneroid reading and temperature observation at each height the density is obtained. The reading of the airspeed indicator is then corrected by dividing by the square root of the density.
   - (*c*) These corrected results are plotted against the average height in feet. An example of such a test is given in Tables LX. and LXI.

2. Rate of climb.
   - (*a*) The aneroid height every 1000 feet is observed, together with the corresponding times from the start.
   - (*b*) The observed times are then plotted against aneroid heights. From the curve obtained, the rate of climb at any point can be obtained from the tangent to the curve at that point.

Table LXII. gives the results of a Rate of Climb Test.

Table LX.—Calibration of an Airspeed Indicator by Direct Test.

Run No.	Measured ground speed m.p.h.	Measured wind-speed.	Wind direction.	Corrected true speed.	Observed height (aneroid).	Observed temperature.	% Standard density.	Observed air-speed.	$\frac{\text{Airspeed.}}{\sqrt{\text{Density}}}$.	Correction.
1	59·1	31·0	161·5°	89·2	5100	31·0°	0·879	80	83·6	3·6
2	123·4	28·6	5·5°	93·7	5100	31·0°	0·879	85	87·8	2·8
3	62·0	32·3	168·5°	93·8	5050	31·0°	0·881	85	88·1	3·1
4	124·7	32·3	21·0°	95·6	5000	31·0°	0·882	86	88·8	2·8

Mean = 3·1

Table LXI.—Airspeed at Heights.

Aneroid height (feet).	Observed temperature (F.).	Density.	Corresponding standard height.	Observed airspeed.	From calibration tests.	Corrected for density.	R.P.M. of engine.
3000	39°	·935	2900	95	98	101·5	1280
			3000			103·0	1290
5000	35°	·875	4900	93	96	102·5	1280
			6500			100·5	1250
7000	30°	·821	6900	88	91	100·5	1240
9200	24°	·767	9000	81	84	96·0	1220
			10000			96·5	1215
10800	19°	·731	10400	80	83	97·0	1220
12800	17°	·682	12600	72	75	92·0	1200
			13000			94·0	1180
13800	12°	·664	13400	68	72	88·5	1180
			15000			86·0	1160
15200	8°	·636	14800	64	69	86·5	1160

TABLE LXII.—RATE OF CLIMB TEST.

Height in feet aneroid.	Observed temperature (F.).	% Standard density.	Observed time (minutes).	Rate of climb feet per minute.
1000	37°	101·0	1·00	814
2000	38°	97·2	2·10	718
3000	36°	94.2	3·70	622
4000	36°	90·7	5·40	544
5000	36°	87·4	7·25	495
6000	33°	84·7	9·4	435
7000	30°	82·1	11·9	389
8000	26°	79·9	14·25	347
9000	26°	77·6	17·00	312
10000	23°	74·7	20·25	294
11000	21°	72·2	23·6	264
12000	20°	69·8	27·4	216
13000	17°	67·7	31·9	182
14000	12°	65·9	37·9	139
15000	8°	64·1	45·25	101

CHAPTER XIII.

General Lay-out of Machines.

The process of laying out an aeroplane varies considerably in different drawing offices, some of the methods adopted being excellent examples of correct procedure, while in many other cases 'rule-of-thumb' ideas prevail. As a painful illustration of the latter method, or perhaps more correctly lack of method, we outline how a machine is designed in an aeronautical drawing office with which we are acquainted.

The designer decides upon a new machine, and guesses at the complete weight. The area of the wings is then obtained by dividing this weight by seven, probably in order to give an approximate loading of seven pounds per square foot. A draughtsman is then summoned, and instructed to get out a side elevation, and sometimes a plan, being told the type of engine, the number of passengers, the quantity of petrol to be carried, the stagger and the chord. The draughtsman is then compelled to arrange his weights by a process of wangling, and usually puts in the size of the fin, rudder, and tail plane by 'eye.' This drawing is then passed on to the fuselage expert, who runs out a drawing of this unit, while the first draughtsman stresses the wings and settles the section, spars, and other details. The whole staff is then employed on preparing detail drawings for the shops, and on completion the building of the first machine is commenced. At this stage the designer has a walk round, and promptly proceeds to alter the majority of the details, fresh drawings are prepared, and the process is repeated. After several alterations the machine approaches completion, and then possibly a general arrangement is prepared. In the hands of a genius such a manner of lay-out may produce excellent results, but it is neither scientific nor up-to-date.

In order to produce an economical, successful, and scientific design, requiring very few alterations while in course of manufacture in the shops, careful attention must be paid to the points outlined in the preceding chapters, and we will now show how to apply these chapters to the design of machines. For the purpose of illustration we will consider the design of a biplane having a speed of 120 miles per hour at 10,000 feet, a landing speed of 50 miles per hour, a radius of action of 480 miles, and capable of carrying at least 500 lbs. of useful load, excluding fuel. Referring to Table XL., we see that the useful load represents approximately 14% of the total weight of the machine, so that we have

$$\text{Total weight} = \frac{100}{14} \times 500$$
$$= 3570 \text{ lbs.}$$

For the present this weight will be taken as 3500 lbs., and at once from Table XL. we get the following estimate of the weights of the various components :

	lbs.	lbs.
I. THE POWER PLANT.		
(*a*) Engine	700	
(*b*) Radiators	87·5	
(*c*) Cooling water	70	
(*d*) Tanks, etc.	105	
(*e*) Airscrew, etc.	87·5	
		1050
II. THE GLIDER.		
(*a*) The wings	455	
(*b*) The wing bracing ...	105	
(*c*) The tail unit	70	
(*d*) The body	455	
(*e*) The chassis	140	
		1225
III. USEFUL LOAD.		
(*a*) Fuel	700	
(*b*) Passengers, etc. ...	490	
		1190
IV. Instruments, etc.		35
Total weight		3500

Before proceeding further it is necessary to determine whether the estimated weight of power plant will permit of an engine of sufficient power to give the required performance. This brings us to a consideration of the supporting surfaces.

In Chapter III., on wing sections, we saw that the essential features of a wing section, to give a good range of speed, were as follows :

(*a*) A high value of the maximum lift coefficient (K_y max.) ;
(*b*) At small angles of incidence the value of K_y may be small, but the value of the L/D ratio must be large.

The maximum landing speed required will determine the first of these requirements, while the relative merits of various aerofoils, in order to fulfil the second requirement to the best advantage, may be investigated as follows. The most efficient aerofoil at the speed required will be the one which offers the least resistance (drag). The lift on the wings is equal to the weight of the machine, and is therefore the same on each aerofoil section. The best type of aerofoil to use, therefore, is the one which has the highest value of L/D at the required speed 'V', that is, at a value of

$$K_y = K_y\,(\text{max.}) \times \left(\frac{V_L}{V}\right)^2$$

where V_L is the landing speed.

By examining the characteristics of a number of aerofoils by means of this equation, the most suitable section from a theoretical standpoint is determined. Practical considerations, such as ease of manufacture of ribs, spars, etc., may lead to modification in the type selected, but the underlying principles of wing design should be based on such an investigation.

The Wing Sections shown graphically at the conclusion of Chapter III. have been investigated with this end in view, and Fig. 76 (Section No. 10) represents the section and aerodynamic characteristics most suitable for the present design.

It will be seen that the maximum value of K_y is 0·63. For a landing speed of 50 m.p.h. the necessary wing area is given by the equation

$$\text{Area} = \frac{W}{\frac{\rho}{g} K_y V^2}$$

$$= \frac{3500}{\cdot 00237 \times 0\cdot 63 \times 73\cdot 3 \times 73\cdot 3}$$

$$= 435 \text{ square feet.}$$

Allowing for loss of efficiency of aerofoil due to the biplane arrangement, and taking a factor of ·8, we find that the area of supporting surface required

$$= 540 \text{ square feet.}$$

Having decided upon the most suitable wing section, we are now in a position to form an estimate as to the engine horsepower necessary to enable the required performance to be obtained.

This can be roughly investigated as follows: The value of the lift coefficient required at a speed of 120 m.p.h. when flying at 10,000 feet, where the value of ρ/g is ·00177,

$$= K_y = \frac{3500}{\cdot 00177 \times 540 \times 176 \times 176}$$

$$= \cdot 118$$

On looking at our curve of aerofoil characteristics, we see that for a value of $K_y = \cdot 118$ the corresponding L/D ratio is approximately 9·6, hence the drag of the wings under these conditions is 3500/9·6 = 365 lbs.

For the most economical speed of flight, namely, that corresponding to maximum L/D, the wing and body resistance are approximately equal. Upon this basis the total resistance of the machine will be twice that of the wings, that is, 730 lbs. This resistance must be balanced by the thrust of the airscrew, that is,

$$730 = \frac{\text{H.P. of engine} \times 550 \times \text{efficiency of airscrew}}{\text{Maximum flying speed}}$$

whence horse-power of engine required

$$= \frac{730 \times 176}{550 \times 0{\cdot}8}$$

$$= 292$$

The assumption made above, that the resistance of the body is equal to that of the wings, is approximately true only for the most economical speed of flight, and for speeds greater than this the body resistance will probably be greater than that of the wings; hence the total resistance assumed above is somewhat less than the true value at top speed. It is therefore advisable to insert an engine possessing greater power than that given above in order to be sure of obtaining the desired performance, and to have a reserve of power for unexpected contingencies.

Reference to Table XLI. shows that the most suitable water-cooled engines are the 350 h.p. Rolls-Royce and the 300 h.p. Hispano-Suiza; whereas, if an air-cooled engine were to be adopted, the 320 h.p. A.B.C. Dragonfly should be sufficient.

Using the particulars given in Table XLI., the following table showing the relative merits of these three engines for the purpose of the present design can be prepared:

	350 R.-R. lbs.	300 H.-S. lbs.	320 A.B.C. lbs.
Weight of power unit ...	933	596	600
Weight of fuel for 4 hours...	740	690	742
Total weight ...	1673	1286	1342

An examination of these particulars shows that the A.B.C. Dragonfly engine is the most suitable for our purpose, there being the additional advantage that it is an air-cooled engine, and therefore the weight allowed for radiator and cooling water will be available for useful load.

If this machine were intended for fighting purposes it would perhaps be advisable to use the 350 Rolls-Royce, in order to have a reserve of power for emergencies, and in order to be quite sure of obtaining the desired performance.

Having checked the estimated weights of the power plant, attention must be turned to the determination of the principal dimensions of the machine.

The total wing area having been already fixed, the next step is to decide upon the span and the chord. A suitable aspect ratio is 7, so that we have

$$S = 7\,C \quad \text{(i.)}$$
$$2\,S \times C = 540 \quad \text{(ii.)}$$

Solving these equations, we have

$$S = 44 \text{ feet.}$$
$$C = 6{\cdot}25 \text{ feet.}$$

In order to allow for 'end effect' and loss of centre portion we will make span 45 feet, and chord 6 ft. 3 in.

Gap.—It is next necessary to fix the amount of gap required. General aeronautical practice to-day makes the gap equal to the chord. When the gap is equal to the chord the loss in efficiency is equal to ·8 which was the figure adopted in calculating the extra area required on account of the biplane arrangement. We shall therefore make the gap equal to the chord, that is equal to 6 ft. 3 ins.

Stagger.—For fighting purposes a good field of view is essential, and as this is also a desirable attribute for general utility purposes we shall adopt a small amount of positive stagger, say one foot. When we come to consider the position of the centre of gravity of the machine at a later stage it may be necessary to modify this amount.

Dihedral.—Considerations relating to lateral stability make it advisable to give a small dihedral angle to the wings. A dihedral angle of 3° will therefore be adopted for the purpose of preliminary design.

The next step is to settle the length of the fuselage required. Generally speaking, it is found that in order to obtain a reasonable degree of controllability, the distance from the C.G. of the machine to the C.P. of the tail plane varies from one-half to one-third of the wing span. The span of our machine is 45 feet, hence a length of fuselage of 16 feet between the trailing edge of the lower wing and the sternpost should be sufficient.

Controls.—The next item in the design is the size of the lateral and longitudinal control surfaces. An empirical formula may be used to arrive at a first estimate of the size of the tail-plane and elevator, or recourse may be had to an investigation into the sizes adopted on similar machines. For our purpose we will use the following formula:

$$\text{Area of tail plane} = \frac{\cdot 4 \times (\text{area of wings} \times \text{chord})}{\text{Dist. between C.P. of wings and tail plane}}$$

$$= \frac{\cdot 4 \times 540 \times 6\cdot 25}{16}$$

$$= 70 \text{ square feet approx.}$$

We shall divide this area as follows:

Area of tail plane, 40 square feet.
Area of elevators, 30 square feet.

A common aspect ratio for the combined tail member is three, which gives us approximately 14 foot span and 5 foot chord. The section should be symmetrical and of sufficient depth to allow of a suitable spar.

RUDDER AND FIN.—The correct area of the rudder and fin is bound up with the question of the lateral stability of the machine, and as we are not yet in a position to investigate this mathematically or experimentally, it is advisable to fall back upon the size adopted in existing machines of similar type and similar dimensions. A suitable area of fin will be 12 square feet, and of rudder 18 square feet.

An alternative and very useful method of arriving at a rough estimate of the fin and rubber area required is as follows: A side view of the machine is drawn to scale on a piece of stiff cardboard. The outline is then cut out with a sharp knife, leaving a fairly wide margin round the proposed shape of the fin and rudder. The cardboard outline is then balanced on the edge of a knife placed perpendicular to the longitudinal axis of the machine, and the margin round the fin and rudder trimmed until balance is obtained at a distance of about 3″ (to the scale used for the model outline) behind the desired position of the centre of gravity of the machine. The weight on each side of the knife-edge approximates to the side force of the wind on the machine and thus gives a rough measure of the fin area required for stability.

It should be carefully noted that these areas for control surfaces are provisional, and before adopting them in the final design every effort must be made to investigate the stability of the machine according to the mathematical theory outlined in Chapter X.

General Arrangement.—We are now sufficiently advanced to lay out a scheme for the G.A. of the machine (see Fig. 287). The wings must first be drawn with their correct relative positions of gap, stagger, etc. It is customary to give them an initial angle of incidence with reference to the datum line of the fuselage, a common angle being 3°. The next step is to determine the mean chord of the biplane arrangement as set out in Chapter XI. The position of the mean chord enables the wing structure to be arranged relative to the remainder of the machine, as it is usual to distribute the weight of the machine

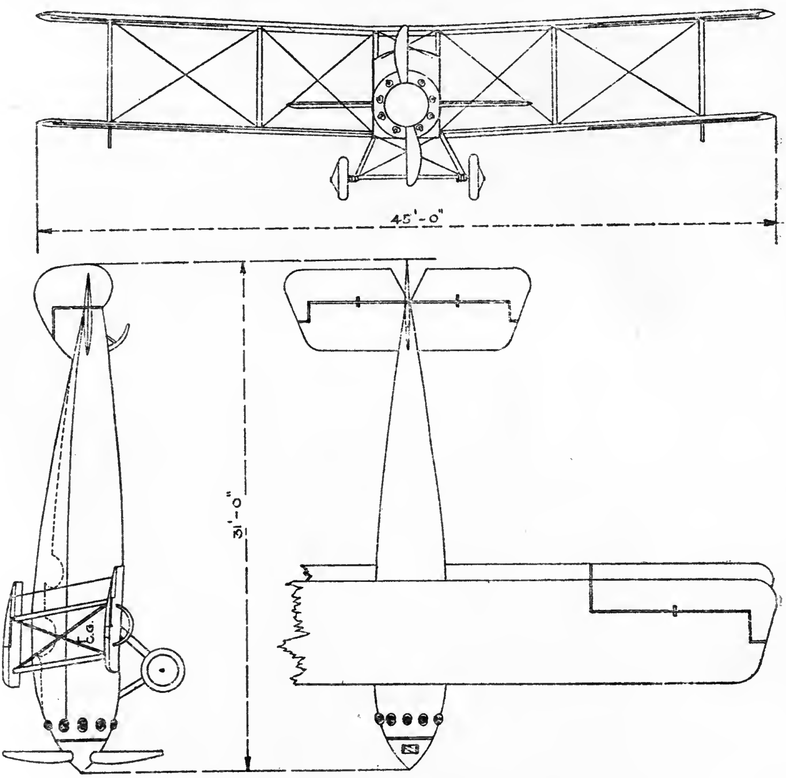

FIG. 287.—Lay-out of Aeroplane.

in such a manner that the C.G. of the whole machine is at a distance of ·35 × mean chord from its leading edge longitudinally and a few inches below vertically. This point is therefore marked on the side view of the wing structure, and the position of the C.G. of the remainder of the machine determined as under. This entails the drawing out of the fuselage and tail unit and the fixing of the various weights in their respective positions. Variable weights such as oil, fuel, passengers, etc., should be placed as near to the C.G. as possible. The cross section of the fuselage will be governed by the space necessary to house the engine, tanks, pilot, and passenger. Having settled these points a preliminary 'balancing up' can be completed.

For this purpose it is customary to take moments about a fixed datum line. A convenient line for this purpose is the vertical line through the nose of the machine. The estimated weight is then multiplied by its distance from this datum line, and thus the moment of each weight about this line is obtained. The sum of all these moments divided by the weight of the complete machine will give the position of the C.G. relative to the datum line selected. The work should be arranged in tabular form as shown in Table LXIII.

TABLE LXIII.—DETERMINATION OF THE POSITION OF THE CENTRE OF GRAVITY.

Description of part.	Weight. lbs.	Distance from datum. feet.	Moment.
Airscrew, etc. ...	87·5	1·0	87·5
Engine... ...	600·0	3·0	1800·0
Fuel	742	7·5	5565·0
Tanks	105	7·5	787·5
Fuselage ...	455	11·0	5005
Pilot	180	8·0	1440
Passenger ...	180	12·5	2250
Tail unit ...	70	28·0	1960
Instruments ...	35	7·0	245
	2454·5		19140

Distance of C.G. from the datum line

$= \bar{x} = 7·8$ feet from nose of machine.

It will be noticed that the chassis has been omitted in the above estimate. This is because its position is determined from the estimated C.G. in the manner set forth in Chapter VIII., and since this component acts close to the final position of the C.G. it can be neglected for the moment, as it will be partly balanced by the wings, which have also been omitted.

The next step is to superpose the drawing of the wing structure upon that of the body so that the longitudinal position of the C.G. of the machine is at ·35 times the mean chord, and also with the bottom of the fuselage resting on the lower plane.

The chassis can now be fixed in position relative to the C.G.

A second balance-up should next be undertaken, the wings and chassis being included this time and the position of the C.G. determined both horizontally and vertically. This is set out in Table LXIV.

As well as the G.A. drawing of the complete machine, general arrangement drawings of the different units should also be prepared, each preferably by an expert designer of each item, and the various details should be handed out to different draughtsmen to prepare. A standard size should be adopted for the G.A. drawings of complete machines, and another size for the G.A. drawings of the different units; while the detail drawings should be neatly arranged upon sheets of the same size as the latter drawings if only one machine is being built, while for quantity production it is advisable to have a separate sheet for each detail. The G.A. drawing of the complete machine should bear the serial number of the design, and the other sheets should all bear this number, and in addition should be lettered and numbered according to some systematic plan. The following scheme of lettering, being practically self-explanatory, has much to recommend it:—

Name of unit.	Distinguishing letter.
Fuselage	F
Tail skid	F—TS
Tanks	F—T
Engine installation	F—EI
Fuselage, stress diagrams	F—SD
Wings	W
Wings, stress diagrams	W—SD
Interplane struts	W—S
Wings, wiring	W—W
Tail-plane unit	TP
Chassis	U
Chassis, stress diagrams	U—SD
Controls	C
Engine controls	C—E
Instrument board	I
Part lists	PL

Detail sheets belonging to each series will be consecutively numbered, the G.A. sheet of the series being number one, of course. For example, the G.A. sheet of the tail-plane unit for a machine whose design number is 55 would be numbered 55—TP—1, and the fifth sheet of details of the same tail-plane unit would be numbered 55—TP—5.

The position of the wing structure relative to the fuselage having now been fixed, the side view of the machine can be completed. It is advisable to make this arrangement as detailed as possible. The main dimensions should be inserted in some decimal unit in order to facilitate calculations, and great care should be taken to see that the drawing is correct to scale.

The fuselage between the rear chassis struts and the nose of the machine should be amply strong, and the engine-bearers should be supported on stout ribs built up of three-ply wood. Longerons should be made of ash about $1\frac{1}{4}''$ square, tapering to about $1''$ square at the sternpost.

The fuel and oil tanks should be drawn in their correct positions, and provision made for strapping to the fuselage.

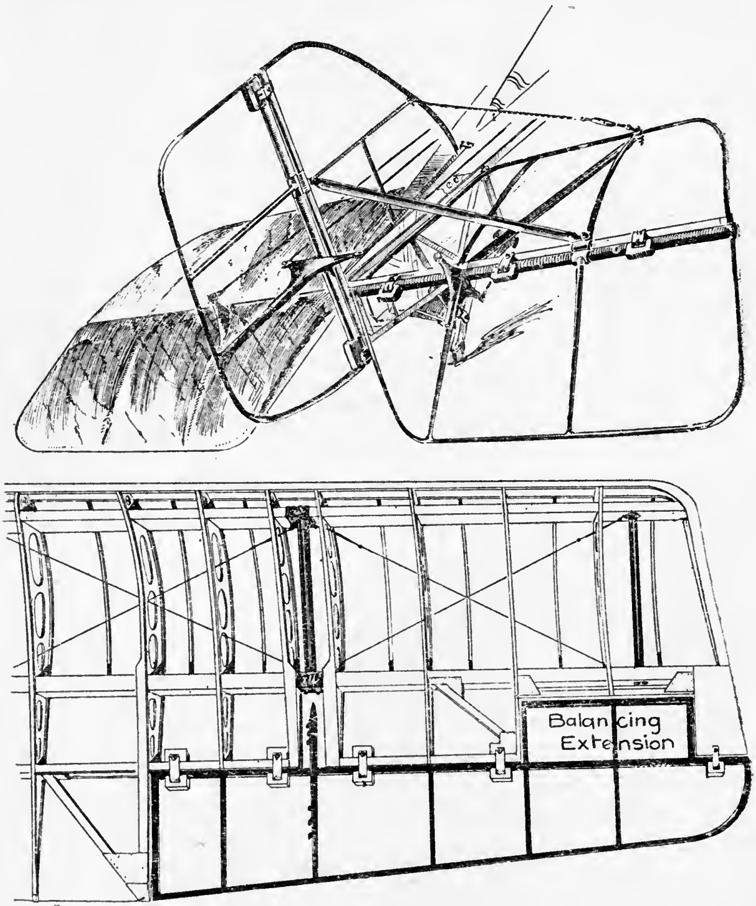

FIG. 274.—Tail Unit Components. (See also p. 379.)

The engine and control connections may with advantage be drawn in red ink. A strong cross strut should be introduced to take the thrust of the rudder bar ; and footboards run in for the pilot and passenger. About $1\frac{1}{4}''$ diameter tube will be suitable for the control lever.

The instrument board position should be drawn in, allowing ample clearance for the control lever and a long-legged pilot's knees. A low shield affixed to the fuselage, and streamlining the forward end of the openings to the cockpits, will spill the air over these openings, and thus reduce resistance in the open design. These openings may be cut out of thin three-ply wood. Elsewhere three-ply should be avoided on account of its weight (except around the engine forward, where it may be used in place of bracing wires), and also on account of its dangerous splinters in the case of a crash.

Join the longerons together forward by means of a nose-plate made of sheet steel of about No. 16 S.W.G., lightened out wherever possible, and with its edges turned up to give stiffness and to act as corner sockets. A ball-bearing for the airscrew shaft may be introduced if required on this plate. The longerons aft should be joined together in pairs and attached to the sternpost. The sternpost may be either tubular or of wood, and the rudder should be hinged to it. The main spar of the tail plane may also be attached at this point, the front spar being attached to a vertical strut in the fuselage.

The elevators are hinged to the rear spar of the tail plane, and 10 mm. tubing may be used for the trailing edges of elevators and rudder. Cable levers should be short and of streamline form.

The sternpost should be streamlined above the fuselage with the fin, and below the fuselage should be used for attachment of a small tail skid. The static moment on this tail skid may be determined by taking moments. Rule a line from the base of the wheels to the end of the skid and project the position of the C.G. of the whole machine on to this line, and the moment at once follows. The tail skid should be designed to withstand a load several times greater than this static load in order that it may survive the shock of a bad bump. It will be advisable to recalculate the position of the C.G. of the machine. If it is found that the machine is coming out nose-heavy—that is, that the C.G. is too far forward—then the balance may be adjusted by moving the engine back. On the other hand, if the machine is coming out tail-heavy, then the engine may be placed further forward. For example:

Let a be distance of the C.G. in front of the required position
W be the total weight of the machine
w be the weight of the engine or other parts to be moved
x be the distance required

then $w\,x = W\,a$

or $x = W\,a/w$

TABLE LXIV.—BALANCING.

Item.	Estimated. Weight. W.	Distance from nose of machine. Ft. D.	Moment. W × D.	Longitudinal.	Measured. Weight. W.	Distance D.	Moment. W × D.
Airscrew ...	87·5	1·0	87·5				
Engine ...	600	3·0	1800	∴ Long$^{\text{l}}$			
Fuel ...	742	7·5	5565	pos$^{\text{n}}$ of C.G.			
Tanks ...	105	7·5	787·5				
Chassis ...	140	6·5	910	$\bar{x} = \frac{24250}{3154 \cdot 5}$			
Wings ...	560	7·5	4200				
Fuselage ...	455	11·0	5005	$= 7 \cdot 70'$			
Pilot ...	180	8·0	1440	from nose			
Passenger..	180	12·5	2250	of machine.			
Tail unit ...	70	28·0	1960				
Instruments	35	7·0	245				
	3154·5		24250				
		Distance from ground.		Vertical.			
Airscrew ...	87·5	6·25	547				
Engine ...	600	6·25	3750	Vert$^{\text{l}}$ pos$^{\text{n}}$			
Fuel ...	742	6·5	4820	of C.G.			
Tanks ...	105	6·5	683				
Chassis ...	140	2·0	280	$\bar{y} = \frac{20211}{3154 \cdot 5}$			
Wings ...	560	7·5	4200				
Fuselage ...	455	6·25	2845	$= 6 \cdot 42'$			
Pilot ...	180	6·75	1215	from			
Passenger...	180	6·75	1215	ground line			
Tail unit ...	70	6·0	420				
Instruments	35	6·75	236				
	3154·5		20211				

The various members should be weighed after construction, and the C.G.'s of assembled parts, such as the wings and fuselage, should be checked experimentally by suspension. The table given for the determination of the C.G. can also be extended to give the longitudinal moment of inertia of the machine, and similar tables will give the vertical position of the C.G. and also the lateral moment of inertia. These moments of inertia are necessary for investigating the stability of the machine.

As it is of extreme importance that the calculated position of the C.G. should agree closely with its actual position upon the completed machine, it is necessary that the true position of the C.G. of the machine should be found before any test flight takes place.

All fittings to spars and longerons should be positively registered in place, and if it is absolutely necessary to pierce the timber to effect this, the cross-sectional dimension must be suitably increased at the hole. Similarly any local strengthening of steel tubing should be securely fastened in position. The radius used upon all plate fittings must not be less than the thickness of the metal employed in such fittings. Whenever it is found necessary to alter the angles or shapes of such fittings during erection, they must always be re-annealed after alteration. The keynote of the lay-out of the control system should be simplicity combined with accessibility. Simplicity in the design of the control devices leads to freedom from jamming, and accessibility ensures that the system receives adequate attention and lubrication. Complicated inspection doors should be avoided. The rudder should be controlled by means of an adjustable foot-bar, provided with leather heel supports; the elevator should be actuated by means of a column moving fore and aft; and the ailerons should be controlled by a sideways movement of the same column or by means of a wheel at the top of the column. For machines weighing over 5000 lbs. it is advisable to use balanced ailerons, rudders, and elevators. The ailerons should be interconnected, and ease of operation of the control column carefully studied.

As part of the fuselage drawings an engine installation drawing should be prepared. The general arrangement will show the leading features of the scheme, on the lines suggested in Chapter VII., and the details sheets will show the bearers, plates, etc. The G.A. drawing might with advantage also show the position of the radiators, tanks, etc. From these diagrams the various stresses can be worked out as required. The mounting of the engine should be of fireproof construction, and accessibility to the various parts of the engine requiring attention, such as magnetos, carburettors, pumps, etc., should be carefully considered. The engine controls should always be operated in a positive manner by means of rods or similar mechanism. Such rods should not exceed three feet in length unless provided with suitable guides to prevent springing. In order to keep the movements of the controls standardised they should conform to Air Ministry practice, that is, the throttle control handle moves forward to open the throttle, the altitude control handle moves forward to weaken the mixture, the magneto control handle moves forward to advance the ignition, and the petrol-cock control handle moves forward for the 'ON' position. The corresponding name plates should be marked SHUT—OPEN; STRONG—WEAK; RETARD—ADVANCE; OFF—ON. The method of coupling up the various controls must be clearly marked on the drawings.

In arranging the disposition of the various tanks, care must be taken to see that petrol will be fed to the engine in any position the machine may assume in flight. Where several tanks are fitted, each should be separately connected to the main supply pipe to the carburettor. In these feed-pipes sharp corners must be avoided, or air-locks will form and cut off the petrol supply. It is a good plan to run them behind the longerons, which will serve as a protection. The clips with which they are attached should be lined with felt or similar material. The tank for the lubricant should be of sufficient size to hold from 15% to 25% more oil than is actually required by the engine for the length of run provided by the petrol tanks. It is a good plan to distinguish the oil pipes from the petrol pipes by using clips of distinctive colours, and the filler caps of the various tanks should be of ample size and clearly marked with the nature of the contents.

A quantity gauge for the petrol tanks should be inserted, also an air-release valve, and a pressure gauge for the oil, both gauges being placed in a convenient position for observation by the pilot.

Where a water-cooled engine is employed, a detail drawing should be prepared showing the radiator system, and reserve water should be carried at the rate of ·25 gallons per 100 h.p. per hour of fuel capacity. Radiator pipes should be clipped in the same manner as the petrol and oil pipes by a clip of a distinctive colour, blue being the colour usually adopted.

In the case of air-cooled engines the efficiency is largely dependent upon the manner in which the cowling is arranged to give an ample supply of air to the engine and oil sump. The cowling should provide protection to the magnetos, sparking plugs, and carburettors from rain, while still allowing easy access to these units by means of doors or quickly removable pieces.

The engine installation diagram should indicate the manner in which the exhaust gases are carried away from the exhaust manifold, and care must be taken to see that this pipe does not approach within six inches of any woodwork or fabric. Riveting is preferable to welding in the case of built-up exhaust pipes.

The engine-makers should provide an earthing switch for each magneto, and it should be possible to earth all the magnetos at once or separately, so that each magneto can be tested in turn. The earthing wires should not be jointed, and the main earth wire from the switch should be carried direct to the engine. All wires should be tested after installation, and must be capable of easy inspection.

From the completed general arrangement (Fig. 287) it is now possible to estimate the resistance of each item, and consequently the total resistance of the complete machine. From these particulars the centre of resistance of the machine can then be calculated. The resistance of each separate item should be estimated as carefully as possible, taking into account the slip-stream and interference effects wherever possible. Moments should then be taken about a fixed datum line in a similar manner to the balancing-up process, and the total moment divided by the sum of the resistances gives the line of action of the centre of resistance.

Body Resistance.—The estimate for the body resistance of the machine under design is shown in Tables LXV. and LXVI.

TABLE LXV.—BODY RESISTANCE. (OUTSIDE SLIP STREAM.)

ITEM.	Size.	Area. Sq. ft.	Resistance. lbs. at 100 ft. per sec. (R).	Distance above datum line (H).	R × H	REMARKS.
	Inches.					
Vheels	30 dia. 6 wide × 2	2·50	10·0	1·25	12·5	
xle	30 × 2	0·417	0·625	1·25	0·78	
ail plane ...	30 × 3	0·625	0·625	5·75	3·60	
nterplane struts outer	1·125 × 72 × 4	2·25	2·093	7·75	22·70	
nterplane struts inner	1·75 × 72 × 4	3·50	4·55	7·25	33·00	
ift wires—						
Front outer ...	134 × 0·09 × 2	0·168	0·545	7·75	4·23	
Front inner ...	72 × 0·14 × 2	0·140	0·455	7·25	3·30	
Rear outer ...	134 × 0·09 × 2	0·168	0·545	7·50	4·09	
Rear inner ...	72 × 0·11 × 2	0·110	0·358	7·0	2·50	
own wires—						
Outer F and R	130 × 0·09 × 4	0·325	1·055	7·75	8·17	
Inner F and R	112 × 0·11 × 4	0·342	1·110	7·25	8·05	
ing struts ...	36 × 1 × 2	0·50	2·50	3·5	8·75	
ileron levers ...	8 × ¾ × 4	0·166	0·415	11·0	4·56	
TOTAL ...	—	—	25·72	—	116·23	

entre of Resistance of Components out of Slip Stream $= \frac{116·23}{25·72} = 4·52'$ from datum.

Table LXVI.—Body Resistance. (In Slip Stream.)

Item.	Size.	Area. Sq. ft.	Resistance. lbs. at 100 ft. sec. out of slip.	Distance above datum line (H) ft.	R × H	Remarks.
	Inches.					
Wheels	0	—	0	—	—	
Axle	54 × 2	0·75	1·125	1·25	1·41	
Front struts (chassis) ...	30 × 1·25 × 2	0·521	0·680	2·75	1·87	
Rear struts ...	30 × 1·25 × 2	0·521	0·680	2·75	1·87	
Bracing lift Wires front ...	42 × 0·14 × 2	0·082	0·266	7·25	1·93	
Bracing lift Wires rear ...	42 × 0·11 × 2	0·064	0·208	7·0	1·46	
Body	—	—	55 lbs.*	6·25	344·00	* Deduced from expts. relating to Aeroplane bodies, Chap. VI.
Tail plane ...	114 × 3	2·38	2·38	5·75	13·70	
Tail-plane levers	8 × $\frac{3}{4}$ × 4	0·167	0·418	5·75	2·40	
Tail skid ...	18 × 2	0·25	1·480	3·5	5·19	
Rudder and fin ...	36 × 3	0·75	0·750	6·5	4·88	
Central wing Struts front ...	36 × 1·1 × 2	0·55	0·715	8·75	6·25	
Central wing Struts rear ...	38 × 1·0 × 2	0·50	0·65	8·50	5·53	
Central wing bracing ...	54 × ·09 × 2	0·067	0·216	8·75	1·91	
Total ...	—	—	64·57	—	392·40	

Centre of Resistance of Components in Slip Stream $= \frac{392 \cdot 4}{64 \cdot 57} = 6 \cdot 08'$ from datum.

In order to arrive at a correct estimate of the resistance it is necessary to take into account the variation of the resistance due to the slip stream of the airscrew. For this purpose the curve given in Fig. 174 may be used, together with Formula 70. The following particulars relating to the airscrew it is proposed to use are also necessary for the evaluation of this formula: Diameter 10 feet, experimental mean pitch 10·1 feet, number of blades 2, revolutions per minute 1650, $k = 4 \cdot 6 \times 10^{-7}$ Substituting in Formula 70, Tractive Power

$$= P = 4 \cdot 6 \times 10^{-7} \left[1 - \left(\frac{V}{\frac{1650}{60} \times 10 \cdot 1} \right)^2 \right] \frac{1650^3}{60} \times 10^5$$

$$= 960 \left[1 - \left(\frac{V^2}{77200} \right) \right]$$

From this relationship the values given in Table LXVII. can be calculated, and the slip-stream coefficient determined from Fig. 174.

TABLE LXVII.—CALCULATION OF SLIP-STREAM COEFFICIENT.

V ft./sec. ...	60	80	100	120	140	160	180
V^2	3600	6400	10000	14400	19600	25600	32400
$V^2/77200$ ...	·047	·083	·130	·187	·254	·332	·420
$1 - (V^2/77200)$...	·953	·917	·870	·813	·746	·668	·580
P	915	880	835	780	715	640	556
$\frac{\text{Tractive power}}{(\text{Airscrew diameter})^2}$	9·15	8.8	8·35	7·8	7·15	6·4	5·56
Slip-stream coeffct.	2·74	2·45	2·16	1·88	1·65	1·5	1·37

The resistance of all components affected by the slip stream from the airscrew must be multiplied by these factors.

From Table LXVI. it is seen that the estimated resistance of the components affected by the slip stream is 64·57 lbs. at 100 feet per second. The resistance at other speeds

$$= \frac{64{\cdot}57 \times V^2}{10^4} \times \text{slip-stream coefficient}$$

and the resistance of the components out of the slip stream

$$= \frac{25{\cdot}72 \times V^2}{10^4}$$

From these two equations the body resistance of the machine at various speeds can be calculated, as shown in Table LVIII.

TABLE LVIII.—BODY RESISTANCE OF MACHINE AT DIFFERENT SPEEDS.

V ft./sec	60	80	100	120	140	160	180
Components in slip-stream	64	101	139	175	209	248	286
Components outside slip-stream	9·2	16·5	25·7	37	50	66	83
Total resistance R_B ...	73	117·5	165	212	259	314	369

Wing Resistance.—From the fundamental equation

$$W = K_y \frac{\rho}{g} A' V^2$$

the necessary lift at any speed can be obtained by putting into the form

$$K_y = \frac{W}{\frac{\rho}{g} A' V^2}$$

$$= \frac{3500}{\cdot 00237 \times 500 \times V^2}$$

$$= \frac{2960}{V^2}$$

and when K_y has been determined, the corresponding K_x can be read directly from the curve of aerodynamic characteristics. Knowing K_x, the drag of the wings R_W can be determined at each speed, and by adding this result to the resistance of the body the total resistance of the machine at ground level can be determined, as shown in Table LXIX.

TABLE LXIX.—CALCULATION OF TOTAL RESISTANCE.

V	70	80	100	120	140	160	180
K_y	·605	·461	·296	·205	·151	·115	·091
K_x	·051	·0294	·0137	·0127	·0118	·0118	·0127
$\frac{\rho}{g}(540) K_x V^2 = R_W$	320	241	175	234	296	387	527
$R_B + R_W$ ...	393	358	340	446	555	701	896

Horse-power.—The horse-power required at the various speeds is obtained by the use of the formula

$$\text{Horse-power required} = \frac{\text{Resistance} \times \text{Velocity}}{550}$$

and the variation in engine power will be assumed to follow the law of the curve shown in Fig. 277. The maximum efficiency of the airscrew will be taken as 80% at a forward speed of 120 miles per hour. The rate of climb in feet per minute

$$= \frac{\text{Horse-power available} \times 33000}{\text{Weight of machine}}$$

Table LXX. can now be prepared.

TABLE LXX.—HORSE-POWER REQUIRED AND AVAILABLE, AND RATE OF CLIMB.

V (ft. per second) ...	70	80	100	120	140	160	180
$\frac{RV}{550}$ = H.P. required ...	50	52	62	97	141	204	293
$V/V_{max.}$	·398	·455	·569	·682	·795	·908	1·0
Power factor	·56	·64	·76	·86	·93	·98	1·0
$320 \times \cdot 8 \times F_p$	143	164	195	220	238	251	256
H.P. available	93	112	133	123	97	47	0
Rate of climb (ft. per min.)	876	1055	1250	1160	914	443	0

The effect of the variation of the slip stream will be to alter the position of the centre of resistance in a vertical plane, and it is therefore necessary to determine its position both at top speed and at slow speed. These positions are obtained by combining the information given in Tables LXV., LXVI.

Resistance of components out of the slip stream
at a speed of 80 f.p.s. = 25·72 × ·64 = 16·5 lbs.
at a speed of 160 f.p s. = 25·72 × 2·56 = 66·0 lbs.
acting at a distance of 4·52 feet from datum line.

Resistance of components in slip stream
at a speed of 80 f.p.s. = 64·57 × ·64 × 2·45 = 101·2 lbs.
at a speed of 160 f.p.s. = 64·57 × 2·56 × 1·5 = 248 lbs.
acting at a distance of 6·08 feet from datum line.

Resistance of wings
at a speed of 80 f.p.s. = 240 lbs.
at a speed of 160 f.p.s. = 400 lbs.
acting at 6·75 feet from datum line.

Taking moments about datum line,

For a speed of 80 feet per second

$$\overline{H}' = \frac{74\cdot5 + 615 + 1620}{357} = 6\cdot46 \text{ feet}$$

For a speed of 160 feet per second

$$\overline{H}' = \frac{298 + 1508 + 2700}{714} = 6\cdot3 \text{ feet}$$

so that there is a variation in the vertical position of the centre of resistance of 0·16 feet or 1·92 inches over the speed range.

Knowledge of the position of the centre of resistance enables the final balancing up of the machine to be obtained and the direction of the tail-loading determined. In this case the line of pull of the airscrew acts at a distance of 6·25 feet from the datum, so that the resulting thrust-resistance couple will be very small, and a small up load on the tail will correct for this effect. The tail-setting for various flight speeds is next calculated in the manner shown in Chapter XI.

The various performance curves for the machine are shown in Fig. 288, from which it will be seen that the estimated flight speed is 117 miles per hour, as against 120 miles per hour required by the design. It will be noted, however, that in the calculation of the resistance and the available horse-power, no allowance has been made for the variation due to the change in

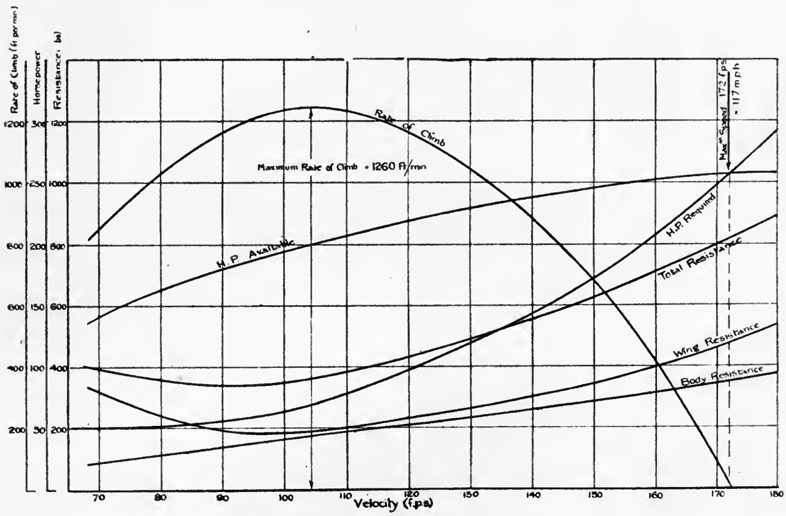

FIG. 288.—Performance Curves.

the density of the atmosphere. As pointed out in Chapter I., these two items will have a neutralising effect upon each other, and as the resistance has, if anything, been over-estimated, it is extremely probable that the desired performance of 120 miles per hour at 10,000 feet will be achieved upon the trial flights of this machine.

In order to reduce the labour of design work to a minimum, it is very desirable that a careful record should be kept of all machines designed and built. For this purpose some such table as that shown in Fig. 289 should be prepared and filled in as the various particulars become available. Data relating to some of the most successful machines yet built is given in Chapter XIV., which will form a nucleus upon which the embryo designer can build his own designs.

Engine:—
Type
B.H.P. R.P.M.
No. fitted Total H.P.
$\frac{\text{Airscrew r.p.m.}}{\text{Engine r.p.m.}}$ = =
Fuel p. B.H.P.
Oil p. B.H.P.

	mls.	hrs.
Range		

Speed
Ground
10000 ft.
15000 ft.
Landing

Climb	Time	Rate
to 5000 ft.		
to 10000 ft.		
to 15000 ft.		
to 20000 ft.		

Ceiling

Aeroplane
Type
No. of wings

	Span	Chord	Incid'ce	Dihedral	Gap	Stagger
Top wing						
Second middle						
Third						
Bottom						

Overall length
Height
$\frac{\text{Gap}}{\text{Chord}}$
Distance from L.E. of lower wing to elevator hinge
Stability
Longitudinal
Lateral

	Areas			Weight lbs.	Wt. Sq. ft.	% Wt.
Structural Unit		Wings	Top plane			
			Second plane			
			Middle plane			
			Third plane			
			Bottom plane			
			Ailerons			
			Struts (No. =)			
			External bracing wires			
			Total Wings ...			
		Controls	Tail plane			
			Elevator			
			Fin			
			Rudder			
			Total Controls ...			
		Body	Fuselage			
			Chassis			
			Tail skid			
			Controls			
			Total Body ...			
	Total Weight of Structural Unit					
Power Unit		Engine	Engine dry			
			Airscrew			
			Radiator, piping, and water			
			Engine accessories			
			Power Unit ...			
		Fuel	Fuel tanks and piping			
			Oil tanks and piping			
			Fuel			
			Oil			
	Total Weight of Power Unit					
Useful Load	Crew					
	Passengers					
	Instruments					
	W.T. do.					
	Luggage					
	Cargo					
	Spares					
	Sundries					
	Total Weight of Load Unit					
	Total Weight of Machine					

Fig. 289.

CHAPTER XIV.

The General Trend of Aeroplane Design.

> 'Soon shall thy arm, unconquered steam, afar
> Drag the slow barge, or draw the rapid car;
> Or on wide waving wings expanded bear
> The flying chariot through the field of air.'
>
> *The Botanic Garden*, by Erasmus Darwin, published 1791.

It seems hardly credible, when one surveys the present science of aeronautics, that it was only in 1903 that the Wright Brothers were making their first experiments in aerodynamics and their flights with gliders at Kitty Hawk. A brief *résumé* of the leading facts of aeronautical history is of more than ordinary interest.

In 1848 a small model was made by Stringfellow which flew for about forty yards under its own steam, but it was not really until the late nineties of the last century that serious attention was devoted to the problem of the 'heavier than air' flying machine. At that time the two most prominent investigators in this new field of science were Langley in America and Hiram Maxim in England. Langley's machine had a wing-surface area of 70 square feet, a steam engine of one horse-power weighing 7 lbs., the whole arrangement weighing 30 lbs. It was designed to carry no passenger, and flew under its own steam-power upon two occasions in 1896; the lengths of the flights being respectively one-half and three-quarters of a mile. Maxim's machine of the same date was much more ambitious in conception. The wing-surface area was 4000 square feet, the steam engine was of 360 horse-power, weighing 1200 pounds, and the whole machine weighed 8000 pounds. It was designed to carry three passengers, and on its trial was anchored down to rails to prevent actual flying. The check rail, however, was torn away and the machine wrecked on its trial. In 1897 Ader constructed an aeroplane weighing complete 1100 pounds, the power unit being a steam engine of 40 horse-power and weighing nearly 300 pounds. This engine was capable of pulling the machine along the ground for short distances, but no flight was accomplished. Meanwhile Langley was still experimenting in America, and produced in 1903 a full-size aeroplane as the result of his researches. With his power-driven models the

FIG. 297.—The Bristol Monoplane.

FIG. 298.—Bristol Fighter fitted with Wireless.

To follow page 424.

method of launching from the top of a house-boat had been adopted with successful results, but when applied to the full-scale machine this plan proved a failure, and Langley abandoned his efforts in this direction.

Then on September 17th, 1903, the Wright Brothers, after many years spent in experiments, succeeded in flying a power-driven machine as stated in Chapter I., the machine weighing 750 pounds and being equipped with a 16 horse-power petrol motor. This first flight lasted but twelve seconds. Rapid progress was now made, and in 1908 Wilbur Wright made his sensational flights in France, and although he was at first treated as a 'bluffer,' a flight lasting for over ninety minutes at Le Mans in the September of that year dispelled all doubts about actual flight.

Since that date the main air marks to record are the crossing of the English Channel by Bleriot on a monoplane in July, 1909; the great development and expansion of aeronautics, owing to the War, from 1914–1918; the flight of a V-1500 Handley-Page from Ipswich to Karachi (India) by stages from December 13th, 1918, to January 16th, 1919; the unsuccessful attempt of Hawker and Grieve to cross the Atlantic on a Sopwith machine on May 19th, 1919; the crossing of the Atlantic on June 14th–15th, 1919, by Alcock and Whitten-Brown in a Vickers-Vimy-Rolls—from St. John's, Newfoundland, to Clifden, Ireland, a distance of about 1900 miles, in 16 hours; the flight of Captain Ross-Smith and three companions from Hounslow (England) to Port Darwin in Australia in a Vickers-Vimy-Rolls, a distance of 11,300 miles, between November 12th and December 10th, 1919.

Civil aviation opened officially in England on May 1st, 1919. Table LXXI. shows the results obtained by private enterprise during the six months ending October 31st, 1919.

TABLE LXXI.—PROGRESS OF CIVIL AVIATION IN ENGLAND, MAY 15TH TO OCTOBER 31ST, 1919.

Number of hours flown	4,000
Number of flights	21,000
Number of passengers	52,000
Approximate mileage	303,000
Total number of accidents	13
Number of fatal accidents	2

It will thus be seen that more than 25,000 passengers were carried for every one fatally injured, so that flying can be regarded to be quite as safe as any other form of locomotion, while offering the advantage of much greater speed.

The Bleriot Machine.—The machine used by Bleriot in his cross-Channel journey was known as a No. XI. type monoplane. The fuselage was of open wooden framework braced by steel wires throughout. The two halves of the main plane were set at a slight dihedral. The span was 28·5 feet, the chord 6·5 feet, and the total surface area 151 square feet.

The tail plane consisted of a fixed plane at the rear of the fuselage of area 17 square feet. The elevators were placed on each side of this fixed tail plane, their total area being 16 square feet. The rudder was rectangular in form, fixed beyond the end of the fuselage, and having an area of 4·5 square feet. Lateral stability was maintained by warping the main planes, as in the case of the Wright machines.

The power plant consisted of a three-cylinder 25 h.p. Anzani air-cooled engine, driving a two-bladed airscrew nearly 7 feet in diameter at 1350 r.p.m.

The total weight of the machine was about 700 lbs., and its maximum speed 40 miles per hour.

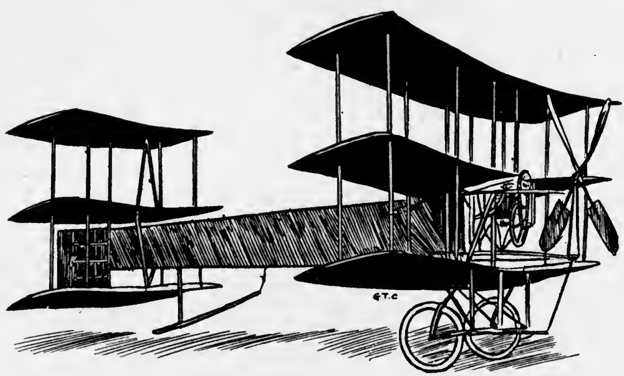

Reproduced by courtesy of 'Flight.'

FIG. 290.—Avro Triplane, 1908.

Avro Machines.—One of the pioneers in England was A. V. Roe, whose early experiments in aviation have led to the development of A. V. Roe & Co., Manchester and Southampton. A study of the various machines produced by this firm illustrates the progress of aeroplane design in an interesting manner.

The 'Bull's Eye,' as the triplane with which Mr. Roe carried out many experiments on the Lea Marshes in 1908–1909 was called, weighed only 200 lbs. It had a surface area of about

300 square feet, while the engine was a 10 h.p. Jap. The fuselage was triangular in section, the pilot being situated some distance behind the main planes. The main planes could be swivelled round a horizontal axis in order to vary the angle of incidence. These main planes could also be warped in order to maintain lateral stability, while directional control was maintained by the rudder at the rear of the tail planes. The triplane tail was of the lifting type, and was rigidly attached to the rear end of the fuselage. Fig. 290 gives a very good idea of the general appearance of this machine.

The first Avro biplane appeared in 1911. It was fitted with a 35 h.p. Green engine, only the nose portion of the fuselage being covered with fabric, while the body was triangular in shape as in the triplane. The tail plane was of the non-lifting

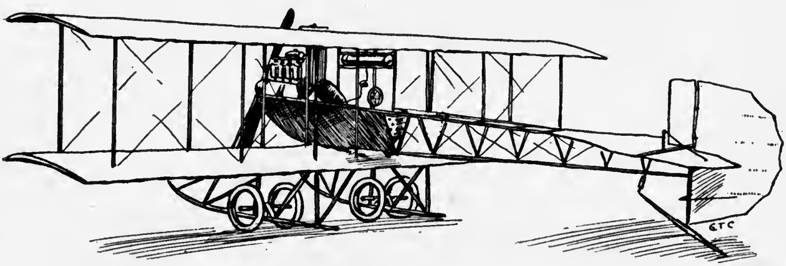

Reproduced by courtesy of 'Flight.'

Fig. 291.—Avro Biplane, 1911.

type fitted with elevators, and lateral stability was obtained by warping the main planes. (See Fig. 291.)

In Fig. 292A is shown the Avro 504 K, which is a modification of the Avro 1913 machine. This machine has been used as the standard training machine for pilots of the Royal Air Force, and is practically the only early machine still in general use. The Avro Spider is shown in Fig. 292B, and embodies an entirely different type of wing-construction. As will be seen, the struts are arranged similarly to the struts in the Wireless Biplane Truss shown in Fig. 101, and the side elevation is of the same type as that illustrated in Fig. 114 (the Nieuport 'V'). Fig. 292C depicts the Avro Manchester Mark II., which represents the probable commercial machine of this firm. It is a twin-engined biplane, and follows orthodox construction except that the ailerons are balanced by means of an auxiliary plane mounted on two short struts from the main aileron and placed slightly ahead of it.

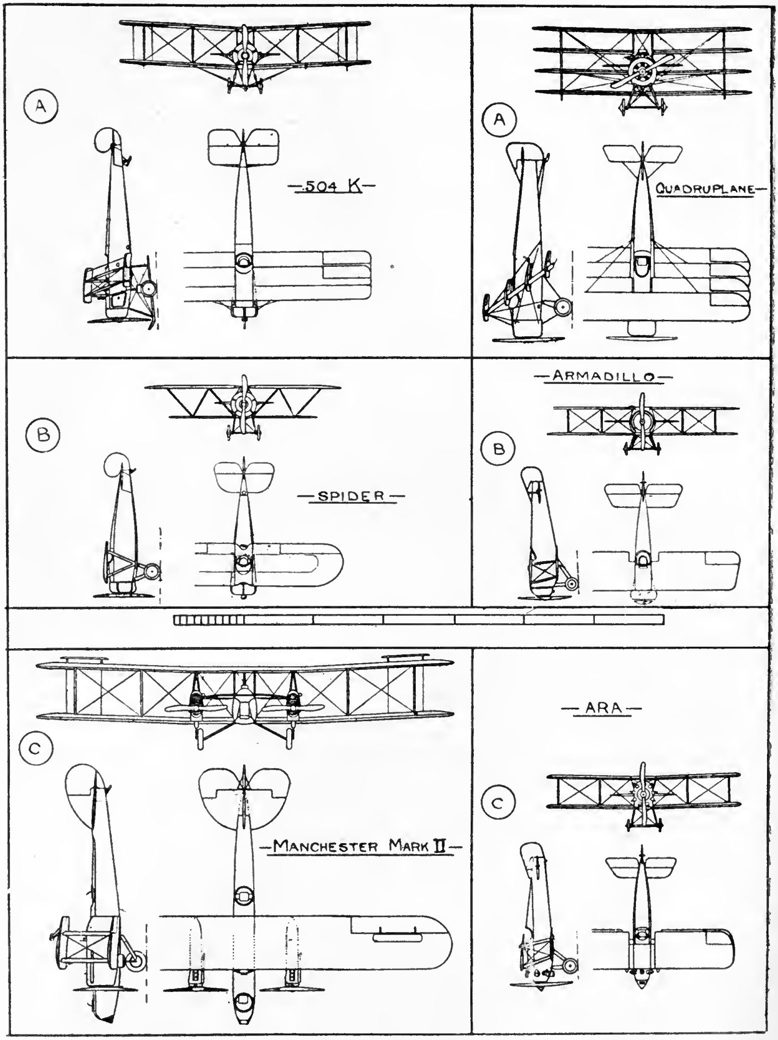

Avro Machines.

FIG. 292.

Armstrong-Whitworth Machines.

FIG. 294.

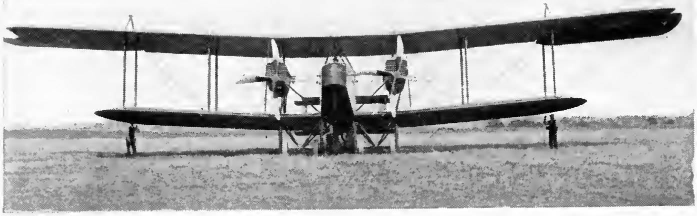

Fig. 300.—0–400 Handley Page.

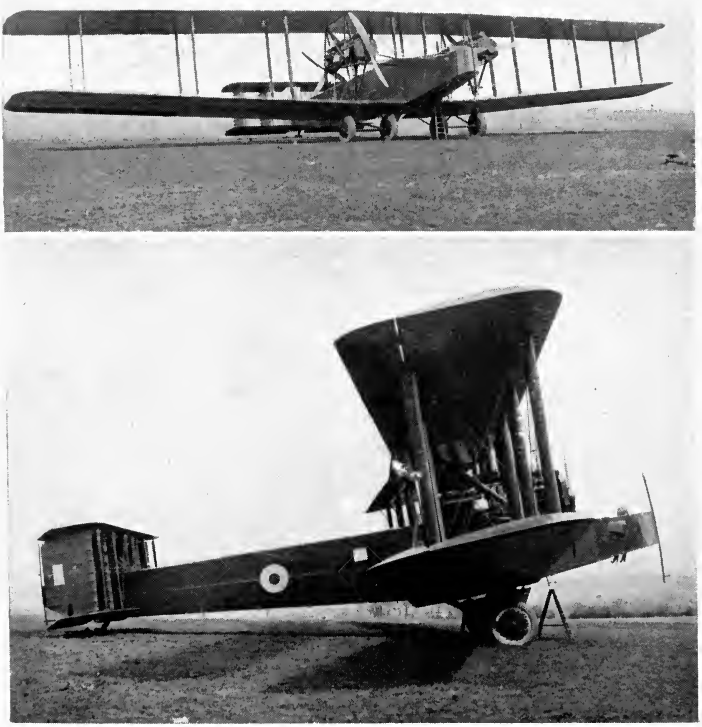

Reproduced by courtesy of Messrs. Handley Page, Ltd.

Fig. 301.—Front and Side Views of V–1500 Handley Page.

In order to illustrate further the general trend of aeroplane design, the most interesting machines of the leading aeronautical firms of Great Britain will be briefly reviewed so far as particulars are available. The general dimensions of the machines dealt with are summarised in Table 72, and their performance and weights are given in Table 73. The line drawings of these machines are due to the courtesy of *Flight* and have all been prepared to the same scale, so that direct comparison is possible.

Airco Machines.—The design of the Airco machines has throughout been the work of Capt. G. de Havilland. They were on this account formerly termed 'de H. machines,' and under this appellation earned a well-deserved reputation during the War. The first of these machines made its appearance early in 1915, and was a two-seater machine of the pusher type fitted with a 70 h.p. Renault engine. It was followed by the de H. 1 A, practically identical in dimensions and construction, but fitted with a 120 h.p. Beardmore engine. The performance of this machine was quite good for the engine power available. (See Fig. 293 A). The de H. 4 machine was one of the most successful machines produced during the war, and was used for all purposes. It is a tractor biplane of good clean design. Various types of engine have been fitted to this machine, the first being a B.H.P. 200 h.p. The engine power has been gradually increased until at the present time some of these machines are fitted with 450 h.p. Napier engines. The engines most frequently fitted are the Rolls-Royce 250 h.p. and 350 h.p. types. (See Fig. 293 B.) Since the war the passenger accommodation on this machine has been enclosed to form a cabin capable of seating two persons, and in this form the de H. 4 was used for many journeys between London and Paris in connection with the Peace negotiations. An Airco 4 R (de H. 4 fitted with the 450 h.p. Napier 'Lion') won the the Aerial Derby in 1919. The de H. 5 is a small tractor scout in which the chief aim in design appears to have been the provision of a clear field of vision for the pilot. The most notable constructional feature of this machine is the large amount of negative stagger, and perhaps it was due to this fact that the machine was not easy to handle. (See Fig. 293 C.) The de H. 9 in its main dimensions was largely a copy of the de H. 4, the chief difference being in the fuselage. The pilot's cockpit is placed further back, and by fitting a vertical engine the front portion of fuselage has been given a much better shape. (See Fig. 293 D.) A modified 9, fitted with Napier 'Lion' engine, piloted by Capt. Gather-

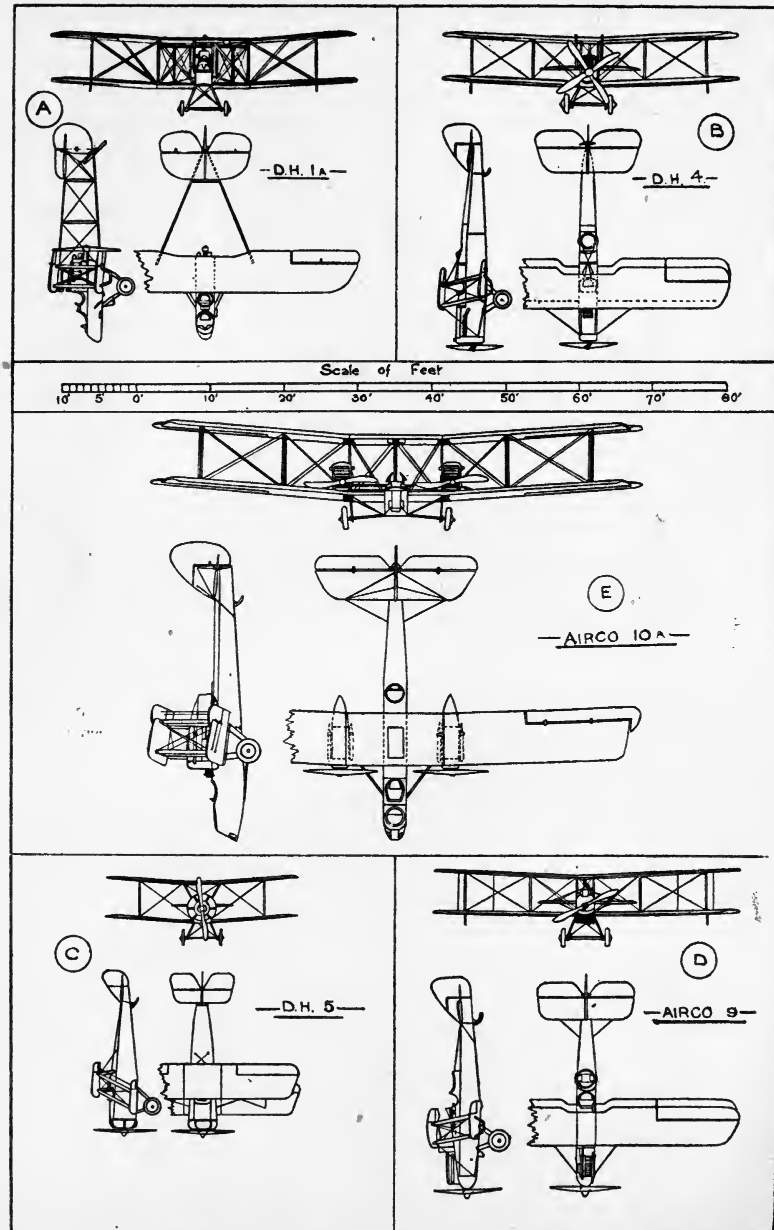

FIG. 293.—Airco Machines.

good, broke eighteen British records in one flight on Nov. 15th, 1919. This machine has attained a speed of 155 m.p.h. The Airco 10 A was designed for long-distance bombing combined with all-round performance. Table LXXIII. shows how well this aim was achieved. It is a twin-engined machine, the Liberty engines being placed out on the lower wing structure, one on each side. (See Fig. 293 E.)

Armstrong-Whitworth Machines.—Since the A.W. Quadruplane is the only example of this type of machine which has been constructed by British aeronautical engineers, its leading features are of considerable interest. On trial it was found that its performance was slightly inferior to that of contemporary triplanes of the same engine power, and much inferior to that of small biplanes. The load per brake horse-power is somewhat high, and it is possible that the fitting of a more highly powered engine would lead to a considerable improvement in its performance. (See Fig. 294 A.) The Armadillo is noteworthy from the fact that the fuselage entirely fills the centre section of the wing structure (see Fig. 294 B); while in the Ara machine there is a slight gap between the top of the fuselage and the top plane. (See Fig. 294 C.) Both of these machines are single-seater tractors, and, as Table LXXIII. shows, their performance under test was good.

Bristol Machines.—Although the monoplane is the most efficient type of aeroplane aerodynamically, it fell into disrepute about 1912 on account of several fatal accidents which occurred in use, owing principally to structural defects. It is therefore very creditable that Captain Barnwell, the designer of the Bristol machines, has produced, in the face of much opposition and prejudice, such a pleasing and efficient monoplane as is shown in Figs. 296 A, 297 (p. 424). As will be seen, the wing section employed allows of deep spars, the wing being fitted with aileron surfaces instead of with warping arrangements as is usual in monoplane practice. Especial care has been devoted to streamlining, and openings are provided in the inner portion of the wings near the sides of the fuselage, resulting in a further increase in the natural range of visibility of the monoplane type. The Bristol Fighter (Figs. 296 B and 298, p. 424) illustrates a machine designed primarily for fighting purposes. The F 2 B, as it was also called, was very largely used for fighting, scouting, and other purposes during the war, and the illustrations show the modifications that have been made in the design of the fuselage and other components in order to render this machine efficient

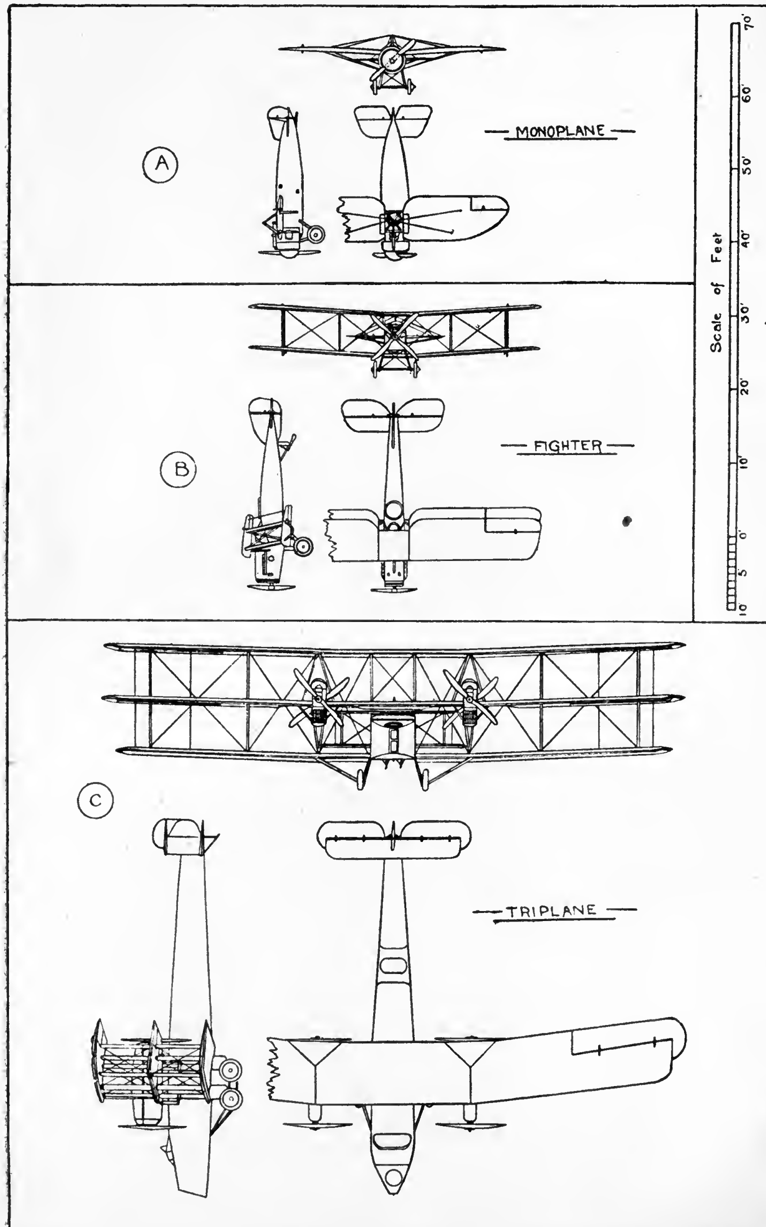

FIG. 296.—Bristol Machines.

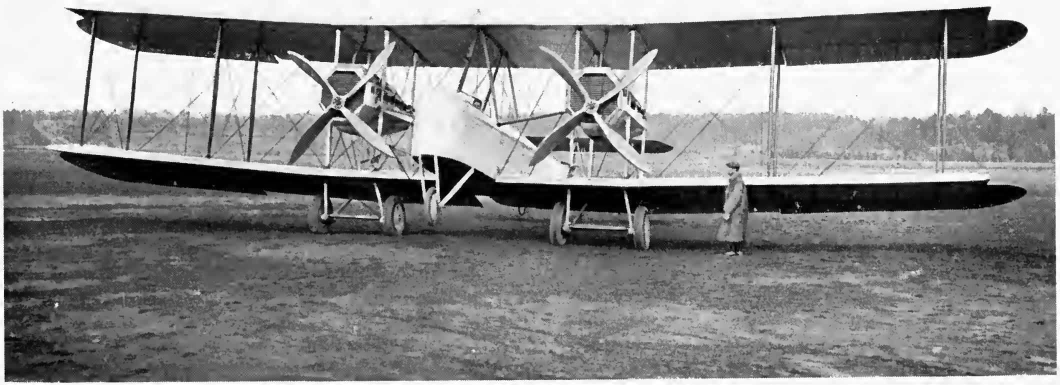

Reproduced by courtesy of Messrs. Vickers, Ltd.

Fig. 304.—The Cross-Atlantic Vickers 'Vimy-Rolls.'

To follow page 432.

for its specific purpose. In particular it will be observed that the lower plane is situated well below the fuselage, resulting in a somewhat more complicated arrangement of the chassis. Pilots report that this machine is very responsive to its controls, while it also possesses a large amount of inherent stability. The Bristol Triplane (Fig. 296C) is a four-engined machine driving two tractor and two pusher airscrews. It was primarily designed for bombing purposes, but is being adapted for other uses.

Handley Page Machines.—From the very inception of his firm Mr. Handley Page has pinned his faith to the future of the large aeroplane. The first Handley Page bombing machines did not make their appearance until December, 1915, and it was not until August of the following year that the first squadron of the O-400 type was formed at Dunkirk. From that date until the conclusion of hostilities, all heavy night bombing on the Western Front was performed with these machines. The V-1500 type was designed originally to bomb Berlin, but is now being adapted for commercial use. One of these machines has carried forty-one passengers to a height of 8000 feet.

A line diagram of the O-400 type is shown in Fig. 299, a front view of the O-400 in Fig. 300, while front and side views of the V-1500 type are shown in Fig. 301 (p. 424). Photographs illustrating the position of the wings in their folded-back position were shown in Figs. 3, 151.

Sopwith Machines.—The Sopwith Tabloid was originally built as a side-by-side two-seater for Mr. Hawker, who has since achieved fame as a first-class test pilot, and whose attempt to be the first airman to cross the Atlantic on a Sopwith machine was only frustrated through radiator failure. In the Tabloid machine lateral control was effected by means of wing-warping. This machine first demonstrated the possibilities of the small single-seater biplane as a rival to the monoplane for high-speed work, while retaining a large range of flying speeds. (See Fig. 302 A.) The $1\frac{1}{2}$ Strutter is so designated because of the type of wing-bracing employed. The top plane was in two halves bolted to the top of a central cabane, and the spars are provided with extra support in the shape of shorter struts running obliquely from the top longerons to the top plane spars. This machine is also interesting owing to the fact that it was fitted with an air brake taking the form of adjustable flaps inserted into the trailing edge of the lower plane close to the fuselage. Another feature incorporated in the $1\frac{1}{2}$ Strutter was the tail-plane variable incidence gear. (See Fig. 302 B.) The Sopwith Pup follows the general lines of the $1\frac{1}{2}$ Strutter and the original Tabloid. It handles remarkably well, and, as will be seen from Table LXXIII.,

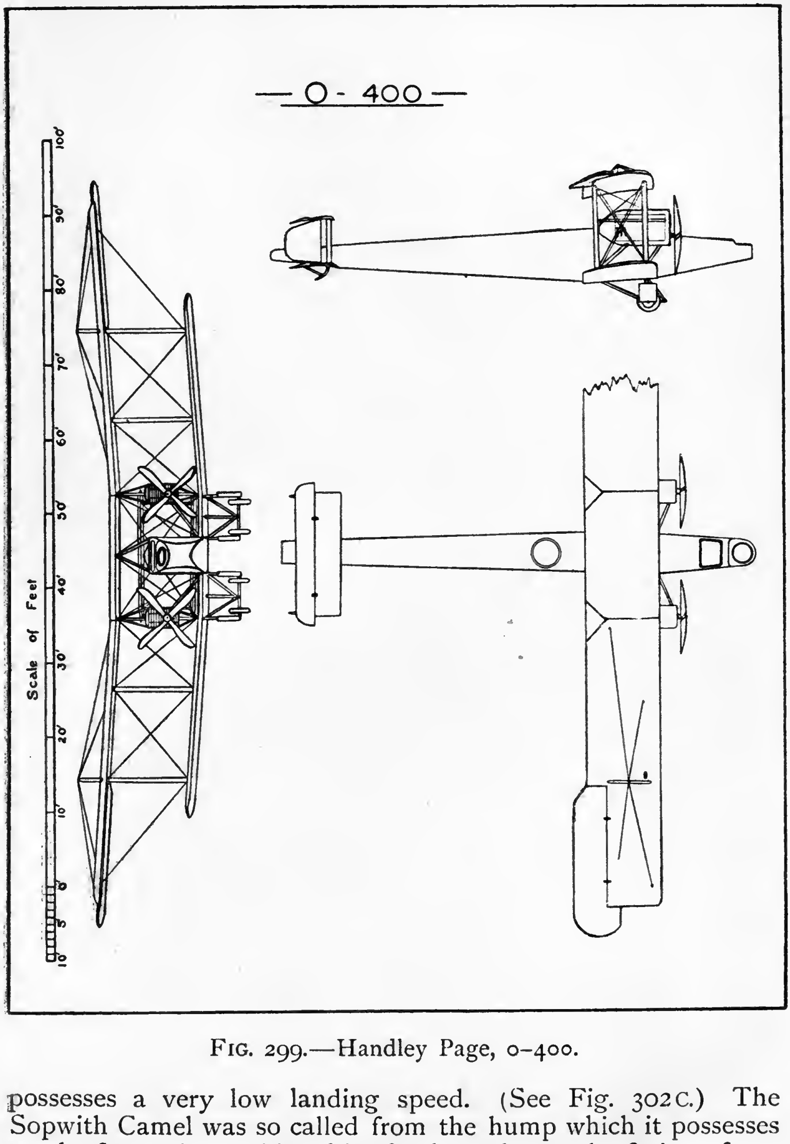

FIG. 299.—Handley Page, 0–400.

possesses a very low landing speed. (See Fig. 302 C.) The Sopwith Camel was so called from the hump which it possesses on the forward top side of its fuselage, due to the fitting of two

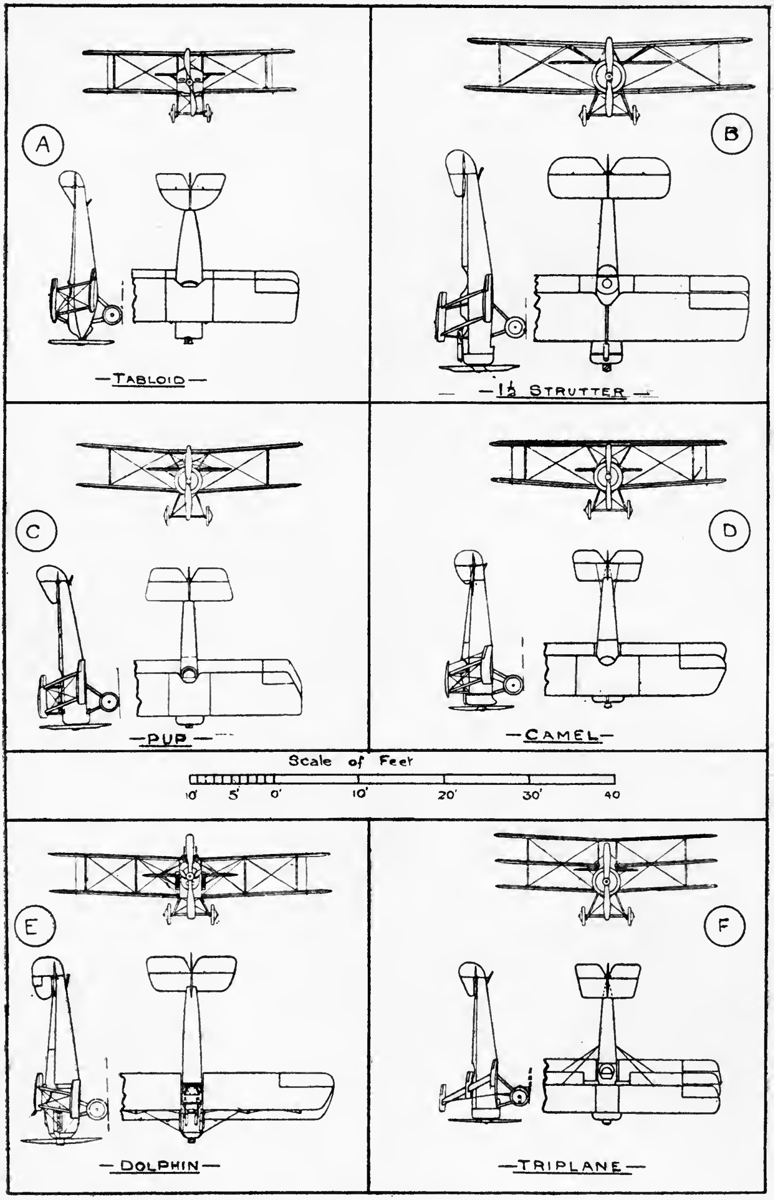

FIG. 302.—Sopwith Machines.

fixed machine guns both firing through the airscrew. It achieved a great reputation during the War, but as a sporting machine the Pup is preferable in many respects. (See Fig. 302D.) The Dolphin (see Fig. 302E) differs considerably from the Camel in structural arrangements. It will be seen in the illustration that a double bay arrangement of struts has been adopted, the gap has been diminished, and negative stagger introduced. The radiator was divided into two portions, placed one on either side of the fuselage opposite the pilot's cockpit, each radiator being fitted with deflectors. The Sopwith Triplane was designed solely to afford good visibility and manœuvrability. As will be seen from the figures and tables, the wing chord has been considerably reduced, and single 'I' struts have been fitted between the planes in place of the more usual pair.

Vickers Machines.—At the commencement of the war the Vickers Gun Bus (F.B. 5) (Fig. 303A) was practically the only fighting aeroplane in existence. It was a pusher machine, the Vickers gun being mounted in the nose of the nacelle, from which position a very wide range of unobstructed fire could be obtained; and its arrival on the Western Front established for the time being the aerial supremacy of the Allies. The F.B. 7 (Fig. 303B) was brought out in August, 1915, and was one of the first twin-engined machines to take the air. It is particularly interesting as being the prototype of the now famous 'Vimy Bomber.' In the experimental model of the F.B. 16 trouble developed owing to the weakness of the leading edge of the main planes. Investigation showed that this weakness resulted from an inadequate factor of safety for the high speed attained by this machine. After remedying this defect, the machine was tested officially and showed a performance better than that obtained by contemporary machines of a similar type. The Vimy Bomber (Figs. 303D, 304, p. 432) was remarkable for its small size when compared with its large lifting capacity. It is claimed that this machine is stable both longitudinally and laterally. The engines are placed out on the wing structure directly over the landing chassis. The fore part of the fuselage is constructed of metal tube and the rear part of special wooden tube. This machine, as used for crossing the Atlantic, is shown in the Frontispiece and Fig. 304, and it is noteworthy that with the fitting of additional fuel tanks only, it succeeded in accomplishing the first direct flight across the Atlantic. An exactly similar type machine accomplished the first flight to Australia. Fig. 305 (p. 432) shows the Vimy as adapted for commercial work. Details of this machine have already been given in Chapter VII.

Boulton and Paul Machines.—Illustrations of two of the machines manufactured by this firm are shown in Figs. 306, 307 (p. 444). It will be noticed from Table LXXIII. that the load

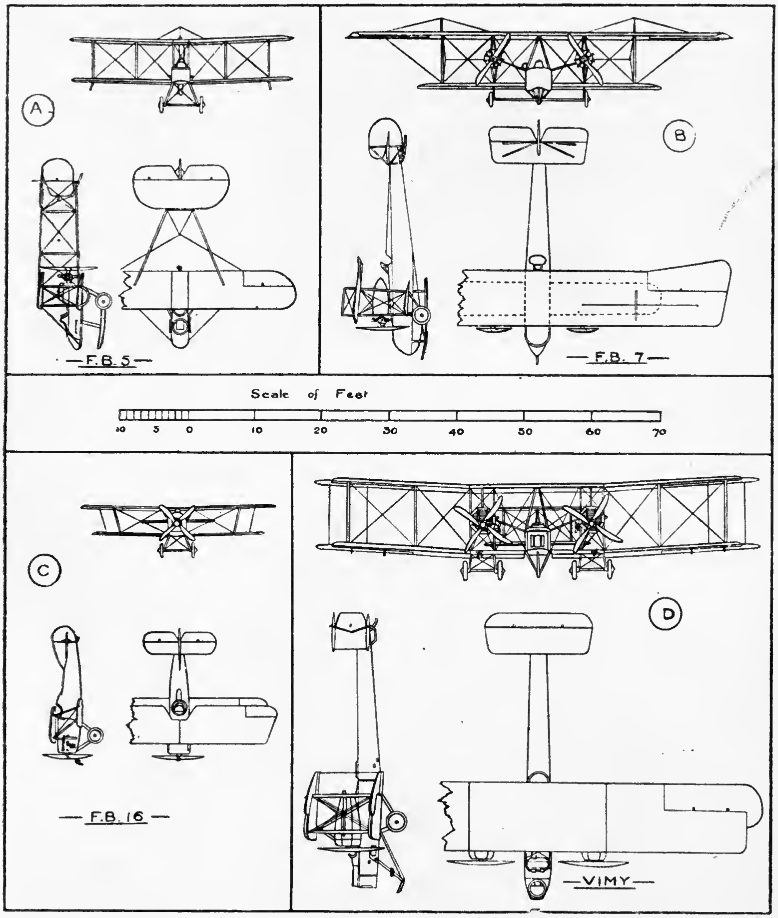

Fig. 303.—Vickers' Machines.

per horse-power for the passenger machine is only 7·8 lbs., which, coupled with particular care in the remainder of the design, in a large measure accounts for the remarkable performance of this type.

TABLE LXXII.

TYPE OF MACHINE.	Over-all length	WING SPAN. Top.	Middle.	Bottom.	WING CHORD. Top.	Middle	Bottom	WING AREA. Top.	Middle	Bottom	Total.
	feet	feet	feet	feet	feet	feet	feet	sq. feet	sq. feet	sq. feet	sq. feet
AVRO											
504 K	28·92	36·0	—	36·0	4·83	—	4·83	171·5	—	158·5	330·0
Spider	20·5	28·5	—	21·5	6·00	—	2·5	162·0	—	46·0	208·0
Manchester Mk. II	37·0	60·0	—	60·0	7·5	—	7·5	430·0	—	387·0	817·0
AIRCO											
1A	29·0	41·0	—	41·0	5·9	—	5·9	187·0	—	175·25	362·25
4	30·0	42·39	—	42·39	5·5	—	5·5	223·0	—	211·0	434·0
5	22·0	25·67	—	25·67	4·5	—	4·5	111·2	—	100·9	212·1
9	30·83	42·39	—	42·39	5·5	—	5·5	223·0	—	211·0	434·0
10A	39·62	65·5	—	65·5	7·0	—	7·0	429·2	—	408·2	837·4
A-WHITWORTH											
Quadruplane ...	22·25	27·83	(2) 27·83 (3) 27·83	27·83	3·58	(2) 3·58 (3) 3·58	3·58	102·6	(2) 92·6 (3) 92·6	102·6	398·4
Armadillo ...	18·83	27·75	—	27·75	5·25	—	4·5	125·0	—	125·0	250·0
Ara	20·25	27·42	—	27·42	5·25	—	4·5	147·0	—	110·0	257·0
BRISTOL											
Monoplane ...	20·33	30·75	—	—	5·92	—	—	145.0	—	—	145·0
Fighter	25·75	39·25	—	39·25	5·5	—	5·5	202·5	—	202·5	405·0
Triplane ...	51·50	81·67	81·67	78·25	8·5	8·5	8·5	650·0	650·0	605·0	1905·0
HANDLEY PAGE											
0-400	62·85	100·0	—	70·0	10·0	—	10·0	1020·0	—	625·0	1645·0
SOPWITH											
Tabloid	20·33	25·5	—	25·5	5·12	—	5·12	128·3	—	113·0	241·3
1½ Strutter ...	25·33	33·5	—	33·5	5·5	—	5·5	183·0	—	170·0	353·0
Pup	19·33	26·5	—	26·5	5·12	—	5·12	132·0	—	122·0	254·0
Camel	18·75	28·0	—	28·0	4·5	—	4·5	125·0	—	115.0	240·0
Dolphin ...	22·25	32·5	—	32·5	4·5	—	4·5	132·0	—	131·0	263·0
Triplane ...	18·83	26·5	26·5	26·5	3·25	3·25	3·25	84·0	72·0	75·0	231·0
VICKERS											
F.B. 5	27·17	36·5	—	36·5	5·5	—	5·5	197·0	—	185·0	382·0
F.B. 7	36·0	59·5	—	37·5	8·3	—	6·0	459·0	—	181·0	640·0
F.B. 16	19·5	25·0	—	22·33	5·5	—	4·17	126·0	—	81·0	207·0
Vimy	43·54	67·17	—	67·17	10·5	—	10·5	686·0	—	644·0	1330·0
BOULTON & PAUL											
Scout	20·0	29·0	—	29·0	5·37	—	4·12	152·0	—	114·0	266·0
Passenger ...	40·0	59·0	—	59·0	8·0	—	6·5	432·0	—	338·0	770·0
S.E. 5	20·92	26·62	—	26·62	5·0	—	5·0	130·0	—	113·0	249·0

TABLE LXXII.

INCIDENCE.					DIHEDRAL.			AREA OF CONTROL SURFACES.						
Top	Middle.	Bottom.	Gap.	Stagger	Top.	Middle.	Bottom	Aileron	Tail plane.	Elevator	Total.	Fin.	Rudder.	Total.
			feet	feet				sq. ft.	sq. ft.	sq. ft.	sq. ft.	sq. ft.	sq. ft.	sq. ft.
4·5°	—	4·5°	5·5	2·17	2·5°	—	2·5°	45·5	26·0	18·0	44·0	—	9·0	9·0
0·0°	—	0·0°	4·22	2·00	0·0°	—	0·0°	22·0	15·2	10·4	25·6	—	7·8	7·8
4·0°	—	4·0°	7·25	0·0	2·5°	—	2·5°	124·0	50·0	35·0	85·0	12·0	16·0	28·0
5·5°	—	5·5°	5·87	0·0	3·0°	—	3·0°	64·0	37·5	23·0	60·5	3·7	15·4	19·1
3·0°	—	3·0°	5·50	1·0	3·0°	—	3·0°	82·0	38·0	24·0	62·0	5·4	13·7	19·1
2·0°	—	2·0°	4·75	−2·25	4·5°	—	4·5°	46·4	13·4	12·2	25·6	2·2	6·3	8·5
3·0°	—	3·0°	5·50	1·0	3·0°	—	3·0°	82·0	38·0	24·0	62·0	5·4	13·7	19·1
7·0°	—	7·0°	7·0	0·0	4·5°	—	4·5°	118·0	75·5	33·1	108·6	10·0	25·75	35·75
3·0°	(2) 3·0° (3) 3·0°	3·0°	2·67	1·42	1·5°	(2) 1·5° (3) 1·5°	1·5°	67·2	—	16·0	16·0	1·9	8·0	9·9
2·25°	—	1·0°	3·92	0·71	0·0°	—	2·0°	36·0	17·0	14·0	31·0	1·6	6·0	7·6
2·75°	—	1·25°	3·88	0·96	1·5°	—	1·5°	20·4	25·0	24·0	49·0	2·5	11·0	13·5
0·0°	—	—	—	—	2·0°	—	—	18·0	20·0	15·0	35·0	5·0	4·5	9·5
1·5°	—	1·5°	5·42	1·42	3·5°	—	3·5°	50·0	22·2	23·2	45·4	10·7	7·2	17·9
2·5°	2·5°	2·5°	7·21	—	2·0°	2·0°	2·0°	192·0	96·5	85·0	181·5	28·2	25·0	53·2
—	—	—	11·0	—	4·0°	—	4·0°	—	123·5	65·3	188·8	14·7	45·7	60·4
1·0°	—	1·0°	4·5	0·92	1·5°	—	1·5°	28·0	11·8	11·8	23·6	1·8	4·3	6·1
2·45	—	2·45°	5·42	2·0	2·45°	—	2·45°	52·0	35·5	21·5	57·0	3·5	7·25	10·75
1·5°	—	1·5°	4·42	1·5	3·0°	—	3·0°	22·0	23·0	11·8	34·8	3·5	4·5	8·0
2·0°	—	2·0°	5−4	1·5	0.0°	—	5·0°	36·0	14·0	10·5	24·5	3·0	4·9	7·9
2·0°	—	2·0°	4·25	−1·0	2·5°	—	2·5°	38·0	17·0	13·5	30·5	3·5	8·0	11·5
2·0°	2·0°	2·0°	3·0	1·5	2·5°	2·5°	2·5°	34·0	14·0	9·6	23·6	2·5	4·5	7·0
4·5	—	4·5°	6·0	0·0	1·0°	—	1·0°	57·0	56·0	24·6	80·6	8·5	13·25	21·75
3·0°	—	3·0°	7·33	0·92	3·0°	—	3·0°	93·0	42·0	28·5	70·5	—	20·0	20·0
2·0°	—	2·0°	3·92	2·5	1·5°	—	1·5°	23·5	18·5	15·3	33·8	6·5	6·0	12·5
3·5°	—	3·5°	10·0	0·0	3·0°	—	3·0°	242·0	114·5	63·0	177·5	2 × 13·5	2 × 10·75	48·5
—	—	—												
5·0°	—	5·0°	4·6	1·5	5·0°	—	5·0°	30·2	5·1	15·1	30·2	6·5	6·0	12·5

TABLE LXXIII.

TYPE OF MACHINE.	ENGINE.			WEIGHT OF MACHINE.		Fuel capacity. Hours.	Range. Miles.
	Name.	No.	H.P.	Empty. Lbs.	Loaded. Lbs.		
AVRO							
504 K	Le Rhone ...	1	110	1230	1820	3·0	225
Spider	Clerget	1	130	963	1517	3·0	330
Manchester Mk. II. ...	Siddeley ...	2	600	4580	7160	3·8	450
AIRCO							
1 A	Beardmore ...	1	120	—	2400	—	—
4	Rolls-Royce ...	1	370	—	3340	4·0	500
5	Le Rhone ...	1	110	—	1490	2·0	200
9	Lion (Napier) ..	1	420	—	3725	—	—
10 A	Liberty	2	800	—	8500	5·0	650
A-WHITWORTH							
Quadruplane	Clerget	1	130	1140	1800	—	—
Armadillo	B.R. 2	1	230	1250	1860	2·75	—
Ara	Dragonfly ...	1	320	1320	1930	3·25	450
BRISTOL							
Monoplane	Le Rhone ...	1	110	—	1300	—	—
Fighter	Rolls-Royce ...	1	250	—	2800	—	—
Triplane...	Siddeley ...	4	1000	9300	16200	—	—
HANDLEY PAGE							
0-400	Rolls Royce ...	2	700	8000	14000	7·0	650
SOPWITH							
Tabloid	Gnome	1	80	730	1120	3·5	320
1½ Strutter	Le Rhone ...	1	110	1280	2200	—	—
Pup	Gnome	1	100	856	1297	2·0	200
Camel	B.R. 1	1	150	—	1470	2·6	310
Dolphin	Hispano Suiza ...	1	200	1406	1880	2·0	230
Triplane...	Clerget	1	130	1100	1540	—	310
VICKERS							
F.B. 5	Gnome	1	100	1220	2050	4·5	330
F.B. 7	Gnome	2	200	2130	3200	2·5	200
F.B. 16	Hispano Suiza ...	1	200	1380	1880	2·25	300
Vimy	Rolls-Royce ...	2	700	6700	12500	11·00	1100
BOULTON & PAUL							
Scout	B.R. 2	1	230	1230	1920	3·5	440
Passenger	Napier Lion ...	2	900	4000	7000	3·0	—
S.E. 5	Hispano Suiza ...	1	200	—	1980	2	250

Table LXXIII.

SPEED.			CLIMB.			Ceiling. Feet.	Landing speed. m.p.h.	LOAD.	
			Minutes to—						
Ground level.	At 10000 ft.	At 15000 ft.	5000 ft.	10000 ft.	15000 ft.			Per sq. ft.	Per H.P.
90	75	65	6·25	16·0	40·0	—	35	5·52	16·5
120	110	—	4·0	9·5	22·0	19000	40	7·78	11·6
125	119	112	6·5	11·15	40·0	17000	45	8·76	11·9
89	—	—	10·0	—	—	—	—	6·6	20·0
—	133	126	—	9·0	16·6	23500	52	7·4	9·4
—	102	89	—	12·4	27·4	17000	50	7·0	13·6
—	140	135	—	8.2	14·6	25300	—	8·5	8·8
—	124	117	—	11·0	20·5	20000	55	10·0	10·6
105	99	—	—	17·0	—	25000	—	4·5	13·9
125	113	—	—	6·5	—	24000	55	7·4	8·0
150	145	—	—	4·5	—	28000	55	7·5	6·0
130	117	—	3·5	9·0	19·0	—	49	8·97	10·8
125	113	—	—	11·5	21·5	—	48	6·92	11·2
106	93	—	—	35·0	—	—	55	8·5	16·2
—	85	—	—	—	—	—	—	8·5	20·0
92	—	—	—	—	—	—	36	4.66	14·0
—	103	—	8·0	18·9	41·5	16000	35	6·4	17·5
110	104	100	5·7	12·4	23·4	18500	30	5·2	12·4
—	120	114	—	8·3	15·8	23000	35	6·14	9·8
—	128	124	3·9	8·25	14·7	23500	40	7·3	9·0
—	106	95	5·0	11·8	22·3	21000	35	6·0	12·4
75	—	—	16·0	—	—	9000	41	5·4	20·5
80	—	—	18·0	—	—	12000	40	5·0	16·0
—	135	126	4·75	10·4	20·75	20000	55	9·1	9·4
105	100	—	15·0	50·0	—	10500	50	9·4	17·9
—	125	110	—	9·5	18·0	21000	50	7·2	8·3
—	149	142	—	8·0	15·0	25000	54	9·1	7·8
—	—	120	5·0	10·8	20·8	21000	—	8.0	9·8

Official Machines.—Probably more controversy has raged round the B.E. 2 C than any other aeroplane built, nevertheless it represents the type of aeroplane that will undoubtedly be largely developed in the near future, namely, the inherently stable machine. Its inception and development was principally due to the efforts of the late Mr. E. T. Busk, of the Royal Aircraft Factory, and it shows in a striking manner the result of a sound application of theory to practice. Table I. illustrates how near the actual performance of this machine approached the calculated values. The S.E. 5 represents the most successful war product of the R.A.E. In general appearance it is similar to the Sopwith $1\frac{1}{2}$ Strutter, and was designed as a single-seater fighting machine. It is inherently stable, a wonderful demonstration of its qualities in this direction being provided when a S.E. 5 machine returned safely to the British lines after its controls had been practically shot away over the German lines.

Having considered the general trend of design with reference to complete machines, there only remains to be considered the question of detail design.

CHOICE OF TYPE.—It would be rash to prophesy whether the monoplane, biplane, or multiplane will be the most largely developed type in the future, since each type possesses advantages peculiar to itself. In comparison with the biplane, the monoplane can carry 5 per cent. more weight per square foot of wing surface, besides giving much better visibility. On the other hand, it is much weaker structurally. In the same way the triplane and quadruplane are about 5 per cent. less efficient than the biplane and triplane respectively, but if well designed should be more manœuvrable.

Generally speaking, it seems probable that the biplane will hold its own for general purposes for some considerable time to come, with the triplane as a rival in the larger sizes.

Wing Design.—The wind channel method of investigation has produced very efficient forms of aerofoils, and it seems probable that seventeen is an optimum value of the Lift/Drag ratio for wings of practical design. Further investigation is needed as to the depth of camber and the nature of the flow in the neighbourhood of the aileron surfaces. It is probable that in the near future metal construction will replace wood for the ribs and spars of large machines at least.

Optical stress analysis has shown that there is considerable divergence between the points of inflexion as calculated from

Reproduced by courtesy of Messrs. Vickers, Lta.

FIG. 305.—The 'Vimy' Commercial Passenger Machine.

the Theorem of Three Moments and the points obtained by loading a spar approximately as in practice, and further inquiry into this discrepancy is required. It seems at least on the safe side to use the Theory of Bending as outlined in Chapter V.

For large machines the saving in weight obtained by using tapered struts is of great importance, and it is hoped that the graphical method of tackling their design, which has been fully explained in Chapter V., will enable all those whose knowledge of the Calculus is limited, or even non-existent, to apply this theory in practice.

Internal bracing is generally effected by either plain or stranded wire in machines of all countries, the Fokker biplane and triplane being notable exceptions. A great improvement in the design of the wings will be the development of a section with a stationary centre of pressure over the range of flying angles. Further improvements likely to follow are:

(i) A practical design for a variable camber of surface, in which the mechanism is simple and reliable, and does not add appreciably to the weight of the machine.

(ii) The elimination of the major portion of the external bracing of the wing structure.

Fuselages.—The design of the fuselage is largely governed by the type of engine employed and the particular purpose for which the machine is intended. Recent investigations tend to show that the circular (or elliptical) body does not possess any material advantage over the square section. Constructionally, either wooden formers, suitably lightened out and of the required cross-sectional shape, support the longerons at regular intervals; or the strut and cross-bracing wire method is used. It may be remarked in passing that enclosing the rear portion of the body of several well-known war machines has led to a reduced overall resistance and consequent improvement in performance.

The monocoque method of fuselage construction, which dispenses with the longerons and employs a moulded three-ply method of construction, offers considerable advantages from the commercial point of view, since internal bracing is not needed, and consequently the space inside the fuselage is left clear for passengers, luggage, and cargo.

Control Surfaces.—As shown in Chapter XI., the attainment of stability by means of a correct disposition of the various control surfaces in relation to the fixed surface areas of the machine itself is now well within the compass of the aeroplane designer. It is also possible to achieve stability by means of external stabilising devices, such as, for example, the use of a gyroscope, but the success of the inherently stable machine has obviated the need for developing such methods.

The Airscrew.—Rapid development has taken place in the design of the airscrew during the war period, and it is now stated that the limit to the speed of the airscrew is fixed by the circumferential velocity of the tip, which must not exceed the velocity of sound (1100 feet per second). Airscrews must therefore be geared down so that the maximum tip speed under no circumstances is greater than 1000 feet per second. Metal airscrews have been manufactured, and will probably be developed for countries where the climatic conditions do not permit of a continued use of a wooden airscrew. There are also several experimental designs of airscrews with variable pitch under trial, of which more will doubtless be heard in the future.

Performance.—With the passing of the special conditions imposed by the War, the need for very rapid climb will disappear, and aeroplanes will cease to be required to operate at 20,000 feet, and to be capable of reaching that height in the minimum time.

The engine employed is a vital factor in the performance of any machine, and it is quite a truism that in all far-reaching developments the aeroplane designer has to wait upon the engine designer.

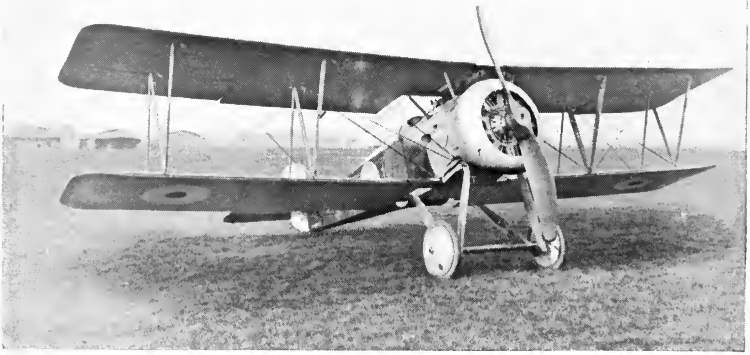

FIG. 306.—Scout.

Reproduced by courtesy of Messrs Boulton & Paul.

FIG. 307.—Passenger.

Boulton & Paul Machines.

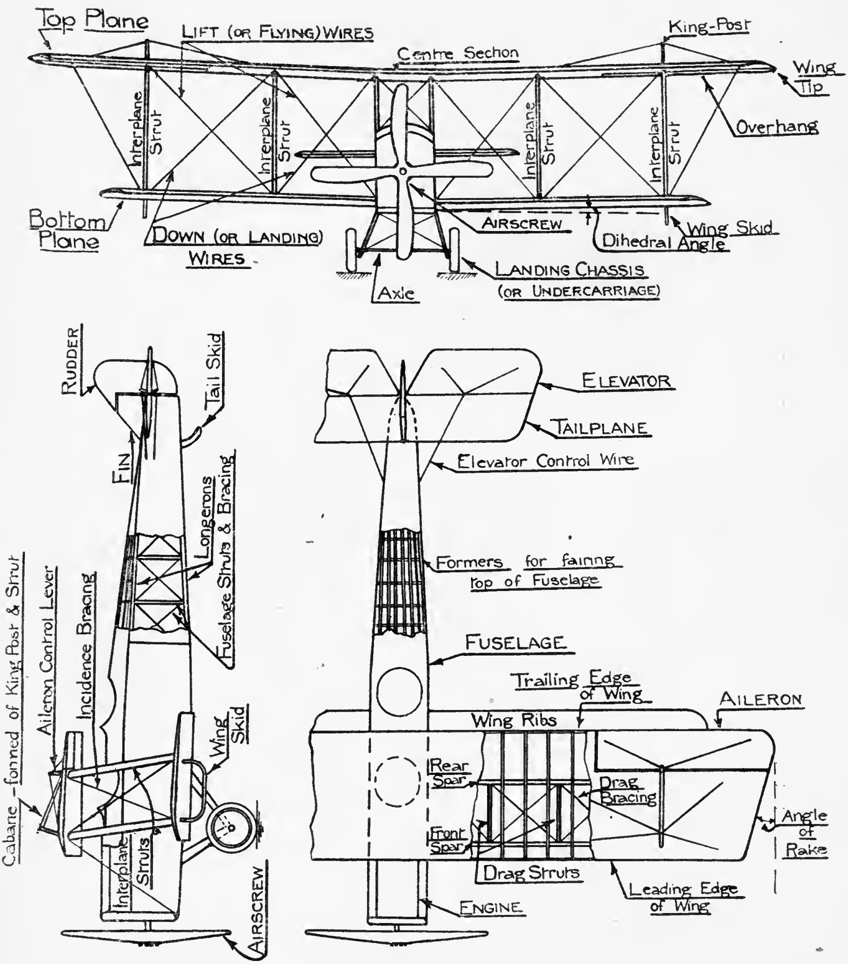

FIG. 308.—Aeroplane Nomenclature.

TABLE LXXIV.—SAFE LOADS IN

Outside diam.	Area. Sq. ins.	Weight. Lbs. run per ft.	LENGTHS 10	20	30	40	50	60
								SAFE LOADS
Inches.						GAUGE 22.	THICKNESS	
1/2 ...	·0415	·141	1300	650	400	250	150	100
3/4 ...	·0635	·216	2800	1800	1000	650	400	300
7/8 ...	·0745	·253	3400	2500	1500	1000	700	500
1 ...	·0855	·291	4000	3250	2200	1450	1000	700
1 1/8 ...	.0965	·328	4600	3850	2850	1900	1350	1000
1 1/4 ...	·1075	·366	5100	4500	3550	2500	1800	1300
1 3/8 ...	·1185	·403	5700	5100	4250	3150	2300	1700
1 1/2 ...	·1295	·440	6300	5750	4950	3800	2900	2150
1 5/8 ...	·1405	·478	6850	6300	5550	4500	3500	2650
1 3/4 ...	·1515	·515	7400	6900	6200	5200	4100	3200
1 7/8 ...	·1625	·553	8000	7500	6900	5900	4750	3800
2 ...	·1735	·590	8500	8050	7500	6550	5500	4400
						GAUGE 20.	THICKNESS	
1/2 ...	·0525	·178	2000	1200	700	450	300	200
3/4 ...	·0807	·275	3900	2500	1450	850	500	350
7/8 ...	·0949	·323	4800	3550	2200	1400	900	650
1 ...	·1090	·371	5600	4500	3000	2000	1400	1000
1 1/8 ...	·1232	·419	6500	5500	4000	2750	1950	1350
1 1/4 ...	·1373	·467	7300	6400	5000	3600	2500	1800
1 3/8 ...	·1514	·515	8200	7300	5950	4500	3300	2400
1 1/2 ...	·1656	·563	9000	8200	6900	5400	4000	3000
1 5/8 ...	·1797	·611	9700	9050	7900	6300	5000	3800
1 3/4 ...	·1938	·659	10600	9850	8800	7300	5800	4600
1 7/8 ...	·2080	.707	11400	10700	9700	8400	6700	5400
2 ...	·2221	·755	12200	11500	10650	9400	7800	6400
						GAUGE 17.	THICKNESS	
1/2 ...	·0781	·401	2000	1000	400	250	200	170
3/4 ...	·1221	·647	5900	3500	1900	1100	800	500
7/8 ...	·1441	·769	7200	5600	3150	1900	1150	800
1 ...	·1661	.892	8700	7000	4500	2900	1950	1350
1 1/8 ...	·1881	1·015	9800	8250	6000	4000	2800	2000
1 1/4 ...	·2101	1·138	11150	9850	7500	5000	3700	2750
1 3/8 ...	·2321	1·261	12600	11200	9000	6600	4750	3500
1 1/2 ...	·2540	1·384	13700	12500	10600	8000	6000	4500
1 5/8 ...	·2760	1·507	14900	13800	12100	9700	7400	5600
1 3/4 ...	·2980	1·629	16300	15200	13700	11250	8900	6900
1 7/8 ...	·3200	1·752	17600	16600	14900	12750	10150	8000
2 ...	·3420	1·875	18800	17850	16400	14250	11800	9500

LBS. FOR TUBULAR STEEL STRUTS.

IN INCHES.

70	80	90	100	110	120	130	140	150
IN LBS.								
OF METAL, 0·028″								
80	70	60	50	40	—	—	—	—
200	1 0	150	120	100	80	—	—	—
350	300	230	200	150	120	100	—	—
500	400	330	280	200	160	130	110	—
750	550	440	350	280	240	180	160	150
1000	800	600	460	360	320	260	220	200
1300	1000	800	650	520	450	340	280	250
1700	1300	1080	830	700	600	500	420	350
2100	1650	1350	1100	870	750	650	560	500
2550	2000	1650	1350	1130	920	800	750	650
3000	2450	2000	1700	1400	1200	1000	880	800
3600	2900	2400	2000	1650	1400	1200	1100	1000
OF METAL, 0·036″								
150	100	90	80	70	—	—	—	—
250	200	200	170	150	130	—	—	—
500	350	300	280	230	200	180	—	—
700	550	450	400	330	280	250	180	—
1000	800	650	550	450	370	320	280	250
1400	1100	850	700	600	500	420	380	300
1800	1400	1150	900	800	650	550	500	450
2300	1800	1500	1200	1000	850	800	700	550
2800	2300	1850	1500	1300	1100	920	800	700
3600	2800	2300	1850	1550	1300	1150	1000	900
4300	3400	2950	2300	1950	1650	1400	1300	1150
5200	4100	3350	2750	2353	2000	1700	1500	1350
OF METAL, 0·056″								
150	120	100	70	—	—	—	—	—
350	250	200	120	100	—	—	—	—
600	500	400	320	300	260	—	—	—
950	800	650	550	500	350	320	—	—
1500	1200	950	800	700	550	500	450	—
2000	1600	1300	1000	850	750	650	570	500
2700	2100	1700	1400	1200	1000	850	750	650
3450	2700	2200	1800	1500	1250	1000	875	800
4300	3500	2800	2300	1900	1650	1350	1150	1000
5300	4300	3500	2850	2400	2000	1700	1500	1250
6500	5100	4250	3550	2000	2500	2100	1850	1600
7700	6200	5000	4200	3600	3050	2600	2300	2000

LIST OF TABLES.

I. Comparison of Calculated and Actual Performance.
II. Weights of Structural Components expressed as Percentages of the Total Weight.
III. Diminution in Weight per H.P. of Aero Engines.
IV. Percentage Resistance of Aeroplane Components.
V. Strength and Weight of Timbers.
VI. Properties of Duralumin.
VII. Specific Tenacity of Different Materials.
VIII. Steels to Standard Specifications.
IX. Brinell Hardness Numbers.
X. Factors of Safety.
XI. Wind Pressures.
XII. Table of Forces.
XIII. Table of Forces.
XIV. Influence of Aspect Ratio on the Normal Pressure of a Flat Plate (Eiffel).
XV. R.A.F.6. Coefficients.
XVI. Influence of Aspect Ratio.
XVII. Camber.
XVIII. Reduction Coefficients due to Biplane Effects.
XIX. Comparison of Lift Coefficients.
XX. Comparison of the Wings of a Triplane.
XXI. Calculations of V/V′.
XXII. Moments of Inertia—Geometrical Sections.
XXIII. Load, Shear Force, Bending Moment and Deflection.
XXIV. Shear, Bending Moment, Slope, and Deflection by Tabular Integration.
XXV. Wing Loading of Modern Machines.
XXVI. Bracing Wires and Tie-rods.
XXVII. Particulars of Strands for Aircraft Purposes.
XXVIII. Strainers.
XXIX. Resistances of Struts.
XXX. Resistance Coefficients for Fuselage Shapes.
XXXI. Monocoque Fuselages without Airscrews.
XXXII. Monocoque Fuselages with Airscrews.
XXXIII. Comparison of Four Fuselage Bodies.
XXXIV. Values of K with Increase of dV.
XXXV. Resistance of Inclined Struts and Wires.

XXXVI. Resistances of Landing Wheels.
XXXVII. Estimate of Body Resistance of B.E.2 at 60 M.P.H.
XXXVIII. Resistance of Aeroplane Components.
XXXIX. Skin Frictional Resistances.
XL. Percentage Weights of Aeroplane Components.
XLI. Weights and Particulars of Leading Aero Engines.
XLII. Elongation of Shock Absorber.
XLIII. Stresses due to Centrifrugal Force.
XLIV. Stresses due to Bending.
XLV. Maximum Stresses in the Airscrew Blade.
XLVI. Stability Nomenclature.
XLVII. (Case I.) Speed 79 m.p.h. Angle of Attack (i) 1°
XLVIII. (Case II.) Speed 45 m.p.h. Angle of Attack (i) 12°.
XLIX. Wing Characteristics.
L. Determination of Angle of Downwash.
LI. " " θ'
LII. " " Angle of Tailplane to Body.
LIII. " " Elevator Moment.
LIV. " " K_y'
LV. Lateral Force of Aeroplane Components.
LVI. Determination of Wing Resistance.
LVII. " " H.P. available.
LVIII. Mean Atmospheric Pressure, Temperature, and Density at Various Heights above Sea Level.
LIX. Percentage of Standard Density due to Change of Altitude.
LX. Calibration of an Airspeed Indicator by Direct Test.
LXI. Airspeed at Heights.
LXII. Rate of Climb Test.
LXIII. Determination of the Position of the Centre of Gravity.
LXIV. Balancing.
LXV. Body Resistance (Outside Slip Stream).
LXVI. Body Resistance (In Slip Stream).
LXVII. Calculation of Slip Stream Coefficient.
LXVIII. Body Resistance of Machine at Different Speeds.
LXIX. Calculation of Total Resistance.
LXX. Horse-power Required and Available, and Rate of Climb.
LXXI. Progress of Civil Aviation in England, May 15th to October 31st, 1919.
LXXII. Data relating to Successful Aeroplanes.
LXXIII. " " " "
LXXIV. Safe Loads in lbs. for Tubular Steel Struts.

INDEX.

ACCELEROMETER, 145.
Aeroplane nomenclature, 445.
Aerodynamic balance, 41-45.
Aero engines, 239.
Aerofoil, 38, *et seq.*
—— characteristics, 3, 50, 59.
—— choice, 84–86.
—— comparison with model, 64.
—— effect of thickening L. E., 73.
—— ,, ,, T. E., 74.
—— full-scale pressure distribution, 62, 63.
—— pressure distribution, 55, 57, 60, 61.
—— superimposed, 79, 80.
—— upper and lower surfaces compared, 65, 66.
—— variation of maximum ordinate, 71, 72.
Ailerons (wing flaps), 372.
—— balanced, 377.
Airco machines, 429, 430.
Airscrew, 7, 280, *et seq.*
—— airscrew balance, 302.
—— angle of attack, 9.
—— construction, 299.
—— design, 285, 286, 295, 296.
—— efficiency, 8, 140, 287, 289.
—— slip ratio, 282, 283.
—— stresses, 295–98.
—— testing, 302.
—— variable pitch, 9.
Airspeed indicator, 390, 392.
—— calibration, 401.
Altimeter, 398, 399.
Alloys, light, 15.
—— steel, 17.
Anemometer, 390.
Aneroid barometer, 397, 398.
Angular accelerations, 308.
Armstrong-Whitworth machines, 137, 428, 431.
Aspect ratio, 5, 47–49, 63–65, 382, 383.
Atlantic flight, 425.
Australian flight, 425.
Avro biplane, 421.
Avro machines, 426, *et seq.*
Avro triplane, 426.

BANKING, 143.
Bairstow, 304, 313, 333.
Bending moment, 110–13, 118, 120, 121, 198.
B.E. 2 biplane, 349.
B.E. 2 fuselage.
B.E. 3 fuselage, 222–27.
Bernouilli's assumption, 144, 155.
Biplane, 5, 80.
—— strutless, 135.
—— trusses, 132.
—— wireless, 134.
Blade element theory, 280, 490, *et seq.*
Bleriot, 131, 425, 426.
—— stability model, 315, 321, 323, 335.
Body resistance, 213, 383, 386, 417, 419.
Boulton & Paul machines, 437, 444.
Bow's notation, 28.
Brinell hardness, 22, 23.
Bristol fighter, 146, 147.
—— machines, 431, 432.
—— monoplane, 424.
—— triplane, 433.
Bryan, 304.
Bulk modulus, 21.

CAMBER, upper service variable, 67–69.
—— lower service variable, 70.
Ceiling, 8.
Centre of gravity, 75, 132, 257, 260, 410.
Centre of pressure, 16, 74, 75, 149, 160, 162, 356, 374.
Centre of resistance, 414, 417, 418.
Chanute, 1, 132.
Chassis, 260.
—— design, 262, *et seq.*
—— location, 261, 262.
—— resistance, 230.

Chassis, stresses, 269-71.
—— types, 264, 269.
Civil aviation, 425.
Clerk Maxwell, 26.
Controllability, 5, 9, 11, 303, 346.
Control surfaces, 346, *et seq.*, 443.
—— balanced, 375.
Controls, 407.
Cowling, 255.
Curtiss, 253.
—— stability model, 339–44.

DECALAGE, 83.
Deflexion, 118, 120, 121.
De Havilland, 429.
Density, standard, 390.
Derivatives, resistance, 301, 314.
—— rotary, 304, 314.
Dihedral, 407.
Dines, 389.
Down-loading stresses, 151, 155–57, 165, 197.
Drag, 4, 7, 49–52, 54, 58.
Drag-bracing, 137, 138, 163, 177, 191, 194.
Drag-struts, 177, 178, 195.
Drawings, general scheme, 411.
Dual control, 378.
Duplication, 161.
Duralumin, 15.

ECCENTRIC loading, 126.
Eddy motion, 59.
Eiffel, 38, 47, 231.
Eiffel laboratory, 45, 46.
Elasticity, 20.
Elevator, 346, 356, 379.
—— settings, 359, *et seq.*
End effect, 62, 287.
End correction factor, 198.
Engine mountings, 250–53.
Equations of motion, 307.
Equivalent chord, 357.
Euler's formula, 125, 126.

FABRIC, 20.
Factor of safety, 23, 24, 140, 141.
Farman, H., 132.
Fin, 368, 379.
Fineness ratio, 129.
Flat plate, force on, 47.
—— inclined, 48.
—— edgewise, 50.
—— resistance, 230.
Forces, 10.
Fuselage design, 237, *et seq.*
—— monocoque, 223, 238, 245, 443.
—— resistance, 213, 215–20, 222.
—— stressing, 247, 249.

GAP, 77, 407.
Grieve, 425.
Gyroscopic action, 257–59.

Handley Page, 424, 425, 433, 434.
—— fuselage, 245.
Hanging on the prop, 8.
Hawker, 433, 435.
Hooke's law, 21, 114.
Horse-power, 7.
—— available, 384, 424, 487.
—— required, 384, 487, 420.

INCIDENCE bracing, 137, 138, 162.
Incidence gears, 363, 379.
Inherently stable, 303.
Interference, 77, 383.
Interplane struts, 165, 171–76, 178, 184–91.

KINEMATIC viscosity, 89.

LANCHESTER, 304.
Langley, 48, 424.
Lateral force, 319, 325, 327, 370.
—— in airscrew, 372.
Lay-out, 403, *et seq.*
Leading edge, 73.
Lift, 4, 7, 49–52, 54, 58.
—— effect of variable camber on, 68–71.
—— bracing, 165.
Lift/Drag, 51, 53, 54.
—— superimposed aerofoils, 83.
Lilienthal, 1.
Linear accelerations, 307.
Load, 118, 122, 27.
—— diagram, 122.
Longitudinal force, 317, 353, 354.

MATERIALS, 13, *et seq.*
Maxim, 424.
Meridian curve (tapered strut), 174.
Method of sections, 35–37.
Moments of inertia, 101, 102, 105–108.
Monoplane, 5, 80.
—— trusses, 130.
Multiplane, 6.

NIEUPORT, 6, 133, 139.
Nomograms, 108, 109.
Normal force, 318, 352, 355.
Nose diving, 144.
National Physical Laboratory, 38.

OLEO gear, 276.
Oscillations, longitudinal, 315.
—— lateral, 313.

PARALLEL axes, 102.
Parasol type, 132.
Performance, 2, 381, *et seq.*, 389, 444.
—— curves, 421.
—— test, full scale, 395.
Perry formula, 129.
Pfalz, 248.
Pitching, 305.
—— moment, 319, 254, 352, 355.
Pitot tube, 56, 392, 393.
Poisson's ratio, 21, 22.
Polar moment of inertia, 105.
Polygon of forces, 26.
Pratt truss, 131, 132.
Pusher, 139, 176, 254.

QUADRUPLANE trusses, 137.

RADIATORS, 255–57.
R.A.F. 6, characteristics, 54, 164.
R.A.F. wires, 167
Rankine-Gordon formula, 126, 127, 249, 250.
Rate of climb, 386, 3)6, 400, 402, 421.
Rayleigh, 88.
Resistance, 6, 208, *et seq.*
—— aeroplane components, 233.
—— complete machine, 232.
—— wires, 228, 229, 382, 420.
Ribs, 177, 203–206.
Rigidity modulus, 21.
Rolling, 305.
—— moment, 320, 325, 327.
Ross-Smith, 425.
Routh's discriminant, 313, 330, 343.
Rudder, 368, 379, 408.

SECTION modulus, 116.
S. E. 4, 369.
S. E. 5, 145, 146, 442.
Shear force, 110–13, 198.
Shear stress, 116, 118.
Shock absorbers, 272–76.
Similitude, 88.
Skin friction, 209, 234–37, 244.
Slip stream, air-screw, 231.
—— coefficient, 234, 419.
Slope, 118, 120, 121.
Sopwith machines, 433, 435.
Spars, 179, 181, 195, 196, 199, 200, 201.
Specific tenacity, 15.
Spiral instability, 334.
Stability, 9, 11, 303, *et seq.*, 346, 408.
—— nomenclature, 305.
—— lateral, 319–21, 323, 333.
—— longitudinal, 315–17, 330, 338.
Stable machine, 303.
Stagger, 83, 84, 164, 383, 407.
Stanton, Dr., 47.
Statoscope, 400.
Steel, 16.
Strain, 20, 101, *et seq.*
Strainers, 169, 170.
Stream lining, 208, *et seq.*
—— chassis, 279.
Stress, 20, 101, *et seq.*, 148.
—— airscrew, 295.
—— beams, 114.
—— chassis, 269-71.
—— fuselage, 247, 249.
Stress diagrams, 26, 34.
—— reciprocal figures, 35.
Struts, 121, 123, 124.
—— tapered, 121, 174–76, 184–87, 189, 191.
—— stream line, 129.
—— interplane, 165, 171–74.
—— inclined, 213, 229.
Strut resistance, 213, 214.
Sturtevant, 246, 253.
Superimposed aerofoils, 79, 80.

TABULAR integration, 120.
Tail-plane incidence gears, 363, 379.
Tail plane, 80, 346, 379.
—— design, 357.
—— interference, 80.
—— loading, 347.
—— skid, 277, 278.
Theorem of three moments, 113, 154, 155.
Tie rods, 167, 168.
Timber, 13, 14.
—— seasoning, 13.
Torque, 286.
Tractive power, 289.
—— airscrew, 231.
Tractor, 139, 176.
Trailing edge, 74.
—— reflexure, 76, 77.
Triangle of forces, 26.
Triplane, 5, 80.
Trusses, 136.
Thrust, 288, 293.

UNITS, 87, 88.

VENTURI meter, 393, 394.
Vickers Vimy-Rolls, 425, 432, 436, 437.
Vimy bomber, 240.
—— commercial, 244, 245, 248, 432.
V. squared law, 210.

WASH from main planes, 349.
Weight, 2, 238.
Wind pressure, 24, 25.
—— tunnel, 38–40.
Wing assembly, 206, 207.
—— design, 130, *et seq.*, 160, 183, 184, 443.
—— folding, 8, 208.
—— resistance, 384, 419.
—— sections and characteristics, 90–100.
—— stresses, 148, 152, 153.
—— structures, 130.
—— tip losses, 287.
Wings, loading, 149, 150.
—— pressure distribution, 62, 63.
—— weights, 149.
Wires resistance, 228, 229.
Wright brothers, 424, 425.
—— glider, 8.

YAWING, 305.
—— moment, 324, 326, 328, 369.
Young's modulus, 21, 114.

ZAHM, 235.